NOVEL INSIGHTS INTO PLANT-GEMINIVIRUS INTERACTIONS

EDITED BY: Jose Trinidad Ascencio-Ibáñez, Alice Kazuko Inoue-Nagata, Rosa Lozano-Durán and Araceli G. Castillo

PUBLISHED IN: Frontiers in Plant Science and Frontiers in Microbiology

frontiers Research Topics

frontiers

ISSN 1664-8714
ISBN 978-2-88966-785-7
DOI 10.3389/978-2-88966-785-7

About Frontiers

Frontiers is more than just an open-access publisher of scholarly articles: it is a pioneering approach to the world of academia, radically improving the way scholarly research is managed. The grand vision of Frontiers is a world where all people have an equal opportunity to seek, share and generate knowledge. Frontiers provides immediate and permanent online open access to all its publications, but this alone is not enough to realize our grand goals.

Frontiers Journal Series

The Frontiers Journal Series is a multi-tier and interdisciplinary set of open-access, online journals, promising a paradigm shift from the current review, selection and dissemination processes in academic publishing. All Frontiers journals are driven by researchers for researchers; therefore, they constitute a service to the scholarly community. At the same time, the Frontiers Journal Series operates on a revolutionary invention, the tiered publishing system, initially addressing specific communities of scholars, and gradually climbing up to broader public understanding, thus serving the interests of the lay society, too.

Dedication to Quality

Each Frontiers article is a landmark of the highest quality, thanks to genuinely collaborative interactions between authors and review editors, who include some of the world's best academicians. Research must be certified by peers before entering a stream of knowledge that may eventually reach the public - and shape society; therefore, Frontiers only applies the most rigorous and unbiased reviews.
Frontiers revolutionizes research publishing by freely delivering the most outstanding research, evaluated with no bias from both the academic and social point of view. By applying the most advanced information technologies, Frontiers is catapulting scholarly publishing into a new generation.

What are Frontiers Research Topics?

Frontiers Research Topics are very popular trademarks of the Frontiers Journals Series: they are collections of at least ten articles, all centered on a particular subject. With their unique mix of varied contributions from Original Research to Review Articles, Frontiers Research Topics unify the most influential researchers, the latest key findings and historical advances in a hot research area! Find out more on how to host your own Frontiers Research Topic or contribute to one as an author by contacting the Frontiers Editorial Office: frontiersin.org/about/contact

NOVEL INSIGHTS INTO PLANT-GEMINIVIRUS INTERACTIONS

Topic Editors:
Jose Trinidad Ascencio-Ibáñez, North Carolina State University, United States
Alice Kazuko Inoue-Nagata, Brazilian Agricultural Research Corporation (EMBRAPA), Brazil
Rosa Lozano-Durán, Shanghai Institute for Biological Sciences, Chinese Academy of Sciences (CAS), China
Araceli G. Castillo, Institute of Subtropical and Mediterranean Horticulture La Mayora, Spain

Citation: Ascencio-Ibáñez, J. T., Inoue-Nagata, A. K., Lozano-Durán, R., Castillo, A. G., eds. (2021). Novel Insights Into Plant-Geminivirus Interactions. Lausanne: Frontiers Media SA. doi: 10.3389/978-2-88966-785-7

Table of Contents

frontiers in Plant Science

MINI REVIEW
published: 08 April 2020
doi: 10.3389/fpls.2020.00398

A Begomovirus Nuclear Shuttle Protein-Interacting Immune Hub: Hijacking Host Transport Activities and Suppressing Incompatible Functions

*Laura G. C. Martins, Gabriel A. S. Raimundo, Nathalia G. A. Ribeiro, Jose Cleydson F. Silva, Nívea C. Euclydes, Virgilio A. P. Loriato, Christiane E. M. Duarte and Elizabeth P. B. Fontes**

Department of Biochemistry and Molecular Biology, National Institute of Science and Technology in Plant-Pest Interactions, Bioagro, Universidade Federal de Viçosa, Viçosa, Brazil

OPEN ACCESS

Edited by:
Rosa Lozano-Durán, Shanghai Institutes for Biological Sciences (CAS), China

Reviewed by:
R. Vinoth Kumar, National Centre For Biological Sciences, India
Björn Krenz, German Collection of Microorganisms and Cell Cultures GmbH (DSMZ), Germany

***Correspondence:**
Elizabeth P. B. Fontes
bbfontes@ufv.br

Specialty section:
This article was submitted to Virology, a section of the journal Frontiers in Plant Science

Received: *14 January 2020*
Accepted: *19 March 2020*
Published: *08 April 2020*

Citation:
Martins LGC, Raimundo GAS, Ribeiro NGA, Silva JCF, Euclydes NC, Loriato VAP, Duarte CEM and Fontes EPB (2020) A Begomovirus Nuclear Shuttle Protein-Interacting Immune Hub: Hijacking Host Transport Activities and Suppressing Incompatible Functions. Front. Plant Sci. 11:398. doi: 10.3389/fpls.2020.00398

Begomoviruses (*Geminiviridae* family) represent a severe constraint to agriculture worldwide. As ssDNA viruses that replicate in the nuclei of infected cells, the nascent viral DNA has to move to the cytoplasm and then to the adjacent cell to cause disease. The begomovirus nuclear shuttle protein (NSP) assists the intracellular transport of viral DNA from the nucleus to the cytoplasm and cooperates with the movement protein (MP) for the cell-to-cell translocation of viral DNA to uninfected cells. As a facilitator of intra- and intercellular transport of viral DNA, NSP is predicted to associate with host proteins from the nuclear export machinery, the intracytoplasmic active transport system, and the cell-to-cell transport complex. Furthermore, NSP functions as a virulence factor that suppresses antiviral immunity against begomoviruses. In this review, we focus on the protein-protein network that converges on NSP with a high degree of centrality and forms an immune hub against begomoviruses. We also describe the compatible host functions hijacked by NSP to promote the nucleocytoplasmic and intracytoplasmic movement of viral DNA. Finally, we discuss the NSP virulence function as a suppressor of the recently described NSP-interacting kinase 1 (NIK1)-mediated antiviral immunity. Understanding the NSP-host protein-protein interaction (PPI) network will probably pave the way for strategies to generate more durable resistance against begomoviruses.

Keywords: nuclear shuttle protein, begomoviruses, immune hub, NSP, NSP-interacting proteins, NIG, NSI, NIK

INTRODUCTION

Begomovirus represents the largest genus of the *Geminiviridae* family and consists of whitefly-transmitted single-stranded DNA viruses, which severely inflict several important crops and vegetables in tropical and subtropical regions (Rojas et al., 2018). Species of the *Begomovirus* genus can be either monopartite (with one single genomic component) or bipartite (two genomic components, referred to as DNA-A and DNA-B) (Zerbini et al., 2017; Kumar, 2019). The nuclear shuttle protein (NSP) is encoded by the DNA-B of bipartite begomoviruses, which also encodes the

movement protein (MP). MP and NSP are required for systemic infection and act cooperatively to mediate the intra- and intercellular trafficking of viral DNA (Lazarowitz and Beachy, 1999; Gafni and Epel, 2002; Sanderfoot et al., 1996). Pioneering studies with the movement proteins from *Bean dwarf mosaic virus* (BDMV) and *Squash leaf curl virus* (SLCV) have established that NSP facilitates the nucleocytoplasmic translocation of viral DNA via nuclear pores, whereas MP is predominantly involved in mediating the cell-to-cell movement of viral DNA via plasmodesmata (Noueiry et al., 1994; Sanderfoot and Lazarowitz, 1995, 1996).

The host range of begomovirus species depends on multiple molecular interactions involved in both co-opting the cellular machinery and evading the innate immune recognition (for reviews see Hanley-Bowdoin et al., 2013; Li et al., 2018; Kumar, 2019). Failure of any one of these steps can decrease or impair the virus proliferation on a given host. NSP is implicated in both pro- and antiviral interactions, which determine host susceptibility to begomovirus. Based on characterized NSP-interacting proteins, we describe here an NSP-interacting immune hub, as one of the influential spreaders of information from the host immune system and begomovirus virulence strategies. As the combinatorial effects of pro- and antiviral interactions may establish the host susceptibility to a virus, the elucidation of the NSP-host protein-protein interaction (PPI) network is expected to shed light on the mechanisms for engineering resistance to begomoviruses.

NSP-INTERACTING PROTEINS DISPLAYING PROVIRAL FUNCTIONS

As begomoviruses replicate in the nuclei of infected cells, the nascent viral DNA (vDNA) must be translocated from the nucleus to the cytosol via nuclear pores, throughout the cytoplasm to the cell periphery and then to the adjacent, uninfected cells via plasmodesmata. To promote this typical cell-to-cell movement, like any other plant virus, the DNA-B of begomoviruses encodes a movement protein that increases the size exclusion limit of the plasmodesmata and mediates the viral nucleic acid translocation into adjacent cells (Noueiry et al., 1994). However, the mechanisms of viral DNA exit from the nucleus and its intracytoplasmic movement to the cell periphery are far less understood. It has been conceptually accepted that NSP facilitates the nuclear exit of newly replicated vDNA via nuclear pores, but interactions of the viral protein with the host nuclear transport machinery have not been reported. Consistent with the NSP-mediated nucleocytoplasmic transport of ss-vDNA, NSPs from BDMV and *Abutilon mosaic virus* (AbMV) interact with ss-vDNA and ds-vDNA presumably in the nuclei of infected cells, whereas NSP from SLCV binds only ss-vDNA *in vitro* (Pascal et al., 1994; Rojas et al., 1998; Hehnle et al., 2004). Immunogold labeling of systemically infected leaves localized SLCV NSP in the nuclei of phloem cells (Pascal et al., 1994) and expression of an epitope-tagged AbMV NSP in *Nicotiana benthamiana* cells confirmed its nuclear localization (Kleinow et al., 2009). In transient assays, NSP from different begomoviruses has been shown to be located in nuclei of cells exclusively expressing NSP fusions but is redirected to the cell periphery in the presence of co-expressed MP (Sanderfoot and Lazarowitz, 1995; Sanderfoot et al., 1996; Lazarowitz and Beachy, 1999; Zhang et al., 2001). The identification of an NSP-interacting GTPase (NIG), which interacts with NSP at the cytosolic side of the nuclear pore complex and shares transport properties with the human Rev-Interacting Protein (hRIP), has shed light on the mechanism for the release of NSP-vDNA complex from the nuclear periphery into the cytoplasm (Carvalho et al., 2008a,b). NSP also interacts with MP in the cytoplasm (Carvalho et al., 2008a), which may promote the directionality of virus translocation to the cell surface (Noueiry et al., 1994; Sanderfoot and Lazarowitz, 1995; Frischmuth et al., 2007).

Consistent with a role in the transport of vDNA-NSP complex, NIG interacts *in vivo* and *in vitro* with different begomovirus NSPs, promotes the translocation of NSP from the nucleus to the cytosol and displays a proviral function (Carvalho et al., 2008a). Furthermore, NIG shares structural features and transport proprieties with hRIP, an essential Rev cofactor that accessorizes the release of HIV-1 RNAs from nuclear-exported complexes into the cytosol (Sánchez-Velar et al., 2004). Therefore, the begomovirus NSP role in plants may be similar to the HIV Rev function in mammals. Both hRIP and NIG exhibit an N-terminal ArfGAP domain, involved in in addressing intracellular protein localization, vesicular trafficking or signaling (Chavrier and Goud, 1999; Turner et al., 2001; Sabe et al., 2006; Bist et al., 2017). Based on its effects on NSP function and transport properties, NIG may function as a facilitator for the disassembly of nuclear-exported complexes at the cytoplasmic side, and/or a positive regulator for addressing these nuclear-exported proteins to specific sites within the cytoplasm (Carvalho et al., 2008a). Nevertheless, cytosolic targets for NIG have not been identified yet, and its proviral function has not been examined in reverse genetics studies, which preclude a conclusive understanding of the underlying mechanism for NIG action. Currently, the only identified NIG partner is a nuclear body-forming protein, AtWWP1 (*Arabidopsis thaliana* WW domain-containing protein 1), which accumulates during viral infection and sequesters NIG into nuclear bodies (Calil et al., 2018).

Cabbage leaf curl virus (CaLCuV) NSP has been demonstrated to interact with a nuclear acetyltransferase, designated nuclear shuttle protein interactor (AtNSI), which may control the ss-vDNA-NSP nuclear export through acetylation of CP and histones (McGarry et al., 2003; Carvalho and Lazarowitz, 2004). AtNSI assembles into highly active multimeric enzyme complexes, which acetylate plant proteins that may be involved in differentiation and/or plant defense (Carvalho et al., 2006). NSP binding to AtNSI prevents its assembly into the highly active enzyme complexes, and hence NSP recruits AtNSI into newly synthesized ss-vDNA to acetylate bound CP. CP acetylation disrupts vDNA-CP interaction to favor vDNA-NSP complex formation and subsequent vDNA trafficking to the cytosol (Carvalho and Lazarowitz, 2004; Carvalho et al., 2006). AtNSI also acetylates histone H3, which is associated with vDNA nucleosome formation and genome assembly into minichromosomes, modulating viral replication

and transcription (McGarry et al., 2003). Nevertheless, H3 also interacts with both NSP and MP from BDMV and has been shown to be part of the vDNA-protein complex that traffics intra- and intercellularly (Zhou et al., 2011). The presence of H3 into an NSP- and MP-containing movement-competent complex might be attributed to the histone packaging ability, thereby assisting the viral genome transport through the nucleoporin complex and subsequentially through plasmodesma. However, attempts to use gene silencing for assessing a direct H3 role in begomovirus infection have not been succeeded, and hence whether the putative proviral function of H3 is essential for infection remains to be determined. Nonetheless, these NSP-interacting host proteins with proviral functions may be in somehow involved in stabilizing the ss-vDNA-NSP complex or actively assisting the nucleocytoplasmic transport function of the viral protein.

Although the mechanism of intra- and intercellular transport of begomoviral DNA may exhibit species specificity in some aspects, a general model for the intracellular trafficking of vDNA holds that, in the nucleus, NSP binds to vDNA and H3, and the complex NSP-H3-vDNA is exported to the cytoplasm via nuclear pores. At the cytosolic side, the release of the trimeric complex is facilitated by NIG; then, NSP binds to MP that also binds to H3. The complex MP-NSP-H3-vDNA traffics to the cell periphery to be translocated to adjacent, uninfected cells via plasmodesmata. In these neighboring cells, NSP shuttles the viral genome to the nucleus to initiate new rounds of viral genome replication via the rolling circle mechanism (Krichevsky et al., 2006; Hanley-Bowdoin et al., 2013). Consistent with the general aspects of the intracellular movement of vDNA, the MP and NSP from AbMV and BDMV have been shown to confer cell-to-cell movement to recombinant mastreviral replicons, which belong to the *Mastrevirus* genus of the *Geminiviridae* family (Diamos et al., 2019). This lack of species specificity of the begomoviral MP and NSP functions depends on the replicon size and a fine-tuning expression of MP and NSP to prevent hypersensitive response and interference with replication and expression from viral replicons.

NSP AS A SUPPRESSOR OF PLANT DEFENSES

A host defense-suppressing function of NSP was first demonstrated through its interaction with the NSP-interacting kinases (NIKs), which belong to the superfamily of the transmembrane leucine-rich repeat receptor-like kinases (LRR-RLK) (Fontes et al., 2004; Mariano et al., 2004). The NSP-binding site on NIK1 from Arabidopsis corresponds to an 80-amino acid sequence delimited by amino acids 422–502, which overlaps with the putative active site for Ser/Thr kinases (subdomain VIb–HrDvKssNxLLD) and the activation loop (subdomain VII–DFGAk/rx, plus subdomain VIII–GtxGyiaPEY). The activation site of NIK1 corresponds to a threonine residue at position 474 within the activation loop of the kinase (Fontes et al., 2004; Santos et al., 2009). As a single-pass transmembrane receptor kinase, NIK1 may dimerize or multimerize with itself and/or receptors to promote transphosphorylation and subsequent kinase activation (Santos et al., 2010). Binding of NSP to NIK1 blocks the phosphorylation of the crucial threonine-474 residue and hence prevents the activation of NIK1 that otherwise would transduce an antiviral signal in response to begomovirus infection. The NSP-NIK complex formation is neither virus-specific nor host-specific (Fontes et al., 2004; Mariano et al., 2004). The binding of NSP to NIKs is conserved among NSP from different begomoviruses, such as CaLCuV, *Tomato golden mosaic virus* (TGMV), *Tomato crinkle yellow leaf virus* (TCrYLV), *Tomato yellow spot virus* (ToYSV), and NIKs from different plant species, including soybean, tomato and Arabidopsis (Fontes et al., 2004; Mariano et al., 2004; Sakamoto et al., 2012). This observation has led to the manipulation of the NIK1 immune receptor-like kinase as a target for engineering broad-range resistance to begomoviruses (Brustolini et al., 2015). As a proof of concept, the constitutive activation of NIK1 by expression of the NIK1-T474D gain-of-function mutant resulted in suppression of general translation and enhanced resistance to different species of tomato-infecting begomoviruses in tomato transgenic lines. Despite 25% suppression of translation, the transgenic lines were phenotypically indistinguishable from untransformed tomato plants under greenhouse optimized growth conditions. In contrast, the constitutive activation of the NIK1-mediated antiviral signaling in Arabidopsis caused stunted growth (Zorzatto et al., 2015). An additional pitfall in engineering NIK1-mediated broad-range resistance to begomoviruses in crops is the finding that NIK1 negatively modulates antibacterial immunity (Li et al., 2019). NIK1 overexpression in Arabidopsis has been shown to enhance susceptibility to bacterial infections, which is not desirable under field conditions where plants are often exposed to simultaneous infections by different pathogens (Li et al., 2019).

Progress in elucidating the NIK1-mediated signaling pathway includes the characterization of the downstream components, the ribosomal protein L10 (RPL10), and the transcription-repressing factor L10-interacting Myb domain-containing protein (LIMYB) (Carvalho et al., 2008c; Rocha et al., 2008; Zorzatto et al., 2015). More recently, the NIK1-mediated antiviral signaling has been demonstrated to be activated by begomovirus-derived nucleic acids that very likely function as pattern-associated molecular patterns (PAMPs) to induce or stabilize the oligomerization of NIK1 as the critical early event that triggers signaling and transduction from a receptor (Teixeira et al., 2019).

The mechanistic model for NIK1 activation and defense assembly holds that, in response to virus infection, begomovirus-derived nucleic acids function as PAMPs to mediate dimerization of NIK1 with itself, its paralog NIK2 or another unknown transmembrane receptor, which may function as a PAMP recognition receptor (PRR) (Teixeira et al., 2019). The NIK1 oligomerization induces the phosphorylation of the NIK1 kinase domain at the key threonine residue at position 474 (Machado et al., 2015, 2017). This phosphorylation-induced activation of NIK1 mediates the phosphorylation of the downstream component RPL10, which, in turn, is reallocated from the cytoplasm to the nucleus, where it binds to LIMYB. The RPL10-LYMIB complex represses the expression of translational

machinery-related genes, including initiation and elongation factors of translation and ribosomal protein genes (Calil and Fontes, 2017; Gouveia et al., 2017). Prolonged downregulation of the translational machinery of plant cells leads to the suppression of global translation (Brustolini et al., 2015; Zorzatto et al., 2015). The viral mRNAs are not able to escape this translational regulatory mechanism of plant cells; they are not efficiently translated, compromising infection (Brustolini et al., 2015). In host-begomovirus compatible interactions, NSP from begomoviruses binds to the NIK1 kinase domain to prevent activation of the NIK1-mediated antiviral signaling creating an environment that is more favorable to virus infection (Fontes et al., 2004; Santos et al., 2009). Therefore, this antiviral signaling pathway is a defense strategy evolutionarily overcome by the virus.

Nuclear shuttle protein has also been shown to interact with two other receptor-like kinases, the brassinosteroid insensitive 1-associated kinase 1 (BAK1) and a PERK-like kinase, designated NSP-associated kinase (NsAK) (Florentino et al., 2006; Li et al., 2019). While the NSP-NsAK complex formation positively contributes to viral infection, the interaction of NSP with BAK1 may be associated with a host defense-suppressing function. BAK1 functions as a co-receptor of several PRRs, such as flagellin sensing 2 (FLS2) and elongation factor thermo unstable receptor (EFR), which perceive specific PAMPs and trigger or amplify PTI (PAMP-triggered immunity), the first layer of the plant innate immune system (Zipfel et al., 2006; Chinchilla et al., 2007). Several lines of evidence indicate that NSP may suppress BAK1 function. First, NIK1 and BAK1 are structurally related; they belong to the same subfamily II of LRR-RLKs and share conserved positions for the activation site of the kinases (Sakamoto et al., 2012). Second, the binding site of NSP on NIK1 and the corresponding sequence on BAK1 are highly conserved (Santos et al., 2010). Third, despite its antiviral function, NIK1 has also been shown to inhibit BAK1-mediated PTI through direct interaction with the co-receptor BAK1 and the PRR FLS2 (Li et al., 2019). The viral NSP suppressor of NIK1 may interfere with the NIK1-BAK1-FLS2 complex formation. Finally, viral infection has been shown to inhibit PTI directly via viral protein suppressors, including the coat protein (CP) from *Plum pox virus* (PPV; Nicaise and Candresse, 2017), the movement protein (MP) from *Cucumber mosaic virus* (CMV; Kong et al., 2018) and P6 from *Cauliflower mosaic virus* (CaMV) (Zvereva et al., 2016). PPV CP has also been shown to function as a viral effector (Avr factor), which activates effector-triggered immunity (ETI), the second layer of the innate immune system, via specific recognition by a host intracellular receptor, the resistance R protein (Decroocq et al., 2009). This finding suggests that viral suppressors may link the suppression of PTI with activation of ETI, as predicted by the zig-zag evolutionary model of plant innate immunity (Jones and Dangl, 2006). NSP from BDMV has also been shown to function as an Avr factor for ETI activation in resistant *Phaseolus vulgaris* genotypes (Garrido-Ramirez et al., 2000), linking a primary mechanism of antiviral immunity at the cell surface (NIK1 and BAK1) with ETI.

Nuclear shuttle protein from CaLCuV also interacts with ASYMMETRIC LEAVES2 (AS2), which regulates positively mRNA decapping and degradation, inhibits siRNA accumulation, and functions as an endogenous suppressor of post-transcriptional gene silencing (PTGS) (Ye et al., 2015). As a suppressor of host defense, NSP induces the expression of AS2 and also causes the nuclear exit of AS2 to activate DCP2 decapping activity and suppress PTGS. Therefore, NSP stimulates the AS2 proviral function and hence increases the susceptibility to begomovirus in Arabidopsis.

Immune-affinity capture of proteins using GFP-tagged-NSP (from AbMV) identified a unique peptide from the Arabidopsis Ras-GAP SH3 domain-binding protein (G3BP) homolog as a candidate for NSP-interacting protein (Krapp et al., 2017). G3BP is a stress granule (SG)-localized protein, which is required for SG assembly, implicated in host defense against animal viruses (Tourrière et al., 2003; Lloyd, 2012). The mRNA-protein aggregates of SGs are formed upon biotic and abiotic stresses in response to stalled translation (Buchan and Parker, 2009). Viral proteins bind G3BP via their FGDF motifs to impair SG assembly (McInerney, 2015; Panas et al., 2015). Additional evidence that AbMV NSP binds AtG3BP *in planta* relies on the observation that mutated NSP on its FGDF-like motif loses the capacity to co-localize with AtG3BP in SG, under stress conditions (Krapp et al., 2017). The biological relevance of the G3BP-NSP interaction has not been investigated; thereby, the proposition that NSP binds to G3BP to inhibit SG formation is reminiscent of functional studies of animal virus-host interactions (Lloyd, 2012; Panas et al., 2015).

AN NSP-INTERACTING IMMUNE HUB AGAINST BEGOMOVIRUSES

Genome-wide studies of plant immunity and pathogen infection strategies have revealed an integrated picture of the plant-pathogen interactions, in which the pathogen effector interactions and plant defense proteins converge to subsets of highly interconnected host proteins, designated hubs (Mukhtar et al., 2011). Based on its intra- and intercellular transport function, NSP from begomoviruses may be an excellent target for identifying components of the basic cellular processes as this viral protein interacts with host factors in different organelles and may represent itself a hub for host protein-protein interactions (**Figure 1**). Accordingly, we summarized here that the NSP-interacting immune hub is formed with proteins located in different subcellular compartments, including the nuclear acetylase, AtNSI (Carvalho and Lazarowitz, 2004), the nuclear Histone H3 (Zhou et al., 2011), the cytosolic GTPase NIG (Carvalho et al., 2008a), the nucleocytoplasmic AS2 (Ye et al., 2015), the cytoplasmic G3BP (Krapp et al., 2017) and the plasma membrane receptor kinases, designated NIKs (Fontes et al., 2004; Mariano et al., 2004) and NsAKs (Florentino et al., 2006). This NSP-interacting immune hub accommodates proviral proteins, including AtNSI, H3, NIG, NsAK, and AS2 and antiviral proteins, such as NIKs, G3BP, and AtWWP1. The proviral factors may facilitate or stabilize NSP binding to vDNA, such as AtNSI and H3, or may direct an active intracellular transport of NSP-vDNA, like NIG. The NIG-NSP interaction seems to be very important during infection because plant cells have evolved a defense

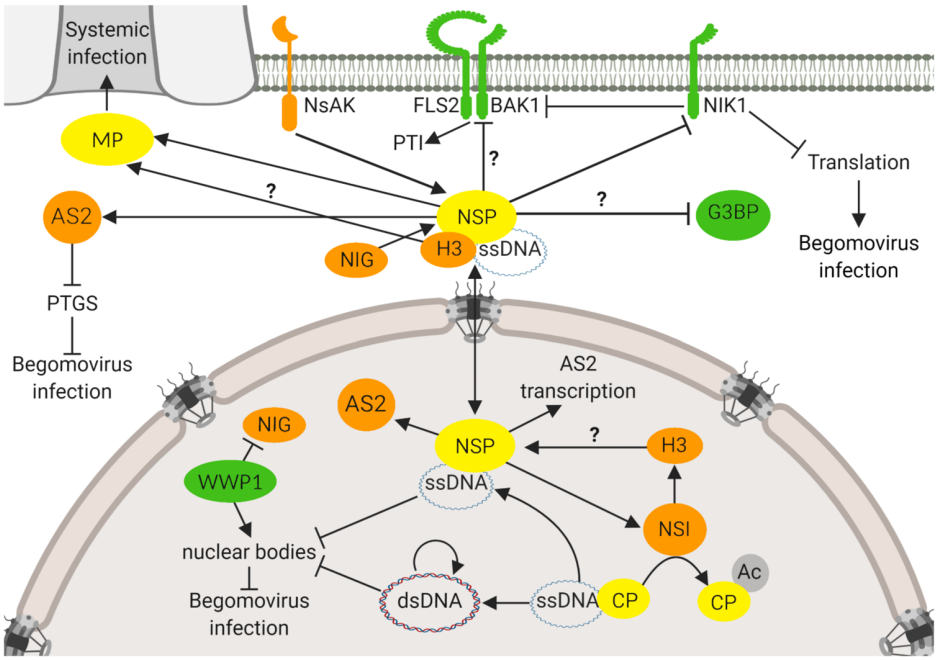

FIGURE 1 | NSP-interacting immune hub. The NSP-interacting immune hub consists of host proteins displaying antiviral functions (green) and proviral functions (orange). Viral proteins are indicated in yellow. In the nucleus, CaLCuV NSP binds to AtNSI to facilitate the acetylation of CP that favors NSP-vDNA complex formation. BDMV NSP also binds to H3. CaLCuV NSP increases the expression of proviral AS2, an inhibitor of PTGS, and also promotes its reallocation to the cytosol. At the cytosolic, perinuclear region, CaLCuV NSP interacts with NIG to facilitate the release of the vDNA-NSP complex from the nuclear pore into the cytosol. To prevent the NIG proviral function, the antiviral protein WWP1 sequesters NIG into nuclear bodies (NB), impairing its cytosolic transport function. As a counter defensive measure, vDNA disrupts the WWP1-NB assembly. At the cytoplasm, NSP may interact with G3BP, a protein required for the assembly of stress granules. NSP also interacts with the viral MP, which may provide the directionality for the NSP-vDNA-H3 complex toward the plasmodesmata for translocation to the neighboring cells. At the plasma membrane, NSP interacts with the receptor-like kinase NIK1 to suppress its kinase activity that otherwise would transduce an antiviral signal against begomoviruses. NIK1 also inhibits PTI, via interaction with BAK1 that may also be a target of the suppressing activity of NSP. NSP may serve as a substrate for another receptor-like kinase, NsAK, at the plasma membrane. Question marks denote not fully characterized proviral or antiviral functions of host proteins. Arrows indicate a positive effect on protein activity, and inhibitor lines denote suppressing activities. Double arrow indicates the double direction of protein movement. The figure was created with BioRender.com.

strategy to prevent the NIG proviral function (Calil et al., 2018). Viral infection promotes the accumulation of a nuclear body (NB)-forming protein, AtWWP1, which relocates NIG from the cytoplasm to the nucleus where it is confined to AtWWP1-NBs, impairing the NIG cytosolic transport function (Calil et al., 2018). The antiviral function of AtWWP1-NBs, however, may be antagonized by the viral infection. As a counter defensive measure, vDNA binds to AtWWP1 and induces either a decrease in the number or disruption of AtWWP1-NBs, restoring the NIG cytosolic localization (Calil et al., 2018). Therefore, the begomoviruses have evolved vDNA-based virulence strategies to overcome nuclear bodies-derived host defense responses.

Likewise, the binding of NSP to defense proteins, such as NIK1 and AS2, leads to suppression of host immunity. In the first case, during infection, NSP inhibits the NIK1 kinase that otherwise would transduce an antiviral signal to protect plants against begomoviruses (Brustolini et al., 2015; Machado et al., 2015, 2017). In the latter case, NSP not only increases AS2 expression, an endogenous suppressor of PTGS, but also can induce nuclear export of AS2 to the cytosol where it interacts with DCP2 to stimulate decapping activity, decrease siRNA accumulation and impair RNA silencing (Ye et al., 2015).

The NSP-interacting immune hub also cross-talks with the antibacterial immune response through interactions between NIK1 and the flagellin receptor FLS2 and its co-receptor BAK1 (Li et al., 2019). In the absence of bacterial and viral infection, NIK1 binds to FLS2 and BAK1 to prevent the activation of an autoimmune response. NIK1 may control FLS2-BAK1 complex formation, as the amplitude of the immune response depends on basal concentrations of NIK1 (Li et al., 2019). The bacterial infection leads to the formation of an active immune complex, between PRR FLS2 and its co-receptor BAK1, which phosphorylates bound NIK1 at the crucial Thr-474 to activate antiviral immunity. Therefore, bacterial infection may promote plant resistance to begomoviruses in a NIK1-dependent manner.

The NSP-interacting immune hub was integrated into the Arabidopsis interactome (BioGRID database)[1] and (Arabidopsis interactome database)[2], and the LRR-based cell surface interaction network (CSILRR; Smakowska-Luzan et al., 2018), using Cytoscape software[3] (**Supplementary Figure 1**

[1]http://www.thebiogrid.org

[2]http://interactome.dfci.harvard.edu/A_thaliana/

[3]https://cytoscape.org/

and **Supplementary Table 1**). This procedure identified the NSP-host protein-protein interaction (PPI) network, containing directly and indirectly NSP-interacting host proteins that converge to relevant hubs of plant-pathogen interactions. Although this *in silico* studies revealed that the functional characterization of a potential NSP-interacting immune hub is far from being complete, these NSP-derived hubs may represent a framework for rationalizing future studies in begomovirus-host interactions.

CONCLUSION

Successful systemic plant infection by viruses depends on spreading their genomes between cells and throughout the plant. Thus, the identification of host factors involved in virus movement that interact direct or indirectly with virus-encoded movement proteins is essential for the establishment of novel antiviral strategies. NSP may use the nuclear export machinery to facilitate the translocation of viral DNA from the nucleus to the cytoplasm. Although some progress in the identification of NSP partners has been made in the last decade, the characterization of a potential NSP-interacting immune hub is far from being complete. For instance, we now know that intracellular trafficking of NSP-DNA complexes is accessorized by NIG at the cytosolic side, but the transport activity and underlying mechanism for NIG function are poorly understood (Carvalho et al., 2008a,b). Evidence that NIG functions in the viral DNA-NSP trafficking relies on the demonstration that NIG interacts *in vivo* and *in vitro* with NSP, is capable of redirecting NSP-DNA complexes from the nucleus to the cytoplasm and functions as a proviral factor during begomovirus infection (Carvalho et al., 2008a,b). These findings suggest that NIG may be a susceptibility gene for engineering resistance to begomovirus. Nevertheless, a conclusive demonstration that NIG is essential for begomovirus infection is lacking, and cytosolic NIG-interacting proteins that could provide an intracellular route for the complex vDNA-NSP trafficking toward the plasmodesmata have not been identified.

The host defense-suppressing function of NSP has also been characterized via protein-protein interaction studies. In this regard, NSP negatively controls virus silencing by inducing the expression and activity of the endogenous inhibitor of PTGS, AS2 (Ye et al., 2015). NSP also negatively modulates innate immune responses by suppressing activity of the immune receptor-like kinases NIK1 and BAK1 (Fontes et al., 2004; Sakamoto et al., 2012). While compelling evidence demonstrates that NSP inhibits the phosphorylation-mediated activation of NIK1 to prevent the receptor from signaling (Calil and Fontes, 2017; Gouveia et al., 2017), evidence that NSP controls negatively PTI is still rudimentary. Although NSP has been shown to interact with BAK1, a co-receptor of PTI, the NSP-mediated suppression of BAK1 function has not been examined yet. Therefore, attempts to deploy the innate immune responses as targets for plant resistance to begomovirus are still in their infancy.

AUTHOR CONTRIBUTIONS

LM, GR, NR, NE, VL, CD, and EF designed the concept and organized the manuscript. JS performed bioinformatic analysis. LM, GR, and EF wrote the manuscript. LM, CD, and EF edited the manuscript.

FUNDING

This work was partially supported by the Brazilian funding agencies: Conselho Nacional de Desenvolvimento Científico e Tecnológico (CNPq), Fundação de Amparo à Pesquisa do Estado de Minas Gerais (FAPEMIG), Coordenação de Aperfeiçoamento de Pessoal de Nível Superior (CAPES), and the National Institute of Science and Technology in Plant-Pest Interactions (INCTIPP).

SUPPLEMENTARY MATERIAL

The Supplementary Material for this article can be found online at: https://www.frontiersin.org/articles/10.3389/fpls.2020.00398/full#supplementary-material

REFERENCES

Bist, P., Kim, S. S., Pulloor, N. K., McCaffrey, K., Nair, S. K., Liu, Y., et al. (2017). ArfGAP domain-containing protein 2 (ADAP2) integrates upstream and downstream modules of RIG-I signaling and facilitates type I interferon production. *Mol. Cell. Biol.* 37:e00537-36.

Brustolini, O. J. B., Machado, J. P. B., Condori-Apfata, J. A., Coco, D., Deguchi, M., Loriato, V. A. P., et al. (2015). Sustained NIK-mediated antiviral signalling confers broad-spectrum tolerance to begomoviruses in cultivated plants. *Plant Biotechnol. J.* 13, 1300–1311. doi: 10.1111/pbi.12349

Buchan, J. R., and Parker, R. (2009). Review eukaryotic stress granules: the ins and outs of translation. *Mol. Cell* 36, 932–941. doi: 10.1016/j.molcel.2009.11.020

Calil, I. P., and Fontes, E. P. B. (2017). Plant immunity against viruses: antiviral immune receptors in focus. *Ann. Bot.* 119, 711–723. doi: 10.1093/aob/mcw200

Calil, I. P., Quadros, I. P. S., Araújo, T. C., Duarte, C. E. M., Gouveia-Mageste, B. C., Silva, J. C. F., et al. (2018). A WW domain-containing protein forms immune nuclear bodies against begomoviruses. *Mol. Plant.* 11, 1449–1465. doi: 10.1016/j.molp.2018.09.009

Carvalho, C. M., Fontenelle, M. R., Florentino, L. H., Santos, A. A., Zerbini, F. M., and Fontes, E. P. B. (2008a). A novel nucleocytoplasmic traffic GTPase identified as a functional target of the bipartite geminivirus nuclear shuttle protein. *Plant J.* 55, 869–880. doi: 10.1111/j.1365-313X.2008.03556.x

Carvalho, C. M., Machado, J. P. B., Zerbini, F. M., and Fontes, E. P. B. (2008b). NSP-interacting GTPase: a cytosolic protein as cofactor for nuclear shuttle proteins. *Plant Signal. Behav.* 3, 752–754. doi: 10.4161/psb.3.9.6641

Carvalho, C. M., Santos, A. A., Pires, S. R., Rocha, C. S., Saraiva, D. I., Machado, J. P. B., et al. (2008c). Regulated nuclear trafficking of rpL10A mediated by NIK1 represents a defense strategy of plant cells against virus. *PLoS Pathog.* 4:e1000247. doi: 10.1371/journal.ppat.1000247

Carvalho, M. F., and Lazarowitz, S. G. (2004). Interaction of the movement protein NSP and the *Arabidopsis* acetyltransferase AtNSI is necessary infection and pathogenicity. *J. Virol.* 78, 11161–11171. doi: 10.1128/JVI.78.20.11161

Carvalho, M. F., Turgeon, R., and Lazarowitz, S. G. (2006). The geminivirus nuclear shuttle protein NSP inhibits the activity of AtNSI, a vascular-expressed *Arabidopsis* acetyltransferase regulated with the sink-to-source transition. *Plant Physiol.* 140, 1317–1330. doi: 10.1104/pp.105.075556

Chavrier, P., and Goud, B. (1999). The role of ARF and Rab GTPases in membrane transport. *Curr. Opin. Cell Biol.* 11, 466–475. doi: 10.1016/S0955-0674(99)80067-2

Chinchilla, D., Zipfel, C., Robatzek, S., Kemmerling, B., Nürnberger, T., Jones, J. D. G., et al. (2007). A flagellin-induced complex of the receptor FLS2 and BAK1 initiates plant defence. *Nature* 448, 497–500. doi: 10.1038/nature05999

Decroocq, V., Salvador, B., Sicard, O., Glasa, M., Cosson, P., Svanella-Dumas, L., et al. (2009). The determinant of potyvirus ability to overcome the RTM resistance of *Arabidopsis thaliana* maps to the N-terminal region of the coat protein. *Mol. Plant Microb. Interact.* 22, 1302–1311. doi: 10.1094/mpmi-22-10-1302

Diamos, A. G., Crawford, J. M., and Mason, H. S. (2019). Fine-tuning expression of begomoviral movement and nuclear shuttle proteins confers cell-to-cell movement to mastreviral replicons in *Nicotiana benthamiana* leaves. *J. Gen. Virol.* 100, 1038–1051. doi: 10.1099/jgv.0.001275

Florentino, L. H., Santos, A. A., Fontenelle, M. R., Pinheiro, G. L., Zerbini, F. M., Baracat-Pereira, M. C., et al. (2006). A PERK-like receptor kinase interacts with the geminivirus nuclear shuttle protein and potentiates viral infection. *J. Virol.* 80, 6648–6656. doi: 10.1128/jvi.00173-06

Fontes, E. P. B., Santos, A. A., Luz, D. F., Waclawovsky, A. J., and Chory, J. (2004). The geminivirus nuclear shuttle protein is a virulence factor that suppresses transmembrane receptor kinase activity. *Genes Dev.* 18, 2545–2556. doi: 10.1101/gad.1245904

Frischmuth, S., Wege, C., Hülser, D., and Jeske, H. (2007). The movement protein BC1 promotes redirection of the nuclear shuttle protein BV1 of *Abutilon mosaic* geminivirus to the plasma membrane in fission yeast. *Protoplasma* 230, 117–123. doi: 10.1007/s00709-006-0223-x

Gafni, Y., and Epel, B. L. (2002). The role of host and viral proteins in intra- and inter-cellular trafficking of geminiviruses. *Physiol. Mol. Plant Pathol.* 60, 231–241. doi: 10.1006/pmpp.2002.0402

Garrido-Ramirez, E. R., Sudarshana, M. R., Lucas, W. J., and Gilbertson, R. L. (2000). Bean dwarf mosaic virus BV1 protein is a determinant of the hypersensitive response and avirulence in *Phaseolus vulgaris*. *Mol. Plant Microb. Interact.* 13, 1184–1194. doi: 10.1094/MPMI.2000.13.11.1184

Gouveia, B. C., Calil, I. P., Machado, J. P. B., Santos, A. A., and Fontes, E. P. B. (2017). Immune receptors and co-receptors in antiviral innate immunity in plants. *Front. Microbiol.* 7:2139. doi: 10.3389/fmicb.2016.02139

Hanley-Bowdoin, L., Bejarano, E. R., Robertson, D., and Mansoor, S. (2013). Geminiviruses: masters at redirecting and reprogramming plant processes. *Nat. Rev. Microbiol.* 11, 777–788. doi: 10.1038/nrmicro3117

Hehnle, S., Wege, C., and Jeske, H. (2004). Interaction of DNA with the movement proteins of geminiviruses revisited. *J. Virol.* 78, 7698–7706. doi: 10.1128/jvi.78.14.7698-7706.2004

Jones, J. D. G., and Dangl, J. L. (2006). The plant immune system. *Nature* 444, 323–329. doi: 10.1038/nature05286

Kleinow, T., Tanwir, F., Kocher, C., Krenz, B., Wege, C., and Jeske, H. (2009). Expression dynamics and ultrastructural localization of epitope-tagged *Abutilon mosaic* virus nuclear shuttle and movement proteins in *Nicotiana benthamiana* cells. *Virology* 391, 212–220. doi: 10.1016/j.virol.2009.06.042

Kong, J., Wei, M., Li, G., Lei, R., Qiu, Y., Wang, C., et al. (2018). The cucumber mosaic virus movement protein suppresses PAMP-triggered immune responses in *Arabidopsis* and tobacco. *Biochem. Biophys. Res. Comm.* 498, 395–401. doi: 10.1016/j.bbrc.2018.01.072

Krapp, S., Greiner, E., Amin, B., Sonnewald, U., and Krenz, B. (2017). The stress granule component G3BP is a novel interaction partner for the nuclear shuttle proteins of the nanovirus pea necrotic yellow dwarf virus and geminivirus *Abutilon mosaic* virus. *Virus Res.* 227, 6–14. doi: 10.1016/j.virusres.2016.09.021

Krichevsky, A., Kozlovsky, S. V., Gafni, Y., and Citovsky, V. (2006). Nuclear import and export of plant virus proteins and genomes. *Mol. Plant Pathol.* 7, 131–146. doi: 10.1111/j.1364-3703.2006.00321.x

Kumar, R. V. (2019). Plant antiviral immunity against geminiviruses and viral counter-defense for survival. *Front. Microbiol.* 10:1460. doi: 10.3389/fmicb.2019.01460

Lazarowitz, S. G., and Beachy, R. N. (1999). Viral movement proteins as probes for intracellular and intercellular trafficking in plants. *Plant Cell* 11, 535–548. doi: 10.1105/tpc.11.4.535

Li, B., Ferreira, M. A., Huang, M., Camargos, L. F., Yu, X., Teixeira, R. M., et al. (2019). The receptor-like kinase NIK1 targets FLS2/BAK1 immune complex and inversely modulates antiviral and antibacterial immunity. *Nat. Commun.* 10:4996. doi: 10.1038/s41467-019-12847-6

Li, F., Yang, X., Bisaro, D. M., and Zhou, X. (2018). The βC1 protein of geminivirus-betasatellite complexes: a target and repressor of host defenses. *Mol. Plant* 11, 1424–1426. doi: 10.1016/j.molp.2018.10.007

Lloyd, R. E. (2012). How do viruses interact with stress-associated RNA granules? *PLoS Pathog.* 8:e1002741. doi: 10.1371/journal.ppat.1002741

Machado, J. P. B., Brustolini, O. J. B., Mendes, G. C., Santos, A. A., and Fontes, E. P. B. (2015). NIK1, a host factor specialized in antiviral defense or a novel general regulator of plant immunity? *Bioessays* 37, 1236–1242. doi: 10.1002/bies.201500066

Machado, J. P. B., Calil, I. P., Santos, A. A., and Fontes, E. P. B. (2017). Translational control in plant antiviral immunity. *Genet. Mol. Biol.* 40, 292–304. doi: 10.1590/1678-4685-gmb-2016-0092

Mariano, A. C., Andrade, M. O., Santos, A. A., Carolino, S. M. B., Oliveira, M. L., Baracat-Pereira, M. C., et al. (2004). Identification of a novel receptor-like protein kinase that interacts with a geminivirus nuclear shuttle protein. *Virology* 318, 24–31. doi: 10.1016/j.virol.2003.09.038

McGarry, R. C., Barron, Y. D., Carvalho, M. F., Hill, J. E., Gold, D., Cheung, E., et al. (2003). A novel *Arabidopsis* acetyltransferase interacts with the geminivirus movement protein NSP. *Plant Cell* 15, 1605–1618. doi: 10.1105/tpc.012120

McInerney, G. M. (2015). FGDF motif regulation of stress granule formation. *DNA Cell Biol.* 34, 1–4. doi: 10.1089/dna.2015.295.7

Mukhtar, M. S., Carvunis, A. R., Dreze, M., Epple, P., Steinbrenner, J., Moore, J., et al. (2011). Independently evolved virulence effectors converge onto hubs in a plant immune system network. *Science* 333, 596–601. doi: 10.1126/science.1203659

Nicaise, V., and Candresse, T. (2017). Plum pox virus capsid protein suppresses plant pathogen-associated molecular pattern (PAMP)-triggered immunity. *Mol. Plant Pathol.* 18, 878–886. doi: 10.1111/mpp.12447

Noueiry, A. O., Lucas, W. J., and Gilbertson, R. L. (1994). Two proteins of a plant DNA virus coordinate nuclear and plasmodesmal transport. *Cell* 76, 925–932. doi: 10.1016/0092-8674(94)90366-2

Panas, M. D., Schulte, T., Thaa, B., Sandalova, T., Kedersha, N., Achour, A., et al. (2015). Viral and cellular proteins containing FGDF motifs bind G3BP to block stress granule formation. *PLoS Pathog.* 11:e004659. doi: 10.1371/journal.ppat.1004659

Pascal, E., Sanderfoot, A. A., Ward, B. M., Medville, R., Turgeon, R., and Lazarowitz, S. G. (1994). The geminivirus BR1 movement protein binds single-stranded DNA and localizes the cell nucleus. *Plant Cell* 6, 995–1006. doi: 10.1105/tpc.6.7.995

Rocha, C. S., Santos, A. A., Machado, J. P. B., and Fontes, E. P. B. (2008). The ribosomal protein L10/QM-like protein is a component of the NIK-mediated antiviral signaling. *Virology* 380, 165–169. doi: 10.1016/j.virol.2008.08.005

Rojas, M. R., Macedo, M. A., Maliano, M. R., Soto-Aguilar, M., Souza, J. O., Briddon, R. W., et al. (2018). World management of geminiviruses. *Annu. Rev. Phytopathol.* 56, 637–677. doi: 10.1146/annurev-phyto-080615-100327

Rojas, M. R., Noueiry, A. O., Lucas, W. J., and Gilbertson, R. L. (1998). Bean dwarf mosaic geminivirus movement proteins recognize DNA in a form- and size-specific manner. *Cell* 95, 105–113. doi: 10.1016/S0092-8674(00)81786-9

Sabe, H., Onodera, Y., Mazaki, Y., and Hashimoto, S. (2006). ArfGAP family proteins in cell adhesion, migration and tumor invasion. *Curr. Opin. Cell Biol.* 18, 558–564. doi: 10.1016/j.ceb.2006.08.002

Sakamoto, T., Deguchi, M., Brustolini, O. J. B., Santos, A. A., Silva, F. F., and Fontes, E. P. B. (2012). The tomato RLK superfamily: phylogeny and functional predictions about the role of the LRRII-RLK subfamily in antiviral defense. *BMC Plant Biol.* 12:229. doi: 10.1186/1471-2229-12-229

Sánchez-Velar, N., Udofia, E. B., Yu, Z., and Zapp, M. L. (2004). hRIP, a cellular cofactor for rev function, promotes release of HIV RNAs from the perinuclear region. *Genes Dev.* 18, 23–34. doi: 10.1101/gad.1149704

Sanderfoot, A. A., Ingham, D. J., and Lazarowitz, S. G. (1996). A viral movement protein as a nuclear shuttle. The geminivirus *BR1* movement protein contains domains essential for interaction with BL1 and nuclear localization. *Plant Physiol.* 110, 23–33. doi: 10.1104/pp.110.1.23

Sanderfoot, A. A., and Lazarowitz, S. G. (1995). Cooperation in viral movement: the geminivirus BL1 movement protein interacts with BR1 and redirects it from the nucleus to the cell periphery. *Plant Cell* 7, 1185–1194. doi: 10.1105/tpc.7.8.1185

Sanderfoot, A. A., and Lazarowitz, S. G. (1996). Getting it together in plant virus movement: cooperative interactions between bipartite geminivirus

movement proteins. *Trends Cell Biol.* 6, 353–358. doi: 10.1016/0962-8924(96)10031-3

Santos, A. A., Carvalho, C. M., Florentino, L. H., Ramos, H. J. O., and Fontes, E. P. B. (2009). Conserved threonine residues within the A-loop of the receptor NIK differentially regulate the kinase function required for antiviral signaling. *PLoS One* 4:e5781. doi: 10.1371/journal.pone.0005781

Santos, A. A., Lopes, K. V. G., Apfata, J. A. C., and Fontes, E. P. B. (2010). NSP-interacting kinase, NIK: a transducer of plant defence signalling. *J. Exp. Bot.* 61, 3839–3845. doi: 10.1093/jxb/erq219

Smakowska-Luzan, E., Mott, G. A., Parys, K., Stegmann, M., Howton, T. C., Layeghifard, M., et al. (2018). An extracellular network of *Arabidopsis leucine*-rich repeat receptor kinases. *Nature* 553, 342–346. doi: 10.1038/nature25184

Teixeira, R. M., Ferreira, M. A., Raimundo, G. A. S., Loriato, V. A. P., Reis, P. A. B., and Fontes, E. P. B. (2019). Virus perception at the cell surface: revisiting the roles of receptor-like kinases as viral pattern recognition receptors. *Mol. Plant Pathol.* 20, 1196–1202. doi: 10.1111/mpp.12816

Tourrière, H., Chebli, K., Zekri, L., Courselaud, B., Blanchard, J. M., Bertrand, E., et al. (2003). The RasGAP-associated endoribonuclease G3BP assembles stress granules. *J. Cell Biol.* 160, 823–831. doi: 10.1083/jcb.200212128

Turner, C. E., West, K. A., and Brown, M. C. (2001). Paxillin-ARF GAP signaling and the cytoskeleton. *Curr. Opin. Cell Biol.* 13, 593–599. doi: 10.1016/S0955-0674(00)00256-8

Ye, J., Yang, J., Sun, Y., Zhao, P., Gao, S., Jung, C., et al. (2015). Geminivirus activates ASYMMETRIC LEAVES 2 to accelerate cytoplasmic DCP2-mediated mRNA turnover and weakens RNA silencing in *Arabidopsis*. *PLoS Pathog.* 11:e1005196. doi: 10.1371/journal.ppat.1005196

Zerbini, F. M., Briddon, R. W., Idris, A., Martin, D. P., Moriones, E., Navas-Castillo, J., et al. (2017). ICTV virus taxonomy profile: geminiviridae. *J. Gen. Virol.* 98, 131–133. doi: 10.1099/jgv.0.000738

Zhang, S. C., Wege, C., and Jeske, H. (2001). Movement proteins (BC1 andBV1) of *Abutilon mosaic* geminivirus are cotransported in and between cells of sink but not of source leaves as detected by green fluorescent protein tagging. *Virology* 290, 249–260. doi: 10.1006/viro.2001.1185

Zhou, Y., Rojas, M. R., Park, M.-R., Seo, Y.-S., Lucas, W. J., and Gilbertson, R. L. (2011). Histone H3 interacts and colocalizes with the nuclear shuttle protein and the movement protein of a geminivirus. *J. Virol.* 85, 11821–11832. doi: 10.1128/jvi.00082-11

Zipfel, C., Kunze, G., Chinchilla, D., Caniard, A., Jones, J. D. G., Boller, T., et al. (2006). Perception of the bacterial PAMP EF-Tu by the receptor EFR restricts Agrobacterium-mediated transformation. *Cell* 125, 749–760. doi: 10.1016/j.cell.2006.03.037

Zorzatto, C., Machado, J. P. B., Lopes, K. V. G., Nascimento, K. J. T., Pereira, W. A., Brustolini, O. J. B., et al. (2015). NIK1-mediated translation suppression functions as a plant antiviral immunity mechanism. *Nature* 520, 679–682. doi: 10.1038/nature14171

Zvereva, A. S., Golyaev, V., Turco, S., Gubaeva, E. G., Rajeswaran, R., Schepetilnikov, M. V., et al. (2016). Viral protein suppresses oxidative burst and salicylic acid-dependent-autophagy and facilitates bacterial growth on virus-infected plants. *New Phytol.* 211, 1020–1034. doi: 10.1111/nph.13967

Conflict of Interest: The authors declare that the research was conducted in the absence of any commercial or financial relationships that could be construed as a potential conflict of interest.

frontiers in Plant Science

HYPOTHESIS AND THEORY
published: 15 April 2020
doi: 10.3389/fpls.2020.00414

Amplifier Hosts May Play an Essential Role in Tomato Begomovirus Epidemics in Brazil

Armando Bergamin Filho, Mônica A. Macedo, Gabriel M. Favara, Daiana Bampi, Felipe F. de Oliveira and Jorge A. M. Rezende*

Department of Plant Pathology and Nematology, E.S.A. "Luiz de Queiroz," University of São Paulo, Piracicaba, Brazil

Current control of tomato golden mosaic disease, caused in Brazil predominantly by tomato severe rugose virus (ToSRV), is dependent on both, planting resistant/tolerant hybrids and intensive insecticide sprays (two to three per week) for controlling *Bemisia tabaci*, the vector of ToSRV. Resistant hybrids only confer moderate resistance to infection by ToSRV and some tolerance to the disease. Insecticide sprays, although widely used, have failed in most tomato production areas in Brazil, as they are unable to reduce primary spread, i.e., infection caused by the influx of viruliferous whiteflies coming from external sources of inoculum. Severe epidemics are recurrently observed in some tomato fields in several Brazilian regions, which prompted us to postulate the existence in the agroecosystem, in some places and time, of amplifier hosts that provide the necessary force of infection for epidemics to occur, even in the absence of secondary spread in the target crop. Amplifier hosts are ideally asymptomatic, occur in high density near the target crop, and support growth of both virus and vector. Soybean and common bean are potential amplifier hosts for begomovirus in tomato crops. Our results support the hypothesis that soybean plants may play an important role as an amplifier host of ToSRV for tomato crops in the field, although this does not seem to be a frequent phenomenon. Successful amplification will depend on several factors, including the soybean cultivar, the soybean stage of development at the moment of infection, the ToSRV isolate, and the perfect synchrony between the beginning of a soybean field and the end of a ToSRV-infected crop, and, later, between the senescence of the ToSRV-infected soybean plants and the new tomato crop. The concept of amplifier hosts has been widely used in ecology of zoonoses but, to our knowledge, has never been used in botanical epidemiology.

Keywords: *Solanum lycopersicum*, *Bemisia tabaci*, Geminiviridae, reservoir, epidemiology

OPEN ACCESS

Edited by:
Araceli G. Castillo, Institute of Subtropical and Mediterranean Horticulture La Mayora, Spain

Reviewed by:
Ana Grande-Pérez, Institute of Subtropical and Mediterranean Horticulture La Mayora, Spain
Anders Kvarnheden, Swedish University of Agricultural Sciences, Sweden
Jesus Mendez-Lozano, National Polytechnic Institute, Mexico

****Correspondence:***
Armando Bergamin Filho
abergami@usp.br

Specialty section:
This article was submitted to Virology, a section of the journal Frontiers in Plant Science

Received: *19 December 2019*
Accepted: *23 March 2020*
Published: *15 April 2020*

Citation:
Bergamin Filho A, Macedo MA, Favara GM, Bampi D, Oliveira FFd and Rezende JAM (2020) Amplifier Hosts May Play an Essential Role in Tomato Begomovirus Epidemics in Brazil. Front. Plant Sci. 11:414. doi: 10.3389/fpls.2020.00414

INTRODUCTION

Tomatoes are one of the most important vegetable crops in Brazil and worldwide. In 2018, approximately 59.7 thousand hectares were planted to tomatoes in the country, and 4.1 million tons of fruit was produced (Instituto Brasileiro de Geografia e Estatística [IBGE], 2018). Tomato production can be affected by several begomoviruses, the most prevalent being tomato severe rugose virus (ToSRV) (Fernandes et al., 2008; Inoue-Nagata et al., 2016; Rojas et al., 2018; Mituti et al., 2019). Begomoviruses are transmitted by the silverleaf whitefly *Bemisia tabaci* in a circulative-persistent manner (Rosen et al., 2015).

In 2003, due to the high incidence of begomovirus in processing tomatoes, a legislative control measure mandating a tomato-free period of 2 months (December and January) was implemented in Goiás state (Inoue-Nagata et al., 2016). Despite the implementation of this legislative control measure, a high incidence of ToSRV (60 to 100%) is recurrently observed in tomato crops (Macedo et al., 2014, 2017c, 2019).

Current control of diseases caused by begomoviruses for processing (determinate growth) and fresh market tomatoes (indeterminate growth) depends almost exclusively on both planting resistant/tolerant hybrids and on intensive insecticide sprays (2 to 3 per week) for controlling *B. tabaci*, the vector of ToSRV, in the target crop. Resistant hybrids possess only moderate resistance to infection with the bipartite begomovirus ToSRV, as well as some tolerance to the disease (Inoue-Nagata et al., 2016). Insecticide sprays, although widely used, have failed in most tomato production areas in Brazil because they are unable to reduce primary spread, i.e., infection caused by the influx of viruliferous whiteflies coming from external sources of inoculum. This failure has been reported for a begomovirus disease in tomato fields in Florida (Polston et al., 1996) and demonstrated under controlled conditions by Gouvêa et al. (2017) in Brazil. As for processing tomatoes, high incidences of ToSRV in fresh market tomatoes are observed annually in some tomato fields in Brazil.

These recurrent and localized abrupt high incidences of ToSRV prompted us to propose a hypothesis for such epidemics: the existence in the agroecosystem, in some places and time, of amplifier hosts that provide the necessary force of infection for epidemics to occur, even in the absence of secondary spread in the target crop. Force of infection is defined as the rate at which susceptible target individuals acquire an infectious disease from a given source (Viana et al., 2014). Amplifier hosts are ideally asymptomatic, occur in high density near the target crop, and support the abundant growth of both virus and vector. The amplifier host acts as an intermediate link between a reservoir host and the target host and provide a strong short-term source of infection. The concept of amplifier hosts has been widely used in ecological studies of zoonoses (Childs et al., 2007; Lambin et al., 2010; Karesh et al., 2012; Jones et al., 2013; Streicker et al., 2013; Wardrop, 2016; Faust et al., 2018), but to our knowledge has never been used in botanical epidemiology.

RESERVOIR AND AMPLIFIER HOSTS IN BOTANICAL EPIDEMIOLOGY

The amplifier-host hypothesis applied to ToSRV epidemiology is based on the premise that secondary spread of the virus in tomato fields with high insecticide input is almost fully prevented by the nearly complete elimination of *B. tabaci* from the tomato fields. Therefore, epidemics, when they occur, are driven by the migration of viruliferous whiteflies from outside the target field (Barbosa et al., 2016; Bergamin Filho et al., 2016; Macedo et al., 2017c, 2019). This indicates the crucial importance of identifying the external sources of inoculum, as recognized recently in landscape botanical epidemiology (Plantegenest et al., 2007; Meentemeyer et al., 2012; Bergamin Filho et al., 2016).

Epidemiology of plant viruses has traditionally considered the reservoir as the main source of primary inoculum; afterward, the epidemic is driven by the secondary inoculum (Duffus, 1971). Reservoir is defined as one or more epidemiologically connected populations (mainly weed hosts in plant virus epidemics) in which the pathogen can be permanently maintained and from which infection is transmitted to the target population (Haydon et al., 2002). Reservoir hosts provide a long-term source of infection to the target population (Reisen, 2010). However, in Brazilian conditions, we have strong evidence that the incidence of ToSRV in populations of weed plants (reservoir) is very low (Macedo et al., 2017c; Rezende, unpublished data), and secondary spread is prevented by intensive and effective insecticide sprays for vector control.

The amplifier-host hypothesis (**Figure 1**) helps to explain the recurrent rapid epidemics that occur in Brazilian conditions, despite both the weak reservoir force of infection and the prevention of secondary spread by insecticide sprays for vector control. The insight to include amplifier hosts in the conceptual model of ToSRV/tomato epidemics was based on two recent surveys carried out in central Brazil, one reporting that 2.9% of asymptomatic common bean plants were infected with ToSRV (Macedo et al., 2017a), and the other reporting that 3.3% of asymptomatic soybean plants were infected with the same begomovirus (Macedo et al., 2017b). Furthermore, data collected in 2018 in the Sumaré region (state of São Paulo) in a senescent soybean crop near a recently transplanted tomato crop (sprayed with insecticide three times per week) showed a > 10% incidence of asymptomatic ToSRV-infected soybean plants and a 57–70% incidence of symptomatic ToSRV-infected tomato plants. Infection of both the soybean and tomato plants with ToSRV was confirmed by means of PCR, using the degenerate primer pairs PAR1c496 and PAL1v1978 for begomoviruses (Rojas et al., 1993), followed by nucleotide sequencing of the amplicons. The approximately 300,000 soybean plants per hectare would provide 30,000 ToSRV-infected plants per hectare as sources of inoculum (amplifier). Tomato fields are often located next to common bean and soybean fields on Brazilian farms. The potential interplay of begomoviruses and these crops has been mentioned previously (Costa, 1975; Gilbertson et al., 1991; Navas-Castillo et al., 1999; Anderson et al., 2004).

SOYBEAN AS AN AMPLIFIER HOST TO TOSRV EPIDEMICS IN TOMATO

In order to obtain further information on the potential of soybean plants to act as an amplifier host, we studied the susceptibility of 42 soybean cultivars to ToSRV infection in three independent experiments performed under greenhouse conditions and in one experiment in the field. Healthy soybean plants were grown from seeds in 3.0-liter pots containing

substrate. After reaching the 3 to 4 true-leaf stage, the plants were inoculated with ToSRV. Virus-free adults of *B. tabaci* MEAM1, reared on collard plants (*Brassica oleracea*) kept in whitefly-proof cages were provided an acquisition access period (AAP) of 24 h on ToSRV-infected tomato leaves. Afterward, these potentially viruliferous insects were transferred to five plants of each cultivar, growing in separate pots that were covered with voile fabric cages. An average of 30 insects per plant were released into the cage. The inoculation access period (IAP) was 96 h. Then, the plants were sprayed with the insecticide Flupyradifurone (Sivanto®) to prevent later colonization by the vector, and kept in whitefly-proof cages in a greenhouse. ToSRV was detected by PCR in total DNA extracted from soybean leaf samples according to Dellaporta et al. (1983), modified according to Favara et al. (2019). Samples of total DNA extracted from ToSRV-infected tomato plants and from healthy plants were used as positive and negative controls, respectively. The PCR was performed with the primer pairs PAR1c496 and PAL1v1978 (Rojas et al., 1993). The amplicons obtained were analyzed by electrophoresis in 1% agarose gels, stained with SYBR® Safe DNA Gel Stain (Invitrogen), and visualized in a UV-transilluminator. Some amplicons were randomly selected, purified, and sent for nucleotide sequencing at Macrogen Inc. (Seoul, South Korea) to confirm the identity of the virus. In the first experiment, ToSRV was also detected by qPCR with the specific primers ToSRV-F 5′-GCAACCGCCTCTAGCACTTC-3′ and ToSRV-R 5′-GACCTGGTCTCCCCAACAAGG-3′ and protocols described by Bampi et al. (2019).

After evaluating the susceptibility of soybean cultivars to ToSRV infection under greenhouse conditions, an experiment was conducted in the field. First, 100 healthy tomato plants were transplanted in the field. Then, 10 ToSRV-infected *Nicandra physaloides*, were transplanted around the tomato plants to act as sources of inoculum. To ensure the presence of the vector, 4 collard plants infested with *B. tabaci* MEAM1 were placed in the field, inside whitefly proof-cages. Once a week the cages were opened to release some insects. The infection of the tomato plants with ToSRV was confirmed by observation of the symptoms and by PCR for randomly chosen plants. Sixty days later, when the rate of ToSRV-infected tomato plants was approximately 100%, soybean plants of 22 cultivars were exposed to natural infection with this virus in the field. The plants were grown from seed in 3.0-liter pots containing substrate. After emergence, ten plants of each cultivar were randomly placed in the field containing ToSRV-infected tomato plants. Ten healthy tomato plants cv. Santa Clara were also placed in the field as control of ToSRV transmission. Virus-free adults of *B. tabaci* MEAM1 were released 3 times (at 5, 10, and 15 days after plant exposure). Then, 40 days after exposing soybean plants to natural infection with ToSRV, PCR was performed with the primer pairs PAR1c496 and PAL1v1978 (Rojas et al., 1993).

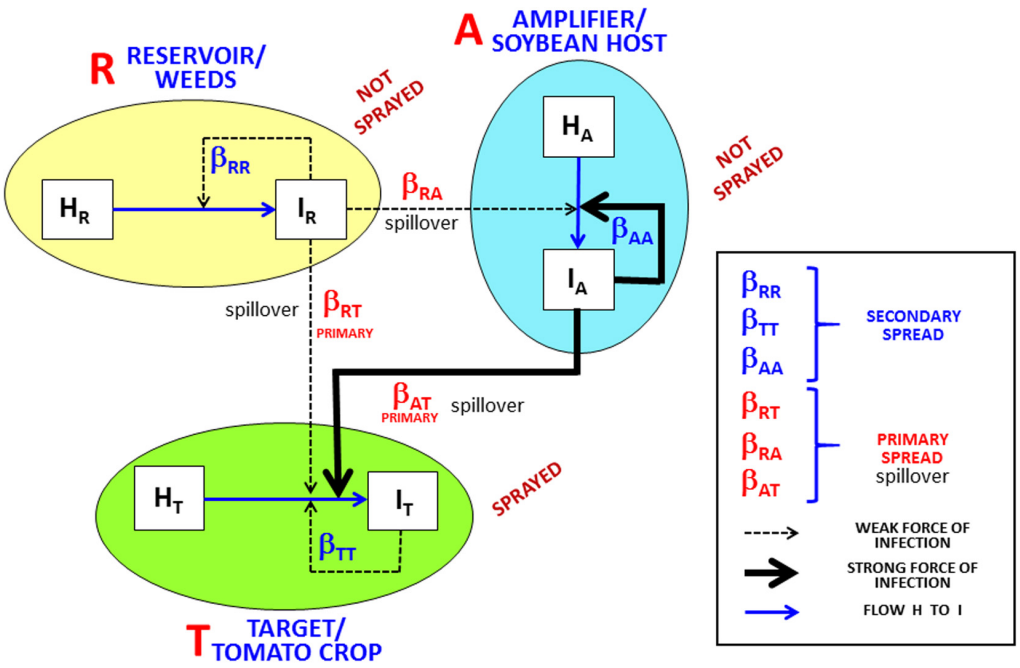

FIGURE 1 | Framework of the target (tomato crop)/reservoir (weeds)/amplifier (soybean host) pathosystem. Target tomato crop (T) receives inoculum influx (spillover) from the reservoir (R), with a weak primary infection force (β_{RT}) due to low infected reservoir density, and from the amplifier (A), with a strong infection force (β_{AT}) due to high infected amplifier density. H and I represent healthy and infected plants, respectively, for target, reservoir, and amplifier. Rates β_{RR}, β_{TT}, and β_{AA} drive secondary infections in R, T, and A, respectively; thin dotted lines in R represent weak forces of secondary infection due to low infected plant density; thin dotted lines in T represent weak forces of secondary infection due to intensive insecticide sprays; thick line in A represents a strong force of secondary infection due to high density of infected plants and absence of insecticide spray. Spillover is defined as a primary infection from a host species to a different host species. Based on Fenton and Pedersen (2005) with addition of the amplifier host concept.

TABLE 1 | Susceptibility of soybean cultivars to infection with tomato severe rugose virus experimentally inoculated using *Bemisia tabaci* MEAM1, and of cultivars exposed to natural infection in the field.

	Greenhouse experiment[a]		Field experiment[b]	
Cultivar	No. infected plants/No. inoculated plants	% Infection	No. infected plants/No. inoculated plants	% Infection
AFS 110	0/15	0	0/10	0
AMS Tibaggi Bayer	0/10	0	nt	nt
BMX Garra	2/10	20	nt	nt
BMX Ícone	2/10	20	nt	nt
BMX Potência	0/15	0	0/10	0
Bonus	0/10	0	nt	nt
BR 4	1/10	10	0/10	0
BR 16	1/10	10	nt	nt
BR 36	0/15	0	0/10	0
BR 132	0/10	0	nt	nt
BR 282	0/10	0	1/10	10
BR 284	0/10	0	1/10	10
BRS 245 RR	0/15	0	0/10	0
BS 2606 Ipro	0/10	0	nt	nt
Campos Gerais	2/15	13	nt	nt
CD 206	0/15	0	0/10	0
Davis	0/15	0	0/10	0
Desafio	0/10	0	nt	nt
Embrapa 48	0/15	0	0/10	0
FT Abyara	0/15	0	0/10	0
FT Cometa	0/15	0	0/10	0
FT-11 Alvorada	0/15	0	0/10	0
IAS3	0/15	0	0/10	0
M 6210 Monsoy	0/10	0	nt	nt
M 7251	0/10	0	nt	nt
M 5892 Ipro	1/10	10	0/10	0
M 72-S1	0/10	0	nt	nt
MG/BR 46 - Conquista	1/10	10	0/10	0
Nidera 5909	1/10	10	0/10	0
NS 6906 Ipro Nidera	0/10	0	nt	nt
NS 6909 Ipro Nidera	0/10	0	nt	nt
Ocepar 3 - Primavera	2/10	20	nt	nt
Ocepar 4 - Iguaçu	2/10	20	nt	nt
Ocepar 5	0/10	0	nt	nt
Paraná	0/15	0	0/10	0
Paraná Marrom	0/15	0	0/10	0
Sambaiba	0/10	0	nt	nt
Santa Rosa	0/15	0	0/10	0
TMG 7062	1/10	10	nt	nt
TMG 7262 RR	4/10	40	2/10	20
TMG 7739	1/10	10	nt	nt
Viçoja	1/10	10	0/10	0

[a] *Three independent experiments.* [b] *One experiment. nt, not tested.*

Of the 42 soybean genotypes evaluated under greenhouse conditions, 14 were susceptible to infection with ToSRV (**Table 1**). The rate of infection ranged from 10% to 40%. Of the 22 cultivars evaluated under field conditions, the cultivars TMG 7262 RR, BRS 282, and BRS 284 were susceptible to ToSRV. The rate of infection ranged from 10% to 20%. The infection rate of tomato plants cv. Santa Clara was 50% (5/10). The susceptibility of soybean cultivars to ToSRV infection under experimental and field conditions varied. Only plants of cultivar TMG 7262 RR were infected under both conditions. All soybean-infected plants, as confirmed by PCR, were symptomless in both assays.

ToSRV-infected soybean plants of the cultivars TMG 7262 RR, Ocepar 4-Iguaçu, Viçoja, MG/BR 46-Conquista and M 5892 Ipro were then evaluated as sources of inoculum for *B. tabaci* MEAM1, for subsequent transmission to 13 healthy tomato plants, using an average of 30 insects per plant. The AAP and IAP were the same as the ones described for the previous experiment. The rates of ToSRV transmission from infected plants of cultivars TMG 7262 RR and Ocepar 4-Iguaçu were 23% (3/13) and 15% (2/13), respectively. The virus was not transmitted from infected plants of cultivars Viçoja, MG/BR 46-Conquista and M5892 Ipro to tomato plants.

DISCUSSION

These results support the hypothesis that soybean plants may play an important role as an amplifier host of ToSRV for tomato crops in the field, although this does not seem to be a frequent phenomenon. Successful amplification will depend on several factors, including:

- the soybean cultivar, since not all of them are susceptible to ToSRV infection; even among susceptible cultivars, not all acted as a source of virus for transmission to tomato by *B. tabaci* MEAM1;
- the soybean stage of development at the moment of infection;
- the ToSRV isolate. Soybean plants of cv. Davis inoculated by biolistics and adults of *B. tabaci* MEAM1 were infected with the ToSRV isolate used by Macedo et al. (2017b). However, plants of the same cultivar were not infected with the ToSRV isolate used in the present study.
- a perfect synchrony must exist between the beginning of a soybean field and the end of a ToSRV-infected tomato crop, and later, between the senescence of the ToSRV-infected soybean plants and the new tomato crop.

The conceptual model proposed here opens up a number of research avenues with the potential to improve both our understanding of the tomato/ToSRV and other related pathosystems (referred as polycyclic diseases with continuous primary spread by Bergamin Filho et al., 2016), and our competence to formulate more rational and sustainable management strategies, especially for intensive agriculture, as follow:

- to investigate other potential amplifier hosts (in addition to soybean and common bean) of ToSRV;
- to quantify the epidemiological effect of different amplifier hosts on tomato crops;
- to determine the influence that the distance between the amplifier host and the tomato crop may have;
- to quantify the effect of vector control (chemical, genetic, biological, etc.) carried out in amplifier hosts on ToSRV incidence in tomato crops;
- to quantify the effect of the absence of the amplifier host (or planting a resistant variety of it) in the vicinity area where tomato is the main crop;
- to verify the influence of delay and/or coincidence of planting dates of tomato and amplifier hosts in the ToSRV epidemics in tomato;
- to assess the effect of a tomato-free-period (legislative control) when amplifier hosts are present in the area.

DATA AVAILABILITY STATEMENT

The datasets generated for this study are available on request to the corresponding author.

AUTHOR CONTRIBUTIONS

AB elaborated the concept of amplifier host for plant virus diseases. MM, GF, FO, and JR conducted field evaluations for amplifier host identification. DB and FO conducted greenhouse and field trials with soybean genotypes. GF, DB, and FO performed molecular analysis. All authors assisted in analyses of data and discussed the results, revised, and contributed to writing the manuscript. MM and DB drafted the manuscript.

FUNDING

This study was supported by the Fundação de Amparo à Pesquisa do Estado de São Paulo (FAPESP), grant numbers 2012/51771-4 and 2018/18274-3. The first and sixty authors are fellows of the Conselho Nacional de Desenvolvimento Científico e Tecnológico (CNPq), grant numbers 303299/2015-0 and 304438/2014-6, respectively.

ACKNOWLEDGMENTS

Our thanks to the Brazilian Agriculture Research Corporation (Embrapa) for the donation of soybean seeds, which was the first and essential step to carry out this research.

REFERENCES

Anderson, P. K., Cunningham, A. A., Patel, N. G., Morales, F. J., Epstein, P. R., and Daszak, P. (2004). Emerging infectious diseases of plants: pathogen pollution, climate change and agrotechnology drivers. *Trends Ecol. Evol.* 19, 535–544. doi: 10.1016/j.tree.2004.07.021

Bampi, D., Favara, G. M., Edwards Molina, J. P., and Rezende, A. M. (2019). Lack of synergistic effects in tomato plants coinfected with *Tomato severe rugose virus* and tomato chlorosis virus. *Plant Pathol.* 68, 1019–1024. doi: 10.1111/ppa.13004

Barbosa, J. C., Rezende, J. A. M., Amorim, L., and Bergamin Filho, A. (2016). Temporal dynamics of *Tomato severe rugose virus* and *Bemisia tabaci* in tomato fields in São Paulo. *Brazil. J. Phytopathol.* 164, 1–10 doi: 10.1111/jph.12402

Bergamin Filho, A., Inoue-Nagata, A. K., Bassanezi, R. B., Belasque, J. Jr., and Amorim, L. (2016). The importance of primary inoculum and area-wide management to crop health and food security. *Food Sec.* 8, 221–238. doi: 10.1007/s12571-015-0544-8

Childs, J. E., Richt, J. A., and Mackenzie, J. S. (2007). Introduction: conceptualizing and partitioning the emergence process of zoonotic viruses from wildlife to humans. *Curr. Top. Microbiol. Immunol.* 315, 1–31. doi: 10.1007/978-3-540-70962-6_1

Costa, A. S. (1975). "Increase in the populational density of Bemisia tabaci, a threat of widespread virus infection of legume crops in Brazil," in *Tropical Diseases of Legumes*, eds J. Bird and K. Maramorosch (New York, NY: Academic Press), 27–50.

Dellaporta, S. L., Wood, J., and Hicks, J. B. (1983). A plant DNA minipreparation: version II. *Plant. Mol. Biol. Rep.* 1, 19–21. doi: 10.1007/bf02712670

Duffus, J. E. (1971). Role of weeds in the incidence of virus diseases. *Annu. Rev. Phytopathol.* 9, 319–340. doi: 10.1146/annurev.py.09.090171.001535

Faust, C. L., McCallum, H. I., Bloomfield, L. S. P., Gottdenker, N. L., Gillespie, T. R., Torney, C. J., et al. (2018). Pathogen spillover during land conversion. *Ecol. Lett.* 21, 471–483. doi: 10.1111/ele.12904

Favara, G. M., Bampi, D., Edwards-Molina, J. P., and Rezende, J. A. M. (2019). Kinetics of systemic invasion and latent and incubation periods of *Tomato severe rugose virus* and *Tomato chlorosis virus* in single and co-infections in tomato plants. *Phytopathology* 109, 480–487. doi: 10.1094/phyto-06-18-0203-r

Fenton, A., and Pedersen, B. (2005). Community epidemiology framework for classifying disease threats. *Emerg. Infect. Dis.* 11, 1815–1821. doi: 10.3201/eid1112.050306

Fernandes, F. R., Albuquerque, L. C., Giordano, L. B., Boiteux, L. S., Ávila, A. C., and Inoue-Nagata, A. K. (2008). Diversity and prevalence of Brazilian bipartite begomovirus species associated to tomatoes. *Virus Genes* 36, 251–258. doi: 10.1007/s11262-007-0184-y

Gilbertson, R. L., Faria, J. C., Hanson, S. F., Morales, F. J., Ahlquist, P., Maxwell, D. P., et al. (1991). Cloning of the complete DNA genomes of four bean-infecting geminiviruses and determining their infectivity by electric discharge particle acceleration. *Phytopathology* 81, 980–985.

Gouvêa, M. M., Freitas, D. M. S., Rezende, J. A. M., Watanabe, L. F. M., and Lourenção, A. L. (2017). Bioassay of insecticides on mortality of *Bemisia tabaci* biotype B and transmission of *Tomato severe rugose virus* (ToSRV) on tomatoes. *Phytoparasitica* 45, 95–101. doi: 10.1007/s12600-017-0562-5

Haydon, D. T., Cleaveland, S., Taylor, L. H., and Laurenson, M. K. (2002). Identifying resevoirs of infection: a conceptual and practical challenge. *Emerg. Infect. Dis.* 8, 1468–1473. doi: 10.3201/eid0812.010317

Inoue-Nagata, A. K., Lima, M. F., and Gilbertson, R. L. (2016). A review of geminivirus (begomovirus) diseases in vegetables and other crops in Brazil: current status and approaches for management. *Hortic. Bras.* 34, 8–18. doi: 10.1590/s0102-053620160000100002

Instituto Brasileiro de Geografia e Estatística [IBGE] (2018). *Levantamento Sistemático da Produção Agrícola*. Avaliable at: https://sidra.ibge.(.)gov.br/tabela/1618#resultado. (accessed on August 9, 2019).

Jones, B. A., Grace, D., Kock, R., Alonso, S., Rushton, J., Said, M. Y., et al. (2013). Zoonosis emergence linked to agricultural intensification and environmental change. *Proc. Natl. Acad. Sci. U.S.A.* 110, 8399–8404. doi: 10.1073/pnas.1208059110

Karesh, W. B., Dobson, A., Lloyd-Smith, J. O., Lubroth, J., Dixon, M. A., Bennett, M., et al. (2012). Ecology of zoonoses: natural and unnatural histories. *Lancet* 380, 1936–1945. doi: 10.1016/s0140-6736(12)61678-x

Lambin, E. F., Tran, A., Vanwambeke, S. O., Linard, C., and Soti, V. (2010). Pathogenic landscapes: interactions between land, people, disease vectors, and their animal hosts. *Int. J. Health Geographics* 9:54. doi: 10.1186/1476-072x-9-54

Macedo, M. A., Barreto, S. S., Costa, T. M., Maliano, M. R., Rojas, M. R., Gilbertson, R. L., et al. (2017a). First report of common beans as a non-symptomatic host of *Tomato severe rugose virus* in Brazil. *Plant Dis.* 101:261. doi: 10.1094/pdis-03-16-0330-pdn

Macedo, M. A., Barreto, S. S., Costa, T. M., Rocha, G. A., Dianese, E. C., Gilbertson, R. L., et al. (2017b). First report of *Tomato severe rugose virus*, a tomato-infecting begomovirus, in soybean plants in Brazil. *Plant Dis.* 101:1958.

Macedo, M. A., Costa, T. M., Barbosa, J. C., Pereira, J. L., Michereff-Filho, M., Gilbertson, R. L., et al. (2017c). Temporal and spatial dynamics of begomovirus disease in tomatoes in central Brazil. *Plant Pathol.* 66, 529–538. doi: 10.1111/ppa.12632

Macedo, M. A., Barreto, S. S., Hallwass, M., and Inoue-Nagata, A. K. (2014). High incidence of *Tomato chlorosis virus* alone and in mixed infection with begomoviruses in two tomato fields in the Federal District and Goiás state. *Brazil. Trop. Plant Pathol.* 39, 9–452.

Macedo, M. A., Inoue-Nagata, A. K., Silva, T. N. Z., Freitas, D. M. S., Rezende, J. A. M., Barbosa, J. C., et al. (2019). Temporal and spatial progress of the diseases caused by the crinivirus tomato chlorosis virus and the begomovirus *Tomato severe rugose virus* in tomatoes in Brazil. *Plant Pathol.* 68, 72–88.

Meentemeyer, R. K., Haas, S. E., and Václavik, T. (2012). Landscape epidemiology of emerging infectious diseases in natural and human-altered ecosystems. *Annu. Rev. Phytopathol.* 50, 379–402. doi: 10.1146/annurev-phyto-081211-172938

Mituti, T., Moura, M. F., Macedo, M. A., Silva, T. N. Z., Pinto, L. R., Costa, H., et al. (2019). Survey of begomoviruses and crinivirus, tomato chlorosis virus, in solanaceous in Southeast/Midwest of Brazil. *Trop. Plant Pathol.* 44, 468–472. doi: 10.1007/s40858-019-00294-z

Navas-Castillo, J., Sánchez-Campos, S., and Díaz, J. A. (1999). Tomato yellow leaf curl vírus-Is causes a novel disease of common bean and severe epidemics in tomato in Spain. *Plant Dis.* 83, 29–32. doi: 10.1094/pdis.1999.83.1.29

Plantegenest, M., May, C. L., and Fabre, F. (2007). Landscape epidemiology of plant diseases. *J. R. Soc. Interface* 4, 963–979.

Polston, J. E., Chellemi, D. O., Schuster, D. J., McGovern, R. J., and Stansly, P. A. (1996). Spatial and temporal dynamics of Tomato mottle geminivirus and *Bemisia tabaci* (Genn.) *in Florida tomato fields*. *Plant Dis.* 80, 1022–1028.

Reisen, W. K. (2010). Landscape epidemiology of vector-borne diseases. *Annu. Rev. Entomol.* 55, 461–483. doi: 10.1146/annurev-ento-112408-085419

Rojas, M. R., Gilbertson, R. J., Russel, D. R., and Maxwell, D. P. (1993). Use of degenerate primers in the polymerase chain reaction to detect whitefly-transmitted geminiviruses. *Plant Dis.* 77, 340–347.

Rojas, M. R., Macedo, M. A., Maliano, M. R., Soto-Aguilar, M., Souza, J. O., Briddon, R. W., et al. (2018). World management of geminiviruses. *Annu. Rev. Phytopathol.* 56, 637–677.

Rosen, R., Kanakala, S., Kliot, A., Pakkianathan, B. C., Farich, B. A., Santana-Magal, N., et al. (2015). Persistent circulative transmission of begomoviruses by whitefly vectors. *Curr. Opin. Virol.* 15, 1–8. doi: 10.1016/j.coviro.2015.06.008

Streicker, D. G., Fenton, A., and Pedersen, A. B. (2013). Differential sources of host species heterogeneity influence the transmission and control of multihost parasites. *Ecol. Letters* 16, 975–984. doi: 10.1111/ele.12122

Viana, M., Mancy, R., Biek, R., Cleaveland, S., Cross, P. C., Lloyd-Smith, J. O., et al. (2014). Assembling evidence for identifying reservoirs of infection. *Trends Ecol. Evol.* 29, 270–279. doi: 10.1016/j.tree.2014.03.002

Wardrop, N. A. (2016). Integrated epidemiology for vector-borne zoonoses. *Trans. R. Soc. Trop. Med. Hyg.* 110, 87–89. doi: 10.1093/trstmh/trv115

Conflict of Interest: The authors declare that the research was conducted in the absence of any commercial or financial relationships that could be construed as a potential conflict of interest.

frontiers in Microbiology

OPINION
published: 05 May 2020
doi: 10.3389/fmicb.2020.00878

Geminivirus-Encoded Proteins: Not All Positional Homologs Are Made Equal

Ana P. Luna[1]* *and Rosa Lozano-Durán*[2]*

[1] Instituto de Hortofruticultura Subtropical y Mediterránea "La Mayora" (IHSM-UMA-CSIC), Area de Genética, Facultad de Ciencias, Universidad de Málaga, Málaga, Spain, [2] Shanghai Center for Plant Stress Biology, CAS Center for Excellence in Molecular Plant Sciences, Chinese Academy of Sciences, Shanghai, China

Keywords: geminivirus, viral protein, positional homolog, silencing suppressor, C2/AC2, V2/AV2, C4/AC4

THE PLANT GEMINIVIRUSES

Geminiviruses are insect-transmitted plant viruses with circular, single-stranded (ss)DNA genomes that cause devastating diseases in major crops worldwide. The family *Geminiviridae* comprises more than 450 species divided in nine genera, based on genome organization, host range, and insect vector: *Begomovirus*, *Mastrevirus*, *Curtovirus*, *Becurtovirus*, *Topocuvirus*, *Turncurtovirus*, *Capulavirus*, *Gablovirus*, and *Eragrovirus* (Zerbini et al., 2017). The most diverse genus in this family is *Begomovirus*, which to date includes 409 different species (reviewed in Zhao et al., 2019). Begomoviruses can be further subdivided in monopartite, with one-molecule genomes, and bipartite, with two-molecule genomes (**Figure 1A**). Regardless of whether they are mono- or bi-partite, the size of each genomic DNA molecule is ∼3 kb.

Apart from the obvious economic and practical interest propelling the study of geminiviruses, this virus family is an excellent model system to gain insight into plant processes. Geminiviruses replicate their DNA genomes in the nucleus by using the plant DNA replication machinery; the geminivirus genome forms minichromosomes that are subjected to epigenetic modifications; geminiviruses are both activators and suppressors of plant defense responses, and modulate plant developmental processes (reviewed in Hanley-Bowdoin et al., 2013). Therefore, geminiviruses can be used as probes to deepen our understanding not only of plant-virus interactions, but also of different aspects of plant biology.

GEMINIVIRUS-ENCODED PROTEINS

As intracellular parasites, geminiviruses have to effectively manipulate plant cell functions to replicate, suppress anti-viral defense, and move throughout the plant, ultimately establishing a systemic infection; their evolved capacity to co-opt and modulate processes in a given host plant will determine the outcome of the plant-virus interaction. In order to hijack the host cell molecular machinery, geminiviruses produce a limited number (between 4 and 8) of small, fast-evolving, multifunctional proteins, encoded by bidirectional and partially overlapping open reading frames (ORFs) (**Figure 1A**). Monopartite begomoviruses encode six proteins, namely C1/Rep, C2/TrAP, C3/REn, C4, V2, and V1/CP. Homologs are encoded in one of the genomic component of bipartite begomoviruses, DNA A (in this case, named AC1/Rep, AC2/TrAP, AC3/REn, AC4, AV2, and AV1/CP); the other component in bipartite species, termed DNA B, encodes two additional proteins: the nuclear shuttle protein (NSP) and the movement protein (MP) (**Figure 1A**). Curiously, monopartite begomoviruses are often found in nature associated with satellite molecules, known as α- and β-satellites, which contribute to or even enable viral pathogenicity through the action of their encoded proteins (α-Rep and β-C1, respectively) (reviewed in Zhou, 2013).

OPEN ACCESS

Edited by:
Ricardo Flores, Polytechnic University of Valencia, Spain

Reviewed by:
F. Murilo Zerbini, Universidade Federal de Viçosa, Brazil
Emanuela Noris, National Research Council (CNR), Italy

***Correspondence:**
Ana P. Luna
analuna@uma.es
Rosa Lozano-Durán
lozano-duran@sibs.ac.cn

Specialty section:
This article was submitted to Virology, a section of the journal Frontiers in Microbiology

Received: *29 February 2020*
Accepted: *15 April 2020*
Published: *05 May 2020*

Citation:
Luna AP and Lozano-Durán R (2020) Geminivirus-Encoded Proteins: Not All Positional Homologs Are Made Equal. Front. Microbiol. 11:878. doi: 10.3389/fmicb.2020.00878

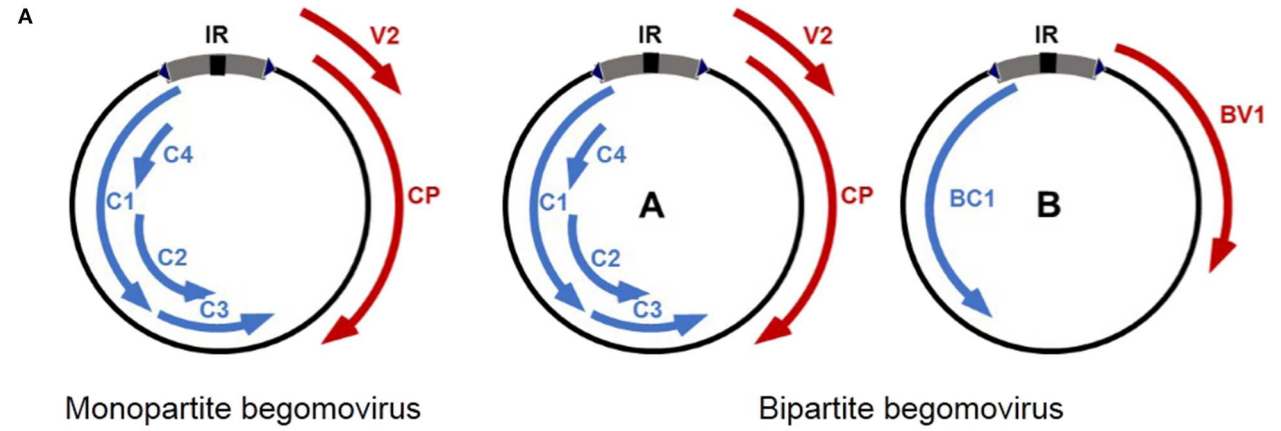

B

Genera	Species	Accession number	C4 protein ID	AA	Myr	cTP
Capulavirus	*French bean severe leaf curl virus*	JX094280	C4 putative protein	97	yes	no
Mastrevirus	*Axonopus compressus streak virus*	KJ437671	C4 putative protein	112	yes	no
Mastrevirus	*Chickpea chlorotic dwarf virus*	DQ458791	C4 putative protein	114	no	23
Curtovirus	*Horseradish curly top virus*	U49907	C4 protein AAB18927	121	no	28
Curtovirus	*Spinach severe curly top virus*	GU734126	C4 protein ADM64622	120	no	no
Becurtovirus	*Beet curly top Iran virus*	KP410285	C4 putative protein	134	yes	no
Becurtovirus	*Spinach curly top Arizona virus*	HQ443515	C4 putative protein	134	yes	no
Eragrovirus	*Eragrostis curvula streak virus*	FJ635634	C4 putative protein	85	yes	24
Begomovirus	*African cassava mosaic virus*	FM877473	AC4 protein CAT00009	171	no	no
Begomovirus	*Bean golden mosaic virus*	FJ635283	C4 protein AIN35540	85	yes	47
Curtovirus	*Pepper yellow dwarf virus*	EU921828	C4 protein ACH48061	85	yes	77
Curtovirus	*Beet curly top virus*	M24597	C4 protein ADD82466	85	yes	69
Turncurtovirus	*Turnip leaf roll virus*	KT388086	C4 protein ALR86872	85	yes	no
Turncurtovirus	*Turnip curly top virus*	GU456685	C4 protein ADJ58422	85	yes	no
Turncurtovirus	*Turnip curly top virus*	KC108902	C4 protein AGA19556	85	yes	no
Begomovirus	*Cotton leaf curl Burewala virus*	JF502373	C4 protein AFB83504	181	no	no
Turncurtovirus	*Turnip leaf roll virus*	KT388088	C4 protein ALR86884	102	no	57
Begomovirus	*Tomato yellow leaf curl virus*	AJ439258	C4 protein CAD33252	97	yes	43
Unclassified	*Apple geminivirus*	KM386645	C4 protein AJZ68901	77	yes	no
Begomovirus	*East African cassava mosaic virus*	AJ717542	AC4 protein CAJ78099	77	yes	49
Topocuvirus	*Tomato pseudo-curly top virus*	X84735	C4 protein CAA59226	85	yes	54
Curtovirus	*Beet curly top virus*	AY548948	C4 protein AAS86157	85	yes	77
Begomovirus	*Sida micrantha mosaic virus*	KC706535	AC4 protein AGH29602	87	no	73

FIGURE 1 | (A) Geminivirus (begomovirus) genome structure in monopartite and bipartite species. Arrows represent open reading frames (ORFs). ORFs in the virion strand are in red; ORFs in the complementary strand are in blue. See text for details. **(B)** Comparison of the C4 proteins from different geminivirus species across genera. The presence of a predicted myristoylation site (Myr) or chloroplast transit peptide (cTP) in the protein sequence is indicated.

In view of the fast pace of evolution of geminivirus genomes (reviewed in Zhao et al., 2019), it is expected that all proteins therein encoded are essential for the viral infection—since otherwise their coding sequence would be eventually lost. This idea is supported by the results obtained in the laboratory with artificially mutated viruses, which generally present a dramatically decreased virulence in their natural hosts and a high rate of reversion. Our current knowledge of the specific molecular function of individual geminivirus-encoded proteins derives from an ever-growing body of work, carried out by multiple research groups worldwide during the past few decades and resulting from the combination of molecular biology, cell biology, virology, and biochemistry.

Considering the biological properties and life cycle of geminiviruses and plant viruses in general, a series of functions that are *conditio sine qua non* for a successful viral infection can be inferred: these include manipulation of the cell cycle, DNA replication, intra- and inter-cellular movement, and suppression of gene silencing and other anti-viral defenses, such as the response to defense-related hormones. Virus-encoded proteins exerting these functions have indeed been identified in different geminivirus species, although in some cases the exact underlying molecular mechanisms remain to be unraveled (reviewed in Hanley-Bowdoin et al., 2013; Yang et al., 2016).

POSITIONAL HOMOLOGS IN GEMINIVIRUSES

Genome structure is conserved among geminiviral species within the same genus, and in some cases even among species

TABLE 1 | Different C2/AC2 functions described in several geminiviral species.

Virus	Function	References
Tomato golden mosaic virus (TGMV); *Mungbean yellow mosaic virus* (MYMV)	Transcriptional activator for viral and some plant host genes	Sunter and Bisaro, 1992, 1997; Trinks et al., 2005
Tomato golden mosaic virus (TGMV) and *Beet curly top virus* (BCTV)	Inactivation of SNF1-related kinase (*Arabidopsis* protein kinase 11 [AKIN11])	Hao et al., 2003; Wang et al., 2003
African cassava mosaic virus (ACMV); *Tomato yellow leaf curl virus* (TYLCV); *Tomato golden mosaic virus* (TGMV); *Beet curly top virus* (BCTV); *Indian cassava mosaic virus* (ICMV) and *East African cassava mosaic Cameroon virus* (EACMCV)	Posttranscriptional gene silencing (PTGS) suppression	Voinnet et al., 1999; Vanitharani et al., 2004; Wang et al., 2005; Luna et al., 2012
Tomato golden mosaic virus (TGMV); *Cabbage leaf curl virus* (CaLCuV), and *Beet curly top virus* (BCTV)	Transcriptional gene silencing (TGS) suppression by interfering with the methyl cycle through inhibition of adenosine kinase (ADK)	Buchmann et al., 2009; Jackel et al., 2015
Beet severe curly top virus (BSCTV)	TGS suppression by interfering with the methyl cycle through attenuation of the proteasome-mediated degradation of S-adenosyl-methionine decarboxylase 1 (SAMDC1)	Zhang et al., 2011
Tomato golden mosaic virus (TGMV); *Cabbage leaf curl virus* (CaLCuV) and *Indian cassava mosaic virus* (strains: ICMV-Dha and ICMV-SG)	TGS suppression by inhibiting the H3K9 histone methyltransferase SUVH4/KYP	Castillo-González et al., 2015; Sun et al., 2015
Beet curly top virus (BCTV)	Creation of a cellular environment permissive to DNA replication	Caracuel et al., 2012; Lozano-Duran et al., 2012

in different genera: genes in the same strand (virion or complementary) and position in different geminivirus species are therefore referred to as positional homologs, have the same name, and the resulting proteins show sequence similarity at the amino acid level (**Figure 1**). Given these shared properties, together with the observation that the biological requirements for a successful geminivirus infection are most likely common to all family members, positional homologs are frequently considered equivalent, and the properties identified for an individual gene are often extrapolated to others. This notion assumes that positional homologs are invariably and necessarily functional homologs; nonetheless, this is at odds with the idea of functional diversification that could result from the fast adaptation of different virus species to their hosts. Without the intention to be exhaustive, some specific examples are briefly discussed below.

Some functions of positional homologs seem indeed to be conserved across geminivirus species and genera: this is the case of Rep, which facilitates replication of the viral genome in all known species by reprogramming the cell cycle and mediating initiation, elongation, and termination of viral DNA replication (reviewed in Hanley-Bowdoin et al., 2013; Ruhel and Chakraborty, 2019); or that of V2, which acts as a suppressor of post-transcriptional gene silencing (PTGS) in all geminivirus species tested to date (Zrachya et al., 2007; Sharma and Ikegami, 2010; Amin et al., 2011; Zhang et al., 2012; Luna et al., 2017; Yang et al., 2018; Zhan et al., 2018; Mubin et al., 2019). Nevertheless, it has to be considered that geminivirus-encoded proteins are multifunctional: Rep, for example, promotes viral transcription (Kushwaha et al., 2017) and works as a suppressor of either transcriptional gene silencing (TGS) or PTGS in certain species (Rodríguez-Negrete et al., 2013; Liu et al., 2014); some V2 proteins act as suppressors of TGS (Wang et al., 2014, 2018, 2020; Mubin et al., 2019), and inhibit a host protease (Bar-Ziv et al., 2015). Therefore, at this point, whether functional homology among Rep or V2 proteins is complete or only partial is unclear.

On the other hand, examples of geminiviral positional homologs with proven partial functional homology are available in the literature. Perhaps the most illustrative case to date is that of the C2/AC2 proteins: in begomoviruses and curtoviruses, C2/AC2 proteins have a conserved zinc-finger motif, despite showing only limited similarity in the overall amino acid sequence; but while AC2, but perhaps not C2, from begomoviruses acts as a transcriptional activator for viral and some plant host genes (Sunter and Bisaro, 1992, 1997; Wartig et al., 1997; Trinks et al., 2005), C2 from curtoviruses lacks an obvious transcriptional activation domain and transcriptional activation activity (Sunter et al., 1994; Baliji et al., 2007). At least in two species, C2/AC2 interacts with and inactivates SNF1-related kinase (also known as Arabidopsis protein kinase 11 [AKIN11]), a global regulator of metabolism (Hao et al., 2003; Wang et al., 2003). Some C2/AC2 proteins are suppressors of PTGS (Voinnet et al., 1999; Vanitharani et al., 2004; Wang et al., 2005; Luna et al., 2012), but not others (Vanitharani et al., 2004; Luna et al., 2012). C2/AC2 has also been shown to suppress TGS by interfering with the methyl cycle in several species, but through at least two different mechanisms, namely the inhibition of adenosine kinase (ADK) (Buchmann et al., 2009; Jackel et al., 2015) and the attenuation of the proteasome-mediated degradation of S-adenosyl-methionine decarboxylase 1 (SAMDC1) (Zhang et al., 2011). A third strategy to suppress TGS is exhibited by the C2/AC2 protein encoded by at least two other species, of which the C2/AC2 proteins interact with and inhibit the H3K9 histone methyltransferase SUVH4/KYP (Castillo-González et al., 2015; Sun et al., 2015). The C2 protein encoded

by a curtovirus creates a cellular environment permissive to DNA replication, but this function is not shared by the protein encoded by the position homologue in begomoviruses (Caracuel et al., 2012; Lozano-Duran et al., 2012) (**Table 1**).

The functions of the geminivirus-encoded C4/AC4 could be at least as varied in different species as those of C2/AC2. Several independent functions have been ascribed to C4/AC4 to date (e.g. Piroux et al., 2007; Teng et al., 2010; Luna et al., 2012; Sunitha et al., 2013; Ismayil et al., 2018; Li et al., 2018; Mei et al., 2018, 2020; Rosas-Diaz et al., 2018), and transgenic *Arabidopsis thaliana* plants expressing C4/AC4 from different geminiviruses display distinct developmental phenotypes (Mills-Lujan and Deom, 2010; Luna et al., 2012). Perhaps even more importantly, the C4/AC4 proteins encoded by different geminivirus species can have non-perfectly overlapping subcellular localizations, depending on specific targeting signals, namely acylation sites and a chloroplast transit peptide (e.g., Fondong et al., 2007; Carluccio et al., 2018; Mei et al., 2018; Rosas-Diaz et al., 2018; Zhan et al., 2018; Medina-Puche et al., 2019) (**Figure 1B**). These differences in subcellular distribution of different C4/AC4 proteins, which can be found associated to membranes, in the cytoplasm, in the nucleus, or in chloroplasts, will in all likelihood have a strong impact on their functionality during infection. Interestingly, C4 is seemingly under positive selection, in stark contrast to other geminiviral proteins (Sanz et al., 1999; Melgarejo et al., 2013; Yang et al., 2014).

In summary, a growing body of experimental data supports the idea that, although positional homologs have a common origin and frequently share functions, this functional overlap is not necessarily complete, since novel roles will have most likely been acquired during evolution. At the same time, not all geminiviral ORFs have positional counterparts (e.g., those in the DNA-B of bipartite geminiviruses), and therefore the essential virulence functions provided by the proteins they encode must be fulfilled by other, non-homologous geminiviral proteins. Hence, caution must be taken when extrapolating functional information to positional homologs, and uncovering the roles of each geminivirus-encoded protein in individual species will in all cases require experimental assessment.

AUTHOR CONTRIBUTIONS

AL and RL-D conceived the idea and prepared the manuscript.

FUNDING

Work in the Lozano-Duran lab is supported by the Shanghai Center for Plant Stress Biology from the Chinese Academy of Sciences, the National Science Foundation China (NSFC grants 31671994 and 31870250), and the Chinese Academy of Sciences Strategic Pilot Science and Technology Special (B) funding (grant No. XDB27040206).

ACKNOWLEDGMENTS

The authors would like to thank Alberto P. Macho for critical reading of the manuscript, Laura Medina-Puche for her invaluable help in the preparation of **Figure 1B**, and Eduardo R. Bejarano, the authors' PhD supervisor, for nurturing their critical thinking abilities in their scientific infancy.

REFERENCES

Amin, I., Hussain, K., Akbergenov, R., Yadav, J. S., Qazi, J., Mansoor, S., et al. (2011). Suppressors of RNA silencing encoded by the components of the cotton leaf curl begomovirus-betasatellite complex. *Mol. Plant Microbe. Interact.* 24, 973–983. doi: 10.1094/MPMI-01-11-0001

Baliji, S., Sunter, J., and Sunter, G. (2007). Transcriptional analysis of complementary sense genes of *Spinach curly top virus* and functional role of C2 in pathogenesis. *Mol. Plant Microbe. Interact.* 20, 194–206. doi: 10.1094/MPMI-20-2-0194

Bar-Ziv, A., Levy, Y., Citovsky, V., and Gafni, Y. (2015). The Tomato Yellow Leaf Curl Virus (TYLCV) V2 protein inhibits enzymatic activity of the host papain-like cysteine protease CYP1. *Biochem. Biophys. Res. Commun.* 460, 525–529. doi: 10.1016/j.bbrc.2015.03.063

Buchmann, R. C., Asad, S., Wolf, J. N., Mohannath, G., and Bisaro, D. M. (2009). Geminivirus AL2 and L2 proteins suppress transcriptional gene silencing and cause genome-wide reductions in cytosine methylation. *J. Virol.* 83, 5005–5013. doi: 10.1128/jvi.01771-08

Caracuel, Z., Lozano-Durán, R., Huguet, S., Arroyo-Mateos, M., Rodríguez-Negrete, E. A., and Bejarano, E. R. (2012). C2 from Beet curly top virus promotes a cell environment suitable for efficient replication of geminiviruses, providing a novel mechanism of viral synergism. *New Phytol.* 194, 846–858. doi: 10.1111/j.1469-8137.2012.04080.x

Carluccio, A. V., Prigigallo, M. I., Rosas-Diaz, T., Lozano-Duran, R., and Stavolone, L. (2018). S-acylation mediates mungbean yellow mosaic virus AC4 localization to the plasma membrane and in turns gene silencing suppression. *PLoS Pathog.* 14:e1007207. doi: 10.1371/journal.ppat.1007207

Castillo-González, C., Liu, X., Huang, C., Zhao, C., Ma, Z., Hu, T., et al. (2015). Geminivirus-encoded TrAP suppressor inhibits the histone methyltransferase SUVH4/KYP to counter host defense. *Elife* 4:e0667. doi: 10.7554/eLife.06671

Fondong, V. N., Reddy, R. V. C., Lu, C., Hankoua, B., Felton, C., Czymmek, K., et al. (2007). The consensus N-myristoylation motif of a geminivirus AC4 protein is required for membrane binding and pathogenicity. *Mol. Plant. Microbe. Interact.* 20, 380–391. doi: 10.1094/MPMI-20-4-0380

Hanley-Bowdoin, L., Bejarano, E. R., Robertson, D., and Mansoor, S. (2013). Geminiviruses: masters at redirecting and reprogramming plant processes. *Nat. Rev. Microbiol.* 11, 777–788. doi: 10.1038/nrmicro3117

Hao, L., Wang, H., Sunter, G., and Bisaro, D. M. (2003). Geminivirus AL2 and L2 proteins interact with and inactivate SNF1 kinase. *Plant Cell.* 15, 1034–1048. doi: 10.1105/tpc.009530

Ismayil, A., Haxim, Y., Wang, Y., Li, H., Qian, L., Han, T., et al. (2018). Cotton leaf curl multan virus C4 protein suppresses both transcriptional and post-transcriptional gene silencing by interacting with SAM synthetase. *PLoS Pathog.* 14:e1007282. doi: 10.1371/journal.ppat.1007282

Jackel, J. N., Buchmann, R. C., Singhal, U., and Bisaro, D. M. (2015). Analysis of geminivirus AL2 and L2 proteins reveals a novel AL2 silencing suppressor activity. *J. Virol.* 89, 3176–3187. doi: 10.1128/jvi.02625-14

Kushwaha, N. K., Bhardwaj, M., and Chakraborty, S. (2017). The replication initiator protein of a geminivirus interacts with host monoubiquitination machinery and stimulates transcription of the viral genome. *PLoS Pathog.* 13:e1006587. doi: 10.1371/journal.ppat.1006587

Li, H., Zeng, R., Chen, Z., Liu, X., Cao, Z., Xie, Q., et al. (2018). S-acylation of a geminivirus C4 protein is essential for regulating the CLAVATA pathway

in symptom determination. *J. Exp. Bot.* 69, 4459–4468. doi: 10.1093/jxb/ery228

Liu, Y., Jin, W., Wang, L., and Wang, X. (2014). Replication-associated proteins encoded by Wheat dwarf virus act as RNA silencing suppressors. *Virus Res.* 190, 34–39. doi: 10.1016/j.virusres.2014.06.014

Lozano-Duran, R., Caracuel, Z., and Bejarano, E. R. (2012). C2 from beet curly top virus meddles with the cell cycle: a novel function for an old pathogenicity factor. *Plant Signal. Behav.* 7, 1705–1708. doi: 10.4161/psb.22100

Luna, A. P., Morilla, G., Voinnet, O., and Bejarano, E. R. (2012). Functional analysis of gene-silencing suppressors from tomato yellow leaf curl disease viruses. *Mol. Plant. Microbe. Interact.* 25, 1294–1306. doi: 10.1094/MPMI-04-12-0094-R

Luna, A. P., Rodríguez-Negrete, E. A., Morilla, G., Wang, L., Lozano-Durán, R., Castillo, A. G., et al. (2017). V2 from a curtovirus is a suppressor of post-transcriptional gene silencing. *J. Gen. Virol.* 98, 2607–2614. doi: 10.1099/jgv.0.000933

Medina-Puche, L., Tan, H., Dogra, V., Wu, M., Rosas-Diaz, T., Wang, L., et al. (2019). A novel pathway linking plasma membrane and chloroplasts is co-opted by pathogens to suppress salicylic acid-dependent defences. *bioRxiv* 837955. doi: 10.1101/837955

Mei, Y., Ma, Z., Wang, Y., and Zhou, X. (2020). Geminivirus C4 antagonizes the HIR1-mediated hypersensitive response by inhibiting the HIR1 self-interaction and promoting degradation of the protein. *New Phytol.* 225, 1311–1326. doi: 10.1111/nph.16208

Mei, Y., Wang, Y., Hu, T., Yang, X., Lozano-Duran, R., Sunter, G., et al. (2018). Nucleocytoplasmic shuttling of geminivirus C4 protein mediated by phosphorylation and myristoylation is critical for viral pathogenicity. *Mol. Plant* 11, 1466–1481. doi: 10.1016/j.molp.2018.10.004

Melgarejo, T. A., Kon, T., Rojas, M. R., Paz-Carrasco, L., Zerbini, F. M., and Gilbertson, R. L. (2013). Characterization of a new world monopartite begomovirus causing leaf curl disease of tomato in Ecuador and Peru reveals a new direction in geminivirus evolution. *J. Virol.* 87, 5397–5413. doi: 10.1128/JVI.00234-13

Mills-Lujan, K., and Deom, C. M. (2010). Geminivirus C4 protein alters arabidopsis development. *Protoplasma* 239, 95–110. doi: 10.1007/s00709-009-0086-z

Mubin, M., Briddon, R. W., and Mansoor, S. (2019). The V2 protein encoded by a monopartite begomovirus is a suppressor of both post-transcriptional and transcriptional gene silencing activity. *Gene* 686, 43–48. doi: 10.1016/j.gene.2018.11.002

Piroux, N., Saunders, K., Page, A., and Stanley, J. (2007). Geminivirus pathogenicity protein C4 interacts with Arabidopsis thaliana shaggy-related protein kinase AtSKη, a component of the brassinosteroid signalling pathway. *Virology* 362, 428–440. doi: 10.1016/j.virol.2006.12.034

Rodríguez-Negrete, E., Lozano-Durán, R., Piedra-Aguilera, A., Cruzado, L., Bejarano, E. R., and Castillo, A. G. (2013). Geminivirus Rep protein interferes with the plant DNA methylation machinery and suppresses transcriptional gene silencing. *New Phytol.* 199, 464–475. doi: 10.1111/nph.12286

Rosas-Diaz, T., Zhang, D., Fan, P., Wang, L., Ding, X., Jiang, Y., et al. (2018). A virus-targeted plant receptor-like kinase promotes cell-to-cell spread of RNAi. *Proc. Natl. Acad. Sci. U.S.A.* 115, 1388–1393. doi: 10.1073/pnas.1715556115

Ruhel, R., and Chakraborty, S. (2019). Multifunctional roles of geminivirus encoded replication initiator protein. *VirusDisease* 30, 66–73. doi: 10.1007/s13337-018-0458-0

Sanz, A. I., Fraile, A., Gallego, J. M., Malpica, J. M., and García-Arenal, F. (1999). Genetic variability of natural populations of cotton leaf curl geminivirus, a single-stranded DNA virus. *J. Mol. Evol.* 9, 672–81. doi: 10.1007/PL00006588

Sharma, P., and Ikegami, M. (2010). Tomato leaf curl Java virus V2 protein is a determinant of virulence, hypersensitive response and suppression of posttranscriptional gene silencing. *Virology* 396, 85–93. doi: 10.1016/j.virol.2009.10.012

Sun, Y.-W., Tee, C.-S., Ma, Y.-H., Wang, G., Yao, X.-M., and Ye, J. (2015). Attenuation of Histone Methyltransferase KRYPTONITE-mediated transcriptional gene silencing by Geminivirus. *Sci. Rep.* 5:16476. doi: 10.1038/srep16476

Sunitha, S., Shanmugapriya, G., Balamani, V., and Veluthambi, K. (2013). Mungbean yellow mosaic virus (MYMV) AC4 suppresses post-transcriptional gene silencing and an AC4 hairpin RNA gene reduces MYMV DNA accumulation in transgenic tobacco. *Virus Genes* 46, 496–504. doi: 10.1007/s11262-013-0889-z

Sunter, G., and Bisaro, D. M. (1992). Transactivation of geminivirus AR1 and BR1 gene expression by the viral AL2 gene product occurs at the level of transcription. *Plant Cell* 4, 1321–1331. doi: 10.2307/3869417

Sunter, G., and Bisaro, D. M. (1997). Regulation of a geminivirus coat protein promoter by AL2 protein (TrAP): evidence for activation and derepression mechanisms. *Virology* 232, 269–280. doi: 10.1006/viro.1997.8549

Sunter, G., Stenger, D. C., and Bisaro, D. M. (1994). Heterologous complementation by geminivirus AL2 and AL3 genes. *Virology* 203, 203–210. doi: 10.1006/viro.1994.1477

Teng, K., Chen, H., Lai, J., Zhang, Z., Fang, Y., Xia, R., et al. (2010). Involvement of C4 protein of Beet severe curly top virus (Family Geminiviridae) in virus movement. *PLoS ONE* 5:e011280. doi: 10.1371/journal.pone.0011280

Trinks, D., Rajeswaran, R., Shivaprasad, P. V., Akbergenov, R., Oakeley, E. J., Veluthambi, K., et al. (2005). Suppression of RNA silencing by a geminivirus nuclear protein, AC2, correlates with transactivation of host genes. *J. Virol.* 79, 2517–2527. doi: 10.1128/JVI.79.4.2517-2527.2005

Vanitharani, R., Chellappan, P., Pita, J. S., and Fauquet, C. M. (2004). Differential roles of AC2 and AC4 of cassava geminiviruses in mediating synergism and suppression of posttranscriptional gene silencing. *J. Virol.* 78, 9487–9498. doi: 10.1128/JVI.78.17.9487-9498.2004

Voinnet, O., Pinto, Y. M., and Baulcombe, D. C. (1999). Suppression of gene silencing: a general strategy used by diverse DNA and RNA viruses of plants. *Proc. Natl. Acad. Sci.U.S.A.* 96, 14147–14152. doi: 10.1073/pnas.96.24.14147

Wang, B., Li, F., Huang, C., Yang, X., Qian, Y., Xie, Y., et al. (2014). V2 of Tomato yellow leaf curl virus can suppress methylation-mediated transcriptional gene silencing in plants. *J. Gen. Virol.* 95, 225–230. doi: 10.1099/vir.0.055798-0

Wang, B., Yang, X., Wang, Y., Xie, Y., and Zhou, X. (2018). Tomato yellow leaf curl virus V2 interacts with host histone deacetylase 6 to suppress methylation-mediated transcriptional gene silencing in plants. *J. Virol.* 92:e00036-18. doi: 10.1128/JVI.00036-18

Wang, H., Buckley, K. J., Yang, X., Buchmann, R. C., and Bisaro, D. M. (2005). Adenosine kinase inhibition and suppression of RNA silencing by geminivirus AL2 and L2 proteins. *J. Virol.* 79, 7410–7418. doi: 10.1128/JVI.79.12.7410-7418.2005

Wang, H., Hao, L., Shung, C.-Y., Sunter, G., and Bisaro, D. M. (2003). Adenosine kinase is inactivated by geminivirus AL2 and L2 proteins. *Plant Cell* 15, 3020–3032. doi: 10.1105/tpc.015180

Wang, L., Ding, Y., He, L., Zhang, G., Zhu, J.-K., and Lozano-Duran, R. (2020). A virus-encoded protein suppresses methylation of the viral genome in the Cajal body through its interaction with AGO4. *bioRxiv* 811091. doi: 10.1101/811091

Wartig, L., Kheyr-Pour, A., Noris, E., De Kouchkovsky, F., Jouanneau, F., Gronenborn, B., et al. (1997). genetic analysis of the monopartite tomato yellow leaf curl geminivirus: roles of V1, V2, and C2 ORFs in viral pathogenesis. *Virology* 228, 132–140. doi: 10.1006/viro.1996.8406

Yang, X., Ren, Y., Sun, S., Wang, D., Zhang, F., Li, D., et al. (2018). Identification of the potential virulence factors and RNA silencing suppressors of mulberry mosaic dwarf-associated geminivirus. *Viruses* 10:472. doi: 10.3390/v10090472

Yang, X., Wang, B., Li, F., Yang, Q., and Zhou, X. (2016). "Research Advances in Geminiviruses," in *Current Research Topics in Plant Virology*, eds A. Wang and X. Zhou (Cham: Springer International Publishing), 251–269. doi: 10.1007/978-3-319-32919-2_11

Yang, X. L., Zhou, M. N., Qian, Y. J., Xie, Y., and Zhou, X. P. (2014). Molecular variability and evolution of a natural population of *Tomato yellow leaf curl virus* in Shanghai, China. *J. Zhejiang Univ. Sci. B* 15, 133–142. doi: 10.1631/jzus.B1300110

Zerbini, F. M., Briddon, R. W., Idris, A., Martin, D. P., Moriones, E., Navas-Castillo, J., et al. (2017). ICTV virus taxonomy profile: geminiviridae. *J. Gen. Virol.* 98, 131–133. doi: 10.1099/jgv.0.000738

Zhan, B., Zhao, W., Li, S., Yang, X., and Zhou, X. (2018). Functional scanning of apple geminivirus proteins as symptom determinants and suppressors of posttranscriptional gene silencing. *Viruses* 10:488. doi: 10.3390/v10090488

Zhang, J., Dong, J., Xu, Y., and Wu, J. (2012). V2 protein encoded by *Tomato yellow leaf curl China virus* is an RNA silencing suppressor. *Virus Res.* 163, 51–58. doi: 10.1016/j.virusres.2011.08.009

Zhang, Z., Chen, H., Huang, X., Xia, R., Zhao, Q., Lai, J., et al. (2011). BSCTV C2 attenuates the degradation of SAMDC1 to Suppress DNA

methylation-mediated gene silencing in Arabidopsis. *Plant Cell* 23, 273–288. doi: 10.1105/tpc.110.081695

Zhao, L., Rosario, K., Breitbart, M., and Duffy, S. (2019). Eukaryotic circular rep-encoding single-stranded DNA (CRESS DNA) viruses: ubiquitous viruses with small genomes and a diverse host range. *Adv. Virus Res.* 103, 71–133. doi: 10.1016/bs.aivir.2018.10.001

Zhou, X. (2013). Advances in understanding begomovirus satellites. *Annu. Rev. Phytopathol.* 51, 357–381. doi: 10.1146/annurev-phyto-082712-102234

Zrachya, A., Glick, E., Levy, Y., Arazi, T., Citovsky, V., and Gafni, Y. (2007). Suppressor of RNA silencing encoded by Tomato yellow leaf curl virus-Israel. *Virology* 358, 159–165. doi: 10.1016/j.virol.2006.08.016

Conflict of Interest: The authors declare that the research was conducted in the absence of any commercial or financial relationships that could be construed as a potential conflict of interest.

frontiers in Microbiology

ORIGINAL RESEARCH
published: 05 May 2020
doi: 10.3389/fmicb.2020.00851

C4, the Pathogenic Determinant of *Tomato Leaf Curl Guangdong Virus*, May Suppress Post-transcriptional Gene Silencing by Interacting With BAM1 Protein

*Zhenggang Li[1,2], Zhenguo Du[1], Yafei Tang[1], Xiaoman She[1], Xiaomei Wang[1], Yanhua Zhu[1], Lin Yu[1], Guobing Lan[1] and Zifu He[1,2]**

[1] Plant Protection Research Institute, Guangdong Academy of Agricultural Sciences, Guangzhou, China, [2] Guangdong Provincial Key Laboratory of High Technology for Plant Protection, Guangdong Academy of Agricultural Sciences, Guangzhou, China

Tomato leaf curl Guangdong virus (ToLCGdV) is a begomovirus associated with a Tomato yellow leaf curl disease (TYLCD) epidemic in Guangdong province, China. Being the least conserved protein among geminivirus proteins, the function of C4 during ToLCGdV infection has not been elucidated. In this study, the infectious clones of ToLCGdV and a ToLCGdV mutant (ToLCGdV$_{mC4}$) with disrupted C4 ORF were constructed. Although ToLCGdV and ToLCGdV$_{mC4}$ could infect *Nicotiana benthamiana* and tomato plants, ToLCGdV$_{mC4}$ elicited much milder symptoms compared with ToLCGdV. To further verify the role of C4 in viral pathogenesis, C4 was expressed in *N. benthamiana* from *Potato virus X* (PVX) vector. The results showed that ToLCGdV C4 enhanced the pathogenicity of PVX and induced more severe developmental abnormalities in plants compared with PVX alone or PVX-mC4. In addition, ToLCGdV C4 suppresses systemic gene silencing in the transgenic *N. benthamiana* line 16c, but not local gene silencing induced by sense GFP in wild-type *N. benthamiana* plants. Moreover, C4 suppresses transcriptional gene silencing (TGS) by reducing the DNA methylation level of 35S promoter in 16c-TGS *N. benthamiana* plants. Furthermore, C4 could also interact with the receptor-like kinase (RLK) BARELY ANY MERISTEM 1 (BAM1), suggesting that C4 may suppress gene silencing by interfering with the function of BAM1 in the cell-to-cell spread of RNAi. All these results suggest that C4 is a pathogenic determinant of ToLCGdV, and C4 may suppress post-transcriptional gene silencing (PTGS) by interacting with BAM1.

Keywords: ***Tomato yellow leaf curl Guangdong virus*, C4, pathogenic determinant, PTGS, TGS, BAM1**

OPEN ACCESS

Edited by:
Rosa Lozano-Durán, Shanghai Institutes for Biological Sciences (CAS), China

Reviewed by:
Pablo A. Manavella, CONICET Santa Fe, Argentina
Xueping Zhou, Zhejiang University, China

***Correspondence:**
Zifu He
hezf@gdppri.com

Specialty section:
This article was submitted to Virology, a section of the journal Frontiers in Microbiology

Received: *12 December 2019*
Accepted: *09 April 2020*
Published: *05 May 2020*

Citation:
Li Z, Du Z, Tang Y, She X, Wang X, Zhu Y, Yu L, Lan G and He Z (2020) C4, the Pathogenic Determinant of Tomato Leaf Curl Guangdong Virus, May Suppress Post-transcriptional Gene Silencing by Interacting With BAM1 Protein. Front. Microbiol. 11:851. doi: 10.3389/fmicb.2020.00851

INTRODUCTION

Geminiviridae constitutes a large family of plant viruses with small, single-stranded and circular DNA (sscDNA) genomes encompassed within characteristic twinned icosahedral particles (Hanley-Bowdoin et al., 1999; Fauquet et al., 2008). Geminiviruses, which are transmitted by insects and could infect both dicots and monocots (John et al., 2001), have emerged as one of

the most important groups of plant pathogens worldwide, especially in tropical and subtropical regions (Boulton, 2003; Varma and Malathi, 2003; Rojas et al., 2005; Mansoor et al., 2006; Fauquet et al., 2008; Navas-Castillo et al., 2011; Sattar et al., 2013). *Geminiviridae* includes nine genera *Becurtovirus*, *Begomovirus*, *Capulavirus*, *Curtovirus*, *Eragrovirus*, *Grablovirus*, *Mastrevirus*, *Topocuvirus*, and *Turncurtovirus* with different genome organization, host range, and insect vectors (Zerbini et al., 2017). Except the genus *Begomovirus*, geminivirus consists of monopartite component with 2.5∼3.0 kb in length (Zerbini et al., 2017).

Begomoviruses, transmitted by the whitefly vector *Bemisia tabaci*, are either monopartite or bipartite and infect only dicots. The DNA A virion-sense strand of bipartite begomovirus encodes the coat protein CP (AV1) and movement protein (AV2), which may both be involved in virus movement. The complementary-sense strand of DNA A component encodes the replication-associated protein (Rep, ORF AC1), transcriptional activator protein (TrAP, ORF AC2), replication enhancer protein (REn, ORF AC3) and C4 protein (ORF AC4). The DNA B component of bipartite begomovirus encodes two proteins, the nuclear shuttle protein (NSP, ORF BV1) on the virion-sense strand and the movement protein (MP, ORF BC1) on the complementary-sense strand (Hanley-Bowdoin et al., 1999). For both DNA A and DNA B, the bidirectionally arranged ORFs are separated by a long intergenic region (IR) which carries key elements for initiating viral replication and transcription (Hanley-Bowdoin et al., 1999). The genome of monopartite begomovirus encodes all information required for the viral infection and consists of a single ssDNA molecule which resembles the DNA A of bipartite begomovirus. However, an increasing number of monopartite begomoviruses have been found to require betasatellites for successful infection and symptom induction in some host plants (Zhou, 2013; Yang et al., 2019).

As one of the least conserved proteins among geminivirus proteins, the function of AC4/C4 protein varies among different geminiviruses. C4 is a major pathogenic determinant in curtoviruses and some monopartite begomoviruses, disruption of C4 reduces viral infections and symptom development (Stanley and Latham, 1992; Teng et al., 2010; Li et al., 2018). Transient expression of *Beet curly top virus* (BCTV) C4 or *Tomato leaf curl Yunnan virus* (TLCYnV) C4 contributes to PVX infection, and induces severe developmental abnormalities similar with phenotypes induced by virus infection in both *N. benthamiana* and *Arabidopsis* (Latham et al., 1997; Piroux et al., 2007; Mills-Lujan and Deom, 2010; Mills-Lujan et al., 2015; Mei et al., 2018b). However, AC4 of the bipartite begomovirus *Tomato golden mosaic virus* (TGMV) has no obvious effect on symptom development (Piroux et al., 2007). More and more studies have found that AC4/C4 induces plant abnormal development by regulating brassinosteroid (BR) signaling pathway through interaction with members of *Arabidopsis* SHAGGY-like protein kinase (AtSK) family (Piroux et al., 2007; Mills-Lujan and Deom, 2010; Deom and Mills-Lujan, 2015; Mills-Lujan et al., 2015; Bi et al., 2017; Mei et al., 2018a,b).

AC4/C4 also functions as a viral suppressor of RNA silencing (VSR) to suppress both post-transcriptional gene silencing (PTGS) and transcriptional gene silencing (TGS) (Vanitharani et al., 2004; Gopal et al., 2007; Yang et al., 2011; Fondong, 2013; Xie et al., 2013). AC4 encoded by *African cassava mosaic virus* (ACMV) and *Sri Lankan cassava mosaic virus* (SLCMV), but not *East African cassava mosaic Cameroon virus* (EACMCV) nor *Indian cassava mosaic virus* (ICMV), have been shown to suppress RNA silencing by specifically binding to the single-stranded miRNAs and siRNAs to block the miRNA-mediated cleavage of target mRNAs (Chellappan et al., 2004, 2005; Vanitharani et al., 2004; Fondong et al., 2007). A recent study also shows that *Tomato yellow leaf curl virus* (TYLCV) C4 interacts with the receptor-like kinases (RLKs) BARELY ANY MERISTEM 1 (BAM1) and its homolog BAM2, interfering with the function of BAM1 and BAM2 in the intercellular spread of RNAi (Rosas-Diaz et al., 2018). Moreover, *Mungbean yellow mosaic virus* (MYMV) AC4 also interacts with BAM1 at plasma membrane (PM), and the PM location of MYMV AC4 depends on S-palmitoylation (Carluccio et al., 2018). AC4/C4 can also reverse methylation-mediated TGS. *Cotton leaf curl Multan virus* (CLCuMuV) C4 have been shown to repress both PTGS and TGS by interacting with S-adenosyl methionine synthetase (SAMS) and inhibiting SAMS activity (Ismayil et al., 2018).

A group of begomoviruses, most of which are monopartite geminiviruses, infect tomato plants and are considered to be responsible for a devastating disease called tomato yellow leaf curl disease (TYLCD) which is a major limiting factor for tomato cultivation worldwide (Navas-Castillo et al., 2011). A new begomovirus which might be responsible for the epidemic of TYLCD in Guangdong province of China during the year 2004–2006 was isolated and named *Tomato leaf curl Guangdong virus* (ToLCGdV) (He et al., 2005). ToLCGdV is a monopartite begomovirus with 2744nt in length and encodes 6 proteins as the other monopartite geminiviruses. As expected, ToLCGdV CP encoded by virion-sense strand shares the highest amino acid identity compared with other begomoviruses, while C4 protein shares the least amino acid identity (He et al., 2005). As the huge diversity of AC4/C4, the function of ToLCGdV C4 is still unknown.

In this study, the infectious clones of ToLCGdV and ToLCGdV$_{mC4}$ were constructed. ToLCGdV C4 is a pathogenic determinant by contributing to ToLCGdV and PVX infection. ToLCGdV C4 is also a VSR by suppressing systemic gene silencing but not local gene silencing. Moreover, ToLCGdV C4 could reverse methylation-mediated TGS. In addition, ToLCGdV C4 suppresses PTGS maybe by interacting with BAM1. These results demonstrate that ToLCGdV C4 plays an important role in virus infection by functioning as both pathogenic determinant and VSR.

MATERIALS AND METHODS

Plasmid Construction

To construct ToLCGdV infectious clones pGreenII-1.3A-ToLCGdV which contains a 1.3-mer tandem repeat of ToLCGdV, the full-length sequence and a 0.8-kb fragment

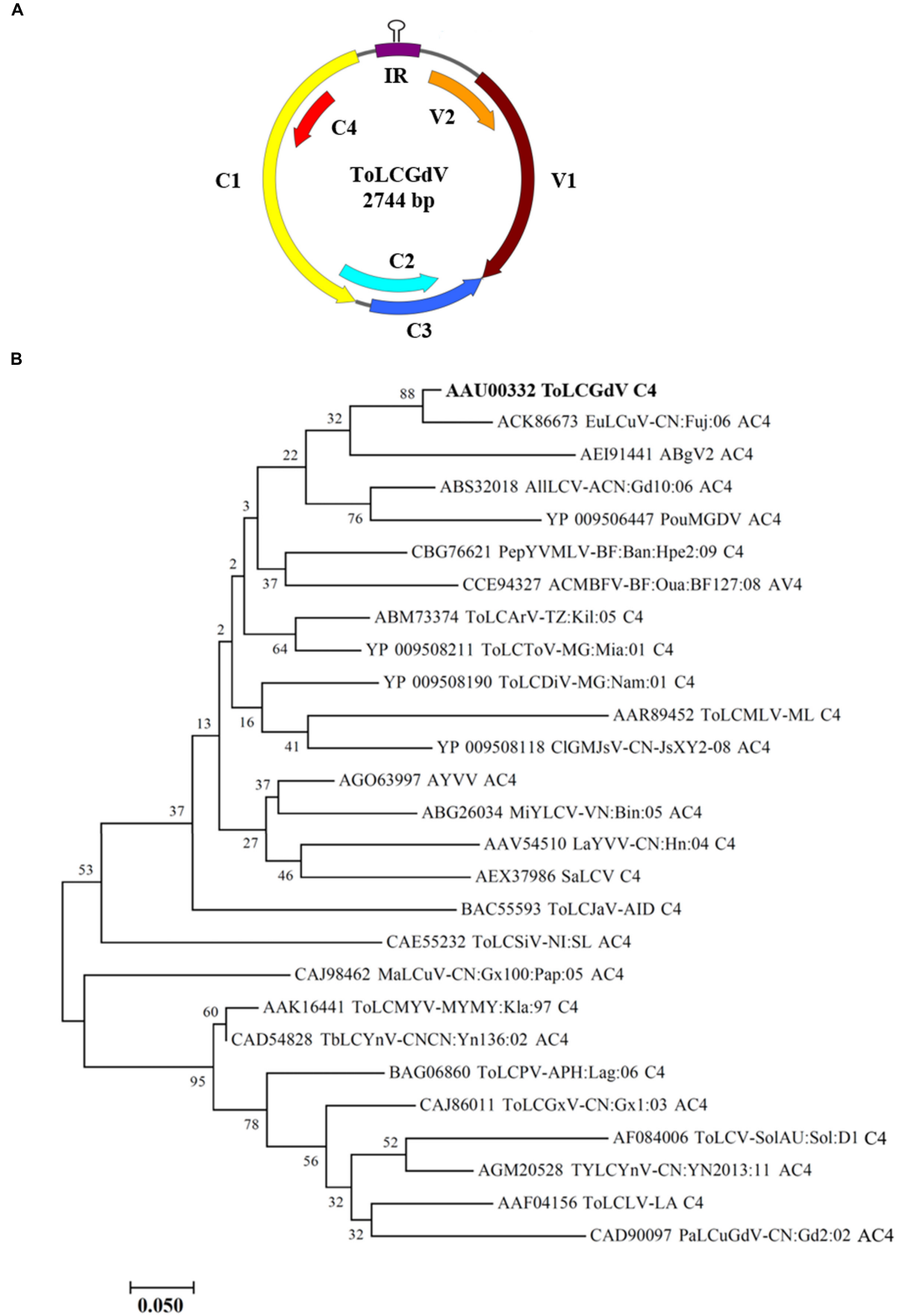

FIGURE 1 | Schematic diagram of ToLCGdV genome and phylogenetic tree constructed from AC4/C4 protein sequences by neighbor-joining method. **(A)** Schematic diagram of ToLCGdV genome. Viral genes are indicated by filled arrows. IR, intergenic region. **(B)** Phylogenetic tree constructed from AC4/C4 protein sequences by neighbor-joining method. Twenty-seven AC4/C4 protein sequences were acquired from the GenBank. Full names and the origins of the begomoviruses used in the phylogenetic analyses are listed in **Table 1**. Numbers on the branches are bootstrap obtained from 1000 replicates. ToLCGdV C4 are marked in bold.

TABLE 1 | Begomoviruses used in the phylogenetic analyses.

Abbreviation	Name	Accession number		Origin
		DNA A	DNA B	
ABgV2	Asystasia begomovirus 2	JF694486		West Africa
ACMBFV-[BF:Oua:BF127:08]	African cassava mosaic Burkina Faso virus	HE616777		Burkina Faso: Ouagadougou
AllLCV-A[CN:Gd10:06]	Allamanda leaf curl virus	EF602306		China: Guangdong
AYVV	*Ageratum yellow vein virus*	KC810890		China: Hainan
ClGMJsV-[CN-JsXY2-08]	*Clerodendrum golden mosaic Jiangsu virus*	FN396966		China: Jiangsu
EuLCuV-[CN:Fuj:06]	*Euphorbia leaf curl virus*	FJ487911		China: Fujian
LaYVV-[CN:Hn:04]	*Lindernia anagallis yellow vein virus*	AY795900		China: Hainan
MaLCuV-[CN:Gx100:Pap:05]	Malvastrum leaf curl virus	AM260699		China: Guangxi
MiYLCV-[VN:Bin:05]	*Mimosa yellow leaf curl virus*	DQ641695		Vietnam: Binhduong
PaLCuGdV-[CN:Gd2:02]	*Papaya leaf curl Guandong virus*	AJ558122		China: Guangdong
PepYVMLV-[BF:Ban:Hpe2:09]	*Pepper yellow vein Mali virus*	FN555173		Burkina Faso: Banfora
PouMGDV	Pouzolzia mosaic Guangdong virus	NC_038453		China: Guangdong
SaLCV	*Sauropus leaf curl virus*	JN809825		Thailand: Kamphaengsaen
TbLCYnV-CN[CN:Yn136:02]	*Tobacco leaf curl Yunnan virus*	AJ512761		China: Yunnan
ToLCArV-[TZ:Kil:05]	*Tomato leaf curl Arusha virus*	EF194760		Tanzania: Kilimandjaro
ToLCDiV-[MG:Nam:01]	Tomato leaf curl Diana virus	AM701765		Madagascar: Namakely
ToLCGdV	*Tomato leaf curl Guangdong virus*	AY602165		China: Guangdong
ToLCGxV-[CN:Gx1:03]	*Tomato leaf curl Guangxi virus*	AM236784		China: Guangxi
ToLCJaV-A[ID]	*Tomato leaf curl Java virus*	AB100304		Indonesia
ToLCLV-[LA]	*Tomato leaf curl Laos virus*	AF195782		Laos
ToLCMLV-[ML]	*Tomato leaf curl Mali virus*	AY502936		Mali
ToLCMYV-MY[MY:Kla:97]	*Tomato leaf curl Malaysia virus*	AF327436		Malaysia
ToLCPV-A[PH:Lag:06]	*Tomato leaf curl Philippines virus*	AB377113		Philippines: Laguna
ToLCSiV-[NI:SL]	*Tomato leaf curl Sinaloa virus*	AJ608286	AJ508783	Nicaragua: Santa Lucia
ToLCToV-[MG:Mia:01]	Tomato leaf curl Toliara virus	AM701768		Madagascar: Miandrivazo
ToLCV-Sol[AU:Sol:D1]	*Tomato leaf curl virus*	AF084006		Australia
TYLCYnV-[CN:YN2013:11]	*Tomato yellow leaf curl Yunnan virus*	KC686705		China: Yunnan

of ToLCGdV were amplified with primer pairs ToLCGDV-F1/R1 and ToLCGDV-F2/R2 (**Supplementary Table 1**), respectively, and introduced into *Sma*I-digested pGreenII (Hellens et al., 2000) by Seamless Cloning and Assembly (Takara). pGreenII-1.3A-ToLCGdV$_{mC4}$ was generated by QuickChange® site-directed mutagenesis (Agilent Technologies) with pGreenII-1.3A-ToLCGdV as templates.

C4 and the mutated C4 nucleotide sequences were amplified from pGreenII-1.3A-ToLCGdV or pGreenII-1.3A-ToLCGdV$_{mC4}$ and introduced into pGR107 (Lu et al., 2003) to obtain PVX-C4 and PVX-mC4. pGD-C4-Myc was generated by inserting C4 sequence into pGD-Myc (Goodin et al., 2002). Subsequently, the sequence of C4-Myc was amplified and introduced into pGR107 to get PVX-C4-Myc.

For bimolecular fluorescence complementation (BiFC) assays, C4 was amplified and cloned into pSPYNE-35S and pSPYCE-35S split YFP destination vectors (Walter et al., 2004). For subcellular localization experiments, C4 was amplified, followed by cloning into pGDGm (Goodin et al., 2002; Fan et al., 2014) with standard protocols.

Primers used for plasmid construction in this study are listed in **Supplementary Table 1**.

Plant Growth Conditions

Nicotiana benthamiana and tomato plants used in this study were grown in a climate chamber with a 13h/11h light/dark photoperiod at 24°C. *N. benthamiana* were agroinfiltrated at 5–6 leaf stage, and tomato plants were inoculated at 6–7 leaf stage.

Western Blot Detection

For western blot detection, samples were taken and weighed, followed by ground in liquid nitrogen. Two volumes of 1 × SDS loading buffer was added and boiled for 10 min. After centrifugation for 10 min at 12 000 rpm, 20 μl supernatant was loaded per lane on the SDS-PAGE gel. Then proteins were transferred to the nitrocellulose membranes. The secondary antibody was purchased from Sigma-Aldrich, Inc., Alkaline phosphatase was visualized with NBT/BCIP (Sangon Biotech, Shanghai, China).

Phylogenetic Analyses

AC4/C4 protein sequences were obtained by searching National Center for Biotechnology Information (NCBI) GenBank using the protein sequence of ToLCGdV C4. Phylogenetic trees were constructed with MEGA7 (Kumar et al., 2016) software using neighbor-joining method based on AC4/C4 protein sequences. 1000 bootstrap replicates were performed to obtain support for the identified phylogenetic relationships.

Quantitative RT-PCR

Total RNA was extracted with Trizol reagent (Takara) and treated with RNase-free rDNase I (Takara) before reverse

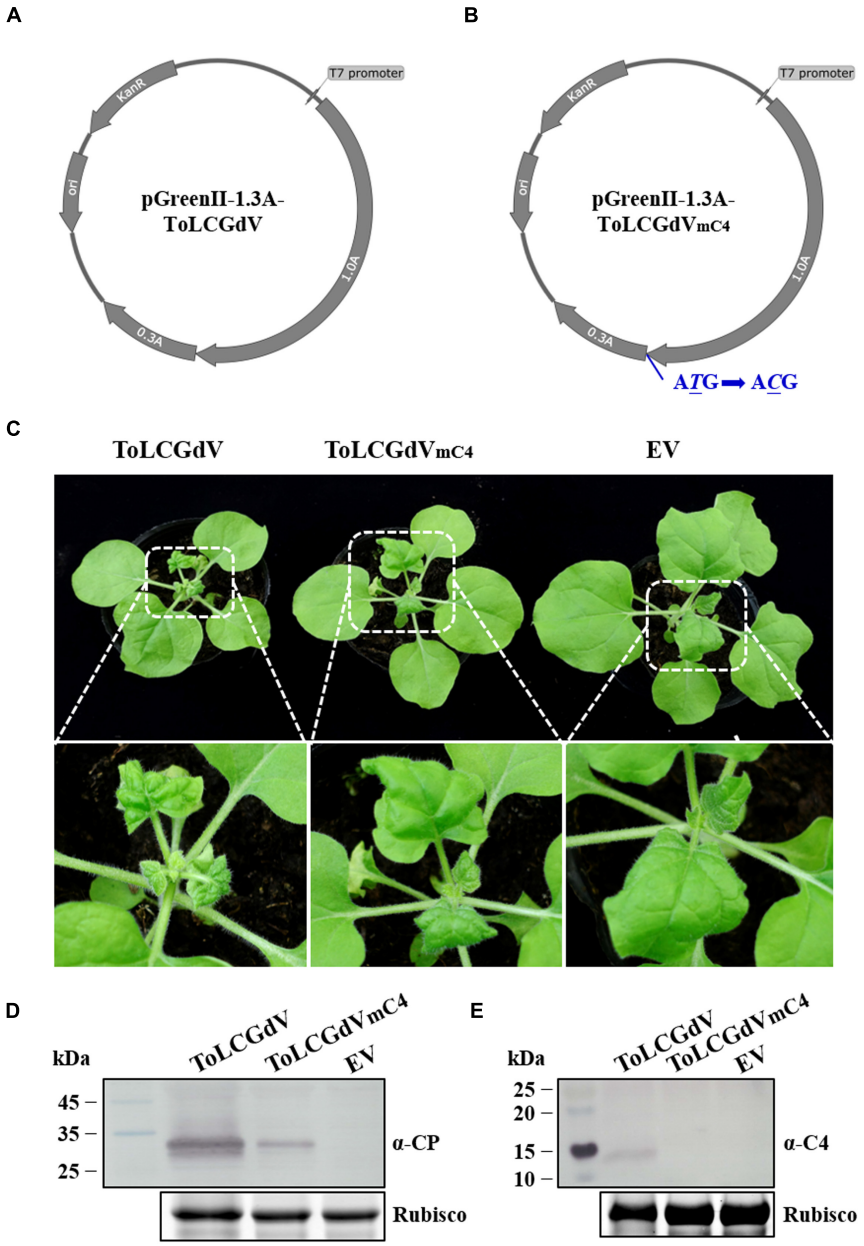

FIGURE 2 | Construction of ToLCGdV and ToLCGdV$_{mC4}$ infectious clones. **(A)** Schematic depiction of pGreenII-1.3A-ToLCGdV. Full-length and 0.3-time sequence of ToLCGdV were amplified and cloned into pGreenII vector (Hellens et al., 2000). *KanR*, kanamycin resistance. *ori*, replication initial origin. **(B)** Schematic depiction of pGreenII-1.3A-ToLCGdV$_{mC4}$. Loss expression of C4 was made by replacing the start codon ATG with ACG, which has no effect on the expression of C1. *KanR*, kanamycin resistance. *ori*, replication initial origin. **(C)** Symptoms of *N. benthamiana* plants agroinfiltrated with pGreenII-1.3A-ToLCGdV or pGreenII-1.3A-ToLCGdV$_{mC4}$. *Agrobacterium* strains harboring pGreenII-1.3A-ToLCGdV or pGreenII-1.3A-ToLCGdV$_{mC4}$ were infiltrated into the leaves of 5–6 leaf-stage *N. benthamiana*. Photos were taken at 13 dpi. The bottom panel shows the magnification of the white dotted frame. EV, empty vector. **(D)** Western blot detection of virus accumulation in the infected plants. The upper leaves were taken at 13 dpi and subjected to western blot detection with anti-ToLCGdV AV1 (CP) antibody. Rubisco shows equal sample loading. Numbers on the left indicate molecular weight. **(E)** Western blot detection of C4 in the upper infected leaves. Leaves were taken at 13 dpi to perform western blot with anti-C4 antibody. Rubisco is used as equal loading. Numbers on the left indicate molecular weight.

transcription reaction. Equal amount of treated RNA was subjected to reverse transcription using PrimeScript RT Reagent Kit (Takara). Real-time RT-PCR was performed with SYBR Premix Ex Taq II (Takara) using CFX96 Real-Time System (Bio-Rad, United States).

GFP Imaging

To identify the suppressor activity of C4, 16c transgenic *N. benthamiana* plants (provided by Dawei Li lab) and 16c-TGS plants were used. 16c-TGS plants were generated as described (Buchmann et al., 2009). *Agrobacterium* infiltration

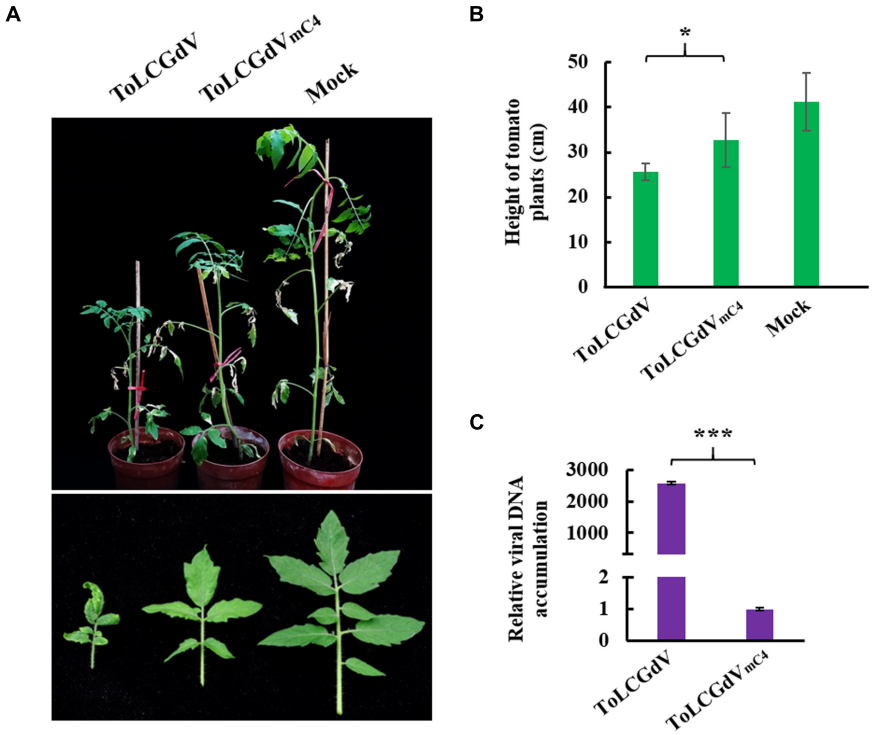

FIGURE 3 | Effects of C4 on ToLCGdV pathogenicity in tomato. **(A)** Symptoms of tomato plants infected by ToLCGdV or ToLCGdV$_{mC4}$. *Agrobacterium* strains harboring pGreenII-1.3A-ToLCGdV or pGreenII-1.3A-ToLCGdV$_{mC4}$ were infiltrated into 4–6-week-old tomato plants. Photos were taken at 30 dpi. **(B)** Statistical analysis of the height of tomato plants infected by ToLCGdV and ToLCGdV$_{mC4}$. Ten plants of each treatment were performed to measure the height. *$p < 0.05$. **(C)** Quantitative PCR to detect the viral DNA accumulation. Samples were taken at 30 dpi and subjected to DNA extraction. 0.2 μg DNA was used to perform real-time PCR. ***$p < 0.001$ (extremely significant).

was performed as described previously (Hamilton et al., 2002). *Tomato bushy stunt virus* (TBSV) p19 and an empty vector (pGD) were used as positive and negative controls, respectively. GFP fluorescence was observed under a long-wave UV lamp (Black Ray model B 100A; UV Products) and photographed using a Nikon D70 digital camera with a Y48 yellow filter.

Confocal Microscopy

Agrobacterium strains harboring the corresponding plasmids were co-infiltrated into 5–6 leaf stage *N. benthamiana* plants. Samples were taken at 3 dpi and visualized under Zeiss LSM710 confocal microscope (Carl Zeiss 710, Germany). Excitation wavelengths were as follows: EYFP, 514 nm; RFP, 561 nm.

Genomic DNA Isolation and Next Generation Sequencing-Based Bisulfite Sequencing PCR (BSP)

Genomic DNA was extracted with a cetyltrimethylammonium bromide (CTAB) method (Doyle and Doyle, 1987). Cytosine methylation level of the 35S promoter region was assayed by next generation sequencing-based BSP method as described previously (Gao et al., 2014, 2015; Pan et al., 2018). Primer pair used to amplify 35S promoter was described previously (Ismayil et al., 2018). PCR products of 35S promoter from different samples were quantified by Qubit 3.0 (Thermo Fisher), followed by bisulfite treatment with EZ DNA Methylation Gold Kit (Zymo Research). Then the products were subjected to adapter ligation by PCR amplification to generate barcoded libraries. Barcoded libraries from different samples were pooled together equally for standard pair-end sequencing with Illumina HiSeq PE150. The acquired data were processed with standard protocols (Li et al., 2010).

Co-immunoprecipitation (Co-IP) Assays

Co-immunoprecipitation assays were performed according to the previously published protocols (Rubio et al., 2005; Hu et al., 2015). Inoculated *N. benthamiana* leaves were collected at 3 dpi to perform Co-IP assays with anti-c-Myc agarose affinity gel (Sigma Aldrich, United States).

RESULTS

Phylogenetic Analysis of ToLCGdV C4

Tomato leaf curl Guangdong virus was firstly reported and named by He et al. (2005), and no satellite molecules were found to be associated with ToLCGdV. ToLCGdV contains 2744 nucleotides and encodes 6 proteins, V1, V2, C1, C2, C3, and C4 (**Figure 1A**). As the least conserved protein among

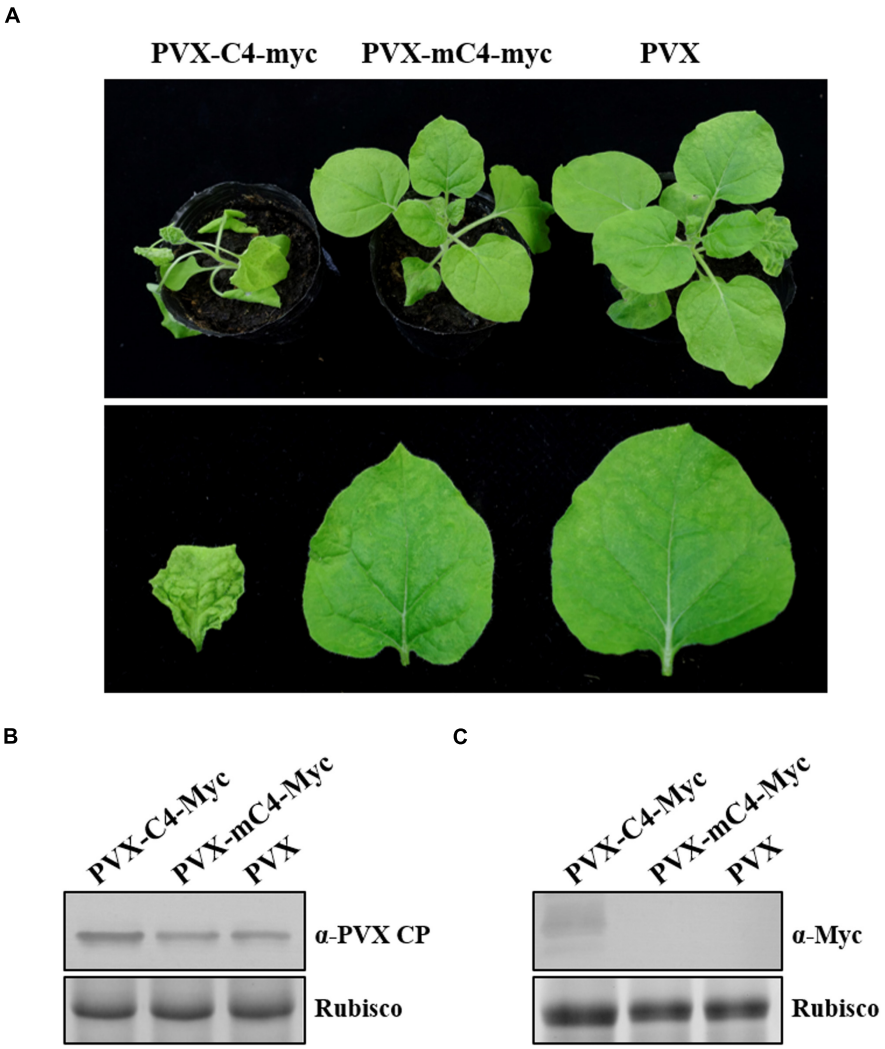

FIGURE 4 | Enhancement of C4 on PVX symptom development. **(A)** Symptoms of *N. benthamiana* plants infected by PVX-C4-Myc, PVX-mC4-Myc, and PVX, respectively. *Agrobacterium* strain harboring PVX-C4-Myc, PVX-mC4-Myc, or PVX was infiltrated into 5–6 leaf-stage *N. benthamiana* plants. Photos were taken at 10 dpi. **(B)** Western blot detection of the upper infected leaves. Samples were taken at 10 dpi and subjected to western blot with anti-PVX CP antibody. Rubisco indicates equal sample loading. **(C)** Western blot to detect C4 expression. Samples were taken at 10 dpi and western blot was performed with anti-Myc antibody. Rubisco indicates equal sample loading.

geminiviruses, the variety of C4 is one of the main reasons that responsible for the diversity of geminiviruses. To explore the relationship of ToLCGdV C4 with other begomoviruses AC4/C4, multiple AC4/C4 protein sequences of different begomoviruses (**Table 1**) were obtained by searching NCBI GenBank using the protein sequence of ToLCGdV C4. Phylogenetic analysis shows that ToLCGdV C4 shares the highest amino acids similarity (92.94%) with AC4 of *Euphorbia leaf curl virus* (EuLCuV) (**Figure 1B**), an *Euphorbia pulcherrima*-infecting monopartite begomovirus firstly identified in China (Ma et al., 2004). ToLCGdV C4 is also close to AC4 proteins encoded by other weed-infecting begomoviruses like Asystasia begomovirus 2 (ABgV2), Allamanda leaf curl virus (AllLCV), and Pouzolzia mosaic Guangdong virus (PouMGDV) (**Figure 1B**). In contrast, ToLCGdV C4 has relatively farther genetic distance with other tomato-infecting begomoviruses (**Figure 1B**). Thus, it is speculated that ToLCGdV may be a recombinant begomovirus originated from the weed-infecting begomoviruses.

C4 Contributes to ToLCGdV Pathogenicity

To study the molecular characteristic of ToLCGdV, the infectious clones of ToLCGdV and ToLCGdV$_{mC4}$ which contains an unexpressed C4 were constructed. pGreenII-1.3A-ToLCGdV (**Figure 2A**) and pGreenII-1.3A-ToLCGdV$_{mC4}$ (**Figure 2B**) were transformed to *Agrobacterium tumefaciens* strain GV3101 and then infiltrated into 5–6 leaf stage *N. benthamiana* plants. Comparing with control plants, plants agroinfiltrated with pGreenII-1.3A-ToLCGdV showed symptoms with stunting,

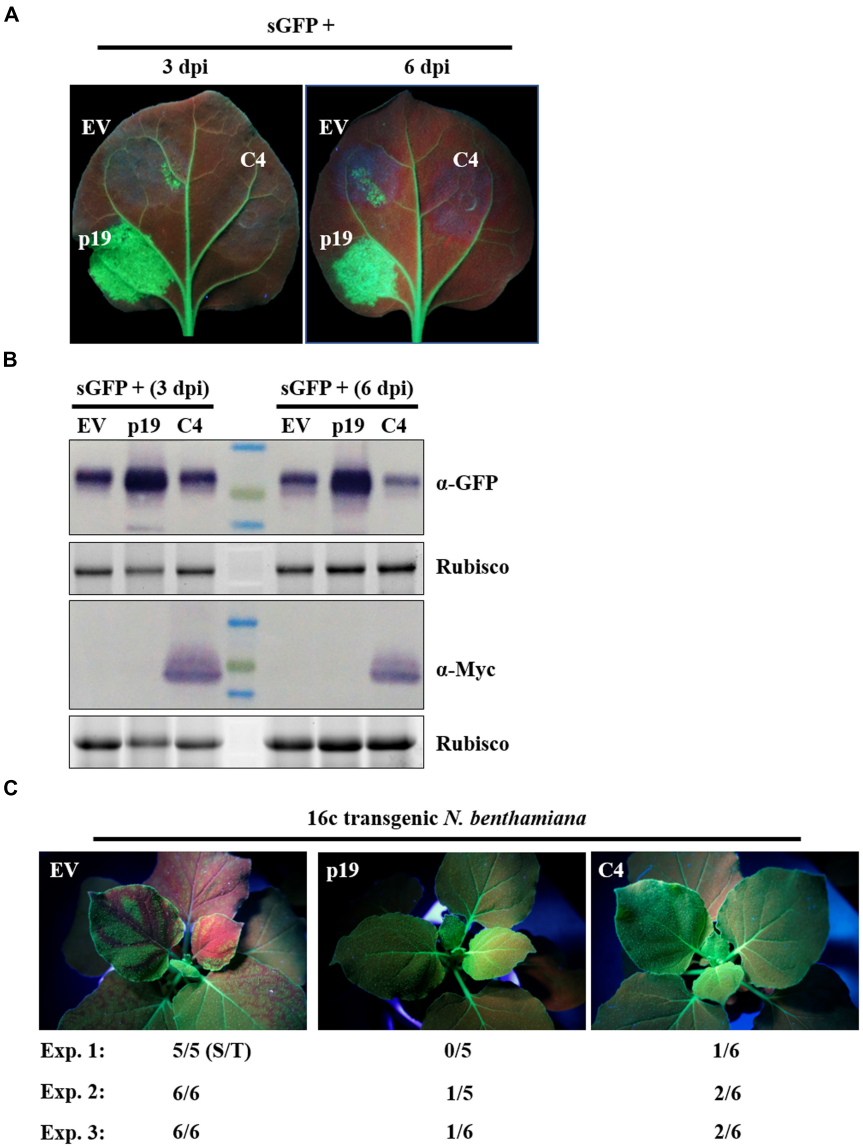

FIGURE 5 | Suppression of ToLCGdV C4 in PTGS. **(A)** Effect of C4 in local gene silencing. *Agrobacterium* strains containing sGFP and p19, sGFP and EV, or sGFP and C4-Myc were co-infiltrated into the same leaf of *N. benthamiana*. EV and p19 were used as negative and positive controls, respectively. Leaves were photographed under UV light at 3 and 6 dpi. **(B)** Western blot assays of GFP and C4 expression in co-infiltrated leaves. Samples taken at 3 and 6 dpi were subjected to western blot with anti-GFP and anti-Myc antibody. Rubisco indicates equal sample loading. **(C)** Suppression of C4 in systemic gene silencing. *Agrobacterium* strains containing sGFP and p19, sGFP and EV, or sGFP and C4-Myc were co-infiltrated into 16c transgenic *N. benthamiana* plants. Inoculated plants were observed under UV light at 12 dpi. Three independent experiments were repeated. The number ratio (S/T) indicates the systemic silencing (S) among the total number of infiltrated plants (T).

newly leaves curly, and yellowing at 10 days post inoculation (dpi) (**Figure 2C**), while plants agroinfiltrated with pGreenII-1.3A-ToLCGdV$_{mC4}$ showed visible symptoms with newly leaves curly until 15 dpi (**Figure 2C**). Western blot detection also confirmed that though the mutant virus can still move systemically to the upper leaves, the virus accumulation reduced significantly due to the loss of C4 (**Figures 2D,E**). In summary, inoculation of *N. benthamiana* verified the validity of the infectious clones and demonstrate that loss of C4 remarkably delay and weaken disease symptoms of ToLCGdV in *N. benthamiana*.

To explore the function of C4 during ToLCGdV infection in its natural host tomato, *Agrobacterium* strain containing pGreenII-1.3A-ToLCGdV or pGreenII-1.3A-ToLCGdV$_{mC4}$ was infiltrated into tomato plants. Tomato plants agroinfiltrated with pGreenII-1.3A-ToLCGdV developed obvious symptoms including leaf curling and yellowing at 30 dpi (**Figure 3A**), indicating the monopartite nature of ToLCGdV. However, tomato plants infected by ToLCGdV$_{mC4}$ showed much milder symptoms compared with plants infected by ToLCGdV or mock-treated (**Figure 3A**). In addition, ToLCGdV$_{mC4}$-infected tomato

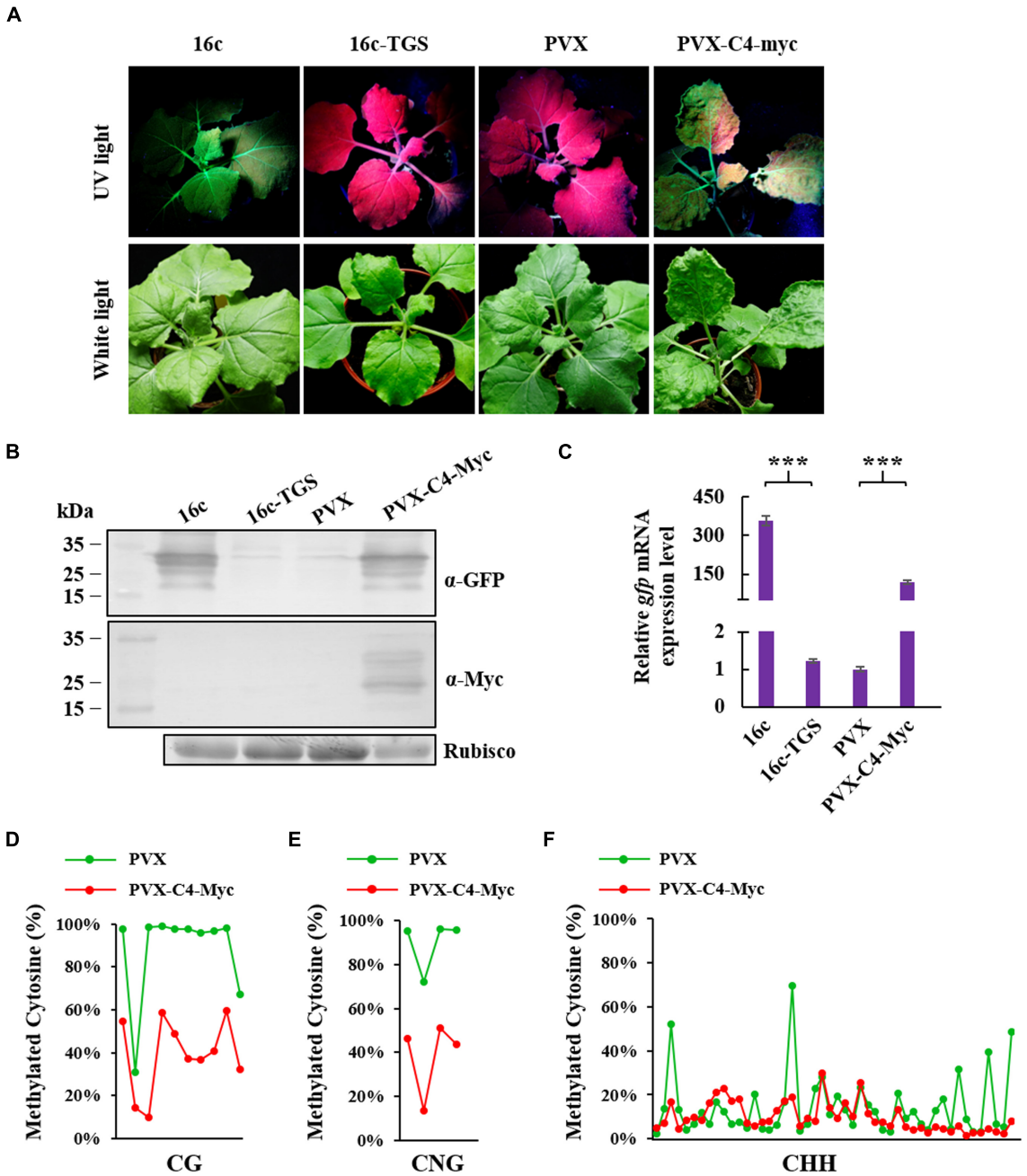

FIGURE 6 | Suppression of ToLCGdV C4 in TGS. **(A)** PVX-based expression of C4 suppressed TGS. *Agrobacterium* strains containing sGFP and p19, sGFP and EV, or sGFP and C4-Myc were co-infiltrated into 16c-TGS *N. benthamiana* plants. At 12 dpi, the infiltrated plants were observed and photographed under UV light and white light. **(B)** Western blot assays to detect the expressions of GFP and C4 in infiltrated plants. Samples were taken at 12 dpi and subjected to western blot with anti-GFP and anti-Myc antibody, respectively. Rubisco was used as a loading control. Numbers on the left indicate molecular weight. **(C)** Real-time RT-PCR detection of GFP mRNA accumulation in infiltrated 16c-TGS plants. Samples were taken at 12 dpi and 2 μg RNA was used to perform detection. ***$p < 0.001$ (extremely significant). Cytosine methylation level of CG sites **(D)**, CNG sites **(E)**, and CHH sites **(F)** in 35S promoter region. Cytosine methylation level was measured by next generation sequencing-based bisulfite sequencing PCR (BSP). Green dots represent the cytosine residues of 35S promoter in 16c-TGS plants infiltrated with PVX, and red dots represents the cytosine residues of 35S promoter in plants infiltrated with PVX-C4-Myc. The detailed methylation level of each CG, CNG, and CHH sites are listed in **Supplementary Table 2**.

plants were not as shortened as ToLCGdV-infected tomato plants (**Figure 3B**). Quantitative PCR also confirmed that loss of C4 significantly reduced viral accumulation (**Figure 3C**). These results implied that though ToLCGdV can still move systemically without C4 expression, C4 plays an important role in ToLCGdV symptom development.

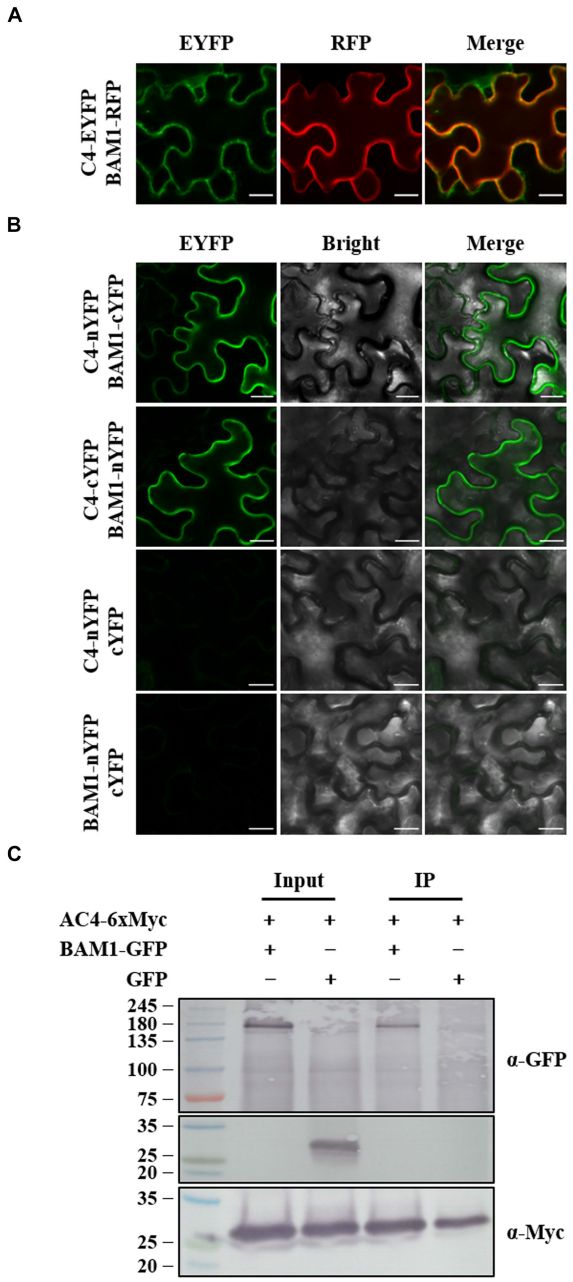

FIGURE 7 | Co-localization and interaction between C4 and BAM1. **(A)** Co-localization of C4 and BAM1. *Agrobacterium* strains harboring C4-EYFP and BAM1-RFP were co-infiltrated into *N. benthamiana* leaves. At 3 dpi, the infiltrated leaves were taken and observed under confocal microscope. Bars = 20 μm. **(B)** Interaction between C4 and BAM1 by BiFC. *Agrobacterium* strains harboring C4-nYFP and BAM1-cYFP, or C4-cYFP and BAM1-nYFP were co-infiltrated into *N. benthamiana* leaves and subjected to confocal microscopy observation at 3 dpi. C4-nYFP and cYFP, and BAM1-nYFP and cYFP were used as negative controls. Bars = 20 μm. **(C)** Co-IP assays to detect the interaction between C4 and BAM1. *Agrobacterium* strains containing AC4-6xMyc and BAM1-GFP, or AC4-6xMyc and GFP were co-infiltrated into *N. benthamiana* leaves. Samples were taken at 3 dpi to perform Co-IP assays. Western blot detections were conducted with anti-GFP and anti-Myc antibodies, respectively. Numbers on the left indicate molecular weight.

ToLCGdV C4 Could Enhance PVX Pathogenicity

To further substantiate the role of C4 in pathogenesis independent of ToLCGdV, C4 fused with Myc tag was cloned into the *Potato virus X* (PVX) vector pGR107 (Lu et al., 2003) to yield PVX-C4-Myc. Moreover, mC4-Myc with start codon mutation was also cloned into pGR107 to make PVX-mC4-Myc. *Agrobacterium* containing PVX-C4-Myc, PVX-mC4-Myc, or PVX was infiltrated into 5–6 leaf-stage *N. benthamiana*. Mild mosaic symptoms on the top leaves of *N. benthamiana* infected by PVX-C4-Myc were first observed at 5 dpi, while no obvious symptoms were observed on plants inoculated with PVX-mC4-Myc or PVX at this time (**Supplementary Figure 1**). At 10 dpi, severe mosaic and curling of the leaves were observed on plants infected by PVX-C4-Myc, while only mild mosaic was observed in plants infected by PVX-mC4-Myc or PVX (**Figure 4A**). At later time, symptoms on the newly emerged leaves of plants inoculated with PVX or PVX-mC4-Myc became very weak and hardly visible (**Supplementary Figure 1**). However, symptoms including mosaic, curling, and distortion caused by PVX-C4-Myc sustained throughout the life of the plants. Western blot experiments performed at 10 dpi with anti-PVX CP antibody and anti-Myc antibody confirmed that C4 could remarkably increase PVX accumulation (**Figures 4B,C**), further implying that C4 may be a pathogenic determinant independent of ToLCGdV infection.

ToLCGdV C4 Suppresses PTGS by Repressing Systemic Gene Silencing but Not Local Gene Silencing

AC4/C4 encoded by some begomoviruses have been reported to function as a VSR (Vanitharani et al., 2004; Bisaro, 2006; Gopal et al., 2007). To explore the function of ToLCGdV C4 in RNA silencing suppression, a widely adopted method based on *Agrobacterium* infiltration was utilized (Johansen, 2001). *Agrobacterium* strains harboring C4-Myc and the positive sense-GFP (sGFP) (Bragg and Jackson, 2004; Dong et al., 2016; Zhang et al., 2017, 2018) were mixed equally and co-infiltrated into *N. benthamiana* leaves. Co-infiltration of p19 and sGFP was used as positive control, while co-infiltration of empty vector (EV) and sGFP was used as negative control. Three days after agroinfiltration, strong GFP fluorescence was observed in regions co-infiltrated with sGFP and p19 (**Figure 5A**). However, no obvious or little fluorescence was observed in leaf patches co-infiltrated with sGFP and C4-Myc or sGFP and EV (**Figure 5A**). The results were the same at 6 dpi. Western blot detection confirmed that C4 had no effect on GFP protein accumulation compared with p19 and EV (**Figure 5B**).

Next, we tested whether C4 suppresses systemic movement of RNA silencing signals. C4-Myc, p19, or EV were mixed with sGFP and co-infiltrated into leaves of 16c transgenic *N. benthamiana* (Voinnet and Baulcombe, 1997). Three independent experiments were repeated to detect the systemic movement of GFP silencing signals. As expected, transient expression of p19, but not the EV, suppressed the movement of GFP silencing signals from infiltrated leaves to upper leaves

at 12 dpi (**Figure 5C**). C4 could also suppressed systemic movement of GFP silencing signals, though not as effective as p19 (**Figure 5C**).

In summary, these results demonstrate that C4 functions as a VSR by repressing systemic gene silencing but not local gene silencing.

ToLCGdV C4 Suppresses Methylation-Mediated TGS

To identify whether ToLCGdV C4 could suppress methylation-mediated TGS, 16c-TGS transgenic *N. benthamiana* plants were used. In 16c-TGS plants, GFP was silenced by TGS, and TGS was induced by *Tobacco rattle virus* (TRV) vector which contains a portion of the 35S promoter sequence (Buchmann et al., 2009; Raja et al., 2010). *Agrobacterium* harboring PVX-C4-Myc or PVX was infiltrated into 16c-TGS plants, and the plants were photographed under white light and UV lamp at 12 dpi. 16c-TGS plants infiltrated with PVX showed no visible GFP fluorescence, while plants infiltrated with PVX-C4-Myc showed obvious GFP fluorescence (**Figure 6A**). 16c and 16c-TGS *N. benthamiana* plants were used as positive and negative controls, respectively. Western blot and real-time RT-PCR confirmed that GFP protein and mRNA expressions were significantly increased in 16c-TGS plants infiltrated with PVX-C4-Myc compared with plants infiltrated with PVX (**Figures 6B,C**).

To further confirm the ability of C4 to reverse methylation-mediated TGS, next generation sequencing-based bisulfite sequencing PCR (BSP) was performed to assess the cytosine methylation level of 35S promoter. Cytosine methylation level of ten CG, four CNG, and forty-eight CHH sites in the 35S promoter region were analyzed. C4 expressed from the PVX vector reduced cytosine methylation remarkably at CG (48%), CNG (51%), and CHH (5%) sites (**Figures 6D–F** and **Supplementary Table 2**). These results indicated that ToLCGdV C4 is able to suppress methylation-mediated TGS.

C4 Colocalizes and Interacts With BAM1

Tomato yellow leaf curl virus C4 and MYMV AC4 have been reported to interact with BAM1 in PM and plasmodesmata (PD) to inhibit the intercellular spread of RNAi (Carluccio et al., 2018; Rosas-Diaz et al., 2018), the interaction between ToLCGdV C4 and BAM1 was also investigated. *Agrobacterium* strains containing C4-EYFP and BAM1-RFP were co-infiltrated into *N. benthamiana* leaves. C4 co-localizes with BAM1 both in PM and PD (**Figure 7A**). BiFC assays found that C4 interacts with BAM1 at PM (**Figure 7B**). Co-IP assays further confirmed the interaction between C4 and BAM1 (**Figure 7C**). These results imply that ToLCGdV C4 may adopt the same strategy as TYLCV C4 to suppress PTGS (Rosas-Diaz et al., 2018).

DISCUSSION

In this study, we report that ToLCGdV may be a recombinant begomovirus originated from some weed-infecting begomoviruses based on phylogenetic analyses of multiple AC4/C4 protein sequences. ToLCGdV C4 is closely related to the AC4 of *Euphorbia leaf curl virus* (EuLCuV), Asystasia begomovirus 2 (ABgV2), Allamanda leaf curl virus (AllLCV), and Pouzolzia mosaic Guangdong virus (PouMGDV). All these begomoviruses are firstly isolated from wild plant hosts (He et al., 2009; Tang et al., 2014; Wyant et al., 2015), demonstrating the frequent recombination between wild hosts and crops (Lefeuvre and Moriones, 2015; Garcia-Arenal and Zerbini, 2019). Recombination is a key process in the evolution of many viruses, especially for geminiviruses which contain a highly compacted genome (∼2.7 kb) (Garcia-Andres et al., 2007; Varsani et al., 2008; Martin et al., 2011). It has been highly speculated that recombination between different geminiviruses in even different hosts is one of the main reasons for the diversification of geminiviruses (Padidam et al., 1999; Briddon et al., 2010). One of the best studied examples is the recombination between TYLCD-associated begomoviruses. *Begomovirus* contains over 320 species and is one of the largest plant virus genera (Zerbini et al., 2017). Begomoviruses are transmitted by whitefly between wild hosts and crops (Perefarres et al., 2012; Rey et al., 2012), which increases the opportunities of mix infection and recombination (Lima et al., 2012). *Tomato leaf curl Yunnan virus* (TLCYnV), a begomovirus firstly isolated from *Malvastrum coromandelianum*, evolved from *Tomato yellow leaf curl China virus* (TYLCCNV) by recombination and is highly infectious to a range of host plants by acquiring a more virulent C4 (Xie et al., 2013). Moreover, a recombinant virus named tomato yellow leaf curl Malaga virus (TYLCMalV) is the recombination of *Tomato yellow leaf curl Sardinia virus* (TYLCSV) and TYLCV (Monci et al., 2002). TYLCMalV exhibits a novel pathogenic phenotype and has an enlarge host range, which contribute to the prevalence in the region where it was detected (Monci et al., 2002). Thus, we speculate that ToLCGdV may be a recombinant virus evolved from two or more wild plant hosts, acquiring more virulence and becoming prevalent in Guangdong province where ToLCGdV was isolated.

We also found that disruption of C4 delayed ToLCGdV symptom development in *N. benthamiana* and significantly reduced viral DNA accumulation in tomato plants. However, the detailed function of C4 during ToLCGdV infection remains unknown. C4 has long been demonstrated to be required for monopartite begomovirus infection (Stanley and Latham, 1992; Teng et al., 2010; Li et al., 2018). Recently, AC4 of EACMCV has been shown to be involved in virus infection, knockout mutation in AC4 ORF delayed virus symptom development and plants recovered from the mutant virus infection (Chen et al., 2019). In addition, AC4 of ACMV (Hipp et al., 2016) and of MYMV (Carluccio et al., 2018) were also required for virus infection.

Tomato leaf curl Guangdong virus C4 expressed from the PVX vector significantly increased PVX concentration, and induced leaf curling and severe mosaic in plants inoculated with PVX-C4-Myc compared with plants inoculated with PVX or PVX-mC4-Myc. This result implies that C4 may be a pathogenic determinant essential for abnormalities in infected plants. Induction of hyperplasia and tumorigenic growth in infected plant tissues by AC4/C4 has been extensively studied (Mills-Lujan et al., 2015). The nature of hyperplasia and tumorigenic growth is uncontrolled DNA replication and loss function of host cell

cycle regulators. AC4/C4 is considered to be the "oncogene" that manipulates the host cell cycle to stimulate DNA replication (Nikitin and Luftig, 2012). However, the mechanism about how AC4/C4 induces abnormalities in infected plants may be variable according to the diversity of AC4/C4. A recent study found that TLCYnV C4 interacts and relocates the glycogen synthase kinase 3 (GSK3)/SHAGGY like kinase, named NbSKη, from the nucleus to membrane. Relocalization of NbSKη affects the degradation of Cyclin D1.1, thereby inducing the cell division (Mei et al., 2018b). Another study found that *Beet severe curly top virus* (BSCTV) C4 induces the expression of a RING finger E3 ligase, RKP, which antagonizes with an inhibitor of cyclin-dependent kinase (CDK) to induce cell cycle (Cheng et al., 2013).

Tomato leaf curl Guangdong virus C4 is a VSR which inhibits both TGS and PTGS. TGS and PTGS are the main pathways exploited by plants to counter virus infection by inducing viral genome methylation or sequence-specific mRNA degradation. TGS acts as defenses against DNA viruses, however, geminiviruses have evolved to encode proteins to interfere with these processes. VSR encoded by begomovirus is often able to suppress DNA methylation-mediated TGS, like βC1 of Tomato yellow leaf curl China virus betasatellite (TYLCCNB) (Yang et al., 2011), C4 of CLCuMuV (Ismayil et al., 2018), and C4 of *Tomato leaf curl Yunnan virus* (Xie et al., 2013). TYLCCNB βC1 interacts and inhibits the activity of a key enzyme required for maintenance of the methyl cycle, S-adenosyl homocysteine hydrolase (SAHH) (Yang et al., 2011).

Tomato leaf curl Guangdong virus C4 inhibits systemic gene silencing but not local gene silencing, this is also the case for TYLCV C4 (Luna et al., 2012). AC4/C4 of TYLCV or MYMV has been found to suppress intercellular spread of RNAi by interacting with BAM1 (Rosas-Diaz et al., 2018). We found that ToLCGdV C4 also colocalizes and interacts with BAM1. However, AC4/C4 encoded by TYLCV, MYMV, and ToLCGdV shares low amino acids identity (**Supplementary Figure 2**), implying that different begomoviruses may adopt the same strategy to suppress PTGS.

DATA AVAILABILITY STATEMENT

All datasets generated for this study are included in the article/**Supplementary Material**.

AUTHOR CONTRIBUTIONS

ZL, ZD, and ZH conceived and designed the experiments. ZL, ZD, YT, and LY conducted the experiments. XS, XW, GL, and YZ analyzed the data. ZL and ZD wrote the manuscript. All authors read and approved the manuscript.

FUNDING

This work was supported by grants from the National Natural Science Foundation of China (31871937 and 31801712), the Key Research and Development Program of Guangdong Province (2018B020202006), the National Key Research and Development Program of China (2018YFD0201209), and Special Fund for Scientific Innovation Strategy-Construction of High-Level Academy of Agriculture Science (R2017YJ-YB3004, R2019PY-QF003, and R2018QD-058).

ACKNOWLEDGMENTS

We are grateful to RL-D (Chinese Academy of Sciences, Shanghai, China) who generously provided BAM1 related *agrobacterium* strains. We would also thank Dr. Yule Liu (Tsinghua University, Beijing, China) for his kind help in the generation of 16c-TGS *N. benthamiana* plants.

SUPPLEMENTARY MATERIAL

The Supplementary Material for this article can be found online at: https://www.frontiersin.org/articles/10.3389/fmicb.2020.00851/full#supplementary-material

FIGURE S1 | Symptoms of *N. benthamiana* infected by PVX-C4-myc, PVX-mC4-myc, and PVX at different times.

FIGURE S2 | Amino acids alignment of AC4/C4 of ToLCGdV, TYLCV, and MYMV.

TABLE S1 | Primers used in this study.

TABLE S2 | Cytosine methylation level of each CG, CNG, and CHH site.

REFERENCES

Bi, H., Fan, W., and Zhang, P. (2017). C4 protein of Sweet potato leaf curl virus regulates brassinosteroid signaling pathway through interaction with ATBIN2 and affects male fertility in *Arabidopsis*. *Front. Plant Sci.* 8:1689. doi: 10.3389/fpls.2017.01689

Bisaro, D. M. (2006). Silencing suppression by geminivirus proteins. *Virology* 344, 158–168. doi: 10.1016/j.virol.2005.09.041

Boulton, M. I. (2003). Geminiviruses: major threats to world agriculture. *Ann. Appl. Biol.* 142, 143–143. doi: 10.1111/j.1744-7348.2003.tb00239.x

Bragg, J. N., and Jackson, A. O. (2004). The C-terminal region of the Barley stripe mosaic virus γb protein participates in homologous interactions and is required for suppression of RNA silencing. *Mol. Plant Pathol.* 5, 465–481. doi: 10.1111/j.1364-3703.2004.00246.x

Briddon, R. W., Patil, B. L., Bagewadi, B., Nawaz-ul-Rehman, M. S., and Fauquet, C. M. (2010). Distinct evolutionary histories of the DNA-A and DNA-B components of bipartite begomoviruses. *BMC Evol. Biol.* 10:97. doi: 10.1186/1471-2148-10-97

Buchmann, R. C., Asad, S., Wolf, J. N., Mohannath, G., and Bisaro, D. M. (2009). Geminivirus AL2 and L2 proteins suppress transcriptional gene silencing and cause genome-wide reductions in cytosine methylation. *J. Virol.* 83, 5005–5013. doi: 10.1128/JVI.01771-1778

Carluccio, A. V., Prigigallo, M. I., Rosas-Diaz, T., Lozano-Duran, R., and Stavolone, L. (2018). S-acylation mediates Mungbean yellow mosaic virus AC4 localization to the plasma membrane and in turns gene silencing suppression. *PLoS Pathog.* 14:e1007207. doi: 10.1371/journal.ppat.1007207

Chellappan, P., Vanitharani, R., and Fauquet, C. M. (2005). MicroRNA-binding viral protein interferes with Arabidopsis development. *Proc. Natl. Acad. Sci. U.S.A.* 102, 10381–10386. doi: 10.1073/pnas.0504439102

Chellappan, P., Vanitharani, R., Pita, J., and Fauquet, C. M. (2004). Short interfering RNA accumulation correlates with host recovery in DNA virus-infected hosts, and gene silencing targets specific viral sequences. *J. Virol.* 78, 7465–7477. doi: 10.1128/JVI.78.14.7465-7477.2004

Chen, K., Khatabi, B., and Fondong, V. N. (2019). The AC4 protein of a cassava geminivirus is required for virus infection. *Mol. Plant Microbe Interact.* 32, 865–875. doi: 10.1094/MPMI-12-18-0354-R

Cheng, Y., Cao, L., Wang, S., Li, Y., Shi, X., Liu, H., et al. (2013). Downregulation of multiple CDK inhibitor ICK/KRP genes upregulates the E2F pathway and increases cell proliferation, and organ and seed sizes in *Arabidopsis*. *Plant J.* 75, 642–655. doi: 10.1111/tpj.12228

Deom, C. M., and Mills-Lujan, K. (2015). Toward understanding the molecular mechanism of a geminivirus C4 protein. *Plant Signal. Behav.* 10, e1109758. doi: 10.1080/15592324.2015.1109758

Dong, K., Wang, Y., Zhang, Z., Chai, L.-X., Tong, X., Xu, J., et al. (2016). Two amino acids near the N-terminus of Cucumber mosaic virus 2b play critical roles in the suppression of RNA silencing and viral infectivity. *Mol. Plant Pathol.* 17, 173–183. doi: 10.1111/mpp.12270

Doyle, J., and Doyle, J. (1987). Genomic plant DNA preparation from fresh tissue-CTAB method. *Phytochem Bull.* 19, 11–15.

Fan, H., Sun, H., Wang, Y., Zhang, Y., Wang, X., Li, D., et al. (2014). Deep sequencing–based transcriptome profiling reveals comprehensive insights into the responses of *Nicotiana benthamiana* to Beet necrotic yellow vein virus infections containing or lacking RNA4. *PLoS One* 9:e85284. doi: 10.1371/journal.pone.0085284

Fauquet, C. M., Briddon, R. W., Brown, J. K., Moriones, E., Stanley, J., Zerbini, M., et al. (2008). Geminivirus strain demarcation and nomenclature. *Arch. Virol.* 153, 783–821. doi: 10.1007/s00705-008-0037-36

Fondong, V. N. (2013). Geminivirus protein structure and function. *Mol. Plant Pathol.* 14, 635–649. doi: 10.1111/mpp.12032

Fondong, V. N., Reddy, R. V., Lu, C., Hankoua, B., Felton, C., Czymmek, K., et al. (2007). The consensus N-myristoylation motif of a geminivirus AC4 protein is required for membrane binding and pathogenicity. *Mol. Plant Microbe Interact.* 20, 380–391. doi: 10.1094/MPMI-20-4-0380

Gao, F., Liang, H., Lu, H., Wang, J., Xia, M., Yuan, Z., et al. (2015). Global analysis of DNA methylation in hepatocellular carcinoma by a liquid hybridization capture-based bisulfite sequencing approach. *Clin. Epigenet.* 7:86. doi: 10.1186/s13148-015-0121-121

Gao, F., Zhang, J., Jiang, P., Gong, D., Wang, J. W., Xia, Y., et al. (2014). Marked methylation changes in intestinal genes during the perinatal period of preterm neonates. *BMC Genomics* 15:716. doi: 10.1186/1471-2164-15-716

Garcia-Andres, S., Accotto, G. P., Navas-Castillo, J., and Moriones, E. (2007). Founder effect, plant host, and recombination shape the emergent population of begomoviruses that cause the tomato yellow leaf curl disease in the Mediterranean basin. *Virology* 359, 302–312. doi: 10.1016/j.virol.2006.09.030

Garcia-Arenal, F., and Zerbini, F. M. (2019). Life on the edge: geminiviruses at the interface between crops and wild plant hosts. *Annu Rev Virol.* 6, 411–433. doi: 10.1146/annurev-virology-092818-15536

Goodin, M. M., Dietzgen, R. G., Schichnes, D., Ruzin, S., and Jackson, A. O. (2002). pGD vectors: versatile tools for the expression of green and red fluorescent protein fusions in agroinfiltrated plant leaves. *Plant J.* 31, 375–383. doi: 10.1046/j.1365-313X.2002.01360.x

Gopal, P., Pravin Kumar, P., Sinilal, B., Jose, J., Kasin Yadunandam, A., and Usha, R. (2007). Differential roles of C4 and βC1 in mediating suppression of post-transcriptional gene silencing: evidence for transactivation by the C2 of Bhendi yellow vein mosaic virus, a monopartite begomovirus. *Virus Res.* 123, 9–18. doi: 10.1016/j.virusres.2006.07.014

Hamilton, A., Voinnet, O., Chappell, L., and Baulcombe, D. (2002). Two classes of short interfering RNA in RNA silencing. *EMBO J.* 21, 4671–4679.

Hanley-Bowdoin, L., Settlage, S. B., Orozco, B. M., Nagar, S., and Robertson, D. (1999). Geminiviruses: models for plant DNA replication, transcription, and cell cycle regulation. *Crit. Rev. Plant Sci.* 18, 71–106. doi: 10.1080/07352689991309162

He, Z. F., Mao, M. J., Yu, H., Li, H. P., and Chen, X. (2009). Molecular characterization of a distinct begomovirus infecting Allamanda cathartica in Guangdong. China. *Arch. Virol.* 154, 1199–1202. doi: 10.1007/s00705-009-0445-442

He, Z. F., Yu, H., and Luo, F. F. (2005). Molecular characteristics of DNA A of Tomato leaf curl Guangdong virus isolate G2. *Wei Sheng Wu Xue Bao.* 45, 48–52.

Hellens, R. P., Edwards, E. A., Leyland, N. R., Bean, S., and Mullineaux, P. M. (2000). pGreen: a versatile and flexible binary Ti vector for Agrobacterium-mediated plant transformation. *Plant Mol. Biol.* 42, 819–832. doi: 10.1023/A:1006496308160

Hipp, K., Rau, P., Schafer, B., Pfannstiel, J., and Jeske, H. (2016). Translation, modification and cellular distribution of two AC4 variants of African cassava mosaic virus in yeast and their pathogenic potential in plants. *Virology* 498, 136–148. doi: 10.1016/j.virol.2016.07.011

Hu, Y., Li, Z., Yuan, C., Jin, X., Yan, L., Zhao, X., et al. (2015). Phosphorylation of TGB1 by protein kinase CK2 promotes Barley stripe mosaic virus movement in monocots and dicots. *J. Exp. Bot.* 66, 4733–4747. doi: 10.1093/jxb/erv237

Ismayil, A., Haxim, Y., Wang, Y., Li, H., Qian, L., Han, T., et al. (2018). Cotton Leaf Curl Multan virus C4 protein suppresses both transcriptional and post-transcriptional gene silencing by interacting with SAM synthetase. *PLoS Pathog.* 14:e1007282. doi: 10.1371/journal.ppat.1007282

Johansen, L. K. (2001). Silencing on the spot. Induction and suppression of RNA silencing in the Agrobacterium-mediated transient expression system. *Plant Physiol.* 126, 930–938. doi: 10.1104/pp.126.3.930

John, S., Margaret, I. B., and Davies, J. W. (2001). "Geminiviridae," in *eLS*, eds Wiley Online Library (Hoboken, NJ: John Wiley & Sons, Ltd).

Kumar, S., Stecher, G., and Tamura, K. (2016). MEGA7: molecular evolutionary genetics analysis version 7.0 for bigger datasets. *Mol. Biol. Evol.* 33, 1870–1874. doi: 10.1093/molbev/msw054

Latham, J. R., Saunders, K., Pinner, M. S., and Stanley, J. (1997). Induction of plant cell division by Beet curly top virus gene C4. *Plant J.* 11, 1273–1283. doi: 10.1046/j.1365-313X.1997.11061273.x

Lefeuvre, P., and Moriones, E. (2015). Recombination as a motor of host switches and virus emergence: geminiviruses as case studies. *Curr. Opin. Virol.* 10, 14–19. doi: 10.1016/j.coviro.2014.12.005

Li, H., Zeng, R., Chen, Z., Liu, X., Cao, Z., Xie, Q., et al. (2018). S-acylation of a geminivirus C4 protein is essential for regulating the CLAVATA pathway in symptom determination. *J. Exp. Bot.* 69, 4459–4468. doi: 10.1093/jxb/ery228

Li, Y., Zhu, J., Tian, G., Li, N., Li, Q., Ye, M., et al. (2010). The DNA methylome of human peripheral blood mononuclear cells. *PLoS Biol.* 8:e1000533. doi: 10.1371/journal.pbio.1000533

Lima, A. T. M., Sobrinho, R. R., Gonzalez-Aguilera, J., Rocha, C. S., Silva, S. J. C., Xavier, C. A. D., et al. (2012). Synonymous site variation due to recombination explains higher genetic variability in begomovirus populations infecting non-cultivated hosts. *J. Gen. Virol.* 94(Pt 2), 418–431. doi: 10.1099/vir.0.047241-47240

Lu, R., Malcuit, I., Moffett, P., Ruiz, M. T., Peart, J., Wu, A. J., et al. (2003). High throughput virus-induced gene silencing implicates heat shock protein 90 in plant disease resistance. *EMBO J.* 22, 5690–5699. doi: 10.1093/emboj/cdg546

Luna, A. P., Morilla, G., Voinnet, O., and Bejarano, E. R. (2012). Functional analysis of gene-silencing suppressors from tomato yellow leaf curl disease viruses. *Mol. Plant Microbe Interact.* 25, 1294–1306. doi: 10.1094/MPMI-04-12-0094-R

Ma, X. Y., Cai, J. H., Li, G. X., Qin, B. X., and Zhou, X. P. (2004). Molecular characterization of a distinct begomovirus infecting Euphorbia pulcherrima in China. *J. Phytopathol.* 152, 215–218. doi: 10.1111/j.1439-0434.2004.00832.x

Mansoor, S., Zafar, Y., and Briddon, R. W. (2006). Geminivirus disease complexes: the threat is spreading. *Trends Plant Sci.* 11, 209–212. doi: 10.1016/j.tplants.2006.03.003

Martin, D. P., Biagini, P., Lefeuvre, P., Golden, M., Roumagnac, P., and Varsani, A. (2011). Recombination in eukaryotic single stranded DNA viruses. *Viruses* 3, 1699–1738. doi: 10.3390/v3091699

Mei, Y., Wang, Y., Hu, T., Yang, X., Lozano-Duran, R., Sunter, G., et al. (2018a). Nucleocytoplasmic shuttling of geminivirus C4 protein mediated by phosphorylation and myristoylation is critical for viral pathogenicity. *Mol Plant* 11, 1466–1481. doi: 10.1016/j.molp.2018.10.004

Mei, Y., Yang, X., Huang, C., Zhang, X., and Zhou, X. (2018b). Tomato leaf curl Yunnan virus-encoded C4 induces cell division through enhancing stability of Cyclin D 1.1 via impairing NbSKη-mediated phosphorylation in *Nicotiana benthamiana*. *PLoS Pathog.* 14:e1006789. doi: 10.1371/journal.ppat.1006789

Mills-Lujan, K., Andrews, D. L., Chou, C. W., and Deom, C. M. (2015). The roles of phosphorylation and SHAGGY-like protein kinases in geminivirus C4

protein induced hyperplasia. *PLoS One* 10:e0122356. doi: 10.1371/journal.pone.0122356

Mills-Lujan, K., and Deom, C. M. (2010). Geminivirus C4 protein alters *Arabidopsis* development. *Protoplasma* 239, 95–110. doi: 10.1007/s00709-009-0086-z

Monci, F., Sánchez-Campos, S., Navas-Castillo, J., and Moriones, E. (2002). A natural recombinant between the geminiviruses Tomato yellow leaf curl *Sardinia* virus and Tomato yellow leaf curl virus exhibits a novel pathogenic phenotype and is becoming prevalent in Spanish populations. *Virology* 303, 317–326. doi: 10.1006/viro.2002.1633

Navas-Castillo, J., Fiallo-Olive, E., and Sanchez-Campos, S. (2011). Emerging virus diseases transmitted by whiteflies. *Annu. Rev. Phytopathol.* 49, 219–248. doi: 10.1146/annurev-phyto-072910-095235

Nikitin, P. A., and Luftig, M. A. (2012). The DNA damage response in viral-induced cellular transformation. *Br. J. Cancer* 106, 429–435. doi: 10.1038/bjc.2011.612

Padidam, M., Sawyer, S., and Fauquet, C. M. (1999). Possible emergence of new geminiviruses by frequent recombination. *Virology* 265, 218–225. doi: 10.1006/viro.1999.0056

Pan, X., Gong, D., Nguyen, D. N., Zhang, X., Hu, Q., Lu, H., et al. (2018). Early microbial colonization affects DNA methylation of genes related to intestinal immunity and metabolism in preterm pigs. *DNA Res.* 25, 287–296. doi: 10.1093/dnares/dsy001

Perefarres, F., Thierry, M., Becker, N., Lefeuvre, P., Reynaud, B., Delatte, H., et al. (2012). Biological invasions of geminiviruses: case study of TYLCV and Bemisia tabaci in Reunion Island. *Viruses* 4, 3665–3688. doi: 10.3390/v4123665

Piroux, N., Saunders, K., Page, A., and Stanley, J. (2007). Geminivirus pathogenicity protein C4 interacts with Arabidopsis thaliana shaggy-related protein kinase AtSKη, a component of the brassinosteroid signalling pathway. *Virology* 362, 428–440. doi: 10.1016/j.virol.2006.12.034

Raja, P., Wolf, J. N., and Bisaro, D. M. (2010). RNA silencing directed against geminiviruses: post-transcriptional and epigenetic components. *Biochim. Biophys. Acta* 1799, 337–351. doi: 10.1016/j.bbagrm.2010.01.004

Rey, M. E. C., Ndunguru, J., Berrie, L. C., Paximadis, M., Berry, S., Cossa, N., et al. (2012). Diversity of dicotyledenous-infecting geminiviruses and their associated DNA molecules in Southern Africa, including the south-west Indian ocean islands. *Viruses* 4, 1753–1791. doi: 10.3390/v4091753

Rojas, M. R., Hagen, C., Lucas, W. J., and Gilbertson, R. L. (2005). Exploiting chinks in the plant's armor: evolution and emergence of geminiviruses. *Annu. Rev. Phytopathol.* 43, 361–394. doi: 10.1146/annurev.phyto.43.040204.135939

Rosas-Diaz, T., Zhang, D., Fan, P., Wang, L., Ding, X., Jiang, Y., et al. (2018). A virus-targeted plant receptor-like kinase promotes cell-to-cell spread of RNAi. *Proc. Natl. Acad. Sci. U.S.A.* 115, 1388–1393. doi: 10.1073/pnas.1715556115

Rubio, V., Shen, Y., Saijo, Y., Liu, Y., Gusmaroli, G., Dinesh-Kumar, S. P., et al. (2005). An alternative tandem affinity purification strategy applied to Arabidopsis protein complex isolation. *Plant J.* 41, 767–778. doi: 10.1111/j.1365-313X.2004.02328.x

Sattar, M. N., Kvarnheden, A., Saeed, M., and Briddon, R. W. (2013). Cotton leaf curl disease - an emerging threat to cotton production worldwide. *J. Gen. Virol.* 94(Pt 4), 695–710. doi: 10.1099/vir.0.049627-49620

Stanley, J., and Latham, J. R. (1992). A symptom variant of beet curly top geminivirus produced by mutation of open reading frame C4. *Virology* 190, 506–509. doi: 10.1016/0042-6822(92)91243-n

Tang, Y. F., Du, Z. G., He, Z. F., Brown, J. K., and She, X. M. (2014). Identification and molecular characterization of two begomoviruses from *Pouzolzia zeylanica* (L.) Benn. exhibiting yellow mosaic symptoms in adjacent regions of China and Vietnam. *Arch. Virol.* 159, 2799–2803. doi: 10.1007/s00705-014-2049-2048

Teng, K., Chen, H., Lai, J., Zhang, Z., Fang, Y., Xia, R., et al. (2010). Involvement of C4 protein of Beet severe curly top virus (family Geminiviridae) in virus movement. *PLoS One* 5:e11280. doi: 10.1371/journal.pone.0011280

Vanitharani, R., Chellappan, P., Pita, J. S., and Fauquet, C. M. (2004). Differential roles of AC2 and AC4 of cassava geminiviruses in mediating synergism and suppression of posttranscriptional gene silencing. *J. Virol.* 78, 9487–9498. doi: 10.1128/JVI.78.17.9487-9498.2004

Varma, A., and Malathi, V. G. (2003). Emerging geminivirus problems: a serious threat to crop production. *Ann. Appl. Biol.* 142, 145–164. doi: 10.1111/j.1744-7348.2003.tb00240.x

Varsani, A., Shepherd, D. N., Monjane, A. L., Owor, B. E., Erdmann, J. B., Rybicki, E. P., et al. (2008). Recombination, decreased host specificity and increased mobility may have driven the emergence of maize streak virus as an agricultural pathogen. *J. Gen. Virol.* 89(Pt 9), 2063–2074. doi: 10.1099/vir.0.2008/003590-3590

Voinnet, O., and Baulcombe, D. C. (1997). Systemic signalling in gene silencing. *Nature* 389, 553–555. doi: 10.1038/39215

Walter, M., Chaban, C., Schutze, K., Batistic, O., Weckermann, K., Nake, C., et al. (2004). Visualization of protein interactions in living plant cells using bimolecular fluorescence complementation. *Plant J.* 40, 428–438. doi: 10.1111/j.1365-313X.2004.02219.x

Wyant, P., Strohmeier, S., Fischer, A., Schafer, B., Briddon, R. W., Krenz, B., et al. (2015). Light-dependent segregation of begomoviruses in *Asystasia gangetica* leaves. *Virus Res.* 195, 225–235. doi: 10.1016/j.virusres.2014.10.024

Xie, Y., Zhao, L., Jiao, X., Jiang, T., Gong, H., Wang, B., et al. (2013). A recombinant begomovirus resulting from exchange of the C4 gene. *J. Gen. Virol.* 94(Pt 8), 1896–1907. doi: 10.1099/vir.0.053181-53180

Yang, X., Guo, W., Li, F., Sunter, G., and Zhou, X. (2019). Geminivirus-associated betasatellites: exploiting chinks in the antiviral arsenal of plants. *Trends Plant Sci.* 24, 519–529. doi: 10.1016/j.tplants.2019.03.010

Yang, X., Xie, Y., Raja, P., Li, S., Wolf, J. N., Shen, Q., et al. (2011). Suppression of methylation-mediated transcriptional gene silencing by βC1-SAHH protein interaction during geminivirus-betasatellite infection. *PLoS Pathog.* 7:e1002329. doi: 10.1371/journal.ppat.1002329

Zerbini, F. M., Briddon, R. W., Idris, A., Martin, D. P., Moriones, E., Navas-Castillo, J., et al. (2017). ICTV virus taxonomy profile: geminiviridae. *J. Gen. Virol.* 98, 131–133. doi: 10.1099/jgv.0.000738

Zhang, K., Zhang, Y., Yang, M., Liu, S., Li, Z., Wang, X., et al. (2017). The Barley stripe mosaic virus γb protein promotes chloroplast-targeted replication by enhancing unwinding of RNA duplexes. *PLoS Pathog.* 13:e1006319. doi: 10.1371/journal.ppat.1006319

Zhang, X., Dong, K., Xu, K., Zhang, K., Jin, X., Yang, M., et al. (2018). Barley stripe mosaic virus infection requires PKA-mediated phosphorylation of γb for suppression of both RNA silencing and the host cell death response. *New Phytol.* 218, 1570–1585. doi: 10.1111/nph.15065

Zhou, X. (2013). Advances in understanding begomovirus satellites. *Annu. Rev. Phytopathol.* 51, 357–381. doi: 10.1146/annurev-phyto-082712-102234

Conflict of Interest: The authors declare that the research was conducted in the absence of any commercial or financial relationships that could be construed as a potential conflict of interest.

frontiers in Plant Science

REVIEW
published: 19 May 2020
doi: 10.3389/fpls.2020.00591

Manipulation of the Plant Host by the Geminivirus AC2/C2 Protein, a Central Player in the Infection Cycle

Jennifer Guerrero[1], Elizabeth Regedanz[2], Liu Lu[3†], Jianhua Ruan[4†], David M. Bisaro[2†] and Garry Sunter[1†]*

[1] Department of Biology, South Texas Center for Emerging Infectious Diseases, University of Texas at San Antonio, San Antonio, TX, United States, [2] Department of Molecular Genetics, Center for Applied Plant Sciences, Center for RNA Biology, Infectious Diseases Institute, The Ohio State University, Columbus, OH, United States, [3] Department of Computer Science, North Dakota State University, Fargo, ND, United States, [4] Department of Computer Science, University of Texas at San Antonio, San Antonio, TX, United States

OPEN ACCESS

Edited by:
Jose Trinidad Ascencio-Ibáñez, North Carolina State University, United States

Reviewed by:
Ramón Gerardo Guevara-Gonzalez, Universidad Autónoma de Querétaro, Mexico
Wei Shen, North Carolina State University, United States

***Correspondence:**
Garry Sunter
garry.sunter@utsa.edu

†ORCID:
Liu Lu
orcid.org/0000-0003-0218-2242
Jianhua Ruan
orcid.org/0000-0002-5622-3137
David M. Bisaro
orcid.org/0000-0002-6765-0548
Garry Sunter
orcid.org/0000-0001-9845-8746

Specialty section:
This article was submitted to Virology, a section of the journal Frontiers in Plant Science

Received: *29 February 2020*
Accepted: *20 April 2020*
Published: *19 May 2020*

Citation:
Guerrero J, Regedanz E, Lu L, Ruan J, Bisaro DM and Sunter G (2020) Manipulation of the Plant Host by the Geminivirus AC2/C2 Protein, a Central Player in the Infection Cycle. Front. Plant Sci. 11:591. doi: 10.3389/fpls.2020.00591

Geminiviruses are a significant group of emergent plant DNA viruses causing devastating diseases in food crops worldwide, including the Southern United States, Central America and the Caribbean. Crop failure due to geminivirus-related disease can be as high as 100%. Improved global transportation has enhanced the spread of geminiviruses and their vectors, supporting the emergence of new, more virulent recombinant strains. With limited coding capacity, geminiviruses encode multifunctional proteins, including the *AC2/C2* gene that plays a central role in the viral replication-cycle through suppression of host defenses and transcriptional regulation of the late viral genes. The AC2/C2 proteins encoded by mono- and bipartite geminiviruses and the curtovirus C2 can be considered virulence factors, and are known to interact with both basal and inducible systems. This review highlights the role of AC2/C2 in affecting the jasmonic acid and salicylic acid (JA and SA) pathways, the ubiquitin/proteasome system (UPS), and RNA silencing pathways. In addition to suppressing host defenses, AC2/C2 play a critical role in regulating expression of the coat protein during the viral life cycle. It is important that the timing of CP expression is regulated to ensure that ssDNA is converted to dsDNA early during an infection and is sequestered late in the infection. How AC2 interacts with host transcription factors to regulate CP expression is discussed along with how computational approaches can help identify critical host networks targeted by geminivirus AC2 proteins. Thus, the role of AC2/C2 in the viral life-cycle is to prevent the host from mounting an efficient defense response to geminivirus infection and to ensure maximal amplification and encapsidation of the viral genome.

Keywords: AC2/C2, pathogenicity factor, transcriptional activation, PTGS, TGS, antiviral defense response

INTRODUCTION

The *Geminiviridae* is a family of single-stranded DNA (ssDNA) viruses that infect agricultural crops in tropical and sub-tropical regions worldwide, and are responsible for billions of dollars in annual losses contributing to famine and loss of life (Legg and Fauquet, 2004; Scholthof et al., 2011). The International Committee on Taxonomy of Viruses (ICTV) currently recognizes nine

genera within the family, classified according to genome organization, genome-wide pairwise sequence identities, insect vector, and host range (Zerbini et al., 2017; Kumar, 2019). The genus *Begomovirus*, with ∼320 species, is by far the largest and its members are the most widely studied (Zerbini et al., 2017; Kumar, 2019). By contrast, the genus *Mastrevirus* consists of ∼30 species, with the remaining genera (*Becurtovirus*, *Capulavirus*, *Curtovirus*, *Eragrovirus*, *Grablovirus*, *Topocuvirus*, and *Turncurtovirus*) having 1–4 species each (Zerbini et al., 2017). Geminiviruses do not encode DNA or RNA polymerases and rely on host machinery to replicate their circular ssDNA genomes through double-stranded DNA (dsDNA) replicative forms (RFs). The RFs associate with host histone proteins to form non-integrating minichromosomes. Most geminiviruses have monopartite genomes except for the begomoviruses, which have either monopartite or bipartite genomes (designated DNA-A and DNA-B), both of which are required for infectivity. Individual genome components of bipartite begomoviruses are typically 2.5–3.0 kb in size and together can encode a total of eight proteins, while monopartite begomovirus genomes are ∼3.0 kb and encode six proteins. Curtovirus genomes, also ∼3.0 kb, are similar in organization to monopartite begomoviruses and encode seven proteins (**Figure 1**). Considerable genetic economy is evident, with genes encoded by both strands of the dsDNA RFs and overlapping genes in different reading frames. Two gene nomenclature systems are in use. One denotes genes and proteins as leftward (L) or rightward (R) relative to conventional genome maps. The other refers to genes as complementary (C) or viral (V) sense, with viral sense indicating the encapsidated strand. The latter system is used in this review. Most viral proteins are also named according to core function.

In all geminiviruses, virion and complementary sense genes are separated by an intergenic region (IR) ∼300 bp in size, a portion of which, called the Common Region (CR), is shared by DNA-A and DNA-B in bipartite begomoviruses. Transcription occurs bidirectionally from promoters within the IR, which also contains the origin of replication. In bipartite begomoviruses, the virion sense strand of DNA-A encodes the capsid protein (CP, also known AV1). In monopartite begomoviruses, the virion sense strand encodes CP/V1 that also acts as a movement factor, as well as an additional movement protein (MP/V2). In all begomoviruses, the complementary strand encodes the replication protein (Rep, AC1/C1), a transcriptional activator protein and pathogenicity factor (TrAP, AC2/C2), a replication enhancer protein (REn, AC3/C3), and AC4/C4, which also appears to function as a pathogenicity determinant. In some begomoviruses, including *African cassava mosaic virus* (ACMV), *Bean golden mosaic virus* (BGMV), *Potato yellow mosaic virus* (PYMV), and *Tomato golden mosaic virus* (TGMV), the *AC4* gene is not critical for virus infection (Elmer et al., 1988; Etessami et al., 1991; Sung and Coutts, 1995; Hoogstraten et al., 1996; Bull et al., 2007). DNA-B of bipartite begomoviruses codes for two proteins, a nuclear shuttle protein (NSP, BV1) in the virion sense, and a movement protein (MP, BC1) in the complementary sense (Stanley and Gay, 1983; Hamilton et al., 1984; Zerbini et al., 2017). In the similarly organized genomes of curtoviruses, the complementary sense strand also codes for Rep/C1, C2, REn/C3, and C4. Rep and REn are highly conserved between the two genera, and the REn proteins are functionally interchangeable (Hormuzdi and Bisaro, 1995). However, while begomovirus TrAP/AC2/C2 and curtovirus C2 share some pathogenicity functions, curtovirus C2 is not a transcriptional activator (Sunter et al., 1994; Baliji et al., 2007). The curtovirus virion sense strand codes for the capsid protein which also functions as a movement protein (CP/V1), a protein that regulates viral ssDNA versus dsDNA levels (V2), and a protein required for systemic spread (V3) (Hormuzdi and Bisaro, 1993, 1995; Baliji et al., 2004).

GEMINIVIRUS AC2/C2 PROTEIN AND THE VIRAL REPLICATION CYCLE

Geminiviruses exhibit a strategy that is common among DNA viruses, where gene expression is separated into early and late phases. Genes that are expressed early, meaning prior to DNA synthesis, typically encode proteins necessary for replication of the viral genome and/or to modulate the host cell environment. After viral DNA replication, the late genes encoding structural proteins needed to package DNA and form virions are expressed. DNA tumor viruses, including polyomaviruses such as SV40 and papilloma viruses, rely on cellular polymerases that are typically expressed during S-phase of the cell cycle. Thus, they have evolved mechanisms to subvert many of the cellular checkpoints that control cell cycle. Geminiviruses have also evolved to produce a protein, Rep, that interferes with cell cycle controls to drive infected cells from quiescence into S-phase in order to promote virus replication (for review see Hanley-Bowdoin et al., 2013). The viral proteins that interfere with cell cycle control, including geminivirus Rep protein, also autoregulate their own expression (Sunter et al., 1993; Eagle et al., 1994). As an example, when the large T-antigen of SV40 reaches a threshold concentration it binds to the early promoter, repressing initiation of transcription (Tjian, 1981). In many cases, products of the viral early genes are also required for expression of the late viral genes, and for suppression of host defenses. We suggest that AC2 protein of geminiviruses provides this critical function in the switch from the early phases of infection, namely transformation of cells to promote viral replication, to the late phases of infection involving virion production. The focus of this review is therefore on the AC2 protein of begomoviruses and the C2 protein of monopartite begomoviruses and curtoviruses, and highlights the central role that AC2 plays in the viral replication cycle through suppression of host defenses and transcriptional regulation of the late viral genes.

FEATURES OF THE AC2/C2 PROTEIN

The *Begomovirus* AC2 protein (also known as AL2 and Transcriptional Activator Protein; TrAP) is ∼15 kDa in size and is conserved among all Begomoviruses. Using the protein of TGMV as a representative, full-length AC2 comprises 129 amino acids with a basic N terminal region (amino acids 13 to 28), a

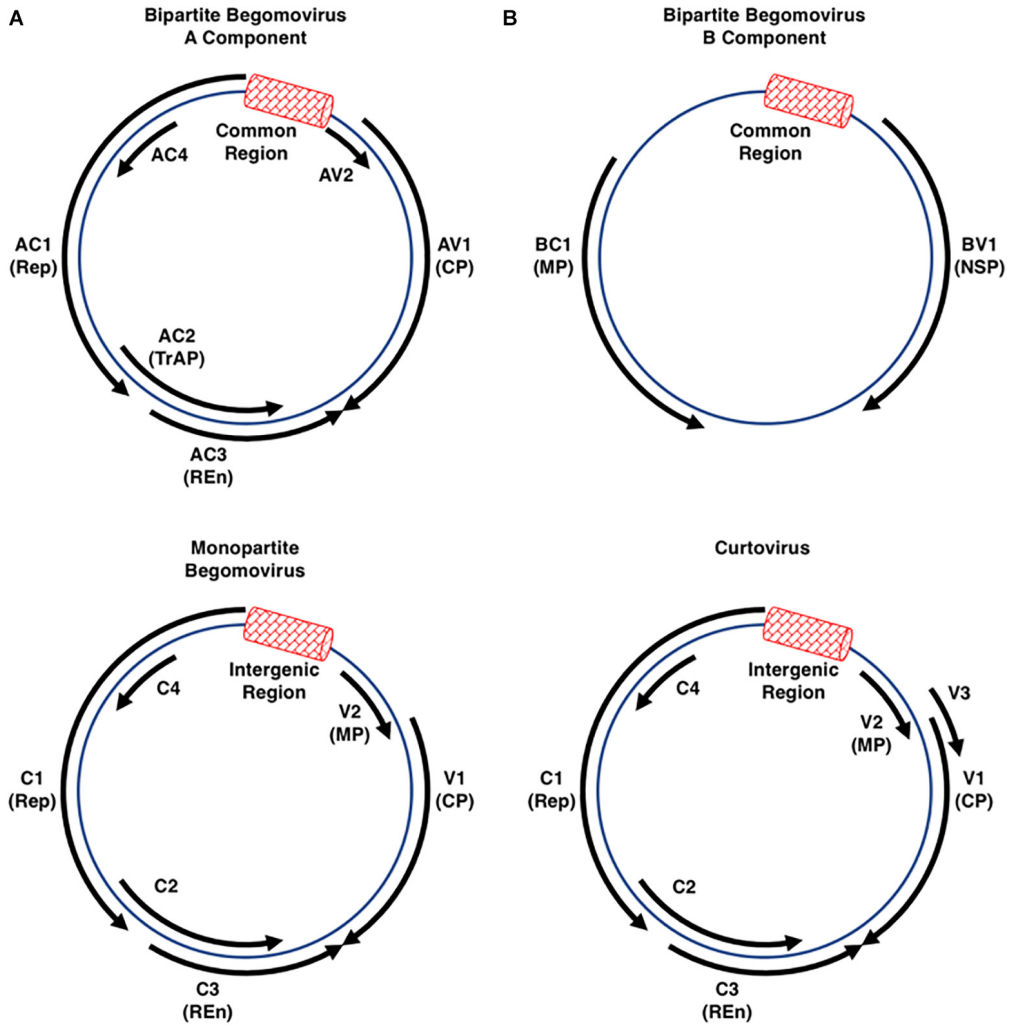

FIGURE 1 | Begomo- and Curtovirus Genome Organization. The circular diagrams represent the double-stranded replicative forms of geminiviruses belonging to the genera *Begomovirus* (mono- or bipartite genomes) and *Curtovirus* (monopartite genomes only). Each has an intergenic region (IR: red box) that contains the origin of rolling-circle replication flanked by divergent promoters that control expression of the virion and complementary sense transcription units. Viruses belonging to each of these genera (see **Table 1** for a list of viruses discussed in this review) encode between six and eight open reading frames (solid black arrows) capable of encoding proteins larger than 10 kDa. The coat protein (CP) forms the viral capsid that mediates vector transmission, and in monopartite viruses also functions as a movement protein. In the monopartite begomoviruses and curtoviruses, the AV2/V2 proteins inhibit gene silencing and also function as movement proteins (MP). The AC1/C1 protein (Replication initiator protein-Rep) is absolutely required for initiation of viral DNA replication, while the AC3/C3 replication enhancer protein (REn) stimulates replication. The AC2 protein in bipartite and monopartite begomoviruses is also called transcriptional activator protein (TrAP) due to its function in transcriptional activation of the CP and, in bipartite viruses, the BV1 gene. AC2 also interferes with transcriptional gene silencing (TGS) and post-transcriptional gene silencing (PTGS), functions it shares with the related C2 protein of the monopartite begomoviruses and curtoviruses. The AC4/C4 protein has been shown to function as a suppressor of PTGS in some, but not all viruses. In bipartite begomoviruses the movement proteins BV1 (Nuclear shuttle protein, NSP) and BC1 (MP) are encoded by DNA-B.

nuclear localization signal (NLS; amino acids 17 to 31), and a C terminal acidic region (amino acids 101 to 129) containing a transcriptional activation domain (TAD, amino acids 115 to 129) (Hartitz et al., 1999).

The central region of AC2 contains a series of conserved cysteine and histidine residues (amino acids 33 to 56) and a zinc finger-like domain (ZFD; amino acids 36 to 53) (**Figure 2**). AC2 has been shown to bind zinc and to be a target for phosphorylation (Hartitz et al., 1999; Wang et al., 2003). Cell localization experiments have shown that a phosphorylated form of AC2 can be detected in the nucleus and that non-phosphorylated AC2 can be found in both the nucleus and cytoplasm (Wang et al., 2003). Interestingly, AC2 is capable of self-interaction, with AC2:AC2 complexes found primarily in the nucleus (Yang et al., 2007). The ZFD is required but not sufficient for self-interaction. In contrast, AC2 interactions with cellular factors that condition antiviral defenses occur in both the nucleus and the cytoplasm (see below). Thus, AC2 localizes to sub-cellular compartments that correlate with known functions of the protein, which are to interact with plant nuclear and cytoplasmic proteins

TABLE 1 | Geminiviruses discussed in this review.

Bipartite begomovirus	Abbreviation	Monopartite begomovirus	Abbreviation	Curtovirus	Abbreviation
African cassava mosaic virus	ACMV	*Cotton leaf curl Kokhran virus*	CLCuKoV	*Beet curly top virus*	BCTV
Bean dwarf mosaic virus	BDMV	*Cotton leaf curl Multan virus*	CLCuMuV	*Beet curly top virus-SpCT*	BCTV-SpCT
Cabbage leaf curl virus	CaLCuV	*Papaya leaf curl virus*	PaLCuV	*Beet severe curly top virus*	BSCTV
Mungbean yellow mosaic virus-Vigna	MYMV	*Tomato yellow leaf curl China virus*	TYLCCNV		
Tomato golden mosaic virus	TGMV	*Tomato yellow leaf curl China betasatellite*	TYLCCNB		
Tomato leaf curl New Delhi virus	ToLCNDV	*Tomato leaf curl Java virus*	TLCJV		
		Tomato yellow leaf curl-Sardinia virus	TYLCSV		
		Tomato yellow leaf curl virus	TYLCV		

Geminiviruses mentioned in this review are listed according to genus and, in the case of begomoviruses, genome type (bipartite or monopartite).

to suppress host defenses, and to activate transcription (Hao et al., 2003; Wang et al., 2003).

The equivalent C2 protein encoded by curtoviruses (**Figure 2**), including *Beet curly top virus* (BCTV) and *Beet curly top virus*-SpCT (BCTV-SpCT), exhibits very little sequence similarity to the AC2 protein, apart from the central region containing the conserved cysteine and histidine residues within the zinc finger-like motif. The limited sequence and structural similarity correlate with the observation that the C2 protein in curtoviruses appears to lack the ability to activate transcription (Sunter et al., 1994). Prediction of protein structures for AC2 and C2 reveals regions of alpha helix with significant stretches of coiled and extended sheet (Combet et al., 2000), but no significant similarities to known 3D structures. The major similarity in predicted secondary structure between the AC2 protein of TGMV and the C2 protein of BCTV is apparent within the ZFD, which is the only significant stretch of amino acid similarity (**Figure 2**). It is likely that solving the 3D structures of AC2 and C2 would provide insight into the different functions assigned to these multifunctional viral proteins.

AC2/C2 AND SUPPRESSION OF PLANT DEFENSE RESPONSES

One of the two major roles identified to date for the AC2/C2 proteins of begomo- and curtoviruses is suppression of host immune responses. Some of the host defense systems that these proteins are known to interact with include both basal and inducible defenses. The latter include the jasmonic acid and salicylic acid (JA and SA) pathways, the ubiquitin/proteasome system (UPS), and RNA silencing pathways. The AC2/C2 proteins encoded by mono- and bipartite geminiviruses and curtovirus C2 have been recognized as pathogenicity determinants based on their capacity to cause damage in a host. Inactivating mutations in the *AC2* gene renders begomoviruses non-infectious due to loss of CP and BR1 expression (Elmer et al., 1988; Sunter et al., 1994), and curtovirus C2 mutants exhibit a recovery phenotype (Hormuzdi and Bisaro, 1995). This suggests that AC2/C2 can be considered virulence factors, based on the definition of a virulence factor as a microbial component that damages the host (Casadevall and Pirofski, 1999). In many cases, virulence factors are microbial effectors that allow the pathogen to inhibit and/or evade host immune responses. Based on the classical zigzag model for plant immunity (Jones and Dangl, 2006), the first line of defense is recognition of pathogen-associated molecular patterns (PAMP) by host pattern recognition receptors (PRRs), resulting in activation of PAMP-triggered immunity (PTI). In response, successful pathogens secrete effectors that act to suppress PTI responses, leading to effector-triggered susceptibility (ETS). As a second line of defense, plants have evolved cytoplasmic R proteins (nucleotide binding–leucine-rich repeat proteins, NB-LRR) that recognize the presence or activity of specific effectors, resulting in effector-triggered immunity (ETI) (Jones and Dangl, 2006). ETI typically leads to a hypersensitive response (HR) and systemic acquired resistance (SAR). More recently, it has been proposed that there is not really a clear distinction between PAMPs and effectors, or between PAMP receptors and resistance proteins (Thomma et al., 2011). This implies that PTI and ETI are not always distinct defense responses but both can be robust or weak, depending on the specific interaction. Therefore, activation of innate immunity in plants can be summed up by recognition of danger signals either directly derived from the microbe (PAMPs and effectors) or from damage or alteration of eukaryotic host structures (Thomma et al., 2011). This definition seems appropriate for geminivirus AC2/C2 proteins, which can be considered viral effectors essential for a productive infection that can also trigger HR in some cases. Currently, the available evidence suggests that the AC2/C2 proteins interact with several host immune pathways to evade host defense responses.

AC2 AND THE HYPERSENSITIVE RESPONSE

Effector-triggered immunity against a plant pathogen is a localized resistance reaction that typically involves a hypersensitive response (HR), characterized by localized cell death that often leads to arrest of the pathogen (Durrant and Dong, 2004). HR is a widespread response which can be induced by effector proteins produced by fungi, oomycetes, bacteria, viruses, and insects (Balint-Kurti, 2019). The response is characterized by a transient burst of reactive oxygen species, strengthening of plant cell walls, and accumulation of antimicrobial phytoalexins (Dangl et al., 1996). Plants exhibiting

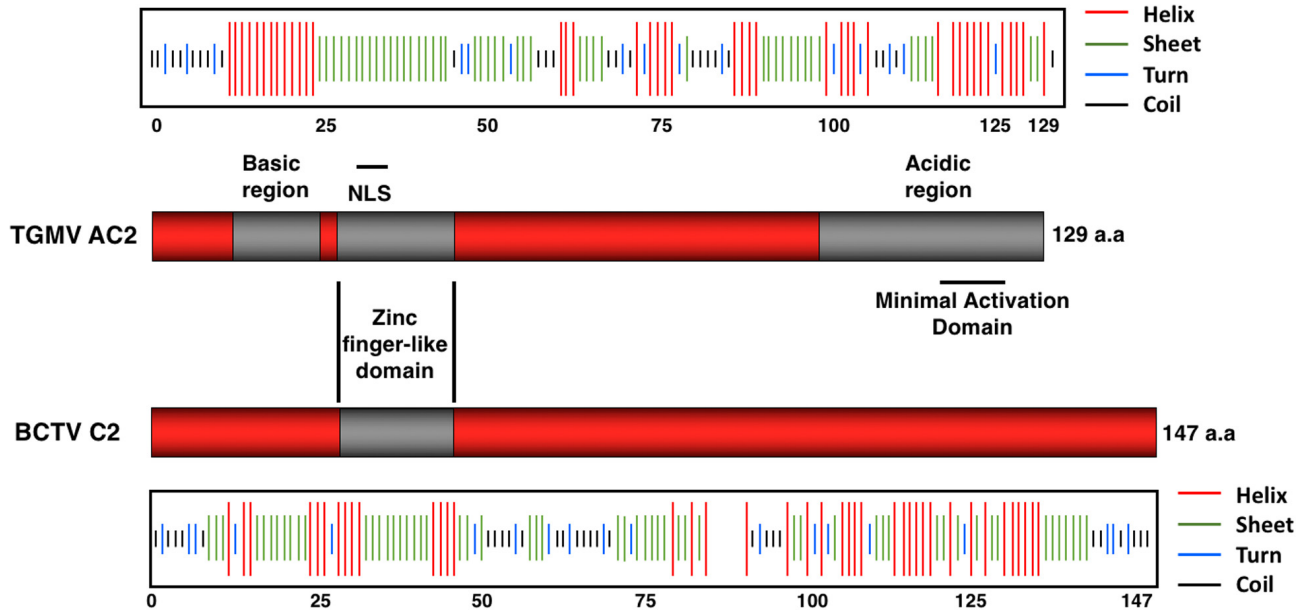

FIGURE 2 | Structural Features of the AC2 and C2 Proteins. The TGMV AC2 protein is 129 amino acids in length and contains three domains: an N-terminal basic region, a zinc-finger-like domain (ZFD) that contains a nuclear localization signal (NLS), and a C-terminal acidic region that contains a minimal transcriptional activation domain. The BCTV C2 protein is 147 amino acids in length and exhibits little similarity with TGMV AC2 other than the ZFD. Secondary structure predictions were obtained using the Network Protein Sequence @nalysis (NPS@). Stretches of amino acids capable of forming helices (red lines), sheets (green lines), turns (blue lines), and coils (black lines) are shown above (AC2) or below (C2) each protein.

HR can develop resistance to a secondary infection through spread of a mobile signal, salicylic acid (SA), to distal tissues, a phenomenon known as systemic acquired resistance (SAR) (Durrant and Dong, 2004). Both SA and its association with the accumulation of pathogenesis-related (PR) proteins are thought to be required for an effective SAR (Durrant and Dong, 2004).

A number of geminivirus proteins, including Rep, NSP, and V2 (Garrido-Ramirez et al., 2000; Amin et al., 2011), have been shown to induce a reaction typical of an HR response when over-expressed, indicating that these proteins could be pathogenicity determinants and a target of host immune defenses, triggering ETI. However, HR is not usually observed in plants infected with geminiviruses, suggesting that induction of an HR through recognition of some viral proteins is usually suppressed by other viral-encoded proteins (Mubin et al., 2010; Matic et al., 2016). For example, the V2 protein of several monopartite begomoviruses, including *Cotton leaf curl Kokhran virus* (CLCuKoV), *Papaya leaf curl virus* (PaLCuV), and *Tomato leaf curl Java virus* (TLCJV), is able to induce HR in *Nicotiana benthamiana* and *N. tabacum* (Mubin et al., 2010; Sharma and Ikegami, 2010). In these monopartite begomoviruses, the C2 protein is able to counter the HR response induced by the V2 protein (Mubin et al., 2010). In the case of the bipartite begomoviruses *Tomato leaf curl New Delhi virus* (ToLCNDV) and *Bean dwarf mosaic virus* (BDMV), it appears as though NSP is the inducer of HR, and the AC2 protein counteracts the HR in an NLS and ZFD-dependent manner (Hussain et al., 2007). In another example, the C2 protein of *Tomato yellow leaf curl-Sardinia virus* (TYLCSV) elicits a strong HR response in *N. benthamiana*, *N. tabacum*, and *A. thaliana*, suggesting that C2 may represent the viral effector (Matic et al., 2016). However, no HR develops during a typical TYLCSV infection, and co-expression of C2 with the Rep or V2 proteins partially counteracts the HR, resulting in chlorosis (Matic et al., 2016). Interestingly, the C2 protein from the closely related *Tomato yellow leaf curl virus* (TYLCV) does not induce HR (Matic et al., 2016). These examples suggest that geminiviruses encode proteins that are potentially recognized by the host as avirulence (*avr*) factors, resulting in development of an HR response that could inhibit viral spread. However, in some cases at least, the virus has developed countermeasures, and the AC2/C2 protein appears to have evolved to avoid or inhibit the HR response, allowing for systemic spread of the virus (**Figure 3A**). While this function does not appear to be unique to AC2/C2, it is clear that these proteins often play a critical role in ensuring evasion of host immune responses. It should be noted that a host protein capable of triggering an HR-like response against a geminivirus has yet to be identified.

C2 AND THE UBIQUITIN/PROTEASOME SYSTEM (UPS)

Plants, and all eukaryotes, rely on a highly dynamic UPS which targets proteins for ubiquitination, a post-translational modification leading to proteolytic degradation by the proteasome [reviewed in (Dreher and Callis (2007)]. This highly enzymatic process is not only a way of regulating endogenous proteins involved in many plant cellular processes,

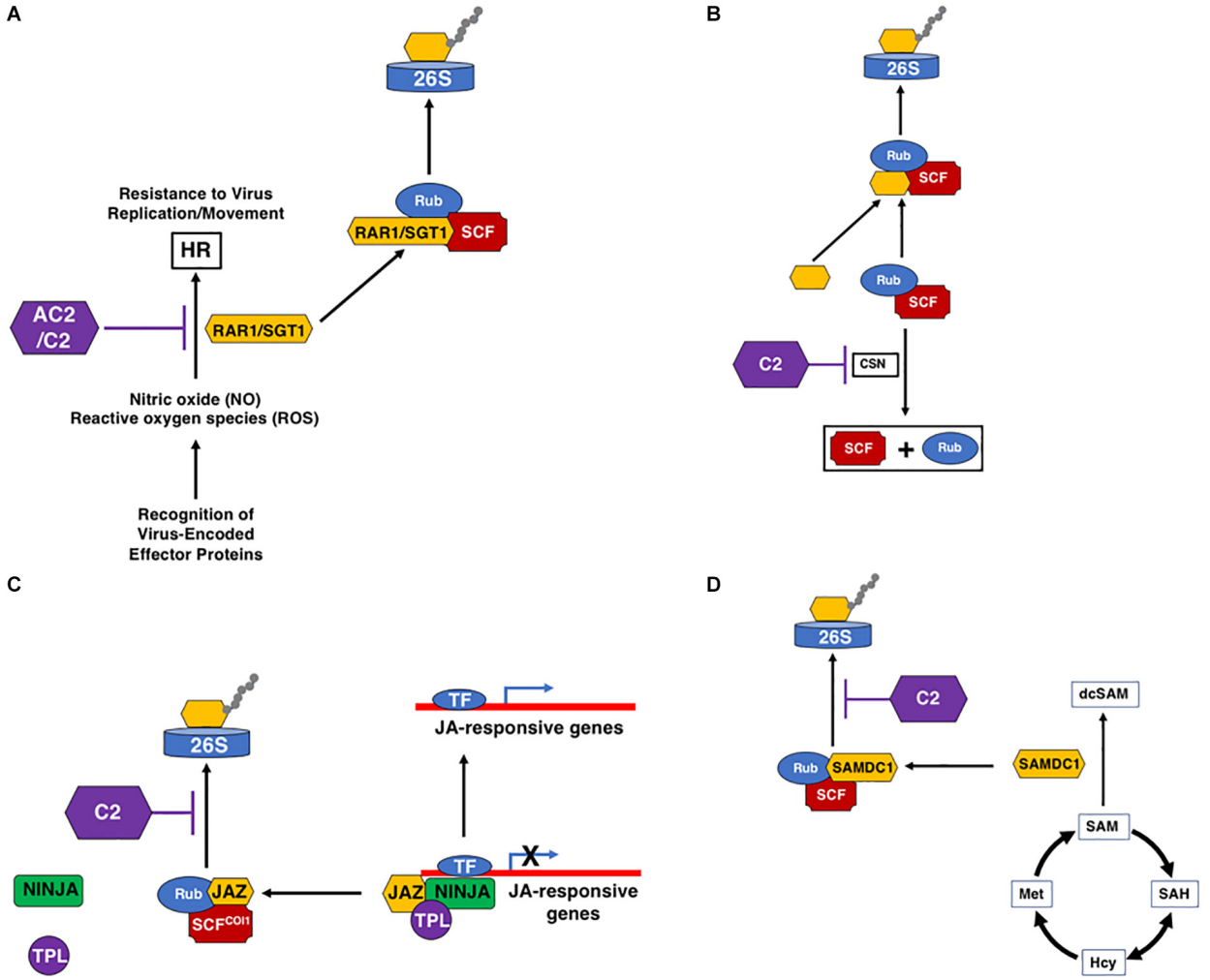

FIGURE 3 | Interactions of AC2/C2 with the Ubiquitin/Proteasome System (UPS). C2 and AC2 can inhibit the UPS at multiple steps through inactivation of the CSN complex. **(A)** Inhibition of the HR response by C2 and AC2. This may be mediated through inhibition of the SCF complex that degrades RAR1/SGT1. **(B)** C2 inhibition of the CSN complex that promotes derubylation of cullin within the SCF complex. **(C)** Inhibition of SCF^{COI1} by C2, which promotes the degradation of JAZ through the 26S proteasome releasing the co-repressors TPL and NINJA. Loss of JAZ promotes the induction of JA-responsive defense genes. **(D)** Stabilization of SAMDC1 by C2 increases levels of decarboxylated SAM (dcSAM) at the expense of SAM. The following acronyms are used: HR, Hypersensitive Response; SCF, SKP1/Cullin/F-Box-; Rub, Related to Ubiquitin; RAR1/SGT1, Required for Mla12 resistance/Suppressor of G_2 allele of Skp1; CSN, COP9 Signalosome Complex; JAZ, Jasmonate-Zim Domain; 26S, 26S Proteosome; SAM, S-Adenosyl Methionine; SAMDC1, SAM Decarboxylase 1; dcSAM, decarboxylated SAM; SAH, S-Adenosyl Homocysteine; Hcy, Homocysteine; Met, Methionine; AC2/C2, geminivirus virulence factors; TF, Transcription Factor; TPL, Topless Co-Repressor; NINJA, Novel Interactor of Jaz. Black arrows represent reactions and/or responses that are induced. Purple lines indicate inhibition through interaction with the geminivirus AC2 and/or C2 proteins.

including hormonal responses [reviewed in Santner and Estelle (2009)], but is also a defense mechanism against pathogenic organisms, including geminiviruses (Lozano-Durán et al., 2011; Mandadi and Scholthof, 2013). In plants, the most abundant family of E3 ligases comprises the multi-subunit Cullin RING Ligases (CRLs) (Dreher and Callis, 2007). Within this family, the most abundant class of SCF complexes is composed of SKP1/ASK (S-phase kinase-associated protein), Cullin1 (CUL1), an F-Box substrate binding protein, and the RING subunit RBX1 (RING box 1). The UPS appears to be a high value target for the geminiviruses (**Figure 3**). The AC2/C2 proteins compromise the activity of several SCF complexes, resulting in altered SCF complexes involved in plant defense and in the signaling pathways of several hormones (Lozano-Durán et al., 2011). The C2 protein of the monopartite begomoviruses TYLCSV and TYLCV, and the curtovirus BCTV, inhibit the activity of CSN5 (**Figure 3B**), the only catalytic subunit of the COP9 signalosome complex (CSN), but does not interfere with the assembly of CSN or SCF complexes (Lozano-Durán et al., 2011). CSN5 is necessary for CSN-mediated removal of a ubiquitin-like moiety, RUB (Related to Ubiquitin), from CUL1, which is the scaffold protein of the CRLs (Dreher and Callis, 2007). Conjugation of RUB to CUL1 upregulates CRL activity and is known to stimulate ubiquitination of substrate proteins by CRLs (Duda et al., 2008).

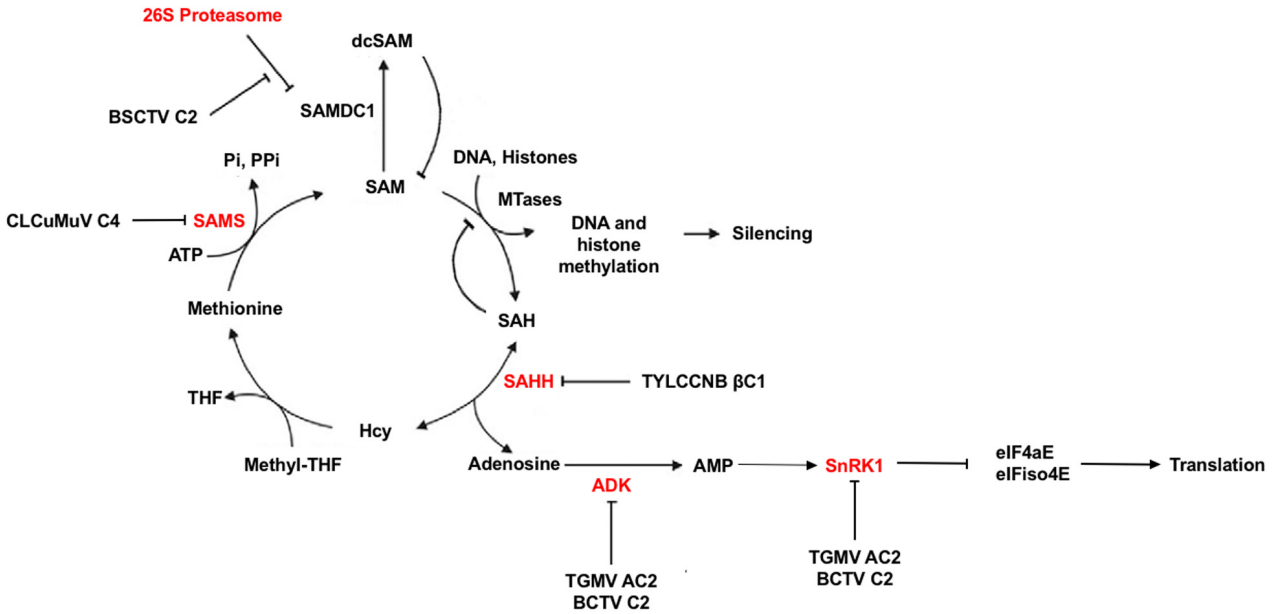

FIGURE 4 | Methyl cycle Inactivation by Geminivirus and Betasatellite Proteins. S-adenosyl methionine (SAM) serves as a methyl group donor for most transmethylation reactions. The product, S-adenosyl homocysteine (SAH), is converted by S-adenosyl homocysteine hydrolase (SAHH) to homocysteine (Hcy) and adenosine. Adenosine phosphorylation by adenosine kinase (ADK) is essential because the reaction catalyzed by SAHH is reversible and the equilibrium lies in the direction of SAH synthesis. In addition, SAH is a competitive inhibitor of methyltransferase (MTase) reactions. Thus, phosphorylation of adenosine promotes flux through the cycle, and inactivation of ADK by TGMV AC2 and BCTV C2 inhibits SAM synthesis. AMP generated by adenosine phosphorylation sustains SNF1-related kinase 1 (SnRK1) activity, which also is directly inhibited by AC2 and C2. SnRK1 phosphorylation of eIF4E/iso4E interferes with protein synthesis. The TYLCCNV betasatellite TYLCCNB encodes the pathogenicity factor βC1, which blocks the methyl cycle by inhibiting SAHH activity. BSCTV C2 antagonizes proteasome-mediated degradation of SAM decarboxylase (SAMDC), increasing levels of decarboxylated SAM (dcSAM). The C4 protein of CLCuMuV interferes with SAM synthetase (SAMS) activity. Based on Yang et al., 2011.

As the CSN complex is one of the regulators of CRL activity, it is essential for function *in vivo* (Hotton and Callis, 2008), and is predicted to act as a negative regulator of SCF complexes. However, genetic data suggests that the CSN acts as a positive regulator of cullin-based SCFs and loss-of-function mutants in CSN subunits mimic mutants in SCF complexes, and result in loss of SCF activity (Cope and Deshaies, 2003). This is observed in C2-mediated inhibition of CSN5, which is predicted to result in reduced derubylation that should increase SCF activity. However, C2 actually appears to inhibit the function of CUL1-based SCF complexes resulting in altered cellular responses, including suppression of JA-responses (Lozano-Durán et al., 2011). One proposed hypothesis is SCF activity is not strictly dependent upon CSN, but that CSN is required for maintaining an optimal pool of active E3 complexes (Cope and Deshaies, 2003). If so, then CSN could act as a positive regulator of some SCF complexes and a negative regulator of others. Therefore, the CSN could be a valuable target for geminiviruses through C2, by inhibiting the activity of select SCF complexes but enhancing the activity of others.

The main SCF-dependent hormone signaling pathway impaired by C2-mediated inhibition of CSN5 is the JA response (Lozano-Durán et al., 2011). This could be particularly significant for viral pathogenesis, as many geminiviruses are limited to phloem cells, the preferential sites of JA biosynthesis, making suppression of the JA response during infection feasible (Hanley-Bowdoin et al., 2013). Plants respond to JA through degradation of the JAZ family of transcriptional regulators by SCF^{COI1} (CORONATINE INSENSITIVE 1), in a proteasome-dependent manner (**Figure 3C**). This suggests that the C2 protein of geminiviruses may alter the JA response by inhibiting the targeting of JAZs for ubiquitination and degradation via the 26S proteasome pathway, thereby interrupting expression of JA-responsive genes (Lozano-Durán et al., 2011; Rosas-Díaz et al., 2016). This is supported by data showing that infection of JA-treated Arabidopsis plants with BCTV resulted in milder symptoms and reduced viral DNA accumulation (Lozano-Durán et al., 2011), and that Arabidopsis plants expressing C2 from TYLCV or TYLCSV show suppression of JA-mediated defense processes and JA-dependent secondary metabolism (Rosas-Díaz et al., 2016). In addition, transcriptomic analysis of transgenic Arabidopsis plants expressing TYLCSV C2 found a subset of repressed genes in processes related to plant defense and response to JA. This is also evident in Arabidopsis plants infected with *Cabbage leaf curl virus* (CaLCuV), where COI1-induced genes are reduced, and transcripts encoding components of the ubiquitin-proteasome pathway, including 32 genes specifying 11 core and 13 regulatory subunits of the 26S proteasome complex, were elevated (Ascencio-Ibañez et al., 2008). Together, this supports repression of the JA pathway by C2, which could provide a biological advantage for viral infection through

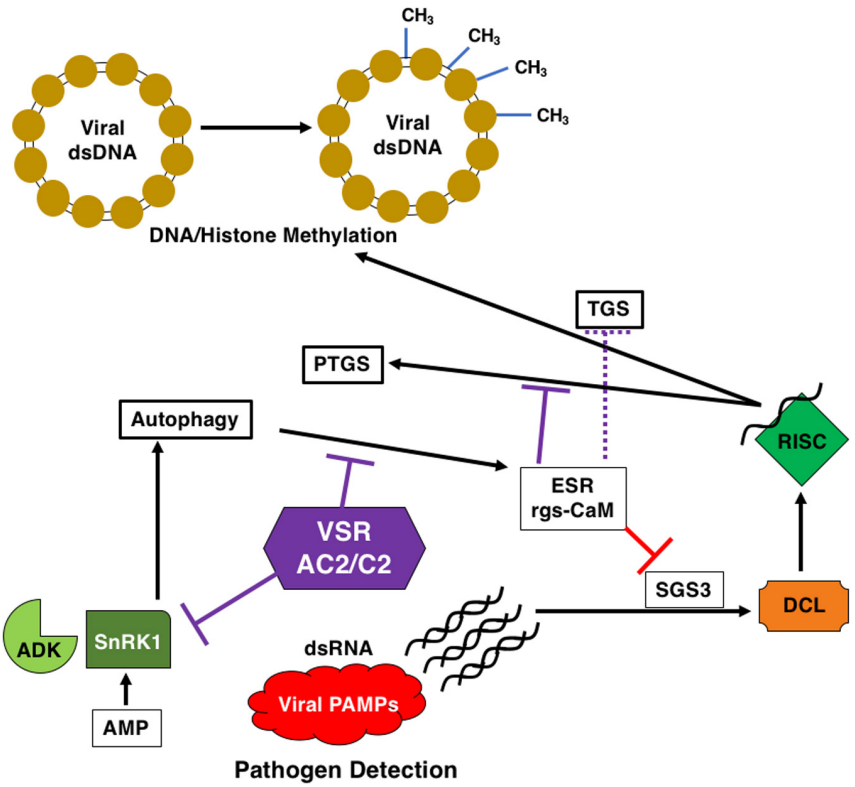

FIGURE 5 | AC2/C2 and Autophagy. AC2/C2 modulate the autophagic pathway to facilitate infection and inhibit antiviral defense pathways. AC2/C2 stabilize endogenous suppressors of RNA silencing to inhibit TGS and PTGS. The following cellular components are shown: ADK, Adenosine Kinase; SnRK1, SNF1-Related Kinase 1; PTGS, Post-Transcriptional Gene Silencing; ESR, Endogenous Suppressor of RNA Silencing; rgs-CaM, Regulator of Gene Silencing Calmodulin-like Protein; TGS,Transcriptional Gene Silencing; SGS3, Suppressor of Gene Silencing 3; DCL, Dicer Like; RISC, RNA-Induced Silencing Complexes; VSR, Viral Suppressor of RNA Silencing; AC2/C2, geminivirus virulence factors; CH_3, methylated DNA in the viral dsDNA minichromosome. Black arrows represent reactions and/or responses that are induced. Red lines indicate inhibition due to the ESR. Purple lines indicate inhibition of ADK and SnRK1 and rgs-CaM through interaction with AC2 and/or C2 proteins.

suppression of hormone-mediated plant defense responses (Lozano-Durán et al., 2011).

A second example of geminiviruses interfering with the UPS to promote virulence is exemplified by the *Beet severe curly top virus* (BSCTV) C2 protein, which interacts with and inhibits UPS-mediated degradation of *S*-adenosyl-methionine decarboxylase 1 (SAMDC1) (Zhang et al., 2011; **Figure 3D**). Levels of *S*-adenosyl-methionine (SAM) are modulated in part through the decarboxylase activity of SAMDC1, which therefore affects host DNA methylation status (Mandadi and Scholthof, 2013). Loss of function of either SAMDC1 or mutation in the BSCTV C2 gene leads to enhanced *de novo* methylation of the BSCTV dsDNA RF, resulting in reduced BSCTV replication and decreased BSCTV infectivity (Zhang et al., 2011). Whether the SCF complex that degrades SAMDC1 is regulated by the same CSN complex that controls SCF-dependent JA-signaling is currently unknown (Lozano-Durán et al., 2011).

An additional hypothesis has also been proposed whereby C2 may redirect certain SCF complexes to degrade specific host proteins producing an environment conducive for viral infection (Lozano-Durán et al., 2011). For example, the tobacco *N* gene–mediated resistance response against *Tobacco mosaic virus* (TMV) requires a functional RAR1/SGT1 (Required for Mla12 resistance/Suppressor of G_2 allele of Skp1) complex (Mandadi and Scholthof, 2013). This complex physically interacts with SKP1 and the CSN (Liu et al., 2002; **Figure 3**). Down-regulation of components of the RAR1/SGT1, SKP1 or CSN complex abolishes *N* gene–mediated resistance, supporting a role for UPS in *N*-mediated HR and resistance responses (Liu et al., 2002). It is interesting to speculate that the ability of AC2/C2 proteins of geminiviruses to counter the HR response is a consequence of interference with the UPS and its function in antiviral immune responses. Thus, C2 interference with derubylation of the SCF complex could result in accumulation of an active SCF complex, and therefore degradation of the RAR1/SGT1 complex, preventing HR.

SULFUR-ENHANCED DEFENSE (SED) AND C2

Based on the established link between jasmonate signaling and sulfur metabolism, it is possible that the geminivirus C2 protein targets the sulfur metabolic pathway by suppressing

the JA response (Lozano-Duran et al., 2012). This could be significant given the importance of the pathway in response to plant pathogens. This is highlighted by the high response of genes related to sulfur metabolism in Arabidopsis plants treated with methyl jasmonate (MeJA), although the mechanism is still unresolved (Jost et al., 2005). Plants assimilate inorganic sulfur from the soil as sulfate which is assimilated into cysteine (Rausch and Wachter, 2005; Lozano-Duran et al., 2012). From cysteine, sulfur is available for synthesis of many different compounds, including methionine, glucosinolates, and phytoalexins as well as sulfur-containing defense compounds (SDCs) such as glutathione (Rausch and Wachter, 2005; Lozano-Duran et al., 2012). Glutathione is an important compound for protection against reactive oxygen species (ROS) that accumulate in response to stress, and so operates as a detoxification mechanism (Rausch and Wachter, 2005). Transgenic Arabidopsis plants expressing TYLCSV C2 protein that exhibit repression of genes involved in the JA response also exhibit repression of genes in the sulfur assimilation pathway (*APS3, APR1*, and *APR3*) (Lozano-Durán et al., 2011; Lozano-Duran et al., 2012). Treatment with MeJA is able to restore expression of genes involved in sulfur assimilation (Lozano-Duran et al., 2012). Thus, the interaction of the geminivirus C2 protein with proteins that function in the ubiquitination pathway appears to have a high value with respect to suppressing JA and sulfur-enhanced defense pathways. During ETI, both JA and SA, which are normally antagonistic defense hormones, accumulate to high levels, and JA appears to be a positive regulator of Resistance to *Pseudomonas syringae* 2 (RPS2)-mediated ETI (Liu et al., 2016). This is again consistent with C2 being a viral effector protein that suppresses ETI leading to effector-triggered sensitivity.

It is important to note that while the UPS appears to be a high value target for geminivirus AC2/C2 proteins, it seems unlikely that a single host protein is impacted. It is possible that geminiviruses need to enhance degradation of some host proteins and inhibit the degradation of others. Thus, a more likely scenario is that AC2/C2 target multiple proteins of the UPS system, similar to AC2/C2 mechanisms that have evolved to interfere with different components of the RNA silencing pathway (Bisaro, 2006; Raja et al., 2010).

AC2/C2 AND METABOLISM

In addition to what may be described as classical defense mechanisms, plants are capable of altering their metabolic systems in times of environmental or parasitic stress. In this regard, geminiviruses have been shown to target and inactivate two proteins important for plant cellular metabolism, sucrose non-fermenting-related kinase 1 (SnRK1) and adenosine kinase (ADK) (**Figure 4**). Specifically, TGMV AC2, and BCTV C2 were found to interact with and inhibit both SnRK1 and ADK (Hao et al., 2003; Wang et al., 2003). SnRK1 is a serine/threonine kinase of the SNF1/AMPK family that plays a key role in metabolism by turning off energy consuming biosynthetic pathways and turning on alternative ATP generating systems in response to nutritional, environmental, and biotic stresses that deplete ATP. This is accomplished by direct phosphorylation and inhibition of key biosynthetic enzymes as well as alteration of the transcriptome (Baena-González and Sheen, 2008; Halford and Hey, 2009; Hulsmans et al., 2016). Cellular energy charge is sensed by relative ATP/ADP/AMP levels, with AMP generally stimulating or maintaining SNF1/AMPK/SnRK1 activity. ADK is a purine nucleoside kinase that catalyzes transfer of γ-phosphate from ATP or GTP to adenosine, producing AMP. ADK is involved in adenosine salvage, which contributes to maintaining cellular energy charge by supporting the synthesis of a variety of biomolecules such as nucleotide cofactors, nucleic acids, polyamines, and enzymes involved with methyl recycling. It also plays a central role in maintaining the methyl cycle and S-adenosyl methionine (SAM)-dependent methyltransferase activity (Weretilnyk et al., 2001; Moffatt et al., 2002; **Figure 4**). A direct link between these two kinases has been established by the observation that SnRK1 and ADK form a cytoplasmic complex that potentially is mutually stimulatory (Mohannath et al., 2014). AMP generated by ADK is known to maintain SnRK1 activity, and SnRK1 was found to stimulate ADK by an unknown non-enzymatic mechanism. That geminiviruses appear to have evolved a dual approach for disabling metabolic responses involving these kinases leads one to conclude that they are an important aspect of plant antiviral defense.

Direct evidence for the involvement of SnRK1 in antiviral defense comes from studies which demonstrated that *N. benthamiana* plants with reduced SnRK1 activity due to expression of an antisense SnRK1 transgene display enhanced susceptibility to geminivirus infection similar to that observed upon expression of TGMV AC2 and BCTV C2 transgenes (Sunter et al., 2001; Hao et al., 2003; Mohannath et al., 2014). As SnRK1 has a plethora of cellular targets, which might be relevant to antiviral defense remains unclear, but the mRNA cap-binding proteins eukaryotic initiation factor 4E (eIF4E) and eIFiso4E were recently identified as promising candidates (**Figure 4**). SnRK1 has been shown to phosphorylate these essential translation initiation factors and inhibit protein synthesis (Bruns et al., 2019). This is possibly analogous to phosphorylation of eIF2α by Protein kinase R (PKR), which blocks protein synthesis in infected mammalian cells as part of the innate immune response. PKR activity, which is not found in plants, is inhibited (or its effects abrogated) by pathogenicity factors of essentially all mammalian viruses.

Interestingly, it has been reported that Arabidopsis SnRK1 can phosphorylate CaLCuV AC2 protein *in vitro*. In addition, a phosphomimic mutation in CaLCuV AC2 delayed symptom appearance in Arabidopsis and reduced viral DNA accumulation in protoplasts, suggesting that phosphorylation of AC2 by SnRK1 hinders the establishment of CaLCuV infection (Shen et al., 2014). By contrast, TGMV AC2 and BCTV C2 are not phosphorylated *in vitro* by SnRK1, and instead inhibit SnRK1 kinase activity (Wang et al., 2003). More recent work confirmed that SnRK1 can phosphorylate CaLCuV AC2 *in vitro*, but not TGMV AC2, BCTV L2, and TYLCV C2 (S. Li and D.M. Bisaro, unpublished). Consistent with this, sequence analysis revealed that the AC2/C2 proteins of some New World begomoviruses (∼20, e.g., TGMV), nearly all Old World begomoviruses

examined (>100, e.g., TYLCV), and all curtoviruses (e.g., BCTV), lack a consensus SnRK1 phosphorylation site. However, the AC2 proteins of some New World begomoviruses (∼40, including CaLCuV) do in fact contain a SnRK1 consensus motif. Thus, the available evidence suggests that the SnRK1:AC2/C2 interaction is in flux: in some systems, SnRK1 may phosphorylate AC2 and reduce virus accumulation, while in most cases the AC2/C2 proteins are likely not phosphorylated and instead may inhibit SnRK1-mediated antiviral defense. That AC2/C2 may be under selection to avoid SnRK1 phosphorylation further highlights the importance of this interaction to viral pathogenesis.

Another potential consequence of inhibiting ADK relates to a possible role in cytokinin metabolism and cell cycle progression (Kwade et al., 2005). Cytokinins are N6-substituted adenine derivatives that promote cell proliferation, and ADK can phosphorylate and convert cytokinins to lower activity nucleotides (von Schwartzenberg et al., 1998). ADK may therefore modulate the relative levels of different cytokinin forms. It follows that inhibition of ADK activity by AC2/C2 could increase the pool of bioactive cytokinins necessary for plant cell cycle progression, on which geminiviruses rely for replication of their DNA genomes. Consistent with this idea, activity of a cytokinin responsive promoter was found to be increased in *adk* mutant Arabidopsis plants and in *N. benthamiana* following transient silencing of ADK expression or treatment with a pharmacological inhibitor of ADK. Similar expression changes were observed following over-expression of begomovirus AC2 and curtovirus C2. It should be noted that over-expression may not reflect the same conditions observed in a host during an actual viral infection with respect to transcript abundance, protein abundance, and/or timing of expression. However, observations that geminivirus infection increased expression of cytokinin responsive genes, and that exogenous application of cytokinin increased susceptibility to infection (Baliji et al., 2010), are consistent with AC2/C2 inhibition of ADK leading to a change in cytokinin responses and a strong indicator for ADK being a high value target for geminiviruses.

AC2/C2 AND GENE SILENCING

RNA silencing refers to a set of mechanistically related, partially overlapping, and evolutionarily conserved processes including post-transcriptional gene silencing (PTGS, also known as RNA interference) and transcriptional gene silencing (TGS) (Brodersen and Voinnet, 2006; Matzke and Mosher, 2014; Pikaard and Mittelsten Scheid, 2014; Fultz et al., 2015). In plants, PTGS typically leads to siRNA-mediated degradation of mRNAs or translation inhibition in the cytoplasm. TGS is an siRNA-mediated nuclear process associated with repressive DNA and histone methylation, which is established by a pathway commonly known as RNA-directed DNA methylation (RdDM). Mechanistic details of these small RNA pathways can be found in the reviews noted above. As antiviral silencing specificity is determined by virus-derived siRNAs, viruses are both inducers and targets of the silencing response. Moreover, as siRNAs can be amplified and spread systemically throughout the plant, they can "prime" silencing-based host defenses in tissues distant from the site of primary infection, greatly enhancing their efficacy (Palaqui et al., 1997; Ratcliff et al., 1997; Molnar et al., 2010). Antiviral roles for both PTGS and TGS are well-established, and their importance is highlighted by the observation that virtually all plant viruses encode silencing suppressor proteins (Díaz-Pendón and Ding, 2008; Ruiz-Ferrer and Voinnet, 2009; Wu et al., 2010; Burgyan and Halveda, 2011). Geminiviruses, which replicate and transcribe their genes in the nucleus and export mRNAs to the cytoplasm, are targeted by both PTGS and TGS and of necessity encode proteins that suppress both pathways (Bisaro, 2006; Raja et al., 2010). These counter-defensive proteins employ multiple mechanisms to block different aspects of RNA silencing.

Post-transcriptional gene silencing was first perceived as a defense against geminiviruses with the observation that the AC2 protein of ACMV could prevent silencing of a green fluorescent protein (GFP) transgene in *N. benthamiana* plants (Voinnet et al., 1999). AC2 was subsequently found to suppress PTGS by multiple mechanisms. One, referred to here as transcription-dependent suppression, involves transactivation of host genes that appear to encode endogenous negative regulators of RNA silencing, including Werner exonuclease-like 1 (*WEL1*) and regulator of gene silencing calmodulin-like protein (*rgs-CaM*) (Trinks et al., 2005; Chung et al., 2014). A second mechanism, referred to as transcription-independent suppression, is shared by AC2 and BCTV C2 which, unlike AC2, is not a transcriptional activator. This mechanism correlates with the ability of AC2 and C2 to interact with and inactivate ADK (Wang et al., 2003, 2005). Interestingly, while both AC2 and C2 can inhibit the establishment of PTGS, only AC2 can block the systemic spread of silencing. That AC2 lacking its transcription activation domain is likewise unable to prevent systemic spread indicates that suppression of this aspect of silencing is transcription-dependent (Jackel et al., 2015). Because silencing spread is a crucial feature of antiviral defense, it is possible that another BCTV protein might be involved in preventing the production and/or trafficking of mobile siRNAs.

Transcriptional gene silencing was first implicated as a defense against geminiviruses with the observation that viral replication in transfected protoplasts is greatly reduced when the inoculum DNA is methylated (Brough et al., 1992). Later studies employing a variety of Arabidopsis mutants lacking components of the RdDM pathway definitively established that viral chromatin methylation is a potent epigenetic defense against geminiviruses (Raja et al., 2008, 2014; Jackel et al., 2016). Repressed viral chromatin is covalently marked with cytosine methylation and histone H3 lysine 9 dimethylation (H3K9me2), both of which are hallmarks of constitutive heterochromatin that are also found on silenced endogenous transposable elements. In addition, viral chromatin containing epigenetic marks indicative of active viral gene expression (including H3K9 acetylation and H3K4me3) coexist with repressed viral chromatin in infected plants, and the equilibrium between them dictates the outcome of infection. A preponderance of repressed chromatin favors symptom remission and host recovery from infection (Raja et al., 2008, 2014; Ceniceros-Ojeda et al., 2016; Jackel et al., 2016; Coursey et al., 2018b). Repressed viral chromatin is highly compacted

relative to active chromatin, and increased physical compaction correlates with reduced viral gene expression (Ceniceros-Ojeda et al., 2016; Coursey et al., 2018b). However, the relationship between active and repressed chromatin may prove more complex than initially realized. EMSY-like 1 (EML1), a histone reader protein that binds a mark often present on active chromatin (H3K36 methylation), was recently found to suppress geminivirus infection. Further, EML1 was shown to diminish viral gene expression by inhibiting the association of RNA polymerase II (Pol II) with viral chromatin (Coursey et al., 2018a). Thus, EML1 may bind viral chromatin marked as active and promote changes that render it less accessible to the cellular transcription machinery.

TGMV and CaLCuV AC2 have been shown to suppress and reverse viral chromatin methylation and TGS by both transcription-dependent and -independent means, while BCTV C2 is again limited to the latter mechanism (Buchmann et al., 2009; Jackel et al., 2015). While transcription-dependent mechanisms are not yet defined, AC2 binds and inhibits the histone methyltransferase responsible for writing repressive H3K9me2, a crucial RdDM pathway component (Castillo-González et al., 2015). Transcription-independent reversal of TGS also correlates with methyl cycle interference due to inhibition of ADK (Wang et al., 2003; Buchmann et al., 2009; **Figure 4**). By phosphorylating adenosine, ADK promotes flux through the methyl cycle that generates SAM, a methyl group donor and essential methyltransferase cofactor (Moffatt et al., 2002). The importance of the methyl cycle for defense against geminiviruses is underscored by the number of pathway enzymes targeted by viral proteins. In addition to ADK targeted by AC2 and BCTV C2, BSCTV C2 inhibits methylation by stabilizing SAM decarboxylase (SAMDC), presumably increasing levels of decarboxylated SAM (dcSAM) at the expense of SAM (Zhang et al., 2011). It should be pointed out that the cellular levels of SAM or dsSAM were not measured directly. Interestingly, the βC1 protein encoded by the TYLCCNV satellite DNAβ (TYLCCNB) interferes with SAM synthesis by interacting with and inhibiting S-adenosyl homocysteine hydrolase (SAHH) (Yang et al., 2011). In this case, C2 encoded by the TYLCCNV helper virus appears to have lost the ability to suppress TGS, relying instead on βC1 to provide this critical function. Yet another geminivirus protein, C4 encoded by *Cotton leaf curl Multan virus* (CLCuMuV), suppresses TGS and PTGS by interacting with SAM synthetase (Ismayil et al., 2018). Clearly, methyl cycle inhibition is a common strategy of begomoviruses and curtoviruses.

AC2/C2, AUTOPHAGY AND RGS-CAM

Recent research has implied a link between autophagy, infection and RNA silencing (**Figure 5**). Autophagy is a cell-based self-degradative process important for energy balance during critical times in development and in response to different stresses, including nutrient deprivation and viral infection (Zhou et al., 2014). RNA silencing as mentioned earlier is part of the innate immune response in plants, and it has been shown that components of the RNA silencing pathway are targeted for degradation by the host autophagic pathway (Li et al., 2014, 2017). Viral RNA silencing suppressors are also targeted by the autophagic pathway, potentially through the action of rgs-CaM (regulator of gene silencing–calmodulin-like) (Anandalakshmi et al., 2000; Nakahara et al., 2012). It has been proposed that rgs-CaM acts as an endogenous negative regulator of RNA silencing, ensuring that this arm of the immune system is inactive in the absence of a viral infection. The HC-Pro protein encoded by the *Tobacco etch virus* (TEV) is a suppressor of PTGS and has been shown to interact with rgs-CaM from *Nicotiana tabacum* (Nt-rgsCaM), and to increase the levels of Nt-rgsCaM (Anandalakshmi et al., 2000). It was later discovered using tobacco cells that rgs-CaM is capable of interacting with other viral RNA silencing suppressors (RSS), including HC-Pro encoded by the potyvirus *Turnip mosaic virus* (TuMV) and *Cucumber mosaic virus* (CMV) 2b protein (Nakahara et al., 2012). This was further extended by the observation that rgsCaM RNA levels are increased *N. benthamiana* infected with the begomoviruses CaLCuV and TGMV, and with the curtovirus BCTV (Chung et al., 2014). This increase was recapitulated when TGMV AC2 was over-expressed in plants (Chung et al., 2014). Further, transcriptomic studies revealed that rgs-CaM is up-regulated in response to HC-Pro, P25 from *Potato virus X* (PVX), and ACMV AC2 (Jada et al., 2013). Binding of rgs-CaM to CMV 2b appears to be mediated through an arginine rich region of the viral protein. Interestingly, the AC2 protein of begomoviruses has a conserved basic region containing a stretch of arginine residues (**Figure 2**). TGMV AC2 is able to interact with rgs-CaM (Chung et al., 2014), although it is not known whether C2 proteins are capable of interacting with rgs-CaM. It is interesting to note at this point that the βC1 protein encoded by the betasatellite TYLCCNB has also been shown to upregulate rgs-CaM in *N. benthamiana* (Nbrgs-CaM), resulting in suppression of RNA silencing through repression of RNA dependent RNA polymerase 6 (RDR6) expression (Li et al., 2014, 2017). Additional studies determined that Nbrgs-CaM is able to interact with and induce autophagic degradation of Suppressor of Gene Silencing 3 (SGS3), a cofactor of RDR6 in PTGS (Li et al., 2017). While the βC1 protein sequence is unrelated to AC2, they both function as silencing suppressors and so autophagic degradation may be a general antiviral response targeting viral suppressors. Interestingly, both rgs-CaM and viral suppressors of PTGS are likely degraded by autophagy-like protein degradation (ALPD) immediately after they form a complex (Nakahara et al., 2012). However, for geminiviruses interaction with AC2 results in a different outcome. While rgs-CaM is able to self-interact in the cytoplasm, AC2 sequesters rgs-CaM to localized regions of the nucleus (Chung et al., 2014). The apparent difference in AC2 interaction outcome as compared to viral suppressors from previous studies could be a consequence of the DNA genome of geminiviruses, or that rgs-CaM inhibits the ability of other suppressors to bind siRNAs (Nakahara et al., 2012). This may well be the case given that TGMV AL2 does not bind siRNAs, even under conditions that support binding by the *Tomato bushy stunt virus* P19 suppressor (Wang et al., 2005). Although we do not know at this time whether nuclear relocalization

of rgs-CaM by AC2 has any role in silencing suppression, another interesting possibility relates to the function of AC2 in suppression of TGS. Given that nucleolus-associated Cajal bodies in plants are possible sites for biogenesis of siRNAs that guide TGS RISC complexes to chromatin (Pontes and Pikaard, 2008), it is tempting to speculate that sequestration of rgsCaM by AC2 could impact the ability of the host to generate siRNAs for silencing in general, or more specifically for TGS. The potential importance of rgs-CaM to host defense against geminivirus infection is highlighted by observations that over-expression in *N. benthamiana* plants leads to enhanced susceptibility to TGMV infection, while *Arabidopsis* plants containing an rgs-CaM T-DNA insertion mutation is are less susceptible to infection by CaLCuV and BCTV (Chung et al., 2014). The role of autophagy in potentially limiting geminivirus infection, the potential inhibition through the function of AC2/C2 and the link to RNA silencing is based on a few limited studies using over-expression strategies, and so additional work is needed to confirm whether autophagy represents a true anti-viral defense against geminiviruses.

Despite the differences, these results are consistent with the involvement of endogenous silencing suppressors in the mechanism of action of viral RNA silencing suppression. Referring back to the zigzag model for plant immunity (Jones and Dangl, 2006), the dsRNA trigger for RNAi could well be regarded as a viral PAMP and RNA silencing considered to be a facet of PAMP-triggered immunity (Nakahara et al., 2012; **Figure 5**). The RNA silencing defense is then countered by viral suppressor proteins like AC2, which can function at different points in the pathway to decrease the availability of siRNAs for the silencing machinery (Bisaro, 2006; Raja et al., 2010). Thus, viral suppressors can be regarded as effectors that facilitate viral infection and replication in plants (Nakahara et al., 2012). As a possible counter-defense, rgs-CaM may be able to recognize AC2 and subsequently target the protein for degradation, but geminiviruses may have evolved different strategies to evade this defense. AC2 from TGMV appears to sequester rgs-CaM in the nucleus, whereas the TYLCCNB βC1 protein promotes degradation of SGS3.

THE GEMINIVIRUS REPLICATION CYCLE IS REGULATED BY TEMPORALLY CONTROLLED GENE EXPRESSION

In addition to the extensive role that AC2 plays in suppression of host immune responses, a major function of AC2 is to regulate expression of the late viral genes, CP and NSP. Early in the infection process, after the viral genomic ssDNA has entered the nucleus, host polymerases use viral DNA as template for complementary strand synthesis to generate dsDNA RF intermediates, which subsequently associate with histones to form minichromosomes (**Figure 6**). Viral minichromosomes serve as template for both transcription and rolling circle replication (RCR). Minichromosomes of bipartite begomoviruses associate with 11 or 12 nucleosomes in two defined structures with open gaps that correlate with promoter structures and the origin of replication in both DNA A and DNA B (Pilartz and Jeske, 2003). One of the nucleosome free regions spans the IR, which contains the origin of replication and divergent promoters for complementary and viral sense transcription. A large complementary sense transcript encodes the early viral genes (Rep and AC3) that promote viral replication and production of genomic ssDNA by RCR. Early in infection, newly synthesized ssDNA is converted to dsDNA to amplify RF intermediates. Subsequent binding of Rep within the IR down-regulates its own expression (Sunter et al., 1993; Eagle et al., 1994), which enables expression from a downstream promoter that generates a transcript capable of expressing AC2. The downstream promoter appears to correlate with the second nucleosome-free region on minichromosomes. AC2 in turn activates expression of late genes (CP and NSP) from the virion sense promoter in the IR. Expression of late genes promotes virus spread and encapsidation of genomic ssDNA (Sunter and Bisaro, 1992). The presence of CP is critical for ssDNA accumulation during RCR. Thus, AC2 is critical for regulating the timing of CP expression to ensure that ssDNA is converted to dsDNA early during an infection and is sequestered late in the infection (**Figure 6**).

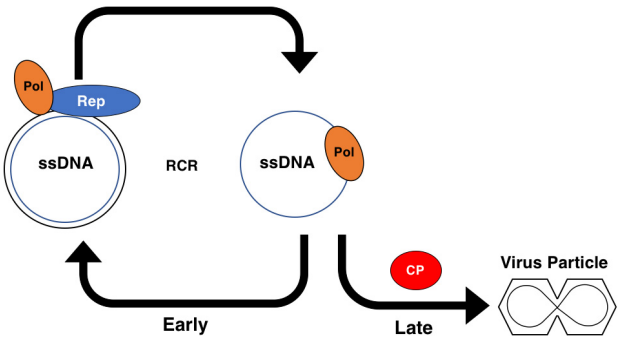

FIGURE 6 | Role of the Geminivirus CP Protein in Rolling Circle Replication. Early in the infection cycle single-stranded (ss)DNA associates with host DNA polymerases (Pol) and is converted to a double-stranded (ds)DNA intermediate. The dsDNA intermediate associates with the viral Rep protein and Pol to serve as a template for amplification via rolling circle replication (RCR). The dsDNA intermediate also serves as a template for transcription and produces the viral coat protein (CP) transcript late in the infection cycle. CP sequesters the viral ssDNA into particles, preventing the ssDNA from participating in RCR.

AC2 AND *CP* PROMOTER REGULATION

AC2-mediated regulation of the *CP* promoter in begomoviruses occurs in all tissues, however the mechanism by which expression is controlled is different in different cell types (Sunter and Bisaro, 1997). It has been determined that AC2 activates the *CP* promoter in mesophyll cells but acts to derepress and activate the *CP* promoter in phloem cells (Sunter and Bisaro, 1997). This is mediated through independent sequences located in two different regions of the viral genome (**Figure 7**). AC2-dependent *CP* promoter activation in both phloem and mesophyll cells is mediated through sequences located proximal

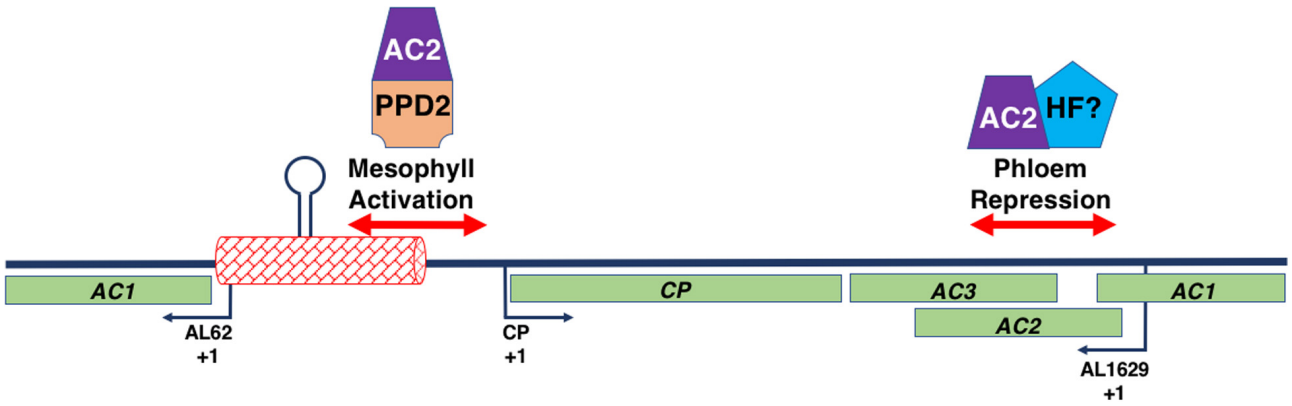

FIGURE 7 | Interaction of the Begomovirus Genome with AC2 and Host Factors. The figure represents a double stranded begomovirus DNA A genome in linear form. The complete CP, AC2, and AC3 open reading frames are shown (light green boxes), along with the AC1 ORF, which is split into two. The transcription initiation sites (+1) for the viral (CP) and complementary (AL62 and AL1629) sense transcripts are indicated by the black arrows. The intergenic region (red box) contains the replication origin including the hairpin and its invariant loop sequence (lollipop). Regions of the begomovirus genome involved in AC2-mediated activation in mesophyll and AC2-mediated de-repression in phloem tissue are shown (double-red arrows). An AC2-PPD2 complex binds sequences with the *CP* promoter involved in AC2-mediated activation. Whether AC2 interacts with a host factor (HF) to mediate de-repression is currently unknown.

to the transcription start site of the *CP* gene, but downstream of the conserved stem-loop structure important for the initiation of replication (Sunter and Bisaro, 1997, Bisaro, 2003; Lacatus and Sunter, 2008). In TGMV, a second element located within a region 590 bp downstream of the CP coding region, within the AC2 and AC3 coding sequences, is necessary for repression of *CP* promoter activity in phloem cells (Sunter and Bisaro, 1997). Repression of CaLCuV *CP* promoter activity in phloem cells is mediated by sequences within 340 bp downstream of the CP coding region, again within the AC2 and AC3 coding sequences (Lacatus and Sunter, 2008). AC2 is also required for activation of the *NSP* promoter (Sunter and Bisaro, 1992) and is dependent on sequences within 144 bp upstream of the NSP transcription start site (Berger and Sunter, 2013). Although the *NSP* promoter appears to exhibit AC2-independent expression in vascular tissue, similar to the CaLCuV and TGMV *CP* promoters (Berger and Sunter, 2013), we do not currently know whether the *NSP* promoter is regulated by independent mechanisms in different tissue types. By comparison, we have previously noted that the C2 protein in curtoviruses appears to lack the ability to activate transcription (Sunter et al., 1994). Further, analysis of the BCTV-SpCT *CP* promoter in transgenic *N. benthamiana* plants demonstrated it is active in the absence of any viral proteins (Rao and Sunter, 2012). Given the assumed necessity to control CP production as outlined for begomoviruses, the *CP* promoter is expected to be repressed in phloem cells, although this has currently not been tested. Therefore, we speculate that late in infection it is possible that C2 acts to derepress the promoter thereby producing CP at the appropriate time.

The interaction of AC2 with two independent sequences within the begomovirus genome, in conjunction with the observation that these sequences appear to bind different nuclear factors, suggests that AC2 is capable of interacting with different components of the host transcription machinery proteins to regulate the viral *CP* promoter (Sunter and Bisaro, 1997; Lacatus and Sunter, 2008; **Figure 7**). As AC2 does not bind dsDNA in a sequence-specific manner (Hartitz et al., 1999), it was assumed that AC2 is directed to responsive promoters through protein-protein interactions with cellular factors (Sunter and Bisaro, 2003). This was confirmed when a genetic screen identified the Arabidopsis PEAPOD2 (PPD2) protein, which is also known as TIFY4B, which specifically binds to sequences within the TGMV and CaLCuV *CP* promoters that mediate AC2-dependent promoter activation (Sunter and Bisaro, 2003; Lacatus and Sunter, 2009). The idea that AC2 is targeted to the *CP* promoter through interaction with PPD2, leading to activation of *CP* gene expression, is supported by evidence that PPD2 is also able to bind sequences necessary for AC2-mediated activation of the TGMV *NSP* promoter (Berger and Sunter, 2013), but not with sequences required for AC2-mediated derepression in phloem (Lacatus and Sunter, 2009). Additional evidence that AC2 is targeted to responsive promoters by PPD2 is provided by results which demonstrate that TGMV AC2 and PPD2 are able to form a complex on sequences containing the *CP* promoter, and that PPD2 localizes to the nucleus but is unable to activate transcription directly (Lacatus and Sunter, 2009). The ability of AC2 proteins from different viruses to transactivate the TGMV *CP* promoter suggests that begomovirus AC2 gene products function through interactions with common host proteins (Sunter et al., 1994). This is consistent with the observation that AC2 proteins from different begomoviruses are able to directly interact with PPD2 (Lacatus and Sunter, 2009).

IMPACT OF AC2 ON THE HOST TRANSCRIPTOME: COMPUTATIONAL ANALYSIS

If AC2 is targeted to the *CP* and *NSP* promoters by a host factor(s), then it is expected that AC2 could also have widespread

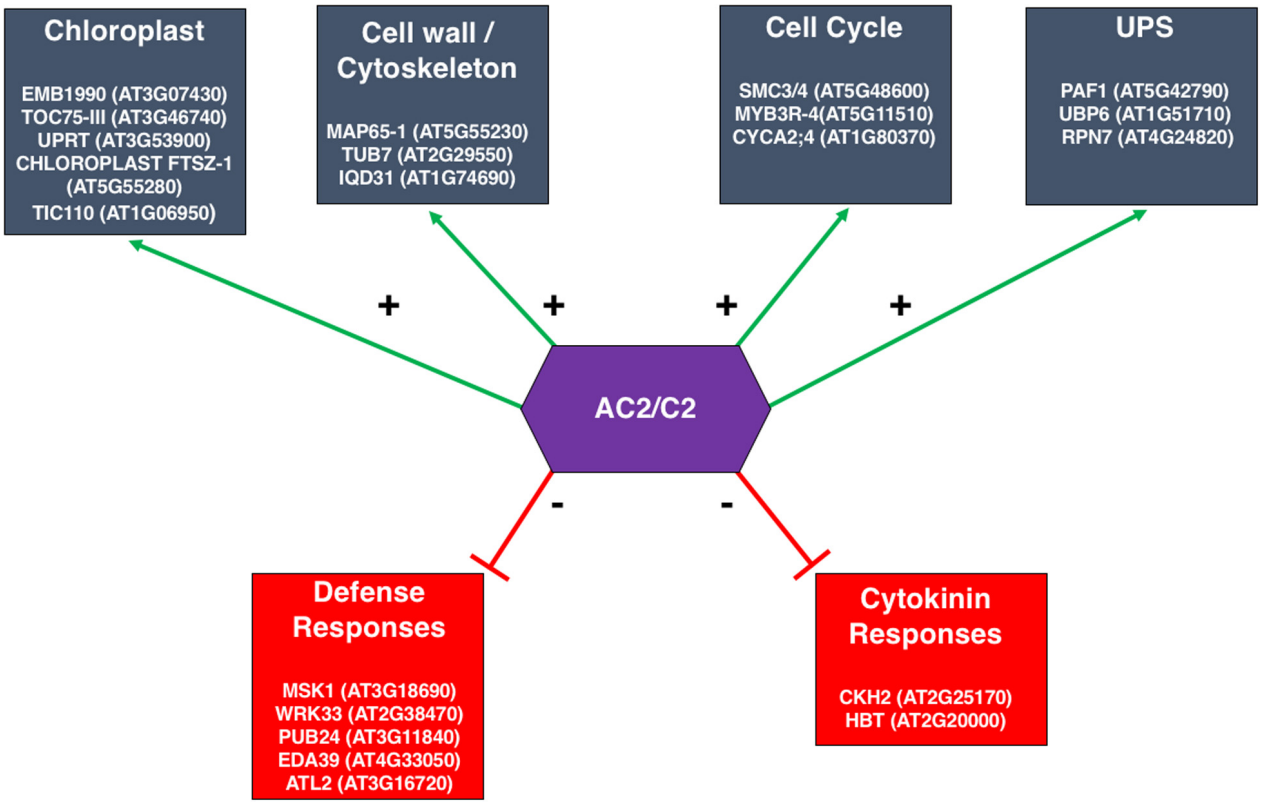

FIGURE 8 | Sub-networks of Genes Differentially Expressed in the Arabidopsis Genome in Response to the Transcription Function of the CaLCuV AC2 Protein. The response of Arabidopsis transcriptome to full-length CaLCuV AC2 or AC2 with a deletion of the transcriptional activation domain, revealed significant alterations in gene expression that could be attributed to the transcription function of AC2. A network-based analysis identified core gene groups that were up- or down-regulated in response to full length AC2 at 1 and 2 dpi, (Liu et al., 2014). Examples of genes, including gene ID, within these networks are given within each of the boxes shown. Downregulated groups are shown in red, and upregulated groups are in blue.

impact on the host transcriptome. Several large-scale microarray studies have been conducted to survey changes in the host transcriptome induced by the AC2 protein or its homologs (Trinks et al., 2005; Caracuel et al., 2012; Soitamo et al., 2012; Liu et al., 2014). Applying a stringent statistical criterion to a study using AC2 of ACMV and *Mungbean yellow mosaic virus-Vigna* (MYMV), Affymetrix GeneChips (ATH1), and transient expression assays with *Arabidopsis* protoplasts, 55 genes were found to be up-regulated >2-fold by MYMV AC2 (Trinks et al., 2005). Of these 55 genes, 30 were also induced >2-fold by ACMV AC2. With a less stringent criterion, the number of genes upregulated by ACMV increased to 162, of which 139 were also induced by MYMV AC2, including six cold-regulated genes. A second study using Agilent's microarray platform examined expression in transgenic tobacco plants expressing ACMV AC2, and identified a total of 1369 differentially expressed genes in leaves and flowers. Examples of the types of processes whose genes were found to be up-regulated were those related to stress, cell wall modification, and signaling. By contrast, processes associated with genes that were down-regulated were those related to translation, photosynthesis, and transcription (Soitamo et al., 2012). A comparison of the transcriptomic changes in transgenic Arabidopsis plants expressing C2 from the monopartite begomovirus TYLCSV, and its curtovirus counterpart, C2 from BCTV, found that the BCTV C2 up-regulates 444 genes and down-regulates 154 (Caracuel et al., 2012). Among those genes up-regulated, 15 were related to the cell-cycle and 9 were associated with DNA packaging. In contrast, stress response genes are over-represented in both up- and down-regulated genes. However, there was minimal overlap between genes differentially regulated by TYLCSV C2 and BCTV C2 (Caracuel et al., 2012). Although these studies were performed using over-expression of the viral proteins, it is important to validate the differential expression of identified candidate genes during an actual viral infection.

A dilemma frequently faced by genome-wide expression studies is that, due to the problem of multiple hypothesis testing and limited statistical power, very few genes can be selected with stringent statistical significance. On the other hand, with reduced statistical rigor, many more genes can be selected but it is difficult to determine which genes are indeed differentially expressed in response to a given treatment. To address this problem, Liu et al. (2014) developed a network-based analysis to identify core gene groups responding to AC2 expression in Arabidopsis using a

whole plant infusion assay with either the full-length CaLCuV AC2 or a truncated AC2 lacking the C-terminal transcriptional activation domain. Host genes that were differentially expressed due to full-length or truncated AC2 were overlaid to a whole-genome gene co-expression network constructed from more than 1300 microarrays (Ruan et al., 2011). Although hundreds of genes were identified as differentially regulated by full length AC2 but not truncated AC2, most of them were not connected to each other in the network, reflecting the diverse functional processes induced by AC2. Interestingly, a small fraction of the genes appears to be tightly linked to each other, resulting in dense sub-networks that may represent core functional groups co-regulated by the transcriptional activation function of AC2. For example, of the 214 unique genes that were up-regulated in response to full length AC2 at one day post infusion (dpi), five subnetworks were identified, each consisting of between four to eight highly connected genes. Two of these subnetworks contain genes encoding complexes involved in protein import into chloroplasts, which are of potential relevance for geminivirus infections (Krenz et al., 2012). Another sub-network consists of genes associated with the cell wall and/or cytoskeleton (**Figure 8**), consistent with previous findings using ACMV AC2 (Soitamo et al., 2012). This supports the hypothesis that AC2 may induce host genes that are important for cell-to-cell and long-distance movement of the virus. Of the six sub-networks up-regulated by full length AC2 at 2 dpi, one consists of five highly inter-connected genes having functions related to the cell cycle (**Figure 8**), in agreement with microarray results using BCTV C2 (Caracuel et al., 2012). On the other hand, down-regulated genes form a dense sub-network of genes involved in defense responses to pathogen infection (**Figure 8**). Another sub-network of down-regulated genes included cytokinin-hypersensitive 2 and Hobbit. This down-regulation may hint at a potential mechanism whereby AC2 interferes with progression of cell differentiation, shifting the balance in favor of cell proliferation thereby promoting viral replication (**Figure 8**). Many of these genes would not have been thought of as functioning in a network using standard statistical approaches, and therefore a network-based analysis can reveal highly connected genes in co-regulated gene networks that are potentially targeted by geminiviruses during infection.

It is quite clear from several studies that geminiviruses manipulate the host transcriptome, and that some critical networks appear to be high-value targets of the AC2/C2 protein. However, substantial work needs to be done to determine the consequences of these changes in host gene expression for viral pathogenesis.

FUTURE PERSPECTIVES

It is clear that the AC2/C2 proteins encoded by begomoviruses are multifunctional and have critical roles in both suppression of host immune responses and in regulation of the *CP* promoter. While the information gathered to date is extensive and has increased our understanding of the role of AC2 in geminivirus pathogenesis, there are several aspects with respect to AC2 that are currently unknown and are, or we argue should be, under investigation. First, the mechanism(s) by which AC2/C2 interact to disable the UPS are not understood, nor is it clear that we have discovered all of the defense-related pathways that are targeted by these viral proteins. As an example, plant hormones have significant roles in plant–pathogen interactions (Alazem and Lin, 2014), and the known interactions between these hormones along with the interaction of AC2/C2 with the cytokinin, SA, and JA pathways, leads us to believe that geminiviruses may also perturb other hormone pathways as well. Second, additional information is needed on how AC2 reverses TGS at the IR. Third, we do not know whether there are additional host factors that interact with the begomovirus *CP* promoter to mediate activation in mesophyll, and the identity of the host factor(s) that mediates repression in phloem cells is unknown. Fourth, the mechanism by which geminiviruses switch from early to late gene expression requires further study. For example, are there different populations of dsDNA templates for replication and transcription, or is a single population used for both? Lastly, how are the different functions of AC2 regulated? Consider that TGMV AC2 protein can interact with ADK, SnRK1, rgsCaM, and PPD2. We know that AC2 is found in both phosphorylated and non-phosphorylated forms in plant cells (Wang et al., 2003), and that AC2 can form a homo-dimer and higher-order multimers, which is consistent with a role in transcriptional activation (Yang et al., 2007). So, are there different functions associated with phosphorylated and non-phosphorylated forms and/or multimers? Answers to these and other questions will be valuable in extending our knowledge of AC2 function, which may ultimately lead to new ideas on how to effectively combat this devastating group of viruses.

AUTHOR CONTRIBUTIONS

GS: writing and editing entire manuscript, figures, and submission. JG: writing, draft of AC2 and HR, UPS, sulfur and transcription section. ER: writing, draft of metabolism, silencing section, and figures. LL and JR: writing, drafts computational section. DB: writing and editing the entire manuscript.

FUNDING

Work in the GS and JR labs was supported by a grant from the National Science Foundation (DBI-1565076), work in the DB lab was supported by grants from the National Science Foundation (IOS-1354636 and MCB-1158262); and the US Department of Agriculture, National Institute of Food and Agriculture (USDA/NIFA 2015-6703-22999).

REFERENCES

.Alazem, M., and Lin, N.-S. (2014). Roles of plant hormones in the regulation of host-virus interactions. *Mol. Plant Pathol.* 16, 529–540. doi: 10.1111/mpp.12204

Amin, I., Patil, B. L., Briddon, R. W., Mansoor, S., and Fauquet, C. M. (2011). Comparison of phenotypes produced in response to transient expression of genes encoded by four distinct begomoviruses in *Nicotiana benthamiana* and their correlation with the levels of developmental miRNAs. *Virol. J.* 8:238. doi: 10.1186/1743-422X-8-238

Anandalakshmi, R., Marathe, R., Ge, X., Herr, J. M., Mau, C., Mallory, A., et al. (2000). A calmodulin-related protein that suppresses posttranscriptional gene silencing in plants. *Science* 290, 142–144. doi: 10.1126/science.290.5489.142

Ascencio-Ibañez, J. T., Sozzani, R., Lee, T.-J., Chu, T.-M., Wolfinger, R. D., Cellab, R., et al. (2008). Global analysis of Arabidopsis gene expression uncovers a complex array of changes impacting pathogen response and cell cycle during geminivirus infection. *Plant Physiol.* 148, 436–454. doi: 10.1104/pp.108.121038

Baena-González, E., and Sheen, J. (2008). Convergent energy and stress signaling. *Trends Plant Sci.* 13, 474–482. doi: 10.1016/j.tplants.2008.06.006

Baliji, S., Black, M. C., French, R., Stenger, D. C., and Sunter, G. (2004). Spinach curly top virus: a new curtovirus species from southwest Texas displaying incongruent gene phylogenies that suggest a history of recombination among curtoviruses. *Phytopathology* 94, 772–779. doi: 10.1094/PHYTO.2004.94.7.772

Baliji, S., Lacatus, G., and Sunter, G. (2010). The interaction between geminivirus pathogenicity proteins and adenosine kinase leads to increased expression of primary cytokinin responsive genes. *Virology* 402, 238–247. doi: 10.1016/j.virol.2010.03.023

Baliji, S., Sunter, J., and Sunter, G. (2007). Transcriptional analysis of complementary sense genes in Spinach curly top virus and the functional role of C2 in pathogenesis. *Mol. Plant Microbe Interact.* 20, 194–206. doi: 10.1094/MPMI-20-2-0194

Balint-Kurti, P. (2019). The plant hypersensitive response: concepts, control and consequences. *Mol. Plant Pathol.* 20, 1163–1178. doi: 10.1111/mpp.12821

Berger, M. R., and Sunter, G. (2013). Identification of sequences required for AL2-mediated activation of the Tomato golden mosaic virus-yellow vein BR1 promoter. *J. Gen. Virol.* 94(Pt 6), 1398–1406. doi: 10.1099/vir.0.050161-50160

Bisaro, D. M. (2006). Silencing suppression by geminivirus proteins. *Virology* 344, 158–168. doi: 10.1016/j.virol.2005.09.041

Brodersen, P., and Voinnet, O. (2006). The diversity of RNA silencing pathways in plants. *Trends Genet.* 22, 268–280. doi: 10.1016/j.tig.2006.03.003

Brough, C. L., Gardiner, W. E., Inamdar, N., Zhang, X. Y., Ehrlich, M., and Bisaro, D. M. (1992). DNA methylation inhibits propagation of Tomato golden mosaic virus DNA in transfected protoplasts. *Plant Mol. Biol.* 18, 703–712. doi: 10.1007/bf00020012

Bruns, A., Li, S., Mohannath, G., and Bisaro, D. (2019). Phosphorylation of *Arabidopsis* eIF4E and eIFiso4E by SnRK1 inhibits translation. *FEBS J.* 286, 3778–3796. doi: 10.1111/febs.14935

Buchmann, R. C., Asad, S., Wolf, J. N., Mohannath, G., and Bisaro, D. M. (2009). Geminivirus AL2 and L2 proteins suppress transcriptional gene silencing and cause genome-wide reductions in cytosine methylation. *J. Virol.* 83, 5005–5013. doi: 10.1128/JVI.01771-1778

Bull, S. E., Briddon, R. W., Sserubombwe, W. S., Ngugi, K., Markham, P. G., and Stanley, J. (2007). Infectivity, pseudorecombination and mutagenesis of Kenyan cassava mosaic begomoviruses. *J. Gen. Virol.* 88, 1624–1633. doi: 10.1099/vir.0.82662-82660

Burgyan, J., and Halveda, Z. (2011). Viral suppressors of RNA silencing. *Trends Plant Sci.* 16, 265–272. doi: 10.1016/j.tplants.2011.02.010

Caracuel, Z., Lozano-Durán, R., Huguet, S., Arroyo-Mateos, M., Rodríguez-Negrete, E. A., and Bejarano, E. R. (2012). C2 from Beet curly top virus promotes a cell environment suitable for efficient replication of geminiviruses, providing a novel mechanism of viral synergism. *New Phytol.* 194, 846–858. doi: 10.1111/j.1469-8137.2012.04080.x

Casadevall, A., and Pirofski, L. (1999). Host-pathogen interactions: redefining the basic concepts of virulence and pathogenicity. *Infect. Immun.* 67, 3703–3713. doi: 10.1128/IAI.67.8.3703-3713.1999

Castillo-González, C., Liu, X., Huang, C., Zhao, C., Ma, Z., Hu, T., et al. (2015). Geminivirus-encoded TrAP suppressor inhibits the histone methyltransferase SUVH4/KYP to counter host defense. *eLife* 4:e06671. doi: 10.7554/eLife.06671

Ceniceros-Ojeda, E. A., Rodriguez-Negrete, E. A., and Rivera-Bustamante, R. F. (2016). Two populations of viral minichromosomes are present in a geminivirus-infected plant showing symptom remission (recovery). *J. Virol.* 90, 3828–3838. doi: 10.1128/JVI.02385-2315

Chung, H. Y., Lacatus, G., and Sunter, G. (2014). Geminivirus AL2 protein induces expression of, and interacts with, a calmodulin-like gene, an endogenous regulator of gene silencing. *Virology* 461, 108–118. doi: 10.1016/j.virol.2014.04.034

Combet, C., Blanchet, C., Geourjon, C., and Deléage, G. (2000). NPS@: network protein sequence analysis. *Trends Biochem. Sci.* 25, 147–150. doi: 10.1016/s0968-0004(99)01540-1546

Cope, G. A., and Deshaies, R. J. (2003). COP9 signalosome: a multifunctional regulator of SCF and other cullin-based ubiquitin ligases. *Cell* 114, 663–671. doi: 10.1016/s0092-8674(03)00722-720

Coursey, T., Milutinovic, M., Regedanz, E., Brkljacic, J., and Bisaro, D. M. (2018a). Arabidopsis histone reader EMSY-LIKE 1 binds H3K36 and suppresses geminivirus infection. *J. Virol.* 92:e219. doi: 10.1128/JVI.00219-218

Coursey, T., Regedanz, E., and Bisaro, D. M. (2018b). Arabidopsis RNA polymerase V mediates enhanced compaction and silencing of geminivirus and transposon chromatin during host recovery from infection. *J. Virol.* 92:e1320-17. doi: 10.1128/JVI.01320-1317

Dangl, J. L., Dietrich, R. A., and Richberg, M. H. (1996). Death don't have no mercy: cell death programs in plant-microbe interactions. *Plant Cell* 8, 1793–1807. doi: 10.1105/tpc.8.10.1793

Díaz-Pendón, J. A., and Ding, S. W. (2008). Direct and indirect roles of viral suppressors of RNA silencing in pathogenesis. *Ann. Rev. Phytopathol.* 46, 303–326. doi: 10.1146/annurev.phyto.46.081407.104746

Dreher, K. A., and Callis, J. (2007). Ubiquitin, hormones and biotic stress in plants. *Ann. Bot.* 99, 787–822. doi: 10.1093/aob/mcl255

Duda, D. M., Borg, L. A., Scott, D. C., Hunt, H. W., Hammel, M., and Schulman, B. A. (2008). Structural insights into NEDD8 activation of cullin-RING ligases: conformational control of conjugation. *Cell* 134, 995–1006. doi: 10.1016/j.cell.2008.07.022

Durrant, W. E., and Dong, X. (2004). Systemic acquired resistance. *Ann. Rev. Phytopathol.* 42, 185–209. doi: 10.1146/aanurev.phyto.42040803.140421

Eagle, P. A., Orozco, B. M., and Hanley-Bowdoin, L. (1994). A DNA sequence required for geminivirus replication also mediates transcriptional regulation. *Plant Cell* 6, 1157–1170. doi: 10.1105/tpc.6.8.1157

Elmer, J. S., Brand, L., Sunter, G., Gardiner, W. E., Bisaro, D. M., and Rogers, S. G. (1988). Genetic analysis of Tomato golden mosaic virus II. The product of the AL1 coding sequence is required for replication. *Nucl. Acids Res.* 16, 7043–7060. doi: 10.1093/nar/16.14.7043

Etessami, P., Saunders, K., Watts, J., and Stanley, J. (1991). Mutational analysis of complementary-sense genes of African cassava mosaic virus DNA A. *J. Gen. Virol.* 72, 1005–1012. doi: 10.1099/0022-1317-72-5-1005

Fultz, D., Choudury, S., and Slotkin, R. (2015). Silencing of active transposable elements in plants. *Curr. Opin. Plant Biol.* 27, 67–76. doi: 10.1016/j.pbi.2015.05.027

Garrido-Ramirez, E. R., Sudarshana, M. R., Lucas, W. J., and Gilbertson, R. L. (2000). Bean dwarf mosaic virus BV1 protein is a determinant of the hypersensitive response and avirulence in Phaseolus vulgaris. *Mol. Plant Microbe Interact.* 13, 1184–1194. doi: 10.1094/MPMI.2000.13.11.1184

Halford, N., and Hey, S. (2009). SNF1-related protein kinases (SnRKs) act within an intricate network that links metabolic and stress signalling in plants. *Biochem. J.* 419, 247–259. doi: 10.1042/BJ20082408

Hamilton, W. D. O., Stein, V. E., Coutts, R. H. A., and Buck, K. W. (1984). Complete nucleotide sequence of the infectious cloned DNA components of Tomato golden mosaic virus: potential coding regions and regulatory sequences. *EMBO J.* 3, 2197–2205. doi: 10.1002/j.1460-2075.1984.tb02114.x

Hanley-Bowdoin, L., Bejarano, E. R., Robertson, D., and Mansoor, S. (2013). Geminiviruses: masters at redirecting and reprogramming plant processes. *Nat. Rev. Microbiol.* 11, 777–788. doi: 10.1038/nrmicro3117

Hao, L., Wang, H., Sunter, G., and Bisaro, D. M. (2003). Geminivirus AL2 and L2 Proteins interact with and inactivate SNF1 kinase. *Plant Cell* 15, 1034–1048. doi: 10.1105/tpc.009530

Hartitz, M. D., Sunter, G., and Bisaro, D. M. (1999). The geminivirus transactivator (TrAP) is a zinc-binding phosphoprotein with an acidic activation domain. *Virology* 263, 1–14. doi: 10.1006/viro.1999.9925

Hoogstraten, R. A., Hanson, S. F., and Maxwell, D. P. (1996). Mutational analysis of the putative nicking motif in the replication-associated protein (AC1) of Bean golden mosaic geminivirus. *Mol. Plant Microbe Interact.* 9, 594–599. doi: 10.1094/mpmi-9-0594

Hormuzdi, S. G., and Bisaro, D. M. (1993). Genetic analysis of Beet curly top virus: evidence for three virion sense genes involved in movement and regulation of single-and double-stranded DNA levels. *Virology* 193, 900–909. doi: 10.1006/viro.1993.1199

Hormuzdi, S. G., and Bisaro, D. M. (1995). Genetic analysis of Beet curly top virus: examination of the roles of L2 and L3 genes in viral pathogenesis. *Virology* 206, 1044–1054. doi: 10.1006/viro.1995.1027

Hotton, S. K., and Callis, J. (2008). Regulation of cullin RING ligases. *Ann. Rev. Plant Biol.* 59, 467–489. doi: 10.1146/annurev.arplant.58.032806.104011

Hulsmans, S., Rodriguez, M., De Coninck, B., and Rolland, F. (2016). The SnRK1 energy sensor in plant biotic interactions. *Trends Plant Sci.* 21, 648–661. doi: 10.1016/j.tplants.2016.04.008

Hussain, M., Mansoor, S., Iram, S., Zafar, Y., and Briddon, R. W. (2007). The hypersensitive response to Tomato leaf curl New Delhi virus nuclear shuttle protein is inhibited by transcriptional activator protein. *Mol. Plant Microbe Interact.* 20, 1581–1588. doi: 10.1094/MPMI-20-12-1581

Ismayil, A., Haxim, Y., Wang, Y., Li, H., Qian, L., Han, T., et al. (2018). Cotton Leaf Curl Multan virus C4 protein suppresses both transcriptional and post-transcriptional gene silencing by interacting with SAM synthetase. *PLoS Pathog.* 14:e1007282. doi: 10.1371/journal.ppat.1007282

Jackel, J. N., Buchmann, R. C., Singhal, U., and Bisaro, D. M. (2015). Analysis of geminivirus AL2 and L2 proteins reveals a novel AL2 silencing suppressor activity. *J. Virol.* 89, 3176–3187. doi: 10.1128/JVI.02625-2614

Jackel, J. N., Storer, J. M., Coursey, T., and Bisaro, D. M. (2016). Arabidopsis RNA polymerases IV and V are required to establish H3K9 methylation, but not cytosine methylation, on geminivirus chromatin. *J. Virol.* 90, 7529–7540. doi: 10.1128/JVI.00656-616

Jada, B., Soitamo, A. J., and Lehto, K. (2013). Organ-specific alterations in tobacco transcriptome caused by the PVX-derived P25 silencing suppressor transgene. *BMC Plant Biol.* 13:229. doi: 10.1186/1471-2229-13-18

Jones, J. D. G., and Dangl, J. L. (2006). The plant immune system. *Nature* 444, 323–329. doi: 10.1038/nature05286

Jost, R., Altschmied, L., Bloem, E., Bogs, J., Gershenzon, J., Hähnel, U., et al. (2005). Expression profiling of metabolic genes in response to methyl jasmonate reveals regulation of genes of primary and secondary sulfur-related pathways in *Arabidopsis thaliana*. *Photosynth. Res.* 86, 491–508. doi: 10.1007/s11120-005-7386-7388

Krenz, B., Jeske, H., and Kleinow, T. (2012). The induction of stromule formation by a plant DNA-virus in epidermal leaf tissues suggests a novel intra- and intercellular macromolecular trafficking route. *Front. Plant Sci.* 3:291. doi: 10.3389/fpls.2012.00291

Kumar, R. V. (2019). "Classification, taxonomy and gene function of geminiviruses and their satellites," in *Geminiviruses: Impact, Challenges and Approaches*, ed. R. V. Kumar (Cham: Springer), 1–16. doi: 10.1007/978-3-030-18248-9_1

Kwade, Z., Swiatek, A., Azmi, A., Goossens, A., Inze, D., Van Onckelen, H., et al. (2005). Identification of four adenosine kinase isoforms in tobacco By-2 Cells and their putative role in the cell cycle-regulated cytokinin metabolism. *J. Biol. Chem.* 280, 17512–17519. doi: 10.1074/jbc.M411428200

Lacatus, G., and Sunter, G. (2008). Functional analysis of bipartite begomovirus coat protein promoter sequences. *Virology* 376, 79–89. doi: 10.1016/j.virol.2008.03.012

Lacatus, G., and Sunter, G. (2009). The Arabidopsis PEAPOD2 transcription factor interacts with geminivirus AL2 protein and the coat protein promoter. *Virology* 392, 196–202. doi: 10.1016/j.virol.2009.07.004

Legg, J. P., and Fauquet, C. M. (2004). Cassava mosaic geminiviruses in Africa. *Plant Mol. Biol.* 56, 585–599. doi: 10.1007/s11103-004-1651-1657

Li, F., Huang, C., Li, Z., and Zhou, X. (2014). Suppression of RNA silencing by a plant DNA virus satellite requires a host calmodulin-like protein to repress RDR6 Expression. *PLoS Pathog.* 10:e1003921. doi: 10.1371/journal.ppat.1003921

Li, F., Zhao, N., Li, Z., Xu, X., Wang, Y., Yang, X., et al. (2017). A calmodulin-like protein suppresses RNA silencing and promotes geminivirus infection by degrading SGS3 via the autophagy pathway in *Nicotiana benthamiana*. *PLoS Pathog.* 13:6213. doi: 10.1371/journal.ppat.1006213

Liu, L., Chung, H.-Y., Lacatus, G., Baliji, S., and Ruan, J. S. (2014). Altered expression of Arabidopsis genes in response to a multifunctional geminivirus pathogenicity protein. *BMC Plant Biol.* 14:30. doi: 10.1186/s12870-014-0302-307

Liu, L., Sonbol, F.-M., Huot, B., Gu, Y., Withers, J., Mwimba, M., et al. (2016). Salicylic acid receptors activate jasmonic acid signalling through a non-canonical pathway to promote effector-triggered immunity. *Nat. Commun.* 7:13099. doi: 10.1083/ncomms13099

Liu, Y., Schiff, M., Serino, G., Deng, X.-W., and Dinesh-Kumar, S. P. (2002). Role of SCF ubiquitin-ligase and the COP9 signalosome in the N gene-mediated resistance response to Tobacco mosaic virus. *Plant Cell* 14, 1483–1496. doi: 10.1105/tpc.002493

Lozano-Duran, R., Caracuel, Z., and Bejarano, E. R. (2012). C2 from Beet curly top virus meddles with the cell cycle: a novel function for an old pathogenicity factor. *Plant Signal. Behav.* 7, 1705–1708. doi: 10.4161/psb.22100

Lozano-Durán, R., Rosas-Díaz, T., Gusmaroli, G., Luna, A. P., Taconnat, L., Deng, X. W., et al. (2011). Geminiviruses subvert ubiquitination by altering CSN-mediated derubylation of SCF E3 ligase complexes and inhibit jasmonate signaling in *Arabidopsis thaliana*. *Plant Cell* 23, 1014–1032. doi: 10.1105/tpc.110.080267

Mandadi, K. K., and Scholthof, K.-B. G. (2013). Plant immune responses against viruses: how does a virus cause disease? *Plant Cell* 25, 1489–1505. doi: 10.1105/tpc.113.111658

Matic, S., Pegoraro, M., and Noris, E. (2016). The C2 protein of Tomato yellow leaf curl Sardinia virus acts as a pathogenicity determinant and a 16-amino acid domain is responsible for inducing a hypersensitive response in plants. *Virus Res.* 215, 12–19. doi: 10.1016/j.virusres.2016.01.014

Matzke, M., and Mosher, R. (2014). RNA-directed DNA methylation: an epigenetic pathway of increasing complexity. *Nat. Rev. Genet.* 15, 394–408. doi: 10.1038/nrg3683

Moffatt, B. A., Stevens, Y. Y., Allen, M. S., Snider, J. D., Pereira, L. A., Todorova, M. I., et al. (2002). Adenosine kinase deficiency is associated with developmental abnormalities and reduced transmethylation. *Plant Physiol.* 128, 812–821. doi: 10.1104/pp.010880

Mohannath, G., Jackel, J. N., Lee, Y. H., Buchmann, R. C., Wang, H., Patil, V., et al. (2014). A complex containing SNF1-related kinase (SnRK1) and adenosine kinase in *Arabidopsis*. *PLoS One* 9:e87592. doi: 10.1371/journal.pone.0087592

Molnar, A., Melnyk, C. W., Bassett, A., Hardcastle, T. J., Dunn, R., and Baulcombe, D. C. (2010). Small silencing RNAs in plants are mobile and direct epigenetic modification in recipient cells. *Science* 328, 872–875. doi: 10.1126/science.1187959

Mubin, M., Amin, I., Amrao, L., Briddon, R. W., and Mansoor, S. (2010). The hypersensitive response induced by the V2 protein of a monopartite begomovirus is countered by the C2 protein. *Mol. Plant Pathol.* 11, 245–254. doi: 10.1111/j.1364-3703.2009.00601.x

Nakahara, K. S., Masuta, C., Yamada, S., Shimura, H., Kashihara, Y., Wada, T. S., et al. (2012). Tobacco calmodulin-like protein provides secondary defense by binding to and directing degradation of virus RNA silencing suppressors. *Proc. Natl. Acad. Sci. U.S.A.* 109, 10113–10118. doi: 10.1073/pnas.1201628109

Palaqui, J. C., Elmayan, T., Pollien, J. M., and Vaucheret, H. (1997). Systemic acquired silencing: transgene-specific post-transcriptional silencing is transmitted by grafting from silenced stocks to non-silenced scions. *EMBO J.* 16, 4738–4745. doi: 10.1093/emboj/16.15.4738

Pikaard, C., and Mittelsten Scheid, O. (2014). Epigenetic regulation in plants. *Cold Spring Harb. Perspect. Biol.* 6:a019315. doi: 10.1101/cshperspect.a019315

Pilartz, M., and Jeske, H. (2003). Mapping of Abutilon mosaic geminivirus minichromosomes. *J. Virol.* 77, 10808–10818. doi: 10.1128/JVI.77.20.10808-10818

Pontes, O., and Pikaard, C. S. (2008). siRNA and miRNA processing: new functions for Cajal bodies. *Curr. Opin. Genet. Dev.* 18, 197–203. doi: 10.1016/j.gde.2008.01.008

Raja, P., Jackel, J. N., Li, S., Heard, I. M., and Bisaro, D. M. (2014). Arabidopsis double-stranded RNA binding protein DRB3 participates in methylation-mediated defense against geminiviruses. *J. Virol.* 88, 2611–2622. doi: 10.1128/JVI.02305-2313

Raja, P., Sanville, B. C., Buchmann, R. C., and Bisaro, D. M. (2008). Viral genome methylation as an epigenetic defense against geminiviruses. *J. Virol.* 82, 8997–9007. doi: 10.1128/JVI.00719-718

Raja, P., Wolf, J. N., and Bisaro, D. M. (2010). RNA silencing directed against geminiviruses: post-transcriptional and epigenetic components. *Biochim. Biophys. Acta Gene Regul. Mech.* 1799, 337–351. doi: 10.1016/j.bbagrm.2010.01.004

Rao, K., and Sunter, G. (2012). Sequences within the Spinach curly top virus virion sense promoter are necessary for vascular-specific expression of virion sense genes. *Virology* 432, 10–19. doi: 10.1016/j.virol.2012.05.007

Ratcliff, F., Harrison, B. D., and Baulcombe, D. C. (1997). A similarity between viral defense and gene silencing in plants. *Science* 276, 1558–1560. doi: 10.1126/science.276.5318.1558

Rausch, T., and Wachter, A. (2005). Sulfur metabolism: a versatile platform for launching defence operations. *Trends Plant Sci.* 10, 503–509. doi: 10.1016/j.tplants.2005.08.006

Rosas-Díaz, T., Macho, A. P., Beuzón, C. R., Lozano-Durán, R., and Bejarano, E. R. (2016). The C2 protein from the geminivirus Tomato yellow leaf curl sardinia virus decreases sensitivity to jasmonates and suppresses jasmonate-mediated defences. *Plants* 5:8. doi: 10.3390/plants5010008

Ruan, J., Perez, J., Hernandez, B., Lei, C., Sunter, G., and Sponsel, V. (2011). Systematic identification of functional modules and cis-regulatory elements in Arabidopsis thaliana. *BMC Bioinform.* 12(Suppl. 12):52. doi: 10.1186/1471-2105-12-S12-S2

Ruiz-Ferrer, V., and Voinnet, O. (2009). Roles of plant small RNAs in biotic stress responses. *Ann. Rev. Plant Biol.* 60, 485–510. doi: 10.1146/annurev.arplant.043008.092111

Santner, A., and Estelle, M. (2009). Recent advances and emerging trends in plant hormone signalling. *Nature* 459, 1071–1078. doi: 10.1038/nature08122

Scholthof, K. B., Adkins, S., Czosnek, H., Palukaitis, P., Jacquot, E., Hohn, T., et al. (2011). Top 10 plant viruses in molecular plant pathology. *Mol. Plant Pathol.* 12, 938–954. doi: 10.1111/j.1364-3703.2011.00752.x

Sharma, P., and Ikegami, M. (2010). Tomato leaf curl Java virus V2 protein is a determinant of virulence, hypersensitive response and suppression of posttranscriptional gene silencing. *Virology* 396, 85–93. doi: 10.1016/j.virol.2009.10.012

Shen, W., Dallas, M. B., Goshe, M. B., and Hanley-Bowdoin, L. (2014). SnRK1 phosphorylation of AL2 delays Cabbage leaf curl virus infection in *Arabidopsis*. *J. Virol.* 88, 10598–10612. doi: 10.1128/JVI.00671-14

Soitamo, A. J., Jada, B., and Lehto, K. (2012). Expression of geminiviral AC2 RNA silencing suppressor changes sugar and jasmonate responsive gene expression in transgenic tobacco plants. *BMC Plant Biol.* 12:204. doi: 10.1186/1471-2229-12-204

Stanley, J., and Gay, M. R. (1983). Nucleotide sequence of cassava latent virus DNA. *Nature* 301, 260–262. doi: 10.1038/301260a0

Sung, Y. K., and Coutts, R. H. A. (1995). Pseudorecombination and complementation between Potato yellow mosaic geminivirus and Tomato golden mosaic geminivirus. *J. Gen. Virol.* 76, 2809–2815. doi: 10.1099/0022-1317-76-11-2809

Sunter, G., and Bisaro, D. M. (1992). Transactivation of geminivirus AR1 and BR1 gene expression by the viral AL2 gene product occurs at the level of transcription. *Plant Cell* 4, 1321–1331. doi: 10.1105/tpc.4.10.1321

Sunter, G., and Bisaro, D. M. (1997). Regulation of a geminivirus coat protein promoter by AL2 protein (TrAP): evidence for activation and derepression mechanisms. *Virology* 232, 269–280. doi: 10.1006/viro.1997.8549

Sunter, G., and Bisaro, D. M. (2003). Identification of a minimal sequence required for activation of the Tomato golden mosaic virus coat protein promoter in protoplasts. *Virology* 305, 452–462. doi: 10.1006/viro.2002.1757

Sunter, G., Hartitz, M. D., and Bisaro, D. M. (1993). Tomato golden mosaic virus leftward gene expression: autoregulation of geminivirus replication protein. *Virology* 195, 275–280. doi: 10.1006/viro.1993.1374

Sunter, G., Stenger, D. C., and Bisaro, D. M. (1994). Heterologous complementation by geminivirus AL2 and AL3 genes. *Virology* 203, 203–210. doi: 10.1006/viro.1994.1477

Sunter, G., Sunter, J. L., and Bisaro, D. M. (2001). Plants expressing Tomato golden mosaic virus AL2 or Beet curly top virus L2 transgenes show enhanced susceptibility to infection by DNA and RNA viruses. *Virology* 285, 59–70. doi: 10.1006/viro.2001.0950

Thomma, B. P. H. J., Nürnberger, T., and Joosten, M. A. H. J. (2011). Of PAMPs and effectors: the blurred PTI-ETI dichotomy. *Plant Cell* 23, 4–15. doi: 10.1105/tpc.110.082602

Tjian, R. (1981). T antigen binding and the control of SV40 gene expression. *Cell* 26, 1–2. doi: 10.1016/0092-8674(81)90026-x

Trinks, D., Rajeswaran, R., Shivaprasad, P. V., Akbergenov, R., Oakeley, E. J., Veluthambi, K., et al. (2005). Suppression of RNA silencing by a geminivirus nuclear protein, AC2, correlates with transactivation of host genes. *J. Virol.* 79, 2517–2527. doi: 10.1128/JVI.79.4.2517-2527

Voinnet, O., Pinto, Y. M., and Baulcombe, D. C. (1999). Suppression of gene silencing: a general strategy used by diverse DNA and RNA viruses of plants. *PNAS* 96, 14147–14152. doi: 10.1073/pnas.96.24.14147

von Schwartzenberg, K., Kruse, S., Reski, R., Moffatt, B. A., and Laloue, M. (1998). Cloning and characterization of an adenosine kinase from *Physcomitrella* involved in cytokinin metabolism. *Plant J.* 13, 249–257. doi: 10.1023/A:1022576231875

Wang, H., Buckley, K. J., Yang, X., Buchmann, R. C., and Bisaro, D. M. (2005). Adenosine kinase inhibition and suppression of RNA silencing by geminivirus AL2 and L2 proteins. *J. Virol.* 79, 7410–7418. doi: 10.1128/JVI.79.12.7410-7418.2005

Wang, H., Hao, L., Shung, C.-Y., Sunter, G., and Bisaro, D. M. (2003). Adenosine kinase is inactivated by geminivirus AL2 and L2 proteins. *Plant Cell* 15, 3020–3032. doi: 10.1105/tpc.015180

Weretilnyk, E. A., Alexander, K. J., Drebenstedt, M., Snider, J. D., Summers, P. S., and Moffatt, B. A. (2001). Maintaining methylation activities during salt stress. The involvement of adenosine kinase. *Plant Physiol.* 125, 856–865. doi: 10.1104/pp.125.2.856

Wu, J., Du, Z., Wang, C., Cai, L., Hu, M., Lin, Q., et al. (2010). Identification of Pns6, a putative movement protein of RRSV, as a silencing suppressor. *Virol. J.* 7:335. doi: 10.1186/1743-422X-7-335

Yang, X., Baliji, S., Buchmann, R. C., Wang, H., Lindbo, J. A., Sunter, G., et al. (2007). Functional modulation of the geminivirus AL2 transcription factor and silencing suppressor by self-interaction. *J. Virol.* 81, 11972–11981. doi: 10.1128/JVI.00617-617

Yang, X., Xie, Y., Raja, P., Li, S., Wolf, J. N., Shen, Q., et al. (2011). Suppression of methylation-mediated transcriptional gene silencing by βC1-SAHH protein interaction during geminivirus-betasatellite infection. *PLoS Pathog.* 7:e1002329. doi: 10.1371/journal.ppat.1002329

Zerbini, F. M., Briddon, R. W., Idris, A., Martin, D. P., Moriones, E., Navas-Castillo, J., et al. (2017). ICTV virus taxonomy profile: geminiviridae. *J. Gen. Virol.* 98, 131–133. doi: 10.1099/jgv.0.000738

Zhang, Z., Chen, H., Huang, X., Xia, R., Zhao, Q., Lai, J., et al. (2011). BSCTV C2 attenuates the degradation of SAMDC1 to suppress DNA methylation-mediated gene silencing in *Arabidopsis*. *Plant Cell* 23, 273–288. doi: 10.1105/tpc.110.081695

Zhou, J., Yu, J.-Q., and Chen, Z. (2014). The perplexing role of autophagy in plant innate immune responses. *Mol. Plant Pathol.* 15, 637–645. doi: 10.1111/mpp.12118

Conflict of Interest: The authors declare that the research was conducted in the absence of any commercial or financial relationships that could be construed as a potential conflict of interest.

frontiers in Microbiology

ORIGINAL RESEARCH
published: 10 June 2020
doi: 10.3389/fmicb.2020.01243

Tomato Yellow Leaf Curl Virus V2 Protein Plays a Critical Role in the Nuclear Export of V1 Protein and Viral Systemic Infection

Wenhao Zhao[1,2], Shuhua Wu[1], Elizabeth Barton[2], Yongjian Fan[1], Yinghua Ji[1], Xiaofeng Wang[2]* and Yijun Zhou[1]**

[1] Institute of Plant Protection, Jiangsu Academy of Agricultural Sciences, Key Lab of Food Quality and Safety of Jiangsu Province-State Key Laboratory Breeding Base, Nanjing, China, [2] School of Plant and Environmental Sciences, Virginia Tech, Blacksburg, VA, United States

OPEN ACCESS

Edited by:
Rosa Lozano-Durán,
Shanghai Institutes for Biological Sciences (CAS), China

Reviewed by:
Ana P. Luna,
Institute of Subtropical and Mediterranean Horticulture La Mayora, Spain
Ana Grande-Pérez,
Institute of Subtropical and Mediterranean Horticulture La Mayora, Spain
Rena Gorovits,
Hebrew University of Jerusalem, Israel

***Correspondence:**
Yinghua Ji
jiyinghua@jaas.ac.cn
Xiaofeng Wang
reachxw@vt.edu
Yijun Zhou
yjzhou@jaas.ac.cn

Specialty section:
This article was submitted to Virology, a section of the journal Frontiers in Microbiology

Received: 22 January 2020
Accepted: 14 May 2020
Published: 10 June 2020

Citation:
Zhao W, Wu S, Barton E, Fan Y, Ji Y, Wang X and Zhou Y (2020) Tomato Yellow Leaf Curl Virus V2 Protein Plays a Critical Role in the Nuclear Export of V1 Protein and Viral Systemic Infection. Front. Microbiol. 11:1243. doi: 10.3389/fmicb.2020.01243

Geminiviruses are an important group of circular, single-stranded DNA viruses that cause devastating diseases in crops. Geminiviruses replicate their genomic DNA in the nucleus and the newly synthesized viral DNA is subsequently transported to the cytoplasm for further cell-to-cell and long-distance movement to establish systemic infection. Thus, nucleocytoplasmic transportation is crucial for successful infection by geminiviruses. For *Tomato yellow leaf curl virus* (TYLCV), the V1 protein is known to bind and shuttle viral genomic DNA, however, the role of the V2 protein in this process is still unclear. Here, we report that the V1 protein is primarily localized in the nucleus when expressed but the nucleus-localized V1 protein dramatically decreases when co-expressed with V2 protein. Moreover, the V2-facilitated nuclear export of V1 protein depends on host exportin-α and a specific V1-V2 interaction. Chemical inhibition of exportin-α or a substitution at cysteine 85 of the V2 protein, which abolishes the V1-V2 interaction, blocks redistribution of the V1 protein to the perinuclear region and the cytoplasm. When the $V2^{C85S}$ mutation is incorporated into a TYLCV infectious clone, the TYLCV-C85S causes delayed onset of very mild symptoms compared to wild-type TYLCV, suggesting that the V1-V2 interaction and, thus, the V2-mediated nuclear export of the V1 protein is crucial for viral spread and systemic infection. Our data point to a critical role of the V2 protein in promoting the nuclear export of the V1 protein and viral systemic infection, likely by promoting V1 protein-mediated nucleocytoplasmic transportation of TYLCV genomic DNA.

Keywords: ***tomato yellow leaf curl virus*** **(TYLCV), V2 protein, V1 protein, nuclear export, viral systemic infection**

INTRODUCTION

Geminiviruses are a group of plant viruses with a circular, single-stranded DNA genome. Viruses in this family cause devastating diseases in crop plants, leading to worldwide agricultural losses (Nakhla and Maxwell, 1997; Moriones and Navas-Castillo, 2000; Gafni, 2003; Fauquet et al., 2008; Glick et al., 2009; Fondong, 2019; Zeng et al., 2020). While viral protein synthesis occurs in

the cytoplasm, replication of geminiviruses occurs in the nucleus of infected host cells (Hanley-Bowdoin et al., 2013). It is crucial that viral proteins involved in this replication enter the nucleus to execute their functions. In addition, newly synthesized viral genomic DNA is exported from the nucleus to the cytoplasm for further spread to adjacent cells followed by systemic infection through long-distance movement. Therefore, the nucleocytoplasmic shuttling of geminivirus proteins and genomic DNA is of great significance for viral systemic infection and a better understanding of the process will potentially provide new strategies to control viral infections.

Geminiviruses can be divided into two major groups based on their genomic components: one group is the monopartite geminiviruses, while the other group is the bipartite geminiviruses (Hanley-Bowdoin et al., 2013). The movement of bipartite geminiviruses requires two proteins, BV1 and BC1, which are encoded by DNA-B (Brough et al., 1988; Etessami et al., 1988; Padidam et al., 1995; Jeffrey et al., 1996; Sudarshana et al., 1998). BV1 is a nuclear shuttle protein and plays an important role in the nucleocytoplasmic shuttling of viral genomic DNA; BC1 facilitates cell-to-cell movement (Brough et al., 1988; Etessami et al., 1988; Jeffrey et al., 1996; Sudarshana et al., 1998; Lazarowitz and Beachy, 1999).

The genome of monopartite geminiviruses contains only one component, DNA-A. The possible mechanism for viral genomic DNA shuttling between the nucleus and the cytoplasm is not clear even though several monopartite geminiviruses have been examined, such as *Maize streak virus* (MSV) and *Tomato yellow leaf curl virus* (TYLCV) (Liu et al., 2001; Rojas et al., 2001; Gafni and Epel, 2002; Gorovits et al., 2016). It has been reported that the V1 protein, which is the coat protein (CP) of TYLCV, binds to and shuttles viral genomic DNA between the nucleus and cytoplasm in addition to packaging them in viral particles at a later stage (Boulton et al., 1989, 1993; Lazarowitz and Beachy, 1999). It was later reported that host proteins are also required for this process. Nuclear import receptor karyopherin α1 (KAPα) helps TYLCV enter the nucleus (Kunik et al., 1999; Yaakov et al., 2011), HSP70 (heat shock protein) is important for the TYLCV CP shuttle from cytoplasm into nucleus (Gorovits et al., 2016; Gorovits and Czosnek, 2017), and exportin-α is required for the nuclear export of the C4 protein of *Tomato leaf curl Yunnan virus* (TLCYnV) (Mei et al., 2018). In addition, nuclear shuttling of monopartite geminiviruses also involves viral proteins other than V1 protein, such as C4 or V2 protein, suggesting that a protein complex may be involved (Rojas et al., 2001, 2005; Mei et al., 2018). However, it is unclear what viral proteins and how they work together to accomplish the transportation between the nucleus and cytoplasm.

Tomato yellow leaf curl virus is a typical monopartite begomovirus in the family *Geminiviridae*. The single-stranded (ss) DNA genome has six open reading frames (ORFs) and an intergenic region (IR). Two ORFs (V1 and V2) are located on the viral strand and the other four ORFs (C1, C2, C3 and C4) are located on the complementary strand (Navot et al., 1991). Among them, V1 protein facilitates virion assembly and viral trafficking (Gafni, 2003; Rojas et al., 2001; Díaz-Pendón et al., 2010; Scholthof et al., 2011). For the nucleocytoplasmic transportation of TYLCV, V1 protein is well-known as a nuclear shuttle protein and for its role in binding viral genomic DNA (Kunik et al., 1998, 1999; Palanichelvam et al., 1998; Rojas et al., 2001). However, several lines of evidence suggest that other viral proteins, such as V2, are also involved (Kunik et al., 1999; Rojas et al., 2001; Jeske, 2009; Fondong, 2013; Hanley-Bowdoin et al., 2013; Sahu et al., 2014). Rojas et al. (2001) found that the efficiency of nuclear export of viral DNA was enhanced 20–30% in the presence of V2 protein, suggesting a role for V2 protein in the V1 protein-mediated nuclear export of viral genomic DNA. However, the mechanism whereby V2 protein facilitates the V1-mediated viral genomic DNA trafficking out of the nucleus is unknown.

In this study, we demonstrate that V2 protein affects the subcellular localization of V1 protein by dramatically decreasing the nucleus-localized V1 protein in *Nicotiana benthamiana* cells, possibly through host exportin-α (XPO I), which often mediates the nuclear export of proteins. A specific interaction between V2 and V1 proteins has been identified by co-immunoprecipitation (Co-IP) and bimolecular fluorescence complementation (BiFC). Substitutions for cystine 85 in V2 protein inhibit the V1-V2 interaction, block the effect of V2 protein on the subcellular localization of V1 protein, and cause delayed and mild symptom in plants. Our results indicate that the V2 protein interacts with V1 protein, promotes the nuclear export of V1 protein, and plays an important role in viral systemic infection.

RESULTS

V2 Protein Affects the Nuclear Localization of V1 Protein

Tomato yellow leaf curl virus V1 protein is known as a nucleocytoplasmic shuttle protein that facilitates the transport of viral genomic DNA into and out of the nucleus. When expressed in cells of *N. benthamiana* by agroinfiltration as a YFP-tagged protein, V1-YFP, the signal was found in both the nucleus and cytoplasm at 40 h post agroinfiltration (hpai) (**Figure 1A**), consistent with its role in the nuclear transportation of viral genomic DNA. Among 100 cells with a clear nuclear region, strong YFP signal was detected in all cells (**Figure 1A**).

Since V2 protein was reported to facilitate the export of viral genomic DNA from the nucleus (Rojas et al., 2001), we tested whether V2 protein does so by promoting the nucleus export of the V1 protein. We first tested for the subcellular localization of V2 protein as a YFP-tag (V2-YFP) in *N. benthamiana* cells via agroinfiltration. The fluorescence signal was observed under a laser confocal microscope at 40 hpai. Large aggregates of V2-YFP were easily observed when high concentrations of agrobacteria were used for infiltration (**Supplementary Figure S1**). However, fewer aggregates were observed at OD_{600} = 0.5 for infiltration (**Supplementary Figure S1**). In addition, V2-YFP was mainly present in the cytoplasm and perinuclear regions, but a much weaker signal was also present in the nucleus (**Figure 1B**). To better examine the distribution of V2-YFP in the nuclear region, V2-YFP was expressed by infiltration of agrobacterium at OD_{600} = 0.5.

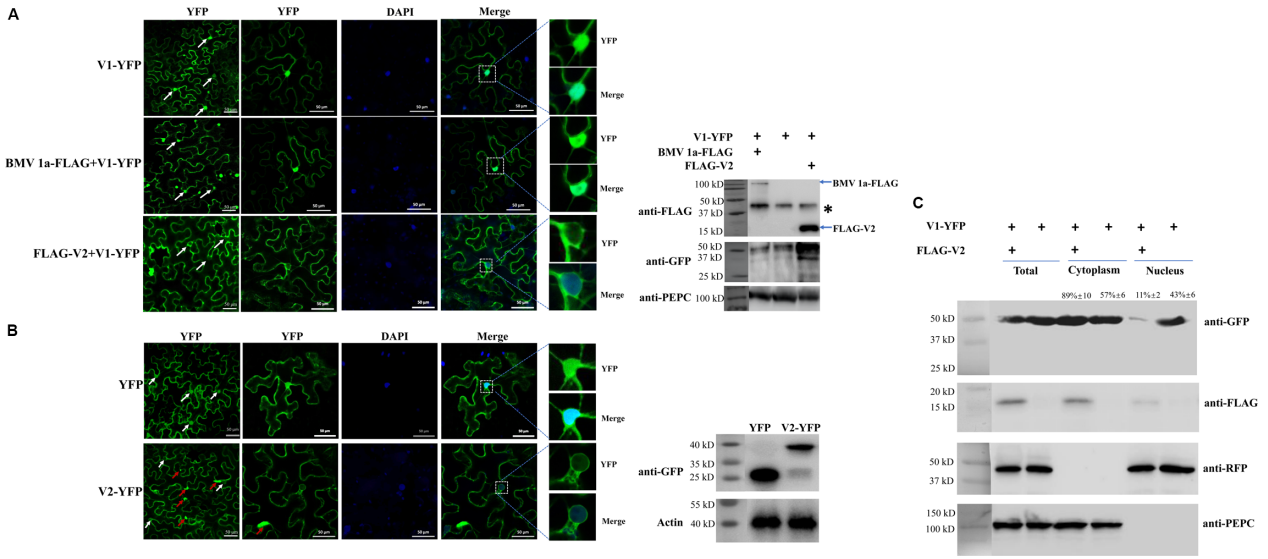

FIGURE 1 | The effect of V2 protein on the nuclear distribution of V1 protein. **(A)** Localization of the V1 protein in the absence or presence of the V2 protein in *N. benthamiana* cells. V1-YFP expressed alone, co-expressed with BMV 1a-FLAG or FLAG-V2, detected either by confocal microscopy (left panel) or by western blotting using an anti-GFP polyclonal antibody (right panel). Arrows point to the nuclear areas in cells. DAPI stains DNA in the nucleus. PEPC serves as a control for equal loading of total lysates. Asterisk indicates a non-specific bands detected in all samples. Bars: 50 μm. **(B)** Localization of V2 in *N. benthamiana* cells. The expressed YFP or V2-YFP in epidermal cells of *N. benthamiana* leaves was detected either by confocal microscopy (left panel) or by western blotting using an anti-GFP polyclonal antibody (right panel). White arrows point to the nuclear areas in cells as shown in left column. Red arrows point to V2 aggregates. DAPI stains DNA in the nucleus. Bars: 50 μm. **(C)** Distribution of V1 protein in the absence or presence of FLAG-V2 in H2B-RFP transgenic *N. benthamiana* plants as analyzed by using a nuclear-cytoplasmic fractionation assay. Nuclei were purified using percoll density gradient centrifugation. Western blotting was conducted with antibodies specific to the indicated proteins. PEPC and H2B-RFP were used as a marker for the cytoplasmic and nuclear fraction, respectively. The intensity of protein signal was measured by using ImageQuant TL (GE healthcare), with levels of the cytoplasm plus the nucleus levels totaling 100%.

To further clarify the function of V2 protein in the nuclear export of TYLCV, we co-expressed FLAG-tagged V2 protein (FLAG-V2) with V1-YFP. Interestingly, a strong nuclear YFP signal was only detected in ∼13% of cells (n = 100). In about 87% of cells, only a weak fluorescence signal of the V1 protein was found in the nucleus compared to that of V1 protein alone (**Figure 1A**). To rule out the possibility that the weaker signal of V1-YFP in the nucleus was due to a decreased expression and/or stability in the presence of V2, we checked the accumulation of V1-YFP by western blotting. Our results showed that both V2 and V1 proteins were accumulated well when co-expressed (**Figure 1A**). Because V2 protein functions as a gene silencing suppressor, an increased accumulation of V1-YFP was noticed when it was co-expressed with FLAG-V2, indicating that the lower V1-YFP signal in the nucleus was not due to its decreased accumulation in the presence of FLAG-V2. To further rule out the possibility that overexpression of any protein may affect the distribution of V1 protein, we included replication protein 1a of *Brome mosaic virus* (BMV) (Diaz and Wang, 2014; Zhang et al., 2019). BMV 1a is an ER membrane-associated protein and redistributes specific host proteins to perinuclear ER membrane-invaginated viral replication complexes (Diaz and Wang, 2014; Diaz et al., 2015; Zhang et al., 2016). However, when co-expressed with V1-YFP, FLAG-tagged BMV 1a (BMV 1a-FLAG) did not show any effect on the localization of V1-YFP, as a strong signal was detected in the nucleus in all cells with detectable YFP signal (n = 100, **Figure 1A**), indicating that the redistribution of V1 protein is specifically mediated by V2 protein.

To confirm our visual observations, we performed a fractionation assay to separate the nucleus from the cytoplasm (Mei et al., 2018) and tested the localization of V1-YFP in the absence and presence of V2 protein. To this end, we expressed FLAG-V2 and V1-YFP in Histone 2B (H2B)-RFP transgenic plants (Martin et al., 2009). As shown in **Figure 1C**, we only detected H2B-RFP in the nuclear fraction but not the cytoplasmic fraction; a cytoplasmic marker, phosphoenolpyruvate carboxylase (PEPC), was only present in the cytoplasm fraction. Under such conditions, FLAG-V2 was primarily detected in the cytoplasm fraction but only weakly in the nucleus. Although V1-YFP was detected in both fractions when expressed alone, the amount in the nuclear fraction significantly decreased in the presence of FLAG-V2, which was consistent with the results based on fluorescence microscopy (**Figure 1C**). To provide a numeric reading, we set the sum of V1-YFP signal intensity in the cytoplasm and nucleus at 100%. In the absence of FLAG-V2, we found that 43% of V1-YFP was associated with the nuclear fraction but decreased to 11% in the presence of FLAG-V2. We concluded from these results that V2 protein is able to change the localization of V1 protein.

V2 Protein Interacts With V1 Protein

We then set out to understand the underlying mechanism by which V2 protein affects the subcellular localization of V1 protein

by first testing whether there is an interaction between V2 and V1 proteins. We used a co-immunoprecipitation (Co-IP) assay because V1 protein is self-activating in the yeast two-hybrid (Y2H) system. FLAG-tagged V2 protein (FLAG-V2) was co-expressed with YFP or V1-YFP in *N. benthamiana*. Total protein extracts were subject to immunoprecipitation by using FLAG-trap beads, and the resulting precipitates were analyzed by an anti-GFP antibody or an anti-FLAG antibody. Although a similar amount of FLAG-V2 was pulled down with FLAG-trap beads, only V1-YFP, and not YFP, was pulled down along with FLAG-V2 (**Figure 2A**).

The fact that the V1 protein was co-precipitated with V2 protein suggests that V2 protein may bind to V1 protein to form a V1-V2 protein complex. To confirm the V1-V2 interaction and identify the location where V1 and V2 proteins may form a complex, we used a bimolecular fluorescence complementation (BiFC) assay. A positive interaction between nYFP-V1 and cYFP-V2 was observed in both the cytoplasm and perinuclear region, as indicated by the presence of reconstituted fluorescence (**Figure 2B**). We also noticed a faint fluorescence signal inside the nucleus. It should be noted that V1-YFP also localized in the cytoplasm and the perinuclear region when it was co-infiltrated with FLAG-V2 (**Figure 1A**), suggesting that V2 protein binds V1 protein at the perinucleus and the cytoplasm. No fluorescence signal was generated when nYFP-V1 and cYFP, or nYFP and cYFP-V2, or nYFP and cYFP were co-expressed (**Figure 2B**), reinforcing a specific interaction between V2 and V1 proteins in plant cells.

V2 Protein Mediates the Nuclear Export of V1 Protein Through Host Exportin-α

The fact that V2 protein hanged the nuclear localization of the V1 protein, raised the possibility that V2 protein might help V1 protein to export from the nucleus to the cytoplasm or block the entrance of V1 protein into the nucleus. Because the nuclear export of proteins is often mediated by exportin-α, we tested the subcellular localization of V2 protein upon treatment with leptomycin B (LMB), an inhibitor of exportin-α (Mathew and Ghildyal, 2017). As expected, the level of nucleus-localized V2-YFP increased after LMB treatment (**Figure 3A**), suggesting that V2 protein depends on exportin-α to move out of the nucleus. To confirm our observation, we performed a nuclear-cytoplasmic fractionation assay on H2B-RFP transgenic *N. benthamiana* plants expressing V2-YFP with or without LMB treatment. As shown in **Figure 3B**, H2B-RFP and PEPC were specifically detected, as expected, in the nuclear and cytoplasmic fractions, respectively. About 32% of the total V2-YFP accumulated in the nucleus but increased to 54% with the LMB treatment (**Figure 3B**), agreeing well with our imaging results (**Figure 3A**).

We also checked whether V2-mediated V1-YFP relocalization can be affected by the LMB treatment. Co-expressed with FLAG-V2, V1-YFP had very low accumulation in the nucleus (top panel, **Figure 3C**), but a strong nuclear signal was observed after treatment with LMB (second panel, -DMSO, **Figure 3C**), suggesting that V2-mediated nuclear relocalization of V1 protein is similar to the V2 protein export, which depends on exportin-α. The fact that both V1 and V2 proteins accumulated in the nucleus in the presence of LMB strongly suggested that V2 protein did not block the nuclear import of V1 protein but rather promoted the nuclear egress of V1 protein.

To confirm the specific effect of LMB on localizations of V1 and V2 proteins, we further infiltrated LMB-treated cells with 0.5% dimethyl sulfoxide (DMSO), which makes LMB unstable and thus, LMB becomes inactive (Mei et al., 2018). As expected, the V1-YFP signal was detected in the nucleus in the presence of FLAG-V2 and LMB at the beginning of the DMSO treatment (second panel, -DMSO, **Figure 3C**). However, the V1-YFP signal in the nucleus decreased gradually after a longer DMSO treatment that eliminated the inhibitory effect of LMB (**Figure 3C**).

To verify the nucleocytoplasmic shuttling of the V1-V2 complex, we performed a BiFC assay applying the same treatments as above. In the presence of LMB only, the reconstituted YFP signal was strongly detected in the nucleus (**Figure 3D**), indicating that the V1-V2 complex was also present in the nucleus as well as in the cytoplasm and perinuclear region (**Figure 2B**). After DMSO treatment for 2 h, the nucleus-localized YFP signal substantially decreased, which was accompanied by a ∼13% increase of the signal intensity in the cytoplasmic region, suggesting an exportin-α-mediated nuclear export of the V1-V2 complex (**Figure 3D**). These results indicated that the nucleocytoplasmic shuttling of V1 protein is dependent on the V2 protein and exportin-α.

A V2 C85A Mutant Abolishes the V1-V2 Interaction

To verify that the V1-V2 interaction plays a crucial role in the nuclear export of V1 protein and to identify the approximate sites in V2 protein that are responsible for the interaction, we constructed six V2 mutants from a region (**Figure 4A**) that plays an important role in the V2-V2 self-interaction (Zhao et al., 2018) and the interaction between V2 and host proteins (Glick et al., 2008). We then tested their interactions with V1 protein using the Co-IP assay. Among the six V2 mutants, five of them (G70A, S71A, K73A, C84AC86A, and T96A) interacted with V1 protein as well as that of wt (data not shown). However, the $V2^{C85A}$ mutant, which has a cysteine to alanine substitution in the residue at position 85, was not pulled down well along with FLAG-V1 because only a much weaker band was detected compare to that of wt V2-YFP (**Figure 4B**). The alanine substitution did not affect expression and stability of the $V2^{C85A}$ mutant because V2-YFP and $V2^{C85A}$-YFP accumulated at similar levels (top, Input panel, **Figure 4B**).

It is well-known that V2 protein is involved in PTGS by binding to tomato SGS3 (SlSGS3), an ortholog of the Arabidopsis SGS3 protein (Glick et al., 2008). It was confirmed that a double mutant of V2, $V2^{C84SC86S}$, does not interact with SlSGS3 and lost its function as a suppressor of gene silencing (Glick et al., 2008). Given the fact that C85 is adjacent to C84 and C86, it is possible that $V2^{C85A}$ may be dysfunctional not only in interacting with V1 protein but also with SlSGS3. To this end, we confirmed that $V2^{C85A}$, but not $V2^{C84AC86A}$,

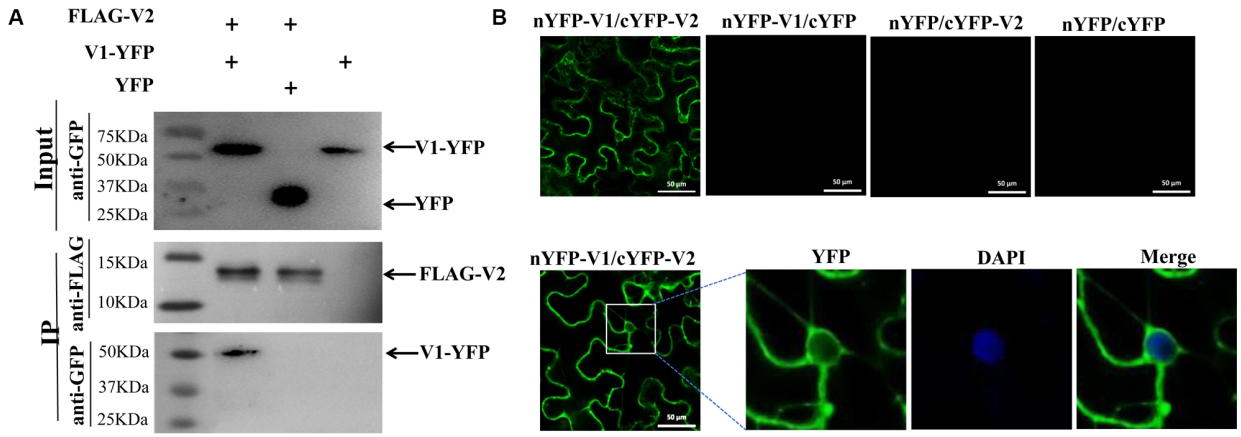

FIGURE 2 | Identification of the interaction between V2 and V1 proteins. **(A)** Co-IP analysis of the interaction between FLAG-V2 and V1-YFP. *N. benthamiana* leaves were co-infiltrated with FLAG-V2 and V1-YFP (Lane 1), FLAG-V2 and YFP (Lane 2), or V1-YFP alone (Lane 3). Cell lysates were incubated with FLAG-trap beads and subsequently washed extensively. Samples before (Input) and after (IP) immunoprecipitation were analyzed using anti-GFP or -FLAG antibody. **(B)** BiFC assays for the interaction between V1 and V2 proteins in *N. benthamiana* cells. The V1-V2 interaction leads to a reconstituted fluorescence signal. DAPI stains DNA in the nucleus. Bars: 50 μm.

interacted with SlSGS3 in the Y2H system (**Figure 4C**), indicating that the C85A substitution specifically blocked the V1-V2 interaction but did not disrupt other functions of the V2 protein, such as the ability to interact with SlSGS3, which leads to a block of host gene silencing-mediated host defense. To directly test whether C85A may disrupt the activity of V2 protein in suppressing gene silencing, we transiently expressed wt V2 or $V2^{C85A}$ in GFP-silenced 16c *N. benthamiana* plants (Nawaz-ul-Rehman et al., 2010). To induce gene silencing of GFP, *Agrobacterium* harboring a GFP expression vector was transiently infiltrated into the GFP transgenic line 16c at a 4-leaf stage. After five days post agroinfiltration, GFP expression was systematically silenced and no fluorescence signal was detected (**Supplementary Figure S2a**). These GFP-silenced leaves were then infiltrated with *Agrobacterium* harboring the vector expressing wt V2 or $V2^{C85A}$. Strong GFP signal was recovered when the p19 protein of *Tomato bushy stunt virus* (TBSV) was expressed as a positive control (**Supplementary Figure S2b**). As expected, the expression of wt V2 led to a detectable GFP signal in the infiltrated region, even though not as strong as that of the p19-infiltrated area (**Supplementary Figure S2b**; Zrachya et al., 2007). Expressing $V2^{C85A}$ also recovered GFP signal to the level similar to that of wt V2. Quantitative reverse transcription-PCR (qRT-PCR) further confirmed that similar levels of GFP transcripts were accumulated in the plants expressing wt V2 or the $V2^{C85A}$ mutant (**Supplementary Figure S2c**), consistent with the note that C85A mutant had no effect on the gene silencing suppression activity of V2 protein.

To further confirm that C85, but not C84 and C86, is crucial for the V1-V2 interaction, we also tested the ability of $V2^{C84AC86A}$ (**Figure 4A**) to interact with the V1 protein. The Co-IP assay indicated that the $V2^{C84AC86A}$ mutant interacted with the V1 protein (**Figure 4D**). Taken together, the activities of the V2 protein in interacting with the V1 protein and SlSGS3 can be separated, where the C85A mutation blocks V2 protein's interaction with V1 protein but not with SlSGS3.

The $V2^{C85A}$ Mutant Fails to Redistribute the V1 Protein

After confirming that $V2^{C85A}$ accumulated well and interacted with SlSGS3 but not V1 protein, we next checked the localization of $V2^{C85A}$ by expressing YFP-tagged $V2^{C85A}$ ($V2^{C85A}$-YFP) in *N. benthamiana* cells. In 56% of cells expressing $V2^{C85A}$-YFP (**Figure 5B**), a fluorescence signal was observed in the cytoplasm and perinuclear region (**Figure 5A**), similar to that of wild-type (wt) V2-YFP. In 44% of cells, however, the fluorescence signal was more spread than that of V2-YFP and was also observed in an elongated region beyond the DAPI-stained nucleus (**Figure 5A**). The nature of the localization remains to be determined. It needs to note that the C85A mutation did not affect the expression or stability of V2-YFP because $V2^{C85A}$-YFP accumulated at a similar level as V2-YFP (**Figures 4B**, **5C**). These results indicated that C85 has some effects on the perinuclear localization of the V2 protein.

To test the effect of C85A substitution in V2 protein on the localization of V1, FLAG- $V2^{C85A}$ was co-expressed with V1-YFP in *N. benthamiana* cells. A strong V1-YFP signal was detected in the nucleus in the presence of FLAG- $V2^{C85A}$, similar to that when V1-YFP was expressed alone (**Figure 5D**). Among 50 cells that were examined for the localization of V1 protein, no obvious difference in the V1-YFP distribution pattern was observed in the absence or presence of $V2^{C85A}$ (**Figure 5E**), suggesting that $V2^{C85A}$ was not able to affect the nuclear localization of V1 protein. Because V1-YFP accumulated at a higher level in the presence of $V2^{C85A}$ compared to that in the absence of $V2^{C85A}$ (**Figure 5F**), we propose that the disrupted V1-V2 interaction is responsible for the failed redistribution of V1-YFP. However, we cannot totally rule out the possibility that other uncharacterized functions might be affected by alanine replacement.

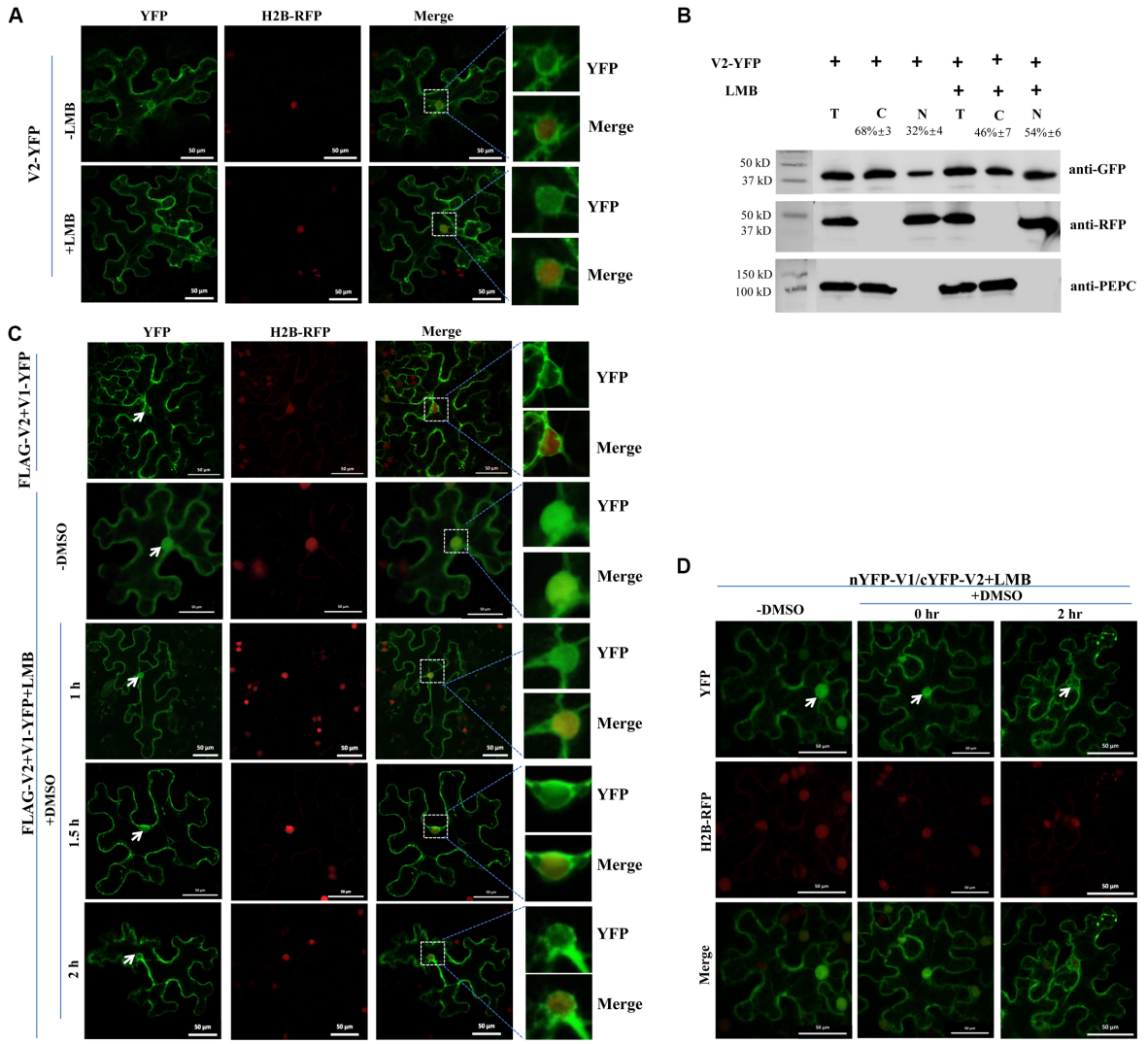

FIGURE 3 | The V2-mediated nuclear export of V1 protein is dependent on exportin-α. **(A)** Subcellular distribution of V2-YFP without or with the LMB treatment in cells of the H2B-RFP transgenic *N. benthamiana* plant. Leaf tissues were first agroinfiltrated with V2-YFP for 40 h, followed by 10 nM LMB for 2 hours. The H2B-RFP signal represents the nucleus. Bars: 50 μm. **(B)** Nuclear-cytoplasmic fractionation analysis of the distribution of V2 with or without LMB treatment in H2B-RFP transgenic *N. benthamiana* plants. Western blotting analysis was conducted with antibodies specific to the indicated proteins. PEPC and H2B-RFP were used as a marker for the cytoplasmic and nuclear fraction, respectively. The intensity of protein signal was measured by using ImageQuant TL (GE healthcare), with levels of the cytoplasm plus the nucleus totaling 100%. **(C)** Subcellular distribution of V1-YFP co-expressed with FLAG-V2 upon the treatment of LMB and DMSO in H2B-RFP transgenic *N. benthamiana* cells. Leaf tissues expressing FLAG-V2 and V1-YFP were first infiltrated with 10 nM LMB for 2 hours and followed by infiltration of 0.5% DMSO to degrade LMB. The YFP signal was observed at specific time points as indicated. Arrows indicate the V1-YFP signal in or around the nucleus at different time points. H2B-RFP signal represents the nucleus. Bars: 50 μm. **(D)** Effects of LMB treatment on the V1-V2 interaction as shown by BiFC in H2B-RFP transgenic *N. benthamiana* plants. Plant tissues co-expressing nYFP-V1 with cYFP-V2 were treated with LMB for 2 h to inactivate exportin-α and then infiltrated with 0.5% DMSO to degrade LMB. Confocal micrographs were taken at the indicated time points. Arrows indicate the reconstituted YFP signal in or around the nucleus at different time points. The H2B-RFP signal represents the nucleus. Bars: 50 μm.

A C85 Substitution in V2 Protein Delays Viral Systemic Infection

To assess the role of the V1-V2 interaction in viral infection, we incorporated a substitution in the C85 of the V2 ORF in the backbone of an infectious TYLCV clone. As the V2 ORF overlaps with the V1 ORF in the TYLCV genome, mutations in V2 may affect V1 amino acid sequence. To ensure that a specific change in C85 has no effect on the V1 protein in TYLCV genome, the C85S mutation, instead of the C85A mutation, was introduced into a TYLCV clone to generate TYLCV-C85S. It needs to be addressed that the $V2^{C85S}$ mutant did not interact with V1 protein (**Supplementary Figure S3a**), but interacted with SlSGS3 (**Supplementary Figure S3b**), and in turn, maintained its activity as a suppressor of gene silencing (**Supplementary Figures S2b,c**). Most importantly, the $V2^{C85S}$ mutant did not affect the subcellular localization of V1-YFP

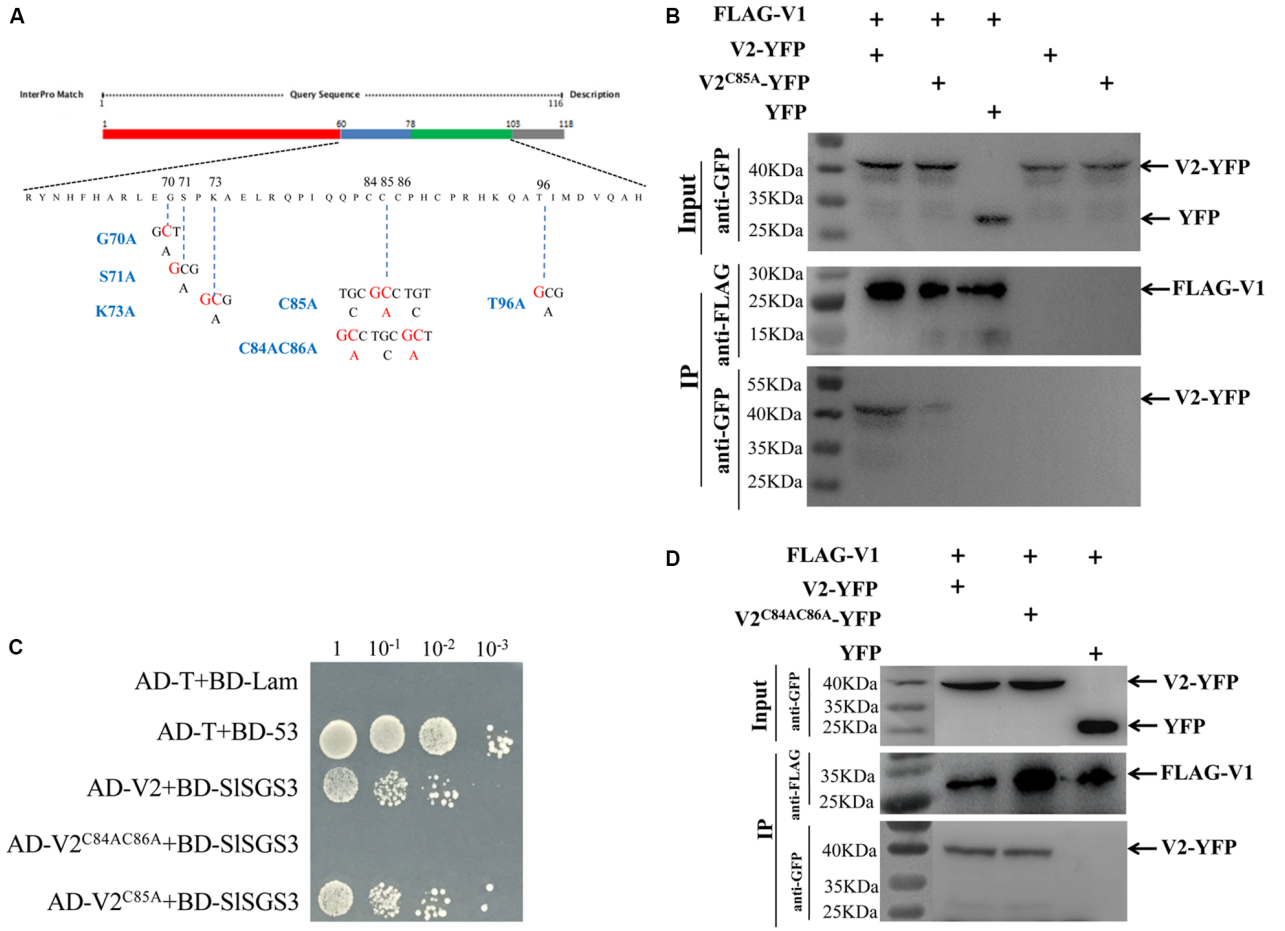

FIGURE 4 | Identification of critical sites in the V2 protein responsible for the V1-V2 interaction. **(A)** Schematic illustration of the V2 protein. Nucleic acid and amino acid sequences of V2 mutants, $V2^{G70A}$, $V2^{S71A}$, $V2^{K73A}$, $V2^{C85A}$, $V2^{C84AC86A}$, and $V2^{T96A}$ are shown. **(B)** The interaction between V1 and wt V2 or $V2^{C85A}$ is examined by a co-IP assay. The Co-IP assay was performed as in **Figure 2A**. **(C)** Y2H detecting possible interactions between SlSGS3 and $V2^{C85A}$ or $V2^{C84AC86A}$. $V2^{C85A}$ and $V2^{C84AC86A}$ were fused with a GAL4 activation domain (AD-$V2^{C85A}$ and AD-$V2^{C84AC86A}$), and SlSGS3 was fused to a GAL4-binding domain (BD-SlSGS3), respectively. AH109 cells co-transformed with the indicated plasmids were subjected to 10-fold serial dilutions and plated on synthetic-defined medium SD/-His/-Leu/-Trp medium to screen for positive interactions. Yeast cells co-transformed with AD-T + BD-53 or AD-T + BD-Lam serve as positive control or negative controls, respectively. **(D)** Co-IP assay to show the interaction between V1 and V2 or $V2^{C84AC86A}$. The Co-IP assay was performed as in **Figure 2A**.

(**Supplementary Figure S3c**), similar to the properties of $V2^{C85A}$. TYLCV-C85S and TYLCV were subsequently used to inoculate tomato (*Solanum lycopersicum*) and *N. benthamiana* plants.

Fifteen tomato plants were inoculated with either wt TYLCV or TYLCV-C85S. Symptoms such as chlorosis on leaves were obviously observed at 13 days post-infection (dpi) on tomato plants inoculated with wt TYLCV but not in the plants inoculated with TYLCV-C85S. The vast majority of TYLCV-C85S-inoculated tomato plants remained symptomless even at 33 dpi and only 1-2 plants among 15 eventually developed mild symptoms, such as leaf yellowing (**Figures 6A,B**). In addition, the average height of TYLCV-C85S-inoculated tomato plants was 32 ± 3.4 cm, which was higher than that of TYLCV-inoculated plants at 22 ± 2.0 cm (**Figure 6C**). Real-time PCR showed that levels of viral genomic DNA were much lower in systemic leaves of plants inoculated with TYLCV-C85S than those in plants inoculated with wt TYLCV at 13, 23, and 33 dpi (**Figure 6D**). These were consistent with the presence of typical symptoms in wt TYLCV-infected plants but no or very mild symptoms in TYLCV-C85S-infected plants at 33 dpi (**Figures 6A,B**).

Similar results were also obtained in TYLCV-C85S-inoculated *N. benthamiana* plants. All wt TYLCV-inoculated plants showed symptoms as early as 13 dpi, such as leaf yellowing and curling as shown in **Figure 7A**. However, only 3-4 out of fifteen plants inoculated with TYLCV-C85S showed mild symptoms (**Figure 7B**). We did notice that plants infected by TYLCV-C85S were shorter (18 ± 1.1 cm) compared to healthy plants at 30 ± 2.0 cm (**Figure 7C**). The accumulated TYLCV genomic DNA (**Figure 7D**) in systemic leaves of TYLCV-C85S-inoculated plants were much lower than those in wt TYLCV-inoculated plants at 13, 23, and 33 dpi, consistent with the presence of typical symptoms in systemic leaves of wt TYLCV-inoculated plants but no or very mild symptoms in systemic leaves of TYLCV-C85S-inoculated plants (**Figure 7A**).

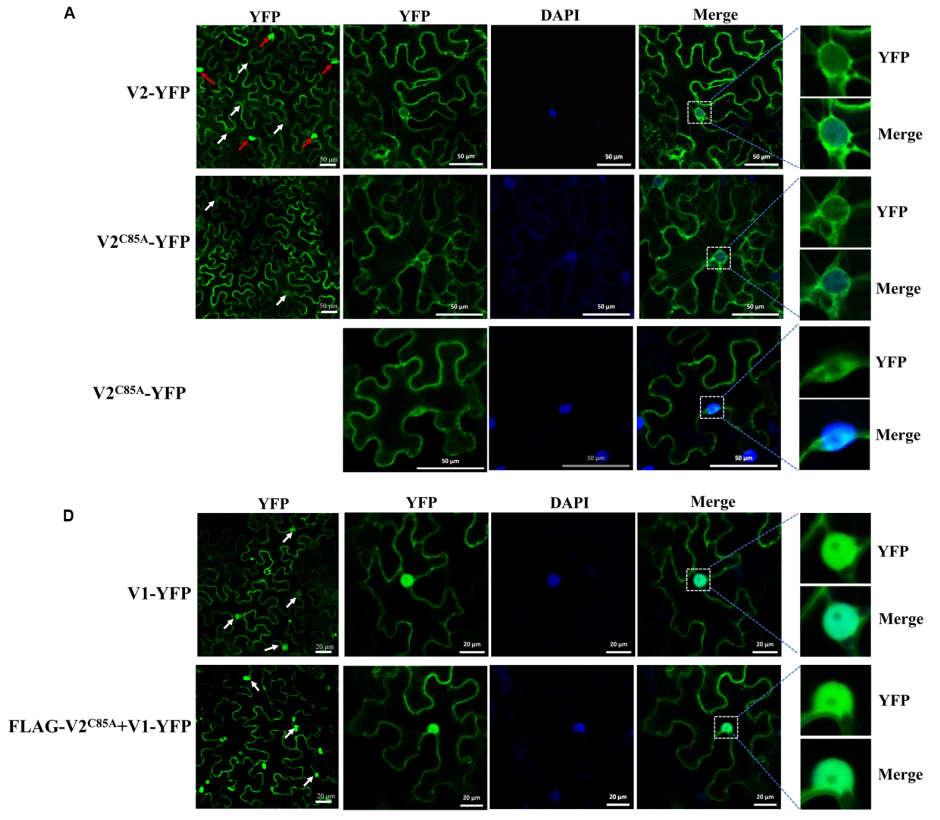

FIGURE 5 | Characterization of the V2^{C85A} mutant. **(A)** Subcellular localization of V2 and V2^{C85A}. DAPI stains DNA in the nucleus. White arrows in the left column point to the nuclear areas in cells. Red arrows point to V2 aggregates. Bars: 50 μm. **(B)** Quantification of perinuclear distribution of V2 and V2^{C85A}. The number of cells with perinuclear distribution in different samples as in a. Experiments were repeated three times and 30 cells were observed in each repeat. Values represent percentages of cells with a perinuclear distribution of YFP signal ± SD (standard deviation). Data were analyzed using Student's *t*-test and asterisks denote significant differences between V2-YFP- and V2^{C85A}-YFP-infiltrated leaves (*$P < 0.05$). **(C)** Western blot analysis showing accumulated V2 and V2^{C85A} using anti-GFP polyclonal antibody. Actin serves as a control for equal loading. **(D)** Localization of V1-YFP expressed alone or co-expressed with V2^{C85A} in *N. benthamiana* leaves. Arrows in the left column point to the nuclear areas in cells. Bars: 20 μm. **(E)** Comparison of the nucleus-localized V1-YFP in the absence or presence of V2^{C85A}. At least 150 cells were analyzed from three independent repeats. Values represent the mean ± SD in plants infiltrated with V1-YFP in the absence or presence of V2^{C85A}. The data were analyzed using Student's *t*-test. **(F)** The accumulated V1-YFP and FLAG- V2^{C85A} as shown by western blot analysis.

Collectively, these results showed that the mutation at C85 of the V2 protein causes significantly low levels of virus accumulation in the systemic leaves and a dramatic decrease in the infection efficiency with delayed and mild symptoms.

DISCUSSION

Because genome replication of geminiviruses takes place in the nucleus of the infected host cells (Hanley-Bowdoin et al., 2013), it is crucial to transport the viral offspring DNA from the nucleus back to the cytoplasm for intracellular, cell-to-cell, and long-distance movement. In bipartite geminiviruses, it is well-known that the BV1 protein facilitates trafficking of the viral genome into and out of the host nucleus (Brough et al., 1988; Etessami et al., 1988; Sudarshana et al., 1998; Jeffrey et al., 1996; Ye et al., 2015). In monopartite geminiviruses, it has been reported that the V1 protein mediates the import and export of viral DNA (Kunik et al., 1998, 1999; Rojas et al., 2001). However, V1 protein might not be the only viral protein that is involved in the nucleocytoplasmic shuttling of TYLCV. Previous reports based on triple microinjection experiments revealed that the nuclear export of viral DNA was enhanced 20–30% in the presence of V2 and V1 proteins compared to that with V1 protein only (Rojas et al., 2001). However, the mechanism by which the V2 protein promotes viral DNA export is unclear. Our results suggest that V2 protein may facilitate viral DNA export by interacting with V1 protein and promote the nuclear export of V1 protein.

In this study, we found that the V2 protein localized primarily in the perinuclear region and the cytoplasm (**Figure 1B**). A very weak signal was also present in the nucleus (**Figures 1B,C**), but upon treatment with the exportin-α inhibitor LMB, the amount of nucleus-localized V2 protein increased significantly (**Figure 3A**), suggesting that V2 protein shuttles between the nucleus and the cytoplasm but is quickly exported out of the nucleus via exportin-α. It is unclear, however, how V2 protein is imported into the nucleus.

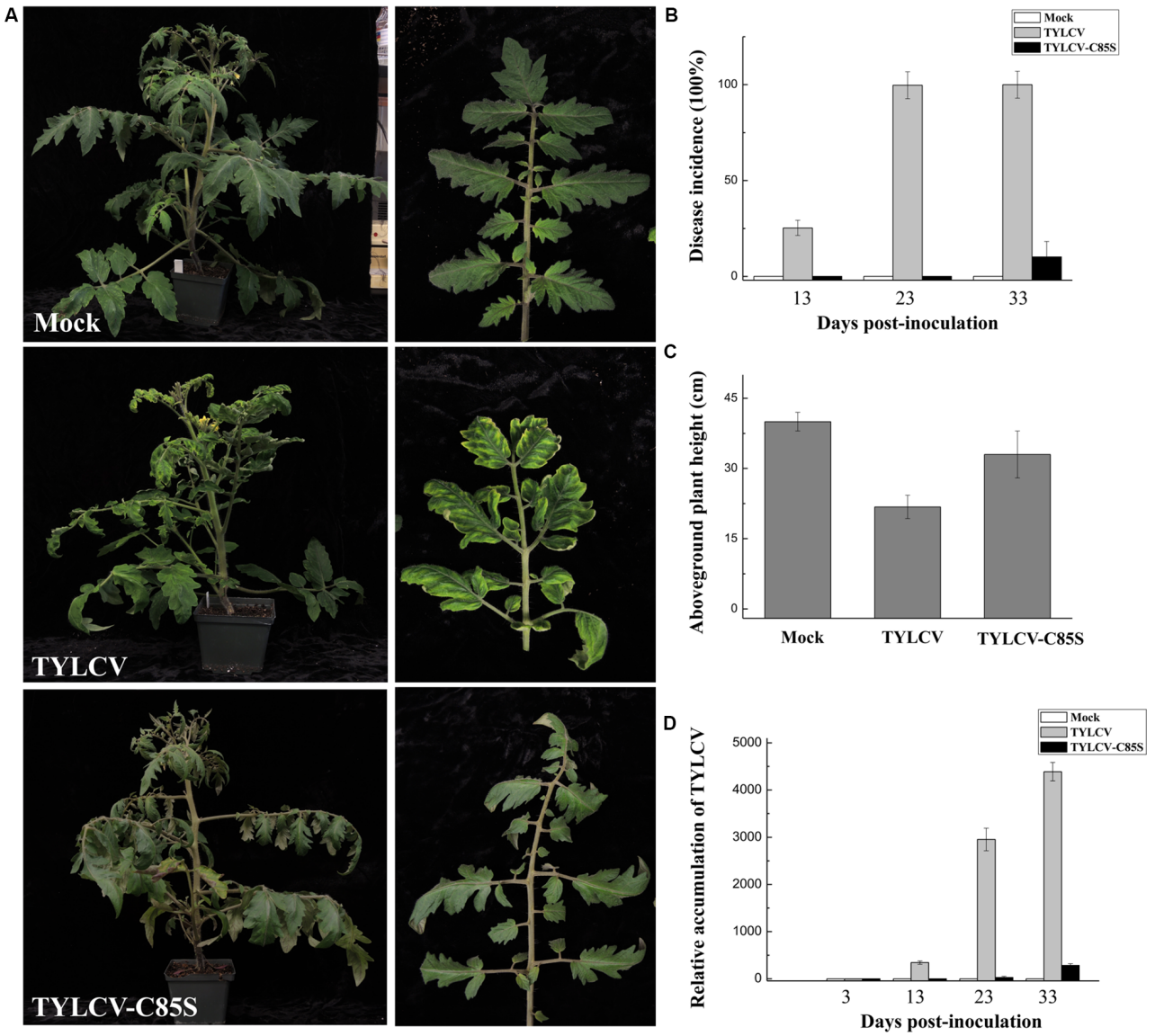

FIGURE 6 | Effects of the C85S mutation on viral infection and viral accumulation in TYLCV-inoculated tomato plants. **(A)** Symptoms in plants that were agroinoculated with wt TYLCV or TYLCV-C85S at 33 dpi. Mock represents mock-inoculated plants. Enlarged images show the yellowing and curling leaves. **(B)** The time course of wt TYLCV or TYLCV-C85S infection. Values representing percentages of systemically infected plants at different dpi are given as mean ± SD of triplicate experiments. In each experiment, 15 plants were inoculated and four independent repeats were performed. **(C)** The aboveground plant heights of Mock-, TYLCV-, or TYLCV-C85S-inoculated tomato plants as measured at 33 dpi. **(D)** The accumulated viral DNA in plants as measured by qPCR. Accumulated levels of viral DNA were tested in TYLCV-, TYLCV- C85S-, or mock-inoculated plants at 3, 13, 23, and 33 dpi. Total DNA was extracted from newly emerged systemic leaves. Values represent the mean relative to the Mock-treated plants (n = 3 biological replicates) and were normalized with *SlActin* as an internal reference.

Our work found that V1 protein was primarily localized in the nucleus when expressed alone, but the nucleus-localized V1 disappeared when co-expressed with V2 protein (**Figure 1A**), suggesting that V2 either promoted the nuclear export of V1 or inhibited the nuclear entry of V1 protein. Although we cannot totally rule out the possibility that V2 may prevent V1 protein from entering the nucleus, our data suggest that V2 protein plays a critical role in the nuclear export of V1 protein as the nucleus-localized V1 diminished when V2 was present (**Figure 1A**). In addition, V1 protein was still accumulated in the nucleus when expressed along with V2 in the presence of LMB (**Figure 3C**), suggesting that V2 protein enhances the nuclear export of V1 but not the nuclear import. We also showed that the specific V1-V2 interaction is closely correlated with V1 trafficking. The V1-V2 interaction primarily occurred in the perinuclear region and the cytoplasm (**Figure 2B**) but was strongly detected in the nucleus upon LMB treatment (**Figure 3D**), suggesting that they may be in a complex or complexes throughout viral replication and movement in infected cells. In addition, it also suggests that LMB only specifically blocked the V2's transport out of the nucleus but

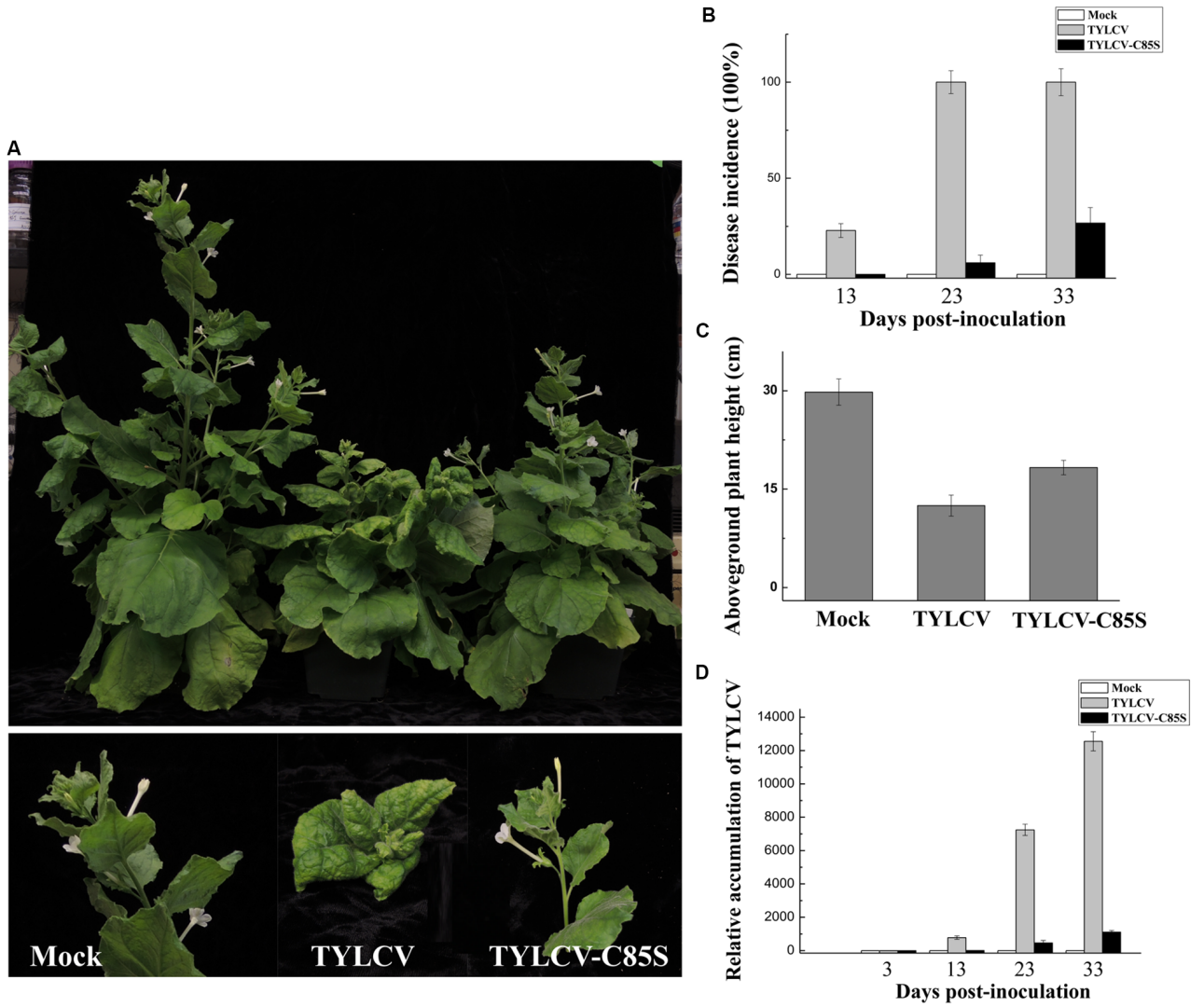

FIGURE 7 | Effects of the C85S mutation on viral infection and viral accumulation in TYLCV-inoculated *N. benthamiana*. **(A)** Symptoms in plants that were agroinoculated with wt TYLCV or TYLCV-C85S at 33 dpi. Mock represents mock-inoculated plants. **(B)** The time course of wt TYLCV or TYLCV-C85S infection. Values represent percentages of systemically infected plants as performed in **Figure 6B**. **(C)** The aboveground plant heights of mock-, TYLCV-, or TYLCV-C85S-inoculated *N. benthamiana* plants as measured at 33 dpi. **(D)** The accumulated viral DNA in plants was measured by qPCR. qPCR was done as **Figure 6D**. *NbActin* as an internal reference.

had no effect on the V1-V2 interaction. However, our data were not able to determine whether V2 protein mediates the nuclear import of V1 protein. In addition, our results do not rule out the possibility that other viral proteins, such as the C4 protein, may also be involved in this process.

Cysteine85 of V2 protein was found to be crucial for the V1-V2 interaction because substitutions of Cys85 with alanine (**Figure 4B**) or serine (**Supplementary Figure S3**a) led to a substantially inhibited interaction with V1 and thus, its ability to facilitate V1's transport out of the nucleus (**Figures 5D,E** for C85A and **Supplementary Figure S3c** for C85S). Because V1 protein is known for binding to and facilitating nucleocytoplasmic trafficking of viral DNA (Kunik et al., 1998, 1999; Rojas et al., 2001), and because V2 facilitates the nuclear export of viral DNA along with V1 protein (Rojas et al., 2001), we propose that the V2-promoted nuclear export of viral DNA is likely via the V1-V2 interaction. Our hypothesis is consistent with our results that the TYLCV-C85S mutant, which has the C85S mutation incorporated into an infectious TYLCV clone, led to the delayed onset of symptoms and reduced viral accumulation (**Figures 6**, **7**). These results indicated that C85 of V2 protein plays an important role in viral systemic infection.

In monopartite geminiviruses, V2 protein is a multifunctional protein that is involved in suppressing host PTGS and TGS, pathogenicity and systemic infection (Wartig et al., 1997; Zrachya et al., 2007; Bar-Ziv et al., 2012; Wang et al., 2014, 2018). Substitution in cysteine 85 may affect functions other than its interaction with V1 protein, especially since Cys84 and Cys86

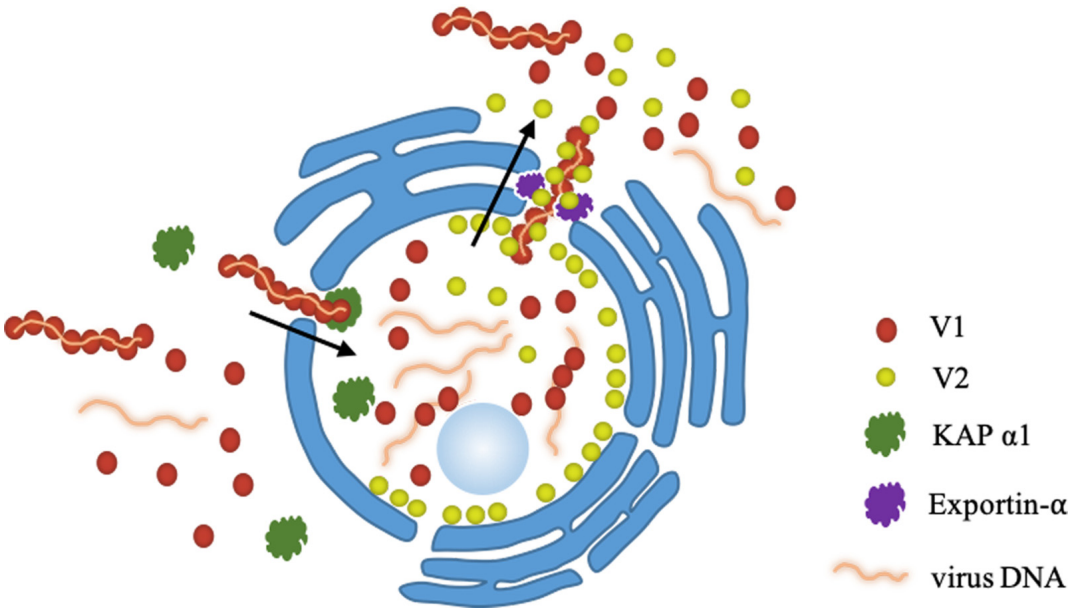

FIGURE 8 | A working model proposed for the V2-mediated nucleocytoplasmic trafficking of the V1 protein. Viral genomic DNAs are bound by V1 and import into the nucleus with the help of KAP α1 via the specific interaction between V1 and V2, leading the formation of a V2-V1-ssDNA complex. With the help of exportin-α, V2 facilitates the V1-ssDNA complex to exit the nucleus to the perinucleus and the cytoplasm.

are critical for interacting with SlSGS3 and the suppression of gene silencing (Glick et al., 2008). We found that even though the C85A (**Figure 4B**) or C85S (**Supplementary Figure S3a**) mutants failed to interact with V1 protein and thus, V1's trafficking out of the nucleus (**Figures 5D,E**; **Supplementary Figure S3c**), both maintained their activity as a suppressor of gene silencing (**Figure 4C**; **Supplementary Figures S3b, S2**). These results are also consistent with the notion that the C85S mutation delays viral systemic infection by affecting V1-mediated viral genomic DNA transportation from the nucleus to the cytoplasm, not by disturbing gene silencing-mediated host defense. However, we cannot totally rule out the possibility that other V2-mediated viral infection step(s) besides viral DNA trafficking are affected by the C85S mutation.

Our data also showed that the V2 C84AC86A double mutant interacted with V1 (**Figure 4D**) but not SlSGS3 (**Figure 4C**), indicating that C84 and C86 are not related to V2's ability to interact with V1 protein. Our results therefore revealed that motifs responsible for V1's nuclear export and the suppressor activity of gene silencing may be independent from one another.

The TYLCV V2 protein was found to be associated with large cytoplasmic aggregates (Moshe et al., 2015; Zhao et al., 2018). We demonstrated that the number of V2 aggregates is related to the *Agrobacterium* concentration used for infiltration (**Supplementary Figure S1**). It is well known that many viruses induce the formation of aggregates/inclusion bodies in the infected cells, which might be involved in viral replication and eventually related to viral infection (Wileman, 2006; Gorovits et al., 2013). However, the aggregates induced by the overexpressed V2 protein localized primarily in the cytoplasm but not the nucleus, where TYLCV replication occurs, suggesting that these aggregates might not be associated with viral replication. The relationship between V2 aggregates and viral infection needs further study.

Our results indicated that V2 protein binds to V1 protein and facilitates the nuclear export of V1 protein. During TYLCV infection, V1 mediates both nuclear import and export of viral DNA. The equilibrium between nuclear targeting and egress is changed upon completion of replication and the V1-V2 interaction can improve the nuclear export of the V1-DNA complex. Thus, viral DNA will be preferentially transported out of the nucleus for subsequent infection events. In the presence of the $V2^{C85S}$ mutant, the nuclear export of V1 is slowed down or eliminated and therefore, viral DNA and subsequent viral cell-to-cell and systemic movement is delayed. However, we cannot totally rule out that the V1-V2 complex is also required for intracellular, cell-to-cell, and/or long-distance movement besides nuclear export of V1 protein and V1-mediated viral offspring DNAs.

Based on our findings here, we propose a working model for the role of V2 protein in V1-mediated nuclear export of TYLCV genomic DNA (**Figure 8**). When offspring viral genomic DNA is produced in the nucleus, they are bound by V1 protein (Palanichelvam et al., 1998). A V2-V1-viral DNA complex is subsequently formed via a specific interaction between V1 and V2 and, with the help of exportin-α, V2 facilitates the V1-viral DNA complex to egress from the nucleus to the perinucleus and the cytoplasm with enhanced efficiency. Eventually, TYLCV spreads to adjacent cells and

upper leaves, which results in a systemic infection. The infection efficiency and the accumulation of TYLCV in the systemic leaves are dramatically inhibited with a defective V2-V1 interaction.

In summary, our results reveal that one mechanism of V2 protein's involvement in viral DNA transportation is to promote V1-mediated viral egress from the nucleus to the perinuclear region and the cytoplasm through a specific interaction with V1 protein, in the form of a V2-V1-viral DNA complex, and via host exportin-α. However, whether V2 promotes the ability of V1 to bind viral DNA and whether the V1-V2 interaction works after nuclear transportation require further research.

EXPERIMENTAL PROCEDURES

Plasmid Construction

The coding sequences of TYLCV V2 and V1 genes were amplified from the cDNA of a TYLCV-infected tomato plant from Jiangsu Province, China (GenBank accession number GU111505) (Ji et al., 2008), using corresponding primers (**Supplementary Table S1**). Site-specific mutants of $V2^{G70A}$, $V2^{S71A}$, $V2^{K73A}$, $V2^{C85A}$, $V2^{C84AC86A}$, $V2^{C85S}$, and $V2^{T96A}$ were synthesized (Invitrogen, China) and confirmed by sequencing (**Figure 4A**). For more details, see the electronic supporting information.

Subcellular Localization of Proteins

The expression vectors p1300-YFP, V2-YFP, V1-YFP, $V2^{C84AC86A}$-YFP, $V2^{C85A}$-YFP and $V2^{C85S}$-YFP were individually introduced into *A. tumefaciens* strain GV3101 through electroporation. Leaves of 4-week-old *N. benthamiana* were infiltrated with *A. tumefaciens* harboring the designated constructs. At 40 hpai, leaves were excised and YFP fluorescence was examined in epidermal cells using confocal microscopy (Zeiss LSM 710). The microscope was configured with a 458–515 nm dichroic mirror for dual excitation and a 488-nm beam splitter to help separate YFP fluorescence.

Bimolecular Fluorescence Complementation (BiFC) Assay

Bimolecular Fluorescence Complementation experiments were performed as previously described (Shen et al., 2012) with minor modifications. The constructs nYFP-V1 and cYFP-V2 were introduced individually into GV3101 by electroporation. After overnight growth and activation, agrobacterium cultures were combined and infiltrated into leaves of *N. benthamiana*. After agroinfiltration, *N. benthamiana* were grown in a growth chamber with a 16 h light/8 h dark cycle. YFP fluorescence was observed and photographed using confocal microscopy (Zeiss LSM 710) at 48 hpai. YFP was observed under a mercury lamp light using a 488-nm excitation filter. Photographic images were prepared using ZEN 2011SP1.

Co-immunoprecipitation Assay

The Co-IP assay was performed as previously described (Zhao et al., 2018). The infiltrated *N. benthamiana* leaves were harvested at 40 hpai. Proteins were extracted in IP buffer (40 mM Tris-HCl at pH 7.5, 100 mM NaCl, 5 mM $MgCl_2$, 2 mM EDTA, 2 × EDTA-free proteinase inhibitor, 1 mM PMSF, 4 mM DTT, 1% glycerol, 0.5% Triton-X100). After centrifugation, the supernatant was mixed with FLAG-trap beads (Sigma, United States). After 1 h incubation at 4°C, the beads were washed with IP buffer and resuspended in 2 × SDS loading buffer. The samples were loaded onto a 12% (vol/vol) SDS/PAGE gel and target proteins were detected using a polyclonal anti-GFP antibody (GenScript, United States) or a monoclonal anti-FLAG (Sigma, Unites States) antibody.

Yeast Two-Hybrid Assay

The yeast two-hybrid system was used to examine interactions between V2, $V2^{C85A}$, $V2^{C84AC86A}$ and SlSGS3. V2, $V2^{C85A}$, and $V2^{C84AC86A}$ were cloned into the activation domain (AD) vector and SlSGS3 was cloned into the vector harboring the DNA binding domain (BD). Both constructs were transformed into the yeast strain AH109. The plasmid pair of BD-53 and AD-recT served as a positive control, while BD-Lam and AD-recT was used as a negative control. Transformants were grown at 30°C for 72 h on synthetic defined medium lacking Histine, Leucine and Tryptophan (SD/-His/-Leu/-Trp) to test protein-protein interactions.

Nuclear-Cytoplasmic Fractionation Assay

Nuclear-cytoplasmic fractionation assays were performed as described previously (Wang et al., 2011) with minor modifications. Infiltrated leaves were harvested and mixed with 2 mL/g of lysis buffer (20 mM Tris-HCl, pH 7.5, 20 mM KCl, 2 mM EDTA, 2.5 mM $MgCl_2$, 25% glycerol, 250 mM Sucrose, 5 mM DTT, 10 mM protease inhibitor). The centrifuged pellet was resuspended with 500 μL of NRB2 and overlaid on top of 500 μL NRB3. The final nuclear pellet was resuspended in lysis buffer. As quality controls for the fractionation assays, PEPC protein and H2B-RFP were used as a cytoplasmic and a nuclear marker, respectively. For more details, see the electronic supporting information.

Leptomycin B Treatment Assays

Leptomycin B (LMB) Treatment Assays were performed as previously described (Mei et al., 2018) with minor modifications. LMB (Fisher Scientific, United States) was dissolved in ethanol to prepare 10 mM stock solutions. For *in vivo* treatment of *N. benthamiana* leaves, stock solutions were diluted in water to prepare a working solution of 10 nM LMB. Agroinfiltrated *N. benthamiana* leaves expressing the protein of interest at 40 hpai were infiltrated with 10 nM LMB. Two hours after LMB treatment, the infiltrated leaves were cut and mounted on a glass slide for confocal imaging. When needed, DMSO was further infiltrated into LMB-treated leaves and tissues were harvested at the specified time points.

TYLCV Constructs for *Agrobacterium*-Mediated Inoculation

To make a DNA clone of TYLCV containing $V2^{C85S}$, a full-length TYLCV mutant, TYLCV-C85S was synthesized (Invitrogen, China). The TYLCV-C85S and wt TYLCV infectious clone were constructed as previously described (Zhao et al., 2018). For more details, see the electronic supporting information.

Agrobacterium cultures harboring TYLCV constructs were injected into the stem of tomato and *N. benthamiana* with a syringe. Inoculated plants were grown in an insect-free cabinet with supplementary lighting corresponding to a 16-hour light and 8-hour dark schedule.

Quantitative PCR

Total DNA was extracted from mock (*Agrobacterium*-carrying empty vector)-, wt TYLCV- or TYLCV-C85S-infiltrated tomato or *N. benthamiana* leaves at different time points. RCR reaction mixes consisted of 6 μl of SYBR Green supermix (BIO-RAD, United States), 0.10 μl of each primer (10 pmol) and 1.5 μl of DNA sample (10 ng/μl) in a total volume of 12 μl.

PCR reactions were done in an Applied Biosystems 7500 (Life Technologies) real-time PCR detection system. *SlActin* or *NbActin* was used as an internal control for tomato or *N. benthamiana*, respectively. Data analysis was performed using Applied Biosystems 7500 software version 2.0.6.

DATA AVAILABILITY STATEMENT

The coding sequences of TYLCV V2 and V1 can be accessed at the NCBI database with the accession number GU111505.

AUTHOR CONTRIBUTIONS

YZ, YJ, XW, and WZ designed the project. WZ, SW, and EB conducted experiments. All authors analyzed the data and reviewed the manuscript. WZ, YJ, and XW wrote the manuscript.

FUNDING

This study was financially supported by grants from the National Natural Science Foundation of China (Nos. 31572074 and 31770168), National Key R&D Program of China (No. 2018YFD0201208), Jiangsu Agriculture Science and Technology Innovation Fund [No. CX(18)2005], China Agriculture Research System (No. CARS-24-C-01) and Jiangsu Academy of Agricultural Sciences Fund (No. 6111614).

ACKNOWLEDGMENTS

We thank Drs. Sue Tolin and Janet Webster at Virginia Tech, United States for critical reading of the manuscript. We also thank Dr. Hernan Garcia-Ruiz at University of Nebraska-Lincoln for providing pZAP-GFP.

SUPPLEMENTARY MATERIAL

The Supplementary Material for this article can be found online at: https://www.frontiersin.org/articles/10.3389/fmicb.2020.01243/full#supplementary-material

REFERENCES

Bar-Ziv, A., Levy, Y., Hak, H., Mett, A., Belausov, E., Citovsky, V., et al. (2012). The (TYLCV) V2 protein interacts with the host papain-like cysteine protease CYP1. *Plant Signal. Behav.* 7, 983–989. doi: 10.4161/psb.20935

Boulton, M. I., Pallaghy, C. K., Chatani, M., MacFarlane, S., and Davies, J. W. (1993). Replication of Maize streak virus mutants in maize protoplasts: evidence for a movement protein. *Virology* 192, 85–93. doi: 10.1006/viro.1993.1010

Boulton, M. I., Steinkellner, J., Donson, J., Markham, P. G., King, D. I., and Davies, J. W. (1989). Mutational analysis of virion-sense genes of maize streak virus. *J. Gen. Virol.* 70, 2309–2323. doi: 10.1099/0022-1317-70-9-2309

Brough, C. L., Hayes, R. J., Morgan, A. J., Coutts, R. H. A., and Buck, K. W. (1988). Effects of mutagenesis in vitro on the ability of cloned tomato golden mosaic virus DNA to infect *Nicotiana benthamiana* plants. *J. Gen. Virol.* 69, 503–514. doi: 10.1099/0022-1317-69-3-503

Diaz, A., and Wang, X. (2014). Bromovirus-induced remodeling of host membranes during viral RNA replication. *Curr. Opin. Virol.* 9, 104–110. doi: 10.1016/j.coviro.2014.09.018

Diaz, A., Zhang, J., Ollwerther, A., Wang, X., and Ahlquist, P. (2015). Host ESCRT proteins are required for bromovirus RNA replication compartment assembly and function. *PLoS Pathog.* 11:e1004742. doi: 10.1371/journal.ppat.1004742

Díaz-Pendón, J. A., Cañizares, M. C., Moriones, E., Bejarano, E. R., Czosnek, H., and Navas-Castillo, J. (2010). Tomato yellow leaf curl viruses: ménage a trois between the virus complex, the plant and the whitefly vector. *Mol. Plant Pathol.* 11, 441–450. doi: 10.1111/j.1364-3703.2010.00618.x

Etessami, P., Callis, R., Ellwood, S., and Stanley, J. (1988). Delimitation of essential genes of cassava latent virus DNA 2. *Nucleic Acids Res.* 16, 4811–4829. doi: 10.1093/nar/16.11.4811

Fauquet, C. M., Briddon, R. W., Brown, J. K., Moriones, E., Stanley, J., Zerbini, M., et al. (2008). Geminivirus strain demarcation and nomenclature. *Arch. Virol.* 153, 783–821. doi: 10.1007/s00705-008-0037-6

Fondong, V. N. (2013). Geminivirus protein structure and function. *Mol. Plant Pathol.* 14, 635–649. doi: 10.1111/mpp.12032

Fondong, V. N. (2019). The ever-expanding role of C4/AC4 in geminivirus infection: punching above its weight? *Mol. Plant* 12, 145–147. doi: 10.1016/j.molp.2018.12.006

Gafni, Y. (2003). Tomato yellow leaf curl virus, the intracellular dynamics of a plant DNA virus. *Mol. Plant Pathol.* 4, 9–15. doi: 10.1046/j.1364-3703.2003.00147.x

Gafni, Y., and Epel, B. L. (2002). The role of host and viral proteins in intra- and inter-cellular trafficking of geminiviruses. *Mol. Plant Pathol.* 60, 231–241. doi: 10.1006/pmpp.2002.0402

Glick, E., Levy, Y., and Gafni, Y. (2009). The viral etiology of Tomato yellow leaf curl disease-a review. *Plant Protoc. Sci.* 45, 81–97. doi: 10.17221/26/2009-pps

Glick, E., Zrachya, A., Levy, Y., Mett, A., Gidoni, D., Belausov, E., et al. (2008). Interaction with host SGS3 is required for suppression of RNA silencing by tomato yellow leaf curl virus V2 protein. *PNAS* 105, 157–161. doi: 10.1073/pnas.0709036105

Gorovits, R., and Czosnek, H. (2017). The involvement of heat shock proteins in the establishment of Tomato yellow leaf curl virus infection. *Front. Plant Sci.* 8:355. doi: 10.3389/fpls.2017.00355

Gorovits, R., Liu, Y., and Czosnek, H. (2016). "The involvement of HSP70 and HSP90 in tomato yellow leaf curl virus infection in tomato plants and insect vectors," in *Heat Shock Proteins and Plants*, eds A. Asea, P. Kaur, and S. Calderwood (Cham: Springer), 189–207. doi: 10.1007/978-3-319-46340-7_10

Gorovits, R., Moshe, A., Kolot, M., Sobol, I., and Czosnek, H. (2013). Progressive aggregation of Tomato yellow leaf curl virus coat protein in systemically

infected tomato plants, susceptible and resistant to the virus. *Virus Res.* 171, 33–43. doi: 10.1016/j.virusres.2012.09.017

Hanley-Bowdoin, L., Bejarano, E. R., Robertson, D., and Mansoor, S. (2013). Geminiviruses: masters at redirecting and reprogramming plant processes. *Nat. Rev. Microbiol.* 11, 777–788. doi: 10.1038/nrmicro3117

Jeffrey, J. L., Pooma, W., and Petty, I. T. D. (1996). Genetic requirements for local and systemic movement of tomato golden mosaic virus in infected plants. *Virology* 223, 208–218. doi: 10.1006/viro.1996.0469

Jeske, H. (2009). Geminiviruses. *Curr. Top. Microbiol. Immunol.* 331, 185–226.

Ji, Y., Xiong, R., Cheng, Z., Zhou, T., Zhao, T., Yu, W., et al. (2008). Molecular diagnosis of Tomato yellow leaf curl disease in Jiangsu province. *Acta Hortic.* 35, 1815–1818.

Kunik, T., Mizrachy, L., Citovsky, V., and Gafni, Y. (1999). Characterization of a tomato karyopherin that interacts with the Tomato yellow leaf curl virus (TYLCV) capsid protein. *J. Exp. Bot.* 50, 731–732. doi: 10.1093/jexbot/50.334.731

Kunik, T., Palanichelvam, K., Czosnek, H., Citovsky, V., and Gafni, Y. (1998). Nuclear import of the capsid protein of Tomato yellow leaf curl virus (TYLCV) in plant cells. *Plant J.* 13, 393–399. doi: 10.1046/j.1365-313x.1998.00037.x

Lazarowitz, S. G., and Beachy, R. N. (1999). Viral movement proteins as probes for intracellular and intercellular trafficking in plants. *Plant Cell* 11, 535–548. doi: 10.1105/tpc.11.4.535

Liu, H., Boulton, M. I., Oparka, K. J., and Davies, J. W. (2001). Interaction of the movement and coat proteins of Maize streak virus: implications for the transport of viral DNA. *J. Gen. Virol.* 82, 35–44. doi: 10.1099/0022-1317-82-1-35

Martin, K., Kopperud, K., Chakrabarty, R., Banerjee, R., Brooks, R., and Goodin, M. M. (2009). Transient expression in *Nicotiana benthamiana* fluorescent marker lines provides enhanced definition of protein localization, movement and interactions in planta. *Plant J.* 59, 150–162. doi: 10.1111/j.1365-313x.2009.03850.x

Mathew, C., and Ghildyal, R. (2017). CRM1 inhibitors for antiviral therapy. *Front. Microbiol.* 8:1171. doi: 10.3389/fmicb.2017.01171

Mei, Y., Wang, Y., Hu, T., Yang, X., Lozano-Duran, R., Sunter, G., et al. (2018). Nucleocytoplasmic shuttling of geminivirus C4 protein Mediated by phosphorylation and myristoylation is critical for viral pathogenicity. *Mol. Plant* 11, 1466–1481. doi: 10.1016/j.molp.2018.10.004

Moriones, E., and Navas-Castillo, J. (2000). Tomato yellow leaf curl virus, an emerging virus complex causing epidemics worldwide. *Virus Res.* 71, 123–134. doi: 10.1016/s0168-1702(00)00193-3

Moshe, A., Belausov, E., Niehl, A., Heinlein, M., Czosnek, H., and Gorovits, R. (2015). The Tomato yellow leaf curl virus V2 protein forms aggregates depending on the cytoskeleton integrity and binds viral genomic DNA. *Sci. Rep.* 5, 1–13.

Nakhla, M. K., and Maxwell, D. P. (1997). Epidemiology and management of tomato yellow leaf curl disease. *Plant Virus Dis. Control* 43, 565–583.

Navot, N., Pichersky, E., Zeidan, M., Zamir, D., and Czosnek, H. (1991). Tomato yellow leaf curl virus: a whitefly-transmitted geminivirus with a single genomic component. *Virology* 185, 151–161. doi: 10.1016/0042-6822(91)90763-2

Nawaz-ul-Rehman, M. S., Nahid, N., Mansoor, S., Briddon, R. W., and Fauquet, C. M. (2010). Post-transcriptional gene silencing suppressor activity of two non-pathogenic alphasatellites associated with a begomovirus. *Virology* 405, 300–308. doi: 10.1016/j.virol.2010.06.024

Padidam, M., Beachy, R. N., and Fauquet, C. M. (1995). Tomato leaf curl geminivirus from India has a bipartite genome and coat protein is not essential for infectivity. *J. Gen. Virol.* 76, 25–35. doi: 10.1099/0022-1317-76-1-25

Palanichelvam, K., Kunik, T., Citovsky, V., and Gafni, Y. (1998). The capsid protein of tomato yellow leaf curl virus binds cooperatively to single-stranded DNA. *J. Gen. Virol.* 79, 2829–2833. doi: 10.1099/0022-1317-79-11-2829

Rojas, M. R., Hagen, C., Lucas, W. J., and Gilbertson, R. L. (2005). Exploiting chinks in the plant's armor: evolution and emergence of Geminiviruses. *Annu. Rev. Phytopathol.* 43, 361–394. doi: 10.1146/annurev.phyto.43.040204.135939

Rojas, M. R., Jiang, H., Salati, R., Xoconostle-Cazares, B., Sudarshana, M. R., Lucas, W. J., et al. (2001). Functional analysis of proteins involved in movement of the monopartite begomovirus, Tomato yellow leaf curl virus. *Virology* 291, 110–125. doi: 10.1006/viro.2001.1194

Sahu, P. P., Sharma, N., Puranik, S., Muthamilarasan, M., and Prasad, M. (2014). Involvement of host regulatory pathways during geminivirus infection: a novel platform for generating durable resistance. *Funct. Integr. Genomics* 14, 47–58. doi: 10.1007/s10142-013-0346-z

Scholthof, K. B. G., Scott, A., Henryk, C., Palukaitis, P., Jacquot, E., Hohn, T., et al. (2011). Top 10 plant viruses in molecular plant pathology. *Mol. Plant Pathol.* 12, 938–944.

Shen, Q., Liu, Z., Song, F., Xie, Q., Hanley-Bowdoin, L., and Zhou, X. (2012). Tomato SlSnRK1 protein interacts with and phosphorylates βC1, a pathogenesis protein encoded by a geminivirus β-satellite. *Plant Physiol.* 157, 1394–1406. doi: 10.1104/pp.111.184648

Sudarshana, M. R., Wang, H. L., Lucas, W. J., and Gilbertson, R. L. (1998). Dynamics of bean dwarf mosaic geminivirus cell-to-cell and long-distance movement in *Phaseolus vulgaris* revealed, using the green fluorescent protein. *Mol. Plant Microbe. Interact.* 11, 277–291. doi: 10.1094/mpmi.1998.11.4.277

Wang, B., Li, F., Huang, C., Yang, X., Qian, Y., Xie, Y., et al. (2014). V2 of tomato yellow leaf curl virus can suppress methylation-mediated transcriptional gene silencing in plants. *J. Gen. Virol.* 95, 225–230. doi: 10.1099/vir.0.055798-0

Wang, B., Yang, X., Wang, Y., Xie, Y., and Zhou, X. (2018). Tomato yellow leaf curl virus V2 interacts with host histone deacetylase 6 to suppress methylation-mediated transcriptional gene silencing in plants. *J. Virol.* 92:e0036-18.

Wang, W., Ye, R., Xin, Y., Fang, X., Li, C., Shi, H., et al. (2011). An importin ß protein negatively regulates microRNA activity in *Arabidopsis*. *Plant Cell* 23, 3565–3576. doi: 10.1105/tpc.111.091058

Wartig, L., Kheyr, P. A., Noris, E., Kouchkovsky, F. D., Jouanneau, F., Gronenborn, B., et al. (1997). Genetic analysis of the monopartite tomato yellow leaf curl geminivirus: roles of V1, V2, and C2 ORFs in viral pathogenesis. *Virology* 228, 132–140. doi: 10.1006/viro.1996.8406

Wileman, T. (2006). Aggresomes and autophagy generate sites for virus replication. *Science* 312, 875–878. doi: 10.1126/science.1126766

Yaakov, N., Levy, Y., Belausov, E., Gaba, V., Lapidot, M., and Gafni, Y. (2011). Effect of a single amino acid substitution in the NLS domain of Tomato yellow leaf curl virus-Israel (TYLCV-IL) capsid protein (CP) on its activity and on the virus life cycle. *Virus Res.* 158, 8–11. doi: 10.1016/j.virusres.2011.02.016

Ye, J., Yang, J., Sun, Y., Zhao, P., Gao, S., Jung, C., et al. (2015). Geminivirus activates ASYMMETRIC LEAVES 2 to accelerate cytoplasmic DCP2-mediated mRNA turnover and weakens RNA silencing in *Arabidopsis*. *PLoS Pathog.* 11:e1005196. doi: 10.1371/journal.ppat.1005196

Zeng, R., Liu, X., Li, H., Wu, S., Huang, W., Zhai, Z., et al. (2020). Danger peptide signaling enhances internalization of a geminivirus symptom determinant in plant cells during infection. *J. Exp. Bot.* 71, 2817–2827. doi: 10.1093/jxb/eraa053

Zhang, J., Zhang, Z., Chukkapalli, V., Nchoutmboube, J. A., Li, J., Randall, G., et al. (2016). Positive-strand RNA viruses stimulate host phosphatidylcholine synthesis at viral replication sites. *PNAS* 113, E1064–E1073.

Zhang, Z., He, G., Filipowicz, N., Randall, G., Belov, G., Kopek, B., et al. (2019). Host lipids in positive-strand RNA virus genome replication. *Front. Microbiol.* 10:286. doi: 10.3389/fmicb.2019.00286

Zhao, W., Ji, Y., Wu, S., Ma, X., Li, S., Sun, F., et al. (2018). Single amino acid in V2 encoded by TYLCV is responsible for its self-interaction, aggregates and pathogenicity. *Sci. Rep.* 8:3561.

Zrachya, A., Glick, E., Levy, Y., Arazi, T., Citovsky, V., and Gafni, Y. (2007). Suppressor of RNA silencing encoded by Tomato yellow leaf curl virus-Israel. *Virology* 358, 159–165. doi: 10.1016/j.virol.2006.08.016

Conflict of Interest: The authors declare that the research was conducted in the absence of any commercial or financial relationships that could be construed as a potential conflict of interest.

frontiers in Plant Science

ORIGINAL RESEARCH
published: 16 June 2020
doi: 10.3389/fpls.2020.00840

Dynamic Subcellular Localization, Accumulation, and Interactions of Proteins From *Tomato Yellow Leaf Curl China Virus* and Its Associated Betasatellite

Hao Li[1†], Fangfang Li[1†], Mingzhen Zhang[1], Pan Gong[1] and Xueping Zhou[1,2*]*

[1] State Key Laboratory for Biology of Plant Diseases and Insect Pests, Institute of Plant Protection, Chinese Academy of Agricultural Sciences, Beijing, China, [2] State Key Laboratory of Rice Biology, Institute of Biotechnology, Zhejiang University, Hangzhou, China

OPEN ACCESS

Edited by:
Alice Kazuko Inoue-Nagata, Brazilian Agricultural Research Corporation (EMBRAPA), Brazil

Reviewed by:
Gong-Yin Ye, Zhejiang University, China
Gian Paolo Accotto, Institute for Sustainable Plant Protection, Italian National Research Council, Italy
Eduardo Rodriguez Bejarano, University of Malaga, Spain

***Correspondence:**
Fangfang Li
ffli@ippcaas.cn;
Elva1988@163.com
Xueping Zhou
zzhou@zju.edu.cn

[†] These authors have contributed equally to this work

Specialty section:
This article was submitted to Virology, a section of the journal Frontiers in Plant Science

Received: 19 January 2020
Accepted: 26 May 2020
Published: 16 June 2020

Citation:
Li H, Li F, Zhang M, Gong P and Zhou X (2020) Dynamic Subcellular Localization, Accumulation, and Interactions of Proteins From Tomato Yellow Leaf Curl China Virus and Its Associated Betasatellite. Front. Plant Sci. 11:840. doi: 10.3389/fpls.2020.00840

Geminiviruses contain the largest number of species of plant viruses, and cause devastating crop diseases worldwide. The development of resistance to these viruses will require a clear understanding of viral protein function and interactions. Tomato yellow leaf curl China virus (TYLCCNV) is a typical monopartite geminivirus, which is associated with a tomato yellow leaf curl China betasatellite (TYLCCNB) in the field; the complex infection of TYLCCNV/TYLCCNB leads to serious economic losses in solanaceous plants. The functions of each protein encoded by the TYLCCNV/TYLCCNB complex have not yet been examined in a targeted manner. Here, we show the dynamic subcellular localization and accumulation of six viral proteins encoded by TYLCCNV and the βC1 protein encoded by TYLCCNB in plants over time, and analyzed the effect of TYLCCNV or TYLCCNV/TYLCCNB infection on these parameters. The interaction among the seven viral proteins was also tested in this study: C2 acts as a central player in the viral protein interaction network, since it interacts with C3, C4, V2, and βC1. Self-interactions were also found for C1, C2, and V2. Together, the data presented here provide a template for investigating the function of viral proteins with or without viral infection over time, and points at C2 as a pivotal protein potentially playing a central role in the coordination of the viral life cycle.

Keywords: tomato yellow leaf curl China virus, tomato yellow leaf curl China betasatellite, dynamic subcellular localization, protein accumulation, interaction assay

INTRODUCTION

Geminiviruses are a group of plant viruses with single-stranded circular DNA genomes that are encapsidated in twinned viral particles, transmitted by insect vectors and causing devastating crop diseases worldwide. Based on their genome organization, transmission insect vectors, and host range, geminiviruses are divided into nine genera[1]. The genus *Begomovirus* comprises by far the largest number of species, many of which cause devastating diseases in economically important

[1] https://talk.ictvonline.org/taxonomy/

crops. The genome of bipartite begomoviruses consists of two DNA molecules, referred to as DNA A and DNA B, while that of monopartite begomoviruses consists of one DNA molecule, similar to the DNA A. Many monopartite begomoviruses are associated with betasatellites, forming a disease complex in the field (Zhou, 2013).

Tomato yellow leaf curl China virus (TYLCCNV) is a typical monopartite geminivirus, which appears associated with a tomato yellow leaf curl China betasatellite (TYLCCNB) in the field (Cui et al., 2004). Tobacco or tomato plants infected by TYLCCNV/TYLCCNB display dwarfing, leaf curling, yellow mosaic patterns and stem distortion symptoms. However, infection by TYLCCNV alone in tobacco or tomato plants fails to induce any obvious symptoms and accumulate less viral DNA (Cui et al., 2004). The TYLCCNV genome contains six open reading frames (ORFs), two in the virion sense orientation (V1 and V2) and four in the complementary sense orientation (C1, C2, C3, and C4), while TYLCCNB encodes the βC1 protein in the complementary sense orientation. The functions of βC1 are well characterized (Zhou, 2013; Li et al., 2018a); for example, TYLCCNB βC1 suppresses transcriptional gene silencing (TGS) by inhibiting the activity of *S*-adenosylhomocysteine hydrolase (SAHH) to restrict the production of *S*-adenosyl methionine, an essential methyltransferase co-factor (Yang et al., 2011); TYLCCNB βC1 also inhibits post-transcriptional gene silencing (PTGS) by up-regulating the expression of an endogenous RNA silencing suppressor, *rgs-CaM*, which can not only reduce the transcription of *NbRDR6* (Li et al., 2014), but also interact with NbSGS3 to guide its autophagic degradation (Li et al., 2017).

Although the function of TYLCCNV-encoded proteins was not investigated in detail, potential roles have been assigned to their positional homologs in other geminivirus species. For example, C1 encodes a replication initiator protein (Rep), which is required for the replication of the viral DNA. C1 does not possess DNA polymerase activity, and heavily relies on the host DNA replication machinery for viral multiplication. Therefore, C1 can interact with host factors and recruit them to replicate the viral genome; these factors include retinoblastoma-related proteins (RBR), which negatively regulate cell cycle (Kong et al., 2000). C2 encodes a transcriptional activator protein (TrAP), which transactivates expression of the coat protein (CP) and movement protein (MP) genes (Sunter and Bisaro, 1997). Interestingly, beet curly top virus (BCTV) C2 has a novel function in the promotion of viral replication, probably by restoring the DNA replication competency of the infected cells and thus creating a favorable cell environment for viral spread. Therefore, C2 seems to have a broad impact on the replication of geminiviruses, and this mechanism might have important epidemiological implications (Trinks et al., 2005; Caracuel et al., 2012). C3 is a replication enhancer protein (REn), which promotes the accumulation of the virus. C4 is found to be a major symptom determinant (Lai et al., 2009). V1, as the viral coat protein (CP), is responsible for packing viral particles, and can also serve as the viral MP to mediate the shuttle of viral DNA/protein complex from the nucleus to the cytoplasm (Zhou et al., 2011). Besides these roles, geminiviral V1 is the protein recognized by the insect vector during virus acquisition, and hence determines vector specificity (Briddon et al., 1990). V2 is an RNA silencing suppressor (Glick et al., 2008; Zhang et al., 2012), and in some monopartite begomoviruses is involved in the movement of the virus and capable of inducing a hypersensitive response (HR) (Harrison and Robinson, 2002; Mubin et al., 2010; Matić et al., 2016).

In addition to performing essential functions to facilitate viral replication, transcription, movement, or spread, viral proteins can exert other roles. For example, viral proteins can counter host defenses including TGS, PTGS, HR, and protein degradation mechanisms. It has been found that C1, C2, C4, and V2 can suppress TGS, and C2, C4, and V2 can suppress PTGS. C1 reduces the expression of the plant maintenance DNA methyltransferases, METHYLTRANSFERASE 1 (MET1) and CHROMOMETHYLASE 3 (CMT3), in both locally and systemically infected tissues, in turn suppressing TGS (Rodríguez-Negrete et al., 2013). The tomato yellow leaf curl virus (TYLCV) V2 protein interacts with the host histone deacetylase 6 and inhibits methylation-mediated TGS in plants (Wang et al., 2018); it also suppresses PTGS by interacting and interfering with SGS3 (Glick et al., 2008). The tomato leaf curl Yunnan virus (TLCYnV) C4 protein can impair the HIR1-mediated cell death through promoting the degradation of HIR1 via physical interaction with this host protein (Mei et al., 2019).

A clear and dynamic description of the subcellular localization of viral proteins is important to understand the virus infection cycle. For example, in animal viruses, changes in the subcellular localization of some CPs may be related to the progression of the viral infection (Wistuba et al., 1997). TYLCV V1 is localized in the nucleolus and weakly in the nucleoplasm when expressed alone, while it is re-localized outside of the nucleolus and into discrete nuclear foci in the presence of TYLCV (Wang et al., 2017). Protein–protein interactions among viral proteins also play pivotal roles during viral infection. For example, it has been revealed that the potyvirus turnip mosaic virus (TuMV) P3N-PIPO is a plasmodesmata (PD)-localized protein that physically interacts with the virus-encoded cylindrical inclusion (CI) protein *in planta*; the CI and P3N-PIPO complex coordinates the formation of PD-associated structures that facilitate the intercellular movement of TuMV in infected plants (Wei et al., 2010).

In this study, we fused a YFP tag to each protein encoded by TYLCCNV/TYLCCNB and then transiently expressed them in *Nicotiana benthamiana* plants. Subcellular localization and protein accumulation were examined in real-time in the presence or absence of the viral infection complex. We found that the fluorescent signal and protein accumulation of C1, C2, V1, and βC1 decreased, while those of C3 and V2 increased, and those of C4 did not display obvious changes after 48 h post infiltration. The concomitant viral infection enhanced the fluorescent signal and protein accumulation of most viral proteins (C1, C2, C4, V1, V2, and βC1). The potential interaction among viral proteins was tested by yeast two-hybrid (Y2H) and bimolecular fluorescence complementation (BiFC) assays; we found that the C2 protein can serve as a network hub by interacting with itself and several other viral proteins. Furthermore, we also observed the self-interactions of C1 and V2. In summary, our work provides useful

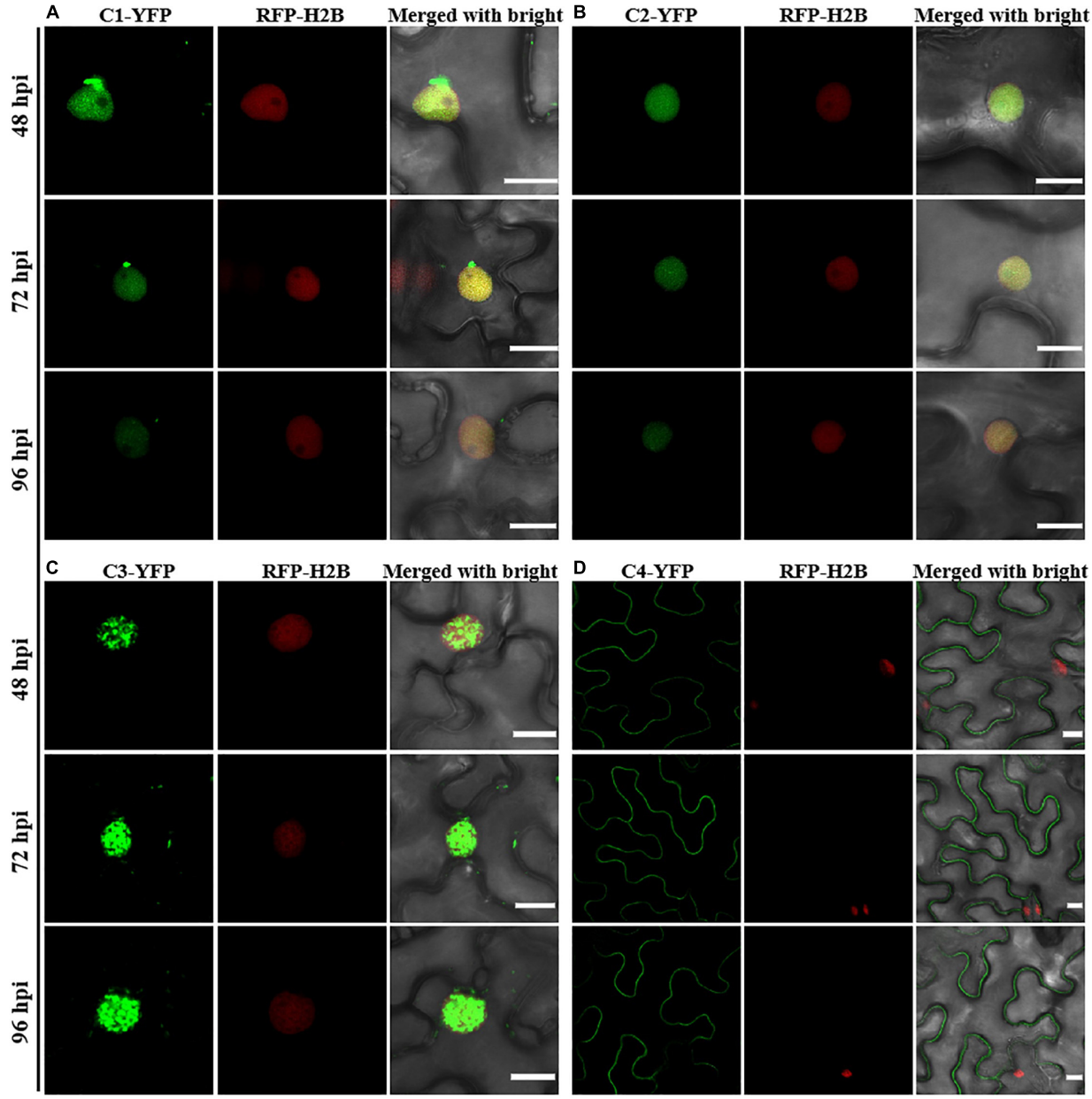

FIGURE 1 | Confocal images of TYLCCNV C1, C2, C3, or C4 proteins fused with YFP. RFP-H2B transgenic *Nicotiana benthamiana* leaves were infiltrated with *Agrobacterium* cultures to express C1-YFP **(A)**, C2-YFP **(B)**, C3-YFP **(C)**, or C4-YFP **(D)**. Confocal images were taken at 48, 72, and 96 h post infiltration (hpi). YFP signal is shown in green. Nuclei of tobacco leaf epidermal cells are marked by RFP-H2B (red). This experiment was repeated three times independently, and more than 20 cells per sample were observed each time; representative results are shown. Scale bar: 10 μm.

data for further studies investigating the role of each geminiviral protein in the context of the viral infection.

MATERIALS AND METHODS

Plant Materials and Growth Conditions

Wild-type and transgenic *N. benthamiana* seedlings expressing RFP-H2B (Martin et al., 2009; Anderson et al., 2018) were potted in soil and placed in an insect-free greenhouse at 25°C and 60% relative humidity under a 16 h light/8 h dark photo-period.

Plasmid Constructs

The infectious clone plasmids pBinPLUS-Y10-1.7A, including 1.7 copies of the TYLCCNV isolate Y10 genome in tandem (10A), and pBinPLUS-Y10-1.7A+1.0b, including 1.7 copies of the TYLCCNV genome and 2 copies of the TYLCCNB sequences (10Aβ) in tandem, are described previously (Zhou et al., 2003).

The full-length sequence information of TYLCCNV (accession number: AJ319675) and TYLCCNB (accession number: AJ781300) can be found in GenBank. Gateway technology was used in this study to construct all vectors required for Y2H assays, subcellular localization experiments, and BiFC experiments. The genomic DNA regions of C1, C2, C3, C4, V1, V2, and βC1 were amplified from the plasmid of pBinPLUS-Y10-1.7A+1.0b by PCR using the KOD high-fidelity enzyme (Takara, Beijing, China). The PCR products were subcloned into the pDONR221 vector by BP Clonase® (Invitrogen, Beijing, China) following the manufacturer's protocol. The resulting pDONR221 constructs were verified by sequencing and linearized by *Mlu*I. The linearized fragments including the specific DNA sequences were transferred by recombination to the indicated binary destination vectors using LR Clonase II (Invitrogen, Beijing, China). To construct plant transient expression plasmids expressing recombinant proteins tagged with C-terminal YFP, C-terminal YFP-N (YN), or C-terminal YFP-C (YC), the linearized fragments were recombined into the binary destination vector pEarleygate101, 35S-YN gateway, or 35S-YC gateway (Earley et al., 2006; Lu et al., 2010), respectively. To construct plasmids for Y2H experiments, these linearized fragments were recombined to pGADT7 gateway or pGBKT7 gateway vectors (Lu et al., 2010). All primers used in this study can be found in **Supplementary Table S1**.

Y2H Assays

Y2H assays were performed as described previously (Shen et al., 2011). Briefly, the pGADT7-DEST and pGBKT7-DEST recombinant constructs expressing the viral proteins were co-transformed into yeast cells (strain Y2H gold), and plated on selective medium lacking tryptophan and leucine (SD/-Trp/-Leu) used to select for co-transformants. The co-transformed yeast cells were further diluted in the selective medium (SD/-Trp/-Leu) and the high-stringency selective medium lacking tryptophan, leucine, histidine, and adenine (SD/-Trp/-Leu/-His/-Ade) to test the interactions. Pictures were taken at 4 days after dilution.

Confocal Microscopy

The observation of subcellular localization of viral proteins and BiFC assays was conducted by confocal microscopy as described previously (Li et al., 2018b). The genes of interest were transiently expressed in the transgenic RFP-H2B *N. benthamiana* leaves, and 1–2 cm^2 sections of the infiltrated leaves were excised and examined by confocal microscopy (Carl Zeiss LSM T-PMT, Germany) at 48 h post-infiltration (hpi), 72 and 96 hpi. YFP was excited at 518 nm, and the emitted light was captured at 565–585 nm. RFP was excited at 552 nm, and the emitted light was captured at 590–630 nm. Generally, at least 20 cells were examined for each experiment. The collected images were analyzed using the ZEN 2 (Carl Zeiss Microscope GmbH-2011) software.

Western Blot Analysis

Total proteins were extracted from the infiltrated areas expressing the viral factors at 48, 72, and 96 hpi, using protein extraction buffer [50 mM Tris-HCl (pH 6.8), 9 M urea, 4.5% SDS and 7.5% β-mercaptoethanol], as described previously (Xiong et al., 2009). Proteins were separated by electrophoresis in 12.5% SDS-PAGE, transferred to PVDF membranes, and probed with mouse anti-GFP monoclonal antibodies at a 1:8000 (v/v) dilution (Roche Applied Science, Basel, Switzerland). The secondary antibody was a goat anti-mouse IgG conjugated with peroxidase at 1:10000 (v/v) dilution (Cell Signaling Technology, Boston, MA, United States). Detection was performed using a high-sig ECL western blotting substrate (Tanon, Shanghai, China) by a chemiluminescence detection system (Tianneng, Shanghai, China). The relative quantification of the target protein in each gel lane was calculated using the Image J software as previously described (Shimoji et al., 2006), and the accumulation of viral proteins when co-infiltrated with mock solution were set to 100.

RT-qPCR Analysis

Total RNA was extracted from the infiltrated leaves using Trizol reagent (Invitrogen, Carlsbad, CA, United States) and 1 mg of RNA was retrotranscribed into cDNA using the PrimeScript™ reagent kit with gDNA eraser (TaKaRa, Dalian, Japan) according to the manufacturer's protocol. The RT-qPCR was performed in triplicates using a Roche Light Cycler 96 system (Roche Applied Science, Basel, Switzerland) with the following program: 30 s at 95°C, 45 cycles of 5 s at 95°C, 30 s at 58°C, and 10 s at 72°C. The specificity of primer pairs was verified by RT-qPCR dissociation curve. The relative expression level was calculated using the comparative Cq ($2^{-\Delta\Delta Cq}$) method. *NbActin* was used as an internal standard. The information of the primers used in the RT-qPCR experiments is listed in **Supplementary Table S1**.

RESULTS

Subcellular Localization of TYLCCNV/TYLCCNB-Encoded Viral Proteins

To gain insight into the functions of the proteins encoded by TYLCCNV/TYLCCNB, their subcellular localization was analyzed. Firstly, the 7 viral open reading frames (ORFs) were cloned into pDNOR221 vector by BP reaction (Invitrogen), followed by recombination and in-frame fusion to the coding sequence of yellow fluorescence protein (YFP) by LR reaction (Invitrogen). The recombinant proteins were expressed transiently in leaves of transgenic RFP-H2B *N. benthamiana* plants which stably expressed RFP-H2B in the nucleus as a nuclear marker (Martin et al., 2009; Anderson et al., 2018), and fluorescent signals were observed at 48, 72, and 96 hpi, by confocal microscopy.

Consistent with a previous study (Li et al., 2020), C1-YFP was mainly distributed in the nucleus at 48 hpi, but a few granules could be observed in the cytoplasm after 48 hpi (**Figure 1A**). C2-YFP was only present in the nucleus and did not change its localization over time, being uniformly distributed in this compartment (**Figure 1B**). Similar to C1-YFP, C3-YFP was mainly present in the nucleus, and C3-YFP-containing granules began to move out of the nucleus after 72 hpi. Interestingly,

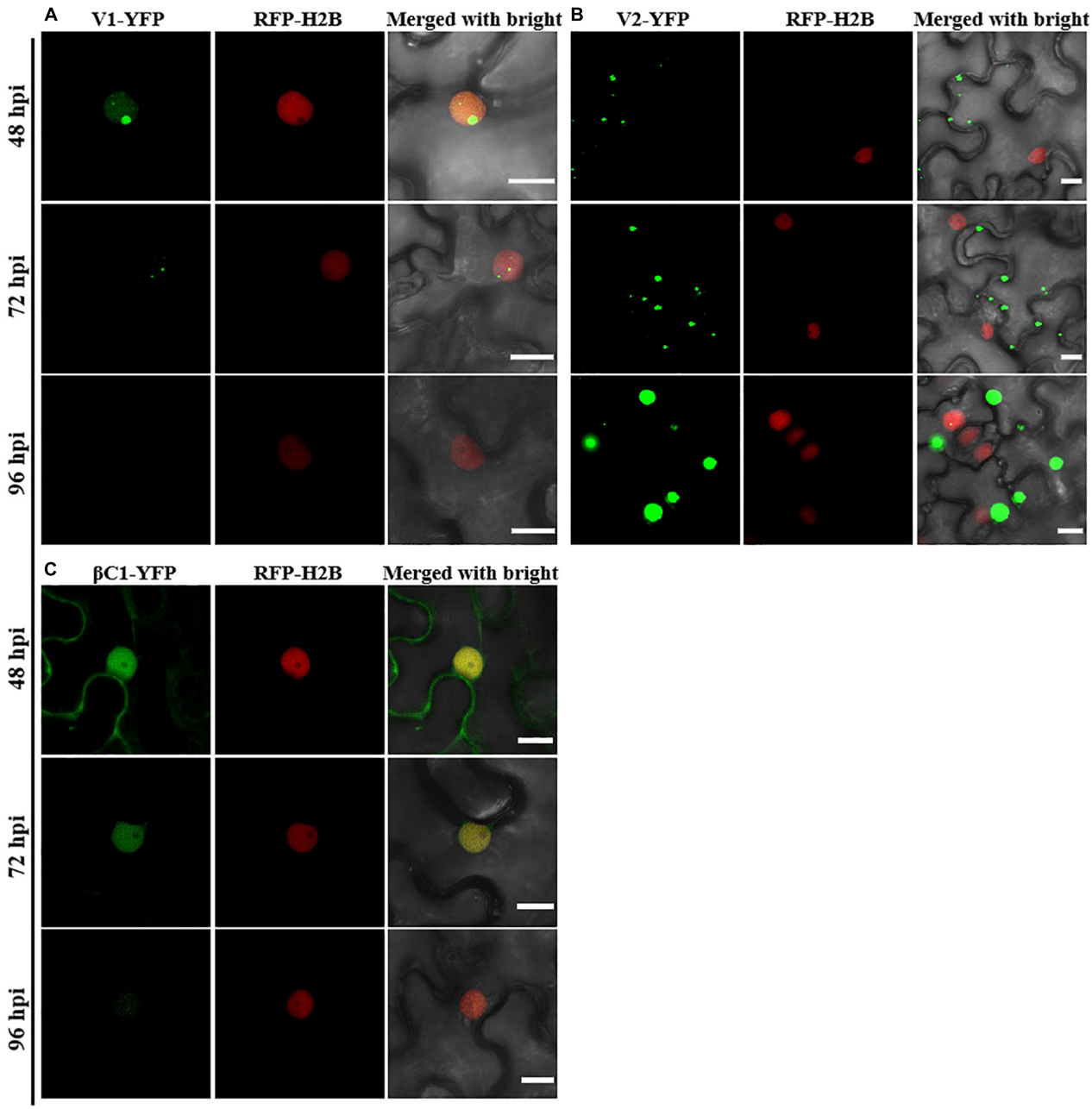

FIGURE 2 | Confocal images of TYLCCNV V1, V2, or TYLCCNB βC1 fused with YFP. RFP-H2B transgenic *N. benthamiana* leaves were infiltrated with *Agrobacterium* cultures to express V1-YFP **(A)**, V2-YFP **(B)**, or βC1-YFP **(C)**. Confocal images were taken at 48, 72, and 96 hpi. YFP signal is shown in green. Nuclei of tobacco leaf epidermal cells are marked by RFP-H2B (red). This experiment was repeated three times independently, and more than 20 cells per sample were observed each time; representative results are shown. Scale bar: 10 μm.

C3-YFP formed irregular and speckled granules in the nucleus, a distribution different to that of C1-YFP (**Figure 1C**). C4-YFP localized exclusively to the plasma membrane, as previously reported for other geminivirus C4 proteins (Mei et al., 2018), and this did not change in time (**Figure 1D**). V1-YFP was localized in the nucleoplasm and in the nucleolus at 48 hpi. The V1-YFP fluorescent signal decreased in the nucleoplasm, appearing in the nucleolus only, at 72 hpi. No fluorescence in V1-YFP-infiltrated leaves was observed at 96 hpi (**Figure 2A**). Different from the protein localization described above, V2-YFP formed some small granules in the cytoplasm, and the fluorescence of these granules became brighter after 48 hpi (**Figure 2B**). The βC1-YFP protein was distributed in both the nucleus and cytoplasm at 48 hpi (**Figure 2C**). It is worth noting that the fluorescence intensity of each YFP-fused protein changed differently over time (note: unless otherwise indicated, confocal images presented in the same

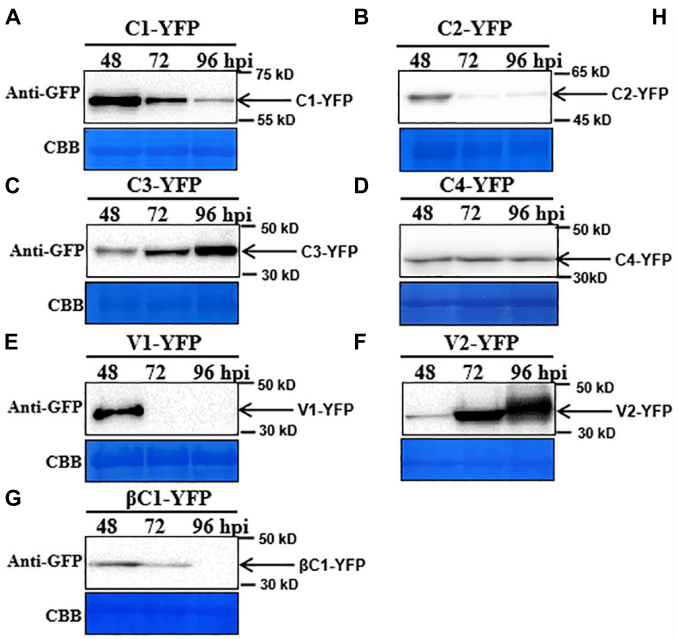

H

	48 hpi	72 hpi	96 hpi
C1-YFP (≈68 kD)	100	46±1	15±1
C2-YFP (≈57 kD)	100	11±1	10±1
C3-YFP (≈42 kD)	100	179±3	272±8
C4-YFP (≈40 kD)	100	101±5	95±1
V1-YFP (≈43 kD)	100	5±1	5±1
V2-YFP (≈41 kD)	100	712±14	981±18
βC1-YFP (≈40 kD)	100	45±1	4±1

FIGURE 3 | Dynamic changes in the accumulation of viral proteins. **(A–G)** *N. benthamiana* leaves were infiltrated with 0.5 ml of *Agrobacterium* cultures to express C1-YFP, C2-YFP, C3-YFP, C4-YFP, V1-YFP, V2-YFP, or βC1-YFP adjusted to an optical density at 600 nm (OD_{600}) = 0.8. Total proteins were extracted from C1-YFP, C2-YFP, C3-YFP, C4-YFP, V1-YFP, V2-YFP, or βC1-YFP infiltrated zones at 48, 72, or 96 hpi. C1-YFP **(A)**, C2-YFP **(B)**, C3-YFP **(C)**, C4-YFP **(D)**, V1-YFP **(E)**, V2-YFP **(F)**, or βC1-YFP **(G)** at 48, 72, or 96 hpi were detected with an anti-GFP antibody. Arrows indicate the expected protein size. All immunoblotting assays in these figures were repeated at least three times, and each experimental sample was derived from three individual infiltrations. One representative blot is shown. Coomassie brilliant blue (CBB)-stained Rubisco large subunit was used as a loading control. **(H)** Accumulation of the specific proteins quantified from the western blot images by Image J, relative to the value of each protein at 48 hpi (set to 100).

figure panel were taken and processed with the same settings). For example, the fluorescent signal of C1-YFP, C2-YFP, V1-YFP, and βC1-YFP gradually decreased after 48 hpi (**Figures 1**, **2**). However, the fluorescent signal of C3-YFP and V2-YFP gradually increased from 48 to 96 hpi (**Figure 1**). No obvious change in the fluorescence intensity of C4-YFP was observed from 48 to 96 hpi (**Figure 1D**).

Dynamic Changes on the Accumulation of TYLCCNV/TYLCCNB-Encoded Proteins

To observe the dynamic changes in the accumulation of the TYLCCNV/TYLCCNB-encoded proteins, total proteins were extracted from C1-YFP, C2-YFP, C3-YFP, C4-YFP, V1-YFP, V2-YFP, or βC1-YFP-expressing leaves at 48, 72, and 96 hpi. Protein levels from 48 to 96 hpi are shown in **Figure 3**. The accumulation of C1-YFP, C2-YFP, V1-YFP, and βC1-YFP decreased after 48 hpi. The accumulation of C1-YFP, V1-YFP, and βC1-YFP was almost undetectable at 96 hpi (**Figures 3A,B,E,G**), while that of V1-YFP and βC1-YFP decreased significantly over time. The amount of C3-YFP and V2-YFP increased after 48 hpi (**Figures 3C,F**). No obvious change in the accumulation of C4-YFP was detected (**Figure 3D**). To evaluate the observed changes in more detail, we quantified the relative protein accumulation by Image J with the data at 72 and 96 hpi normalized to those at 48 hpi (set to 100) (**Figure 3H**). These data were consistent with the confocal observation. To further determine whether the decreased protein accumulation of viral proteins was due to decreased transcript accumulation. RT-qPCR analysis was carried out, and decreased RNA levels of *C1-YFP*, *C2-YFP*, *V1-YFP*, and β*C1-YFP* were observed from 48 to 96 hpi (**Supplementary Figure S1**), suggesting that RNA-mediated degradation was involved in lower accumulation of the protein.

TYLCCNV/TYLCCNB Infection Enhances the Accumulation of Viral Proteins

In order to better determine the localization and expression of each protein in the context of the virus infection, *Agrobacterium* cultures that express the YFP-fused viral proteins were co-infiltrated with *Agrobacterium* cultures carrying an empty vector (Mock), or TYLCCNV (10A), or TYLCCNV/TYLCCNB (10Aβ) infectious clones into RFP-H2B transgenic *N. benthamiana* leaves and infiltrated leaves were examined by confocal microscope at 48 and 72 hpi. Viral intercellular movement may take place after 72 hpi, with replicating viruses moving onto neighboring areas or systemic leaves from the infiltrated zones. Therefore, we chose 48 and 72 hpi, rather than 96 hpi, to analyze the effects of virus infection on the expression and subcellular location of TYLCCNV/TYLCCNB-encoded proteins in the infiltrated leaves. Co-infiltration with TYLCCNV or TYLCCNV/TYLCCNB had no obvious effect on the localization or protein accumulation of C1-YFP at 48 hpi compared

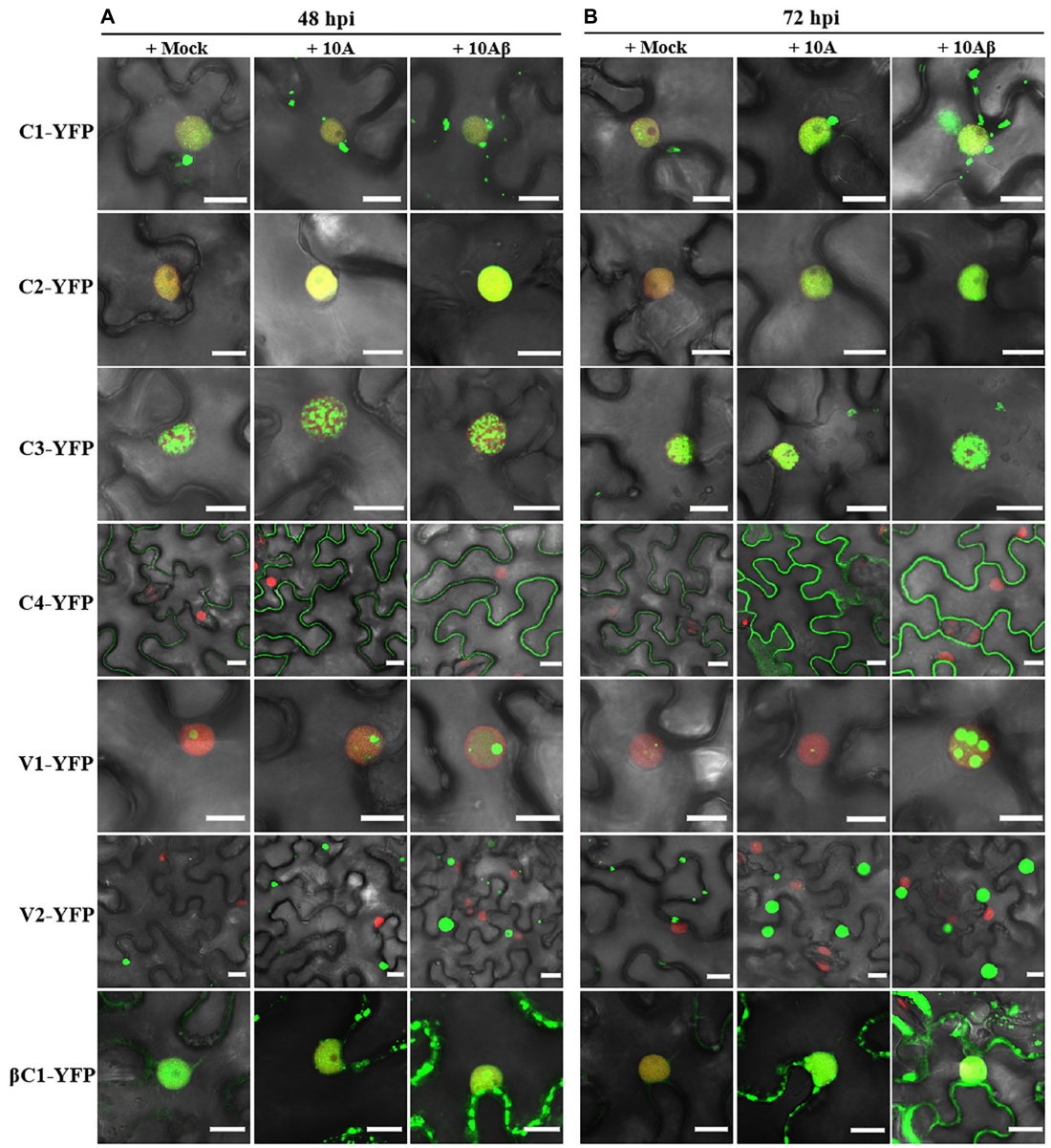

FIGURE 4 | Confocal images of viral proteins fused with YFP in the presence or absence of TYLCCNV (10A), or TYLCCNV/TYLCCNB (10Aβ). **(A,B)** RFP-H2B *N. benthamiana* leaves were co-infiltrated with *Agrobacterium* cultures carrying the indicated constructs, and then examined by confocal microscopy at 48 hpi **(A)** and 72 hpi **(B)**. All *Agrobacterium* cultures were adjusted to an optical density at 600 nm (OD600) = 0.8 and 0.5 ml of *Agrobacterium* cultures were infiltrated into leaves. These experiments were repeated three times by three independent infiltrations, and more than 20 cells per sample were observed in each replicate; representative results are shown. Scale bar: 10 μm.

to that with Mock (**Figures 4A**, **5A**), but enhanced C1-YFP fluorescence and increased protein accumulation were observed at 72 hpi (**Figures 4A**, **5A**). Increased fluorescent signal and protein accumulation of C2-YFP were observed in the presence of TYLCCNV or TYLCCNV/TYLCCNB at 48 and 72 hpi (**Figures 4A,B**, **5B**). Similarly, co-expression with TYLCCNV or TYLCCNV/TYLCCNB increased the fluorescent signal and protein accumulation of C3-YFP, but to a lower extent (**Figures 4A,B**, **5B,C**). It was also obvious that the virus infection enhanced the fluorescence intensity and increased the protein accumulation of C4-YFP at 48 and 72 hpi (**Figure 5D**). There was no significant difference in the subcellular localization and protein accumulation of V1-YFP in the presence or absence of TYLCCNV at 48 hpi (**Figures 4A,B**). However, TYLCCNV/TYLCCNB, but not TYLCCNV alone, at 72 hpi could change the subcellular localization and increase the protein accumulation of V1-YFP, which formed larger and more abundant granules in the nucleus, at 72 hpi. This result indicates that the enhanced fluorescence and increased protein level of V1-YFP at 72 hpi is dependent on TYLCCNB (**Figure 5E**).

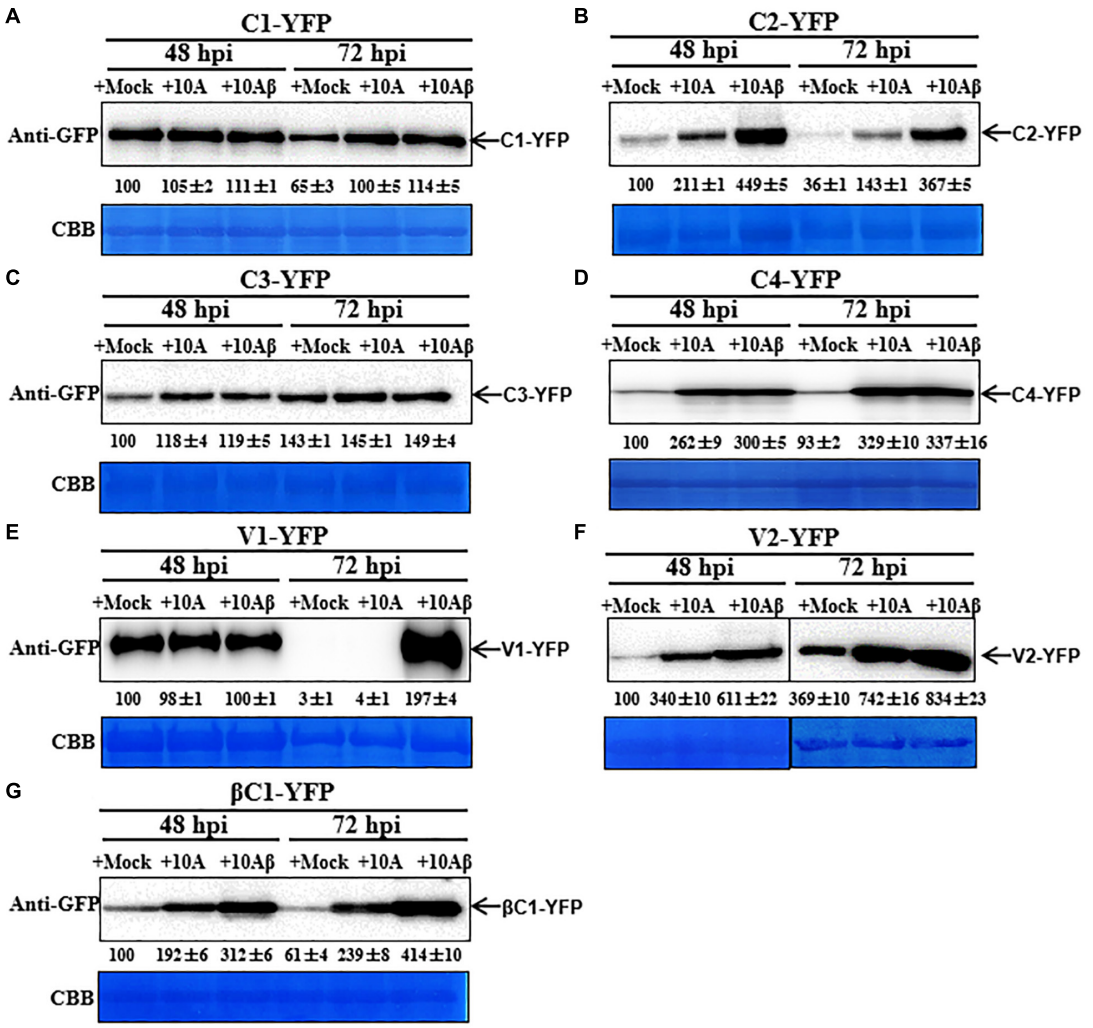

FIGURE 5 | Dynamic changes in the accumulation of viral proteins in the presence or absence of TYLCCNV (10A) or TYLCCNV/TYLCCNB (10Aβ). Wild type *N. benthamiana* leaves were infiltrated with *Agrobacterium* cultures to express C1-YFP, C2-YFP, C3-YFP, C4-YFP, V1-YFP, V2-YFP, or βC1-YFP together with those harboring an empty vector (Mock), or TYLCCNV or TYLCCNV/TYLCCNB infectious clones. **(A–G)** C1-YFP, C2-YFP, C3-YFP, C4-YFP, V1-YFP V2-YFP, or βC1-YFP proteins detected by western blot. Total proteins were extracted from infiltrated leaves as indicated at 48 and 72 hpi, and detected with an anti-GFP antibody. The sample volume was 20 μl **(A–E)** or 10 μl **(F,G)**. All immunoblotting assays in these figures were repeated at least three times, and each experimental sample derived from three individual infiltrations. One representative blot is shown. CBB-stained Rubisco large subunit was used as a loading control. The values of C1-YFP, C2-YFP, C3-YFP, C4-YFP, V1-YFP, V2-YFP, or βC1-YFP at 48 hpi were quantified by Image J and set to 100 for normalization.

The presence of TYLCCNV or TYLCCNV/TYLCCNB increased the fluorescence and protein accumulation of V2-YFP and βC1-YFP at 48 and 72 hpi (**Figures 4A,B**, **5F,G**). Taken together, these data indicate that the accumulation of all viral proteins is enhanced during the viral infection, especially in the presence of TYLCCNB.

Interactions Among TYLCCNV/TYLCCNB-Encoded Proteins

To screen for possible interactions among the seven viral proteins encoded by TYLCCNV/TYLCCNB, yeast two-hybrid (Y2H) assays were conducted. All these viral proteins were fused with the GAL4 transcription activation domain (AD) and the GAL4 DNA binding domain (BD), respectively. As summarized in **Figures 6A,B**, interactions among TYLCCNV/TYLCCNB-encoded proteins were identified. The C2 protein acted as an interaction hub, since it can interact with most proteins including C3, C4, V2, and βC1 (**Figures 6B,C**). In addition, the interaction between C4 and V2, and self-interactions of C1, C2, and V2 were also found (**Figures 6B,C**). Unexpectedly, we did not detect interactions between the V1 (CP) with any other viral protein, or with itself, although the self-interaction of TYLCV V1 was previously reported (Hallan and Gafni, 2001).

All the interactions identified by Y2H were further confirmed by bimolecular fluorescence complementation (BiFC) in transgenic *N. benthamiana* plants expressing RFP-H2B as a nuclear marker. The C2–C3, C2–C4, and C2–βC1 interactions,

A

	BD	BD-C1	BD-C2	BD-C3	BD-C4	BD-V1	BD-V2	BD-βC1
AD	–	–	–	–	–	–	–	–
AD-C1	–	+	-	-	-	-	-	-
AD-C2	–	–	+	+	+	-	+	+
AD-C3	–	–	–	–	–	–	–	–
AD-C4	–	–	–	–	–	–	–	–
AD-V1	–	–	-	–	–	–	–	–
AD-V2	–	–	+	-	+	-	+	-
AD-βC1	–	–	–	–	–	–	–	–

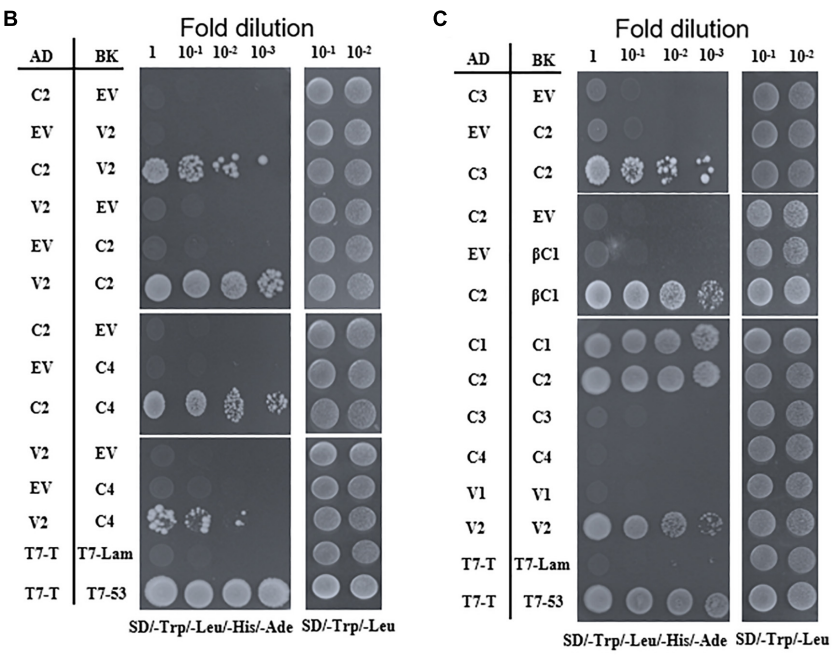

FIGURE 6 | Yeast two-hybrid assays among TYLCCNV/TYLCCNB-encoded proteins. **(A)** Summary of Y2H assay results. "–" means no positive interaction was detected; "+" means a positive interaction was detected. The Y2H assays summarized in this table were repeated at least three times by each independent transformation. **(B)** Interactions between C2 and V2, C2 and C4, and V2 and C4 by Y2H. **(C)** Interactions between C2 and C3, C2 and βC1, and self-interactions of C1, C2, and V2 by Y2H. The Y2H Gold yeast strain cells co-transformed with the indicated plasmids were plated on synthetic dextrose (SD)/-Trp, -Leu, -His, -Ade medium to identify protein interactions. Photographs were taken at 4 days post-transformation. Yeast cells co-transformed with pGADT7-T and pGBKT7-Lam were used as negative controls, and with pGADT7-T and pGBKT7-53 were used as positive controls **(B,C)**.

as well as the C1 and C2 self-interactions, were detected in the nucleus (**Figures 7A,B**). The interaction between C2 and V2 was localized in the nucleus and in the cytoplasm (**Figure 7A**). The interaction between C4 and V2, and the V2 self-interaction were observed in the cytoplasm (**Figures 7A,B**). As a negative control, no YFP fluorescence was observed when the movement protein P3N-PIPO from TuMV (Wei et al., 2015) was co-expressed with C1, C2, C3, C4, V2, or βC1 (**Supplementary Figure S2**).

DISCUSSION

Although the subcellular localization of many geminivirus proteins has been analyzed, the subcellular localization of TYLCCNV/TYLCCNB-encoded proteins has not been reported yet. In this study, the subcellular localization of all TYLCCNV/TYLCCNB-encoded proteins and the effects of the viral infection on the subcellular localization and

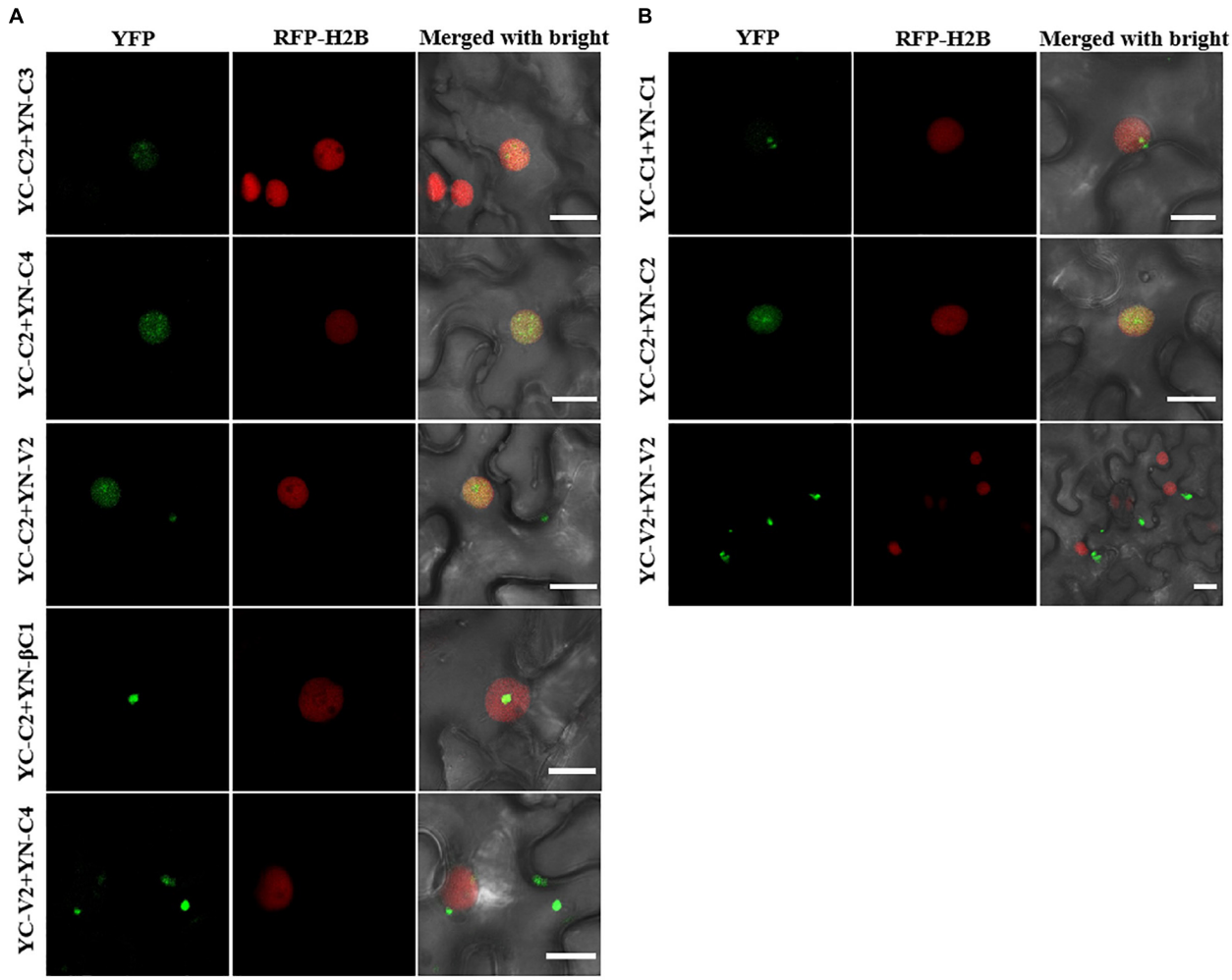

FIGURE 7 | BiFC assays to confirm the interactions among TYLCCNV/TYLCCNB-encoded proteins. **(A)** Confocal visualization of the interaction between C2 and C3, C2 and C4, C2 and V2, C2 and βC1, and C4 and V2 in RFP-H2B transgenic *N. benthamiana* leaves. The fused proteins indicated above were transiently expressed in RFP-H2B transgenic *N. benthamiana* leaves. Images were taken at 48 hpi. Yellow fluorescence (in green) was found in the leaf cells co-expressing C2 + C3, C2 + C4, C2 + V2, C2 + βC1, and C4 + V2. Nuclei of tobacco leaf epidermal cells are indicated by RFP-H2B (red). Bars, 10 μm. **(B)** Confocal visualization of the self-interaction of C1, C2, and V2. C1, C2, and V2 were fused with YN or YC, respectively. Yellow fluorescence (in green) was found upon pairwise expression of YN-C1 + YC – C1, YN – C2 + YC – C2, and YN – V2 + YC – V2 at 48 hpi. Bars, 10 μm. These experiments were repeated three times by three independent infiltrations; one representative result is shown **(A,B)**.

accumulation of each protein were investigated. C1, as a replication initiation protein (Rep) involved in the replication of the geminivirus genome in the nucleus, was initially localized in this subcellular compartment, and then partially localized outside of the nucleus with decreasing fluorescence intensity over time (**Figure 1**). We found that both in the protein level and RNA level of TYLCCNV C1-YFP decreased from 48 to 96 hpi (**Figure 3** and **Supplementary Figure S1**), suggesting that the expression of C1-YFP is susceptible to both RNA and protein-mediated degradation. Similarly, C2-YFP was also localized in the nucleus with decreasing fluorescence intensity, RNA accumulation and protein accumulation after 48 hpi (**Figures 1**, **3**). In contrast, C3-YFP formed speckled granules in the nucleus with increasing fluorescence intensity and protein accumulation, showing that C3 is probably resistant to host RNA and protein-mediated degradation mechanisms. C4-YFP was localized at the plasma membrane, and no obvious change was observed in the C4-YFP subcellular localization or C4-YFP protein accumulation over time (**Figures 2**, **3**). Decreased fluorescent signal, protein accumulation and RNA levels of V1-YFP and βC1-YFP were also observed (**Figures 2**, **3** and **Supplementary Figure S1**). Based on the above results, we speculate that transiently expressed viral proteins can be targets of host RNA and protein degradation systems. Three major RNA degradation pathways including RNA silencing, RNA decay, and RNA quality control can target exogenous RNAs in plants, and mediate degradation of target transcripts (Li and Wang, 2019). The ubiquitin-proteasome system (UPS) and autophagy are reported to be involved in the degradation of many viral protein in plants (Shen et al., 2016;

Cheng and Wang, 2017; Haxim et al., 2017; Yang et al., 2018; Li et al., 2020). For example, autophagy was involved in the degradation of several geminivirus C1 proteins, including C1 of TLCYnV, TYLCV, tobacco curly shoot virus (TbCSV), and mungbean yellow mosaic India virus (MYMIV), which directly interacted with the autophagy protein ATG8h (Li et al., 2020). The geminivirus βC1 can be the target of both the UPS and autophagy, which leads to its degradation (Shen et al., 2016; Haxim et al., 2017). In addition, TYLCV infection in whiteflies activated autophagy to lead to the degradation of the V1 protein and viral genomic DNA (Wang et al., 2016). However, an increased number of fluorescent aggregates and higher protein accumulation of V2-YFP were observed in our experiments (**Figures 2**, **3**), suggesting that V2 can suppress host RNA or protein degradation mechanisms. Indeed, TYLCCNV and TYLCV V2 acts as a strong RNA silencing suppressor (Glick et al., 2008; Zhang et al., 2012).

The observation of the subcellular localization of viral proteins in the context of the viral infection is important to understand their biological roles. In this study, we noticed that the fluorescent signals of almost all viral proteins can be enhanced when TYLCCNV alone or TYLCCNV/TYLCCNB are present, especially the fluorescent intensity of V1-YFP and βC1-YFP (**Figures 4**, **5**), which were consistent with their protein accumulation. Viral proteins encoded in TYLCCNV or TYLCCNB such as V2 and βC1, are able to suppress RNA silencing (Cui et al., 2005; Zhang et al., 2012), so it is reasonable that co-infection of TYLCCNV or TYLCCNV/TYLCCNB enhances the fluorescence intensity and protein expression. It is worth noting that the V1-YFP protein levels were particularly sensitive to TYLCCNV/TYLCCNB infection. At 72 hpi, different from other viral proteins, TYLCCNV alone could not block the sharp decrease of the V1-YFP protein accumulation, while TYLCCNV/TYLCCNB could increase it to a higher level compared to that at 48 hpi (**Figure 5E**). These results indicate that TYLCCNV/TYLCCNB is required for the accumulation of the V1-YFP protein. In addition, V1-YFP was localized in the nucleoplasm and nucleolus, while TYLCCNV/TYLCCNB infection caused the appearance of more bright granules in the nucleus (**Figure 4**). Geminivirus infection changed the subnuclear localization of V1, which has also been reported previously (Wang et al., 2017), suggesting the conserved functions of different geminiviruses. Except for V1, there was no obvious difference in the subcellular localization observed for TYLCCNV/TYLCCNB-encoded proteins in the presence of TYLCCNV alone or TYLCCNV/TYLCCNB, indicating that the unique localization of viral proteins contributes to the viral infection.

Protein–protein interactions during the viral infection are important ways to link different viral proteins together to cooperatively participate in the viral life cycle. We found that several interactions among different viral proteins exist, and C2 serves as an interaction hub, associating with most viral proteins (**Figures 6**, **7**). The geminivirus transcriptional activator C2 protein is a multifunctional protein, which can bind DNA, suppress TGS and PTGS, and also act as a pathogenicity factor (Noris et al., 1996; van et al., 2002; Fondong, 2013). For example, C2 positional homologs of some geminiviruses interact with and inactivate adenosine kinase (ADK) which is required for efficient production of *S*-adenosyl methionine, an essential methyltransferase cofactor. Therefore, C2 homologs can suppress TGS and cause a genome-wide reduction in cytosine methylation (Buchmann et al., 2009). C2 encoded by beet severe curly top virus (BSCTV) interacts with *S*-adenosyl-methionine decarboxylase 1 (SAMDC1) and interferes with the host defense mechanism of DNA methylation-mediated gene silencing through attenuating its 26S proteasome-mediated degradation of SAMDC1 (Zhang et al., 2011). Therefore, the interaction between C2 and C3 probably facilitates the replication of the viral genome and the transcription of viral RNAs by suppressing host TGS and PTGS responses. Geminivirus C4, V2, or βC1 can repress many host defenses with different mechanisms (Zhang et al., 2012; Li et al., 2018a; Wang et al., 2018; Fondong, 2019), so the interactions between C2 and C4, C2 and V2, or C2 and βC1 might enhance viral pathogenicity by forming strong counter-defense complexes to suppress host defense responses. The interaction between V2 and C4 was observed as bright granules localized in the cytoplasm (**Figure 5A**). V2 has been reported as involved in viral movement, and is also able to suppress TGS and PTGS. For example, cotton leaf curl Multan virus (CLCuMuV) V2 protein inhibits TGS by interacting with AGO4 (Wang et al., 2019); TYLCV V2 can achieve PTGS inhibition by interacting with the host SGS3 (Glick et al., 2008), and interacts with *N. benthamiana* histone deacetylase 6 to inhibit methylation-mediated TGS (Wang et al., 2018). C4 has been reported as a movement protein (Jupin et al., 1994; Rojas et al., 2001), so the interaction between C4 and V2 may participate in the movement of the virus and counter host defense responses. Based on the subcellular localization of V2 and C4, we speculate that V2 probably transports the encapsulated virus particles to the cell membrane, where C4 transports them to the neighboring cells.

Self-interactions of TYLCCNV C1, C2, and V2 were also found (**Figures 6**, **7**). It has been shown that the self-interaction of C1 encoded by abutilon mosaic virus (AMV) is involved in initiating the replication in the nucleus (Krenz et al., 2011). Geminivirus C1 is a multifunctional protein with site-specific nicking and ligase activity, helicase activity, site-specific DNA binding activity, and ATPase activity, and it can recruit several host proteins to usurp the host replication machinery for viral proliferation (Hanley-Bowdoin et al., 2013). Therefore, the self-interaction of TYLCCNV C1 is probably involved in its multifunctional activities, which are necessary for the establishment of functional virus replication complexes. The TYLCCNV C2–C2 interaction complexes accumulated primarily in the nucleus, which was consistent with the previous observation that the self-interaction of C2 positional homologs correlates with their nuclear localization and efficient activation of transcription, whereas their monomers can suppress local silencing by

interacting with ADK in the cytoplasm (Yang et al., 2007). The self-interaction of TYLCCNV V2 was also observed in this study (**Figures 6**, **7**), similar to what has been observed for TYLCV V2. A single amino acid in V2 encoded by TYLCV is responsible for its self-interaction, aggregates formation, and pathogenicity (Zhao et al., 2018). The self-interaction of TYLCV CP (V1) was found in a previous report, which identified the N-terminal region of CP as necessary (Hallan and Gafni, 2001). However, no self-interaction of TYLCCNV V1 was found in this study. One possible explanation is sequence differences between these viral proteins, since TYLCCNV V1 shares 76.7% amino acid identity to TYLCV V1 (**Supplementary Figure S3**).

In brief, we have determined the dynamic localization and protein accumulation of TYLCCNV/TYLCCNB-encoded proteins over time with or without the viral infection, and explored the potential roles of each protein in virus replication and infection based on their interactions. Therefore, this study provides solid and useful information for further works on the biological significance of the viral proteins during the viral infection.

DATA AVAILABILITY STATEMENT

The datasets generated for this study can be found in the TYLCCNV (accession number: AJ319675) and TYLCCNB (accession number: AJ781300) can be found in GenBank.

AUTHOR CONTRIBUTIONS

HL, FL, MZ, and PG performed all experiments. FL, HL, and XZ contributed to experimental design and interpretation. FL and XZ conceived the project. HL, FL, and XZ wrote the manuscript with contributions from all authors.

FUNDING

This work was funded by the National Natural Science Foundation of China (31930089 and 31972244).

ACKNOWLEDGMENTS

We thank Michael M. Goodin (University of Kentucky, United States) for the seeds of RFP-H2B transgenic *N. benthamiana*.

SUPPLEMENTARY MATERIAL

The Supplementary Material for this article can be found online at: https://www.frontiersin.org/articles/10.3389/fpls.2020.00840/full#supplementary-material

FIGURE S1 | Dynamic changes in the transcripts of viral genes. RT-qPCR analysis of the YFP RNA fused with C1, C2, V1, and βC1. The values of C1-YFP, C2-YFP, V1-YFP, and βC1-YFP at 48 hpi were normalized against *NbActin* transcripts in the same sample. Three independent experiments, each consisting of three biological replicates, were carried out. Values from one representative result were used to plot a histogram. Statistical analysis was performed using GraphPad Prism 6 software followed by ANOVA using Student's *t*-test (two-sided, $^{*}P < 0.05$, $^{**}P < 0.01$, $^{***}P < 0.001$).

FIGURE S2 | Interaction assays of P3N-PIPO and C1, C2, C3, C4, V2, or βC1. BiFC assays in RFP-H2B transgenic *N. benthamiana* leaves expressing P3N-PIPO and C1, C2, C3, C4, V2, or βC1 at 48 h post infiltration (hpi). Bars = 20 μm. No YFP fluorescence was detected.

FIGURE S3 | Amino acid sequence alignment of TYLCV-V1 and TYLCCNV-V1 was performed in MegAlign (Lasergene) and sequence distances were conducted in MegAlign using the Clustal V Method.

TABLE S1 | Primers used in plasmid construction and other experiments in this study.

REFERENCES

Anderson, G., Jang, C., Wang, R., and Goodin, M. (2018). Mapping the nuclear localization signal in the matrix protein of potato yellow dwarf virus. *J. Gen. Virol.* 99, 743–752. doi: 10.1099/jgv.0.001051

Briddon, R. W., Pinner, M. S., Stanley, J., and Markham, P. G. (1990). Geminivirus coat protein gene replacement alters insect specificity. *Virology* 177, 85–94. doi: 10.1016/0042-6822(90)90462-z

Buchmann, R. C., Asad, S., Wolf, J. N., Mohannath, G., and Bisaro, D. M. (2009). Geminivirus AL2 and L2 proteins suppress transcriptional gene silencing and cause genome-wide reductions in cytosine methylation. *J. Virol.* 83, 5005–5013. doi: 10.1128/JVI.01771-08

Caracuel, Z., Lozano-Durán, R., Huguet, S., Arroyo-Mateos, M., Rodríguez-Negrete, E. A., and Bejarano, E. R. (2012). C2 from Beet curly top virus promotes a cell environment suitable for efficient replication of geminiviruses, providing a novel mechanism of viral synergism. *New Phytol.* 194, 846–858. doi: 10.1111/j.1469-8137.2012.04080.x

Cheng, X., and Wang, A. (2017). The potyvirus silencing suppressor protein VPg mediates degradation of SGS3 via ubiquitination and autophagy pathways. *J. Virol.* 91:e01478-16. doi: 10.1128/JVI.01478-16

Cui, X., Li, G., Wang, D., Hu, D., and Zhou, X. (2005). A begomovirus DNA β-encoded protein binds DNA, functions as a suppressor of RNA silencing, and targets the cell nucleus. *J. Virol.* 79, 10764–10775. doi: 10.1128/JVI.79.16.10764-10775.2005

Cui, X., Tao, X., Xie, Y., Fauquet, C. M., and Zhou, X. (2004). A DNA-beta associated with tomato yellow leaf curl China virus is required for symptom induction. *J. Virol.* 78, 13966–13974. doi: 10.1128/JVI.78.24.13966-13974.2004

Earley, K. W., Haag, J. R., Pontes, O., Opper, K., Juehne, T., Song, K., et al. (2006). Gateway-compatible vectors for plant functional genomics and proteomics. *Plant J.* 45, 616–629. doi: 10.1111/j.1365-313X.2005.02617.x

Fondong, V. N. (2013). Geminivirus protein structure and function. *Mol. Plant Pathol.* 14, 635–649. doi: 10.1111/mpp.12032

Fondong, V. N. (2019). The ever-expanding role of C4/AC4 in geminivirus infection: punching above its weight? *Mol. Plant* 12, 145–147. doi: 10.1016/j.molp.2018.12.006

Glick, E., Zrachya, A., Levy, Y., Mett, A., Gidoni, D., Belausov, E., et al. (2008). Interaction with host SGS3 is required for suppression of RNA silencing by tomato yellow leaf curl virus V2 protein. *Proc. Natl. Acad. Sci. U.S.A.* 105, 157–161. doi: 10.1073/pnas.0709036105

Hallan, V., and Gafni, Y. (2001). Tomato yellow leaf curl virus (TYLCV) capsid protein (CP) subunit interactions: implications for viral assembly. *Arch. Virol.* 146, 1765–1773. doi: 10.1007/s007050170062

Hanley-Bowdoin, L., Bejarano, E. R., Robertson, D., and Mansoor, S. (2013). Geminiviruses: masters at redirecting and reprogramming plant processes. *Nat. Rev. Microbiol.* 11, 777–788. doi: 10.1038/nrmicro3117

Harrison, B. D., and Robinson, D. J. (2002). Green shoots of geminivirology. *Mol. Plant Pathol.* 60, 215–218. doi: 10.1006/pmpp.2002.0400

Haxim, Y., Ismayil, A., Jia, Q., Wang, Y., Zheng, X., Chen, T., et al. (2017). Autophagy functions as an antiviral mechanism against geminiviruses in plants. *eLife* 28:e23897. doi: 10.7554/eLife.23897

Jupin, I., Kouchovsky, F., Jouanneau, F., and Gronenborn, B. (1994). Movement of tomato yellow leaf curl geminivirus (TYLCV): involvement of the protein encoded by ORF C4. *Virology* 204, 82–90. doi: 10.1006/viro.1994.1512

Kong, L. J., Orozco, B. M., Roe, J. R., Nagar, S., Ou, S., Feiler, H. S., et al. (2000). A geminivirus replication protein interacts with the retinoblastoma protein through a novel domain to determine symptoms and tissue specificity of infection in plants. *EMBO J.* 19, 3485–3495. doi: 10.1093/emboj/19.13.3485

Krenz, B., Neugart, F., Kleinow, T., and Jeske, H. (2011). Self-interaction of abutilon mosaic virus replication initiator protein (Rep) in plant cell nuclei. *Virus Res.* 161, 194–197. doi: 10.1016/j.virusres.2011.07.020

Lai, J., Chen, H., Teng, K., Zhao, Q., Zhang, Z., Li, Y., et al. (2009). RKP, a RING finger E3 ligase induced by BSCTV C4 protein, affects geminivirus infection by regulation of the plant cell cycle. *Plant J.* 57, 905–917. doi: 10.1111/j.1365-313X.2008.03737.x

Li, F., Huang, C., Li, Z., and Zhou, X. (2014). Suppression of RNA silencing by a plant DNA virus satellite requires a host calmodulin-like protein to repress RDR6 expression. *PLoS Pathog.* 10:e1003921. doi: 10.1371/journal.ppat.1003921

Li, F., and Wang, A. (2019). RNA-targeted antiviral immunity: more than just RNA silencing. *Trends Microbiol.* 27, 792–805. doi: 10.1016/j.tim.2019.05.007

Li, F., Yang, X., Bisaro, D. M., and Zhou, X. (2018a). The βC1 protein of geminivirus-betasatellite complexes: a target and repressor of host defenses. *Mol. Plant* 11, 1424–1426. doi: 10.1016/j.molp.2018.10.007

Li, F., Zhang, C., Li, Y., Wu, G., Hou, X., Zhou, X., et al. (2018b). Beclin1 restricts RNA virus infection in plants through suppression and degradation of the viral polymerase. *Nat. Commun.* 9:1268. doi: 10.1038/s41467-018-03658-2

Li, F., Zhang, M., Zhang, C., and Zhou, X. (2020). Nuclear autophagy degrades a geminivirus nuclear protein to restrict viral infection in Solanaceous plants. *New Phytol.* 225, 1746–1761. doi: 10.1111/nph.16268

Li, F., Zhao, N., Li, Z., Xu, X., Wang, Y., Yang, X., et al. (2017). A calmodulin-like protein suppresses RNA silencing and promotes geminivirus infection by degrading SGS3 via the autophagy pathway in *Nicotiana benthamiana*. *PLoS Pathog.* 13:e1006213. doi: 10.1371/journal.ppat.1006213

Lu, Q., Tang, X., Tian, G., Wang, F., Liu, K., Nguyen, V., et al. (2010). Arabidopsis homolog of the yeast TREX-2 mRNA export complex: components and anchoring nucleoporin. *Plant J.* 61, 259–270. doi: 10.1111/j.1365-313X.2009.04048

Martin, K., Kopperud, K., Chakrabarty, R., Banerjee, R., Brooks, R., and Goodin, M. M. (2009). Transient expression in *Nicotiana benthamiana* fluorescent marker lines provides enhanced definition of protein localization, movement and interactions in planta. *Plant J.* 59, 150–162. doi: 10.1111/j.1365-313X.2009.03850

Matić, S., Pegoraro, M., and Noris, E. (2016). The C2 protein of tomato yellow leaf curl Sardinia virus acts as a pathogenicity determinant and a 16-amino acid domain is responsible for inducing a hypersensitive response in plants. *Virus Res.* 215, 12–19. doi: 10.1016/j.virusres.2016.01.014

Mei, Y., Ma, Z., Wang, Y., and Zhou, X. (2019). Geminivirus C4 antagonizes the HIR1-mediated hypersensitive response by inhibiting the HIR1 self-interaction and promoting degradation of the protein. *New Phytol.* 225, 1311–1326. doi: 10.1111/nph.16208

Mei, Y., Wang, Y., Hu, T., Yang, X., Lozano-Duran, R., Sunter, G., et al. (2018). Nucleocytoplasmic shuttling of geminivirus C4 protein Mediated by phosphorylation and myristoylation is critical for viral pathogenicity. *Mol. Plant* 11, 1466–1481. doi: 10.1016/j.molp.2018.10.004

Mubin, M., Amin, I., Amrao, L., Briddon, R. W., and Mansoor, S. (2010). The hypersensitive response induced by the V2 protein of a monopartite begomovirus is countered by the C2 protein. *Mol. Plant. Pathol.* 11, 245–254. doi: 10.1111/j.1364-3703.2009.00601.x

Noris, E., Jupin, I., Accotto, G. P., and Gronenborn, B. (1996). DNA-binding activity of the C2 protein of tomato yellow leaf curl geminivirus. *Virology* 217, 607–612. doi: 10.1006/viro.1996.0157

Rodríguez-Negrete, E., Lozano-Durán, R., Piedra-Aguilera, A., Cruzado, L., Bejarano, E. R., and Castillo, A. G. (2013). Geminivirus Rep protein interferes with the plant DNA methylation machinery and suppresses transcriptional gene silencing. *New Phytol.* 199, 464–475. doi: 10.1111/nph.12286

Rojas, M. R., Jiang, H., Salati, R., Xoconostle-Cázares, B., Sudarshana, M. R., Lucas, W. J., et al. (2001). Functional analysis of proteins involved in movement of the monopartite begomovirus, tomato yellow leaf curl virus. *Virology* 291, 110–125. doi: 10.1006/viro.2001.1194

Shen, Q., Hu, T., Bao, M., Cao, L., Zhang, H., Song, F., et al. (2016). Tobacco RING E3 ligase NtRFP1 mediates ubiquitination and proteasomal degradation of a geminivirus-encoded βC1. *Mol. Plant* 9, 911–925. doi: 10.1016/j.molp.2016.03.008

Shen, Q., Liu, Z., Song, F., Xie, Q., Hanley-Bowdoin, L., and Zhou, X. (2011). Tomato SlSnRK1 protein interacts with and phosphorylates βC1, a pathogenesis protein encoded by a geminivirus-satellite. *Plant Physiol.* 157, 1394–1406. doi: 10.1104/pp.111.184648

Shimoji, H., Tokuda, G., Tanaka, Y., Moshiri, B., and Yamasaki, H. (2006). A simple method for two-dimensional color analyses of plant leaves. *Russ. J. Plant Physl.* 53, 126–133. doi: 10.3390/s130202117

Sunter, G., and Bisaro, D. M. (1997). Rugulation of a geminivirus coat protein promoter by AL2 protein (TrAP): evidence for activation and derepression mechanisms. *Virology* 232, 269–280. doi: 10.1006/viro.1997.8549

Trinks, D., Rajeswaran, R., Shivaprasad, P. V., Akbergenov, R., Oakeley, E. J., Veluthambi, K., et al. (2005). Suppression of RNA silencing by a geminivirus nuclear protein, AC2, correlates with transactivation of host genes. *J. Virol.* 79, 2517–2527. doi: 10.1128/JVI.79.4.2517-2527.2005

van, W. R., Dong, X., Liu, H., Tien, P., Stanley, J., and Hong, Y. (2002). Mutation of three cysteine residues in tomato yellow leaf curl virus-China C2 protein causes dysfunction in pathogenesis and posttranscriptional gene-silencing suppression. *Mol. Plant Microbe Interact.* 15, 203–208. doi: 10.1094/MPMI.2002.15.3.203

Wang, B., Yang, X., Wang, Y., Xie, Y., and Zhou, X. (2018). Tomato yellow leaf curl virus V2 interacts with host histone deacetylase 6 to suppress methylation-mediated transcriptional gene silencing in plants. *J. Virol.* 92:e00036-18. doi: 10.1128/JVI.00036-18

Wang, L., Tan, H., Wu, M., Jimenez-Gongora, T., Tan, L., and Lozano-Duran, R. (2017). Dynamic virus-dependent subnuclear localization of the capsid protein from a geminivirus. *Front. Plant Sci.* 8:2165. doi: 10.3389/fpls.2017.02165

Wang, L., Wang, X., Wei, X., Huang, H., Wu, J., Chen, X., et al. (2016). The autophagy pathway participates in resistance to Tomato yellow leaf curl virus infection in whiteflies. *Autophagy* 12, 1560–1574. doi: 10.1080/15548627.2016.1192749

Wang, Y., Wu, Y., Gong, Q., Ismayil, A., Yuan, Y., Lian, B., et al. (2019). Geminiviral V2 protein suppresses transcriptional gene silencing through interaction with AGO4. *J. Virol.* 93:e01675-18. doi: 10.1128/JVI.01675-18

Wei, J., Wang, X. W., and Liu, S. (2015). Research progress in geminivirus transmission by whiteflies (hemiptera: aleyrodidae) and the underlying molecular mechanisms. *Acta Entomol. Sin.* 58, 445–453.

Wei, T., Zhang, C., Hong, J., Xiong, R., Kasschau, K. D., Zhou, X., et al. (2010). Formation of complexes at plasmodesmata for potyvirus intercellular movement is mediated by the viral protein P3N-PIPO. *PLoS Pathog.* 6:e1000962. doi: 10.1371/journal.ppat.1000962

Wistuba, A., Kern, A., Weger, S., Grimm, D., and Kleinschmidt, J. A. (1997). Subcellular compartmentalization of adeno-associated virus type 2 assembly. *J. Virol.* 71, 1341–1352. doi: 10.1128/jvi.71.2.1341-1352.1997

Xiong, R., Wu, J., Zhou, Y., and Zhou, X. (2009). Characterization and subcellular localization of an RNA silencing suppressor encoded by rice stripe tenuivirus. *Virology* 387, 29–40. doi: 10.1016/j.virol.2009.01.045

Yang, M., Zhang, Y., Xie, X., Yue, N., Li, J., Wang, X., et al. (2018). γb protein subverts autophagy to promote viral infection by disrupting the ATG7-ATG8 interaction. *Plant Cell* 30, 1582–1595. doi: 10.1105/tpc.18.00122

Yang, X., Baliji, S., Buchmann, R. C., Wang, H., Lindbo, J. A., and Sunter, G. (2007). Functional modulation of the geminivirus AL2 transcription factor and silencing suppressor by self-interaction. *J. Virol.* 81, 11972–11981. doi: 10.1128/JVI.00617-07

Yang, X., Xie, Y., Raja, P., Li, S., Wolf, J., Shen, Q., et al. (2011). Suppression of methylation-mediated transcriptional gene silencing by βC1-SAHH protein interaction during geminivirus-betasatellite infection. *PLoS Pathog.* 7:e1002329. doi: 10.1371/journal.ppat.1002329

Zhang, J., Dong, J., Xu, Y., and Wu, J. (2012). V2 protein encoded by Tomato yellow leaf curl China virus is an RNA silencing suppressor. *Virus Res.* 163, 51–58. doi: 10.1016/j.virusres.2011.08.009

Zhang, Z., Chen, H., Huang, X., Xia, R., Zhao, Q., Lai, J., et al. (2011). BSCTV C2 attenuates the degradation of SAMDC1 to suppress DNA methylation-mediated gene silencing in *Arabidopsis*. *Plant Cell* 23, 273–288. doi: 10.1105/tpc.110.081695

Zhao, W., Ji, Y., Wu, S., Ma, X., Li, S., Sun, F., et al. (2018). Single amino acid in V2 encoded by TYLCV is responsible for its self-interaction, aggregates and pathogenicity. *Sci. Rep.* 23:3561. doi: 10.1038/s41598-018-21446-2

Zhou, X. (2013). Advances in understanding begomovirus satellites. *Annu. Rev. Phytopathol.* 51, 357–381. doi: 10.1146/annurev-phyto-082712-102234

Zhou, X., Xie, Y., Tao, X., Zhang, Z., Li, Z., and Fauquet, C. M. (2003). Characterization of DNAβ associated with begomoviruses in China and evidence for co-evolution with their cognate viral DNA-A. *J. Gen. Virol.* 84, 237–247. doi: 10.1099/vir.0.18608-0

Zhou, Y., Rojas, M. R., Park, M. R., Seo, Y. S., Lucas, W. J., and Gilbertson, R. L. (2011). Histone H3 interacts and colocalizes with the nuclear shuttle protein and the movement protein of a geminivirus. *J. Virol.* 85, 11821–11832. doi: 10.1128/JVI.00082-11

Conflict of Interest: The authors declare that the research was conducted in the absence of any commercial or financial relationships that could be construed as a potential conflict of interest.

frontiers in Plant Science

ORIGINAL RESEARCH
published: 19 June 2020
doi: 10.3389/fpls.2020.00835

Characterization of Curtovirus V2 Protein, a Functional Homolog of Begomovirus V2

Ana P. Luna[1†], Beatriz Romero-Rodríguez[1†], Tábata Rosas-Díaz[1], Laura Cerero[1], Edgar A. Rodríguez-Negrete[2], Araceli G. Castillo[1] and Eduardo R. Bejarano[1*]*

[1] Departamento de Genética, Facultad de Ciencias, Instituto de Hortofruticultura Subtropical y Mediterránea "La Mayora" (IHSM-UMA-CSIC), Universidad de Málaga, Málaga, Spain, [2] CONACyT, Departamento de Biotecnología Agrícola, Instituto Politécnico Nacional, CIIDIR-Unidad Sinaloa, Guasave, Mexico

OPEN ACCESS

Edited by:
Henryk Hanokh Czosnek, The Hebrew University of Jerusalem, Israel

Reviewed by:
Pradeep Sharma, Indian Institute of Wheat and Barley Research (ICAR), India
Rena Gorovits, The Hebrew University of Jerusalem, Israel

***Correspondence:**
Araceli G. Castillo
ara@uma.es
Eduardo R. Bejarano
edu_rodri@uma.es

[†] These authors have contributed equally to this work

Specialty section:
This article was submitted to Virology, a section of the journal Frontiers in Plant Science

Received: 29 February 2020
Accepted: 25 May 2020
Published: 19 June 2020

Citation:
Luna AP, Romero-Rodríguez B, Rosas-Díaz T, Cerero L, Rodríguez-Negrete EA, Castillo AG and Bejarano ER (2020) Characterization of Curtovirus V2 Protein, a Functional Homolog of Begomovirus V2. Front. Plant Sci. 11:835. doi: 10.3389/fpls.2020.00835

Geminiviruses are single-stranded DNA plant viruses with circular genomes packaged within geminate particles. Among the *Geminiviridae* family, *Begomovirus* and *Curtovirus* comprise the two best characterized genera. Curtovirus and Old World begomovirus possess similar genome structures with six to seven open-reading frames (ORF). Among them, begomovirus and curtovirus V2 ORFs share the same location in the viral genome, encode proteins of similar size, but show extremely poor sequence homology between the genera. V2 from *Beet curly top virus* (BCTV), the model species for the *Curtovirus* genus, as it begomoviral counterpart, suppresses post-transcriptional gene silencing (PTGS) by impairing the RDR6/SGS3 pathway and localizes in the nucleus spanning from the perinuclear region to the cell periphery. By aminoacid sequence comparison we have identified that curtoviral and begomoviral V2 proteins shared two hydrophobic domains and a putative phosphorylation motif. These three domains are essential for BCTV V2 silencing suppression activity, for the proper nuclear localization of the protein and for systemic infection. The lack of suppression activity in the mutated versions of V2 is complemented by the impaired function of RDR6 in *Nicotiana benthamiana* but the ability of the viral mutants to produce a systemic infection is not recovered in gene silencing mutant backgrounds. We have also demonstrated that, as its begomoviral homolog, V2 from BCTV is able to induce systemic symptoms and necrosis associated with a hypersensitive response-like (HR-like) when expressed from *Potato virus X* vector in *N. benthamiana*, and that this pathogenicity activity does not dependent of its ability to supress PTGS.

Keywords: geminivirus, BCTV, RNA-silencing, suppressor, V2, RDR6, pathogenesis

INTRODUCTION

Geminiviruses constitute a group of circular single-stranded DNA plant viruses that infect a wide range of plants and cause substantial yield losses worldwide (Rojas et al., 2018; García-Arenal and Zerbini, 2019). The family *Geminiviridae* is divided into nine genera based on their genome features and biological properties (Varsani et al., 2017; Zerbini et al., 2017). Among them, *Begomovirus* and *Curtovirus* include a large number of the viral species capable to infect economically relevant

dicotyledonous plants. Curtoviruses are important pathogens for many cultivated and wild plant species. Although this genus only has three species, including the model species *Beet curly top virus* (BCTV), it has an enormously wide host range within dicot plants, including around 300 species in more than 40 plant families, as well as a broad geographical distribution that includes the Indian subcontinent, North and Central America and the Mediterranean region (Varsani et al., 2014).

All monopartite and Old World bipartite geminiviruses have similar genome structures, encoding 6 or 7 multifunctional proteins (Fondong, 2013; Varsani et al., 2017; Zerbini et al., 2017). In most cases, the virion sense strand contains two ORFs (V2 and V1, that encodes the coat protein, CP), and a third one (V3) which is only present in some of the nine genera, including *Curtovirus* but not *Begomovirus*. The complementary sense strand encompasses up to four ORFs (C1, C2, C3, and C4).

V2 from begomoviruses encodes a multifunctional protein required for full infection that is able to suppress gene silencing at the transcriptional (TGS) and post-transcriptional (PTGS) level (Zrachya et al., 2007; Chowda-Reddy et al., 2008; Sharma and Ikegami, 2010; Sharma et al., 2010; Amin et al., 2011; Luna et al., 2012; Zhang et al., 2012; Wang et al., 2014, 2018; Saeed et al., 2015; Zhan et al., 2018; Mubin et al., 2019). Additionally, it has been described that V2 protein is required for viral movement and spreading of the virus throughout the plant (Padidam et al., 1996; Rojas et al., 2001; Rothenstein et al., 2007; Moshe et al., 2015), it is involved in the regulation of host defense responses (Bar-Ziv et al., 2012; Roshan et al., 2018) and it elicits symptoms of hypersensitive response (HR)-like cell death phenotype in *Nicotiana benthamiana* plants, when expressed from a *Potato virus X* (PVX)-derived vector (Zrachya et al., 2007; Chowda-Reddy et al., 2008; Mubin et al., 2010; Amin et al., 2011; Luna et al., 2012; Zhang et al., 2012; Roshan et al., 2018).

Less is known about the function of curtovirus V2. Based on genome location and length, begomovirus and curtovirus V2 ORFs seem to be orthologous. However, their homology at the protein level, which is high within each genus, is extremely low. As its begomovirus counterpart, curtovirus V2 is needed for full systemic infection (Stanley et al., 1992; Hormuzdi and Bisaro, 1993; Luna et al., 2017) and it functions as a strong PTGS suppressor by a similar mechanism: impairing the RDR6 (RNA-dependent RNA polymerase 6)/suppressor of gene silencing 3 (SGS3) pathway (Luna et al., 2017).

Here we show that BCTV V2, besides functioning as a PTGS suppressor, also produces an HR-like cell death phenotype in *N. benthamiana* when expressed from PVX, similar to that produced by the expression of its begomoviral equivalent. The functional analysis of the mutated versions of V2 indicated that a putative phosphorylation motif and two N-terminal hydrophobic domains conserved also in V2 from begomovirus, are required for the PTGS suppression activity, viral pathogenicity, V2 subcellular localization and for systemic infection of *N. benthamiana* and *Arabidopsis thaliana* plants. Collectively, these results suggest that begomovirus and curtovirus V2 proteins, in spite of their low sequence homology, have evolved to target the same cellular processes through similar mechanisms, providing a putative example of convergent protein evolution.

MATERIALS AND METHODS

Microorganisms, Plant Material, and Growth Conditions

Manipulation of *Escherichia coli* strains were carried out according to standard methods (Sambrook and Russell, 2001). *E. coli* strain DH5-α was used for subcloning. The *Agrobacterium tumefaciens* GV3101 strain was used for the agroinfiltration and agroinoculation/infection assays.

Plants used in this study were *A. thaliana* Columbia (Col-0) ecotype and *Nicotiana benthamiana*. Plants were grown in chambers at 24°C in long-day conditions (16 h light/8 h dark) before and after agroinfiltration/infection. The *Arabidopsis* mutant lines used for geminiviral infection, *rdr6–15* and the double mutant *dcl2/4,* were described elsewhere (Allen et al., 2004; Deleris et al., 2006, respectively). *N. benthamiana* RDR6i transgenic line was described in Schwach et al., 2005).

Plasmids and Cloning

Supplementary Tables S1, S2 summarize the constructs and the primers used in this work, respectively. All PCR-amplified fragments cloned in this work were fully sequenced. The binary vector expressing green fluorescent protein (GFP) (pBin-35S-mGFP5) (Haseloff et al., 1997) and the nuclear envelope marker AtSUN1–tagRFP (Oda and Fukuda, 2011) were kindly provided by Olivier Voinnet (Zurich, Switzerland) and by Björn Krenz (Braunschweig, Germany), respectively. V2 single mutants, except V2P1D, were generated using two-sided splicing by over-lap extension (Ho et al., 1989). Primers used for both amplification rounds are shown in **Supplementary Tables S2, S3**. The V2P1D mutant and the BCTV V2 mutant viruses were produced by site-directed mutagenesis using QuikChange Lightning Site-Directed Mutagenesis kit (Stratagene, Agilent biotechnologies) with specific primers (see **Supplementary Tables S2, S4**).

Analysis of Nucleic Acids and Proteins

Nucleic acid manipulation was performed according to standard methods (Sambrook and Russell, 2001). For BCTV replication and infection analyses, plant DNA was extracted from the infiltrated (local) or the apical (systemic) leaves of the infected plants at 4 or 28 days post-infiltration (dpi), respectively, digested with *Dpn*I to remove bacterial DNA in the infiltrated tissues (local infection) and then subjected to qPCR analysis using primers described on **Supplementary Table S2** and the 25SrDNA and actin genes as normalizers for *N. benthamiana* and *A. thaliana* samples, respectively (Luna et al., 2017). Expression of BCTV V2 (wild-type or mutants) and GFP in agroinfiltrated tissues was determined by RT-qPCR using the primers described on **Supplementary**

Table S2 and the E1Fa gene as a normalizer (Luna et al., 2017). The analysis of PVX transcript levels and recombinant virus integrity were done by semi quantitative RT-PCR as described in Luna et al., 2012 using specific primers (**Supplementary Table S2**).

For western blot analysis, 100 mg of leaf tissue per sample were used. Total protein was extracted with two volumes of extraction buffer (100 mM Tris–HCl pH 7.5, 150 mM NaCl, 10% glycerol, 0.5 mM EDTA pH 8, 1 mM DTT, 0.5 mM PMSF, 1%[v/v] P9599 protease inhibitor cocktail [Sigma-Aldrich]; 0.2%[v/v] triton X-100). Samples were centrifuged 15 min at 4°C at 16000 *g*. Approximately 150 μl of total protein was recovered, mixed with an equal volume of 2X Laemmli buffer and heated at 95°C for 10 min. 20 μl of total protein was loaded and resolved by 12% SDS-PAGE gel electrophoresis, and transferred by electroblotting onto a PVDF membrane (Immobilon-P, Millipore, MA, United States). Proteins were stained by Coomassie blue and immunoblotted with anti-GFP mouse monoclonal antibody (1:600, clone B-2; sc-9996, Santa Cruz Biotechnology) and anti-mouse IgG whole molecule-peroxidase secondary antibody (1:80,000; A9044, Sigma-Aldrich).

Agroinfiltration and Infection Assays

For PTGS local suppression assays and PVX infections, *N. benthamiana* leaves were agroinfiltrated as previously described (Voinnet et al., 1998; Luna et al., 2012). Long-wave UV lamp was used for the detection of GFP fluorescence (Black Ray model B 100 AP, Upland, United States).

To quantify the hypersensitive-response (HR) in PVX-infected plants, conductivity (mS/cm) was measured using a conductivity meter Crison CM35 (Hach-Lange, Barcelona, Spain). Leaf discs were cut from infiltrated (local tissue) or apical leaves (systemic tissue), washed for 30 min in 6 mL of deionized water, and then transferred to 6 mL of deionized water and the conductivity was measured every 24 h for a total of 3 days, starting at 6 dpi (local tissue) or 8 dpi (systemic tissue). For BCTV infection in *A. thaliana* plants, 4-5-week-old plants were agroinoculated by needle puncture in wounds produced in the rosette crown. 2–3 drops of an overnight grown *A. tumefaciens* culture were placed over these wounds, plants were covered in plastic film for 2–3 days and then plastic was removed. BCTV infection in *N. benthamiana* was done by agroinoculation as described by Elmer et al., 1988.

Subcellular Localization

For immunolocalization, *A. tumefaciens* was transformed with binary vectors containing V2 mutants fused to GFP. *N. benthamiana* leaves were agroinfiltrated with cultures at OD_{600} 0.5–1. For co-localization experiments Agrobacterium cultures containing V2-GFP constructs and the nuclear envelope marker AtSUN1–tagRFP (Oda and Fukuda, 2011) were mixed (1:1 ratio) prior to infiltration. In both cases, fluorescence was detected in epidermal cells 2–3 days after infiltration, using a confocal microscope (Zeiss LSM 880).

Phylogenetic Analysis

The ClustalW algorithm was used to align V2 homolog proteins[1]. The prediction of the putative phosphorylation motives was done by Scan Prosite tool[2]. The hydrophobic domains were identified by ProtScale software[3].

RESULTS

A Phosphorylation Motif and Two Hydrophobic Domains of BCTV V2 Protein Are Essential for Its Silencing Suppression Activity

Suppression of PTGS activity has been described for V2 proteins from several species of begomovirus and the curtovirus *Beet curly top virus* (BCTV) (see section "Introduction" for references). Despite sharing a similar function, the protein homology, which is highly conserved within each genus (**Supplementary Figures S1, S2**), is extremely poor when V2 from begomovirus and curtovirus are compared (**Figure 1A**). In begomoviral V2, two highly conserved protein domains have been identified to be essential for its activity as PTGS suppressor (**Supplementary Figure S1**): (i) a putative CK2/PKC (protein kinase CK2/protein kinase C) phosphorylation motif (Chowda-Reddy et al., 2008) and (ii) a CxC motif (Glick et al., 2008) that is also required for full infection (Hak et al., 2015). Sequence analysis revealed that V2 from curtoviruses lacks the CxC motif, but it contains several putative phosphorylation sites (**Supplementary Figure S2**). Sequence alignment showed that one CK2/PKC motif (hereafter named P1) is conserved in all curtoviral species (**Supplementary Figure S2**) and seems to be homologous to the begomoviral CK2/PKC motif (**Figure 1** and **Supplementary Figure S1**). On the other hand, the other two putative CK2 and PKC phosphorilation motifs predicted in BCTV V2 (named P2 and P3, respectively), seemed to be specific, since they are not conserved in the other two curtoviral species neither in the begomoviral V2 (**Figure 1** and **Supplementary Figure S2**). Interestingly, when hydrophobic profiles of begomoviral and curtoviral V2 proteins are compared, a similar disposition consisting of two hydrophobic domains in the N-terminal region (hereafter named H1 and H2) followed by a long hydrophilic domain in the C-terminus is revealed (**Figure 1A**). A broader alignment of V2 from 29 begomovirus and 3 curtovirus species, displayed a similar distribution of the hydrophobic-hydrophilic domains (**Supplementary Figures S1, S2**).

To determine the functional relevance of the hydrophobic domains and the phosphorylation motifs in the PTGS suppression activity of BCTV V2, we generated point mutants in the mentioned domains (**Figure 1B** and **Supplementary Table S3**). Non-polar residues from the hydrophobic domains, leucine and valine from H1 and two isoleucines from H2, were substituted by either polar-charged amino acids such as glutamic

[1]www.genebee.msu.su/clustal/advanced.html

[2]https://prosite.expasy.org/scanprosite/

[3]https://web.expasy.org/protscale/

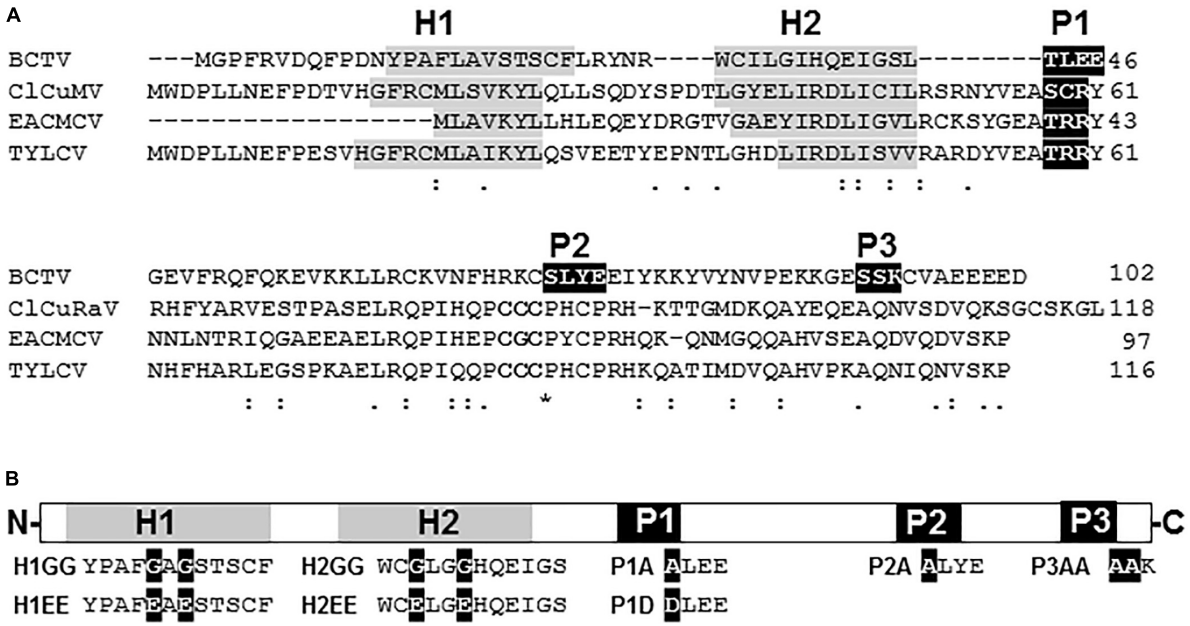

FIGURE 1 | V2 sequence from curtovirus and begomovirus. **(A)** Alignment of the aminoacid sequences of the V2 proteins from the curtovirus *Beet curly top virus* (BCTV; M24597) and the begomoviruses, *Cotton leaf curl Multan virus* (CLCuMV-Fai[PK:Fai2]; AJ496287), *East African cassava mosaic Cameroon virus* (EACMCV; AF112354) and *Tomato yellow leaf curl virus* (TYLCV; X15656). Gaps (-) were introduced to optimize the alignment. The positions of the predicted putative phosphorylation motifs P1 (protein kinase CK2/protein kinase C), P2 (protein kinase CK2) and P3 (protein kinase C) are depicted in white letters inside black boxes. The CxC motif from begomoviruses (Padidam et al., 1996; Zrachya et al., 2007) is underlined. The hydrophobic domains (H1 and H2) are shadowed in gray. **(B)** Schematic view of BCTV V2 aminoacidic sequence. Hydrophobic domains (H1 and H2) are depicted as gray squares. Putative phosphorylation motifs (P1, P2 and P3) are presented as black squares. Amino acid substitutions for each mutant (H1GG, H1EE, H2GG, H2EE, P1A, P1D, P2A, and P3AA) are indicated as white letters in black squares.

acid (H1EE and H2EE) or by a non-polar such as glycine (H1GG and H2GG). The serine/threonine residues in the three hypothetical phosphorylation motifs were replaced by alanines (P1A, P2A, and P3AA) or by aspartic acid in the case of P1 (P1D) to create a phosphomimic mutation. Finally, as a control, an insertion of two nucleotides (AT) at position 395 in BCTV genome, generated a premature stop signal that produced a peptide of 17 aminoacids whose first 5, correspond to V2 protein.

To evaluate the gene silencing suppressor activity of the V2 mutants, *N. benthamiana* wild-type leaves were co-agroinfiltrated as described in Luna et al. (2012) with constructs that expressed GFP and the desired V2 mutant protein from the 35S CaMV promoter. As a negative control the 35S-GFP construct was also co-agroinfiltrated on each leaf with an empty binary vector (ev and C) (**Figure 2A**). As expected, 5 days after the infiltration (5 dpi) leaf patches agroinfiltrated with the 35S-GFP construct and wild-type V2, displayed stronger green fluorescence compared to those infiltrated with the empty vector and 35S-GFP (**Figure 2A**; Luna et al., 2017). A similar result was observed in tissues expressing P2A and P3AA, but not in tissues infiltrated with V2stop, P1A, P1D or any of the V2 mutants at the hydrophobic domains, where the GFP signal was similar to the one observed in the control (**Figure 2A**). To confirm that P2A and P3AA motifs are not required for the suppressor activity of V2, we generated a double mutant (P2A/P3AA) and analyzed its ability to suppress GFP silencing. The level of fluorescence at the leaf patches co-agroinfiltrated with 35S-GFP and the double mutant P2A/P3AA were similar to that obtained in tissues expressing wild-type V2 (**Figure 2A**). The ability of the V2 mutants to supress gene silencing was also determined by measuring the relative transcript levels of GFP by reverse transcription quantitative real-time PCR (RT-qPCR). Transcripts accumulated to a similar extend in the tissues expressing wild-type V2 or the single or double mutants P2A/P3AA and to a lesser extend in tissues agroinfiltrated with any of the other V2 mutants (**Figure 2B**). A similar result was obtained with the relative amount of V2 transcripts, indicating that when functional, V2 also suppresses its own silencing. To determine whether the low level of transcript accumulation of the V2 mutants was due to the lack of PTGS suppression activity and not to a reduction in the transcript generation, we measured the accumulation of V2 transcripts at 1 dpi, before gene silencing is stablished (**Supplementary Figure S3**). The results indicated that, although we detected some variation, the level of V2 transcript from the mutants and wild-type were similar and they do not correlate with their ability to suppress GFP expression, confirming that the differences observed at 5 dpi are due to the lack of gene silencing suppression activity of V2 mutants.

Previous data suggested that, in *Arabidopsis thaliana*, V2 from BCTV suppresses PTGS by interfering with the RDR6-dependent amplification pathway (Luna et al., 2017). To confirm that this pathway was also required for the gene silencing suppression

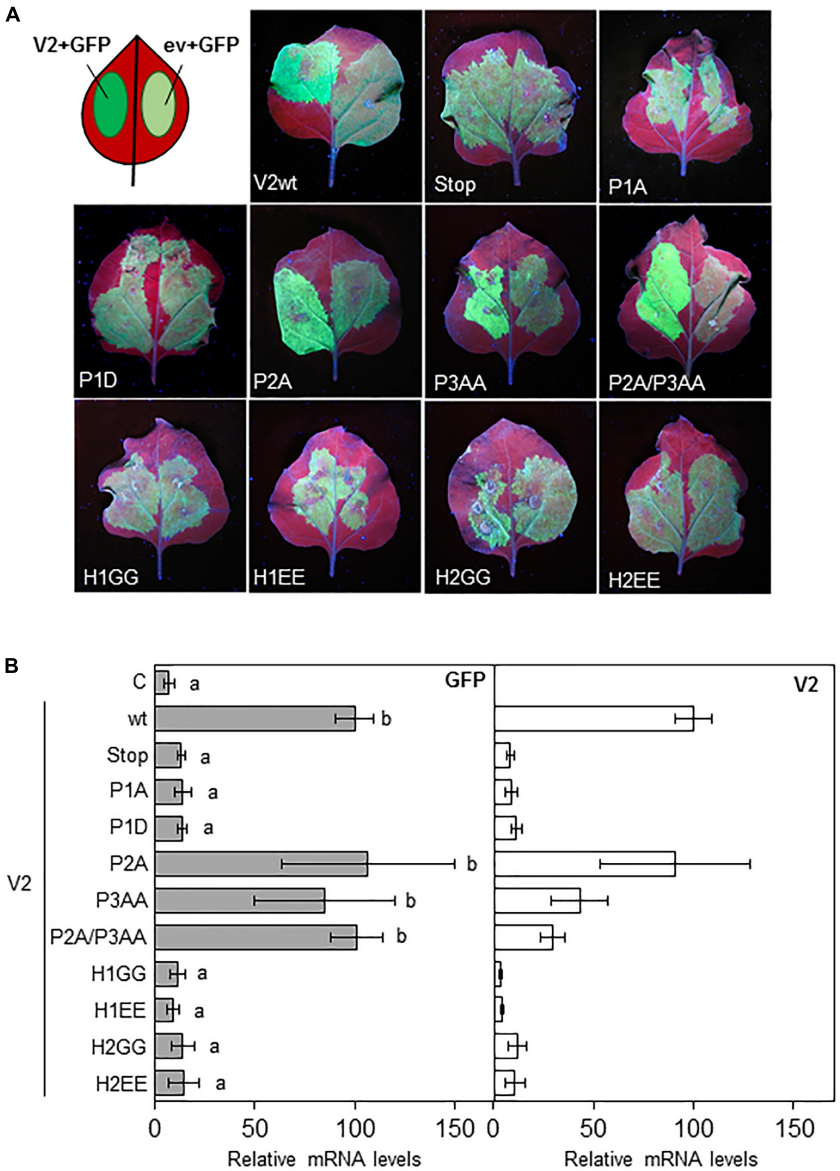

FIGURE 2 | Local PTGS suppression activity of V2 mutants in wild-type *N. benthamiana* plants. **(A)** Leaves from *N. benthamiana* plants infiltrated with a mixture of two *A. tumefaciens* cultures expressing GFP and the indicated version of V2, were photographed under UV light at 5 dpi. Wild-type V2 protein (wt) and the empty vector (C) were used as a positive and negative control, respectively. **(B)** Relative *GFP* and *V2* mRNA levels (RT-qPCR) in infiltrated tissues at 5 dpi. *GFP* or *V2* transcript levels were normalized to *EF1* and are presented as the relative amount of transcripts compared with the amount found in wild-type V2 (wt) samples (set to 100%). Bars represent mean values ± standard error (SE) for 4–8 pools of two leaves from 3 to 4 plants each one. Mean values marked with different letter (a or b) indicate results significantly different from each other, as established by One Way ANOVA (Dunnett's Multiple Comparison Test; $P < 0.05$).

mechanism in *N. benthamiana,* we took advantage of the RDR6i line (Schwach et al., 2005), in which *NbRDR6* expression is reduced by an RNAi hairpin construct. Leaves from wild-type and RDR6i plants were co-infiltrated with two Agrobacterium cultures harboring plasmids to express GFP and the wild-type or the mutated V2 (only one mutant for each domain, P1A, H1GG and H2GG, were included in the analysis as the two type of mutations on each domain, were unable to suppress gene silencing) (**Figure 2**). As expected, leaf patches agroinfiltrated with wild-type V2 showed stronger green fluorescence compared to tissues co-infiltrated with any of the four mutants in *N. benthamiana* wild-type plants (**Figure 3A**). On the other hand, the green fluorescence signal of the patches that expressed the mutated versions of V2 in the RDR6i background was similar to that shown by wild-type V2 (**Figure 3B**). The relative quantification of GFP transcripts accumulated in the infiltrated tissues, confirmed these observations, as the increase of GFP transcript levels in P1A, H1GG and H2GG mutants reached similar levels to the ones from the V2 wild-type protein in the RDR6i background (**Figure 3C**), indicating that the lack of

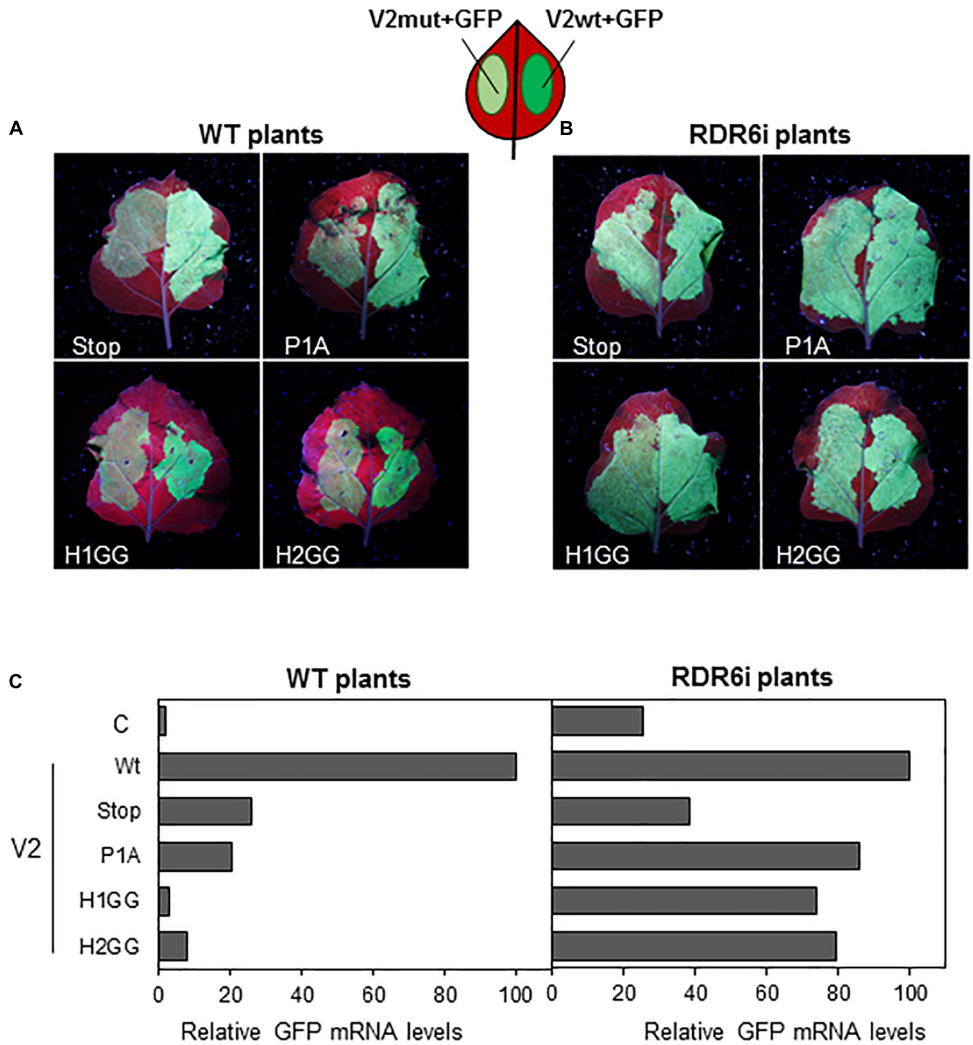

FIGURE 3 | Local PTGS suppression activity of V2 mutants in wild-type (WT) and RDR6i *N. benthamiana* plants. Leaves from WT **(A)** and RDR6i **(B)** *N. benthamiana* plants infiltrated with a mixture of two *A. tumefaciens* cultures containing GFP and the desired V2 construct, were photographed under UV light at 5 dpi. Wild-type V2 protein (wt) was used as a positive control. **(C)** Relative GFP mRNA levels in infiltrated tissues at 5 dpi. GFP levels were normalized to *EF1* and are presented as the relative amount of transcripts compared with the amount found in wild-type V2 (wt) samples (set to 100%). Bars represent mean values from a pool of 2–3 leaves obtained from 4 plants for each combination. Similar results were obtained in two independent experiments.

silencing suppression activity of V2 mutants, is complemented by the impaired RDR6 function in the RDR6i line. These results support the view that BCTV V2-mediated silencing suppression operates via hindrance of the RDR6 function in *N. benthamiana*, and it is in accordance with our previous data from *A. thaliana* (Luna et al., 2017).

Pathogenicity of BCTV V2 Does Not Dependent of Its Ability to Supress PTGS

Previous results indicated that begomoviral V2 is involved in pathogenicity as the ectopic expression in *N. benthamiana* of V2 from several begomoviruses using a *Potato virus X* (PVX)-derived vector, caused localized cell death in the infiltrated area and induced systemic symptoms and necrosis associated with a hypersensitive response-like (HR-like) phenotype (Mubin et al., 2010; Sharma and Ikegami, 2010; Luna et al., 2012; Roshan et al., 2018). Although stable expression of BCTV V2 in transgenic *A. thaliana* Col-0 plants do not alter the plant phenotype (Luna et al., 2017), we studied whether the curtoviral protein, as its begomoviral equivalent, induces symptoms and local or systemic necrosis, when it is expressed from a PVX-derived vector. Tissues infiltrated with the PVX empty vector (control, C) developed the typical local yellowing symptoms but the presence of V2 produced a HR-like cell death phenotype in the infiltrated *N. benthamiana* leaves (**Figure 4A**, local panels). At a systemic level, PVX infection (control, C) produced mild mosaic symptoms that came to be asymptomatic in some leaves due to recovery from viral infection. On the other hand, when BCTV V2 was expressed from PVX, plants did not recuperate

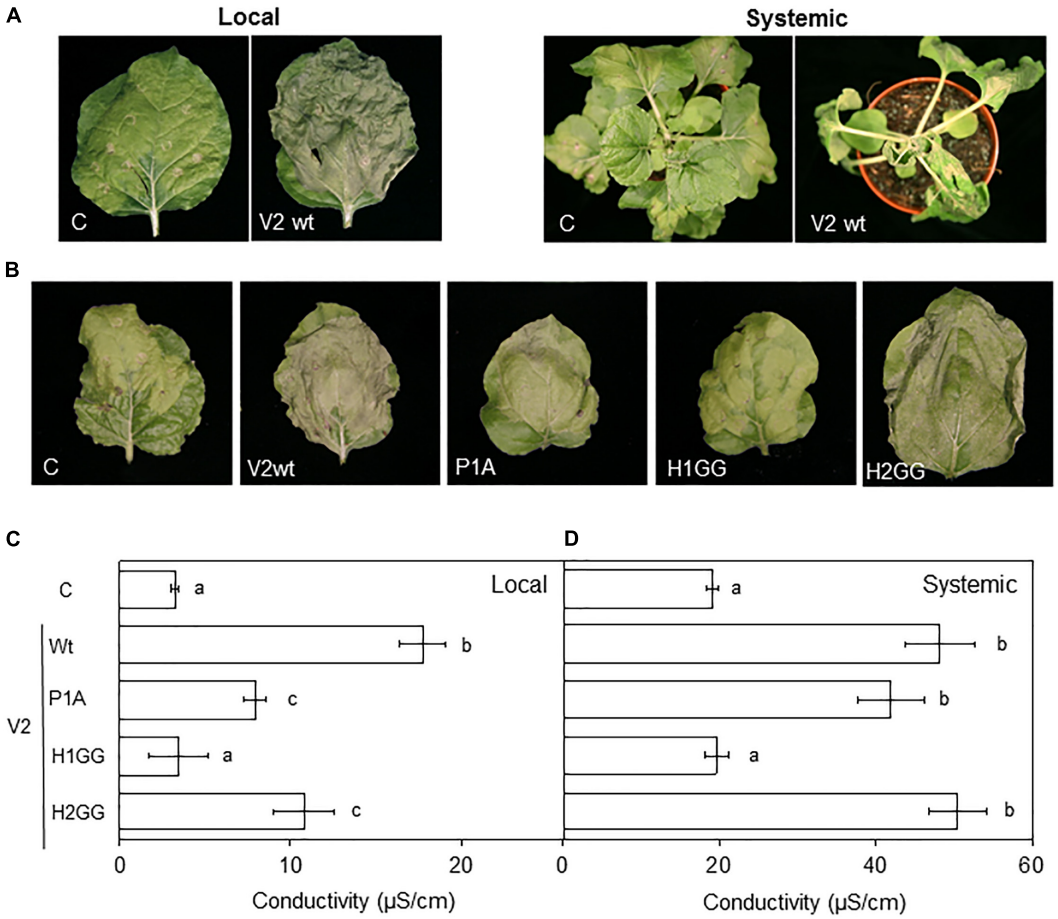

FIGURE 4 | Expression of BCTV V2 mutants from PVX. Wild-type or mutated versions of V2 were expressed from a PVX vector and tested individually in *N. benthamiana* leaves. **(A)** Infiltrated tissue (local) at 6 dpi or apical tissue at 10 dpi (systemic) with the empty PVX vector (C) or with a recombinant PVX virus expressing the wild-type V2 protein (V2wt). **(B)** Infiltrated tissue (local) at 6 dpi with the empty PVX vector (C) or with a recombinant PVX virus expressing the wild-type (V2wt) or the mutated versions (P1A, H1GG, H2GG) of V2. **(C,D)** Measurement of the conductivity from leaf discs extracted from local **(C)** or systemically infected **(D)** tissues. Seven to eight plants were infected with each PVX-derived construct and conductivity (µS/cm) was measured in two pools of four leaf discs per plant. Bars represent mean values ± standard error (SE) for seven to eight plants (four discs per leaf were pooled and two leaves per plant were used) per recombinant PVX construct. Mean values marked with different letter (a, b, or c) indicate results significantly different from each other, as established by One Way ANOVA (Dunnett's Multiple Comparison Test; $P < 0.05$). Similar results were obtained in two independent experiments.

from viral infection, collapsing at 8–10 dpi (**Figure 4A**, systemic panels). Therefore, we can conclude that as its begomoviral counterpart, V2 from curtovirus induces an HR-like phenotype in *N. benthamiana* when is expressed from PVX.

In order to determine the relevance that the selected protein domains have in V2 pathogenicity and if that function is related to the gene silencing suppressor activity, we expressed the curtoviral V2 mutant proteins (P1A, H1GG, and H2GG) from a PVX-derived vector in *N. benthamiana* plants. Local and systemic necrosis was observed in samples expressing wild-type V2 and the P1A and H2GG V2 mutants but not the H1GG mutant (**Figure 4B** and data not shown). To quantify the HR caused by wild-type and mutants in V2, we measured the changes in the conductivity of the water that are produced by the release of cellular electrolytes in the presence of a pathogenic factor (Baker et al., 1991; Mackey et al., 2002). Conductivity of the leaf discs extracted from the local (6dpi) or systemically infected (9 dpi) tissues was measured. In the infiltrated tissue (local infection), the maximum electrolyte leakage was elicited by the V2 wild-type protein and the initiation of the response reaction seemed to be delayed in P1A and H2GG mutants (**Figure 4C**). In apical tissue (systemic infection) the V2 wild-type protein and the P1A and H2GG mutants elicited a similar HR in terms of electrolyte leakage (**Figure 4D**). As previously observed by symptoms (**Figure 4B**), there were not significant differences between the conductivity levels detected in the H1GG mutant expressed from PVX and PVX, either locally or systemically (**Figures 4C,D**, respectively).

Symptoms intensification produced by PVX-recombinant viruses expressing other viral proteins has been related to a larger accumulation of genomic RNA from PVX (Cañizares et al., 2008; Zhang et al., 2012). To rule out this possibility,

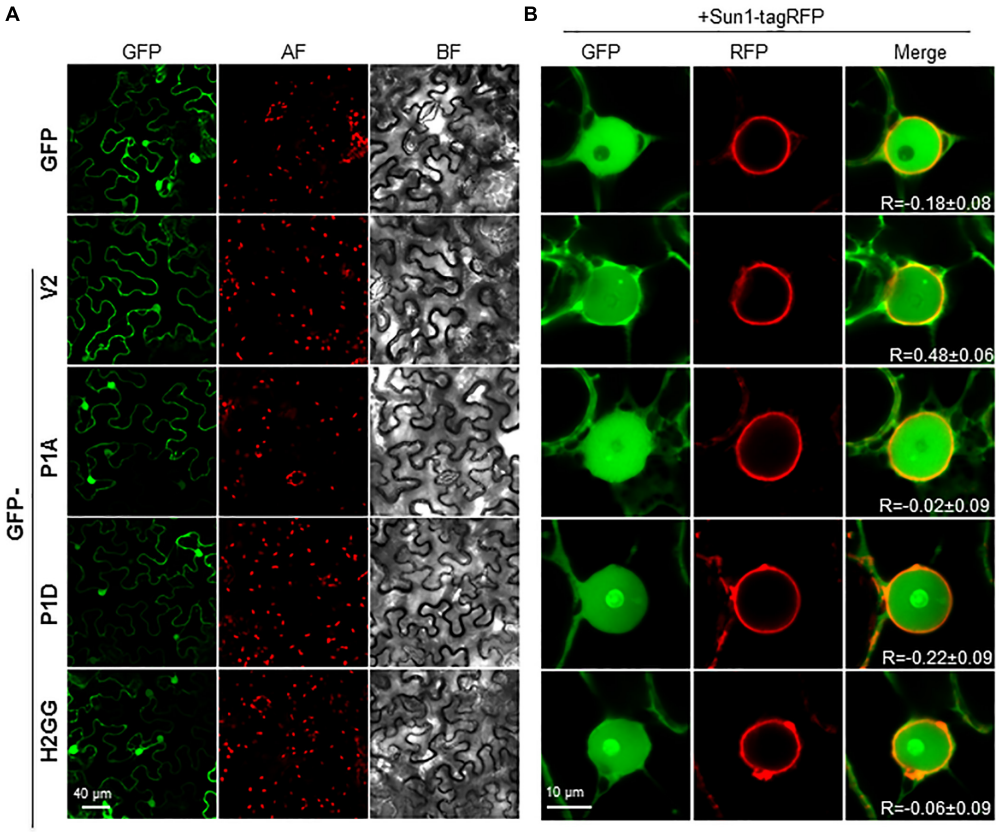

FIGURE 5 | Subcellular localization of V2 mutants fused to GFP protein in epidermal cells of *N. benthamiana.* **(A)** Leaves were agroinfiltrated with a construct expressing the 35S:GFP (GFP), 35S:GFP-V2 fusion protein or the 35S:GFP-V2 mutants. Samples were observed under the confocal microscope at 2 dpi. GFP fluorescence (GFP), autofluorescence (AF) and the bright field channel (BF) are shown. **(B)** Co-localization of 35S:GFP-V2 (wt and mutants) and the nuclear envelope marker 35S:AtSUN1–tagRFP. Leaves were agroinfiltrated with a construct expressing the GFP-V2 fusion protein or the GFP-V2 mutants and the nuclear envelope marker AtSUN1–tagRFP and observed under the confocal microscope at 3 dpi. GFP fluorescence (GFP), RFP fluorescence (RFP), and merge are shown. R stands for the Pearson's correlation coefficient for GFP-fusions and SUN1-tagRFP (mean values ± standard error (SE) from 6 to 9 nuclei).

total RNA was obtained from the systemically infected tissue and PVX was detected by RT-PCR. We did not detect an increase in PVX genomic RNA accumulation with respect to the control samples (**Supplementary Figure S4**). Amplification using primers flanking the PVX vector cloning site, confirmed the integrity of V2 sequences in the recombinant viruses (**Supplementary Figure S4**).

Mutations in P1 or H2 Domains Alter the Subcellular Localization of V2 Protein

We have previously shown that BCTV V2 localizes in the ER network and in the nucleus, from the perinuclear region to the cell periphery (Luna et al., 2017). We addressed whether mutations in the H1, H2 or P1 domains could change the subcellular localization of the protein by transiently expressing GFP-fused versions of BCTV V2 in *N. benthamiana*. Leaves were agroinfiltrated, collected 2–3 days later and visualized using a confocal microscope. Wild-type GFP-V2 localized in the nucleus and in the cellular periphery and not significant differences were observed in the localization of the mutated V2 proteins (**Figure 5A**). However, a close-up of the images showed some differences between the nuclear localization of wild-type V2 and the mutants, as GFP-P1A, GFP-P1D and GFP-H2GG, lose their nuclear periphery localization. To confirm this observation, we transitorily co-expressed the different GFP-V2 proteins with the nuclear envelope marker AtSUN1 tagged with RFP (Oda and Fukuda, 2011). Upon co-expression, overlapping of the fluorescent signals from GFP and RFP was detected for wild-type GFP-V2 protein but not for GFP-H2GG, GFP-P1A, or GFP-P1D mutants, which showed similar values for the Pearson's correlation coefficient to GFP and SUN1-RFP (**Figure 5B** and **Supplementary Figure S5**). Moreover, the GFP-V2 protein accumulated to a greater extend in the nucleolus in GFP-P1D but not in the GFP-P1A mutant, suggesting that the phosphorylation status of the P1 domain can play a role in the nuclear localization of BCTV V2 (**Figure 5B**). The GFP-H2GG mutant also accumulated in the nucleolus to a greater extent than the wild-type protein, indicating the importance of this hydrophobic domain for the proper localization of V2 protein. We could not determine the significance of the H1 domain as we were not able to detect the GFP-fused mutant

protein (**Supplementary Figure S6**). It has been shown that in addition to the nucleoplasm, nuclear periphery and cytoplasm, V2 from the begomovirus TYLCV localizes in the Cajal body, upon transient expression in *N. benthamiana* (Wang et al., 2019, BioRxiv). Interestingly, we could observe that the wild-type and the mutated versions of V2, also localize in a discrete subnuclear compartment, that resembles the Cajal body (**Figure 5B** and data not shown) suggesting that BCTV V2 shares the same subcellular localization as its begomoviral equivalent.

The Hydrophobic Domains H1 and H2 and the P1 Phosphorylation Motif of V2 Protein Are Essential for Systemic but Not for Local Infection of BCTV

To determine the biological relevance of V2 domains, we infected *N. benthamiana* with BCTV wild-type or BCTV mutated in the V2 hydrophobic or phosphorylation motifs. Plants inoculated with wild-type virus developed typical symptoms of BCTV infection by 14 to 21 dpi. Viruses containing single or the double mutations in P2 and P3 domains, caused symptoms indistinguishable from those produced by the wild-type virus, indicating that these mutations do not affect the systemic infection. In contrast, plants inoculated with the virus containing a mutation in the hydrophobic domain H2 (H2GG) developed only mild leaf curling and chlorosis. Viruses containing the premature stop codon in V2 (V2stop), the mutations in the P1 phosphorylation motif (P1A and P1D) or in the hydrophobic domain H1 (H1GG) did not produce any detectable symptoms at 28 dpi (**Supplementary Figure S7**). To quantify BCTV DNA levels in infected *N. benthamiana* plants, samples from apical leaves were analyzed by qPCR at 28 dpi. Accumulation of viral DNA correlated with symptoms intensity. Plants infected with wild-type or P2A, P3AA, or P2A/P3AA mutant viruses, accumulated equivalent amounts of viral DNA (**Figure 6A**). A reduction in viral DNA levels was detected in plants infected with the H2GG mutant, suggesting that mild symptoms are associated with lower amount of viral DNA. No viral DNA was observed in any of the plants infected with the P1A, P1D, H1GG or V2stop mutants (**Figure 6A**). We confirmed by sequencing the V2 ORF, that in plants infected with the P2A, P3AA, P2A/P3AA, or H2GG mutants the viral DNA did not result from the replication of revertants, as all the analyzed fragments contained the proper mutation, confirming that these mutations are stable in infected plants.

To discern if the lessen or absent viral DNA levels in plants infected with the mutants was due to a defect in replication and/or spreading throughout the plant, we quantified the viral DNA in the agroinfiltrated leaves at 4 dpi (local infection, from the same *N. benthamiana* plants used in the systemic infection assay, **Figure 6A**). DNA was extracted and analyzed by qPCR. As presented in **Figure 6B**, all the mutants supported viral replication, indicating that the total or partial inability of P1A, P1D, H1GG, H2GG, and V2stop mutant viruses to infect *N. benthamiana* plants was not due to a replication defect. These findings suggested that the impairment of the BCTV V2 mutants to systemically infect the plant is related with the movement and dissemination of the viruses through the plant tissues.

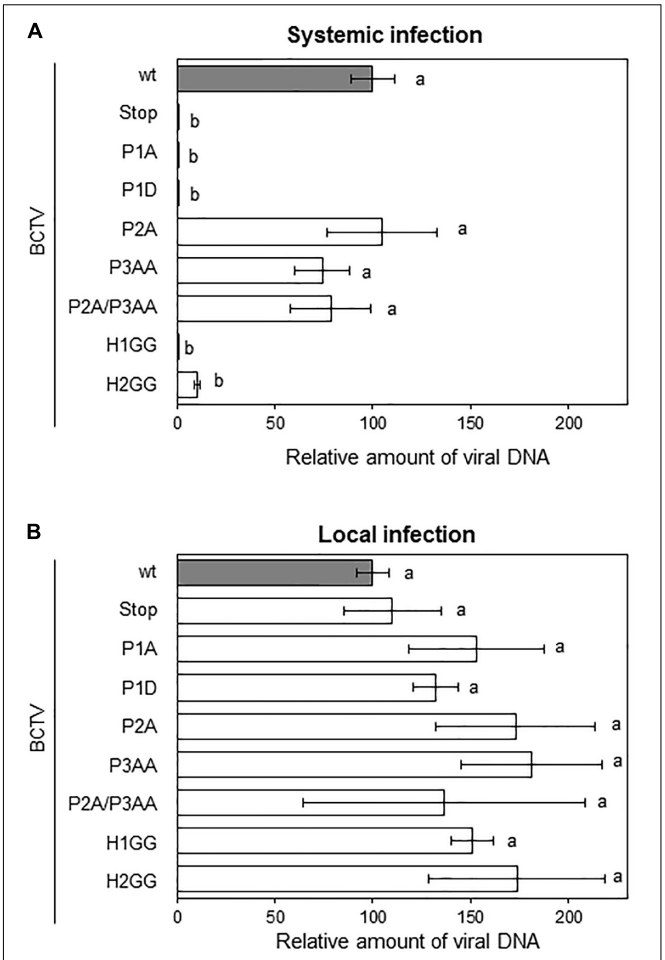

FIGURE 6 | Infection of *N. benthamiana* plants with BCTV V2 mutants. Plants were agroinoculated with wild-type or V2 mutated BCTV infective clones. Relative viral DNA accumulation in apical leaves (systemic infection) at 28 dpi **(A)** or at the infiltrated leaves (local infection) at 4 dpi **(B)**. BCTV accumulation was measured by qPCR. DNA levels were normalized to 25S ribosomal DNA interspacer (ITS) and are presented as the relative amount of virus compared with the amount found in wild-type BCTV (wt) samples (in gray, set to 100%). Bars represent mean values ± standard error (SE) for 4–8 pools of two leaves from 3 to 4 plants each one. Mean values marked with different letter (a or b) indicate results significantly different from each other, as established by One Way ANOVA (Dunnett's Multiple Comparison Test; $P < 0.05$).

We have previously demonstrated that V2 from BCTV suppresses PTGS by interfering with the RDR6-dependent amplification pathway in *A. thaliana* (Luna et al., 2017). Our data indicate that the lack of silencing suppression activity of the V2 mutants P1A, H1GG and H2GG, is complemented by the impaired function of RDR6 in the *N. benthamiana* RDR6i line (**Figure 3**). As an additional approach to analyze whether the lack of these components of the antiviral silencing pathway, could genetically complement the defective systemic infection of BCTV V2 mutants, we infected *A. thaliana* mutants deficient in RDR6 (*rdr6-15*) and DCL2 and DCL4 (double mutant

dcl2-1/dcl4-2 or *dcl2/4*) with BCTV wild-type and V2 mutants unable to systemically infect *N. benthamiana*. *A. thaliana* Col-0 plants infected with BCTV were clearly symptomatic, whereas plants infected with any of the BCTV mutants did not develop symptoms (data not shown). The qPCR results from the infected plants indicated that, as it occurs in *N. benthamiana*, mutant virus in P1 phosphorylation site (P1A and P1D) or any of the two hydrophobic domains (H1GG and H2GG) were impaired in systemic infection of *A. thaliana* (**Figure 7**). The differences on viral DNA accumulation among the wild-type and viral mutants were maintained when *rdr6-15* or the *dcl2/4* mutant plants were infected (**Figure 7**), indicating that the deficiency in viral infection caused by mutations in P1, H1, or H2 domains of V2, is not complemented by the impairment of the antiviral silencing pathway.

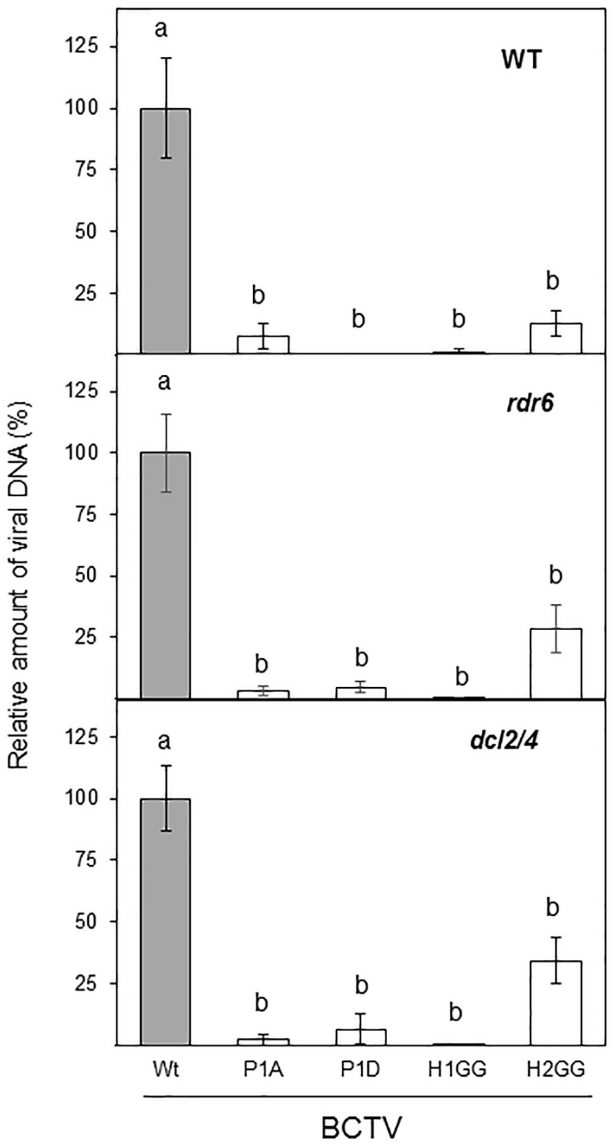

FIGURE 7 | Infection of *A. thaliana* wild-type (WT), *dcl2/4* (*dcl2-1/dcl4-2*) and *rdr6 (rdr6-15)* mutants with wild-type or BCTV V2 mutants. The relative viral DNA accumulation at 28 dpi was quantified by qPCR in WT, *rdr6* and *dcl2/4* backgrounds. DNA levels were normalized to actin gene and are presented as the relative amount of virus compared with the amount found in wild-type BCTV (wt) samples (in gray, set to 100%). Bars represent mean values ± standard error (SE) for eight to twelve plants per biological replicate. Data from three biological replicate are shown. Mean values marked with different letter (a or b) indicate results significantly different from each other, as established by One Way ANOVA (Dunnett's Multiple Comparison Test; $P < 0.05$).

DISCUSSION

In this work, we have identified and characterized three domains of V2 from curtovirus required for PTGS suppression activity, subcellular localization and systemic, but not local infection. These results indicate that curtoviral V2 is, as its functional homolog the begomoviral V2, required for viral spreading in the plant.

The highly conserved protein kinase C (PKC) motif (P1) is required for the PTGS suppression activity of V2, as the replacement of the threonine residues of this motif impairs V2 ability to suppress GFP gene silencing in *N. benthamiana* leaves. The loss of PTGS suppression activity of P1A mutant is completely recovered in a RDR6-defective background, indicating that BCTV V2 suppresses PTGS through a mechanism that involves the RDR6-mediated pathway (Luna et al., 2017). However, the lack of suppression activity produced by the P1A mutation does not seem to be the cause of the lack on infectivity of this mutant, since infectivity is not even partially recovered in plants impaired in gene silencing (*rdr6* and *dcl2/4* mutants). Similar phenotypes are produced by the phosphomimic mutation of the P1 domain (P1D) suggesting that constitutive phosphorylation of the threonine 43 residue is not recovering the suppression activity, neither the ability to propagate the virus during the infection. In Old World begomovirus, this motif has been described to be involved in viral pathogenicity (Chowda-Reddy et al., 2008; Mubin et al., 2010) but studies have not been carried out to determine whether the domain is needed for PTGS suppression or systemic infection.

The analysis of V2 protein sequences drove us to study two hydrophobic domains (H1 and H2) located in the N-terminus, that are presented in all geminiviral V2 proteins. Replacement of two of the non-polar residues of those domains, dramatically affect the PTGS suppression activity of V2 and, as in the case of the P1 mutation, the activity is fully recovered when RDR6 activity is impaired. When *N. benthamiana* wild-type plants were infected with BCTV containing the H1GG or the H2GG V2 mutations, systemic infection was compromised although some differences were observed. While in wild-type *N. benthamiana* H1GG was fully impaired for systemic infection to a similar level than the null V2 mutant (V2stop), the virus containing the H2GG mutation showed a slightly more, although not statistically significant, viral DNA accumulation. This difference among both mutated viruses was more noticeable when *A. thaliana* plants impaired in gene silencing were infected. In wild-type plants infected with the H2GG mutant, the amount of viral DNA is

only 12.6 ± 5.1% of the viral DNA accumulated in plants infected with the wild-type virus. However, in *rdr6* and *dcl2/4* mutants the quantity of H2GG viral DNA represented 28.3 ± 9.6% and 34.3 ± 9.2%, respectively. This indicated that the failure of H2GG to produce a systemic infection is partially recovered by the inhibition of PTGS antiviral activity. Altogether, these results indicated that the inability of these mutants to systemically infect the plant is not due to the lack of PTGS suppression activity. Therefore, other V2 function required for the viral movement is altered by those mutations. Interestingly, mutations in these domains, also provoked changes in the subcellular localization of V2 protein. As begomoviral V2, BCTV V2 protein localizes in the nucleoplasm and in the cell periphery, mainly associated to ER. Additionally, accumulation in the Cajal body (Guo et al., 2015; Wang et al., 2019, BioRxiv) and nuclear periphery (Zhou et al., 2011; Hak et al., 2015; Zhao et al., 2019, BioRxiv) have been reported for V2 from the begomoviruses TYLCV and Grapevine red blotch-associated virus. Here we describe that curtoviral V2 also accumulates in the nuclear periphery and in a discrete nuclear structure that could correspond to the Cajal body. Mutations in the P1 and H2 domains prevent the localization of the protein in the nuclear edge (**Figure 5**) but do not affect the accumulation in this nuclear body (data not shown). Begomoviral V2 interacts with the viral CP, a protein that seems to function as a nuclear shuttle protein that mediates nuclear import and export of viral DNA similarly to BV1, a protein encoded by the B-component of bipartite begomovirus (Rojas et al., 2001; Moshe et al., 2015; Zhao et al., 2019). In begomovirus, V2 affects the nuclear localization of CP and it enhances CP capacity to mediate nuclear export by a mechanism that depends on V2-CP interaction (Zhao et al., 2019). Mutation of cysteine residue (C85A) placed at the "x" position of the CxC motif from TYLCV V2, abolishes the interaction between CP and V2 and affects the nuclear export function and the perinuclear localization of V2. This mutation also causes delayed onset of very mild symptoms, indicating that the interaction between CP and V2 and, as a consequence, the V2-mediated nuclear export of CP is essential for viral spread in the plant. Curiously, our mutants in P1 and H2 displayed a surprisingly similar phenotype. Although curtoviral V2 lacks of a CxC motif, there is a cysteine residue (C71) conserved at a similar position. Considering the functional and structural similarities between curtoviral and begomoviral V2 proteins, a tantalizing possibility is that the BCTV V2 would also participate or mediate the nuclear export of the virus. This function could explain the impairment on viral systemic movement detected in BCTV V2 mutants. Further experiments to determine whether BCTV V2 interacts with CP and if this interaction is affected in the mutants, are in progress.

Hypersensitive response (HR) is an active defense reaction derived from the activation of defense-related pathways, which lead to cell death (CD) (reviewed in Heath, 2000). HR, which is characterized by rapid and localized cell death at the site of infection, arises after the interaction with an incompatible pathogen. Our results indicate that BCTV V2 functions as a pathogenicity determinant and possibly as an avirulence factor. Similar to the results reported for begomoviral V2, ectopic expression of BCTV V2 "*via*" a PVX-derived vector provoked the induction of local and systemic necrosis in the *N. benthamiana* leaves. Interestingly, BCTV infection in *A. thaliana* or *N. benthamiana* plants does not produce cell-death phenotype on systemically infected plants, maybe due to the limited number of cells that harbor its infection. Transient or permanent expression of V2 from a 35S CaMV promoter in *N. benthamiana* or *A. thaliana,* should increase the number of cells expressing V2 and bypass the tissue specificity. However, in none of the occasions in which BCTV V2 was expressed from those type of constructs a necrotic reaction was observed (**Figure 2**; Luna et al., 2017). This raises the concern of different levels of V2 protein accumulation in systemically infected tissues when PVX is used as the vector to express this curtoviral protein.

Interestingly, V2-induced HR is incapable to limit the long-distance movement of PVX-V2 resulting in systemic plant death (**Figure 4**). This function of BCTV V2 as pathogenicity determinant is similar to that described for V2 of Old World begomoviruses. However, the protein domains involved in this activity appear to be at least partially different. In begomovirus, deletion analysis and site-directed mutagenesis of the sequences encompassing the PKC phosphorylation motif (P1) have been shown to abolish or reduce the viral pathogenicity (induction of virus-like symptoms) and the ability to initiate HR (Chowda-Reddy et al., 2008; Mubin et al., 2010). Nevertheless, the mutation of the P1A or H2GG motifs of BCTV V2 reduced, but not abolished local, and did not affect systemic necrosis compared to the wild-type V2. This result suggests that the P1 motif and the H2 region of curtovirus are not fully required for the V2 to function as a pathogenicity determinant. On the contrary, expression of H1GG mutant displayed the same phenotype as the plants infected with non-recombinant PVX. Although this suggests that the H1 domain is absolutely required for the V2-induced HR, this result has to be taken cautiously, since we have not been able to detect a consistent expression of GFP-V2 fused protein containing the H1GG mutation. We cannot discard the possibility that the absence of HR induction by H1GG mutants is due to a lower protein level, in spite of that no difference with the wild-type V2 were observed at a transcriptional level (**Supplementary Figure S3**). Unfortunately, we do not have the antibodies against BCTV-V2 required to determine the protein level of V2H1GG. Although we cannot explain yet how V2 induces a response defense, our results clearly indicate that the ability of curtoviral V2 to induce HR is not dependent of its activity as PTGS suppressor since the PVX-derived expression of P1A and H2GG V2 mutants, that are heavily impaired in their suppression activity, showed similar values for conductivity and similar HR-like phenotype to the wild-type V2 (**Figure 4**).

The results presented here, confirm that V2 proteins from curtovirus and begomovirus are functional homologs. In spite of a very low level of sequence homology, they both are required for viral movement, present similar subcellular distribution and possess similar functions (PTGS suppressor and pathogenicity determinant). The fact that V2 ORF is present in Old World begomovirus and curtovirus, could suggest that this gene was already present in a common ancestor of both viral genera. However, the high level of conservation at the protein

level among the species of each genus, but not between genera, and the absence of ORF V2 homologs in the genome of New World begomoviruses, argue against this hypothesis and suggest that V2 from curtovirus and begomovirus could have evolved independently.

DATA AVAILABILITY STATEMENT

All datasets generated for this study are included in the article/**Supplementary Material**.

AUTHOR CONTRIBUTIONS

AL, BR-R, and TR-D have performed the experiments, analyzed the data, and participated in the writing and critical reading of the manuscript. LC have provided technical assistance in the experimental procedures. ER-N has collaborated in some experiments and participated in the critical reading of the manuscript. EB and AC have planned and directed the experimental design of the work, have done the writing and the critical lecture of the manuscript. All authors contributed to the article and approved the submitted version.

FUNDING

This research was supported by a grant from the spanish "Ministerio de Economía, Industria y Competitividad/FEDER" (AGL2016-75819-C2-1-R). BR-R was awarded with a Predoctoral Fellowship from the Spanish Ministerio de Educación y Formación Profesional. TR-D was supported by "Programa Juan de la Cierva" (IJCI-2017-33367) from the spanish "Ministerio de Economía, Industria y Competitividad."

ACKNOWLEDGMENTS

The authors thank Lucia Cruzado and Pablo García Vallejo for excellent technical assistance.

SUPPLEMENTARY MATERIAL

The Supplementary Material for this article can be found online at: https://www.frontiersin.org/articles/10.3389/fpls.2020.00835/full#supplementary-material

FIGURE S1 | Alignment of the aminoacidic sequence of V2 from 29 begomovirus species: *Ageratum yellow vein virus-China* (AYVV/Gx; AJ495813), *Tomato yellow leaf curl Sardinia virus* (TYLCSaV; L27708), *Papaya leaf curl Guandong virus* (PaLCuGdV; AJ558122), *Indian cassava mosaic virus* (ICMV; AJ314739), *Cotton leaf curl Gezira virus* (CLCuGeV/Ca; AJ542539.1), *Honeysuckle yellow vein virus*-[UK] (HYVV-UK; AJ543429), *Tomato leaf curl virus*-Australia (ToLCV/To; S53251), *East African cassava mosaic Zanzibar virus* (EACMZV; AJ717559): *Tomato leaf curl Mayotte virus* (ToLCYTV; AJ620912), East African cassava mosaic Cameroon virus (EACMCV; AF112354); *Hibiscus rosa-sinensis mosaic virus)* (HRSMV; DQ022659), *Tomato leaf curl Laos virus* (ToLCLV; AF195782), *Tomato leaf curl Java virus* (ToLCJV; AB100304), *Tomato leaf curl China virus* (ToLCCNV; AJ811910), *Tomato leaf curl Taiwan virus* (ToLCTWV; DQ866127), *Spilanthes yellow vein virus* (SpYVV; DQ641694), *Sida yellow vein Vietnam virus* (SiYVVV; DQ641696), *Alternanthera yellow vein virus* (AlYVV; AM691015), *Tomato leaf curl Bangalore virus* (ToLCBV; AY428770), *Lindernia anagallis yellow vein virus* (LaYVV; AY795900), *Siegesbeckia yellow vein virus* (SgYVV; AM183224), *Tomato leaf curl New Delhi virus* (ToLCNDV; AY286316), *Tomato yellow leaf curl Indonesia virus* (TYLCIDV; AF189018), *Tomato leaf curl Hsinchu virus* (ToLCV; DQ866131), *Senecio yellow mosaic virus* (SeYMV; AJ876550), *Vernonia yellow vein virus* (VeYVV; AM182232), *Cotton leaf curl Multan virus* (CLCuMV; EF465535), *Ludwigia yellow vein virus* (LuYVV; AJ965539) and *Clerodendron yellow mosaic virus* (ClYMV; EF408037). Gaps (-) were introduced to optimize the alignment. The positions of the predicted putative phosphorilation motif P1 (protein kinase CK2/protein kinase C) are depicted in white letters inside black boxes. The CxC motif (Padidam et al., 1996; Zrachya et al., 2007) is underlined. The hydrophobic domains (H1 and H2) are shadowed in gray.

FIGURE S2 | Alignment of the aminoacidic sequence of V2 from three curtovirus species: *Beet curly top virus*-California [Logan] (BCTV/CA/Logan; M24597), *Spinach severe curly top virus* (SpSCTV; GU734126) and *Horseradish curly top virus* (HCTV; U49907). The positions of the predicted putative phosphorylation motifs P1 (protein kinase CK2/protein kinase C), P2 (protein kinase CK2) and P3 (protein kinase C) are depicted in white letters inside black boxes. The hydrophobic domains (H1 and H2) are shadowed in gray.

FIGURE S3 | Relative *V2* mRNA levels in *N. benthamiana* leaves. Leaves from *N. benthamiana* plants were infiltrated with a mixture of two *A. tumefaciens* cultures expressing GFP and the indicated version of V2 and relative *V2* mRNA levels were measured by RT-qPCR in the infiltrated tissues at 1 dpi. Wild-type V2 protein (wt) and the empty vector (C) were used as a positive and negative controls, respectively. *V2* transcript levels were normalized to *EF1* and are presented as the relative amount of transcripts compared with the amount found in wild-type V2 (wt) samples (set to 100%). Bars represent the mean ± SD for three different pools from 2 to 3 leaves obtained from 3–4 plants each one. One Way ANOVA (Dunnett's Multiple Comparison Test ($P < 0.05$) was performed and showed no significant differences between the experiments and the control condition (V2 wild-type plants).

FIGURE S4 | RT-PCR from recombinant PVX-infected *N. benthamiana* plants. Molecular analysis of plants infected with PVX-recombinant viruses expressing *V2* and *V2* mutants from BCTV. Total RNA was extracted from apical leaves of *N. benthamiana* plants infected with PVX-recombinant viruses expressing *V2* and *V2* mutated versions from BCTV. RT-PCR with specific primers for PVX was performed to quantify viral titer. As an internal control *N. benthamiana* gene *EF1* was used. Primers hybridizing at both sides of the MCS (*V2*) were also used to detect the retention of the geminiviral protein in the recombinant viruses.

FIGURE S5 | Pearson's correlation coefficient (R) for the co-localization of GFP and SUN1-tagRFP. Leaves were agroinfiltrated with a construct expressing the GFP-V2 fusion protein or the GFP-V2 mutants and the nuclear envelope marker AtSUN1–tagRFP and observed under the confocal microscope at 3 dpi. R was quantified and represented by box plots. Each box represents the mean values ± standard error (SE) from 6 to 9 nuclei.

FIGURE S6 | Western blot from V2 protein (wild-type or mutated) fused to GFP. of samples of V2 mutants fused to GFP expressed in epidermal cells of *N. benthamiana* (**Figure 5A**). Leaves were agroinfiltrated with a construct expressing the 35S:GFP (GFP), 35S:GFP-V2 fusion protein or the 35S:GFP-V2 mutants (P1A, P1D, H1GG or H2GG). Samples were taken at 2 dpi (the same ones shown in **Figure 5A**) and total protein was extracted, loaded, resolved by 12% SDS-PAGE gel electrophoresis, and transferred by electroblotting onto a polyvinylidene diflouride membrane. Proteins were stained by Coomassie blue (CBB) and immunoblotted with anti-GFP mouse monoclonal antibody (α-GFP).

FIGURE S7 | Infection of *N. benthamiana* plants with BCTV V2 mutants. Plants were agroinoculated with wild-type or V2 mutated BCTV clones. Number of symptomatic plants observed at 28 dpi. The asterisk indicates symptoms milder than the caused by the wild-type virus.

REFERENCES

Allen, E., Xie, Z., Gustafson, A. M., Sung, G.-H., Spatafora, J. W., and Carrington, J. C. (2004). Evolution of microRNA genes by inverted duplication of target gene sequences in *Arabidopsis thaliana*. *Nat. Genet.* 36, 1282–1290. doi: 10.1038/ng1478

Amin, I., Hussain, K., Akbergenov, R., Yadav, J. S., Qazi, J., Mansoor, S., et al. (2011). Suppressors of RNA silencing encoded by the components of the cotton leaf curl begomovirus-betasatellite complex. *Mol. Plant. Microbe. Interact.* 24, 973–983. doi: 10.1094/MPMI-01-11-0001

Baker, C. J., O'Neill, N. R., Keppler, L. D., and Orlandi, E. W. (1991). Early responses during plant-bacteria interactions in tobacco cell suspensions. *Physiol. Biochem.* 81, 1504–1507.

Bar-Ziv, A., Levy, Y., Hak, H., Mett, A., Belausov, E., Citovsky, V., et al. (2012). The Tomato yellow leaf curl virus (TYLCV) V2 protein interacts with the host papain-like cysteine protease CYP1. *Plant Signal. Behav.* 7, 983–989. doi: 10.4161/psb.20935

Cañizares, M. C., Navas-Castillo, J., and Moriones, E. (2008). Multiple suppressors of RNA silencing encoded by both genomic RNAs of the crinivirus, tomato chlorosis virus. *Virology* 379, 168–174. doi: 10.1016/j.virol.2008.06.020

Chowda-Reddy, R. V., Achenjang, F., Felton, C., Etarock, M. T., Anangfac, M.-T., Nugent, P., et al. (2008). Role of a geminivirus AV2 protein putative protein kinase C motif on subcellular localization and pathogenicity. *Virus Res.* 135, 115–124. doi: 10.1016/j.virusres.2008.02.014

Deleris, A., Gallego-Bartolome, J., Bao, J., Kasschau, K. D., Carrington, J. C., and Voinnet, O. (2006). Hierarchical action and inhibition of plant dicer-like proteins in antiviral defense. *Science* 313, 68–71. doi: 10.1126/science.1128214

Elmer, J. S., Brand, L., Sunter, G., Gardiner, W. E., Bisaro, D. M., and Rogers, S. G. (1988). Genetic analysis of the tomato golden mosaic virus. II. The product of the AL1 coding sequence is required for replication. *Nucleic Acids Res.* 16, 7043–7060. doi: 10.1093/nar/16.14.7043

Fondong, V. N. (2013). Geminivirus protein structure and function. *Mol. Plant Pathol.* 14, 635–649. doi: 10.1111/mpp.12032

García-Arenal, F., and Zerbini, F. M. (2019). Life on the edge: geminiviruses at the interface between crops and wild plant hosts. *Annu. Rev. Virol.* 6, 411–433. doi: 10.1146/annurev-virology-092818-015536

Glick, E., Zrachya, A., Levy, Y., Mett, A., Gidoni, D., Belausov, E., et al. (2008). Interaction with host SGS3 is required for suppression of RNA silencing by tomato yellow leaf curl virus V2 protein. *Proc. Natl. Acad. Sci. U.S.A.* 105, 157–161. doi: 10.1073/pnas.0709036105

Guo, T. W., Vimalesvaran, D., Thompson, J. R., Perry, K. L., and Krenz, B. (2015). Subcellular localization of grapevine red blotch-associated virus ORFs V2 and V3. *Virus Genes* 51, 156–158. doi: 10.1007/s11262-015-1205-x

Hak, H., Levy, Y., Chandran, S. A., Belausov, E., Loyter, A., Lapidot, M., et al. (2015). TYLCV-Is movement in planta does not require V2 protein. *Virology* 477, 56–60. doi: 10.1016/j.virol.2015.01.007

Haseloff, J., Siemering, K. R., Prasher, D. C., and Hodge, S. (1997). Removal of a cryptic intron and subcellular localization of green fluorescent protein are required to mark transgenic *Arabidopsis* plants brightly. *Proc. Natl. Acad. Sci. U.S.A.* 94, 2122–2127. doi: 10.1073/pnas.94.6.2122

Heath, M. C. (2000). "Hypersensitive response-related death," in *Programmed Cell Death in Higher Plants*, eds E. Lam, H. Fukuda, and J. Greenberg (Dordrecht: Springer Netherlands), 77–90. doi: 10.1007/978-94-010-0934-8_6

Ho, S. N., Hunt, H. D., Horton, R. M., Pullen, J. K., and Pease, L. R. (1989). Site-directed mutagenesis by overlap extension using the polymerase chain reaction. *Gene* 77, 51–59. doi: 10.1016/0378-1119(89)90358-2

Hormuzdi, S. G., and Bisaro, D. M. (1993). Genetic analysis of beet curly top virus: evidence for three virion sense genes involved in movement and regulation of single- and double-stranded dna levels. *Virology* 193, 900–909. doi: 10.1006/viro.1993.1199

Luna, A. P., Morilla, G., Voinnet, O., and Bejarano, E. R. (2012). Functional analysis of gene-silencing suppressors from tomato yellow leaf curl disease viruses. *Mol. Plant Microbe Interact.* 25, 1294–1306. doi: 10.1094/MPMI-04-12-0094-R

Luna, A. P., Rodríguez-Negrete, E. A., Morilla, G., Wang, L., Lozano-Durán, R., Castillo, A. G., et al. (2017). V2 from a curtovirus is a suppressor of post-transcriptional gene silencing. *J. Gen. Virol.* 98, 2607–2614. doi: 10.1099/jgv.0.000933

Mackey, D., Holt, B. F., Wiig, A., and Dangl, J. L. (2002). RIN4 interacts with *Pseudomonas syringae* type III effector molecules and is required for RPM1-mediated resistance in *Arabidopsis*. *Cell* 108, 743–754. doi: 10.1016/S0092-8674(02)00661-X

Moshe, A., Belausov, E., Niehl, A., Heinlein, M., Czosnek, H., and Gorovits, R. (2015). The Tomato yellow leaf curl virus V2 protein forms aggregates depending on the cytoskeleton integrity and binds viral genomic DNA. *Sci. Rep.* 5:9967. doi: 10.1038/srep09967

Mubin, M., Amin, I., Amrao, L., Briddon, R. W., and Mansoor, S. (2010). The hypersensitive response induced by the V2 protein of a monopartite begomovirus is countered by the C2 protein. *Mol. Plant Pathol.* 11, 245–254. doi: 10.1111/j.1364-3703.2009.00601.x

Mubin, M., Briddon, R. W., and Mansoor, S. (2019). The V2 protein encoded by a monopartite begomovirus is a suppressor of both post-transcriptional and transcriptional gene silencing activity. *Gene* 686, 43–48. doi: 10.1016/j.gene.2018.11.002

Oda, Y., and Fukuda, H. (2011). Dynamics of *Arabidopsis* SUN proteins during mitosis and their involvement in nuclear shaping. *Plant J.* 66, 629–641. doi: 10.1111/j.1365-313X.2011.04523.x

Padidam, M., Beachy, R. N., and Fauquet, C. M. (1996). The role of AV2 ("Precoat") and coat protein in viral replication and movement in tomato leaf curl geminivirus. *Virology* 224, 390–404. doi: 10.1006/viro.1996.0546

Rojas, M. R., Jiang, H., Salati, R., Xoconostle-Cázares, B., Sudarshana, M. R., Lucas, W. J., et al. (2001). Functional analysis of proteins involved in movement of the monopartite begomovirus, Tomato yellow leaf curl virus. *Virology* 291, 110–125. doi: 10.1006/viro.2001.1194

Rojas, M. R., Macedo, M. A., Maliano, M. R., Soto-Aguilar, M., Souza, J. O., Briddon, R. W., et al. (2018). World management of geminiviruses. *Annu. Rev. Phytopathol.* 56, 637–677. doi: 10.1146/annurev-phyto-080615-100327

Roshan, P., Kulshreshtha, A., Kumar, S., Purohit, R., and Hallan, V. (2018). AV2 protein of tomato leaf curl Palampur virus promotes systemic necrosis in *Nicotiana benthamiana* and interacts with host Catalase2. *Sci. Rep.* 8:1273. doi: 10.1038/s41598-018-19292-3

Rothenstein, D., Krenz, B., Selchow, O., and Jeske, H. (2007). Tissue and cell tropism of Indian cassava mosaic virus (ICMV) and its AV2 (precoat) gene product. *Virology* 359, 137–145. doi: 10.1016/j.virol.2006.09.014

Saeed, M., Krczal, G., and Wassenegger, M. (2015). Three gene products of a begomovirus–betasatellite complex restore expression of a transcriptionally silenced green fluorescent protein transgene in *Nicotiana benthamiana*. *Virus Genes* 50, 340–344. doi: 10.1007/s11262-014-1155-8

Sambrook, J., and Russell, D. W. (2001). *Molecular Cloning: A Laboratory Manual, Third Edition*. New York, NY: Cold Spring Harbor Laboratory Press.

Schwach, F., Vaistij, F. E., Jones, L., and Baulcombe, D. C. (2005). An RNA-dependent RNA polymerase prevents meristem invasion by potato virus X and is required for the activity but not the production of a systemic silencing signal. *Plant Physiol.* 138, 1842–1852. doi: 10.1104/pp.105.063537

Sharma, P., and Ikegami, M. (2010). Tomato leaf curl Java virus V2 protein is a determinant of virulence, hypersensitive response and suppression of posttranscriptional gene silencing. *Virology* 396, 85–93. doi: 10.1016/j.virol.2009.10.012

Sharma, P., Ikegami, M., and Kon, T. (2010). Identification of the virulence factors and suppressors of posttranscriptional gene silencing encoded by Ageratum yellow vein virus, a monopartite begomovirus. *Virus Res.* 149, 19–27. doi: 10.1016/j.virusres.2009.12.008

Stanley, J., Latham, J. R., Pinner, M. S., Bedford, I., and Markham, P. G. (1992). Mutational analysis of the monopartite geminivirus beet curly top virus. *Virology* 191, 396–405. doi: 10.1016/0042-6822(92)90201-Y

Varsani, A., Martin, D. P., Navas-Castillo, J., Moriones, E., Hernández-Zepeda, C., Idris, A., et al. (2014). Revisiting the classification of curtoviruses based on genome-wide pairwise identity. *Arch. Virol.* 159, 1873–1882. doi: 10.1007/s00705-014-1982-x

Varsani, A., Roumagnac, P., Fuchs, M., Navas-Castillo, J., Moriones, E., Idris, A., et al. (2017). Capulavirus and grablovirus: two new genera in the family Geminiviridae. *Arch. Virol.* 162, 1819–1831. doi: 10.1007/s00705-017-3268-6

Voinnet, O., Vain, P., Angell, S., and Baulcombe, D. C. (1998). Systemic spread of sequence-specific transgene RNA degradation in plants is initiated by localized

introduction of ectopic promoterless DNA. *Cell* 95, 177–187. doi: 10.1016/s0092-8674(00)81749-3

Wang, B., Li, F., Huang, C., Yang, X., Qian, Y., Xie, Y., et al. (2014). V2 of tomato yellow leaf curl virus can suppress methylation-mediated transcriptional gene silencing in plants. *J. Gen. Virol.* 95, 225–230. doi: 10.1099/vir.0.055798-0

Wang, B., Yang, X., Wang, Y., Xie, Y., and Zhou, X. (2018). Tomato yellow leaf curl virus V2 interacts with host histone deacetylase 6 to suppress methylation-mediated transcriptional gene silencing in plants. *J. Virol.* 92, 36–54. doi: 10.1128/jvi.00036-18

Wang, L., Ding, Y., He, L., Zhang, G., Zhu, J.-K., and Lozano-Duran, R. (2019). A virus-encoded protein suppresses methylation of the viral genome through its interaction with AGO4 in the Cajal body. *bioRxiv* [Preprint]. doi: 10.1101/811091

Zerbini, F. M., Briddon, R. W., Idris, A., Martin, D. P., Moriones, E., Navas-Castillo, J., et al. (2017). ICTV virus taxonomy profile: geminiviridae. *J. Gen. Virol.* 98, 131–133. doi: 10.1099/jgv.0.000738

Zhan, B., Zhao, W., Li, S., Yang, X., and Zhou, X. (2018). Functional scanning of apple geminivirus proteins as symptom determinants and suppressors of posttranscriptional gene silencing. *Viruses* 10:488. doi: 10.3390/v10090488

Zhang, J., Dong, J., Xu, Y., and Wu, J. (2012). V2 protein encoded by Tomato yellow leaf curl China virus is an RNA silencing suppressor. *Virus Res.* 163, 51–58. doi: 10.1016/j.virusres.2011.08.009

Zhao, W., Ji, Y., Wu, S., Barton, E., and Fan, Y. (2019). Tomato yellow leaf curl virus V2 protein plays a critical role in the nuclear export of V1 protein and viral systemic infection. *bioRxiv* [Preprint]. doi: 10.1101/669754

Zhou, Y., Rojas, M. R., Park, M.-R., Seo, Y.-S., Lucas, W. J., and Gilbertson, R. L. (2011). Histone H3 interacts and colocalizes with the nuclear shuttle protein and the movement protein of a geminivirus. *J. Virol.* 85, 11821–11832. doi: 10.1128/JVI.00082-11

Zrachya, A., Glick, E., Levy, Y., Arazi, T., Citovsky, V., and Gafni, Y. (2007). Suppressor of RNA silencing encoded by Tomato yellow leaf curl virus-Israel. *Virology* 358, 159–165. doi: 10.1016/j.virol.2006.08.016

Conflict of Interest: The authors declare that the research was conducted in the absence of any commercial or financial relationships that could be construed as a potential conflict of interest.

frontiers in Plant Science

ORIGINAL RESEARCH
published: 15 July 2020
doi: 10.3389/fpls.2020.01069

Identification of Tomato Proteins That Interact With Replication Initiator Protein (Rep) of the Geminivirus TYLCV

Francesca Maio[1†], Tieme A. Helderman[1], Manuel Arroyo-Mateos[1], Miguel van der Wolf[1], Sjef Boeren[2], Marcel Prins[1,3] and Harrold A. van den Burg[1]*

[1] Molecular Plant Pathology, Swammerdam Institute for Life Sciences (SILS), University of Amsterdam, Amsterdam, Netherlands, [2] Laboratory of Biochemistry, Wageningen University, Wageningen, Netherlands, [3] Keygene N.V., Wageningen, Netherlands

Geminiviruses are plant-infecting DNA viruses that reshape the intracellular environment of their host in order to create favorable conditions for viral replication and propagation. Viral manipulation is largely mediated *via* interactions between viral and host proteins. Identification of this protein network helps us to understand how these viruses manipulate their host and therefore provides us potentially with novel leads for resistance against this class of pathogens, as genetic variation in the corresponding plant genes could subvert viral manipulation. Different studies have already yielded a list of host proteins that interact with one of the geminiviral proteins. Here, we use affinity purification followed by mass spectrometry (AP-MS) to further expand this list of interacting proteins, focusing on an important host (tomato) and the Replication initiator protein (Rep, AL1, C1) from *Tomato yellow leaf curl virus* (TYLCV). Rep is the only geminiviral protein proven to be essential for geminiviral replication and it forms an integral part of viral replisomes, a protein complex that consists of plant and viral proteins that allows for viral DNA replication. Using AP-MS, fifty-four 'high confidence' tomato proteins were identified that specifically co-purified with Rep. For two of them, an unknown EWS-like RNA-binding protein (called Geminivirus Rep interacting EWS-like protein 1 or GRIEP1) and an isoform of the THO complex subunit 4A (ALY1), we were able to confirm this interaction with Rep *in planta* using a second method, bimolecular fluorescence complementation (BiFC). The THO subunit 4 is part of the THO/TREX (TRanscription-EXport) complex, which controls RNA splicing and nuclear export of mRNA to the cytoplasm and is also connected to plant disease resistance. This work represents the first step towards characterization of novel host factors with a putative role in the life cycle of TYLCV and possibly other geminiviruses.

Keywords: geminivirus, *Tomato yellow leaf curl virus*, viral replication, proteomics, PCNA, Rep, interactome

OPEN ACCESS

Edited by:
Araceli G. Castillo, Institute of Subtropical and Mediterranean Horticulture La Mayora, Spain

Reviewed by:
Björn Krenz, German Collection of Microorganisms and Cell Cultures GmbH (DSMZ), Germany
Christina Wege, University of Stuttgart, Germany
Linda Hanley-Bowdoin, North Carolina State University, United States

***Correspondence:**
Harrold A. van den Burg
H.A.vandenBurg@uva.nl

***Present address:**
Francesca Maio, Spark Genetics B.V., Utrecht, Netherlands

Specialty section:
This article was submitted to Virology, a section of the journal Frontiers in Plant Science

Received: *28 February 2020*
Accepted: *29 June 2020*
Published: *15 July 2020*

Citation:
Maio F, Helderman TA, Arroyo-Mateos M, van der Wolf M, Boeren S, Prins M and van den Burg HA (2020) Identification of Tomato Proteins That Interact With Replication Initiator Protein (Rep) of the Geminivirus TYLCV. Front. Plant Sci. 11:1069. doi: 10.3389/fpls.2020.01069

INTRODUCTION

During the past twenty years, geminiviruses (family *Geminiviridae*) have emerged as one of the most destructive plant-infecting virus families (Rojas et al., 2005). They infect numerous plant species causing significant yield losses in many economically important crops, both monocots and dicots (Mansoor et al., 2003; Mansoor et al., 2006). Geminiviruses are transmitted between host plants by insect vectors, for example leafhoppers, treehoppers and whiteflies. Based on these vectors and their genome organization, they are currently classified into nine genera (Zerbini et al., 2017). Viral transmission of the largest genus, *Begomoviruses* (>380 species), is mediated by the whitefly *Bemisia tabaci*, a highly polyphagous and worldwide spread insect (Zhao et al., 2019). Correspondingly, *Begomoviruses* have a wide host range, infecting many plant species found in the (sub)tropical regions and in more temperate climate zones (Navas-Castillo et al., 2011). Traditionally, begomovirus infestation was (to some extent effectively) controlled in the field by a combination of (a) insecticide rotation to control whitefly populations and (b) agricultural practices that reduce virus reservoirs in weeds. The success rate of these combined measures varies a lot between crops, cropping systems, and geographical regions (Rojas et al., 2018). To support these aforementioned control measures, they need to be complemented with genetic resistance in crops. So far, few resistance traits against the *Tomato yellow leaf curl virus* (TYLCV) have been identified and introduced in cultivated crops. Among them were the allelic genes *Ty-1* and *Ty-3*, which encode an RNA-dependent RNA polymerase (Verlaan et al., 2013). Introgression of these genes into tomato cultivars conferred resistance to TYLCV by increasing cytosine DNA methylation of the viral genome, thus acting through viral transcriptional gene silencing (Caro et al., 2015). Another example of a TYLCV resistance locus is *Ty-2*, which was genetically linked to the gene *TYNBS1* that encodes a NB-LRR (Nucleotide-Binding domain and Leucine-Rich Repeat-containing) type plant immune receptor (Yamaguchi et al., 2018). However, following the introduction of the resistance genes *Ty-1/3* and *Ty2* in tomato cultivars, resistance-breaking strains of TYLCV have emerged in recent years under field conditions, suggesting that these genes do not confer durable resistance against TYLCV (Verlaan et al., 2013; Butterbach et al., 2014; Belabess et al., 2016; Ohnishi et al., 2016). To increase our arsenal of genetic resources for breeding and to help reduce insecticide usage, new genetic strategies are thus needed. One strategy is to screen for resistance based on natural variation in *Susceptibility* (S) genes (van Schie and Takken, 2014), in this particular case for host genes that are critical for geminiviruses to complete their life cycle in plant cells.

Geminiviruses are typified by their capsid composed of a twinned icosahedral particle that encapsidates the viral genome composed of circular single-stranded DNA (ssDNA) molecule. Within the genus *Begomovirus*, this genome can either be *monopartite* (~2.8 kb) encoding six proteins that jointly control viral replication, movement, transmission, and pathogenesis, or *bipartite* with an 'A *component*' that encodes five or six viral proteins and a 'B *component*' that encodes for two additional proteins (both components being 2.5–2.8 kb in size) (Jeske, 2009). Geminivirus infections start foremost in terminally differentiated cells, i.e. plant cells that are in the G1 phase of the mitotic cell cycle or in the G phase of the endocycle—a variation of the cell cycle characterized by increased ploidy levels and cell expansion without cell division. In order to orchestrate replication of its viral genome, the virus thus needs to reprogram the host cell cycle to promote progression into the S phase of the cell cycle (Hanley-Bowdoin et al., 2004; Hanley-Bowdoin et al., 2013). Only one viral protein, the Replication initiator protein (Rep), is strictly required for viral replication to occur. In fact, Rep is the most conserved geminiviral protein and it is critical for assembly of *viral replisomes*, a complex of viral and host proteins that forms a DNA replication fork at viral DNA (Rizvi et al., 2015; Ruhel and Chakraborty, 2019). Numerous studies have been attempted to characterize the composition and mode-of-action of this viral replisome. At least one other viral protein, REn (Replication enhancer protein), is known to promote viral replication and as such it is likely also part of viral replisomes (Sunter et al., 1990).

Previous studies support that both Rep and REn interact with host factors in order to create a cellular environment favorable for virus replication, e.g. by up-regulating expression of several host DNA polymerases and DNA replication accessory proteins (Gutierrez, 2000a; Gutierrez, 2000b). One critical component of viral replisomes is the protein PCNA (Proliferating cell nuclear antigen), which acts as a processivity factor of eukaryotic DNA polymerases and forms a DNA clamp at replication forks (Castillo et al., 2003; Morilla et al., 2006). PCNA is a highly conserved protein in eukaryotes that controls the cell cycle, DNA replication and DNA repair pathways (Choe and Moldovan, 2017). Different studies have shown that both Rep and REn from different geminiviruses (TYLCV, *Tomato yellow leaf curl Sardinia virus* [TYLCSV], *Tomato Golden Mosaic Virus* [TGMV], *Indian mung bean yellow mosaic virus* [IMYMV]) interact with PCNA (Castillo et al., 2003; Bagewadi et al., 2004; Settlage et al., 2005) and that Rep from two different *Begomoviruses* (TYLCV and TGMV) manipulates the SUMOylation status of PCNA—a conserved protein modification of PCNA that directly modulates PCNA function (Arroyo-Mateos et al., 2018). Other host factors that are recruited by members of the Rep protein family to viral replisomes include among others the Replication factor C, RFC (Luque et al., 2002), Replication protein A32, RPA32 (Singh et al., 2007), the recombination and DNA repair related proteins Rad51 and Rad54 (Kaliappan et al., 2012; Suyal et al., 2013a) and the Minichromosome maintenance protein 2, MCM2 (Suyal et al., 2013b). Moreover, Rep also reprograms the host cell cycle by binding transcriptional regulators of the cell cycle like the Retinoblastoma-related protein (RBR) (Xie et al., 1996; Kong et al., 2000) and several members of the NAC family of transcription factors (GRAB1, GRAB2, NAC083) (Suyal et al., 2014) and by interacting with proteins involved in post-translational modification mechanisms, such as ubiquitination and sumoylation (Castillo et al., 2004; Sánchez-Durán et al., 2011; Kushwaha et al., 2017). Besides, Rep from TGMV was also shown to suppress expression of certain viral genes by binding to the viral DNA (Eagle et al., 1994; Shung and Sunter,

2007). Finally, Rep from different geminiviruses was shown to suppress methylation-mediated transcriptional gene silencing (TGS) by reducing the expression of the responsible DNA methyltransferases (MET1 and CMT3) in the plant species *Nicotiana benthamiana* and *Arabidopsis thaliana* (Rodríguez-Negrete et al., 2013).

Clearly, the geminivirus-plant interaction is intrinsically complex involving a multitude of cellular pathways (Hanley-Bowdoin et al., 2013). To better understand how geminiviruses redirect these pathways, we need to characterize in more detail the protein network of the viral proteins with host proteins. A detailed characterization of this network will aid in the identification of key steps needed for viral replication and allows exploitation of this knowledge to attain durable and broad resistance to these viruses e.g. *via* mutagenesis or natural variation of the underlying genes to ultimately disrupt the viral life cycle. Affinity-based purification followed by mass spectrometry-based protein identification (AP-MS) forms a well-suited technique to characterize the composition of these protein complexes under native conditions (Gavin et al., 2011; Dunham et al., 2012). In the context of plant–virus interactions, AP-MS has been used for example to define the interactome of the NIa protein from the potyvirus *Tobacco etch virus* (Martínez et al., 2016) and to characterize the global landscape of interactions between TYLCV and one of its host plants, *N. benthamiana* (Wang et al., 2017a).

Here we expand this list of potential host-interacting proteins by using an AP-MS approach to compose a list of 'high-confidence' tomato proteins that co-purify with TYLCV Rep in combination with tomato PCNA. For a small subset of these tomato proteins, (i) an EWS (Ewing Sarcoma protein)-like RNA-binding protein (hereafter named Geminivirus Rep-interacting EWS-like protein 1 [GRIEP1]), and (ii) the THO/TREX (TRanscription-EXport) subunit 4A (ALY1), we confirmed that they interact with Rep and PCNA *in planta* using an independent method, *i.e.* the bimolecular fluorescence complementation (BiFC). The THO/TREX complex is involved in mRNA splicing and subsequent export of mRNAs to the cytoplasm and several lines of evidence indicate that nucleocytosolic mRNA transport contributes to the regulation of plant immunity (Ehrnsberger et al., 2019). Moreover, ALY proteins have been shown to play an important role during viral infections (Xu et al., 2020). This work thus extends our inventory of Rep interactions and represents a first step towards characterization of these host factors.

MATERIALS AND METHODS

Tomato Protoplast Isolation and Transfection

Protoplasts were isolated from *in vitro* shoot cultures of tomato as described (Shahin, 1985; Tan et al., 1987). A total of 4×10^7 protoplasts per sample were subjected to Polyethylene-glycol (PEG4000) mediated transformation (Negrutiu et al., 1987) with the following plasmids: (i) pK7FWG2 (Karimi et al., 2002) containing *Rep* from TYLCV (Genbank ID: FJ956702.1) fused to enhanced *GFP* (EGFP) (referred to as Rep-GFP), (ii) Rep-GFP + pJL-TRBO (Lindbo, 2007) containing tomato (*Sl*)*PCNA* fused to the FLAG tag at its N-terminus, referred to as FLAG-PCNA (positive control for interaction), and (iii) FLAG-PCNA as a negative control. Transfected protoplasts were incubated in Gamborg B5 (Duchefa Biochemie) liquid medium at 25°C overnight in dark conditions. Three independent protoplasts isolations and DNA transfections were performed on three different days. The next day the protoplasts were collected in 1.5 ml reaction vials by centrifugation (5 min at 85 g) and frozen at −80°C till further usage.

Protoplasts Protein Extraction and Immunoprecipitation

Protoplasts were defrosted and resuspended in 1 ml per 10^7 protoplasts of Triton X-buffer (20 mM Tris–HCl pH 7.5, 10 mM KCl, 10% glycerol, 1 mM DTT, 10 mM $MgCl_2$, 2 mM EDTA, 1% Triton X-100, 1 mM PMSF, and 1 mM NaF). Protoplast mixtures were incubated on ice for 30 min and sonicated twice for 15 s. NaCl 2M solution was added to the protoplast suspension at a final concentration of 420 mM and tubes were incubated on ice for 1 h with occasional mixing. All protein sample extracts were then centrifuged at 10,000*g* for 30 min at 4°C and the supernatant, containing the extracted proteins, was transferred into a fresh tube. Expression of FLAG-PCNA was confirmed with immunoblotting as previously described (Arroyo-Mateos et al., 2018). For mass spectrometry-based identification of the proteins that co-purify with Rep-GFP, 1 ml of total protein extract from each sample was incubated for 1 h with 25 µl (50% slurry) of GFP-Trap_M® beads (Chromotek) at 4°C. After incubation, the beads were captured with a magnetic rack and washed three times in 0.5 ml of washing buffer (10 mM Tris–HCl pH 7.5, 150 mM NaCl, 0.5 mM EDTA, 1 mM PMSF protease inhibitor). Antibodies used were anti-Flag (F7425; Sigma-Aldrich) and anti-GFP (3H9; Chromotek).

Tryptic Digestion of the Immunopurified Proteins

The affinity purified proteins were subjected to on-bead tryptic digestion. Briefly, the GFP-Trap_M beads were washed twice with 400 µl of 50 mM ammonium bicarbonate buffer pH 8 (ABC), after which the beads were resuspended in 10 µl 50 mM dithiothreitol (DTT) in 50 mM ABC and incubated at 60°C for 1 h. Subsequentely, 12 µl of 50 mM iodoacetamide in 50 mM ABC was added and the sample incubated at room temperature in the dark for 1 h. Then, 14 µl 50 mM cysteine in ABC was added and the bound proteins were digested overnight at 20°C after adding 1 µl of a Trypsin (Roche, sequencing grade) solution (0.5 µg/µl in 1 mM HCl). Peptide digestion was terminated by acidification to pH3 by adding 1 µl 10% trifluoroacetic acid. The tryptic peptides were concentrated and cleaned using home-made µColumns (Lu et al., 2011). These µColumns were prepared by stacking in a 200 µl tip two 3M™ Empore™ C18

extraction disks and 4 µl of a LiChroprep® RP-18 50% (Merck Millipor) slurry in methanol. The µColumns were washed with 100% methanol and equilibrated with 100 µl of 0.1% formic acid in water. Protein samples were added and eluted through the µColumns. The µColumns were washed with 0.1% formic acid in water and the bound peptides were eluted by adding 1:1 mixture of acetonitrile and 0.1% formic acid in water. The acetonitrile content of the samples was reduced by putting the samples in a centrifuge concentrator (Speed-Vac) at 45°C for 2 h and redissolved into 50 µl 1 ml/l formic acid in water.

Mass Spectrometry Analysis and Data Processing

Digested peptides were analyzed using a nano LC-MS/MS LTQ-Orbitrap XL (Thermo Fisher), as previously described (Gawehns et al., 2015). All tryptic digests were sequentially run as one batch of samples on the nLC-MS machine to minimize technical variation. The MaxQuant software 1.5.2.8 (Cox and Mann, 2008; Hubner et al., 2010) was used to analyze the raw data from the LTQ-Orbitrap (Thermo Fisher) for protein identification and label-free quantification (LFQ). The Uniprot proteome database of tomato (UP000004994) and an *in-house* made database of contaminants (Peng et al., 2012) were included in the Andromeda search engine (Cox et al., 2014). The mass spectrometry proteomics data have been deposited to the ProteomeXchange Consortium *via* the PRIDE (Vizcaino et al., 2016) partner repository with the dataset identifier PXD018011.

Data filtering from the MaxQuant output was carried out with Perseus 1.5.5.3 (http://www.perseus-framework.org). Only the LFQ values of the proteins that were identified with at least two tryptic peptides, of which one should be unique and one unmodified, were log10 transformed for further analysis. Proteins that showed a ΔLFQ (log10 LFQ in the sample – log10 LFQ in the control) equal or higher than the ΔLFQ of FLAG-PCNA (*internal control*) in at least one out of three biological replicates were annotated as 'putative interactors' of Rep and included for further analysis.

Computational Analysis

Gene ontology (GO) terms for biological process and cellular component were assigned to the co-purifying tomato proteins using Panther (Mi et al., 2017) and QuickGO (EMBL-EBI, https://www.ebi.ac.uk/QuickGO) tools. GO term enrichment was represented for every sample in a bar graph using Prism 7.0v (GraphPad) software. Venn diagrams were drawn using InteractiVenn (http://www.interactivenn.net/) (Heberle et al., 2015). A manually curated protein–protein interaction network was constructed with Cytoscape (Shannon et al., 2003). For that, the interaction network of every putative host interactor and the known Rep-interactors, as reported by Ruhel and Chakraborty (2019) were retrieved from the STRING protein database (https://string-db.org/). The resulting nodes (proteins) and edges (interactions) were arranged according to the force-directed layout. The protein sequence of the Arabidopsis gene model At4g28990 (closest Arabidopsis homologue of GRIEP1) was analyzed using the InterPro database (https://www.ebi.ac.uk/interpro/) to identify known protein domains in GRIEP1.

Construction of Clones Used for Confocal Microscopy

All molecular DNA cloning techniques were performed using standard methods using (Sambrook et al., 2001). The *E. coli* strain DH5α was used for subcloning. The CDS of *EF1A* (XM_004251106; Solyc11g069700.1.1), *Nucleolin-like 2* (NM_001319854.1; Solyc02g014310.2.1), *Rep-interacting protein 1* (XM_004239224; Solyc05g018340.2.1) and *THO complex subunit 4A* (a.k.a. *SlALY1*) (Bruhn et al., 1997) (NM_001347950.1; Solyc10g086400.1.1) were amplified from tomato cDNA by PCR using Phusion DNA polymerase (Thermo Fisher) and the primers listed in **Table S1** that contained *attB1* and *attB2* recombination sites for Gateway-directed cloning. The resulting PCR products were recombined with the Gateway vector pDONR207 (Thermo Fisher) using BP Clonase II (Thermo Fisher) and the resulting pENTR plasmids confirmed by DNA sequencing. The cDNA clones were then introduced into the destination vectors pGWB452 (Nakamura et al., 2010) and pDEST-SCYNE^{GW} (Gehl et al., 2009) using LR Clonase II (Thermo Fisher). All plasmids generated and used in this work are listed in **Table S2**.

Transient Expression in *N. benthamiana* by Agroinfiltration and Confocal Microscopy

For transient expression in *N. benthamiana* plants, the binary constructs were introduced in *Agrobacterium tumefaciens* GV3101, as previously described (Maio et al., 2019). Briefly, single colonies of *A. tumefaciens* were grown overnight to an OD_{600} of 0.8–1.5 in low salt (2.5 g/l NaCl) LB medium and resuspended in infiltration medium (1× MS [Murashige and Skoog] salts (Duchefa), 10 mM MES pH 5.6, 2% w/v sucrose, 200 µM acetosyringone) and incubated at room temperature for at least 2 h. Fully expanded leaves of 4-week old *N. benthamiana* plants were then syringe-infiltrated with these *A. tumefaciens* cell suspensions at an OD_{600} = 1 for all constructs. When two cultures were co-infiltrated for BiFC analysis, they were mixed at a ratio 1:1 to a final OD_{600} = 1. A. *tumefaciens* strain carrying the pBIN61 binary vector to express the P19 silencing suppressor (referred to as pBIN61:P19) of Tomato bushy stunt virus (TBSV) was added to every sample at a final OD_{600} = 0.5. Three days post-infiltration *N. benthamiana* leaf material was collected for microscopy. Subcellular localization of the GFP-tagged proteins and the reconstituted SCFP fluorophores was detected using a confocal laser scanning microscopy (Zeiss LSM510) with a c-Apochromat 40× 1.2 water-immersion Korr objective. The following beam/filter settings were used: GFP-excitation at 488 nm (argon laser), primary beam-splitting mirrors 405/488, secondary beam splitter 490 nm, band filter BP 505–550 nm; SCFP-excitation at 458 nm (argon laser), primary beam-splitting mirrors 458/514, secondary beam splitter 515 nm, band filter BP 470–500 nm. The experiments were repeated three times with a similar result.

Virus-Induced Gene Silencing in *N. benthamiana*

For virus-induced gene silencing (VIGS), PCR-amplicons of 300 nucleotides length were designed (https://vigs.solgenomics.net/) (Fernandez-Pozo et al., 2015) and amplified from *N. benthamiana* cDNA for the closest homologues of the tomato candidate genes *GRIEP1* (Nbv6.1trP35301) and *SlALY1* (Nbv6.1trP36214) using the primers given in **Table S2**. These fragments were cloned into the *SmaI* site of pYL156 (Liu et al., 2002). The resulting vectors TRV2::*NbALY1* and TRV2::*NbGRIEP1* were confirmed by sequencing and transformed to *A. tumefaciens* GV3101. The different VIGS constructs were mixed in a 1:1 ratio with *A. tumefaciens* strain containing pTRV1 at a final OD_{600} of 0.8 per construct, as described (Liu et al., 2002). This bacterial suspension was syringe-infiltrated in the two first true leaves of two-week old transgenic *N. benthamiana* plants that contain the *2IR-35S:GFP* viral reporter cassette for monitoring TYLCV (isolate Almeria; AJ489258) replication and systemic movement (Maio et al., 2019). As negative control, a TRV2 construct was used that targets the non-plant gene *E. coli* β-glucuronidase (TRV2::*GUS*) (Tameling and Baulcombe, 2007), as the latter clone is less aggressive than TRV2 without insert. The VIGS experiment was repeated twice with 14 plants per silencing construct.

Measurement of Viral Replication Activity of Rep in 2IR-GFP Plants

Two weeks post agroinoculation, one half of a fully expended systemic leaf was infiltrated with REP^{TYLCV}-RFP, while the other half was infiltrated with KtoA triple mutant of REP^{TYLCV}-RFP (K65A K69AK99A) at an OD_{600} of 1.0 (Maio et al., 2019). This latter KtoA triple mutant can no longer replicate the 2IR-GFP cassette (negative control). The replication efficiency of Rep of the viral 2IR-GFP cassette was then estimated indirectly using a radiometric method in which the ratio of RFP fluorescence (Rep levels) over the GFP fluorescence (GFP protein expression from extrachromosomal replisomes) was determined. To this end, in total eight leaf discs (each from a different plant) with a diameter of 5 mm were taken and placed in a 96-wells plate (Perkin-Elmer Optiplate™ 96) containing 100 µl double-distilled water three days post *A. tumefaciens* infiltration. Fluorescence was measured using microplate reader (BioTek Synergy™ H1 Hybrid multi-mode). GFP fluorescence was excited at 485 nm and the emission was measured at 528 nm (BP16 nm monochromator), while RFP fluorescence was excited at 555 nm and the emission measured at 583 nm (BP 16 nm monochromator). The data was compared by using a student t-test. The experiment was repeated twice with eight plants per silencing construct.

Gene Expression Analysis Using Real Time PCR

In order to quantify the transcript levels of *NbALY1* or *NbGRIEP1*, a total of 100 mg of systemic leaf tissue was collected from 4-week old *N. benthamiana* plants (2-week post TRV inoculation). Following tissue grinding (Qiagen Tissuelyser II bead mill), total RNA was extracted using TRIzol LS (Thermo Fisher). RNA concentrations were determined measuring the absorbance at 260 nm (A260) using a NanoDrop (Thermo Fisher). A total of 1 µg of RNA was used for cDNA synthesis using RevertAid H reverse transcriptase (Thermo Fisher) following the manufacturer's instructions. Real time PCR was performed with a QuantStudio™ 3 system (Thermo Fisher) using the EvaGreen kit (Biotium) according to the supplier's instructions. Melting curves were analyzed to ensure amplification specificity and absence of primer-dimer formation. Primer PCR efficiencies were determined using a serial dilution of a mixed cDNA sample (1:2, 1:4, 1:8 & 1:16) and the qPCR reactions were conducted in duplicate (technical replicate) for four samples (biological replicates). Water and no-template controls were used as negative controls for each primer set. Cycle threshold (Ct) values were calculated using the auto baseline function (Quant studio software). Duplicates for which the Ct value different more than 0.5 were not considered and removed from the analysis. Finally, relative gene expression levels were calculated using the obtained Ct values using qBase+ (Biogazelle, Belgium) applying a method that corrects for primer efficiencies. Finally, the gene expression data was normalized using the *N. benthamiana APR* as reference gene (Liu et al., 2012). The VIGS experiment was repeated three times with a similar result. The *2IR-GFP* extrachromosomical molecules (ECMs) were quantified as described previously (Maio et al., 2019). Primers for the ECMs and the internal reference gene, *25S rRNA*, are given in **Table S2**. The qPCR and data analyses were performed using qBase+ software as described above.

N. benthamiana Protein Extraction and Immunoblotting

Two leaf disks (approximately 50 mg) of *N. benthamiana* leaf material were harvested, snap frozen in liquid nitrogen and homogenized with plastic pestles. Laemmli buffer (0.1 M Tris pH 6.8, 20% glycerol, 4% SDS, 100 mM DTT, 0.001% Bromophenol blue) was added to each sample (100 µl of buffer per sample). Tubes were vortexed vigorously and heated for 10 min at 96°C. The extracts were then centrifugated at 14,000 rpm at 4°C for 5 min. A total of 10 µl of the protein extract was separated on 10% SDS-PAGE gels and subsequently transferred onto a PVDF membrane. Immunodetection of the proteins was performed according to standard protocols using anti-RFP antibody (Chromotek 6G6; 1:1,000) to detect the Rep-RFP fusion proteins, anti-GFP (Chromotek 3H9; 1:1,000) antibody for GFP and GFP-fusions as primary antibodies and anti-Rat (Pierce 31470; 1:10,000) or anti-Mouse (Pierce 31430; 1:10,000) as secondary antibodies. The labeled proteins were visualized using enhanced chemiluminescence (ECL, 0.1 M Tris–HCl pH 8.5, 1.25 mM luminol [Sigma-Aldrich 09253] in DMSO, 0.2 mM p-Coumaric acid [Sigma C9008] in DMSO, 0.01% H_2O_2) and detected using MXBE Kodak films (Carestream). Equal loading of the extracted proteins was confirmed by estimating the total amount of Rubisco in each sample using Ponceau S or Coomassie Brilliant Blue staining of the membrane.

RESULTS

Identification of Novel Tomato Proteins That Interact With TYLCV Rep

In order to identify novel host proteins that interact with TYLCV Rep, we isolated tomato protoplasts from *in vitro* cultured plants and transfected them with plasmid DNA to express Rep-GFP alone or in combination with FLAG-PCNA (**Figure 1**). PCNA was co-expressed together with Rep to have an internal positive control for a Rep interacting protein, but also to promote assembly of viral replisomes. Accumulation of Rep-GFP was visually inspected in every sample by using fluorescence microscopy prior to the affinity purification, while FLAG-PCNA accumulation was confirmed by immunoblotting (**Figure S1**). The total protein fraction was extracted from three experimental replicates and subjected to affinity purification using anti-GFP resin followed by tryptic digestion in combination with a nano LC–MS/MS analysis. Identification and quantification of the (co)purifying proteins was then performed using MaxQuant. Rep was readily detected in every sample expressing Rep, while PCNA was enriched in the Rep-PCNA samples in comparison to the negative control (PCNA alone) in two out of three biological replicates. In total we identified 427 candidate interactors. To obtain a set of high-confidence interacting proteins, we used as selection criterion that their abundance after the pull-down should be similar or higher than PCNA in one of the replicates. This yielded a total of 54 tomato proteins (**Table 1**): 27 proteins in the sample expressing Rep-GFP alone, 40 in the sample in which Rep-GFP was expressed together with FLAG-PCNA, and 13 proteins were in present in both samples (**Figure 2A**). For eight of these interacting proteins, a close homolog was previously identified in a related pull-down experiment for TYLCV Rep in *N. benthamiana* (Wang et al., 2017a) (**Figure 2B** and **Table 2**).

Functional Annotation and Protein Network Analysis of the Rep Interactome

In order to gain insight into the cellular processes affected by overexpression of TYLCV Rep in tomato protoplasts, a gene ontology (GO) analysis was conducted assigning functional categories to each interactor. The GO terms "Biological process" and "Cellular component" were assigned and the proportion of plant proteins per GO category (%) was calculated (**Table 3**). The largest GO category for "Biological process" was formed by proteins belonging to "RNA metabolism", in particular the subclasses "involved in spliceosome and ribosome assembly", "regulation of RNA polymerase" and "mRNA/rRNA processing" (**Figure 2C**). These categories were followed by "protein metabolic processes", "photosynthesis', "metabolic processes", "translation" and "cellular component organization". Only two GO categories were significantly overrepresented (p-value <0.05), i.e. "RNA metabolic processes" and "metabolic processes". In total 30% of the identified proteins was assigned to be nucleus based on their annotation (**Figure 2D**). In order to visualize the Rep-interactome, we plotted the 54 tomato proteins in a protein interaction network (**Figure 2E**) with the nodes

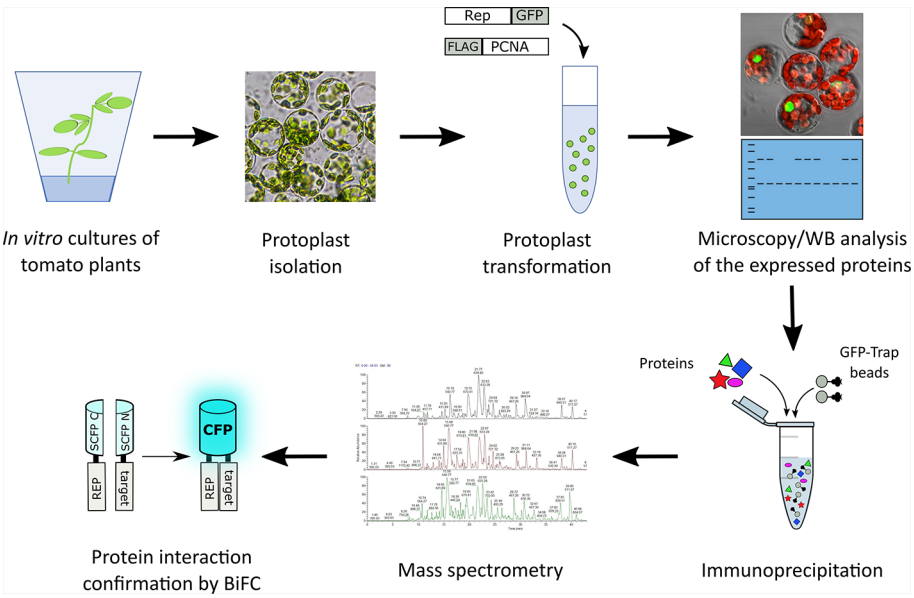

FIGURE 1 | Schematic representation of the strategy followed to identify novel interactors of TYLCV Rep using affinity purification followed by mass spectrometry. Rep fused to GFP was expressed in the presence and absence of FLAG tagged PCNA in tomato protoplasts. The next day, the transfected protoplasts were inspected for a GFP signal using fluorescence microscopy and the total protein fraction was extracted, analyzed for the presence of the overexpressed proteins using immunoblotting (WB) and then subjected to affinity purification using anti-GFP resin (in three independent experiments). Co-purifying proteins were identified after tryptic digestion by tandem mass spectrometry (MS/MS). For a subset of interactors their interaction with Rep was confirmed using bimolecular fluorescence complementation (BiFC). The tryptic digests were prepared in parallel and the resulting peptide samples were analyzed as one batch of runs on the LC-MS.

TABLE 1 | List of the putative interactors of Rep identified by affinity purifications/MS analysis. Proteins in bold were selected for further protein–protein interaction studies.

Protein ID (TrEMBL)	Functional gene description/annotation	Rep[1]	Rep-PCNA[2]
K4CJ02	Photosystem I reaction center subunit		+
K4DB32	Histone 2A	+	
Q2MIA1	P700 chlorophyll a		+
K4DG37	Glycosyltransferase	+	
K4B6B8	**Nucleolin-like**		+
K4ATJ4	Peptidylin-prolyl cis-trans isomerase	+	
K4D6D0	Putative Prohibitin-3		+
K4CVT4	MAR-binding protein		+
K4BCZ4	Protein CROWDED NUCLEI 4		+
K4BFN2	Small nuclear ribonucleoprotein Sm D3		+
K4DAC6	**Elongation factor 1-alpha**		+
P12372	Photosystem I reaction center subunit II		+
K4BPK3	Actin-41		+
K4B256	Glycine-rich RNA-binding protein RZ1A	+	
K4D472	**THO complex subunit 4A, *S*/ALY1**		+
P26300	Enolase		+
K4C2T0	Chlorophyll a-b binding protein		+
K4CFD4	Aconitate hydratase		+
K4DHM2	Serine hydroxymethyltransferase	+	
K4CV90	Small nuclear ribonucleoprotein Sm D2		+
K4BXD4	Serine/threonine-protein phosphatase	+	+
K4B375	Prosequence protease 1		+
K4D383	NDR1/HIN1-like protein	+	
K4BTU2	Serine/arginine-rich splicing factor SC35	+	
K4AZV6	Rhodanese-like domain-containing protein 4		+
K4C9J5	Histone H2B	+	+
K4CAF0	Photosystem I reaction center subunit XI		+
K4BJL2	50S ribosomal protein L29	+	+
K4ATF8	Pre-mRNA cleavage factor Im		+
K4C144	Malic enzyme		+
K4BRF6	Putative methyltransferase	+	
P49212	60S ribosomal protein L37	+	+
K4BA51	H/ACA ribonucleoprotein complex subunit 4		+
K4BZ89	**RNA-binding protein EWS-like, GRIEP1**	+	
K4BBI1	50S ribosomal protein L12	+	
K4AYG3	50S ribosomal protein L1	+	+
P54776	26S proteasome regulatory subunit 6A		+
K4CAT6	Small nuclear ribonucleoprotein Sm D1		+
K4CUW3	60S ribosomal protein L23	+	+
K4C4X4	60S ribosomal protein L36	+	+
K4BA70	40S ribosomal protein S15		+
K4B3P9	Fructose-bisphosphate aldolase	+	
K4D576	Protein RNA-directed DNA methylation 3	+	+
K4AYP1	Dynamin-related protein 1E		+
Q2MIB8	30S ribosomal protein S16	+	+
K4CED0	Uncharacterized protein		+
K4DBB5	Zinc finger CCCH domain-containing protein	+	+
P07370	Chlorophyll a-b protein 1B		+
K4CX06	Ribosome biogenesis protein NSA2 homolog	+	
K4CAC1	26S proteasome regulatory subunit 6B	+	+
P20721	Low-temperature-induced cysteine proteinase	+	+
K4CFR0	26S proteasome non-ATPase regulatory subunit 2	+	
K4DG14	ATP synthase delta chain	+	
Q38MV0	Tubulin beta chain	+	+

[1]*Found in the samples expressing REP-GFP alone.*
[2]*Found in the samples expressing REP-GFP together with PCNA.*

representing (i) the newly identified host proteins (green and yellow), (ii) 16 Rep-interactors derived from previous studies (pink) (reviewed by Ruhel and Chakraborty, 2019) and (iii) Rep (blue). In total, seventy known interactions with Rep (Ruhel and Chakraborty, 2019) were included in this protein network (blue edges and dotted edges) and a total of 148 plant protein interactions (grey edges) were retrieved from the STRING database (**Table S3**). This network contained two major clusters. The first cluster comprises (mostly) known Rep interactors involved in DNA metabolism, such as DNA replication and repair, while the second cluster is primarily formed by newly-identified candidates implicated in RNA metabolic processes, which hints to that Rep potentially regulates RNA biogenesis in an unknown manner.

Examples of Novel Rep Interactors Linked to Viral DNA Replication and RNA Metabolic Processes

Our list of TYLCV Rep interactors contained several proteins linked to DNA replication and pathogenesis. For example, Elongation factor 1-alpha (EF1A), found in the sample Rep-PCNA, participates in cellular functions like translation, nuclear export, transcription but also apoptosis in virus-infected cells (reviewed in Sasikumar et al., 2012). EF1A is also involved in the propagation of certain positive-strand RNA viruses, as it has been found to interact with viral RNA and certain virus-encoded RNA-dependent RNA polymerases (Abbas et al., 2015).

Another putative novel Rep interactor detected in the AP-MS with Rep-PCNA is Nucleolin-like 2, a major nucleolar protein that regulates the rDNA chromatin structure, rRNA gene expression, pre-rRNA processing and assembly of ribosome particles (Durut and Sáez-Vásquez, 2015). Interestingly, Nucleolin interacts also with PCNA and the Replication protein A 32 (RPA32) during replication stress in human cell lines (Kawamura et al., 2019). These authors also provided evidence that Nucleolin is recruited to damaged replication forks and that recruitment of Nucleolin controls the activation of homologous recombination, a process that is also promoted by geminiviruses in infected cells (Richter et al., 2014). These observations argue for a functional link between Rep and Nucleolin-like 2. Possibly related, the coat protein (CP) of TYLCV was shown to be recruited to the nucleolus in the absence of the virus, while in the presence of the virus it was recruited to discrete nuclear foci (Rojas et al., 2001; Wang et al., 2017b). Expression of Rep was already sufficient to exclude CP from the nucleolus, but its localization in foci was only seen during a TYLCV infection (Wang et al., 2017b). In fact, a plethora of animal and plant viruses but also virus-encoded proteins reside in the nucleolus where they interact with nucleolar proteins and several viral proteins have been shown to co-localize with, reorganize and re-distribute nucleolar proteins such as Nucleolin (Hiscox, 2002; Kim et al., 2004; Chaudhry et al., 2018).

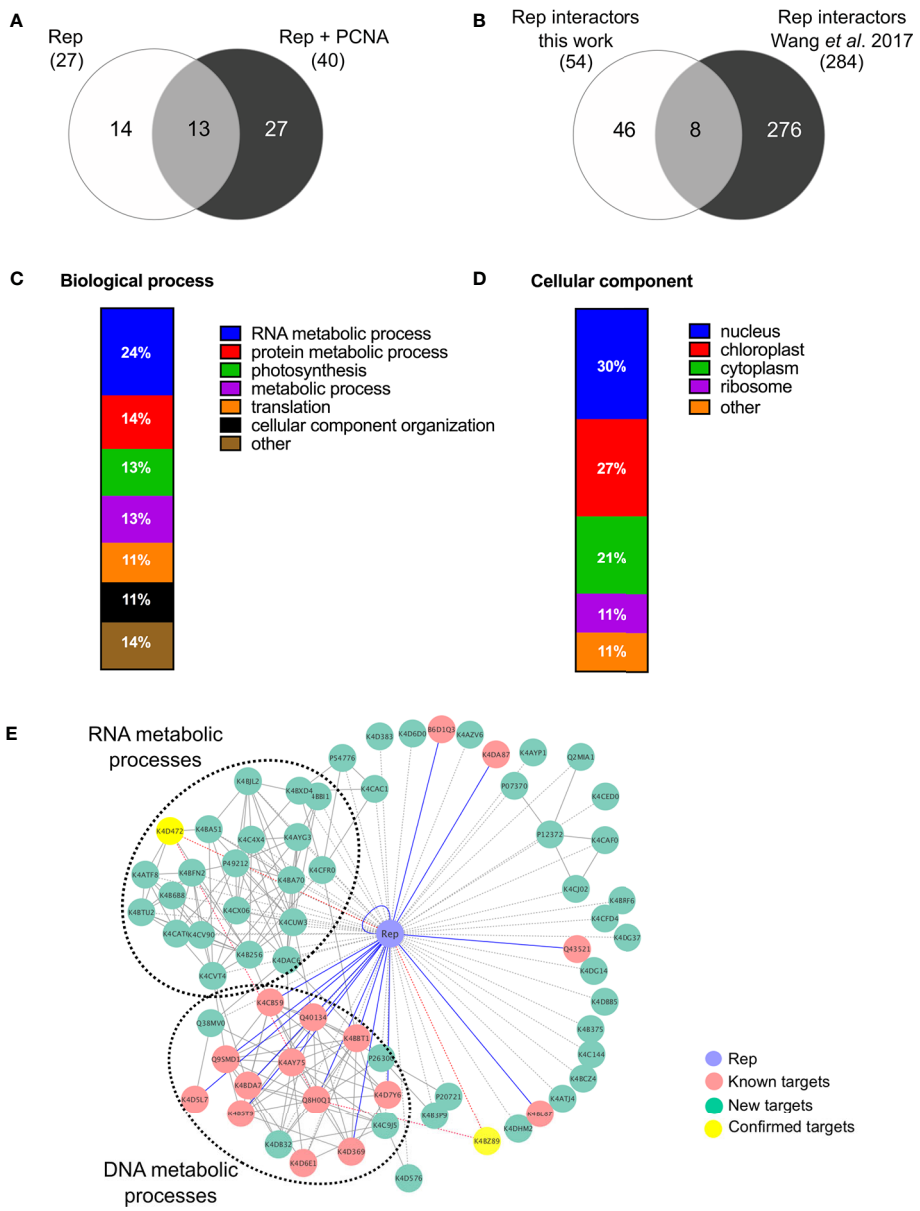

FIGURE 2 | Functional annotation of the tomato interactomes of 'Rep' and 'Rep+PCNA'. **(A)** Venn diagram depicting the number of interacting proteins that were enriched in the samples expressing 'Rep' alone and/or 'Rep + PCNA'. **(B)** Venn diagram representing the number of Rep interactors that overlapped with a similar approach taken by Wang et al. (2017a), who purified TYLCV Rep from *N. benthamiana* cell extracts. **(C)** Bar chart depicting the proportion of proteins (%) in a subclass of the GO term "Biological process" for the tomato interactors of Rep, combining the two lists of interactors. **(D)** Bar chart showing the proportion of proteins (%) in a subclass of the GO term "Cellular component", combining the two lists of interactors. **(E)** Protein network of the Rep tomato interactome identified in this work (green nodes) and retrieved from the literature (pink nodes). Yellow nodes represent targets whose interaction with Rep was confirmed in this work. Blue lines, known interactions with host proteins; dotted lines, putative interactions with host proteins; red lines, novel confirmed interactions; grey solid lines, protein-protein interactions between plant proteins.

A third interactor again coming from the list of proteins co-purifying with Rep-PCNA and implicated in host-virus interactions is the THO subunit 4A, which is part of the THO core complex of the TREX (TRanscription-EXport) complex. This complex is conserved across eukaryotes and is linked to nuclear export of mRNA (Heath et al., 2016; Sørensen et al., 2017). The THO/TREX complex is targeted by various viral proteins to redirect and control viral mRNA translocation (Schneider and Wolff, 2009; Yarbrough et al., 2014). The closest Arabidopsis homologue of the tomato interactor here identified (THO subunit 4A) is the mRNA export adaptor protein ALY1 (AT5G59950). Once bound to mRNA, the ALY proteins interact with the nuclear export receptor, which then facilitates export of the bound mRNA. Interestingly,

TABLE 2 | List of tomato interactors of TYLCV Rep here found that overlap with the study by Wang et al. (2017a).

S. lycopersicum ID (TrEMBL ID); this study	*N. benthamiana* gene model ID (Wang et al.)	Protein annotation
K4CJ02	NbS00018180g0004.1	Photosystem I reaction center subunit
K4BA70	NbS00016568g0015.1	40S ribosomal protein S15
K4BPK3	NbS00041237g0007.1	Actin-41
K4CFD4	NbS00008022g0007.1	Aconitate hydratase
K4CFR0	NbS00013228g0016.1	26S proteasome non-ATPase regulatory subunit 2
K4D6D0	NbS00032991g0022.1	Putative Prohibitin-3
K4DHM2	NbS00012020g0003.1	Serine hydroxymethyltransferase
P20721	NbS00040506g0007.1	Low-temperature-induced cysteine proteinase

TABLE 3 | List of gene ontology classes assigned to the identified tomato proteins.

GO ID	Biological process	
	GO term	**Protein identifiers (TrEMBL ID)**
GO:0016070	RNA metabolic processes	K4CVT4, K4CAT6, K4BFN2, K4CV90, K4BZ89, K4D576, K4ATF8, K4CX06, K4AYG3, K4BA51, K4BTU2, K4D472, K4DBB5
GO:0019538	protein metabolic processes	K4B375, K4CFR0, P54776, K4CAC1, P20721, K4BXD4, K4DAC6
GO:0015979	photosynthesis	K4CJ02, K4CAF0, P12372, Q2MIA1, A0A0J9YZP9, P07370, K4DG14
GO:0008152	metabolic processes	K4DG37, K4CFD4, K4C144, K4B3P9, P26300, K4DHM2, K4AZV6
GO:0006412	translation	P49212, K4BJL2, Q2MIB8, K4CUW3, K4BBI1, K4C4X4
GO:0016043	cellular component organization	K4BPK3, K4BCZ4, K4BA70, K4B6B8, K4AYP1, Q38MV0
GO:0006259	DNA metabolic process	K4CED0, K4DB32, K4C9J5
_	Other	K4ATJ4, K4BRF6, K4D383, K4D6D0, K4B256
GO ID	**Cellular component**	
	GO term	**Protein identifiers (TrEMBL ID)**
GO:0005840	ribosome	K4BJL2, K4BBI1, K4BA70, K4CUW3, P49212, K4C4X4,
GO:0005634	nucleus	K4CED0, K4CFR0, K4C9J5, K4ATF8, K4D576, K4CAT6, K4BFN2, K4CV90, K4BZ89, K4BTU2, K4B6B8, K4B256, K4BXD4, K4BCZ4, K4CX06, K4CVT4, K4DB32
GO:0005737	cytoplasm	K4AYP1, K4BRF6, K4DAC6, Q38MV0, P26300, K4BA51, K4CFD4, P20721, K4DHM2, K4B6B8, K4B256, K4BXD4
GO:0009507	chloroplast	K4C144, Q2MIB8, K4AYG3, P07370, K4DG14, A0A0J9YZP9, Q2MIA1, K4CJ02, P12372, K4B375, K4B3P9, K4ATJ4, K4D472, K4BCZ4, P20721
_	Other	K4DBB5, K4AZV6, K4D383, K4D6D0, K4CAF0,K4DHM2

compromised *ALY1* gene function in Arabidopsis results in loss of RNA-dependent DNA methylation (RdDM) due to deficient export of *Argonaute6* mRNA (Choudury et al., 2019). In line with this connection, Rodríguez-Negrete and co-workers (2013) demonstrated that TYLCSV Rep displays transcriptional gene silencing (TGS) suppressor activity by interfering with the host DNA methylation machinery during infection. In particular, Rep down regulates the transcript levels of key enzymes that maintain this modification, namely the DNA methyltransferases *MET1* and *CMT3*. Arguably, TYLCV Rep might thus inhibit tomato ALY1 function to modulate RdDM activity.

Finally, our list of candidate interactors that interacted with Rep in the absence of PCNA overexpression contained an uncharacterized protein, here called Geminivirus Rep interacting EWS-like protein 1 (GRIEP1), that shows sequence homology to the human RNA-binding protein EWS (Ewing Sarcoma protein). This mammalian protein acts as transcriptional repressor that regulates pri-miRNA processing and plays a role in tumorigenic processes (Ohno et al., 1994; Ouyang et al., 2017). The closest homolog of GRIEP1 in Arabidopsis is At4g28990, a predicted 395 amino acid protein with a predicted Zinc finger domain of the RanBP2-type that groups with the multifunctional TET protein family (TAF15/EWS/TLS; Interpro IPR034870) (Law et al., 2006). This protein family is implicated in transcription, (alternative) splicing, mRNA transport but also DNA repair (Kovar, 2011). To our knowledge this protein has not been studied in any plant species yet. Based on their potential role on DNA replication and/or Rep activity, we selected these four proteins to corroborate their interaction *in planta* (bold in **Table 1**).

Confirmation of the Interaction Between Rep and the Putative Interactors

To assess in an independent assay the specificity of the interactions, we used bimolecular fluorescence complementation (BiFC), as it also provides information on where the interaction occurs in the cell. First, we assessed their subcellular localization pattern in *N. benthamiana* expressing GFP-labelled variants of these proteins. As expected, GFP-EF1A localized to the cytoplasm, while GFP-Nucleolin-like 2 localized exclusively to the nucleolus (**Figure 3A**). *Sl*ALY1 was uniformly distributed in the nucleoplasm with occasionally some small nuclear speckles. GRIEP1 resided, however, in large nuclear bodies (or aggregates) of unknown function or origin. Using immunoblotting, we confirmed that these GFP-fusions accumulated at the expected protein mass in *N. benthamiana* (**Figure S2**). We then fused the N-terminal half of the super Cyan fluorescent protein ($SCFP^N$) to the N-terminus of the candidate proteins and the resulting fusion proteins were expressed in *N. benthamiana* epidermal cells together with Rep or PCNA fused to the C-terminal half of SCFP ($SCFP^C$) (**Figure 3B**). As negative control, the $SCFP^N$ fusion proteins were co-expressed with a non-plant protein ($SCFP^C$-tagged β-Glucuronidase from *E. coli*). We detected no BiFC signal for any of these four interactors in combination with GUS in any cellular compartment. For $SCFP^N$-EF1A and $SCFP^N$-Nucleolin-like 2, only a faint SCFP signal was observed in some nuclei in combination with TYLCV Rep or

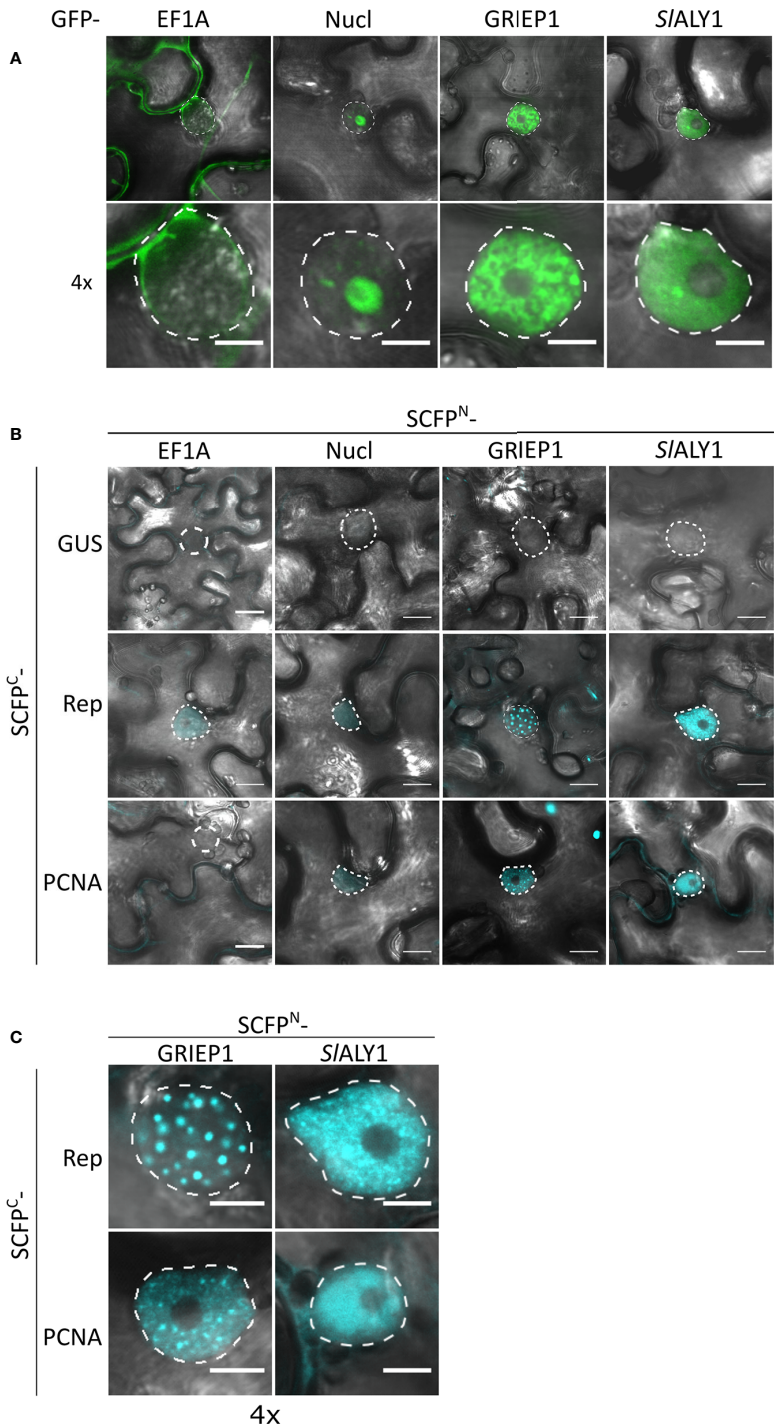

FIGURE 3 | Cellular localization and BiFC protein interaction assay of the Rep-interacting proteins EF1A, Nucleolin-like 2, GRIEP1 and THO. **(A)** Subcellular localization of GFP-tagged tomato EF1A, Nucleolin-like 2 (Nucl), GRIEP1 and *Sl*ALY1 proteins in *N. benthamiana* epidermal cells upon transient overexpression. Image shown represents a typical cell (top) and a 4× zoom showing only its nucleus (bottom). **(B)** In a BiFC assay, EF1A and Nucleolin-like 2 do not seem to interact with TYLCV Rep nor PCNA since only a faint background fluorescence signal was detected, whereas GRIEP1 and *Sl*ALY1 show strong reconstitution of SCFP fluorophore in combination with Rep and PCNA in nuclei of the transfected cells. **(C)** 4× zoom of the nuclei of the positive BiFC interaction pairs shown in **(B)**. Scale bar is 5 μm for **(A, C)** and 20 μm for **(B)**. Dotted lines outline the nucleus. These experiments were repeated three times independently; for each combination, a minimum of 50 cells was analyzed in each experiment.

PCNA. In contrast, the BiFC couple GRIEP1-Rep showed a strong and specific CFP fluorescence signal in distinct (large) nuclear bodies (NBs) and, to a minor extent, in the cytoplasm. Also, the combination of GRIEP1 and PCNA yielded a strong CFP fluorescence signal in the nucleus with some speckles and a weaker fluorescence signal in the cytoplasm (**Figures 3B, C**). Finally, *Sl*ALY1 interacted with Rep in the nucleoplasm and with PCNA in both the cytoplasm and nucleoplasm. These BiFC experiments thus corroborate our MS data that GRIEP1 and *Sl*ALY1 interact specifically and directly with Rep.

Next, we used VIGS to assess whether reduced transcript levels of these two confirmed Rep-interactors (GRIEP1 and *Sl*ALY) would alter DNA replication activity of Rep. To this end, we took advantage of *N. benthamiana* expressing a *2IR-GFP* reporter cassette (Maio et al., 2019), which allows monitoring of viral replication *in situ* as a result of TYLCV Rep expressio,. The VIGS constructs caused indeed effective gene silencing of *SlALY1* and *GRIEP1* without negatively impacting the plant development (**Figures S3A, B**). Two weeks post TRV inoculation, Rep-RFP was transiently expressed in a fully expanded leaf and 3 days later replication of the viral reporter was (indirectly) quantified by comparing the signal intensities of the GFP and RFP fluorescence (**Figure S3C**). Plants silenced for *GRIEP1* or *SlALY1* did not exhibit any reduced Rep replication activity, as measured either by accumulation extrachromosomal circular DNA molecules (ECMs) that derive from the *2IR-GFP* cassette or GFP fluorescence (**Figures S3E, F**). In fact, silencing of *GRIEP1* did significantly increase ECM accumulation compared to GUS silenced plants (p-value = 0.0137), and silencing of *ALY1* resulted in significantly increased GFP intensity (nearly 2.5-fold increase). These data thus argue that both *GRIEP1* and *ALY1* might act as inhibitors of Rep DNA replication activity, but we cannot exclude that they impact functions of Rep other than replication activity. Future work should reveal if overexpression of GRIEP1 and ALY1 can repress Rep activity.

DISCUSSION

This work describes an AP-MS proteomics approach to identify novel host proteins that (in)directly interact with TYLCV Rep and to explore their role for geminivirus replication. This yielded 54 putative interactors of TYLCV Rep of which 40 were detected in cells overexpressing Rep together with tomato PCNA and two were confirmed to interact with both Rep and PCNA in the BiFC assay. The majority of the interactors are involved in RNA biogenesis, such as spliceosomal complex assembly, regulation of DNA-dependent RNA polymerase, rRNA expression and maturation and RNA binding, or in protein metabolic processes like catabolic activity, enzyme regulation and proteasome complex. These findings align in part with the proteomics results obtained by Wang and co-workers (2017a), who found that their list of TYLCV Rep interactors in *N. benthamiana* was enriched for the GO terms belonging to 'protein catabolic processes' but not for 'RNA metabolism'. Moreover, for eight of the Rep interactors here identified a close homolog was found to interact with TYLCV Rep in *N. benthamiana* (Wang et al., 2017a). Several arguments support the validity of our findings. First, we were able to specifically co-purify PCNA with Rep in two out of three of the independent affinity purifications compared to the negative control, demonstrating that the pulldown conditions were suitable to identify interactors of Rep. In addition, some of the AP-MS hits found were previously found to interact with Rep, e.g. the Histones 2A and 2B (Kong and Hanley-Bowdoin, 2002). Second, a substantial proportion of the putative Rep-interactors were predicted to be nuclear localized *in silico*. This agrees with the known subcellular localization of Rep and the viral replisome (Kushwaha et al., 2017; Maio et al., 2019). Third, we were able to confirm the interaction between Rep and two selected candidates *in planta* using the BiFC system and to detect formation of this complex in the nucleus. These two proteins also interacted with PCNA in our BiFC, suggesting that they might be part of viral replisomes or transiently interact with them. GRIEP1 is apparently not required for the Rep-mediated viral DNA replication activity, as the latter remained unchanged in *GRIEP1*-silenced plants. As well, it was not possible from our experiment to unambiguously determine whether Rep activity was altered as a result of *SlALY1*-silencing in *N. benthamiana*. Future studies should reveal if this latter interaction is really involved in viral replication or suppression of transcriptional gene silencing, as reported for other viral proteins (Xu et al., 2020).

Despite the identification of novel interactors of TYLCV Rep in tomato, several limitations apply to our approach. First, we also detected chloroplastic proteins implicated in photosynthesis and proteins involved in ribosome assembly and biogenesis. As a connection is lacking between Rep and photosynthesis and given the difference in compartmentalization of these processes, these proteins likely represent false positives. In fact, photosynthesis-related and ribosomal proteins are highly abundant plant proteins and as such common contaminants picked up in proteomics methods such as AP-MS (Smaczniak et al., 2012). At the same time, many true interactors could easily have been missed due to the stringency of our selection criterium, low protein levels in non-dividing mesophyll cells, weak or transient interactions with Rep or the presence of the tag on Rep, which all could prevent detection of protein-protein interactions. The identified host proteins may also indirectly bind to TYLCV Rep. For example, for Elongation factor 1A and Nucleolin-like 2, we were not able to confirm their interaction using BiFC. This notion of an indirect interaction is corroborated by the observation that, in our interaction network, EF1A is connected to two known interactors of Rep, Ubiquitin conjugation enzyme 2 (UBC2) and Histone 3 (H3). The last aspect to consider is that our experimental results derive from the analysis of epidermal tomato protoplasts that express Rep in the absence of a viral infection. To obtain a more comprehensive picture of the host proteins that interact with Rep, the interactions should also be studied in the context of a virus-infection in phloem cells.

Interestingly, two RNA-binding proteins were confirmed as interacting proteins of both Rep and PCNA. The first one, GRIEP1, is an unknown conserved protein with an EWS-like RNA-binding protein that contains a Zinc finger domain of the RanBP2 type. Interestingly, in Arabidopsis *GRIEP1* is mostly expressed in the shoot apex and floral tissues (data available on ePlant, http://bar.utoronto.ca/eplant/), where meristematic cells are dividing, suggesting that the Arabidopsis homolog has a potential role in cell division or differentiation. Moreover, the BiFC couple between Rep and this EWS-like protein resided in nuclear bodies (NBs). We reported previously that the BiFC pair Rep-SCE1 (SUMO E2 conjugating enzyme 1) also aggregates in NBs (Maio et al., 2019). Co-localization studies with marker proteins of different NBs should elucidate the nature and biological function of these different NBs.

The other confirmed interactor is a subunit of the THO complex, *Sl*ALY1. The biological function of this THO/TREX complex is well characterized in eukaryotes, where it is recruited to nascent mRNA, where it connects transcriptional elongation to export of mature mRNA (Jimeno et al., 2002; Strässer et al., 2002). This complex is also essential for the nuclear export of the Kaposi's sarcoma-associated herpes virus mRNAs and for viral DNA replication (Boyne et al., 2008). In plants, the THO/TREX complex has been shown to influence the production of trans-acting small interfering RNAs (Yelina et al., 2010) and a component of this complex appears to be involved in plant disease resistance against powdery mildew pathogen (Pan et al., 2012). As Rep is known to act as suppressor of RNA silencing (Liu et al., 2014), additional studies are needed to elucidate the mechanism and biological consequence of this Rep-THO/TREX interaction.

DATA AVAILABILITY STATEMENT

The mass spectrometry proteomics data have been deposited to the ProteomeXchange Consortium *via* the PRIDE (Vizcaino et al., 2016) partner repository with the dataset identifier PXD018011.

AUTHOR CONTRIBUTIONS

FM, HB, and MP designed the experiments. FM performed the protoplast isolations and transfections, and prepared the protein samples for nLC-MS/MS measurements. SB performed the nLC-MS/MS measurements. FM and SB analyzed the MS/MS data. FM, TH, MW, and MA-M performed the cloning, agroinfiltration, microscopy analysis, silencing, and qPCR analysis. FM, HB, and MP wrote the manuscript. All authors contributed to the article and approved the submitted version.

FUNDING

The Topsector T&U program Better Plants for Demands (grant 1409-036 to HB), including the partnering breeding companies, supported this work. FM was financially supported by Keygene N.V. (The Netherlands).

ACKNOWLEDGMENTS

We are grateful to L. Tikovsky and H. Lemereis for taking care of our plants; LCAM-FNWI (Molecular Cytology, SILS, University of Amsterdam) for maintenance and support with confocal microscopy. We thank R. Sevenier (Keygene N.V.) for the protoplast isolation and transfection protocol; M. de Vos (Keygene N.V.) for helping with the MS analysis; F. de Lamo for critical review of the manuscript. We thank E. Bejarano (Univeristy of Malaga), D. Baulcome (University of Cambridge, UK), J. Kudla (WWU Muenster, Germany), T. Nagakawa (Shimane University, Japan), J Lindbo for sharing plasmids.

SUPPLEMENTARY MATERIAL

The Supplementary Material for this article can be found online at: https://www.frontiersin.org/articles/10.3389/fpls.2020.01069/full#supplementary-material

REFERENCES

Abbas, W., Kumar, A., and Herbein, G. (2015). The eEF1A Proteins: At the crossroads of oncogenesis, apoptosis, and viral infections. *Front. Oncol.* 5, 75. doi: 10.3389/fonc.2015.00075

Arroyo-Mateos, M., Sabarit, B., Maio, F., Sánchez-Durán, M. A., Rosas-Díaz, T., Prins, M., et al. (2018). Geminivirus Replication Protein impairs SUMO Conjugation of PCNA at two acceptor sites. *J. Virol.* 92, e00611–e00618. doi: 10.1101/305789

Bagewadi, B., Chen, S., Lal, S. K., Choudhury, N. R., and Mukherjee, S. K. (2004). PCNA interacts with Indian mung bean yellow mosaic virus rep and downregulates Rep activity. *J. Virol.* 78, 11890–11903. doi: 10.1128/JVI.78.21.11890-11903.2004

Belabess, Z., Peterschmitt, M., Granier, M., Tahiri, A., Blenzar, A., and Urbino, C. (2016). The non-canonical tomato yellow leaf curl virus recombinant that displaced its parental viruses in southern Morocco exhibits a high selective advantage in experimental conditions. *J. Gen. Virol.* 97, 3433–3445. doi: 10.1099/jgv.0.000633

Boyne, J. R., Colgan, K. J., and Whitehouse, A. (2008). Recruitment of the complete hTREX Complex is required for Kaposi's Sarcoma-Associated Herpesvirus intronless mRNA Nuclear Export and vVirus replication. *PLoS Pathog.* 4, e1000194. doi: 10.1371/journal.ppat.1000194

Bruhn, L., Munnerlyn, A., and Grosschedl, R. (1997). ALY, a context-dependent coactivator of LEF-1 and AML-1, is required for TCRalpha enhancer function. *Genes Dev.* 11, 640–653. doi: 10.1101/gad.11.5.640

Butterbach, P., Verlaan, M. G., Dullemans, A., Lohuis, D., Visser, R. G. F., Bai, Y., et al. (2014). Tomato yellow leaf curl virus resistance by *Ty-1* involves increased cytosine methylation of viral genomes and is compromised by cucumber mosaic virus infection. *Proc. Natl. Acad. Sci. U. S. A.* 111, 12942–12947. doi: 10.1073/pnas.1400894111

Caro, M., Verlaan, M. G., Julián, O., Finkers, R., Wolters, A. M. A., Hutton, S. F., et al. (2015). Assessing the genetic variation of *Ty-1* and *Ty-3* alleles conferring resistance to tomato yellow leaf curl virus in a broad tomato germplasm. *Mol. Breed.* 35, 132. doi: 10.1007/s11032-015-0329-y

Castillo, A. G., Collinet, D., Deret, S., Kashoggi, A., and Bejarano, E. R. (2003). Dual interaction of plant PCNA with geminivirus replication accessory protein

(Ren) and viral replication protein (Rep). *Virology* 312, 381–394. doi: 10.1016/S0042-6822(03)00234-4

Castillo, A. G., Kong, L. J., Hanley-Bowdoin, L., and Bejarano, E. R. (2004). Interaction between a geminivirus replication protein and the plant sumoylation system. *J. Virol.* 78, 2758–2769. doi: 10.1128/JVI.78.6.2758-2769.2004

Chaudhry, U., Malik, D. A., Saleem, N., and Malik, M. T. (2018). Nucleolin: Role in Bacterial and Viral Infections. *EC Microbiol.* 14, 631–640.

Choe, K. N., and Moldovan, G. L. (2017). Forging Ahead through Darkness: PCNA, Still the Principal Conductor at the Replication Fork. *Mol. Cell* 65, 380–392. doi: 10.1016/j.molcel.2016.12.020

Choudury, S. G., Shahid, S., Cuerda-Gil, D., Panda, K., Cullen, A., Ashraf, Q., et al. (2019). The RNA export factor ALY1 enables genome-wide RNA-directed DNA methylation. *Plant Cell* 31, 759–774. doi: 10.1105/tpc.18.00624

Cox, J., and Mann, M. (2008). MaxQuant enables high peptide identification rates, individualized p.p.b.-range mass accuracies and proteome-wide protein quantification. *Nat. Biotechnol.* 26, 1367–1372. doi: 10.1038/nbt.1511

Cox, J., Hein, M. Y., Luber, C. A., Paron, I., Nagaraj, N., and Mann, M. (2014). Accurate Proteome-wide Label-free Quantification by Delayed Normalization and Maximal Peptide Ratio Extraction, Termed MaxLFQ. *Mol. Cell Proteomics* 13, 2513–2526. doi: 10.1074/mcp.M113.031591

Dunham, W. H., Mullin, M., and Gingras, A. C. (2012). Affinity-purification coupled to mass spectrometry: Basic principles and strategies. *Proteomics* 12, 1576–1590. doi: 10.1002/pmic.201100523

Durut, N., and Sáez-Vásquez, J. (2015). Nucleolin: dual roles in rDNA chromatin transcription. *Gene* 556, 7–12. doi: 10.1016/j.gene.2014.09.023

Eagle, P. A., Orozco, B. M., and Hanley-Bowdoin, L. (1994). A DNA sequence required for geminivirus replication also mediates transcriptional regulation. *Plant Cell* 6, 1157–1170. doi: 10.1105/tpc.6.8.1157

Ehrnsberger, H. F., Grasser, M., and Grasser, K. D. (2019). Nucleocytosolic mRNA transport in plants: export factors and their influence on growth and development. *J. Exp. Bot.* 70, 3757–3763. doi: 10.1093/jxb/erz173

Fernandez-Pozo, N., Rosli, H. G., Martin, G. B., and Mueller, L. A. (2015). The SGN VIGS Tool: User-Friendly Software to Design Virus-Induced Gene Silencing (VIGS) Constructs for Functional Genomics. *Mol. Plant* 8, 486–488. doi: 10.1016/j.molp.2014.11.024

Gavin, A. C., Maeda, K., and Kuhner, S. (2011). Recent advances in charting protein-protein interaction: mass spectrometry-based approaches. *Curr. Opin. Biotechnol.* 22, 42–49. doi: 10.1016/j.copbio.2010.09.007

Gawehns, F., Ma, L., Bruning, O., Houterman, P. M., Boeren, S., Cornelissen, B. J. C., et al. (2015). The effector repertoire of *Fusarium oxysporum* determines the tomato xylem proteome composition following infection. *Front. Plant Sci.* 6, 967. doi: 10.3389/fpls.2015.00967

Gehl, C., Waadt, R., Kudla, J., Mendel, R. R., and Hänsch, R. (2009). New GATEWAY vectors for high throughput analyses of protein-protein interactions by bimolecular fluorescence complementation. *Mol. Plant* 2, 1051–1058. doi: 10.1093/mp/ssp040

Gutierrez, C. (2000a). DNA replication and cell cycle in plants: learning from geminiviruses. *EMBO J.* 19, 792–799. doi: 10.1093/emboj/19.5.792

Gutierrez, C. (2000b). Geminiviruses and the plant cell cycle. *Plant Mol. Biol.* 43, 763–772. doi: 10.1023/A:1006462028363

Hanley-Bowdoin, L., Settlage, S. B., and Robertson, D. (2004). Reprogramming plant gene expression: a prerequisite to geminivirus DNA replication. *Mol. Plant Pathol.* 5, 149–156. doi: 10.1111/j.1364-3703.2004.00214.x

Hanley-Bowdoin, L., Bejarano, E. R., Robertson, D., and Mansoor, S. (2013). Geminiviruses: masters at redirecting and reprogramming plant processes. *Nat. Rev. Microbiol.* 11, 777–788. doi: 10.1038/nrmicro3117

Heath, C. G., Viphakone, N., and Wilson, S. A. (2016). The role of TREX in gene expression and disease. *Biochem. J.* 473, 2911–2935. doi: 10.1042/BCJ20160010

Heberle, H., Meirelles, G. V., da Silva, F. R., Telles, G. P., and Minghim, R. (2015). InteractiVenn: a web-based tool for the analysis of sets through Venn diagrams. *BMC Bioinf.* 16, 169. doi: 10.1186/s12859-015-0611-3

Hiscox, J. A. (2002). The nucleolus - a gateway to viral infection? *Arch. Virol* 147, 1077–1089. doi: 10.1007/s00705-001-0792-0

Hubner, N. C., Bird, A. W., Cox, J., Splettstoesser, B., Bandilla, P., Poser, I., et al. (2010). Quantitative proteomics combined with BAC TransgeneOmics reveals in vivo protein interactions. *J. Cell Biol.* 189, 739–754. doi: 10.1083/jcb.200911091

Jeske, H. (2009). Geminiviruses. *Curr. Top. Microbiol. Immunol.* 331, 185–226. doi: 10.1007/978-3-540-70972-5_11

Jimeno, S., Rondón, A. G., Luna, R., and Aguilera, A. (2002). The yeast THO complex and mRNA export factors link RNA metabolism with transcription and genome instability. *EMBO J.* 21, 3526–3535. doi: 10.1093/emboj/cdf335

Kaliappan, K., Choudhury, N. R., Suyal, G., and Mukherjee, S. K. (2012). A novel role for RAD54: this host protein modulates geminiviral DNA replication. *FASEB J.* 26, 1142–1160. doi: 10.1096/fj.11-188508

Karimi, M., Inzé, D., and Depicker, A. (2002). GATEWAY^{TM} vectors for *Agrobacterium*-mediated plant transformation. *Trends Plant Sci.* 7, 193–195. doi: 10.1016/S1360-1385(02)02251-3

Kawamura, K., Qi, F., Meng, Q., Hayashi, I., and Kobayashi, J. (2019). Nucleolar protein nucleolin functions in replication stress–induced DNA damage responses. *J. Radiat. Res.* 60, 281–288. doi: 10.1093/jrr/rry114

Kim, S. H., Ryabov, E. V., Brown, J. W. S., and Taliansky, M. (2004). Involvement of the nucleolus in plant virus systemic infection. *Biochem. Soc. Trans.* 32, 557–560. doi: 10.1042/BST0320557

Kong, L. J., and Hanley-Bowdoin, L. (2002). A Geminivirus Replication Protein Interacts with a Protein Kinase and a Motor Protein That Display Different Expression Patterns during Plant Development and Infection. *Plant Cell* 14, 1817–1832. doi: 10.1105/tpc.003681

Kong, L. J., Orozco, B. M., Roe, J. L., Nagar, S., Ou, S., Feiler, H. S., et al. (2000). A geminivirus replication protein interacts with the retinoblastoma protein through a novel domain to determine symptoms and tissue specificity of infection in plants. *EMBO J.* 19, 3485–3495. doi: 10.1093/emboj/19.13.3485

Kovar, H. (2011). Dr. Jekyll and Mr. Hyde: The Two Faces of the FUS/EWS/TAF15 Protein Family. *Sarcoma* 2011, 837474. doi: 10.1155/2011/837474

Kushwaha, N. K., Mansi,, and Chakraborty, S. (2017). The replication initiator protein of a geminivirus interacts with host monoubiquitination machinery and stimulates transcription of the viral genome. *PLoS Pathog.* 13, e1006587. doi: 10.1371/journal.ppat.1006587

Law, W. J., Cann, K. L., and Hicks, G. G. (2006). TLS, EWS and TAF15: a model for transcriptional integration of gene expression. *Brief Funct. Genomic Proteomic* 5, 8–14. doi: 10.1093/bfgp/ell015

Lindbo, J. A. (2007). TRBO: a high-efficiency tobacco mosaic virus RNA-based overexpression vector. *Plant Physiol.* 145, 1232–1240. doi: 10.1104/pp.107.106377

Liu, Y., Schiff, M., and Dinesh-Kumar, S. P. (2002). Virus-induced gene silencing in tomato. *Plant J.* 31, 777–786. doi: 10.1046/j.1365-313X.2002.01394.x

Liu, D., Shi, L., Han, C., Yu, J., Li, D., and Zhang, Y. (2012). Validation of Reference Genes for Gene Expression Studies in Virus-Infected Nicotiana benthamiana Using Quantitative Real-Time PCR. *PLoS One* 7, e46451. doi: 10.1371/journal.pone.0046451

Liu, Y., Jin, W., Wang, L., and Wang, X. F. (2014). Replication-associated proteins encoded by *Wheat dwarf virus* act as RNA silencing suppressors. *Virus Res.* 190, 34–39. doi: 10.1016/j.virusres.2014.06.014

Lu, J., Boeren, S., de Vries, S. C., van Valenberg, H. J. F., Vervoort, J., and Hettinga, K. (2011). Filter-aided sample preparation with dimethyl labeling to identify and quantify milk fat globule membrane proteins. *J. Proteomics* 75, 34–43. doi: 10.1016/j.jprot.2011.07.031

Luque, A., Sanz-Burgos, A. P., Ramirez-Parra, E., Castellano, M. M., and Gutierrez, C. (2002). Interaction of geminivirus Rep protein with replication factor C and its potential role during geminivirus DNA replication. *Virology* 302, 83–94. doi: 10.1006/viro.2002.1599

Maio, F., Arroyo-Mateos, M., Bobay, B. G., Bejarano, E. R., Prins, M., and van den Burg, H. A. (2019). A lysine residue essential for geminivirus replication also controls nuclear localization of the TYLCV Rep protein. *J. Virol* 93, e01910–e01918. doi: 10.1128/JVI.01910-18

Mansoor, S., Briddon, R. W., Zafar, Y., and Stanley, J. (2003). Geminivirus disease complexes: an emerging threat. *Trends Plant Sci.* 8, 128–134. doi: 10.1016/S1360-1385(03)00007-4

Mansoor, S., Zafar, Y., and Briddon, R. W. (2006). Geminivirus disease complexes: the threat is spreading. *Trends Plant Sci.* 11, 209–212. doi: 10.1016/j.tplants.2006.03.003

Martínez, F., Rodrigo, G., Aragonés, V., Ruiz, M., Lodewijk, I., Fernández, U., et al. (2016). Interaction network of tobacco etch potyvirus NIa protein with the host proteome during infection. *BMC Genomics* 17, 87. doi: 10.1186/s12864-016-2394-y

Mi, H., Huang, X., Muruganujan, A., Tang, H., Mills, C., Kang, D., et al. (2017). PANTHER version 11: expanded annotation data from Gene Ontology and Reactome pathways, and data analysis tool enhancements. *Nucleic Acids Res.* 45, D183–D189. doi: 10.1093/nar/gkw1138

Morilla, G., Castillo, A. G., Preiss, W., Jeske, H., and Bejarano, E. R. (2006). A versatile transreplication-based system to identify cellular proteins involved in geminivirus replication. *J. Virol* 80, 3624–3633. doi: 10.1128/JVI.80.7.3624-3633.2006

Nakamura, S., Mano, S., Tanaka, Y., Ohnishi, M., Nakamori, C., Araki, M., et al. (2010). Gateway binary vectors with the bialaphos resistance gene, bar, as a selection marker for plant transformation. *Biosci. Biotechnol. Biochem.* 74, 1315–1319. doi: 10.1271/bbb.100184

Navas-Castillo, J., Fiallo-Olivé, E., and Sánchez-Campos, S. (2011). Emerging virus diseases transmitted by whiteflies. *Annu. Rev. Phytopathol.* 49, 219–248. doi: 10.1146/annurev-phyto-072910-095235

Negrutiu, I., Shillito, R., Potrykus, I., Biasini, G., and Sala, F. (1987). Hybrid genes in the analysis of transformation conditions. *Plant Mol. Biol.* 8, 363–373. doi: 10.1007/BF00015814

Ohnishi, J., Yamaguchi, H., and Saito, A. (2016). Analysis of the Mild strain of tomato yellow leaf curl virus, which overcomes Ty-2 gene–mediated resistance in tomato line H24. *Arch. Virol* 161, 2207–2217. doi: 10.1007/s00705-016-2898-4

Ohno, T., Ouchida, M., Lee, L., Gatalica, Z., Rao, V. N., and Reddy, E. S. (1994). The Ews Gene, Involved in Ewing Family of Tumors, Malignant-Melanoma of Soft Parts and Desmoplastic Small Round-Cell Tumors, Codes for an Rna-Binding Protein with Novel Regulatory Domains. *Oncogene* 9, 3087–3097.

Ouyang, H., Zhang, K., Fox-Walsh, K., Yang, Y., Zhang, C., Huang, J., et al. (2017). The RNA binding protein EWS is broadly involved in the regulation of pri-miRNA processing in mammalian cells. *Nucleic Acids Res.* 45, 12481–12495. doi: 10.1093/nar/gkx912

Pan, H. R., Liu, S. M., and Tang, D. (2012). HPR1, a component of the THO/TREX complex, plays an important role in disease resistance and senescence in Arabidopsis. *Plant J.* 69, 831–843. doi: 10.1111/j.1365-313X.2011.04835.x

Peng, K., van Lent, J. W. M., Boeren, S., Fang, M., Theilmann, D. A., Erlandson, M. A., et al. (2012). Characterization of Novel Components of the Baculovirus Per Os Infectivity Factor Complex. *J. Virol* 86, 4981–4988. doi: 10.1128/JVI.06801-11

Richter, K. S., Kleinow, T., and Jeske, H. (2014). Somatic homologous recombination in plants is promoted by a geminivirus in a tissue-selective manner. *Virology* 452–453, 287–296. doi: 10.1016/j.virol.2014.01.024

Rizvi, I., Choudhury, N. R., and Tuteja, N. (2015). Insights into the functional characteristics of geminivirus rolling-circle replication initiator protein and its interaction with host factors affecting viral DNA replication. *Arch. Virol.* 160, 375–387. doi: 10.1007/s00705-014-2297-7

Rodríguez-Negrete, E., Lozano-Durán, R., Piedra-Aguilera, A., Cruzado, L., Bejarano, E. R., and Castillo, A. G. (2013). Geminivirus Rep protein interferes with the plant DNA methylation machinery and suppresses transcriptional gene silencing. *New Phytol.* 199, 464–475. doi: 10.1111/nph.12286

Rojas, M. R., Jiang, H., Salati, R., Xoconostle-Cázares, B., Sudarshana, M. R., Lucas, W. J., et al. (2001). Functional analysis of proteins involved in movement of the monopartite begomovirus, *Tomato yellow leaf curl virus*‘. *Virology* 291, 110–125. doi: 10.1006/viro.2001.1194

Rojas, M. R., Hagen, C., Lucas, W. J., and Gilbertson, R. L. (2005). Exploiting chinks in the plant's armor: evolution and emergence of geminiviruses. *Annu. Rev. Phytopathol.* 43, 361–394. doi: 10.1146/annurev.phyto.43.040204.135939

Rojas, M. R., Macedo, M. A., Maliano, M. R., Soto-Aguilar, M., Souza, J. O., Briddon, R. W., et al. (2018). World Management of Geminiviruses. *Annu. Rev. Phytopathol.* 56, 637–677. doi: 10.1146/annurev-phyto-080615-100327

Ruhel, R., and Chakraborty, S. (2019). Multifunctional roles of geminivirus encoded replication initiator protein. *VirusDis* 30, 66–73. doi: 10.1007/s13337-018-0458-0

Sánchez-Durán, M. A., Dallas, M. B., Ascencio-Ibañez, J. T., Reyes, M.II, Arroyo-Mateos, M., Ruiz-Albert, J., et al. (2011). Interaction between geminivirus replication protein and the SUMO-conjugating enzyme is required for viral infection. *J. Virol.* 85, 9789–9800. doi: 10.1128/JVI.02566-10

Sørensen, B. B., Ehrnsberger, H. F., Esposito, S., Pfab, A., Bruckmann, A., Hauptmann, J., et al. (2017). The Arabidopsis THO/TREX component TEX1 functionally interacts with MOS11 and modulates mRNA export and alternative splicing events. *Plant Mol. Biol.* 93, 283–298. doi: 10.1007/s11103-016-0561-9

Sambrook, J., Russel, David, W., and Maniatis, T. (2001). *Molecular cloning* Vol. vol. 1-3 (New York: Cold Spring Habour Laboratory Press).

Sasikumar, A. N., Perez, W. B., and Kinzy, T. G. (2012). The many roles of the eukaryotic elongation factor 1 complex. *WIREs RNA* 3, 543–555. doi: 10.1002/wrna.1118

Schneider, J., and Wolff, T. (2009). Nuclear functions of the influenza A and B viruses NS1 proteins: do they play a role in viral mRNA export? *Vaccine* 27, 6312–6316. doi: 10.1016/j.vaccine.2009.01.015

Settlage, S. B., See, R. G., and Hanley-Bowdoin, L. (2005). Geminivirus C3 protein: replication enhancement and protein interactions. *J. Virol.* 79, 9885–9895. doi: 10.1128/JVI.79.15.9885-9895.2005

Shahin, E. A. (1985). Totipotency of Tomato Protoplasts. *Theor. Appl. Genet.* 69, 235–240. doi: 10.1007/BF00662431

Shannon, P., Markiel, A., Ozier, O., Baliga, N. S., Wang, J. T., Ramage, D., et al. (2003). Cytoscape: a software environment for integrated models of biomolecular interaction networks. *Genome Res.* 13, 2498–2504. doi: 10.1101/gr.1239303

Shung, C. Y., and Sunter, G. (2007). AL1-dependent repression of transcription enhances expression of Tomato golden mosaic virus AL2 and AL3. *Virology* 364, 112–122. doi: 10.1016/j.virol.2007.03.006

Singh, D. K., Islam, M. N., Choudhury, N. R., Karjee, S., and Mukherjee, S. K. (2007). The 32 kDa subunit of replication protein A (RPA) participates in the DNA replication of Mung bean yellow mosaic India virus (MYMIV) by interacting with the viral Rep protein. *Nucleic Acids Res.* 35, 755–770. doi: 10.1093/nar/gkl1088

Smaczniak, C., Li, N., Boeren, S., America, T., van Dongen, W., Goerdayal, S. S., et al. (2012). Proteomics-based identification of low-abundance signaling and regulatory protein complexes in native plant tissues. *Nat. Protoc.* 7, 2144–2158. doi: 10.1038/nprot.2012.129

Strässer, K., Masuda, S., Mason, P., Pfannstiel, J., Oppizzi, M., Rodriguez-Navarro, S., et al. (2002). TREX is a conserved complex coupling transcription with messenger RNA export. *Nature* 417, 304–308. doi: 10.1038/nature746

Sunter, G., Hartitz, M. D., Hormuzdi, S. G., Brough, C. L., and Bisaro, D. M. (1990). Genetic-Analysis of Tomato Golden Mosaic-Virus: ORF AL2 Is Required for Coat Protein Accumulation While ORF AL3 Is Necessary for Efficient DNA Replication. *Virology* 179, 69–77. doi: 10.1016/0042-6822(90)90275-V

Suyal, G., Mukherjee, S. K., and Choudhury, N. R. (2013a). The host factor RAD51 is involved in mungbean yellow mosaic India virus (MYMIV) DNA replication. *Arch. Virol.* 158, 1931–1941. doi: 10.1007/s00705-013-1675-x

Suyal, G., Mukherjee, S. K., Srivastava, P. S., and Choudhury, N. R. (2013b). *Arabidopsis thaliana* MCM2 plays role(s) in mungbean yellow mosaic India virus (MYMIV) DNA replication. *Arch. Virol.* 158, 981–992. doi: 10.1007/s00705-012-1563-9

Suyal, G., Rana, V. S., Mukherjee, S. K., Wajid, S., and Choudhury, N. R. (2014). *Arabidopsis thaliana* NAC083 protein interacts with *Mungbean yellow mosaic India virus* (MYMIV) Rep protein. *Virus Genes* 48, 486–493. doi: 10.1007/s11262-013-1028-6

Tameling, W.II, and Baulcombe, D. C. (2007). Physical association of the NB-LRR resistance protein Rx with a Ran GTPase–activating protein is required for extreme resistance to *Potato virus X*‘. *Plant Cell* 19, 1682–1694. doi: 10.1105/tpc.107.050880

Tan, M. L. M. C., Rietveld, E. M., Vanmarrewijk, G. A. M., and Kool, A. J. (1987). Regeneration of Leaf Mesophyll Protoplasts of Tomato Cultivars (*L. esculentum*) Factors Important for Efficient Protoplast Culture and Plant Regeneration. *Plant Cell Rep.* 6, 172–175. doi: 10.1007/BF00268470

van Schie, C. C. N., and Takken, F. L. W. (2014). Susceptibility genes 101: how to be a good host. *Annu. Rev. Phytopathol.* 52, 551–581. doi: 10.1146/annurev-phyto-102313-045854

Verlaan, M. G., Hutton, S. F., Ibrahem, R. M., Kormelink, R., Visser, R. G. F., Scott, J. W., et al. (2013). The Tomato Yellow Leaf Curl Virus resistance genes *Ty-1* and *Ty-3* are allelic and code for DFDGD-class RNA-dependent RNA polymerases. *PLoS Genet.* 9, e1003399. doi: 10.1371/journal.pgen.1003399

Vizcaino, J. A., Csordas, A., Del-Toro, N., Dianes, J. A., Griss, J., Lavidas, I., et al. (2016). 2016 update of the pride database and its related tools. *Nucleic Acids Res.* 44, D447–D456. doi: 10.1093/nar/gkw880

Wang, L., Ding, X., Xiao, J., Jiménez-Góngora, T., Liu, R. Y., and Lozano-Durán, R. (2017a). Inference of a Geminivirus-Host Protein-Protein Interaction Network through Affinity Purification and Mass Spectrometry Analysis. *Viruses* 9, 275. doi: 10.3390/v9100275

Wang, L., Tan, H., Wu, M., Jimenez-Gongora, T., Tan, L., and Lozano-Duran, R. (2017b). Dynamic Virus-Dependent Subnuclear Localization of the Capsid Protein from a Geminivirus. *Front. Plant Sci.* 8, 2165. doi: 10.3389/fpls.2017.02165

Xie, Q., Sanz-Burgos, A. P., Hannon, G. J., and Gutiérrez, C. (1996). Plant cells contain a novel member of the retinoblastoma family of growth regulatory proteins. *EMBO J.* 15, 4900–4908. doi: 10.1002/j.1460-2075.1996.tb00870.x

Xu, M., Mazur, M. J., Tao, X., and Kormelink, R. (2020). Cellular RNA Hubs: Friends and Foes of Plant Viruses. *Mol. Plant Microbe Interact.* 33, 40–54. doi: 10.1094/MPMI-06-19-0161-FI

Yamaguchi, H., Ohnishi, J., Saito, A., Ohyama, A., Nunome, T., Miyatake, K., et al. (2018). An NB-LRR gene, *TYNBS1*, is responsible for resistance mediated by the *Ty-2 Begomovirus* resistance locus of tomato. *Theor. Appl. Genet.* 131, 1345–1362. doi: 10.1007/s00122-018-3082-x

Yarbrough, M. L., Mata, M. A., Sakthivel, R., and Fontoura, B. M. A. (2014). Viral subversion of nucleocytoplasmic trafficking. *Traffic* 15, 127–140. doi: 10.1111/tra.12137

Yelina, N. E., Smith, L. M., Jones, A. M. E., Patel, K., Kelly, K. A., and Baulcombe, D. C. (2010). Putative Arabidopsis THO/TREX mRNA export complex is involved in transgene and endogenous siRNA biosynthesis. *Proc. Natl. Acad. Sci. U. S. A.* 107, 13948–13953. doi: 10.1073/pnas.0911341107

Zerbini, F. M., Briddon, R. W., Idris, A., Martin, D. P., Moriones, E., Navas-Castillo, J., et al. (2017). ICTV Virus Taxonomy Profile: *Geminiviridae*. *J. Gen. Virol.* 98, 131–133. doi: 10.1099/jgv.0.000738

Zhao, L., Rosario, K., Breitbart, M., and Duffy, S. (2019). Eukaryotic circular Rep-encoding single-stranded DNA (CRESS DNA) viruses: Ubiquitous viruses with small genomes and a diverse host range. *Adv. Virus Res.* 103, 71–133. doi: 10.1016/bs.aivir.2018.10.001

Conflict of Interest: Author MP is employed by the company Keygene N.V.

The remaining authors declare that the research was conducted in the absence of any commercial or financial relationships that could be construed as a potential conflict of interest.

frontiers in Plant Science

MINI REVIEW
published: 23 July 2020
doi: 10.3389/fpls.2020.01131

Geminivirus Resistance: A Minireview

*Kayla Beam and José Trinidad Ascencio-Ibáñez**

Department of Molecular and Structural Biology, North Carolina State University, Raleigh, NC, United States

A continuing challenge to crop production worldwide is the spectrum of diseases caused by geminiviruses, a large family of small circular single-stranded DNA viruses. These viruses are quite diverse, some containing mono- or bi-partite genomes, and infecting a multitude of monocot and dicot plants. There are currently many efforts directed at controlling these diseases. While some of the methods include controlling the insect vector using pesticides or genetic insect resistance (Rodríguez-López et al., 2011), this review will focus on the generation of plants that are resistant to geminiviruses themselves. Genetic resistance was traditionally found by surveying the wild relatives of modern crops for resistance loci; this method is still widely used and successful. However, the quick rate of virus evolution demands a rapid turnover of resistance genes. With better information about virus-host interactions, scientists are now able to target early stages of geminivirus infection in the host, preventing symptom development and viral DNA accumulation.

Keywords: geminivirus, resistance, genetic resistance, agriculture, genetic engineering

OPEN ACCESS

Edited by:
Mario Tavazza,
Energy and Sustainable Economic Development (ENEA), Italy

Reviewed by:
Manoj Prasad,
National Institute of Plant Genome Research (NIPGR), India
Enrique Moriones,
La Mayora Experimental Station, Spain

***Correspondence:**
José Trinidad Ascencio-Ibáñez
jtascenc@ncsu.edu

Specialty section:
This article was submitted to Virology, a section of the journal Frontiers in Plant Science

Received: *28 February 2020*
Accepted: *10 July 2020*
Published: *23 July 2020*

Citation:
Beam K and Ascencio-Ibáñez JT (2020) Geminivirus Resistance: A Minireview. Front. Plant Sci. 11:1131. doi: 10.3389/fpls.2020.01131

INTRODUCTION: VIRAL PROTEINS MAY BE TARGETS FOR RESISTANCE

Geminiviruses are circular single-stranded DNA viruses that infect a wide range of plant species including many important crops. Damages attributed to geminiviruses include over $300 million in loss in the Indian bean industry (Patil et al., 2014), up to 100% loss of tomato crop in Italy and the Dominican Republic (Picó et al., 1996), and nearly $2 billion loss in African cassava production (Patil and Fauquet, 2009). The impact of geminiviruses is widespread and destructive. The family Geminiviridae has nine genera based on viral genome structure and insect vectors. In the case of begomoviruses, genomes can be mono- or bipartite, with each circular DNA (~2.5 Kb) packaged in a twinned icosahedral particle (Zerbini et al., 2017).

Geminivirus infection begins when an insect vector containing virions feeds on a host plant. The viral genome is deposited and unpackaged in the phloem cells. A complementary strand is synthesized, then the dsDNA is replicated and packaged into mini-chromosomes using host histones (reviewed in Jeske, 2009 and Hanley-Bowdoin et al., 2013). The viral genes are transcribed by host RNA Polymerase II. The viral genome is replicated by rolling-circle and recombination-dependent replication systems (Jeske et al., 2001). These processes require both host and viral proteins. See **Figure 1** for an overview of the geminivirus life cycle.

The most critical geminiviral protein for virus replication is the replication initiator protein (Rep). It initiates replication by binding the origin sequence, nicking the DNA, and associating with host factors (Laufs et al., 1995; Kong et al., 2000; Arguello-Astorga et al., 2004; Desvoyes et al., 2006). The geminiviral transcriptional activator protein (TrAP) is involved in pathogenicity and suppresses both transcriptional and post transcriptional gene silencing (Sunter and Bisaro, 1992; Hong et al., 1996; Voinnet et al., 1999; Shivaprasad et al., 2005; Trinks et al., 2005; Wang et al., 2005; Chowda-Reddy et al., 2009; Castillo-González et al., 2015; Kumar et al., 2015). Furthermore, the replication enhancer

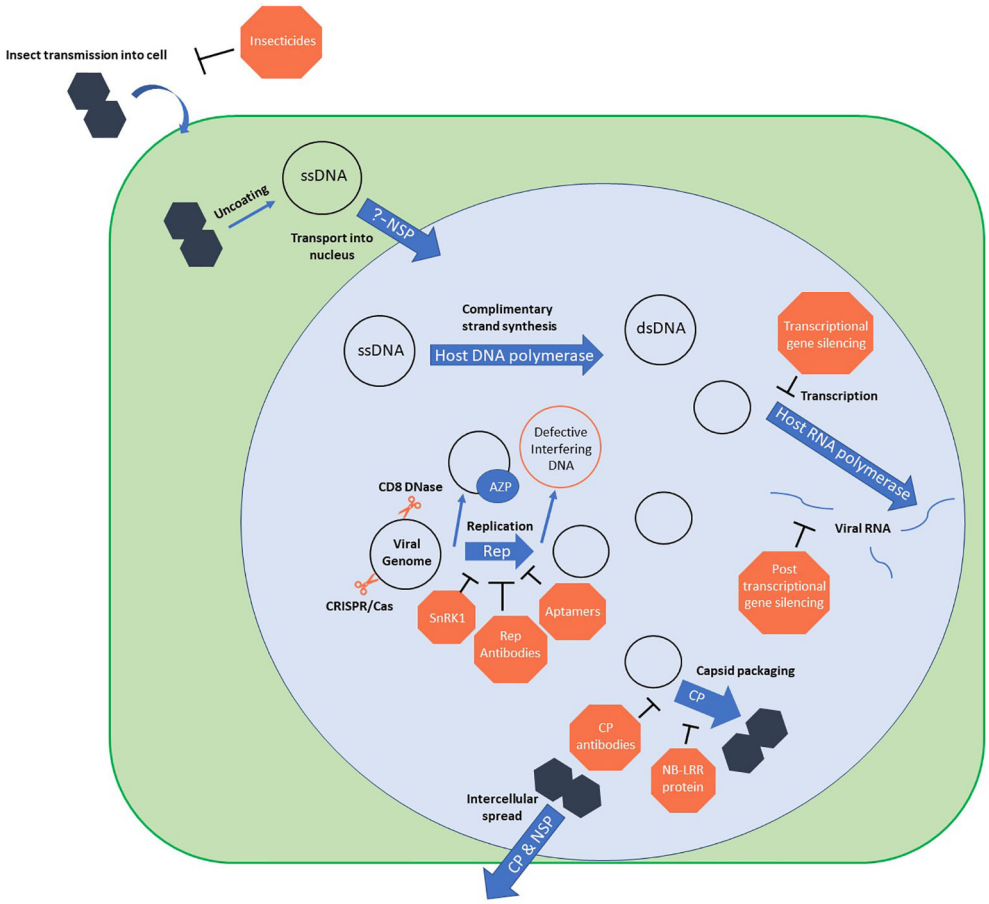

FIGURE 1 | Geminivirus life cycle with points of resistance. Orange blocks show points where known resistance mechanisms interfere with the virus. ssDNA, single stranded DNA; dsDNA, double stranded DNA; NSP, nuclear shuttle protein; AZP, artificial zinc-finger protein; Rep, replication-associated protein; CP, coat protein.

protein (REn) contributes to increased viral replication and interacts with host factors and with Rep. Geminiviruses also encode proteins for packaging and movement. The coat protein (CP) comprises the viral capsid and is critical for vector specificity (Noris et al., 1998) and viral nuclear import (Liu et al., 1999) and is also required for symptom development. In bipartite geminiviruses, the nuclear shuttle protein (NSP) is responsible for nuclear import by binding ssDNA. It also aids in intercellular movement by interacting with the movement protein (MP) at the membrane. MP is responsible primarily for the intercellular spread of viral DNA (Noueiry et al., 1994) by increasing the size exclusion limit of plasmodesmata (Rojas et al., 2001). For excellent reviews in these subjects please see Hanley-Bowdoin et al., 2013; Czosnek et al., 2017; Rojas et al., 2018, and Martins et al., 2020.

NATURALLY OCCURRING RESISTANCE

In the process of crop domestication, traits that are not directly beneficial are often bred out in favor of those increasing yield in particular conditions. When a new challenge arises, breeders search wild relatives for traits that increase survival. This is the case with geminiviruses: there are multiple geminivirus resistance genes from undomesticated relatives that are utilized in agriculture. Examples include many crops like beans (reviewed by Blair and Morales, 2008) or cotton (Zaidi et al., 2020). This minireview will cover resistance genes in tomato and cassava in detail. A selected list of resistance genes for these crops is presented in **Table 1**.

Solanum chilense is the most popular wild tomato relative for introgressing Tomato yellow leaf curl virus (TYLCV) resistance, as over 80% of its accessions are resistant (Yan et al., 2018). Many of the *Ty* family of resistance loci are from this plant. *Ty-1* was introgressed into tomato from *S. chilense* and mapped to chromosome 6. It confers a tolerant symptomless response against TYLCV in homozygous plants (Zamir et al., 1994). *Ty-1* is allelic with another resistance gene from *S. chilense*, *Ty-3*. These genes encode an RNA-dependent RNA polymerase (RDR) similar to RDRs 3, 4, and 5 in *Arabidopsis thaliana*, implying a role for RNA interference (Verlaan et al., 2013). *A. thaliana* itself may be a source for resistance as found by Reyes et al. (2017) in an accession showing immunity to Cabbage leaf curl virus (CbLCV) and Beet

TABLE 1 | List of genes involved in geminivirus resistance and geminiviral suppressors of silencing.

Gene	Protein	Plant	Virus	Reference
Ty-1, Ty-3	RNA-dependent polymerase	*S. lycopersicum*	TYLCV	(Zamir et al., 1994; Verlaan et al., 2013; Butterbach et al., 2014)
Ty-2	NB-LRR class protein	*S. lycopersicum*	TYLCV	(Yang et al., 2014; Yamaguchi et al., 2018)
Ty-4		*S. lycopersicum*	TYLCV	(Ji et al., 2009)
ty-5	pelota	*S. lycopersicum*	TYLCV	(Hutton et al., 2012; Scott et al., 2015; Lapidot et al., 2015)
Ty-6		*S. lycopersicum*	TYLCV	(Scott et al., 2015)
CMD1, CMD3		*M. esculenta*	ACMV	(Fregene et al., 2000; Akano et al., 2002; Okogbenin et al., 2012)
CMD2		*M. esculenta*	ACMV	(Akano et al., 2002; Kuria et al., 2017)
CchGLP	MN-SOD	*C. chinense*	PHYVV, PepGMV	(León-Galván et al., 2011; Guevara-Olvera et al., 2012; Mejía-Teniente et al., 2015)
SlSnRK1	SnRK1	*S. lycopersicum*	TYLCV, CaLCuV	(Shen et al., 2011; Shen et al., 2014; Hulsmans et al., 2016)
Permease-1 like		*S. habrochaites* introgressed *S. lycopersicum*	TYLCV	(Eybishtz et al., 2009)
LeHT1	hexose transporter	*S. lycopersicum*	TYLCV	(Eybishtz et al., 2010; Sade et al., 2012)
SlVSRLip	lipocalin-like	*S. lycopersicum*	TYLCV	(Sade et al., 2012)
NIK	NSP-interacting kinase	*A. thaliana, S. lycopersicum, G. max*	begomoviruses	(Brustolini et al., 2015)
SGS3	RNA binding protein in PTGS	*N. benthamiana*	TYLCV	(Li et al., 2017)
WRKY	Group III transcription factors	*S. lycopersicum*	TYLCV	(Huang et al., 2016)

curly top virus (BCTV). *Ty-1* plants have increased siRNA levels in comparison to non-resistant cultivars, corresponding with high levels of viral DNA methylation. This indicates transcriptional gene silencing (TGS) is likely involved in *Ty-1/Ty-3* mediated resistance (Butterbach et al., 2014).

Ty-2 is a TYLCV resistance locus on tomato chromosome 11 introgressed from *Solanum habrochaites* (Yang et al., 2014). This locus hosts a gene known as *TYNBS1* that encodes an Nucleotide Binding, Leucine Rich Repeat (NB-LRR) protein, known elsewhere to provide pathogen resistance (Yamaguchi et al., 2018). The recessive *ty-5* locus from a hybrid tomato known as Tyking has been mapped to chromosome 4. It is closely tied to the Quantitative trait loci (QTL) marker *SlNAC1* (Anbinder et al., 2009; Hutton et al., 2012). The gene responsible for *ty-5* resistance is *pelota*, which encodes an mRNA surveillance factor homolog (Lapidot et al., 2015; Wang Y. et al., 2018). *Ty-4* and *Ty-6* are other resistances genes from *S. chilense* that are less understood. *Ty-4* is a minor locus on tomato chromosome 3 (Ji et al., 2009). *Ty-6* lies on chromosome 10, has incomplete dominance, and protects tomatoes against Tomato mottle virus (ToMoV) and TYLCV (Scott et al., 2015; Gill et al., 2019).

Cassava mosaic disease (CMD) is caused by multiple cassava mosaic geminiviruses, often in complexes. *CMD* has only three markers in cassava known to confer resistance. *CMD2* is a single locus preferred by breeders due to its dominance (Akano et al., 2002). However, *CMD2* is monogenic and thus at risk of viral evolution overcoming resistance. Monogenic resistance is not sufficient for long-term disease resistance, requiring constant innovation to keep ahead of viral evolution. The newest marker associated with CMD resistance is *CMD3* (Okogbenin et al., 2012). It arose through crossbreeding of cultivars with the *CMD2* locus and another recessive resistance locus, *CMD1*, and appears to provide the highest resistance level of the three (Kuria et al., 2017).

The *CMD2*-provided resistance is lost when the plants are regenerated through somatic embryogenesis (Beyene et al., 2016). The mechanism for this change is unknown. The other CMD resistance alleles (*CMD1* and *CMD3*) are unaffected and still reliable for use. The loss of *CMD2*-based resistance could provide a method to predict if other traits will share the same phenomenon (Chauhan et al., 2018). There are several potential mechanisms for this effect including somaclonal variation, which

is caused by epigenetic changes when the cell undergoes the disorganized regeneration phase in tissue culture (Bairu et al., 2011; Lee and Seo, 2018). However, virus evolution through pseudorecombination or recombination and not changes in the host can also be at play to break resistance in the field.

This ability to overcome genetic resistance is a very challenging aspect in geminivirus-plant interactions. One such example is the discovery of sequences enhancing geminivirus symptoms (SEGS) during CMD infection. These SEGS (encoded in the cassava genome) enabled the virus to cause symptoms in otherwise resistant cultivars, breaking the resistance (Ndunguru et al., 2016). Viruses themselves also have a high rate of mutation that can change the virus-host interactions to evade resistance. For TYLCV, the mean rate of genomic substitutions is estimated to be 2.88 x 10^{-4} nucleotide substitutions per site every year (Duffy and Holmes, 2008). This ability of geminiviruses to overcome genetic resistance has led to a resurgence of Cotton leaf curl disease (CLCuD) in south Asia after it had been nearly eradicated (Amrao et al., 2010).

GEMINIVIRUS-PLANT INTERACTIONS AND UNDERSTANDING HOST RESISTANCE

Reverse genetics is a common method for identifying genes involved in viral infection. Eybishtz et al. used this method in 2009 to identify Permease I-like protein as a resistance factor against TYLCV. In knockout resistant plants, viral genomic titer increased and resulted in susceptibility (Eybishtz et al., 2009). Similarly, the hexose transporter *LeHT1* was also identified as a resistance gene. In *LeHT1*-knockout plants, TYLCV accumulates and causes a necrotic response. This implies programmed cell death may be a factor in geminiviral response (Eybishtz et al., 2010). A downstream gene in the same *LeHT1* pathway, a lipocalin-like gene, also results in a necrotic response to TYLCV when mutated from the resistant tomato (Sade et al., 2012).

A separate geminivirus resistance gene that also involves programmed cell death includes the germin-like *CchGLP* gene found in resistant peppers. This protein has manganese superoxide reductase activity which increases upon infection by Pepper golden mosaic virus or Pepper huasteco yellow vein virus in resistant plants only (León-Galván et al., 2011). Resistant peppers with knocked-out *CchGLP* develop symptoms, indicating this gene has an important role in defense (Mejía-Teniente et al., 2015). When transferred into susceptible tobacco plants, *CchGLP* conferred a mild symptom phenotype with increased reactive oxygen levels and expression of systemic acquired resistance-related genes (Guevara-Olvera et al., 2012). Reactive oxygen species promote programmed cell death, a general defense mechanism to prevent the spread of infectious entities such as bacteria or viruses (Lam, 2004). Tomato leaf curl New Delhi Virus (ToLCNDV) resistance protein SlRPT4, a 26S proteasome, is also shown to regulate programmed cell death and ROS production. This is in addition to its inhibitory binding of the viral genome (Sahu et al., 2016).

SnRK1 is a major regulator of energy and nutrients in the plant cell. It is also emerging with a role in plant response to biotic stress (Hulsmans et al., 2016). When challenged with geminivirus infection, *A. thaliana* SnRK1 has been shown to phosphorylate TrAP of CbLCV, delaying and attenuating symptoms (Shen et al., 2014). TrAP is an RNA silencing suppressor and acts as a transcription factor for two other geminiviral proteins (Fondong, 2013). In tomato, the analogue SlSnRK1 was shown to interact with the geminivirus satellite pathogenicity factor βC1. SlSnRK1 is shown to phosphorylate βC1, leading to symptom delay and viral DNA load reduction (Shen et al., 2011). Additionally, SnRK1 phosphorylates the Tomato golden mosaic virus Rep protein and interferes with its dsDNA binding function. This reduces viral DNA replication and symptoms (Shen et al., 2018). These features make SnRK1 an important factor in geminivirus defense. Other aspects of the host response like SUMOylation, senescence response and autophagy (reviewed by Kumar, 2019) may be used against the virus but viable resistance strategies have yet to be developed.

Another receptor kinase that is known to counteract geminivirus infection is the NSP-interacting kinase (NIK) family (Santos et al., 2010). *A. thaliana* NIKs are activated *via* oligomerization and autophosphorylation upon begomovirus infection (Brustolini et al., 2015). The downstream target of NIK is the ribosomal protein L10, which enters the nucleus and downregulates translation-related genes to slow down the infection (Santos et al., 2010; Brustolini et al., 2015). The begomovirus has evolved alongside NIK to suppress its antiviral activity by binding to the critical threonine 474, preventing the phosphorylation required for NIK activation (Santos et al., 2010). This same T474 when changed to phosphomimetic aspartate constitutively activates antiviral response genes, circumvents interference by NSP, and confers tolerance to begomovirus infection (Brustolini et al., 2015). Furthermore, a GTPase that interacts with NSP can also be conceived as a target to develop resistance against geminiviruses (Martins et al., 2020). These responses exemplify that understanding and changing genetic interactions can provide new solutions for disease management.

The status of the plant hormones in response to geminiviruses has not been exhaustively assessed. Hormone changes related to pathogen response fall within the salicylic acid (SA), jasmonic acid (JA), and ethylene pathways (ET), where SA pathway is upregulated during CbLCV infection in *A. thaliana*, JA is downregulated, and ET has both responses in a transcriptomic study (Ascencio-Ibáñez et al., 2008). Plants overexpressing SA (cpr1 mutants) displayed a substantial delay in symptom appearance upon infection, suggesting that plants with SA pathway always on may have partial protection against geminiviruses. On the other side, the CbLCV depletes the production of jasmonate. JA is known for deterring insects and reducing the transmissibility of geminiviruses (Escobar-Bravo et al., 2016) so it could be used to reduce infection and impact transmission of the virus (Sun et al., 2017). The issue is that SA and JA seemed to be antagonistic on the plants, which will make a plant producing both simultaneously at high levels not a viable

alternative. Auxins, gibberellins, cytokinins, brassinosteroids, abscisic acid, and strigolactones are all involved in the plant responses. However, not enough information is available yet to derive a putative resistance path.

ENGINEERED RESISTANCE

Natural defense mechanisms are often utilized to engineer a plant with geminivirus resistance. This review will briefly cover selected examples of engineered geminivirus resistance that interfere with the viral replication cycle. **Figure 1** puts these mechanisms in context with geminiviral life cycle. For a more detailed look at these approaches, see Loriato et al. (2020).

Interfering With Viral Proteins

Engineered resistance can act on proteins required for viral replication or on viral DNA itself. In an approach known as "immunomodulation", transgenic plants express antibodies against viral proteins. Single-chain antibodies generated against the geminiviral coat protein were shown to bind and provide resistance *in vivo* (Zakri et al., 2012). Similarly, anti-Rep antibody expression can provide resistance, but the response varies between lines due to variable transgene expression (Safarnejad et al., 2009). DNase 3D8 is a recombinant antibody with single- and double-stranded non-specific DNase activity that has been tested against geminiviruses BCTV and Beet severe curly top virus. Though the expression levels had to be kept low to protect host nucleic acid, 3D8 expression prevented high levels of viral DNA accumulation (Lee et al., 2013).

Peptide aptamers are engineered peptide sequences to be expressed by the host to interfere with the activity of a protein of interest. These are significantly smaller than single-chain antibodies, but work similarly. They have been developed and tested to disrupt functions of geminivirus proteins, one of which is Rep from Tomato Golden Mosaic Virus. The aptamers bound Rep *in vivo* and lowered viral DNA production (Lopez-Ochoa et al., 2006). In transgenic tomato, peptide aptamers were also effective against TYLCV and ToMoV by reducing viral symptoms and viral load (Reyes et al., 2013). Another approach for replication interference is by competition, as has been shown with subgenomic DNA. However, this approach is highly virus-specific, making its practical use limited and inefficient (Stanley et al., 1990; Stenger, 1994).

Viral infection can also be impeded by sequestration of protein targets. Rep can be out-competed for origin binding by artificial zinc-finger proteins with specific DNA binding, and one has been shown with greater affinity for the TYLCV origin than Rep (Mori et al., 2013). A plant expressing it or a similar protein may inhibit geminivirus replication. Mendoza-Figueroa et al. found a globulin-derived peptide with high affinity for the TYLCV origin and that reduced viral load when applied to infected plants. This indicates that the peptide may not need to be expressed by the plant, but rather can be applied exogenously to interfere with Rep activity (Mendoza-Figueroa et al., 2018).

Viral Responses Against Gene Silencing Rendered by the Host

Gene silencing regulates host processes by eliminating mRNA before translation and is a defense against viral RNA. Dicer-like proteins cleave dsRNA sequences into short interfering RNA (siRNA) molecules 21–24 nt in length (Rey and Fondong, 2018). The siRNA is loaded into a complex with Argonaute proteins, which are then directed to complimentary DNA or RNA sequences. This results in several outcomes, including degradation or sequestration of existing RNAs (post-transcriptional gene silencing) or targeting DNA for methylation (transcriptional gene silencing) (Mathieu and Bender, 2004; Raja et al., 2010). RDRs spread silencing throughout the plant by multiplying the secondary siRNA signal (Rey and Fondong, 2018).

To counteract silencing, geminiviruses have evolved viral suppressors of RNA silencing which are often pathogenicity factors. For example, V2 of Tomato yellow leaf curl China virus interacts with and sequesters secondary siRNAs, hindering the spread of silencing. V2 of TYLCV suppresses gene silencing by interacting with host proteins suppressor of gene silencing 3 and histone deacetylase 6 (Fondong, 2013; Wieczorek and Obrępalska-Stęplowska, 2015; Li et al., 2017; Wang B. et al., 2018). Another example of RNA silencing suppression is TrAP of Mungbean yellow mosaic Indian virus. It slows siRNA production by blocking RDR6-mediated biogenesis of siRNA, binds to Argonaute 1 to prevent its action, and lowers global DNA methylation levels (Buchmann et al., 2009; Kumar et al., 2015). C4 protein of Cotton leaf curl Multan virus, Cassava mosaic viruses, Tomato leaf curl New Delhi virus, and BCTV is also known to suppress silencing (Vanitharani et al., 2004; Ismayil et al., 2018; Vinutha et al., 2018) and can be a symptom determinant in infection (Mills-Lujan and Deom, 2010).

Upon geminivirus challenge, an increase in siRNA is correlated with a decrease in symptoms (Chellappan et al., 2004). Resistance and recovery phenotypes are strongly associated with RNA silencing. The intergenic region of the BCTV is targeted by transcriptional gene silencing, evidenced by a greater proportion of siRNAs produced for this region along with a heavier methylation load in recovered plants (Yadav and Chattopadhyay, 2011; Coursey et al., 2018). There is a significant inverse relation between the viral DNA methylation and the disease progression, measured by symptom severity and viral titer (Rodríguez-Negrete et al., 2009; Yadav and Chattopadhyay, 2011).

Transgenic approaches have been developed in multiple systems to generate plants that produce antiviral siRNAs, artificial miRNAs, long non-coding RNAs, synthetic trans-acting small interfering RNAs, etc., with different levels of success (some reviewed in Kumar and Khan, 2019). This concept has been proven in transgenic beans against Bean golden mosaic virus (Aragão et al., 2013). In general, a viral gene is expressed in the host to initiate PTGS quicker and to a higher degree when challenged by the virus. The plants expressing the gene in hairpin form had the highest levels of resistance and siRNA, with some plants showing no symptoms at all (Leibman et al., 2015; Tomar et al., 2018). However, this is

apparently dosage-dependent, as multiple studies have shown that resistance is inversely correlated with siRNA level and can be broken by high viral titer (Vanderschuren et al., 2009; Leibman et al., 2015). Furthermore, it has been described that the resistance is sequence dependent and only covers a single species of virus (Fuentes et al., 2016). This limits the use of the technology but does not preclude its application when the prevalent virus is a single species.

The recent advent of the clustered regularly interspaced short palindromic repeats (CRISPR)/Cas system has introduced new tools for generating resistance to geminiviruses. It has potential as a specific editing tool, and has shown to be effective against several different geminiviruses when expressed in plants (reviewed by Zaidi et al., 2016). In all cases, the presence of the Cas endonuclease and targeted short guide RNAs (sgRNAs) reduced viral titer and symptom development. Studies suggest that the level of Cas9 expression was a deciding factor in the level of symptom reduction (Baltes et al., 2015; Ji et al., 2015). Not only is this system effective in reducing geminivirus infection but confers multiple-virus resistance when the conserved nonanucleotide sequence was targeted. This was demonstrated in a dual infection with TYLCV and BCTV. (Ali et al., 2015).

CRISPR/Cas9 offers a great tool to integrate geminivirus resistance into susceptible plants, yet it is not perfect. Zhang et al. described in 2018 that their high-specificity gRNA was still showing off-target effects when expressed in *A. thaliana*. These were reduced by using a modified gRNA scaffold (expressing the gRNA adjacent to tRNA9met) and using the SpCas9 mutant (Zhang et al., 2018). Another unintended consequence of CRISPR-based viral resistance is the evolution of the virus to evade sgRNA. This adaptation renders the resistance useless (Mehta et al., 2019).

CONCLUSIONS

Although geminiviruses are very successful at infecting their hosts, plants also evolve to overcome or tolerate infection. Protective measures are introduced by humans as we seek to maintain our crop productivity. It is important to continue innovating to keep pace with the rapid viral evolution. Resistance based on DNA sequence is at a disadvantage as it relies on sequence to remain unchanged. These also tend to be very virus-specific, making it difficult to protect crops against mixed infections that are common. Antibody-based systems and peptide aptamers may hold better long-term resistance since they put more indirect evolutionary pressure on the geminivirus genome. Additionally, the peptide aptamers showed a broader base of effectiveness (Reyes et al., 2013), which may be effective at fighting mixed infections. Aptamers can be improved and mixed or re-designed using in silico approaches to increase its affinity. However, the long history of virus/host competitive evolution shows that protein-based resistance can still be overcome. To continue developing more resistant crops, we must gain a greater basic understanding of how these viruses infect the plants and how the plant responds to and harbors viral replication. An ideal resistance would prevent initial viral replication, eliminating the opportunity for the virus to evolve. Furthermore, a combinatorial or additive approach targeting both the virus and the vector may provide with a better opportunity to impair the infection and provide a longer lasting protection to crops.

AUTHOR CONTRIBUTIONS

JA-I conceived and supervised the review topics. KB wrote the first draft. All authors contributed to the article and approved the submitted version.

FUNDING

This work was partially funded by the Bill and Melinda Gates Foundation (CPT005698) and by the T&E Biochemistry Foundation.

ACKNOWLEDGMENTS

The authors thank Drs. Niki Robertson, Wei Shen, and Maria Reyes for the critical review of the manuscript. We also apologize to any authors and work that was not cited due to restrictions in the size of the manuscript.

REFERENCES

Akano, A. O., Dixon, A. G. O., Mba, C., Barrera, E., and Fregene, M. (2002). Genetic Mapping of a Dominant Gene Conferring Resistance to Cassava Mosaic Disease. *Theor. Appl. Genet.* 105 (4), 521–525. doi: 10.1007/s00122-002-0891-7

Ali, Z., Abulfaraj, A., Idris, A., Ali, S., Tashkandi, M., and Mahfouz, M. M. (2015). CRISPR/Cas9-Mediated Viral Interference in Plants. *Genome Biol.* 16, 238–248. doi: 10.1186/s13059-015-0799-6

Amrao, L., Amin, I., Shahid, M.S., Briddon, R. W., and Mansoor, S. (2010). Cotton Leaf Curl Disease in Resistant Cotton Is Associated with a Single Begomovirus That Lacks an Intact Transcriptional Activator Protein. *Virus Res.* 152 (1–2), 153–163. doi: 10.1016/j.virusres.2010.06.019

Anbinder, I., Reuveni, M., Azari, R., Paran, I., Nahon, S., Shlomo, H., et al (2009). Molecular Dissection of Tomato Leaf Curl Virus Resistance in Tomato Line TY172 Derived from Solanum Peruvianum. *Theor. Appl. Genet.* 119, 519–530. doi: 10.1007/s00122-009-1060-z

Aragão, F. J. L., Nogueira, E. O. P. L., Tinoco, M. L. P., and Faria, J. C. (2013). Molecular Characterization of the First Commercial Transgenic Common Bean Immune to the Bean Golden Mosaic Virus. *J. Biotechnol.* 166 (1–2), 42–50. doi: 10.1016/j.jbiotec.2013.04.009

Arguello-Astorga, G., Lopez-Ochoa, L., Kong, L.-J., Orozco, B. M., Settlage, S. B., and Hanley-Bowdoin, L. (2004). A Novel Motif in Geminivirus Replication Proteins Interacts with the Plant Retinoblastoma-Related Protein. *J. Virol.* 78 (9), 4817–4826. doi: 10.1128/JVI.78.9.4817-4826.2004

Ascencio-Ibáñez, J. T., Sozzani, R., Lee, T.-J., Chu, T.-M., Wolfinger, R. D., Cella, R., et al (2008). Global Analysis of Arabidopsis Gene Expression Uncovers a Complex Array of Changes Impacting Pathogen Response and Cell Cycle during Geminivirus Infection. *Plant Physiol.* 148 (1), 436–454. doi: 10.1104/pp.108.121038

Bairu, M. W., Aremu, A. O., and Staden, J. V. (2011). Somaclonal Variation in Plants: Causes and Detection Methods. *Plant Growth Regulation no* 63, 147–173. doi: 10.1007/s10725-010-9554-x

Baltes, N. J., Hummel, A. W., Konecna, E., Cegan, R., Bruns, A. N., Bisaro, D. M., et al (2015). Conferring Resistance to Geminiviruses with the CRISPR–Cas Prokaryotic Immune System. *Nat. Plants* 1 (10), 15145. doi: 10.1038/nplants.2015.145

Beyene, G., Chauhan, R. D., Wagaba, H., Moll, T., Alicai, T., Miano, D., et al (2016). Loss of CMD2-Mediated Resistance to Cassava Mosaic Disease in Plants Regenerated through Somatic Embryogenesis. *Mol. Plant Pathol.* 17 (7), 1095–1110. doi: 10.1111/mpp.12353

Blair, M. W., and Morales, F. J. (2008). "Geminivirus Resistance Breeding in Common Bean," in *CAB Reviews: Perspectives in Agriculture, Veterinary Science, Nutrition and Natural Resources*, (CABI Wallingford UK) vol. 3. doi: 10.1079/PAVSNNR20083089

Brustolini, O. J. B., Machado, J. P. B., Condori-Apfata, J. A., Coco, D., Deguchi, M., Loriato, V. A. P., et al (2015). Sustained NIK-Mediated Antiviral Signalling Confers Broad-Spectrum Tolerance to Begomoviruses in Cultivated Plants. *Plant Biotechnol. J.* 13 (9), 1300–1311. doi: 10.1111/pbi.12349

Buchmann, R.C., Asad, S., Wolf, J. N., Mohannath, G., and Bisaro, D. M. (2009). Geminivirus AL2 and L2 Proteins Suppress Transcriptional Gene Silencing and Cause Genome-Wide Reductions in Cytosine Methylation. *J. Virol.* 83 (10), 5005–5013. doi: 10.1128/JVI.01771-08

Butterbach, P., Verlaan, M. G., Dullemans, A., Lohuis, D., Visser, R. G.F., Bai, Y., et al (2014). Tomato Yellow Leaf Curl Virus Resistance by Ty-1 Involves Increased Cytosine Methylation of Viral Genomes and Is Compromised by Cucumber Mosaic Virus Infection. *Proc. Natl. Acad. Sci. United States America* 111 (35), 12942–12947. doi: 10.1073/pnas.1400894111

Castillo-González, C., Liu, X., Huang, C., Zhao, C., Ma, Z., Hu, T., et al (2015). Geminivirus-Encoded TrAP Suppressor Inhibits the Histone Methyltransferase SUVH4/KYP to Counter Host Defense. *ELife* 4, e06671. doi: 10.7554/eLife.06671

Chauhan, R. D., Beyene, G., and Taylor, N. J. (2018). Multiple Morphogenic Culture Systems Cause Loss of Resistance to Cassava Mosaic Disease. *BMC Plant Biol.* 18 (1), 132. doi: 10.1186/s12870-018-1354-x

Chellappan, P., Vanitharani, R., and Fauquet, C. M. (2004). Short Interfering RNA Accumulation Correlates with Host Recovery in DNA Virus-Infected Hosts, and Gene Silencing Targets Specific Viral Sequences. *J. Virol.* 78 (14), 7465–7477. doi: 10.1128/JVI.78.14.7465-7477.2004

Chowda-Reddy, R. V., Dong, W., Felton, C., Ryman, D., Ballard, K., and Fondong, V. N. (2009). Characterization of the Cassava Geminivirus Transcription Activation Protein Putative Nuclear Localization Signal. *Virus Res.* 145 (2), 270–278. doi: 10.1016/j.virusres.2009.07.022

Coursey, T., Regedanz, E., and Bisaro, D. M. (2018). Arabidopsis RNA Polymerase V Mediates Enhanced Compaction and Silencing of Geminivirus and Transposon Chromatin during Host Recovery from Infection. *J. Virol.* 92 (7), e01320–e01317. doi: 10.1128/JVI.01320-17

Czosnek, H., Hariton-Shalev, A., Sobol, I., Gorovits, R., and Ghanim, M. (2017). The Incredible Journey of Begomoviruses in Their Whitefly Vector. *Viruses* 9 (10), 273–291. doi: 10.3390/v9100273

Desvoyes, B., Ramirez-Parra, E., Xie, Qi, Chua, N. H., and Gutierrez, C. (2006). Cell Type-Specific Role of the Retinoblastoma/E2F Pathway during Arabidopsis Leaf Development. *Plant Physiol.* 140 (1), 67–80. doi: 10.1104/pp.105.071027

Duffy, S., and Holmes, E. C. (2008). Phylogenetic Evidence for Rapid Rates of Molecular Evolution in the Single-Stranded DNA Begomovirus Tomato Yellow Leaf Curl Virus. *J. Virol.* 82 (2), 957–965. doi: 10.1128/JVI.01929-07

Escobar-Bravo, R., Alba, J. M., Pons, C., Granell, A., Kant, M. R., Moriones, E., et al (2016). A Jasmonate-Inducible Defense Trait Transferred from Wild into Cultivated Tomato Establishes Increased Whitefly Resistance and Reduced Viral Disease Incidence. *Front. Plant Sci.* 7:1732:1732. doi: 10.3389/fpls.2016.01732

Eybishtz, A., Peretz, Y., Sade, D., Akad, F., and Czosnek, H. (2009). Silencing of a Single Gene in Tomato Plants Resistant to Tomato Yellow Leaf Curl Virus Renders Them Susceptible to the Virus. *Plant Mol. Biol.* 71 (1–2), 157–171. doi: 10.1007/s11103-009-9515-9

Eybishtz, A., Peretz, Y., Sade, D., Gorovits, R., and Czosnek, H. (2010). Tomato Yellow Leaf Curl Virus Infection of a Resistant Tomato Line with a Silenced Sucrose Transporter Gene LeHT1 Results in Inhibition of Growth, Enhanced Virus Spread, and Necrosis. *Planta* 231 (3), 537–548. doi: 10.1007/s00425-009-1072-6

Fondong, V. N. (2013). Geminivirus Protein Structure and Function. *Mol. Plant Pathol.* 14 (6), 635–649. doi: 10.1111/mpp.12032

Fregene, M., Bernal, A., Duque, M., Dixon, A., and Tohme, J. (2000). AFLP Analysis of African Cassava (Manihot Esculenta Crantz) Germplasm Resistant to the Cassava Mosaic Disease (CMD). *Theor. Appl. Genet.* 100, 678–685. doi: 10.1007/s001220051339

Fuentes, A., Carlos, N., Ruiz, Y., Callard, D., Anchez, Y., Ia, M., et al (2016). Field Trial and Molecular Characterization of RNAi-Transgenic Tomato Plants That Exhibit Resistance to Tomato Yellow Leaf Curl Geminivirus. *Mol. Plant-Microbe Interact.* 29 (3), 197–209. doi: 10.1094/MPMI-08-15-0181-R

Gill, U., Scott, J. W., Shekasteband, R., Ogundiwin, E., Schuit, C., Francis, D. M., et al (2019). Ty-6, a Major Begomovirus Resistance Gene on Chromosome 10, Is Effective against Tomato Yellow Leaf Curl Virus and Tomato Mottle Virus. *Theor. Appl. Genet.* 132 (5), 1543–1554. doi: 10.1007/s00122-019-03298-0

Guevara-Olvera, L., Ruíz-Nito, M. L., Rangel-Cano, R. M., Torres-Pacheco, I., Rivera-Bustamante, R. F., Muñoz-Sánchez, C. I., et al (2012). Expression of a Germin-like Protein Gene (CchGLP) from a Geminivirus-Resistant Pepper (Capsicum Chinense Jacq.) Enhances Tolerance to Geminivirus Infection in Transgenic Tobacco. *Physiol. Mol. Plant Pathol.* 78, 45–50. doi: 10.1016/J.PMPP.2012.01.005

Hanley-Bowdoin, L., Bejarano, E. R., Robertson, D., and Mansoor, S. (2013). Geminiviruses: Masters at Redirecting and Reprogramming Plant Processes. *Nat. Rev. Microbiol.* 11, 777–788. doi: 10.1038/nrmicro3117

Hong, Y., Saunders, K., Hartley, M. R., and Stanley, J. (1996). Resistance to Geminivirus Infection by Virus-Induced Expression of Dianthin in Transgenic Plants. *Virology* 220, 119–127. doi: 10.1006/viro.1996.0292

Huang, Y., Li, M.-Y., Wu, P., Xu, Z.-S., Que, F., Wang, F., et al (2016). Members of WRKY Group III Transcription Factors Are Important in TYLCV Defense Signaling Pathway in Tomato (Solanum Lycopersicum). *BMC Genomics* 17 (1), 788. doi: 10.1186/s12864-016-3123-2

Hulsmans, S., Rodriguez, M., Coninck, B. De, and Rolland, F. (2016). The SnRK1 Energy Sensor in Plant Biotic Interactions. *Trends Plant Sci.* 21 (8), 648–661. doi: 10.1016/J.TPLANTS.2016.04.008

Hutton, S. F., Scott, J. W., and Schuster, D. J. (2012). Recessive Resistance to Tomato Yellow Leaf Curl Virus from the Tomato Cultivar Tyking Is Located in the Same Region as *Ty*-5 on Chromosome 4. *HortScience* 47 (3), 324–327. doi: 10.21273/HORTSCI.47.3.324

Ismayil, A., Haxim, Y., Wang, Y., Li, H., Qian, L., Han, T., et al (2018). Cotton Leaf Curl Multan Virus C4 Protein Suppresses Both Transcriptional and Post-Transcriptional Gene Silencing by Interacting with SAM Synthetase. *PloS Pathog.* 14 (8), e1007282. doi: 10.1371/journal.ppat.1007282

Jeske, H., Lütgemeier, M., and Preiß, W. (2001). DNA Forms Indicate Rolling Circle and Recombination-Dependent Replication of Abutilon Mosaic Virus. *EMBO J.* 20 (21), 6158–6167. doi: 10.1093/emboj/20.21.6158

Jeske, H. (2009). "Geminiviruses," in *TT Viruses. Current Topics in Microbiology and Immunology*, vol. 331 . Eds. E. M. de Villiers and H. Hausen (Berlin, Heidelberg: Springer), 185–226. doi: 10.1007/978-3-540-70972-5_11

Ji, Y., Scott, J. W., Schuster, D. J., and Maxwell, D. P. (2009). Molecular Mapping of Ty-4, a New Tomato Yellow Leaf Curl Virus Resistance Locus on Chromosome 3 of Tomato. *J. Am. Soc. Hortic. Sci.* 134 (2), 281–288. doi: 10.21273/JASHS.134.2.281

Ji, X., Zhang, H., Zhang, Yi, Wang, Y., and Gao, C. (2015). Establishing a CRISPR–Cas-like Immune System Conferring DNA Virus Resistance in Plants. *Nat. Plants* 1 (10). 15144 doi: 10.1038/nplants.2015.144

Kong, L.-J., Orozco, B. M., Roe, J. L., Nagar, S., Ou, S., Feiler, H. S., et al (2000). A Geminivirus Replication Protein Interacts with the Retinoblastoma Protein through a Novel Domain to Determine Symptoms and Tissue Specificity of Infection in Plants. *EMBO J.* 19 (13), 3485–3495. doi: 10.1093/emboj/19.13.3485

Kumar, A., and Khan, J. A. (2019). "Geminivirus Resistance Strategies," in *Geminiviruses*. Ed. R. Kumar (Springer Nature Switzerland: Springer International Publishing), 197–218. doi: 10.1007/978-3-030-18248-9_11

Kumar, V., Mishra, S. K., Rahman, J., Taneja, J., Sundaresan, G., Sanan Mishra, N., et al (2015). Mungbean Yellow Mosaic Indian Virus Encoded AC2 Protein Suppresses RNA Silencing by Inhibiting Arabidopsis RDR6 and AGO1 Activities. *Virology* 486, 158–172. doi: 10.1016/J.VIROL.2015.08.015

Kumar, R.V. (2019). Plant Antiviral Immunity against Geminiviruses and Viral Counter-Defense for Survival. *Front. Microbiol.* 10 :1460:1460. doi: 10.3389/fmicb.2019.01460

Kuria, P., Ilyas, M., Ateka, E., Miano, D., Onguso, J., Carrington, J. C., et al (2017). Differential Response of Cassava Genotypes to Infection by Cassava Mosaic Geminiviruses. *Virus Res.* 227, 69–81. doi: 10.1016/J.VIRUSRES.2016.09.022

Lam, E. (2004). Controlled Cell Death, Plant Survival and Development. *Nat. Rev.* 5 (4), 305–315. doi: 10.1038/nrm1358

Lapidot, M., Karniel, U., Gelbart, D., Fogel, D., Evenor, D., Kutsher, Y., et al (2015). A Novel Route Controlling Begomovirus Resistance by the Messenger RNA Surveillance Factor Pelota. *PloS Genet.* 11 (10), e1005538. doi: 10.1371/journal.pgen.1005538

Laufs, J., Traut, W., Heyraud, F., Matzeit, V., Rogers, S. G., Schell, J., et al (1995). In Vitro Cleavage and Joining at the Viral Origin of Replication by the Replication Initiator Protein of Tomato Yellow Leaf Curl Virus. *Proc. Natl. Acad. Sci. United States America* 92, 3879–3883. doi: 10.1073/pnas.92.9.3879

Lee, K., and Seo, P. J. (2018). Dynamic Epigenetic Changes during Plant Regeneration. *Trends Plant Sci.* 23 (3), 235–247. doi: 10.1016/j.tplants.2017.11.009

Lee, G., Shim, H.-K., Kwon, M.-H., Son, S.-H., Kim, K.-Y., Park, E.-Y., et al (2013). A Nucleic Acid Hydrolyzing Recombinant Antibody Confers Resistance to Curtovirus Infection in Tobacco. *Plant Cell Tissue Organ Culture (PCTOC)* 115 (2), 179–187. doi: 10.1007/s11240-013-0357-4

Leibman, D., Prakash, S., Wolf, D., Zelcer, A., Anfoka, G., Haviv, S., et al (2015). Immunity to Tomato Yellow Leaf Curl Virus in Transgenic Tomato Is Associated with Accumulation of Transgene Small RNA. *Arch. Virol.* 160 (11), 2727–2739. doi: 10.1007/s00705-015-2551-7

León-Galván, F., De, A., Joaquín-Ramos, J., Torres-Pacheco, I., De La Rosa, A. P.B., Guevara-Olvera, L., et al (2011). A Germin-Like Protein Gene (CchGLP) of Capsicum Chinense Jacq. Is Induced during Incompatible Interactions and Displays Mn-Superoxide Dismutase Activity. *Int. J. Mol. Sci.* 12, 7301–7313. doi: 10.3390/ijms12117301

Li, F., Wang, Y., and Zhou, X. (2017). SGS3 Cooperates with RDR6 in Triggering Geminivirus-Induced Gene Silencing and in Suppressing Geminivirus Infection in Nicotiana Benthamiana. *Viruses* 9 (9). doi: 10.3390/v9090247

Liu, H., Boulton, M.II, Thomas, C. L., Prior, D. A. M., Oparka, K. J., and Davies, J. W. (1999). Maize Streak Virus Coat Protein Is Karyophyllic and Facilitates Nuclear Transport of Viral DNA. *Mol. Plant-Microbe Interact.* 12 (10), 894–900. doi: 10.1094/MPMI.1999.12.10.894

Lopez-Ochoa, L., Ramirez-Prado, J., and Hanley-Bowdoin, L. (2006). Peptide Aptamers That Bind to a Geminivirus Replication Protein Interfere with Viral Replication in Plant Cells. *J. Virol.* 80 (12), 5841–5853. doi: 10.1128/JVI.02698-05

Loriato, V. A. P., Martins, L. G. C., Euclydes, N. C., Reis, P. A. B., Duarte, C. E. M., and Fontes, E. P. B. (2020). Engineering Resistance against Geminiviruses: A Review of Suppressed Natural Defenses and the Use of RNAi and the CRISPR/Cas System. *Plant Sci.* 292:110410. doi: 10.1016/j.plantsci.2020.110410

Martins, L. G. C., Raimundo, G. A. S., Ribeiro, N. G. A., Silva, J. C. F., Euclydes, N. C., Loriato, V. A. P., et al (2020). A Begomovirus Nuclear Shuttle Protein-Interacting Immune Hub: Hijacking Host Transport Activities and Suppressing Incompatible Functions. *Front. Plant Sci.* 11:398. doi: 10.3389/fpls.2020.00398

Mathieu, O., and Bender, J. (2004). RNA-Directed DNA Methylation. *J. Cell Sci.* 117, 4881–4888. doi: 10.1242/jcs.01479

Mehta, D., Stürchler, A., Anjanappa, R. B., Zaidi, S. S.-e., Hirsch-Hoffmann, M., Gruissem, W., et al (2019). Linking CRISPR-Cas9 Interference in Cassava to the Evolution of Editing-Resistant Geminiviruses. *Genome Biol.* 20 (1), 80. doi: 10.1186/s13059-019-1678-3

Mejía-Teniente, L., Joaquin-Ramos, A., Torres-Pacheco, I., Rivera-Bustamante, R., Guevara-Olvera, L., Rico-García, E., et al (2015). Silencing of a Germin-Like Protein Gene (CchGLP) in Geminivirus-Resistant Pepper (Capsicum Chinense Jacq.) BG-3821 Increases Susceptibility to Single and Mixed Infections by Geminiviruses PHYVV and PepGMV. *Viruses* 7 (12), 6141–6151. doi: 10.3390/v7122930

Mendoza-Figueroa, J. S., Kvarnheden, A., Méndez-Lozano, J., Rodríguez-Negrete, E.-A., Arreguín-Espinosa De Los Monteros, R., and Soriano-García, M. (2018). A Peptide Derived from Enzymatic Digestion of Globulins from Amaranth Shows Strong Affinity Binding to the Replication Origin of Tomato Yellow Leaf Curl Virus Reducing Viral Replication in Nicotiana Benthamiana. *Pesticide Biochem. Physiol.* 145, 56–65. doi: 10.1016/j.pestbp.2018.01.005

Mills-Lujan, K., and Deom, C. M. (2010). Geminivirus C4 Protein Alters Arabidopsis Development. *Protoplasma* 239 (1–4), 95–110. doi: 10.1007/s00709-009-0086-z

Mori, T., Takenaka, K., Domoto, F., Aoyama, Y., and Sera, T. (2013). Inhibition of Binding of Tomato Yellow Leaf Curl Virus Rep to Its Replication Origin by Artificial Zinc-Finger Protein. *Mol. Biotechnol.* 54 (2), 198–203. doi: 10.1007/s12033-012-9552-5

Ndunguru, J., León, L. D., Doyle, C. D., Sseruwagi, P., Plata, G., Legg, J. P., et al (2016). Two Novel DNAs That Enhance Symptoms and Overcome CMD2 Resistance to Cassava Mosaic Disease. *J. Virol.* 90 (8), 4160–4173. doi: 10.1128/JVI.02834-15

Noris, E., Vaira, A. M., Caciagli, P., Masenga, V., Gronenborn, B., and Accotto, G. P. (1998). Amino Acids in the Capsid Protein of Tomato Yellow Leaf Curl Virus That Are Crucial for Systemic Infection, Particle Formation, and Insect Transmission. *J. Virol.* 72 (12), 10050–10057. doi: 10.1128/JVI.72.12.10050-10057.1998

Noueiry, A. O., Lucas, W. J., and Gilbertson, R. L. (1994). Two Proteins of a Plant DNA Virus Coordinate Nuclear and Plasmodesmal Transport. *Cell* 76 (5), 925–932. doi: 10.1016/0092-8674(94)90366-2

Okogbenin, E., Egesi, C. N., Olasanmi, B., Ogundapo, O., Kahya, S., Hurtado, P., et al (2012). Molecular Marker Analysis and Validation of Resistance to Cassava Mosaic Disease in Elite Cassava Genotypes in Nigeria. *Crop Sci.* 52 (6), 2576–2586. doi: 10.2135/cropsci2011.11.0586

Patil, B. L., and Fauquet, C. M. (2009). Cassava Mosaic Geminiviruses: Actual Knowledge and Perspectives. *Mol. Plant Pathol.* 10 (5), 685–701. doi: 10.1111/j.1364-3703.2009.00559.x

Patil, B. L., Kumar, L., Hema, M., Sreenivasulu, P., Kumar, P.L., and Reddy, D. V.R. (2014). Tropical Food Legumes: Virus Diseases of Economic Importance and Their Control. *Adv. Virus Res.* 90, 431–505. doi: 10.1016/B978-0-12-801246-8.00009-3

Picó, B., Díez, M. J., and Nuez, F. (1996). Viral Diseases Causing the Greatest Economic Losses to the Tomato Crop. II. The Tomato Yellow Leaf Curl Virus - A Review. *Scientia Hortic.* 67 (3–4), 151–196. doi: 10.1016/S0304-4238(96)00945-4

Raja, P., Wolf, J. N., and Bisaro, D. M. (2010). RNA Silencing Directed against Geminiviruses: Post-Transcriptional and Epigenetic Components. *Biochim. Biophys. Acta (BBA) - Gene Regul. Mech.* 1799 (3–4), 337–351. doi: 10.1016/J.BBAGRM.2010.01.004

Rey, M. E. C., and Fondong, V. N. (2018). "Mechanisms of Virus Resistance in Plants," in *Genes, Genetics and Transgenics for Virus Resistance in Plants*. Ed. B. L. Patil (Norfolk, UK: Caister Academic Press), 1–23. doi: 10.21775/9781910190814.01

Reyes, M.II, Nash, T. E., Dallas, M. M., Ascencio-Ibáñez, J.T., and Hanley-Bowdoin, L. (2013). Peptide Aptamers That Bind to Geminivirus Replication Proteins Confer a Resistance Phenotype to Tomato Yellow Leaf Curl Virus and Tomato Mottle Virus Infection in Tomato. *J. Virol.* 87 (17), 9691–9706. doi: 10.1128/JVI.01095-13

Reyes, M.II, Flores-Vergara, M. A., Guerra-Peraza, O., Rajabu, C., Desai, J., Hiromoto-Ruiz, Y. H., et al (2017). A VIGS Screen Identifies Immunity in the Arabidopsis Pla-1 Accession to Viruses in Two Different Genera of the Geminiviridae. *Plant J.* 92 (5), 796–807. doi: 10.1111/tpj.13716

Rodríguez-López, M. J., Garzo, E., Bonani, J. P., Fereres, A., Fernández-Muñoz, R., and Moriones, E. (2011). Whitefly Resistance Traits Derived from the Wild Tomato Solanum Pimpinellifolium Affect the Preference and Feeding Behavior of Bemisia Tabaci and Reduce the Spread of Tomato Yellow Leaf Curl Virus. *Virology* 101 (10), 1191. doi: 10.1094/PHYTO-01-11-0028

Rodríguez-Negrete, E. A., Carrillo-Tripp, J., and Rivera-Bustamante, R. F. (2009). RNA Silencing against Geminivirus: Complementary Action of Posttranscriptional Gene Silencing and Transcriptional Gene Silencing in Host Recovery. *J. Virol.* 83 (3), 1332–1340. doi: 10.1128/JVI.01474-08

Rojas, M. R., Jiang, H., Salati, R., Xoconostle-Cá, B., Sudarshana, M. R., Lucas, W. J., et al (2001). Functional Analysis of Proteins Involved in Movement of the Monopartite Begomovirus, Tomato Yellow Leaf Curl Virus. *Virology* 291, 110–125. doi: 10.1006/viro.2001.1194

Rojas, M. R., Macedo, M. A., Maliano, M. R., Soto-Aguilar, M., Souza, J. O., Rob, W., et al (2018). World Management of Geminiviruses. *Annu. Rev. Phytopathol.* 56 (1), 637–677. doi: 10.1146/annurev-phyto-080615-100327

Sade, D., Eybishtz, A., Gorovits, R., Sobol, I., and Czosnek, H. (2012). A Developmentally Regulated Lipocalin-like Gene Is Overexpressed in Tomato

Yellow Leaf Curl Virus-Resistant Tomato Plants upon Virus Inoculation, and Its Silencing Abolishes Resistance. *Plant Mol. Biol.* 80 (3), 273–287. doi: 10.1007/s11103-012-9946-6

Safarnejad, M. R., Fischer, R., and Commandeur, U. (2009). Recombinant-Antibody-Mediated Resistance against Tomato Yellow Leaf Curl Virus in Nicotiana Benthamiana. *Arch. Virol.* 154 (3), 457–467. doi: 10.1007/s00705-009-0330-z

Sahu, P. P., Sharma, N., Puranik, S., Chakraborty, S., and Prasad, M. (2016). Tomato 26S Proteasome Subunit RPT4a Regulates ToLCNDV Transcription and Activates Hypersensitive Response in Tomato. *Sci. Rep.* 6 (1), 1–12. doi: 10.1038/srep27078

Santos, A. A., Lopes, K. V. G., Apfata, J. A. C., and Fontes, E. P. B. (2010). NSP-Interacting Kinase, NIK: A Transducer of Plant Defence Signalling. *J. Exp. Bot.* 61 (14), 3839–3845. doi: 10.1093/jxb/erq219

Scott, J. W., Hutton, S. F., and Freeman, J. H. (2015). Fla. 8638B and Fla. 8624 Tomato Breeding Lines with Begomovirus Resistance Genes Ty-5 Plus Ty-6 and Ty-6, Respectively. *HortScience* 50 (9), 1405–1407. doi: 10.21273/HORTSCI.50.9.1405

Shen, Q., Liu, Z., Song, F., Xie, Qi, Hanley-Bowdoin, L., and Zhou, X. (2011). Tomato SlSnRK1 Protein Interacts with and Phosphorylates βC1, a Pathogenesis Protein Encoded by a Geminivirus β-Satellite. *Plant Physiol.* 157 (3), 1394–1406. doi: 10.1104/pp.111.184648

Shen, W., Dallas, M. B., Goshe, M. B., and Hanley-Bowdoin, L. (2014). SnRK1 Phosphorylation of AL2 Delays Cabbage Leaf Curl Virus Infection in Arabidopsis. *J. Virol.* 88 (18), 10598–10612. doi: 10.1128/JVI.00761-14

Shen, W., Bobay, B. G., Greeley, L. A., Reyes, M.II, Rajabu, C. A., Blackburn, R.K., et al (2018). Sucrose Nonfermenting 1-Related Protein Kinase 1 Phosphorylates a Geminivirus Rep Protein to Impair Viral Replication and Infection. *Plant Physiol.* 178 (1), 372–389. doi: 10.1104/pp.18.00268

Shivaprasad, P. V., Akbergenov, R., Trinks, D., Rajeswaran, R., Veluthambi, K., Hohn, T., et al (2005). Promoters, Transcripts, and Regulatory Proteins of Mungbean Yellow Mosaic Geminivirus. *J. Virol.* 79 (13), 8149–8163. doi: 10.1128/jvi.79.13.8149-8163.2005

Stanley, J., Frischmuth, T., and Ellwood, S. (1990). Defective Viral DNA Ameliorates Symptoms of Geminivirus Infection in Transgenic Plants. *Proc. Natl. Acad. Sci. United States America* 87 (16), 6291–6295. doi: 10.1073/PNAS.87.16.6291

Stenger, D. C. (1994). Strain-Specific Mobilization and AmpLification of a Transgenic Defective-Interfering DNA of the Geminivirus Beet Curly Top Virus. *Virology* 203 (2), 397–402. doi: 10.1006/VIRO.1994.1501

Sun, H., Chen, L., Li, J., Hu, M., Ullah, A., He, X., et al (2017). The JASMONATE ZIM-Domain Gene Family Mediates JA Signaling and Stress Response in Cotton. *Plant Cell Physiol.* 58 (12), 2139–2154. doi: 10.1093/pcp/pcx148

Sunter, G., and Bisaro, D. M. (1992). Transactivation of Geminivirus AR1 and BRI Gene Expression by the Viral AL2 Gene Product Occurs at the Leve1 of Transcription. *Plant Cell* 4, 1321–1331. doi: 10.1105/tpc.4.10.1321

Tomar, G., Chakrabarti, S. K., Sharma, N. N., Jeevalatha, A., Sundaresha, S., Vyas, K., et al (2018). RNAi-Based Transgene Conferred Extreme Resistance to the Geminivirus Causing Apical Leaf Curl Disease in Potato. *Plant Biotechnol. Rep.* 12 (3), 195–205. doi: 10.1007/s11816-018-0485-8

Trinks, D., Rajeswaran, R., Shivaprasad, P. V., Akbergenov, R., Oakeley, E. J., Veluthambi, K., et al (2005). Suppression of RNA Silencing by a Geminivirus Nuclear Protein, AC2, Correlates with Transactivation of Host Genes. *J. Virol.* 79 (4), 2517–2527. doi: 10.1128/jvi.79.4.2517-2527.2005

Vanderschuren, H., Alder, A., Zhang, P., and Gruissem, W. (2009). Dose-Dependent RNAi-Mediated Geminivirus Resistance in the Tropical Root Crop Cassava. *Plant Mol. Biol.* 70 (3), 265–272. doi: 10.1007/s11103-009-9472-3

Vanitharani, R., Chellappan, P., Pita, J. S., and Fauquet, C. M. (2004). Differential Roles of AC2 and AC4 of Cassava Geminiviruses in Mediating Synergism and Suppression of Posttranscriptional Gene Silencing Downloaded From. *J. Virol.* 78 (17), 9487–9498. doi: 10.1128/JVI.78.17.9487-9498.2004

Verlaan, M. G., Hutton, S. F., Ibrahem, R. M., Kormelink, R., Visser, R. G.F., Scott, J. W., et al (2013). The Tomato Yellow Leaf Curl Virus Resistance Genes Ty-1 and Ty-3 Are Allelic and Code for DFDGD-Class RNA–Dependent RNA Polymerases. *PloS Genet.* 9 (3), e1003399. doi: 10.1371/journal.pgen.1003399

Vinutha, T., Kumar, G., Garg, V., Canto, T., Palukaitis, P., Ramesh, S. V., et al (2018). Tomato Geminivirus Encoded RNAi Suppressor Protein, AC4 Interacts with Host AGO4 and Precludes Viral DNA Methylation. *Gene* 678, 184–195. doi: 10.1016/j.gene.2018.08.009

Voinnet, O., Pinto, Y. M., and Baulcombe, D. C. (1999). Suppression of Gene Silencing: A General Strategy Used by Diverse DNA and RNA Viruses of Plants. *Proc. Natl. Acad. Sci. United States America* 96 (24), 14147–14152. doi: 10.1073/PNAS.96.24.14147

Wang, H., Buckley, K. J., Yang, X., Buchmann, R.C., and Bisaro, D. M. (2005). Adenosine Kinase Inhibition and Suppression of RNA Silencing by Geminivirus AL2 and L2 Proteins. *J. Virol.* 79 (12), 7410–7418. doi: 10.1128/JVI.79.12.7410-7418.2005

Wang, B., Yang, X., Wang, Y., Xie, Y., and Zhou, X. (2018). Tomato Yellow Leaf Curl Virus V2 Interacts with Host Histone Deacetylase 6 To Suppress Methylation-Mediated Transcriptional Gene Silencing in Plants. *J. Virol.* 92 (18), e00036–e00018. doi: 10.1128/jvi.00036-18

Wang, Y., Jiang, J., Zhao, L., Zhou, R., Yu, W., and Zhao, T. (2018). Application of Whole Genome Resequencing in Mapping of a Tomato Yellow Leaf Curl Virus Resistance Gene. *Sci. Rep.* 8 (9592), JVI.00036–18. doi: 10.1038/s41598-018-27925-w

Wieczorek, P., and Obrępalska-Stęplowska, A. (2015). Suppress to Survive—Implication of Plant Viruses in PTGS. *Plant Mol. Biol. Rep.* 33 (3), 335–346. doi: 10.1007/s11105-014-0755-8

Yadav, R. K., and Chattopadhyay, D. (2011). Enhanced Viral Intergenic Region–Specific Short Interfering RNA Accumulation and DNA Methylation Correlates with Resistance Against a Geminivirus. *Mol. Plant-Microbe Interact.* 24 (10), 1189–1197. doi: 10.1094/MPMI-03-11-0075

Yamaguchi, H., Ohnishi, J., Saito, A., Ohyama, A., Nunome, T., Miyatake, K., et al (2018). An NB-LRR Gene, TYNBS1, Is Responsible for Resistance Mediated by the Ty-2 Begomovirus Resistance Locus of Tomato. *Theor. Appl. Genet.* 131 (6), 1345–1362. doi: 10.1007/s00122-018-3082-x

Yan, Z., Pérez-de-Castro, A., Díez, M. J., Hutton, S. F., Visser, R. G. F., Wolters, A. M. A., et al (2018). Resistance to Tomato Yellow Leaf Curl Virus in Tomato Germplasm. *Front. Plant Sci.* 9 (1198), 9–1198. doi: 10.3389/fpls.2018.01198

Yang, X., Caro, M., Hutton, S. F., Scott, J. W., Guo, Y., Wang, X., et al (2014). Fine Mapping of the Tomato Yellow Leaf Curl Virus Resistance Gene Ty-2 on Chromosome 11 of Tomato. *Mol. Breed.* 34 (2), 749–760. doi: 10.1007/s11032-014-0072-9

Zaidi, S. S.-e., Mansoor, S., Ali, Z., Tashkandi, M., and Mahfouz, M. M. (2016). Engineering Plants for Geminivirus Resistance with CRISPR/Cas9 System. *Trends Plant Sci.* 21 (4), 279–281. doi: 10.1016/J.TPLANTS.2016.01.023

Zaidi, S. S. e., Naqvi, R. Z., Asif, M., Strickler, S., Shakir, S., Shafiq, M., et al (2020). Molecular Insight into Cotton Leaf Curl Geminivirus Disease Resistance in Cultivated Cotton (Gossypium Hirsutum). *Plant Biotechnol. J.* 18 (3), 691–706. doi: 10.1111/pbi.13236

Zakri, A. M., Ziegler, A., Commandeur, U., Fischer, R., and Torrance, L. (2012). In Vivo Expression and Binding Activity of ScFv-RWAV, Which Recognizes the Coat Protein of Tomato Leaf Curl New Delhi Virus (Family Geminiviridae). *Arch. Virol.* 157 (7), 1291–1299. doi: 10.1007/s00705-012-1310-2

Zamir, D., Ekstein-Michelson, I., Zakay, Y., Navot, N., Zeidan, M., Sarfatti, M., et al (1994). Mapping and Introgression of a Tomato Yellow Leaf Curl Virus Tolerance Gene, TY-1. *Theor. Appl. Genet.* 88 (2), 141–146. doi: 10.1007/BF00225889

Zerbini, F.M., Briddon, R. W., Idris, A., Martin, D. P., Moriones, E., Navas-Castillo, J., et al (2017). ICTV Virus Taxonomy Profile: Geminiviridae. *J. Gen. Virol.* 98, 131–133. doi: 10.1099/jgv.0.000738

Zhang, Q., Xing, H.-L., Wang, Z.-P., Zhang, H.-Y., Yang, F., Wang, X.-C., et al (2018). Potential High-Frequency off-Target Mutagenesis Induced by CRISPR/Cas9 in Arabidopsis and Its Prevention. *Plant Mol. Biol.* 96 (4–5), 445–456. doi: 10.1007/s11103-018-0709-x

Conflict of Interest: The authors declare that the research was conducted in the absence of any commercial or financial relationships that could be construed as a potential conflict of interest.

frontiers in Plant Science

ORIGINAL RESEARCH
published: 31 July 2020
doi: 10.3389/fpls.2020.01155

Phosphorylations of the Abutilon Mosaic Virus Movement Protein Affect Its Self-Interaction, Symptom Development, Viral DNA Accumulation, and Host Range

Tatjana Kleinow, Andrea Happle, Sigrid Kober, Luise Linzmeier, Tina M. Rehm, Jacques Fritze, Patrick C. F. Buchholz, Gabi Kepp, Holger Jeske and Christina Wege*

Institute of Biomaterials and Biomolecular Systems, University of Stuttgart, Stuttgart, Germany

OPEN ACCESS

Edited by:
Alice Kazuko Inoue-Nagata, Brazilian Agricultural Research Corporation (EMBRAPA), Brazil

Reviewed by:
John Hammond, United States Department of Agriculture, United States
Jung-Youn Lee, University of Delaware, United States

****Correspondence:***
Tatjana Kleinow
tatjana.kleinow@bio.uni-stuttgart.de

Specialty section:
This article was submitted to Virology, a section of the journal Frontiers in Plant Science

Received: *19 March 2020*
Accepted: *15 July 2020*
Published: *31 July 2020*

Citation:
Kleinow T, Happle A, Kober S, Linzmeier L, Rehm TM, Fritze J, Buchholz PCF, Kepp G, Jeske H and Wege C (2020) Phosphorylations of the Abutilon Mosaic Virus Movement Protein Affect Its Self-Interaction, Symptom Development, Viral DNA Accumulation, and Host Range. Front. Plant Sci. 11:1155. doi: 10.3389/fpls.2020.01155

The genome of bipartite geminiviruses in the genus *Begomovirus* comprises two circular DNAs: DNA-A and DNA-B. The DNA-B component encodes a nuclear shuttle protein (NSP) and a movement protein (MP), which cooperate for systemic spread of infectious nucleic acids within host plants and affect pathogenicity. MP mediates multiple functions during intra- and intercellular trafficking, such as binding of viral nucleoprotein complexes, targeting to and modification of plasmodesmata, and release of the cargo after cell-to-cell transfer. For Abutilon mosaic virus (AbMV), phosphorylation of MP expressed in bacteria, yeast, and *Nicotiana benthamiana* plants, respectively, has been demonstrated in previous studies. Three phosphorylation sites (T221, S223, and S250) were identified in its C-terminal oligomerization domain by mass spectrometry, suggesting a regulation of MP by posttranslational modification. To examine the influence of the three sites on the self-interaction in more detail, MP mutants were tested for their interaction in yeast by two-hybrid assays, or by Förster resonance energy transfer (FRET) techniques *in planta*. Expression constructs with point mutations leading to simultaneous (triple) exchange of T221, S223, and S250 to either uncharged alanine (MP^{AAA}), or phosphorylation charge-mimicking aspartate residues (MP^{DDD}) were compared. MP^{DDD} interfered with MP-MP binding in contrast to MP^{AAA}. The roles of the phosphorylation sites for the viral life cycle were studied further, using plant-infectious AbMV DNA-B variants with the same triple mutants each. When co-inoculated with wild-type DNA-A, both mutants infected *N. benthamiana* plants systemically, but were unable to do so for some other plant species of the families Solanaceae or Malvaceae. Systemically infected plants developed symptoms and viral DNA levels different from those of wild-type AbMV for most virus-plant combinations. The results indicate a regulation of diverse MP functions by posttranslational modifications and underscore their biological relevance for a complex host plant-geminivirus interaction.

Keywords: geminivirus transport, host plant-virus interaction, plant-derived posttranslational modification, mutagenesis, Förster resonance energy transfer (FRET)

INTRODUCTION

Geminiviruses constitute an economically important group of plant-infecting viruses (Rojas et al., 2018; Garcia-Arenal and Zerbini, 2019). Their genomes consist of either one or two (DNA-A & DNA-B) circular single-stranded (ss) DNA molecules, which are packaged into uniquely shaped "geminate", i.e., double-icosahedral particles (Jeske, 2009; Hanley-Bowdoin et al., 2013; Hipp et al., 2017; Hesketh et al., 2018; Xu et al., 2019). Within nuclei of plant host cells, viral DNAs (vDNAs) replicate *via* double-stranded (ds) intermediates that adopt minichromosome organization (Pilartz and Jeske, 1992; Pilartz and Jeske, 2003; Jeske, 2009; Hanley-Bowdoin et al., 2013).

Based on the currently available data, it can be assumed that geminiviruses have developed manifold and redundant strategies for transferring newly replicated vDNA from the nucleus towards the cell periphery and across plasmodesmata into adjacent cells, as well as for vDNA long-distance spread *via* phloem tissues (Rojas et al., 2005; Wege, 2007; Jeske, 2009; Krenz et al., 2012; Hanley-Bowdoin et al., 2013). Depending on the gene composition within mono- or bipartite genomes of Old and New World geminiviruses, the portfolio of viral proteins mediating intra- and intercellular transport may vary (Jeske, 2009; Hanley-Bowdoin et al., 2013). It is generally accepted that monopartite geminiviruses utilize their coat protein (CP; V1) to shuttle vDNA between nuclei and cytoplasm, whereas bipartite members (in the genus *Begomovirus*) mainly employ the DNA-B-encoded nuclear shuttle protein NSP (NSP; BV1) for this task. Subsequent cytoplasmic trafficking of the nucleoprotein complexes towards and through plasmodesmata (PD) might be mediated primarily either by the pre-coat protein (PCP; [A]V2) in especially in monopartite virus species, or by the DNA-B encoded movement protein (MP; BC1) in bipartite ones. Among those, only Old World members express a PCP that could take over certain functions in cell-to-cell spread (Jeske, 2009). The PCP may be assisted in its action by the (A)C4 protein (Jupin et al., 1994; Rojas et al., 2001; Teng et al., 2010). Due to the lack of an *AV2* gene, begomoviruses of the New World, such as the Abutilon mosaic virus (AbMV), rely on their MP for intra- and intercellular trafficking. The nuclear shuttle function can be mediated by NSP or redundantly by CP in case of a defective NSP (Qin et al., 1998). Besides their coordinated action during viral spread, NSP and MP determine viral pathogenicity collaboratively (Rojas et al., 2005; Zhou et al., 2007; Jeske, 2009; Hanley-Bowdoin et al., 2013).

Geminivirus genomes have a limited coding capacity (five to eight genes) causing a strong dependency on host cellular processes and factors for propagation and systemic invasion of host tissues. The viral proteins fulfill multiple functions and interact in a highly coordinated manner with a variety of plant proteins. The membrane-associated MPs of bipartite begomoviruses are prime examples in this regard. They enable for instance the targeting of viral transport complexes to PD, modify PDs in order to allow passage, and release the infectious cargo after successful cell-to-cell transfer (Jeske, 2009; Krenz et al., 2012; Hanley-Bowdoin et al., 2013). Some MP interacting host proteins have been discovered: histone H3 (Zhou et al., 2011), a synaptotagmin (Lewis and Lazarowitz, 2010), and a chaperone, i.e., the heat shock cognate 70kDa protein cpHSC70-1 (Krenz et al., 2010). Such multifaceted properties do not only apply to geminiviral proteins, but are characteristic of many membrane-targeted proteins of various virus species that can frequently self-interact, and bind other viral proteins and host factors (Laliberte and Sanfacon, 2010; Laliberte and Zheng, 2014).

For AbMV MP, selected as a model in our study, several of these features have been described. MP and NSP cooperate for intra- and intercellular traffic (Zhang et al., 2001). Self-interaction of MP *via* its C-terminal domain was demonstrated in yeast systems (Frischmuth et al., 2004), and for the full-length MP *in planta* by bimolecular fluorescence complementation (BiFC) and Förster resonance energy transfer (FRET) techniques (Happle et al., submitted; Krenz et al., 2010). Membrane association is mediated by the central part of the protein (named anchor domain; **Figure 1A**) as uncovered *in planta* by studying the subcellular localization of green fluorescent protein (GFP)-tagged MP deletion mutants (Zhang et al., 2002). Computer-based analysis predicted an amphiphilic helix structure for this domain, suggesting the MP is a monotopic membrane protein with N- and C-termini located at the cytoplasmic membrane face, as shown in fission yeast by freeze-fracture immunolabeling in both the plasma membrane and microsomes (Aberle et al., 2002; Frischmuth et al., 2004). High resolution fluorescence and electron microscopy-based analysis of either fluorescent protein- or epitope-tagged MP confirmed its localization at the plasma membrane and plasmodesmata of plant cells (Happle et al., submitted; Zhang et al., 2001; Kleinow et al., 2009c). Additionally, the MP was found surrounding nuclei, associated with chloroplasts, and clustered in mobile vesicle-like structures, with the latter most likely representing microsomes trafficking *via* the endoplasmic reticulum (ER)/actin network (Happle et al., submitted; Zhang et al., 2001; Krenz et al., 2010).

Upon systemic infection of a permissive host, vDNA passes through various stages of replication, transcription, transport, and encapsidation, which need to be temporally organized. It can be expected that in the course of these processes, the viral MPs need to switch between several functional options in order to regulate their subcellular distribution and control distinct protein-protein interactions. Posttranslational modifications (PTMs) and especially sequence-specific and reversible phosphorylation play important regulatory roles in many processes in plants, e.g. in subcellular localization, stability and interaction of proteins, metabolic regulation, defense signal transduction, RNA and carbon metabolism (Link et al., 2011; Burch-Smith and Zambryski, 2012; Lofke et al., 2013; Nemes et al., 2017; Ott, 2017; Arsova et al., 2018; Perraki et al., 2018; Zhukovsky et al., 2019). Accordingly, numerous examples of specific PTMs were uncovered to regulate plant endogenous macromolecular trafficking and viral spread (Lee and Lucas, 2001; Waigmann et al., 2004; Lee et al., 2005; Taoka et al.,

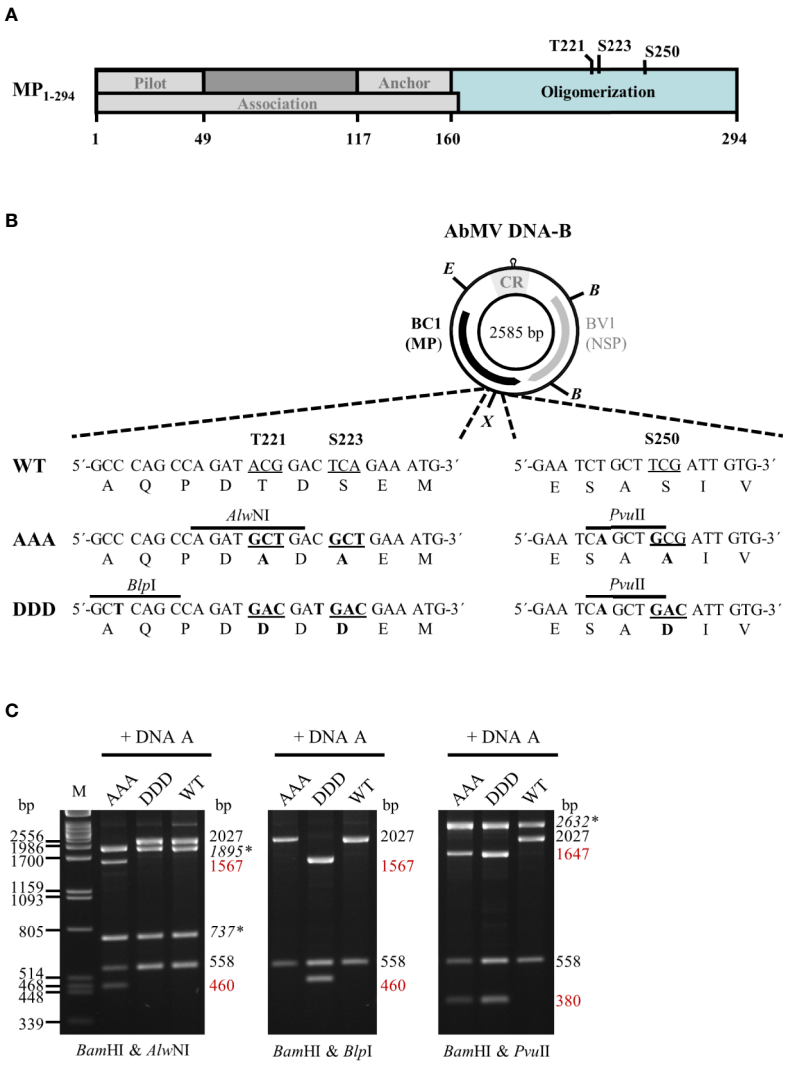

FIGURE 1 | (A) Schematic overview of previously described functional regions and phosphorylation sites identified within full-length AbMV MP (Zhang et al., 2001; Frischmuth et al., 2004; Kleinow et al., 2009b; Krenz et al., 2010; Krapp et al., 2017). **(B)** Schematic representation of the organization of DNA-B encoding the movement protein (MP; BC1) and the nuclear shuttle protein (NSP; BV1). *Eco* RV (E) and *Xba* I (X) sites used for cloning of DNA-B versions with triple phosphorylation site mutations [T221, S223, and S250 exchanged against alanine (AAA) or aspartate (DDD)] for MP are indicated. Details of the site-directed mutagenesis (nucleotide and amino acid changes shown in bold) and newly introduced mutagenesis-specific restriction sites are depicted below. CR: common region; B: *Bam* HI **(C)** Representative RCA-RFLP analysis using *Bam* HI combined with either of the mutagenesis-specific restriction enzymes to monitor the presence of DNA-A and DNA-B variants within total nucleic acids from infected plants (Kleinow et al., 2009b). Sizes of expected fragments are indicated. DNA-A-derived fragments are labelled (italics and asterisks), with those specifically originating from mutagenesis within *BC1* displayed in red. RCA-RFLP analysis was carried out for all samples out of the experiments listed in **Tables 1** and **2**.

2007; Amari et al., 2010). Phosphorylation is the most widespread one, identified in proteins of distinct plant DNA- and RNA-viruses. Several MPs of the 30K family (Melcher, 2000), to which the geminiviral MPs belong, were shown to appear as phosphoproteins *in planta* (Waigmann et al., 2004; Kleinow et al., 2009b; Nemes et al., 2017; and references therein). Well studied examples in the 30K family are MPs of the tobamoviruses tobacco mosaic virus (TMV) and tomato mosaic virus (ToMV), for which roles of phosphorylation in modulation of RNA affinity, subcellular distribution, membrane association, plasmodesmata targeting, and transport activity have been delimited (Karpova et al., 1999; Kawakami et al., 1999; Karger et al., 2003; Waigmann et al., 2004; Trutnyeva et al., 2005; Fujiki et al., 2006). For bipartite begomoviruses, however, studies on the incidence of PTMs and their putative regulatory impact on MPs are scarce. A phosphorylation of MPs was uncovered by metabolic labelling experiments for squash leaf curl virus in insect cells (Pascal et al., 1994), for AbMV in bacteria and yeast (Wege and Jeske, 1998; Kleinow et al., 2008) and by *in vitro* phosphorylation assays using a plasmodesmal-associated protein kinase for bean dwarf mosaic virus (BDMV) (Lee et al., 2005). In addition, phosphorylation on serine and

threonine residues *in planta* could be shown for AbMV MP by Western blot analysis using phospho-amino acid-specific antibodies (Kleinow et al., 2009b). Follow-up work identified three phosphorylation sites, T221, S223, and S250 (**Figure 1A**) within the oligomerization domain of AbMV MP that are each differentially important for symptom development and vDNA accumulation in *Nicotiana benthamiana* Domin (Kleinow et al., 2009b), indicating a functional role of the phosphorylation status at these positions, and a possible effect on intra- and intercellular spread of the virus. The biological relevance of the three sites was examined by introducing point mutations into the MP gene of infectious DNA-B clones, in order to compare the "constant-off of charge" (replacement by uncharged alanine residues) or the "constant-on of charge" status of the negative charges (replacement by aspartate residues) with the regulated wild-type (WT) function for the three MP amino acid positions (Kleinow et al., 2009b).

In the previously described experiments (Kleinow et al., 2009b), single and double mutants were compared. Five out of the six tested combinations of DNA-A with DNA-B variants for T221 and/or S223 enhanced symptoms, and three out of these five elevated the steady-state vDNA content as well. Only the combination of DNA-A & DNA-B S223A did not alter symptoms considerably in comparison to AbMV^{WT}, although the vDNA level was reduced. At amino acid position S250, both mutations attenuated symptom development and reduced the vDNA titer. Overall, the results showed that the respective phosphorylation sites may trigger opposite effects, with intensifying (T221 and S223) or weakening (S250) AbMV pathogenicity.

To further examine the complexity of the differential MP phosphorylation, we have generated AbMV DNA-Bs encoding MPs with triple mutations of the phosphorylation sites, and analyzed their effects on systemic virus infections in plants. In order to detect possible host-dependent differences, a number of plant species has been included. The localization of the mutations within the MP oligomerization domain may suggest an impact of the phosphorylation status on self-interaction, which was analyzed using the yeast two-hybrid system and a FRET measurement approach *in planta*.

MATERIALS AND METHODS

Cloning Procedure

AbMV DNA-B variants encoding triple phosphorylation site mutations of MP (Uniprot P21946) [T221A/S223A/S250A (MP^{AAA}) or T221D/S223D/S250D (MP^{DDD})] were generated by a Phi29 polymerase-based rolling circle amplification (RCA) strategy and thereby a cell-free cloning approach, which preserves the quasi-species nature of geminiviral DNAs (Jeske et al., 2010; Jeske, 2018). DNA-Bs encoding single or double phosphorylation site MP mutants (T221A/S223A, S250A, T221D/S223D or S250D) (Kleinow et al., 2009b) were amplified by RCA from total nucleic acids isolated *via* a CTAB-based extraction protocol (2.3) from *N. benthamiana* systemically infected with the respective AbMV mutant version (Kleinow et al., 2009b). The RCA products were cut by *Eco* RV and *Xba* I according to supplier´s recommendation (New England Biolabs, Ipswich, MA, USA). The resulting two 1,726 bp-fragments comprising mutated sites T221A/S223A or T221D/S223D, and the two 859 bp-fragments including the position encoding for S250A or S250D (**Figure 1**) were gel-purified. To create MP^{AAA}- or MP^{DDD}-DNA-B variants, the DNA fragments harboring double mutations at T221 and S223 were ligated with those comprising the appropriate S250 mutant. For purification of the desired DNA-B types, molecules circularized by ligation were RCA-amplified and digested with the mutant-specific restriction enzyme *Pvu* II (**Figure 1**). Linearized DNA-B fragments were gel-purified, again re-ligated to circular DNAs and amplified by RCA. The correctness of the obtained DNA-B variants was confirmed by restriction analysis using *Bam* HI in combination with either of the three mutant-specific restriction enzymes (*Alw* NI, *Blp* I and *Pvu* II; **Figure 1**) and direct sequencing of RCA products (Schubert et al., 2007). DNA-Bs confirmed to encode either MP^{AAA} or MP^{DDD} were used for biolistic plant inoculation (2.2).

Two-hybrid expression constructs were obtained by Gateway cloning (ThermoFisher Scientific/Invitrogen, Carlsbad, CA, USA). To create entry vectors containing partial *MP* genes coding for the oligomerization domain (BC1-CD; **Figure 1A**) with triple exchanges at positions T221, S223, and S250 against either aspartate (DDD) or alanine (AAA) residues, a PCR-based site-directed mutagenesis strategy using back-to-back orientated primers according to Kleinow et al. (2009b) was applied. Briefly, in each of the various primer pairs used for amplification, one primer introduced the intended mutation and an additional unique restriction site for selection (**Figure 1B**) (Kleinow et al., 2009b). The vector pENTR11-BC1-CD^{WT} (**Supplementary Table S1**) was subjected to two rounds of mutagenesis PCR (a first round introducing changes at positions T221 and S223, and a second one for additional replacement at amino acid position S250) to yield triple mutants. All PCR products were gel-purified, their 5´-ends phosphorylated, re-ligated to obtain circular plasmids and transformed into *Escherichia coli* (DH5α; ThermoFisher Scientific/Invitrogen). Plasmid DNAs from the resulting clones were subjected to mutant-specific restriction analysis and sequencing. From correct entry constructs containing *BC1-CD^{DDD}* or *BC1-CD^{AAA}*, these DNA fragments were recombined by LR reactions into the Gateway-compatible yeast two hybrid vectors pcACT2 (Leu$^+$; N-terminal fusion to Gal4 activation domain [GAD]::hemagglutinin epitope (HA) yielding GAD::HA::BC1-CD$^{DDD/AAA}$) and pAS2-1 (Trp$^+$; N-terminal fusion to Gal4 DNA binding domain [GBD] yielding GBD::BC1-CD$^{DDD/AAA}$). Other two-hybrid constructs used in this study were described previously (Kleinow, 2000; Frischmuth et al., 2004).

In planta expression constructs of MP variants for analyzing subcellular co-localization and protein interactions by FRET were prepared *via* a Gateway recombination-based two-in-one-vector system (Hecker et al., 2015). Genes encoding full-length MP^{WT}, MP^{AAA} or MP^{DDD} from respective pDONR207-BC1 templates were PCR-amplified (1 min at 98°C, 30 cycles of 10 s at 98°C, 30 s at 54°C, and 1 min at 72°C followed by 5 min at

72°C) using Q5 polymerase (New England Biolabs) with primer pairs adding either attB1 & attB4, or attB3 & attB2 sites, respectively, to produce ends applicable in the Gateway recombination system (ThermoFisher Scientific/Invitrogen) (for templates and primers see **Supplementary Table S1**). All ORFs were amplified in two versions, i.e., with and without stop codon to allow later expression in N- as well as C-terminal fusion to a fluorescent reporter protein. The four different PCR products per MP type were purified (PCR purification kit, Qiagen, Hilden, Germany) and introduced *via* a BP reaction into the compatible pDONR221 vector (pDONR221-P1P4 for attB1 and attB4-containing fragments, or pDONR221-P3P2 for attB3- and attB2-harboring fragments) (Hecker et al., 2015) according to manufacturer´s recommendations (ThermoFisher Scientific/Invitrogen). The various entry constructs were confirmed by restriction analysis and sequencing. Verified *MP* genes were transferred by LR reactions into the compatible binary FRET expression vectors (molar ratio of vector to entry clones of 1:3:3; Grefen and Blatt, 2012; Hecker et al., 2015). The vectors allow from one T-DNA dual expression of the test proteins in four different combinations of either N- or C-terminal fusions to the FRET fluorophore pair monomeric Venus (mVenus; acceptor) and monomeric Turquoise2 (donor) (pFRETtv-2-in-1 -NN: both N-terminal, pFRETtv-2-in-1 -NC: C-terminal mVenus & N-terminal mTurquoise2, pFRETtv-2-in-1 -CN: N-terminal mVenus & C-terminal mTurquoise2 or pFRETtv-2-in-1 -CC: both C-terminal). After confirmation by restriction analysis and sequencing, the resulting FRET expression constructs were introduced into chemically competent *Agrobacterium tumefaciens* GV3101 (pMP90) (Koncz et al., 1994) *via* transformation. Construct integrity in agrobacteria was rechecked by colony PCR.

Plant Material and Infection

Plants of *N. benthamiana*, *Malva parviflora* L., *Datura stramonium* L., and *Nicandra physaloides* L. were cultivated in an insect-free biosafety S2 containment greenhouse with supplementary lighting (100 kW/h, 16 h photoperiod at 25°C and a night-time reduction to 20°C) at 60% rel. humidity.

Plants were inoculated with RCA products of DNA-A mixed with RCA products of the respective DNA-Bs (2.1) in a four leaf-stage using particle bombardment as described previously (Kleinow et al., 2009b). AbMV DNA-A (X15984) RCA products for inoculation were amplified from *N. benthamiana* plants confirmed to be systemically infected with DNA-A alone following agro-inoculation (Evans and Jeske, 1993; Kleinow et al., 2009b). Plants inoculated with either gold microcarriers devoid of DNA, or with DNA-B^{WT} alone served as mock-treated controls. All RCA inocula applied in this study were generated using the same template and polymerase source, and were prepared in sufficient amounts to conduct at minimum two completely independent infection experiments per batch. Each inoculum batch was verified by RCA-restriction fragment length polymorphism (RCA-RFLP) testing and direct sequencing (2.4). In total, nine independent experiments were carried out for *N. benthamiana*, and for the other plant species at minimum four experiments (**Tables 1** and **2**). For the host *N. benthamiana*, RCA products from plants systemically infected with AbMV variants encoding either MP^{AAA} or MP^{DDD} were passaged by biolistic inoculation to a secondary set of *N. benthamiana* (four plants per selected sample). Three independent viral progenies per AbMV triple mutant type were subjected to these secondary infection experiments. All plants were evaluated for symptom development weekly and tested for infection with the proper AbMV variant as described below (2.3 and 2.4).

TABLE 1 | Infectivity and symptom phenotype classification of AbMV DNA-B encoded MP phosphorylation site mutants in *N. benthamiana*.

AbMV DNA-B variant[i]	No. of plants (8 expts.)		Infection rate (%)	Symptom class (no. of plants)[iii]				
	Inoculated	Infected		0	I	II	III	IV
Mock-treated	32	0	0					
WT	41[ii]	41	100	0	0	41	0	0
T221A/S223A[iv]	26	20	77	0	1	4	4	11
S250A[iv]	27	18	67	0	12	4	2	0
T221A/S223A/S250A	54[ii]	52	96	40	12	0	0	0
T221D/S223D[iv]	30	22	73	0	3	2	2	15
S250D[iv]	27	21	78	0	13	3	4	1
T221D/S223D/S250D	54[ii]	51	94	0	2	31	8	10

[i] *DNA-B variants were co-inoculated with AbMV DNA-A^{WT}.*
[ii] *Including an additional ninth passage experiment (virus progenies from three independent primary-inoculated plants were used as inoculum for a secondary set of plants [for each inoculum four plants]); per triple mutant variant in total 42 primary (eight experiments [expts.]) and 12 secondary-inoculated plants (one expt.), and for WT in total 29 primary-(eight expts.) and 12 secondary-inoculated plants (one expt.).*
[iii] *AbMV symptoms (stunting, yellow-green leaf mosaic and leaf deformation) were classified as follows: class 0: all features significantly milder than WT, nearly symptomless; class I: one to two features significantly milder than WT; class II: similar to WT; class III: at least one feature significantly more intense than WT; class IV: two to three features significantly more severe than WT.*
[iv] *Single and double mutants used as a reference were characterized previously in Kleinow et al. (2009b).*

TABLE 2 | Infectivity of AbMV DNA-B encoding MP phosphorylation site mutants in various host plants.

Host plant species	No of expts.	AbMV DNA-B variant[i]	No. of plants		Infection rate (%)
			Inoculated	Infected	
Nicotiana benthamiana (Solanaceae)	9	Mock-treated	32	0	0
		WT	41	41	100
		AAA	54	52	96
		DDD	54	51	94
Malva parviflora (Malvaceae)	5	Mock-treated	15	0	0
		WT	67	37	55
		AAA	188	0[ii]	0[ii]
		DDD	108	24	22
Datura stramonium (Solanaceae)	5	Mock-treated	15	0	0
		WT	45	20	44
		AAA	66	27	41
		DDD	70	0[ii]	0[ii]
Nicandra physaloides (Solanaceae)	4	Mock-treated	12	0	0
		WT	33	16	48
		AAA	75	9	12
		DDD	63	13	21

[i] *DNA-B variants were co-inoculated with AbMV DNA-A^{WT}.*
[ii] *No systemic infection.*

Extraction of Total Nucleic Acids From Plants

100 mg leaf tissue from newly emerged sink leaves were collected and total nucleic acids (TNA) were extracted by a cetyltrimethylammonium bromide (CTAB)-based protocol according to Kleinow et al. (2009b). All plants (see 2.2, **Tables 1** and **2**) were harvested for TNA preparation and RCA-RFLP testing at 21 and 45 days post-inoculation (2.4). Samples from the independent experiments (see 2.2, **Tables 1** and **2**) from solanaceous hosts, for which a systemic infection with the respective AbMV variant was confirmed, were subjected to semi-quantitative Southern blot analysis at the time points indicated.

RCA-RFLP Analysis and Direct Sequencing of RCA Products

AbMV circular DNA molecules in TNA samples (2.3) served as templates for RCA *via* a TempliPhi DNA amplification kit (GE Healthcare/Amersham Biosciences, Uppsala, Sweden) as described previously (Kleinow et al., 2009b; Jeske, 2018). The presence of the desired AbMV variants in the products was confirmed by RFLP analysis using MP mutant-specific restriction enzymes (*Alw* NI, *Blp* I or *Pvu* II) combined with *Bam* HI (**Figure 1**)(Kleinow et al., 2009b). Additionally, the integrity of each DNA-B encoded MP version was verified by direct sequencing of the RCA products (Schubert et al., 2007).

Semi-Quantitative Southern Blot Analysis of the vDNA Content

TNA (1 µg) extracted from test plants (2.3) were subjected to semi-quantitative Southern blot analysis with DNA-A- and DNA-B-specific DNA probes. Sample separation on an agarose gel, blotting onto nylon membranes, hybridization, chemiluminescent detection of the digoxigenin (DIG)-labelled probes, quantification, and stripping of membranes for re-probing were carried out as detailed earlier (Kleinow et al., 2009b). Numbers of independent experiments are stated in 2.2 and 2.3.

Detection of Protein Interactions in Yeast Two-Hybrid Assays

Yeast two-hybrid analysis using the GAL4-based Matchmaker System (BD Biosciences/Clontech, Palo Alto, CA, USA) were performed as specified (Kleinow et al., 2009a; Krenz et al., 2010). Briefly, yeast two-hybrid expression constructs for GAD::HA fusion proteins (pcACT2 or pACT2 Leu^+) were transformed into *Saccharomyces cerevisiae* strain Y190 (MATa) and those for GBD fusion proteins (pAS2-1, Trp^+) into strain Y187 (MATα) using a LiCl-based protocol. Transformants were selected on synthetic defined (SD) minimal medium plates lacking either Leu or Trp for three to five days at 30°C. Both plasmids were then combined in yeast cells by mating according to the Matchmaker system manual (BD Biosciences/Clontech). Protein interaction was monitored by activation of the reporter genes encoding yeast imidazoleglycerolphosphate dehydratase (HIS3) and bacterial β-galactosidase (lacZ). A colony-lift filter assay was used to test yeast cells grown on SD medium plates depleted for both Leu & Trp (selection for both plasmids) and additionally on plates lacking Leu, Trp & His supplemented with 50 mM 3-amino-triazole (3-AT; His3 activation test, Matchmaker system manual) for β-galactosidase activity. The presence of GAD::HA and GBD fusion proteins was confirmed by Western blot analysis (2.9; **Figure 6**). In total three independent experiments were performed. Each of those included as a positive control the construct GBD::At1g79160 (*Arabidopsis thaliana*), which activates the reporter genes autonomously, and as a negative control GAD::HA and GBD fusions of At3g27500 (*A. thaliana*) (Kleinow, 2000). In total, three independent mating assays and subsequent colony-lift filter tests were carried out.

Transient Expression of AbMV MP in *N. benthamiana*

For transient expression, binary FRET constructs (2.1) were agro-infiltrated at an agrobacterium concentration of OD_{600nm} 0.25 into fully expanded third to fourth leaves of three-weeks old *N. benthamiana* plants according to Schütze et al. (2009). To optimize protein yield, a 35S promoter-driven expression construct for the p19 silencing suppressor of Cymbidium ringspot virus (Silhavy et al., 2002) was co-infiltrated (same agrobacteria concentration as for FRET constructs). Fluorescence microscopy and FRET analysis was performed at three days post agrobacteria infiltration (dpai). Presence of mVenus and mTurquoise2 fusion proteins was confirmed by Western blot analysis and in-gel fluorescence detection (2.9; **Supplementary Figure S1**).

Live-Cell Imaging to Monitor Subcellular Localization and Detection of Protein Interactions *In Planta* by Acceptor Photobleaching-FRET Analysis

For microscopic investigations, leaf discs (diameter 1 cm) were collected from agro-infiltrated *N. benthamiana* plants and infiltrated with perfluorodecalin (PFD) for enhanced optical resolution (Littlejohn et al., 2010). Samples were mounted onto glass slides and sealed with cover slips. High resolution fluorescence microscopy was carried out with an inverted confocal Zeiss AxioObserver CSU-X1 Spinning Disk Unit with UGA-42-Firefly point scanning device (ZEISS Oberkochen, Germany; Rota Yokogawa GmbH & Co. KG, Wehr, Germany; Rapp OptoElectronic GmbH, Wedel, Germany). Collection of fluorescence intensities for FRET analysis and inspection of the subcellular localization of mTurquoise2- and mVenus-tagged proteins was done with the following microscope settings: Fluorescence of the donor mTurquoise2 was obtained with a 445 nm diode excitation laser combined with 485/30 nm emission filter. The acceptor mVenus was excited with a 514 nm laser, and fluorescence recorded upon use of a 562/45 nm emission filter. Images were acquired using an Axiocam 503 mono (CCD) camera in 2x2 binning mode. Bleaching was performed for an area nearly equivalent to the field of view (excluding only a small outer edge, **Figure 7A**), using an accessory high-intensity 514 nm bleaching laser device,

purpose-built for specimen photomanipulation (UGA-42-Firefly point scanning device). 60% laser intensity was applied for ca. 50 s to ensure uniform mVenus bleaching. This bleaching set-up was applied in all experiments to minimize fluorescence recovery within the analyzed area. Fluorescence intensities of mVenus were recorded before and after the bleaching treatment for follow-up evaluation of bleaching efficiencies. A representative example of fluorescence micrographs imaged before and after specific bleaching of mVenus (acceptor) is shown in **Figure 7A**. To quantify FRET signals, the intensity of donor (mTurquoise2) fluorescence was evaluated prior to, and after acceptor photobleaching (**Figure 7A**). Recording of the overall FRET data set for mTurquoise2 and mVenus fluorescence before and after bleaching took around 55 sec per cell. To discrimnate occasional randomly occurring FRET signals from those caused by specific MP-MP interaction, a reference control for background FRET, which may result, e.g., from random accumulation of test proteins in certain membrane domains and thereby close proximity to each other, was applied. Such random FRET events were monitored by the combination of a plasma membrane-targeted soluble N-ethylmaleimide-sensitive-factor attachment receptor (SNARE) protein (*A. thaliana* SYP122; mVenus::SYP122) (Uemura et al., 2004) with mTurquoise::MP^{WT} (Happle et al., submitted). Both were expressed in *N. benthamiana* and analyzed in the same set-up. Only those FRET data sets of MP-MP tests were considered as positive that were significantly different from this control data set (statistical analysis by non-parametric Kruskal-Wallis test followed by Dunn's multiple comparison of ranks). By applying this stringent baseline, the risk of false-positive results was minimized. The previously confirmed self-interaction of MP^{WT} (Krenz et al., 2010) served as a positive control. For each test combination, leaves of three plants were infiltrated per experiment, and at minimum three independent experiments conducted. For each test combination, ten cells were analyzed from every experiment, resulting in a data set of at least 90 cells/images for subsequent evaluation. For each of these cells/images, fluorescence intensities of donor and acceptor were measured in ten squared regions of interest (ROIs; size each 3.1623 × 3.1623 μm [= 10 μm^2]; example shown in **Figure 7B**), along the plasma membrane/cell periphery, at identical positions and within the central part of the area used for acceptor bleaching, in images captured a second before and a second after photobleaching using Fiji (Image J) (Schindelin et al., 2012). Mean fluorescence intensities (F) after background subtraction, and effectiveness of bleaching and FRET efficiencies ($FRET_{eff}$) were calculated using MS Excel (V 16.34) and Graphpad Prism (V8) for Mac. Data of cells with less than 90% bleach efficiency were excluded from the following evaluation. $FRET_{eff}$ was ascertained as follows: $FRET_{eff} = 1-(F^{mTurquoise\ before\ bleaching})/F^{mTurquoise\ post\ bleaching})$. All $FRET_{eff}$ values obtained for each test combination were plotted and the median values with quartiles are determined (**Figure 7C**). The complete data sets collected in the absence and presence of AbMV infection were compared and statistically evaluated using Mann-Whitney tests (Mann and Whitney, 1947).

Western Blot Analysis of Yeast and Plant Total Protein Extracts, and In-Gel Fluorescence Assays

Total proteins from yeast cells from the mating assays described in 2.6 were extracted by a urea/SDS-based method (Printen and Sprague, 1994). Yeast cells were grown in 5 ml Yeast Extract–Peptone–Dextrose (YPD; Matchmaker system manual) medium at 30°C up to a minimal OD_{600nm} of 0.7. Cells were harvested by centrifugation (6 min, 1,490 x*g*, RT). Per OD_{600nm} unit of cells, 13.5 μl extraction buffer (8 M urea, 5% (w/v) SDS, 40 mM Tris-HCl pH 6.8, 0.1 mM EDTA, 0.4 mg/ml bromophenol blue, 1% β-mercaptoethanol; pre-warmed to 70°C) and an 80 μl-volume glass beads (200 nm, acid-cleaned) were added. The suspension was vortexed for 1 min, incubated at 70°C for 10 min and at 40°C for 30 min. The suspension was cleared by centrifugation (5 min, 12,000 x*g*, RT), the supernatant transferred to a fresh tube and either subjected to SDS-PAGE directly or stored at -80°C.

Total proteins from plant samples described in 2.7 were extracted as follows: 100 mg leaf material was homogenized at 4°C in 200 μl extraction buffer (10 mM KCl, 100 mM Tris-HCl pH 8.0, 5 mM $MgCl_2$, 400 mM sucrose, 10% (v/v) glycerol, 0.1% β-mercaptoethanol) using a plastic pestle and the homogenate cleared by centrifugation (5 min, 12,000 x*g*, RT). Prior to electrophoresis, 4x SDS-PAGE loading buffer (8% SDS, 400 mM Tris-HCl pH 8.8, 100 mM DTT, 40% glycerol and 0.064% bromophenol blue) was added to all samples.

After heating to 40°C for 30 min, proteins of yeast or plant extracts were separated on a 12.5% SDS-PAGE and transferred onto nitrocellulose membranes by semi-dry blotting according to Kleinow et al. (2008). Successful transfer was monitored by Ponceau-S staining. Gels containing FRET expression construct samples were analyzed for mVenus- and mTurquoise2-tagged proteins prior to blotting by in-gel fluorescence detection (mTurquoise2: excitation 440 nm/emission 535 nm and mVenus: excitation 480 nm/emission 535 nm; Fusion fx7edge imaging system, Vilber Lourmat, Eberhardzell, Germany; **Supplementary Figure S1**). Western blot analysis was carried out as described (Kleinow et al., 2008) with minor modifications, using a blocking solution with 2.5% bovine serum albumin (BSA, fraction V) in Tris-buffered saline buffer (TBS, 20 mM Tris-HCl, 138 mM NaCl). Yeast-expressed proteins fused to GBD were detected with a monoclonal anti-GBD antibody (RK5C1) from mouse (1:7,000; Santa Cruz Biotechnology, Dallas, TX, USA) and an anti-mouse horseradish peroxidase conjugated antibody from goat (1:10,000; Rockland, Gilbertsville, PA, USA). For immunodetection of GAD::HA fusion proteins, a rat anti-hemagglutinin (HA) high affinity antibody (3F10) (1:2,000; Roche, Mannheim, Germany) was combined with a goat anti-rat secondary IgG coupled to horseradish peroxidase (1:10,000; Sigma, Taufkirchen, Germany). Monoclonal anti-GFP antibodies (mixture of two antibodies 7.1 and 13.1) from mouse (1:1,000; Roche) recognizing both WT and mutant forms of GFP such as mVenus and mTurquoise2, and an anti-mouse horseradish peroxidase conjugated antibody from goat (1:10,000; Rockland) was used for immunodetection of plant-derived FRET

test proteins. Detection of all target proteins was performed *via* an enhanced chemiluminescence method (Luminata™ Crescendo, Merck EMD Millipore, Schwalbach, Germany; Fusion fx7edge imaging system, Vilber Lourmat).

RESULTS

Functional Analysis of DNA-B Variants Encoding Triple Phosphorylation Site Mutations (T221, S223, and S250) of MP *In Planta*

To analyze the functional role of AbMV MP phosphorylation *in planta* in closer detail, two novel infectious DNA-B constructs were generated that encode MPs with triple amino acid substitutions for T221, S223 and S250 against either aspartate (MP^{DDD}; "constant-on of charge") or alanine (MP^{AAA}; "constant-off of charge") in all three positions. There are several examples available in the literature that describe a loss of infectivity for specific host plant species due to clonally selected geminiviral DNA molecules (for a more detailed discussion see Briddon et al., 1992; Briddon et al., 1998; Grigoras et al., 2009; Jeske et al., 2010; Richter et al., 2016a; Richter et al., 2016b; Jeske, 2018). Thus, RCA-based inocula were applied to circumvent such potential limitations of single virus DNA clones, and to preserve the quasi-species nature of the vDNA pool in the experiments. An *in vitro* RCA-based cloning strategy using the previously established mutated DNA-Bs as starting material was applied in order to maintain the vDNA population (**Figure 1**; 2.1) (Kleinow et al., 2009b). According to the preceding experiments described in Kleinow et al. (2009b), *N. benthamiana* plants were biolistically inoculated with RCA products of AbMV DNA-A plus DNA-B, either WT or encoding one of the two triple phosphorylation site MP mutants. Combinations comprising DNA-A and DNA-Bs expressing the formerly investigated single and double phosphorylation site mutants of MP (Kleinow et al., 2009b) and mock-treated plants were processed in parallel as references or healthy controls, respectively. All AbMV test combinations resulted in a systemic infection with the respective variant, as confirmed by RFLP analyses using a mixture of *Bam* HI (cuts twice in DNA-B) and either of the mutant-specific restriction enzymes, as well as by direct sequencing of RCA products amplified from TNA from newly emerging sink leaves (example in **Figure 1**; **Table 1**; 2.2–2.4).

To test the stability of the newly generated DNA-B-MP^{DDD} or -MP^{AAA} versions *in planta*, the virus pools of three individual, primary-inoculated plants per mutant type were amplified by RCA and the products from each of those plants separately passaged *via* biolistic inoculation to another set of four plants (**Table 1**). These secondary-inoculated plants were evaluated for the presence of the correct mutations by RCA-RFLP and sequencing as well, and the results confirmed the maintenance of the respective mutant DNA-B forms. Eight primary inoculation experiments (with in total 42 plants) and one passaging test (with in total 12 plants) per DNA-B encoding an MP triple mutant were performed (**Table 1**).

The symptoms of *N. benthamiana*, proven to be infected with the respective AbMV mutant (2.3–2.4), were scored in comparison to mock-inoculated and $AbMV^{WT}$-infected ones. With respect to the evaluation criteria - severity of stunting; extent of yellow-green leaf mosaic; and leaf deformations - , plants were grouped into five symptom categories (**Table 1**, **Figure 2**). Experiments with primary- and secondary-inoculated plants were combined, as there was no significant difference between them in symptom development and infection rates (**Table 1**, **Figure 2**). Overall, the analyses by RCA-RFLP, direct sequencing of RCA products, evaluation of infectivity, and symptom development did not reveal any instability of the mutated DNA-B versions and showed equivalent reactions of the primary- and secondary-inoculated plants, suggesting a controlled variability within the samples and a dominant influence of the respective MP versions. All tests and the reproducible outcomes indicate uniformity and repeatability in the experimental set-up using RCA products as inocula.

Representative plants are shown in **Figure 2**. As expected from earlier experiments, AbMV encoding MP^{DD} and MP^{AA} double mutants for T221 and S223 exhibited significantly more severe symptoms in the majority of plants (77 and 75%, respectively, in category III and IV), whereas the ones for S250 developed predominantly milder phenotypes (62 and 67% in category I) (**Table 1**, **Figure 2**) (Kleinow et al., 2009b). Both MP triple mutants induced a divergent, amino acid substitution-specific symptom development in contrast to the amino acid position-specific effects observed with the single and double mutants. The $AbMV^{DDD}$ symptoms were similar to those of the WT virus in the majority of plants (61% in category II), enhanced in 36% (category III and IV) and attenuated in around 4% (**Table 1**, **Figure 2**). On the contrary, $AbMV^{AAA}$ induced extremely mild symptoms (100% category I and 0) (**Table 1**, **Figure 2**). Young leaves were symptomless and older ones exhibited some yellow spots or small areas of leaf crinkling only occasionally (example in **Figure 2**, close-up).

The steady-state vDNA content of systemically infected sink leaves was determined by semi-quantitative Southern blot analysis to monitor the impact of three simultaneously altered phosphorylation sites on MP functions and AbMV spread. *N. benthamiana* plants verified to be systemically infected with the correct combination of DNA-A and the respective DNA-B variant (MP^{DDD} or MP^{AAA}) by RCA-RFLP and sequencing were assayed. $AbMV^{WT}$-infected plants served as a reference. Samples from 14, 26, and 49 dpi were analyzed for time-dependent changes in vDNA accumulation.

Systemic infection with AbMV expressing MP^{AAA} resulted in a transiently delayed accumulation of vDNA (**Figure 3A**). The vDNA content was substantially reduced at 14 dpi, but had increased to approximately half of that of $AbMV^{WT}$ at 49 dpi. The $AbMV^{DDD}$ mutant contained slightly reduced vDNA levels at 14 dpi, but accumulated vDNA to higher levels than $AbMV^{WT}$ at later time points (**Figure 3B**). A difference between the time courses of DNA-A and DNA-B accumulation for MP^{AAA} and MP^{DDD} expressing AbMV variants was not detected (**Figure 3**), in contrast to previous results (Kleinow et al., 2009b).

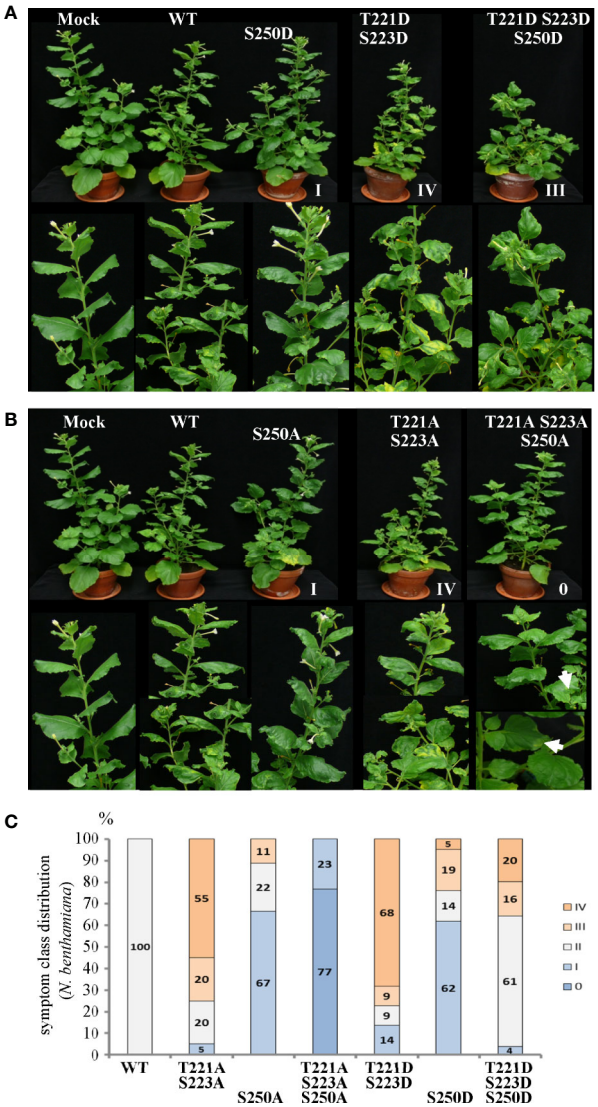

FIGURE 2 | Alterations in AbMV symptom development triggered by MP with either single, dual, or triple aspartate (DDD) or single up to triple alanine (AAA) replacement for amino acid positions T221, S223 and S250. *N. benthamiana* plants were inoculated with AbMV DNA-A plus DNA-B containing a *MP* gene of either wild-type or the distinct mutated versions indicated. The previously described single and double phosphorylation site mutants of MP (Kleinow et al., 2009b) and mock-treated plants served as reference for the novel triple mutation containing MP. The plant classification according to symptom severity (**Table 1**) is indicated. **(A)** Appearance of plants (48 dpi) systemically infected with the indicated phosphorylation-mimicking aspartate replacement mutants, and **(B)** with analogous alanine exchanges. A close-up is shown for symptoms below each plant. Note the nearly symptomless phenotype of MP^{AAA} combination. Small leaf areas displaying yellowing or mild crinkling are marked with an arrow. **(C)** Summary of symptom class distribution for nine independent experiments.

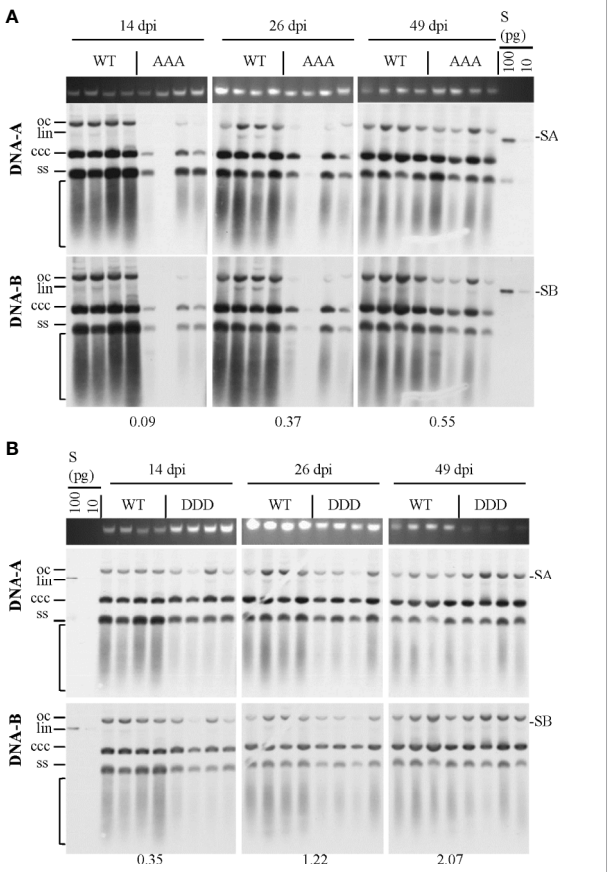

FIGURE 3 | Effect of non-phosphorylation and phospho-charge-mimic MP mutants on AbMV DNA accumulation in *N. benthamiana*. Total nucleic acids were extracted at indicated days post inoculation (dpi) from plants systemically infected with AbMV DNA-A plus one of the three DNA-B variants coding for MP^{WT} **(A, B)**, MP^{AAA} **(A)** or MP^{DDD} **(B)**. Four samples for each combination were separated on an agarose gel in the presence of ethidium bromide, and the area harboring plant genomic DNA served as a loading control (**A**, **B**; upper panel). Semi-quantitative Southern blot analyses were carried out with a DNA-A-specific probe (**A**, **B**; middle panel) and, after stripping and re-hybridization, with a DNA-B-specific probe (**A**, **B**; lower panel). Different vDNA forms are indicated (oc: open circular, lin: linear, ccc: covalently closed-circular and ss: single-stranded). The area indicative of replication by-products is labelled by a bracket. The intensity of hybridization signals was normalized to the amount of DNA loaded. For each sample set, the mean of four typical samples was calculated, and a factor determined for the vDNA difference between WT and triple mutants per time point (displayed below). S: hybridization standards (left to right 100 and 10 pg of standard A [SA]: PCR-amplified DNA A-encoded ORF *AC1* or standard B [SB]: PCR-amplified DNA B lacking sequence of common region). Southern blot analysis was performed for three to four samples per independent experiment with *N. benthamiana* (**Tables 1** and **2**).

Overall, the triple replacements by alanine interfered with pathogenicity and vDNA accumulation, whereas that by aspartate showed a weaker influence on the infection in *N. benthamiana* plants.

The Influence on Symptom Development of MP^{AAA} and MP^{DDD} Depends on the Host Plant Species

For MP^{AAA} and MP^{DDD} variants of AbMV tests were carried out to examine whether these mutations would differentially affect the infection of hosts other than *N. benthamiana* and thus could alter the viral host range. Three plant species susceptible for

AbMV^{WT} in the families Solanaceae (*Datura stramonium* and *Nicandra physaloides*) and Malvaceae (*Malva parviflora*) (Jeske, 2000; Wege et al., 2000) were chosen. Seedlings in the two-to-three-leaf stage were biolistically inoculated with RCA products of viral AbMV DNAs-A and each MP^{AAA}, MP^{DDD}, or MP^{WT} encoding DNAs-B. Mock-treated *N. benthamiana* plants were processed in parallel. The various hosts were inspected for systemic AbMV infection by monitoring symptoms and by testing vDNA from newly emerging sink leaves by RCA-RFLP and Southern blot hybridizations.

AbMV^{WT} infected all hosts with different efficiencies (**Table 2**). For each of the MP mutants the results were plant species specific: For *M. parviflora*, AbMV^{AAA} was not infectious at all, whereas AbMV^{DDD} achieved lower infection rates than AbMV^{WT} (average infection rates 22% versus 55%; **Table 2**). For *D. stramonium,* AbMV^{DDD} was not infectious, and AbMV^{AAA} was similar to AbMV^{WT} (**Table 2**). For *N. physaloides*, both AbMV^{AAA} and AbMV^{DDD} were systemically infectious, although with reduced infection rates (12 or 21%, respectively).

All three plant species developed stronger symptoms upon systemic AbMV^{WT} infection than for *N. benthamiana*. Symptoms comprised more severe stunting, leaf deformations and yellow-green leaf mosaic (**Figure 4**). In contrast, both MP triple mutants caused milder symptoms in the three hosts, if infected. Young sink leaves were nearly symptomless, and older source leaves showed minor wrinkling and small yellow spots rather than a yellow-green mosaic for *D. stramonium* and *N. physaloides* (**Figure 4**).

Southern blot hybridizations were performed for samples from plants infected with the AbMV versions, as verified by RCA RFLP and sequencing, to test for vDNA accumulation. In comparison to AbMV^{WT}, in all AbMV^{AAA}-infected *N. physaloides* and *D. stramonium* the vDNA content was markedly reduced at 44 dpi (**Figure 5**), whereas this effect was less prominent with MP^{DDD} expressing AbMV. No significant difference in those trends was found between DNA-A or DNA-B titers.

In summary, the AbMV triple mutants exerted complex differential effects on hosts, regarding symptom development and vDNA accumulation. Both mutants have lost infectivity for a host susceptible for AbMV^{WT}, suggesting a primary role of the three phosphorylation sites in fine-tuning virus-host interplay and thereby efficiency or even ability of systemic host invasion.

Triple Mutations Influence the Self-Interaction of MP

Both MP mutant types were tested in yeast two-hybrid (Y2H) assays in *S. cerevisiae* cells. To provide the assay functionality, truncated C-terminal domains (MP-CD) were used lacking the membrane anchor domain (Zhang et al., 2002), since full-length MP fusion proteins target to the cell periphery preventing Y2H interactions (Frischmuth et al., 2004). Fusion constructs of all MP-CD variants with either GBD or GAD::HA were tested against each other in all possible combinations. The known self-interaction of MP-CD^{WT} served as positive control, and its combination with an unrelated protein from *A. thaliana* (Cys/His-rich C1 domain family protein, At3g27500) as negative control. Test constructs were combined using single transformations and a mating assay. Yeast cells were tested for reporter gene activation indicative of protein interaction by monitoring histidine prototrophy and ß-galactosidase activity. MP-CD^{AAA} interacted in all combinations with itself or with MP-CD^{WT}. In contrast, no protein interaction was detectable for the DDD variant in any combination (**Figure 6A**). An interaction with the control construct was not detectable likewise (**Figure 6B**, Con). The expression of the GAD::HA- and GBD-fused proteins was confirmed by Western blot analysis (**Figure 6C**). In accordance with previous results (Kleinow et al., 2008; Kleinow et al., 2009b), MP-CD^{WT} showed signals at the expected apparent molecular mass and retarded extra bands (**Figure 6C** right panel). Interestingly, for both mutated MPs only bands with reduced mobility in comparison to the MP-CD^{WT} appeared.

The self-interaction of full-length MP was further tested in living plant cells, using an acceptor photobleaching bleaching FRET detection approach with the fluorophore pair of acceptor mVenus and donor mTurquoise2 (Blatt and Grefen, 2014; Hecker et al., 2015). FRET efficiency measurement is a highly stringent and specific method to assay if two proteins fused to the fluorescent reporters are in close proximity in a protein complex with a distance less than 10 nm (Hecker et al., 2015). When proteins interact only temporally, FRET vanishes upon protein partner dissociation. This additional advantage of FRET allows detecting temporal changes in MP self-interaction *in planta*. The BiFC technique, which had been used previously to confirm MP^{WT}-MP^{WT} interaction in *N. benthamiana* (Krenz et al., 2010), is limited in this respect because complexes of proteins fused to yellow fluorescent protein (YFP) domains may undergo stabilization upon reconstitution of the YFP ß-barrel structure (Hu et al., 2002; Magliery et al., 2005).

The two-in-one FRET binary vector system for the simultaneous expression of two potential interaction partners from a single T-DNA (Hecker et al., 2015) was applied to analyze the fluorescent MP fusion proteins at comparable levels. MP^{DDD} and MP^{AAA} were investigated in comparison to MP^{WT} fusion proteins. To reveal a putative impact of the position and sequence of the fluorescence protein tags on MP-MP interactions, all four possible orientations were generated and assayed for every MP variant: mVenus (acceptor) and mTurquoise2 (donor) tags, respectively, either both located N-terminally (NN) or C-terminally (CC), and additionally N-terminally mVenus plus C-terminally mTurquoise2 (CN) and vice versa (NC) (**Figure 7**, for details see schematic representation). The four FRET constructs for each MP type were transiently and simultaneously expressed after agro-infiltration into epidermal tissues of *N. benthamiana* leaves. To examine if other viral proteins, the vDNA, or AbMV-triggered changes in the cellular environment affected MP-MP interactions, the experiments were done in the absence and in the presence of an AbMV infection. AbMV was inoculated locally by co-infiltration of plasmids delivering infectious

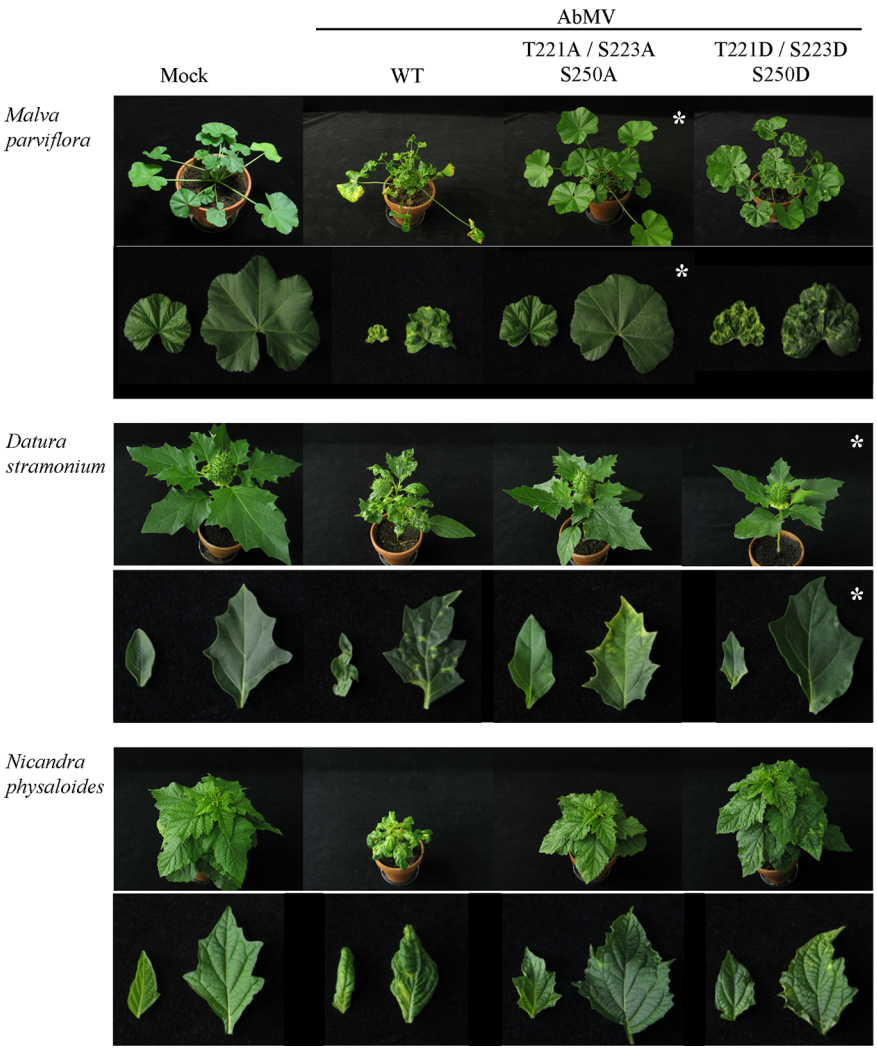

FIGURE 4 | Impact of triple phosphorylation site mutants of MP on AbMV symptom development in host plants other than *N. benthamiana*. *Malva parviflora*, *Datura stramonium*, and *Nicandra physaloides* were inoculated with DNA-A plus DNA-B encoding MP^{WT}, MP^{AAA}, or MP^{DDD} in at minimum four independent experiments (**Table 2**). Mock treatments served as a negative control. Each panel shows the whole plant (35 dpi) and directly below a close-up (right young and left old leaf). Non-infectious virus-host combinations are labeled by an asterisk (compare ; AAA & *M. parviflora*, DDD & *D. stramonium*). Note that all combinations comprising a triple phosphorylation site mutant version of MP exhibit attenuated symptoms in comparison to $AbMV^{WT}$.

DNA-A and a mutant DNA-B with abolished MP^{WT} expression (DNA-BΔMP) (Evans and Jeske, 1993). In order to detect appearance of non-specific FRET, potentially resulting from random accumulation of test proteins in certain membrane domains and thereby close proximity, an additional negative control was included: the plasma membrane-targeted SNARE protein (*Arabidopsis* SYP122; mVenus::SYP122) (Uemura et al., 2004) combined with mTurquoise2::MP^{WT}. MP^{WT} self-interaction (Krenz et al., 2010) was included as a positive control in all layouts tested. High resolution fluorescence microscopy and FRET acceptor photobleaching experiments were performed by imaging samples, before and after photobleaching by a high energy laser beam (example shown in **Figure 7A**). Calculation of FRET efficiencies after background subtraction was done as described in 2.8.

All test layouts showed FRET (NN, CN, NC, and CC, **Figure 7B**) with and without AbMV, indicating that all MP variants were capable for self-interaction. Full-length MP^{DDD} thus differed in the result from that with the partial MP-CD^{DDD} in the yeast two-hybrid assay. Possibly the other MP domains, or plant adapter proteins, rescued the effect of the DDD mutation observed in the yeast system. In the context of an AbMV infection, the variability of FRET efficiencies within each combination was significantly reduced, suggesting a stabilization of the MP complex in the presence of the viral elements. Without AbMV, data for MP combinations with low FRET efficiencies,

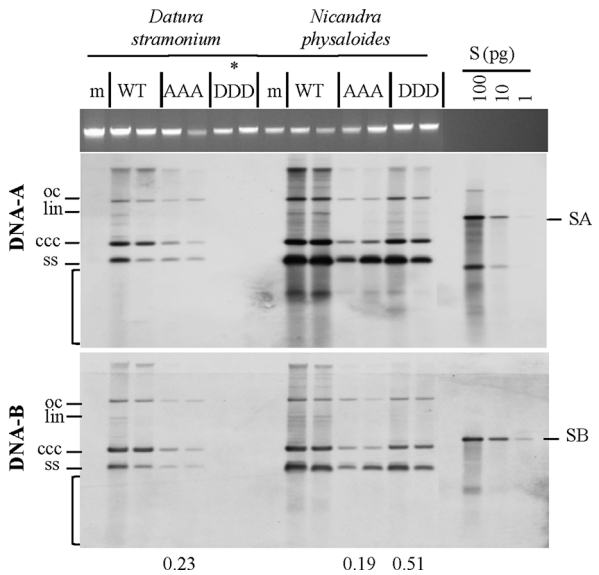

FIGURE 5 | Triple phosphorylation site mutants of MP influence vDNA accumulation in solanaceous host plants. Semi-quantitative Southern blot analyses of total nucleic acids extracted from *D. stramonium* and *N. physaloides* at 44 dpi were carried out as for **Figure 3**. Two plant samples for each combination are shown (m: mock-treated control; WT: AbMV^{WT}; AAA: AbMV^{AAA}; DDD: AbMV^{DDD}). Note that AbMV^{DDD} is non-infectious in *D. stramonium* (asterisks; compare **Table 2**). Different vDNA forms are indicated (oc: open circular, lin: linear, ccc: covalently closed-circular, ss: single-stranded and bracket: area indicative of replication by-products). Data normalization and calculation of factor for the vDNA difference between WT and triple mutants per plant species, as explained in **Figure 3** (displayed below). SA: DNA-A-specific hybridization standard; SB: DNA-B-specific hybridization standard (left to right 100 and 10 pg). Southern blot analysis was done for two to three samples out of each independent experiment (summarized in **Table 2**).

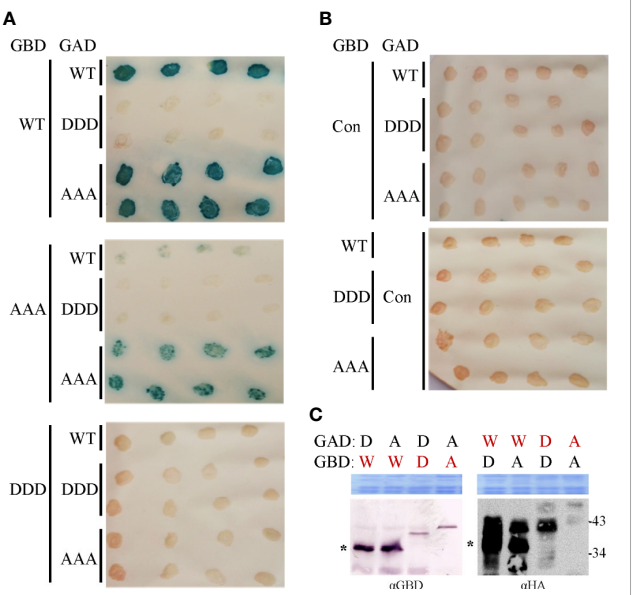

FIGURE 6 | Influence of triple phosphorylation site mutations on MP self-interaction in a yeast-two hybrid system. **(A)** Qualitative colony-lift LacZ filter assay to monitor interactions of GAD::HA and GBD fusions of MP oligomerization domains (MP-CD) between either WT or mutagenized (DDD or AAA) variants. The confirmed interaction of the WT protein served as a positive control. **(B)** Test combinations with GAD::HA and GBD fusions of a Cys/His-rich C1 domain family protein from *A. thaliana* (At3g27500; Con) were tested in parallel as a negative non-interacting control. **(C)** Western blot analysis to assay the presence of the respective GAD::HA and GBD fusion test proteins (depicted in red letters). Expected molecular mass for MP-CD variants fused to GBD is 36.7 kDa and to GAD::HA is 38.7 kDa. W: MP-CD^{WT}; D: MP-CD^{DDD}; A: MP-CD^{AAA}. Asterisk: band position expected in relation to right: (apparent) kDa deduced from molecular weight marker. An area of the Coomassie-stained SDS-PAGE is shown as a loading control. In total three independent experiments were carried out.

namely the CN (mVenus::MP^{variants}/MP^{variants}::mTurquoise2) and NC (MP^{variants}::mVenus/mTurquoise2::MP^{variants}) combinations were not normally distributed and showed FRET values in the range of the negative control. This suggests that in these layouts, MP-MP interactions were impaired, most likely by the opposite positions of the fluorescent protein tags that may influence protein folding or accessibility of domains. A significant difference in FRET efficiency of the same MP-MP combination in the absence or presence of AbMV was detected only for MP^{WT} in the layout NC (**^{*1} label in **Figure 7B**; mean value 36% without vs. 28% with AbMV). Similarly, a significant but moderate difference between MP^{WT}, MP^{AAA}, and MP^{DDD} could be observed in a single layout only (NC with/without AbMV, mean FRET efficiencies: MP^{AAA}: 50/42% without/with AbMV, i.e., significantly higher than that of MP^{WT}: (36/28% without/with AbMV) and MP^{DDD} (14/30% without/with AbMV). For most layouts, no significant difference in FRET efficiencies occurred (**Figure 7B**).

Expression and integrity of the respective test proteins *in planta* were confirmed by Western blot analysis of leaf tissue extracts using an antiGFP antibody reacting with both fusion partners (**Supplementary Figure S1**). Additionally, the presence of the fluorescent protein-tagged MPs in the samples was confirmed by direct in-gel fluorescence detection (**Supplementary Figure S1**). Both assays showed expression of the MP fusion proteins and even allowed discrimination of distinct constructs, although their calculated molecular mass is nearly identical (C-terminally mTurquoise2 or mVenus 61.85 kDa; N-terminally mTurquoise2 or mVenus 61.82 kDa). All MP fusion variants exhibited a clearly different electrophoretic velocity indicative of N- or C-terminal tagging, irrespective if fused to mVenus or mTurquoise2. The C-terminal fusion proteins migrated more slowly than the N-terminally fused ones. All tagged MP variants showed an anomalous migration by comparison to the molecular weight marker.

In order to investigate a potential impact of the phosphorylation sites on the subcellular localization of AbMV MP in living plant cells, high resolution spinning disk confocal microscopy of leaf areas containing fluorescence protein-tagged MP variants was carried out. MP^{DDD} and MP^{AAA} were analyzed in comparison to the WT protein. For this purpose, the four different FRET expression constructs for each MP type were

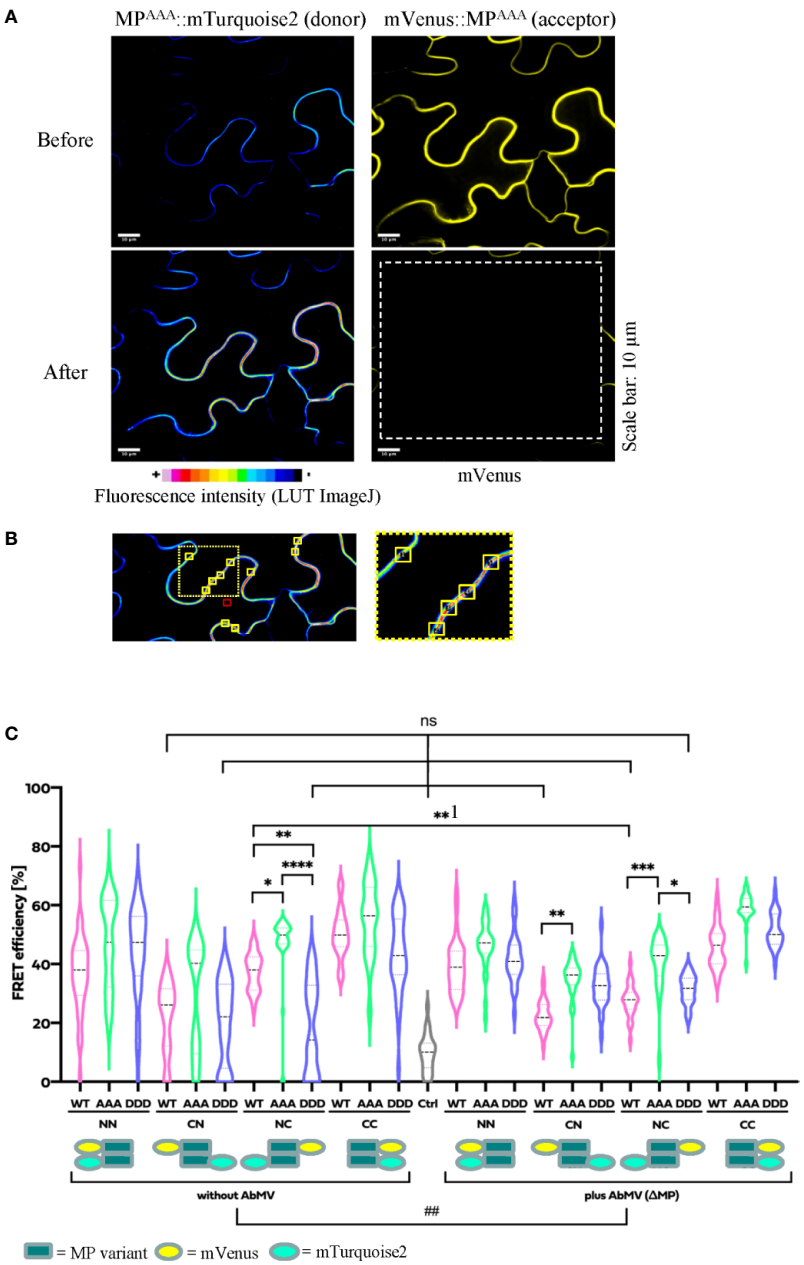

FIGURE 7 | Functional relevance of MP phosphorylation site triple mutants for self-interaction in healthy or AbMV-infected *N. benthamiana*. Protein interaction was assayed by acceptor photobleaching-FRET using the acceptor mVenus and donor mTurquoise2. All four possible combinations of C- and N-terminal fusion to full-length MPs (WT: MP^{WT}; DDD: MP^{DDD}; AAA: MP^{AAA}; see schematic representation) were transiently expressed after agro-infiltration in the absence or presence of AbMV (ΔMP gene) (Evans and Jeske, 1993) infection in leaf epidermal tissues. The combination of a plasma membrane-targeted SNARE protein (*Arabidopsis* SYP122; mVenus::SYP122) (Uemura et al., 2004) with mTurquoise2::MP^{WT} served as a negative control and all combinations of MP^{WT} (Krenz et al., 2010) as a positive control. High resolution spinning disk confocal microscopy was done at three dpai. **(A)** Representative example of fluorescence micrographs (combination MP^{AAA}::mTurquoise2 & mVenus::MP^{AAA}) imaged before and after specific bleaching of mVenus (acceptor; bleaching area marked by a dashed square). **(B)** Ten squared regions of interest (ROIs; size 10 μm^2 each, yellow squares) along the plasma membrane were selected and analyzed per cell. An example is shown for a donor fluorescence micrograph after bleaching (area of close-up to the right indicated by a dotted square). Effectiveness of bleaching and FRET efficiencies were calculated as described in 2.8. Note the increased signal for the donor mTurquoise2 after bleaching the acceptor mVenus. For better visualization of fluorescence intensities, mTurquoise2 is displayed with ImageJ's lookup table (LUT) black to white in 16 colors. Scale bar = 10 µm; images are single optical planes. **(C)** Intensities of acceptor and donor fluorescence were analyzed prior to and after acceptor photobleaching, and the resulting FRET efficiencies were calculated. For each sample, all data points of at minimum three independent experiments are presented as violin plot to better visualize their distribution, and median values with quartiles are depicted. Sample pairs with significant difference are labelled by asterisks: Kruskal-Wallis Test: P value ****<0.0001, ***0.0002, **0.001, *0.01; comparison of only healthy versus AbMV-infected: Mann-Whitney Test; ##P value 0.005; NS, no significant difference.

transiently expressed in epidermal leaf tissues of *N. benthamiana* following agro-infiltration. Experiments were carried out without and with local AbMV infection.

MP^{WT} showed the following subcellular distribution patterns: In cells devoid of AbMV co-infection, fluorescence signals for N- and C-terminally-tagged MP^{WT} localized homogeneously at the cellular periphery, most likely at the cytoplasmic face of the plasma membrane and at plasmodesmata (Happle et al., submitted; Aberle et al., 2002; Frischmuth et al., 2004; Kleinow et al., 2009c) (**Figure 8**; **Supplementary Figure S2**; exemplary fluorescence micrographs for mVenus). Fluorescent protein-tagged MP^{WT} accumulated around nuclei and clustered in small vesicles representing microsomes trafficking *via* the ER/actin network (Happle et al., submitted). The MP vesicles were highly mobile and traveled along the cell periphery and in close vicinity to the nuclear envelope within the cytoplasm. Small spotted structures detected for this fusion protein at the cell periphery exhibited Brownian molecular motion only, considerably different from the trajectories of the N-terminally tagged MP (**Figure 8**; **Supplementary Figure S2**; exemplary fluorescence micrographs for mVenus). As described in detail by Happle et al. (submitted), the proportions of cells with MP fusion proteins accumulating in vesicles, and cells with homogenous MP distribution at the cell periphery varied at three dpai. In the

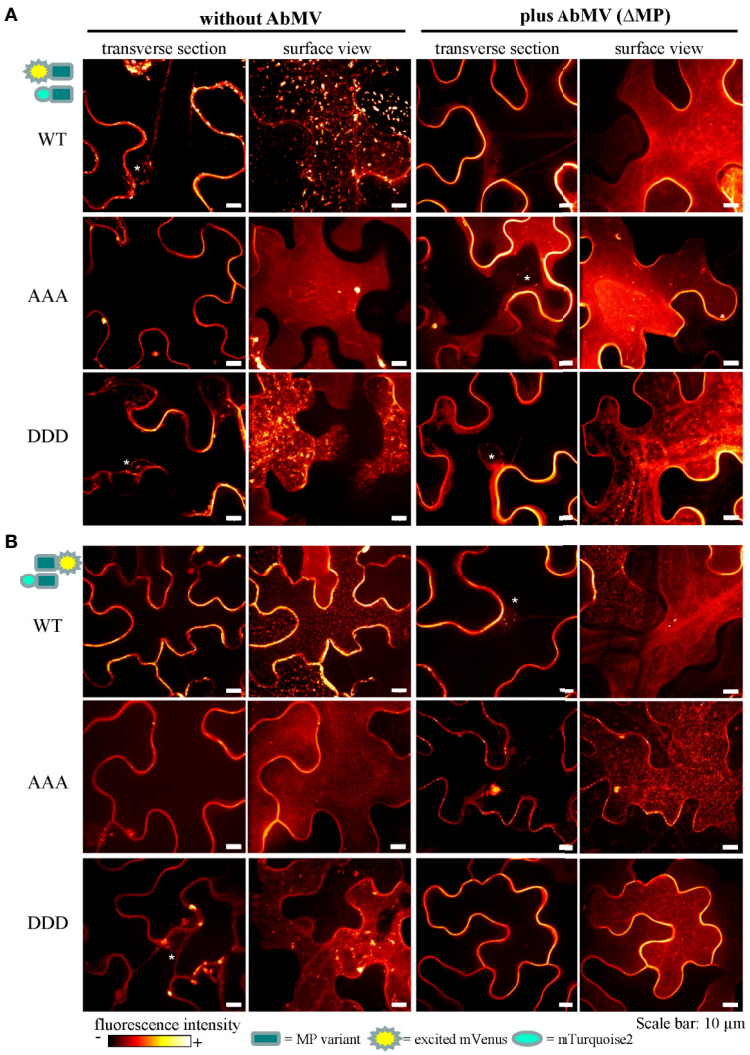

FIGURE 8 | Subcellular localization of AbMV MP phosphorylation site triple mutants. *N. benthamiana* transiently expressing combinations of full-length MP FRET constructs and the negative control set-up (as in **Figure 7**) were analyzed by high resolution spinning disk confocal microscopy at three dpai. Images show the localization of mVenus-tagged test proteins **(A)** mVenus::$MP^{WT/AAA/DDD}$ and **(B)** $MP^{WT/AAA/DDD}$::mVenus, which was indistinguishable from that found with mTurquoise2 fusion proteins (not shown). Additionally, no difference between C- or N-terminal mVenus MP fusion proteins in combinations with either N- or C-terminally mTurquoise2-tagged MP variants was detected (for N- or C-terminally mVenus-tagged MPs combined with same MP type in C-terminal mTurquoise2 fusion, see **Supplement Figure 2**). Exemplary images of representative cells out of at minimum three independent experiments per treatment are shown in transverse section and surface view (displayed in a fluorescence intensity view). Nuclei are labeled by asterisks. Scale bars: 10 µm.

presence of AbMV, MP^{WT} localized predominantly at the cell periphery and formed fewer vesicles.

In all layouts investigated, the subcellular localization of both triple mutants was not significantly altered in comparison to that of MP^{WT}. Exceptionally, a higher abundance of MP-containing vesicles occurred for MP^{AAA}, and MP^{DDD}- or MP^{AAA}-containing filamentous structures at the cell periphery were occasionally detected in different layouts (examples **Figure 8A**, MP^{AAA}; **Supplementary Figure S2A**, MP^{DDD}).

DISCUSSION

Based on our former work that identified three phosphorylation sites in the C-terminal oligomerization domain of MP (T221, S223, and S250) (Kleinow et al., 2009b), this study has focused on triple mutants MPs. Site-directed mutagenesis of the *MP* gene within the infectious AbMV genome has generated a non-phosphorylation ("constant-off of charge"; AAA) or, alternatively, a phospho-charge-mimic ("constant-on of charge", DDD) status for all three amino acid positions simultaneously. Upon systemic infection with $AbMV^{DDD}$, about two thirds of the *N. benthamiana* plants developed symptoms similar to WT, and one third more severe symptoms. Time course experiments indicated changes in the steady-state vDNA content in comparison to $AbMV^{WT}$, slightly reduced at early time points and elevated in later stages of infection. The vDNA content appeared to be independent of the symptom phenotype. In contrast, $AbMV^{AAA}$ resulted in an extreme attenuation of symptoms up to nearly symptomless plants, and accordingly a time-delayed accumulation of vDNA. These results prove a vital role of the three phosphorylation sites located in the C-terminal part of AbMV MP for viral pathogenicity *in planta*. They are in line with other studies that identified the C-terminal part of begomoviral MPs as being important for symptom induction (von Arnim and Stanley, 1992; Ingham and Lazarowitz, 1993; Pascal et al., 1993; Duan et al., 1997; Hou et al., 2000; Saunders et al., 2001).

It is well established that PTMs and especially reversible phosphorylation are important elements in managing a multitude of processes in eukaryotic cells, e.g. altering protein function, stability or subcellular distribution. For MPs in the 30K family of various virus species, phosphorylation on serine and threonine residues was shown to be relevant for *in planta* functionality, including proteins of tobamoviruses (Kawakami et al., 1999; Waigmann et al., 2000; Karger et al., 2003; Kawakami et al., 2003; Trutnyeva et al., 2005; Fujiki et al., 2006), cucumoviruses (Matsushita et al., 2002; Lewsey et al., 2009; Nemes et al., 2017), bromoviruses (Akamatsu et al., 2007) and geminiviruses (Kleinow et al., 2009b). However, details of the regulatory events and reaction cascades triggered by changes of the phosphorylation patterns still need to be investigated.

To some extent, however, these findings for the novel triple phosphorylation site MP mutants contrast with data obtained in our former study (Kleinow et al., 2009b). While for the simultaneous triple changes, mutation-type dependent alterations in pathogenicity dominate the outcome, the previously analyzed single and double mutant versions revealed primarily amino acid position-specific effects on symptom development. On that former basis, we had hypothesized that an interference with phosphorylation-induced ubiquitination of proteins might result in amino acid position-specific effects in plants and change viral symptoms (for a more detailed discussion see Kleinow et al., 2009b). Recent data for the CP of the bipartite begomovirus African cassava mosaic virus support the idea of phosphorylation-mediated proteolysis as an important regulatory cornerstone: a differential CP phosphorylation in plants coinciding with a high turnover rate of the protein indicates its ubiquitin-dependent degradation by the proteasome (Hipp et al., 2019). An ubiquitination and subsequent degradation by the proteasome has also been observed for the CP of the monopartite begomovirus tomato yellow leaf curl virus (Gorovits et al., 2014; Gorovits et al., 2016).

Most interestingly, $AbMV^{AAA}$ and $AbMV^{DDD}$ changed the host ranges, with MP^{AAA} unable to infect *M. parviflora* and MP^{DDD} being non-infectious to *D. stramonium*. It can be speculated that site-selective phosphorylation in the MP oligomerization domain goes along with an adaptation of AbMV to specific plant species, as a prerequisite for successful infection and invasion. To the best of our knowledge, such phosphorylation-dependent host range modulation is shown for a MP of a plant DNA virus for the first time.

For some RNA viruses, however, host dependent phosphorylation of MPs and specific functional consequences e.g. on infectivity and host range, had been found before. Phospho-charge-mimic mutations of three C-terminally located phosphorylation sites in TMV MP affected its ability to gate plasmodesmata for intercellular trafficking in *Nicotiana tabacum*, but not in *N. benthamiana*. This unraveled a host dependency of TMV (genus *Tobamovirus*, family *Virgaviridae)* on specific phosphorylation patterns (Waigmann et al., 2000). For the movement-associated triple gene block protein 1 (TGB1p) of barley stripe mosaic virus (genus *Hordeivirus*, family *Virgaviridae*), two phosphorylation sites were identified (T395 and T401) that upon mutation (non-phosphorylation or phospho-charge-mimic) led to a change in host specificity (Hu et al., 2015). In TGBp3 of potato mop-top virus (genus *Pomovirus* within the *Virgaviridae*), a tyrosine phosphorylation site (Y120) was identified, the alanine substitution of which eliminated infectivity (Samuilova et al., 2013). All these data collectively underscore that MP phosphorylation/dephosphorylation dynamics may have a strong impact on the specific interplay between a virus and the inoculated plant species. The data obtained for AbMV in this study suggest a similar regulation by host-dependent and -specific PTMs of MP, which are needed to mediate infectivity and balance pathogenicity.

For other geminiviral proteins, phosphorylation site-dependent effects on the pathogenicity, the infectivity, or the host range have been observed as well. A point mutation in a protein kinase C recognition motif of East African cassava mosaic Cameroon virus PCP (AV2) influenced the viral pathogenicity (Chowda-Reddy et al., 2008). AC2 proteins of

the two New World bipartite begomoviruses tomato golden mosaic virus (TGMV) and cabbage leaf curl virus (CaLCuV) were both phosphorylated at S109 by an upstream activating kinase of the SUCROSE-NONFERMENTING1-related kinase1 (SnRK1) in plants (Hanley-Bowdoin et al., 2013; Shen et al., 2014). Mutations introduced into the *AC2* gene at this position delayed symptom development and vDNA accumulation upon CaLCuV infection of *Arabidopsis*. S109, however, is not conserved among other (A)C2 proteins. Shen et al. (2014) discussed this as an evolutionary result in specific geminivirus host interactions, an interpretation which might apply to the results for AbMV MP here as well. The Rep of TGMV is phosphorylated at S97 by SnRK1 and its modification impaired its binding to vDNA, but not its cleavage activity (Shen et al., 2018). Interestingly, the TGMV Rep-S97D mutant showed an altered host range and did not infect tomato. This observation is in agreement with our finding that phosphorylation sites in MP influence AbMV infectivity selectively in certain host species. The TGMV Rep-S97D mutant delayed symptom development and vDNA accumulation in *N. benthamiana* considerably, but eventually, systemically infected plants displayed WT-like or even enhanced symptoms. This behavior did not correlate with vDNA contents similar to those of WT TGMV in later stages of the infection: the plants still contained only low levels of vDNA. The ßC1 protein encoded by the tomato yellow leaf curl China ß-satellite (TYLCCNB) was shown to be a substrate for SnRK1 as well (Shen et al., 2011; Shen et al., 2012; Yang et al., 2019). TYLCCNB encoding a phospho-charge-mimic mutant of ßC1 exhibited delayed symptoms and an attenuated phenotype in *N. benthamiana* upon co-infection with tomato yellow leaf curl China virus (TYLCCNV). The plants accumulated lower vDNA titers, whereas those infected with TYLCCNV/mutant TYLCCNB encoding a phosphorylation-negative alanine mutant of ßC1 contained higher vDNA titers. Nevertheless, the latter displayed symptoms resembling those of TYLCCNV/TYLCCNB WT. Such an uncoupling between symptom severity and vDNA content, as described for phosphorylation site mutants of Rep and ßC1, was observed in our previous studies for AbMV MP phosphorylation site double and single mutants as well (Kleinow et al., 2009b). For both novel triple mutants, however, the phenomenon was less pronounced. AbMV^{AAA} caused attenuated symptoms that correlated with reduced vDNA content in all infected host species. In contrast, AbMV^{DDD} induced WT-like or enhanced symptoms in *N. benthamiana*, but vDNA accumulation was transiently reduced in early stages of the infection, and increased to even higher than AbMV^{WT} titers in later stages. In the other plant species tested, AbMV^{DDD} induced milder symptoms in conjunction with lower vDNA titers, comparable to AbMV^{AAA}. This suggests that host-dependent phosphorylation of a begomoviral MP can also impact pathogenicity and efficiency of infection, as detected for other geminiviral proteins before. It remains to be determined whether phosphorylation of AbMV MP affects plant defense mechanisms as suggested by prior studies of TGMV Rep and TYLCCBB βC1.

In a yeast two hybrid system, the DDD mutation abolished MP-CD self-interaction, suggesting that the negative charges introduced by phosphorylation or the respective mutants interfere with the domain's di- or oligomerization. However, this effect was not confirmed in all layouts tested by FRET studies *in planta*. These tests indicated a similar di- or oligomerization for as for MP^{AAA} and MP^{WT}. Most likely, the interaction between MP^{DDD} molecules in plant cells is rescued by the presence of other MP domains, and/or plant adapter proteins which stabilize the MP complex. Which roles MP-MP interactions play within the viral life cycle, still needs to be investigated further.

Overall, fluorescence microscopy showed subcellular distributions of both triple mutants not significantly altered in comparison to MP^{WT}. This indicates that there is no fundamental role of the three phosphorylation sites in targeting MP to subcellular structures, different from some other MPs for which targeting to membranes, plasmodesmata, or nuclear-to-cytoplasmic shuttling was shown to be regulated by phosphorylation (Waigmann et al., 2000; Fujiki et al., 2006; Link et al., 2011; Nemes et al., 2017).

Upon electrophoresis in denaturing SDS polyacrylamide gels, the mobility of MP-CD^{WT} and the MP triple mutants expressed in yeast did not meet the expectations completely. In accordance with previous data (Kleinow et al., 2008; Kleinow et al., 2009b), GAD::HA::MP-CD^{WT} formed retarded extra bands, in addition to a signal at the expected molecular mass (36.7 kDa), most clearly detectable by Western blot analysis (**Figure 6C**, right panel). Interestingly, both MP triple mutants lacked signals corresponding to the expected molecular mass completely and accumulated in a number of bands with retarded migration. GBD fusion proteins behaved similarly (**Figure 6C**, left panel). GBD::MP-CD^{WT} was detected within a single band at the expected molecular mass, whereas both triple mutants showed only single bands migrating with reduced velocity. The complex band pattern of GAD::HA::MP-CD^{WT} resembles that observed for yeast-derived MP before. It was attributed to differential phosphorylation of T221 and S223 as shown by mass spectrometry, and to unidentified PTMs most likely other than phosphorylation (Kleinow et al., 2008; Kleinow et al., 2009b). The results obtained here for the two MP mutants support a presence of such unidentified PTMs reducing electrophoretic mobility. A differentially altered electrophoretic migration was observed for the FRET test proteins, too, in dependence on the fusion proteins' layout with either N- or C-terminal position of the fluorescent protein tags. We suppose that the different layouts influence the accessibility of MP for modifying host enzymes, causing a putatively differential PTM pattern which might lead to the detected differences in electrophoretic mobility. Here, however, no differences were detectable between WT and triple full-length MP mutants. Overall, the results of this study strengthen the assumption that additional PTMs in AbMV MP still need to be uncovered.

A former phylogenetic analysis revealed that the phosphorylation site S250 is present in a highly conserved amino acid context in nearly all bipartite begomoviral MPs, whereas T221 and S223 homologues are found in New World begomoviruses only, with some variability of their exact positions (Kleinow et al., 2009b). This

underscores the functional relevance of all three sites. Which plant kinases target the three phosphorylation sites in AbMV MP is an interesting question, which remains to be answered. The amino acid context of S250 does not correspond to a known kinase recognition motif. In contrast, T221 and S223 exhibit a casein kinase II (CK2) recognition motif (S/T-XX-E/D) (Meggio and Pinna, 2003). Phosphorylation of T221 generates a cluster of negatively charged amino acid residues in a region N-terminal of S223 (D-pT/D-D-S), thereby introducing a casein kinase I (CK1) recognition motif (Gross and Anderson, 1998). This suggests a control of the C-terminal oligomerization domain's state by hierarchical phosphorylation. Members of both casein kinase types were already discovered to phosphorylate viral MPs from various viruses, including for example the +RNA-strand tobamoviruses TMV (Karpova et al., 2002; Lee et al., 2005) and ToMV (Matsushita et al., 2002; Matsushita et al., 2003), the potexvirus potato virus X (PVX) (Modena et al., 2008) and the bipartite DNA begomovirus BDMV (Lee et al., 2005). In addition, other kinases were found to be involved in the geminiviral life cycle as well, suggesting them as further candidates for MP phosphorylation. These include e.g. SnRK1, an upstream activating kinase of SnRK1, shaggy-related protein kinases and various receptor like kinases (Wang et al., 2003; Mariano et al., 2004; Wang et al., 2005; Florentino et al., 2006; Piroux et al., 2007; Shen et al., 2011; Shen et al., 2012; Hanley-Bowdoin et al., 2013; Shen et al., 2014; Shen et al., 2018). The begomoviral AC2 protein and Rep, as well as the satellite-encoded βC1 protein were uncovered to be substrates for SnRK1 (Shen et al., 2011; Shen et al., 2014; Zhong et al., 2017; Shen et al., 2018; Yang et al., 2019). These studies have indicated that phosphorylation by SnRK1 can inhibit viral protein functions, i.e. in vDNA binding for Rep, or in silencing suppression in the case of AC2 protein and ßC1, and have suggested an important role of this kinase in phosphorylation-mediated defense responses against geminivirus infections.

CONCLUSION

The triple mutant MP versions of the bipartite New World begomovirus AbMV turned out to be helpful tools to investigate the functional role of plant-dependent MP phosphorylation in geminivirus–host interaction in closer detail. Our results support the assumption that AbMV MP undergoes a complex, host-dependent pattern of phosphorylation and likely dephosphorylation, and is probably embedded in a regulatory network of diverse host kinases and phosphatases controlling its phosphorylation status and thereby its effect on pathogenicity and vDNA spread, up to its successful establishment within cells. This regulatory node in the begomoviral MP may reflect host adaption aspects and impacts MP di- or oligomerization *via* its C-terminal domain. Other functions of MP may be controlled by phosphorylation as well, however, they are so far a matter of speculation. Future research will be needed to resolve the molecular details.

DATA AVAILABILITY STATEMENT

All datasets presented in this study are included in the article/ **Supplementary Material**.

AUTHOR CONTRIBUTIONS

TK designed and coordinated the research and wrote the manuscript. AH performed research (molecular experiments, microscopy, and FRET analysis) and contributed to writing of the manuscript. SK performed research (molecular experiments, infection, and analysis of plants). LL performed research (molecular experiments, yeast two-hybrid analysis). TR performed research (molecular experiments, yeast two-hybrid analysis). JF performed research (molecular experiments, yeast two-hybrid analysis). PB performed research (molecular experiments, yeast two-hybrid analysis). GK performed research (molecular experiments, infection and analysis of plants). HJ supported research co-ordination, wrote part of and edited the manuscript. CW co-ordinated part of the research, wrote part of and edited the manuscript.

FUNDING

This work was supported by the Deutsche Forschungsgemeinschaft DFG (KL1366/3-1) and by the Landesgraduierten Förderung Baden-Württemberg for AH.

ACKNOWLEDGMENTS

The authors like to thank Sina Homrighausen and Rebecca Hummel for excellent technical assistance, and the gardeners Diether Gotthardt, Marvin Müller and Annika Allinger for taking care of experimental plants. The authors gratefully acknowledge Dr. Stephan Eisler (University of Stuttgart, Stuttgart, Germany) for support in fluorescence microscopy and the Technology Platform "Cellular Analytics" of the Stuttgart Research Center Systems Biology for their support & assistance in this work. We thank Prof. Dr. Christopher Grefen (Ruhr-University Bochum, Germany) for kindly providing plasmids for the two-in-one FRET vector system and the SYP122entry construct, Prof. Dr. József Burgyán (Agricultural Biotechnology Center, Gödöllo, Hungary) for the p19 expression clone and PD Dr. Joachim Uhrig (Georg-August-Universität, Göttingen, Germany) for kindly providing Gateway-compatible yeast two-hybrid vectors pcACT2 and pAS2-1.

SUPPLEMENTARY MATERIAL

The Supplementary Material for this article can be found online at: https://www.frontiersin.org/articles/10.3389/fpls.2020.01155/full#supplementary-material

REFERENCES

Aberle, H. J., Rütz, M. L., Karayavuz, M., Frischmuth, S., Wege, C., Hülser, D., et al. (2002). Localizing BC1 movement proteins of Abutilon mosaic geminivirus in yeasts by subcellular fractionation and freeze-fracture immunolabelling. *Arch. Virol.* 147 (1), 103–107. doi: 10.1007/s705-002-8305-8

Akamatsu, N., Takeda, A., Kishimoto, M., Kaido, M., Okuno, T., and Mise, K. (2007). Phosphorylation and interaction of the movement and coat proteins of brome mosaic virus in infected barley protoplasts. *Arch. Virol.* 152 (11), 2087–2093. doi: 10.1007/s00705-007-1038-6

Amari, K., Boutant, E., Hofmann, C., Schmitt-Keichinger, C., Fernandez-Calvino, L., Didier, P., et al. (2010). A family of plasmodesmal proteins with receptor-like properties for plant viral movement proteins. *PLoS Pathog.* 6 (9), e1001119. doi: 10.1371/journal.ppat.1001119

Arsova, B., Watt, M., and Usadel, B. (2018). Monitoring of plant protein post-translational modifications using targeted proteomics. *Front. Plant Sci.* 9, 1168. doi: 10.3389/fpls.2018.01168

Blatt, M. R., and Grefen, C. (2014). Applications of fluorescent marker proteins in plant cell biology. *Methods Mol. Biol.* 1062, 487–507. doi: 10.1007/978-1-62703-580-4_26

Briddon, R. W., Lunness, P., Chamberlin, L. C., Pinner, M. S., Brundish, H., and Markham, P. G. (1992). The nucleotide sequence of an infectious insect-transmissible clone of the geminivirus Panicum streak virus. *J. Gen. Virol.* 73 (5), 1041–1047. doi: 10.1099/0022-1317-73-5-1041

Briddon, R. W., Liu, S., Pinner, M. S., and Markham, P. G. (1998). Infectivity of African cassava mosaic virus clones to cassava by biolistic inoculation. *Arch. Virol.* 143 (12), 2487–2492. doi: 10.1007/s007050050478

Burch-Smith, T. M., and Zambryski, P. C. (2012). Plasmodesmata paradigm shift: regulation from without versus within. *Annu. Rev. Plant Biol.* 63, 239–260. doi: 10.1146/annurev-arplant-042811-105453

Chowda-Reddy, R. V., Achenjang, F., Felton, C., Etarock, M. T., Anangfac, M. T., Nugent, P., et al. (2008). Role of a geminivirus AV2 protein putative protein kinase C motif on subcellular localization and pathogenicity. *Virus Res.* 135 (1), 115–124. doi: 10.1016/j.virusres.2008.02.014

Duan, Y. P., Powell, C. A., Purcifull, D. E., Broglio, P., and Hiebert, E. (1997). Phenotypic variation in transgenic tobacco expressing mutated geminivirus movement/pathogenicity (BC1) proteins. *Mol. Plant Microbe Interact.* 10 (9), 1065–1074. doi: 10.1094/MPMI.1997.10.9.1065

Evans, D., and Jeske, H. (1993). DNA B facilitates, but is not essential for, the spread of Abutilon mosaic virus in agroinoculated *Nicotiana benthamiana*. *Virology* 194 (2), 752–757. doi: 10.1006/viro.1993.1316

Florentino, L. H., Santos, A. A., Fontenelle, M. R., Pinheiro, G. L., Zerbini, F. M., Baracat-Pereira, M. C., et al. (2006). A PERK-like receptor kinase interacts with the geminivirus nuclear shuttle protein and potentiates viral infection. *J. Virol.* 80 (13), 6648–6656. doi: 10.1128/JVI.00173-06

Frischmuth, S., Kleinow, T., Aberle, H. J., Wege, C., Hulser, D., and Jeske, H. (2004). Yeast two-hybrid systems confirm the membrane- association and oligomerization of BC1 but do not detect an interaction of the movement proteins BC1 and BV1 of Abutilon mosaic geminivirus. *Arch. Virol.* 149 (12), 2349–2364. doi: 10.1007/s00705-004-0381-0

Fujiki, M., Kawakami, S., Kim, R. W., and Beachy, R. N. (2006). Domains of tobacco mosaic virus movement protein essential for its membrane association. *J. Gen. Virol.* 87 (9), 2699–2707. doi: 10.1099/vir.0.81936-0

Garcia-Arenal, F., and Zerbini, F. M. (2019). Life on the edge: Geminiviruses at the interface between crops and wild plant hosts. *Annu. Rev. Virol.* 6 (1), 411–433. doi: 10.1146/annurev-virology-092818-015536

Gorovits, R., Moshe, A., Ghanim, M., and Czosnek, H. (2014). Degradation mechanisms of the tomato yellow leaf curl virus coat protein following inoculation of tomato plants by the whitefly *Bemisia tabaci*. *Pest Manag. Sci.* 70 (10), 1632–1639. doi: 10.1002/ps.3737

Gorovits, R., Fridman, L., Kolot, M., Rotem, O., Ghanim, M., Shriki, O., et al. (2016). Tomato yellow leaf curl virus confronts host degradation by sheltering in small/midsized protein aggregates. *Virus Res.* 213, 304–313. doi: 10.1016/j.virusres.2015.11.020

Grefen, C., and Blatt, M. R. (2012). A 2in1 cloning system enables ratiometric bimolecular fluorescence complementation (rBiFC). *Biotechniques* 53 (5), 311–314. doi: 10.2144/000113941

Grigoras, I., Timchenko, T., Katul, L., Grande-Perez, A., Vetten, H. J., and Gronenborn, B. (2009). Reconstitution of authentic nanovirus from multiple cloned DNAs. *J. Virol.* 83 (20), 10778–10787. doi: 10.1128/JVI.01212-09

Gross, S. D., and Anderson, R. A. (1998). Casein kinase I: spatial organization and positioning of a multifunctional protein kinase family. *Cell Signal* 10 (10), 699–711. doi: 10.1016/s0898-6568(98)00042-4

Hanley-Bowdoin, L., Bejarano, E. R., Robertson, D., and Mansoor, S. (2013). Geminiviruses: masters at redirecting and reprogramming plant processes. *Nat. Rev. Microbiol.* 11 (11), 777–788. doi: 10.1038/nrmicro3117

Hecker, A., Wallmeroth, N., Peter, S., Blatt, M. R., Harter, K., and Grefen, C. (2015). Binary 2in1 vectors improve *in planta* (co)localization and dynamic protein interaction studies. *Plant Physiol.* 168 (3), 776–787. doi: 10.1104/pp.15.00533

Hesketh, E. L., Saunders, K., Fisher, C., Potze, J., Stanley, J., Lomonossoff, G. P., et al. (2018). The 3.3 A structure of a plant geminivirus using cryo-EM. *Nat. Commun.* 9 (1), 2369. doi: 10.1038/s41467-018-04793-6

Hipp, K., Grimm, C., Jeske, H., and Bottcher, B. (2017). Near-atomic resolution structure of a plant geminivirus determined by electron cryomicroscopy. *Structure* 251303-1309 (8), e1303. doi: 10.1016/j.str.2017.06.013

Hipp, K., Zikeli, K., Kepp, G., Schmid, L., Shoeman, R. L., Jurkowski, T. P., et al. (2019). Different forms of African cassava mosaic virus capsid protein within plants and virions. *Virology* 529, 81–90. doi: 10.1016/j.virol.2019.01.018

Hou, Y. M., Sanders, R., Ursin, V. M., and Gilbertson, R. L. (2000). Transgenic plants expressing geminivirus movement proteins: Abnormal phenotypes and delayed infection by tomato mottle virus in transgenic tomatoes expressing the bean dwarf mosaic virus BV1 or BC1 proteins. *Mol. Plant-Microbe Interact.* 13 (3), 297–308. doi: 10.1094/MPMI.2000.13.3.297

Hu, C. D., Chinenov, Y., and Kerppola, T. K. (2002). Visualization of interactions among bZIP and Rel family proteins in living cells using bimolecular fluorescence complementation. *Mol. Cell* 9 (4), 789–798. doi: 10.1016/s1097-2765(02)00496-3

Hu, Y., Li, Z., Yuan, C., Jin, X., Yan, L., Zhao, X., et al. (2015). Phosphorylation of TGB1 by protein kinase CK2 promotes barley stripe mosaic virus movement in monocots and dicots. *J. Exp. Bot.* 66 (15), 4733–4747. doi: 10.1093/jxb/erv237

Ingham, D. J., and Lazarowitz, S. G. (1993). A single missense mutation in the BR1 movement protein alters the host range of the squash leaf curl geminivirus. *Virology* 196 (2), 694–702. doi: 10.1006/viro.1993.1526

Jeske, H., Gotthardt, D., and Kober, S. (2010). *In planta* cloning of geminiviral DNA: the true Sida micrantha mosaic virus. *J. Virol. Methods* 163 (2), 301–308. doi: 10.1016/j.jviromet.2009.10.014

Jeske, H. (2000). Abutilon mosaic virus. *AAB Descr. Plant Viruses*. No. 373.

Jeske, H. (2009). "Geminiviruses," in *Torque Teno Virus: The Still Elusive Human Pathogens*. Eds. H. zur Hausen and E.-M. de Villiers (Berlin: Springer), 185–226.

Jeske, H. (2018). Barcoding of plant viruses with circular single-stranded DNA based on rolling circle amplifcation. *Viruses* 10 (9), 469. doi: 10.3390/v10090469

Jupin, I., De Kouchkovsky, F., Jouanneau, F., and Gronenborn, B. (1994). Movement of tomato yellow leaf curl geminivirus (TYLCV): involvement of the protein encoded by ORF C4. *Virology* 204 (1), 82–90. doi: 10.1006/viro.1994.1512

Karger, E. M., Frolova, O. Y., Fedorova, N. V., Baratova, L. A., Ovchinnikova, T. V., Susi, P., et al. (2003). Dysfunctionality of a tobacco mosaic virus movement protein mutant mimicking threonine 104 phosphorylation. *J. Gen. Virol.* 84 (3), 727–732. doi: 10.1099/vir.0.18972-0

Karpova, O. V., Rodionova, N. P., Ivanov, K. I., Kozlovsky, S. V., Dorokhov, Y. L., and Atabekov, J. G. (1999). Phosphorylation of tobacco mosaic virus movement protein abolishes its translation repressing ability. *Virology* 261 (1), 20–24. doi: 10.1006/viro.1999.9842

Karpova, O. V., Kozlovsky, S. V., Arkhipenko, M. V., Zayakina, O. V., Reshetnikova, V. G., Rodionova, N. P., et al. (2002). Comparative analysis of protein kinases that phosphorylate tobacco mosaic virus movement protein in vitro. *Dokl. Biochem. Biophys.* 386, 293–295. doi: 10.1023/a:1020780132470

Kawakami, S., Padgett, H. S., Hosokawa, D., Okada, Y., Beachy, R. N., and Watanabe, Y. (1999). Phosphorylation and/or presence of serine 37 in the movement protein of tomato mosaic tobamovirus is essential for intracellular localization and stability *in vivo*. *J. Virol.* 73 (8), 6831–6840. doi: 10.1099/0022-1317-81-8-2095

Kawakami, S., Hori, K., Hosokawa, D., Okada, Y., and Watanabe, Y. (2003). Defective tobamovirus movement protein lacking wild-type phosphorylation

sites can be complemented by substitutions found in revertants. *J. Virol.* 77 (2), 1452–1461. doi: 10.1128/jvi.77.2.1452-1461.2003

Kleinow, T., Holeiter, G., Nischang, M., Stein, M., Karayavuz, M., Wege, C., et al. (2008). Post-translational modifications of Abutilon mosaic virus movement protein (BC1) in fission yeast. *Virus Res.* 131 (1), 86–94. doi: 10.1016/j.virusres.2007.08.011

Kleinow, T., Himbert, S., Krenz, B., Jeske, H., and Koncz, C. (2009a). NAC domain transcription factor ATAF1 interacts with SNF1-related kinases and silencing of its subfamily causes severe developmental defects in Arabidopsis. *Plant Sci.* 177 (4), 360–370. doi: 10.1016/j.plantsci.2009.06.011

Kleinow, T., Nischang, M., Beck, A., Kratzer, U., Tanwir, F., Preiss, W., et al. (2009b). Three C-terminal phosphorylation sites in the Abutilon mosaic virus movement protein affect symptom development and viral DNA accumulation. *Virology* 390 (1), 89–101. doi: 10.1016/j.virol.2009.04.018

Kleinow, T., Tanwir, F., Kocher, C., Krenz, B., Wege, C., and Jeske, H. (2009c). Expression dynamics and ultrastructural localization of epitope-tagged Abutilon mosaic virus nuclear shuttle and movement proteins in *Nicotiana benthamiana* cells. *Virology* 391 (2), 212–220. doi: 10.1016/j.virol.2009.06.042

Kleinow, T. (2000). *Identification and characterization of potential components from stress and glucose signal transduction in A. thaliana. PhD thesis (Dr. rer. nat.)* (Cologne, Germany: Faculty of Mathematical and natural science, University of Cologne).

Koncz, C., Martini, N., Szabados, L., Hrouda, M., Bachmair, A., and Schell, J. (1994). "Specialized vectors for gene tagging and expression studies," in *Plant Molecular Biology Manual*. Eds. S. B. Gelvin and R. A. Schilperoort (Dordrecht: Kluwer Academic Publishers), 1–22.

Krapp, S., Schuy, C., Greiner, E., Stephan, I., Alberter, B., Funk, C., et al. (2017). Begomoviral movement protein effects in human and plant cells: Towards new potential interaction partners. *Viruses* 9 (11), 334. doi: 10.3390/v9110334

Krenz, B., Windeisen, V., Wege, C., Jeske, H., and Kleinow, T. (2010). A plastid-targeted heat shock cognate 70kDa protein interacts with the Abutilon mosaic virus movement protein. *Virology* 401 (1), 6–17. doi: 10.1016/j.virol.2010.02.011

Krenz, B., Jeske, H., and Kleinow, T. (2012). The induction of stromule formation by a plant DNA-virus in epidermal leaf tissues suggests a novel intra- and intercellular macromolecular trafficking route. *Front. Plant Sci.* 3, 291. doi: 10.3389/fpls.2012.00291

Laliberte, J. F., and Sanfacon, H. (2010). Cellular remodeling during plant virus infection. *Annu. Rev. Phytopathol.* 48, 69–91. doi: 10.1146/annurev-phyto-073009-114239

Laliberte, J. F., and Zheng, H. (2014). Viral manipulation of plant host membranes. *Annu. Rev. Virol.* 1 (1), 237–259. doi: 10.1146/annurev-virology-031413-085532

Lee, J. Y., and Lucas, W. J. (2001). Phosphorylation of viral movement proteins - regulation of cell-to-cell trafficking. *Trends Microbiol.* 9 (1), 5–8. doi: 10.1016/s0966-842x(00)01901-6

Lee, J. Y., Taoka, K., Yoo, B. C., Ben-Nissan, G., Kim, D. J., and Lucas, W. J. (2005). Plasmodesmal-associated protein kinase in tobacco and Arabidopsis recognizes a subset of non-cell-autonomous proteins. *Plant Cell* 17 (10), 2817–2831. doi: 10.1105/tpc.105.034330

Lewis, J. D., and Lazarowitz, S. G. (2010). Arabidopsis synaptotagmin SYTA regulates endocytosis and virus movement protein cell-to-cell transport. *Proc. Natl. Acad. Sci. U. S. A.* 107 (6), 2491–2496. doi: 10.1073/pnas.0909080107

Lewsey, M., Surette, M., Robertson, F. C., Ziebell, H., Choi, S. H., Ryu, K. H., et al. (2009). The role of the Cucumber mosaic virus 2b protein in viral movement and symptom induction. *Mol. Plant Microbe Interact.* 22 (6), 642–654. doi: 10.1094/MPMI-22-6-0642

Link, K., Vogel, F., and Sonnewald, U. (2011). PD trafficking of potato leaf roll virus movement protein in Arabidopsis depends on site-specific protein phosphorylation. *Front. Plant Sci.* 2, 18. doi: 10.3389/fpls.2011.00018

Littlejohn, G. R., Gouveia, J. D., Edner, C., Smirnoff, N., and Love, J. (2010). Perfluorodecalin enhances in vivo confocal microscopy resolution of *Arabidopsis thaliana* mesophyll. *New Phytol.* 186 (4), 1018–1025. doi: 10.1111/j.1469-8137.2010.03244.x

Lofke, C., Luschnig, C., and Kleine-Vehn, J. (2013). Posttranslational modification and trafficking of PIN auxin efflux carriers. *Mech. Dev.* 130 (1), 82–94. doi: 10.1016/j.mod.2012.02.003

Magliery, T. J., Wilson, C. G., Pan, W., Mishler, D., Ghosh, I., Hamilton, A. D., et al. (2005). Detecting protein-protein interactions with a green fluorescent protein fragment reassembly trap: scope and mechanism. *J. Am. Chem. Soc.* 127 (1), 146–157. doi: 10.1021/ja046699g

Mann, H., and Whitney, D. (1947). On a test of whether one of two random variables is stochastically larger than the other. *Ann. Math Statist.* 18, 50–60. doi: 10.1214/aoms/1177730491

Mariano, A. C., Andrade, M. O., Santos, A. A., Carolino, S. M., Oliveira, M. L., Baracat-Pereira, M. C., et al. (2004). Identification of a novel receptor-like protein kinase that interacts with a geminivirus nuclear shuttle protein. *Virology* 318 (1), 24–31. doi: 10.1016/j.virol.2003.09.038

Matsushita, Y., Yoshioka, K., Shigyo, T., Takahashi, H., and Nyunoy, H. (2002). Phosphorylation of the movement protein of cucumber mosaic virus in transgenic tobacco plants. *Virus Genes* 24 (3), 231–234. doi: 10.1023/a:1015324415110

Matsushita, Y., Ohshima, M., Yoshioka, K., Nishiguchi, M., and Nyunoya, H. (2003). The catalytic subunit of protein kinase CK2 phosphorylates *in vitro* the movement protein of tomato mosaic virus. *J. Gen. Virol.* 84 (2), 497–505. doi: 10.1099/vir.0.18839-0

Meggio, F., and Pinna, L. A. (2003). One-thousand-and-one substrates of protein kinase CK2? *FASEB J.* 17 (3), 349–368. doi: 10.1096/fj.02-0473rev

Melcher, U. (2000). The '30K' superfamily of viral movements proteins. *J. Gen. Virol.* 81 (1), 257–266. doi: 10.1099/0022-1317-81-1-257

Modena, N. A., Zelada, A. M., Conte, F., and Mentaberry, A. (2008). Phosphorylation of the TGBp1 movement protein of potato virus X by a *Nicotiana tabacum* CK2-like activity. *Virus Res.* 137 (1), 16–23. doi: 10.1016/j.virusres.2008.04.007

Nemes, K., Gellert, A., Almasi, A., Vagi, P., Saray, R., Kadar, K., et al. (2017). Phosphorylation regulates the subcellular localization of cucumber mosaic virus 2b protein. *Sci. Rep.* 7 (1), 13444. doi: 10.1038/s41598-017-13870-7

Ott, T. (2017). Membrane nanodomains and microdomains in plant-microbe interactions. *Curr. Opin. Plant Biol.* 40, 82–88. doi: 10.1016/j.pbi.2017.08.008

Pascal, E., Goodlove, P. E., Wu, L. C., and Lazarowitz, S. G. (1993). Transgenic tobacco plants expressing the geminivirus BL1 protein exhibit symptoms of viral disease. *Plant Cell* 5 (7), 795–807. doi: 10.1105/tpc.5.7.795

Pascal, E., Sanderfoot, A. A., Ward, B. M., Medville, R., Turgeon, R., and Lazarowitz, S. G. (1994). The geminivirus BR1 movement protein binds single-stranded DNA and localizes to the cell nucleus. *Plant Cell* 6 (7), 995–1006. doi: 10.1105/tpc.6.7.995

Perraki, A., Gronnier, J., Gouguet, P., Boudsocq, M., Deroubaix, A. F., Simon, V., et al. (2018). REM1.3's phospho-status defines its plasma membrane nanodomain organization and activity in restricting PVX cell-to-cell movement. *PLoS Pathog.* 14 (11), e1007378. doi: 10.1371/journal.ppat.1007378

Pilartz, M., and Jeske, H. (1992). Abutilon mosaic geminivirus double-stranded DNA is packed into minichromosomes. *Virology* 189 (2), 800–802. doi: 10.1016/0042-6822(92)90610-2

Pilartz, M., and Jeske, H. (2003). Mapping of Abutilon mosaic geminivirus minichromosomes. *J. Virol.* 77 (20), 10808–10818. doi: 10.1128/jvi.77.20.10808-10818.2003

Piroux, N., Saunders, K., Page, A., and Stanley, J. (2007). Geminivirus pathogenicity protein C4 interacts with *Arabidopsis thaliana* shaggy-related protein kinase AtSKeta, a component of the brassinosteroid signalling pathway. *Virology* 362 (2), 428–440. doi: 10.1016/j.virol.2006.12.034

Printen, J. A., and Sprague, G. F.Jr. (1994). Protein-protein interactions in the yeast pheromone response pathway: Ste5p interacts with all members of the MAP kinase cascade. *Genetics* 138 (3), 609–619.

Qin, S., Ward, B. M., and Lazarowitz, S. G. (1998). The bipartite geminivirus coat protein aids BR1 function in viral movement by affecting the accumulation of viral single-stranded DNA. *J. Virol.* 72 (11), 9247–9256. doi: 10.1128/JVI.72.11.9247-9256.1998

Richter, K. S., Gotz, M., Winter, S., and Jeske, H. (2016a). The contribution of translesion synthesis polymerases on geminiviral replication. *Virology* 488, 137–148. doi: 10.1016/j.virol.2015.10.027

Richter, K. S., Serra, H., White, C. I., and Jeske, H. (2016b). The recombination mediator RAD51D promotes geminiviral infection. *Virology* 493, 113–127. doi: 10.1016/j.virol.2016.03.014

Rojas, M. R., Jiang, H., Salati, R., Xoconostle-Cazares, B., Sudarshana, M. R., Lucas, W. J., et al. (2001). Functional analysis of proteins involved in movement of the monopartite begomovirus, tomato yellow leaf curl virus. *Virology* 291 (1), 110–125. doi: 10.1006/viro.2001.1194

Rojas, M. R., Hagen, C., Lucas, W. J., and Gilbertson, R. L. (2005). Exploiting chinks in the plant's armor: Evolution and emergence of geminiviruses. *Annu. Rev. Phytopathol.* 43, 361–394. doi: 10.1146/annurev.phyto.43.040204.135939

Rojas, M. R., Macedo, M. A., Maliano, M. R., Soto-Aguilar, M., Souza, J. O., Briddon, R. W., et al. (2018). World management of geminiviruses. *Annu. Rev. Phytopathol.* 56, 637–677. doi: 10.1146/annurev-phyto-080615-100327

Samuilova, O., Santala, J., and Valkonen, J. P. (2013). Tyrosine phosphorylation of the triple gene block protein 3 regulates cell-to-cell movement and protein interactions of potato mop-top virus. *J. Virol.* 87 (8), 4313–4321. doi: 10.1128/JVI.03388-12

Saunders, K., Bedford, I. D., and Stanley, J. (2001). Pathogenicity of a natural recombinant associated with ageratum yellow vein disease: implications for geminivirus evolution and disease aetiology. *Virology* 282 (1), 38–47. doi: 10.1006/viro.2000.0832

Schindelin, J., Arganda-Carreras, I., Frise, E., Kaynig, V., Longair, M., Pietzsch, T., et al. (2012). Fiji: an open-source platform for biological-image analysis. *Nat. Methods* 9 (7), 676–682. doi: 10.1038/nmeth.2019

Schubert, J., Habekuss, A., Kazmaier, K., and Jeske, H. (2007). Surveying cereal-infecting geminiviruses in Germany–diagnostics and direct sequencing using rolling circle amplification. *Virus Res.* 127 (1), 61–70. doi: 10.1016/j.virusres.2007.03.018

Schütze, K., Harter, K., and Chaban, C. (2009). Bimolecular fluorescence complementation (BiFC) to study protein-protein interactions in living plant cells. *Methods Mol. Biol.* 479, 189–202. doi: 10.1007/978-1-59745-289-2_12

Shen, Q., Liu, Z., Song, F., Xie, Q., Hanley-Bowdoin, L., and Zhou, X. (2011). Tomato SlSnRK1 protein interacts with and phosphorylates betaC1, a pathogenesis protein encoded by a geminivirus beta-satellite. *Plant Physiol.* 157 (3), 1394–1406. doi: 10.1104/pp.111.184648

Shen, Q., Bao, M., and Zhou, X. (2012). A plant kinase plays roles in defense response against geminivirus by phosphorylation of a viral pathogenesis protein. *Plant Signal Behav.* 7 (7), 888–892. doi: 10.4161/psb.20646

Shen, W., Dallas, M. B., Goshe, M. B., and Hanley-Bowdoin, L. (2014). SnRK1 phosphorylation of AL2 delays cabbage leaf curl virus infection in Arabidopsis. *J. Virol.* 88 (18), 10598–10612. doi: 10.1128/JVI.00761-14

Shen, W., Bobay, B. G., Greeley, L. A., Reyes, M. I., Rajabu, C. A., Blackburn, R. K., et al. (2018). Sucrose nonfermenting 1-related protein kinase 1 phosphorylates a geminivirus Rep protein to impair viral replication and infection. *Plant Physiol.* 178 (1), 372–389. doi: 10.1104/pp.18.00268

Silhavy, D., Molnar, A., Lucioli, A., Szittya, G., Hornyik, C., Tavazza, M., et al. (2002). A viral protein suppresses RNA silencing and binds silencing-generated, 21- to 25-nucleotide double-stranded RNAs. *EMBO J.* 21 (12), 3070–3080. doi: 10.1093/emboj/cdf312

Taoka, K., Ham, B. K., Xoconostle-Cazares, B., Rojas, M. R., and Lucas, W. J. (2007). Reciprocal phosphorylation and glycosylation recognition motifs control NCAPP1 interaction with pumpkin phloem proteins and their cell-to-cell movement. *Plant Cell* 19 (6), 1866–1884. doi: 10.1105/tpc.107.052522

Teng, K., Chen, H., Lai, J., Zhang, Z., Fang, Y., Xia, R., et al. (2010). Involvement of C4 protein of beet severe curly top virus (family *Geminiviridae*) in virus movement. *PLoS One* 5 (6), e11280. doi: 10.1371/journal.pone.0011280

Trutnyeva, K., Bachmaier, R., and Waigmann, E. (2005). Mimicking carboxyterminal phosphorylation differentially effects subcellular distribution and cell-to-cell movement of tobacco mosaic virus movement protein. *Virology* 332 (2), 563–577. doi: 10.1016/j.virol.2004.11.040

Uemura, T., Ueda, T., Ohniwa, R. L., Nakano, A., Takeyasu, K., and Sato, M. H. (2004). Systematic analysis of SNARE molecules in Arabidopsis: dissection of the post-Golgi network in plant cells. *Cell Struct. Funct.* 29 (2), 49–65. doi: 10.1247/csf.29.49

von Arnim, A., and Stanley, J. (1992). Determinants of tomato golden mosaic virus symptom development located on DNA B. *Virology* 186 (1), 286–293. doi: 10.1016/0042-6822(92)90083-2

Waigmann, E., Chen, M. H., Bachmaier, R., Ghoshroy, S., and Citovsky, V. (2000). Regulation of plasmodesmal transport by phosphorylation of tobacco mosaic virus cell-to-cell movement protein. *EMBO J.* 19 (18), 4875–4884. doi: 10.1093/emboj/19.18.4875

Waigmann, E., Ueki, S., Trutnyeva, K., and Citovsky, V. (2004). The ins and outs of nondestructive cell-to-cell and systemic movement of plant viruses. *Crit. Rev. Plant Sci.* 23195, 250. doi: 10.1080/07352680490452807

Wang, H., Hao, L., Shung, C. Y., Sunter, G., and Bisaro, D. M. (2003). Adenosine kinase is inactivated by geminivirus AL2 and L2 proteins. *Plant Cell* 15 (12), 3020–3032. doi: 10.1105/tpc.015180

Wang, H., Buckley, K. J., Yang, X., Buchmann, R. C., and Bisaro, D. M. (2005). Adenosine kinase inhibition and suppression of RNA silencing by geminivirus AL2 and L2 proteins. *J. Virol.* 79 (12), 7410–7418. doi: 10.1128/JVI.79.12.7410-7418.2005

Wege, C., and Jeske, H. (1998). Abutilon mosaic geminivirus proteins expressed and phosphorylated in *Escherichia coli*. *J. Phytopathol.* 146, 613–621. doi: 10.1111/j.1439-0434.1998.tb04763.x

Wege, C., Gotthardt, R. D., Frischmuth, T., and Jeske, H. (2000). Fulfilling Koch's postulates for Abutilon mosaic virus. *Arch. Virol.* 145 (10), 2217–2225. doi: 10.1007/s007050070052

Wege, C. (2007). "Movement and localization of tomato yellow leaf curl viruses in the infected plant," in *Tomato yellow leaf curl virus disease*. Ed. H. Czosnek (Dordrecht: Springer), 185–206.

Xu, X., Zhang, Q., Hong, J., Li, Z., Zhang, X., and Zhou, X. (2019). Cryo-EM structure of a begomovirus geminate particle. *Int. J. Mol. Sci.* 20 (7), 1738. doi: 10.3390/ijms20071738

Yang, X., Guo, W., Li, F., Sunter, G., and Zhou, X. (2019). Geminivirus-Associated Betasatellites: Exploiting Chinks in the Antiviral Arsenal of Plants. *Trends Plant Sci.* 24 (6), 519–529. doi: 10.1016/j.tplants.2019.03.010

Zhang, S. C., Wege, C., and Jeske, H. (2001). Movement proteins (BC1 and BV1) of Abutilon mosaic geminivirus are cotransported in and between cells of sink but not of source leaves as detected by green fluorescent protein tagging. *Virology* 290 (2), 249–260. doi: 10.1006/viro.2001.1185

Zhang, S. C., Ghosh, R., and Jeske, H. (2002). Subcellular targeting domains of Abutilon mosaic geminivirus movement protein BC1. *Arch. Virol.* 147 (12), 2349–2363. doi: 10.1007/s00705-002-0880-9

Zhong, X., Wang, Z. Q., Xiao, R., Cao, L., Wang, Y., Xie, Y., et al. (2017). Mimic Phosphorylation of a betaC1 Protein Encoded by TYLCCNB Impairs Its Functions as a Viral Suppressor of RNA Silencing and a Symptom Determinant. *J. Virol.* 91 (16), e00300-17. doi: 10.1128/JVI.00300-17

Zhou, Y. C., Garrido-Ramirez, E. R., Sudarshana, M. R., Yendluri, S., and Gilbertson, R. L. (2007). The N-terminus of the begomovirus nuclear shuttle protein (BV1) determines virulence or avirulence in *Phaseolus vulgaris*. *Mol. Plant Microbe Interact.* 20 (12), 1523–1534. doi: 10.1094/MPMI-20-12-1523

Zhou, Y., Rojas, M. R., Park, M. R., Seo, Y. S., Lucas, W. J., and Gilbertson, R. L. (2011). Histone H3 interacts and colocalizes with the nuclear shuttle protein and the movement protein of a geminivirus. *J. Virol.* 85 (22), 11821–11832. doi: 10.1128/JVI.00082-11

Zhukovsky, M. A., Filograna, A., Luini, A., Corda, D., and Valente, C. (2019). Protein Amphipathic Helix Insertion: A Mechanism to Induce Membrane Fission. *Front. Cell Dev. Biol.* 7, 291 (291). doi: 10.3389/fcell.2019.00291

Conflict of Interest: The authors declare that the research was conducted in the absence of any commercial or financial relationships that could be construed as a potential conflict of interest.

frontiers in Microbiology

ORIGINAL RESEARCH
published: 04 August 2020
doi: 10.3389/fmicb.2020.01828

RepA Promotes the Nucleolar Exclusion of the V2 Protein of Mulberry Mosaic Dwarf-Associated Virus

Dongxue Wang[1], Shaoshuang Sun[1], Yanxiang Ren[1,2], Shifang Li[1], Xiuling Yang[1] and Xueping Zhou[1,3]*

[1] State Key Laboratory for Biology of Plant Diseases and Insect Pests, Institute of Plant Protection, Chinese Academy of Agricultural Sciences, Beijing, China, [2] State Key Laboratory of Agro-Biotechnology and Ministry of Agriculture Key Laboratory of Soil Microbiology, College of Biological Sciences, China Agricultural University, Beijing, China, [3] State Key Laboratory of Rice Biology, Institute of Biotechnology, Zhejiang University, Hangzhou, China

Plant viruses have limited coding capacities so that they rely heavily on the expression of multifunctional viral proteins to achieve a successful infection. The functional specification of viral proteins is often related to their differential interaction with plant and viral components and somewhat depends on their localization to various subcellular compartments. In this study, we analyzed the intracellular localization of the V2 protein of *Mulberry mosaic dwarf-associated virus* (MMDaV), an unsigned species of the family *Geminiviridae*. We show that the V2 protein colocalizes with the nucleolar protein fibrillarin (NbFib2) in the nucleolus upon transient expression in the epidermal cells of *Nicotiana benthamiana*. A yeast-two hybrid assay, followed by bimolecular fluorescence complementation assays, demonstrated the specific interaction between V2 and NbFib2. Intriguingly, we find that the presence of MMDaV excludes the V2 protein from the nucleolus to nucleoplasm. We present evidence that the replication-associated protein A (RepA) protein of MMDaV interacts with V2 and enables the nucleolar exclusion of V2. We also show that, while V2 interacts with itself primarily in the nucleolus, the presence of RepA redirects the site of V2–V2 interaction from the nucleolus to the nucleoplasm. We further reveal that RepA promotes V2 out of the nucleolus presumably by directing the NbFib2-V2 complex from the nucleolus to the nucleoplasm. Considering the critical role of the nucleolus in plant virus infection, this RepA-dependent modulation of V2 nucleolar localization would be crucial for understanding the involvement of this subcellular compartment in plant–virus interactions.

Keywords: geminivirus, MMDaV, V2, RepA, nucleolus, protein–protein interactions

OPEN ACCESS

Edited by:
Araceli G. Castillo, Institute of Subtropical and Mediterranean Horticulture La Mayora, Spain

Reviewed by:
Eduardo Rodriguez Bejarano, University of Malaga, Spain
Tatjana Kleinow, University of Stuttgart, Germany

****Correspondence:***
Xiuling Yang
yangxiuling@caas.cn

Specialty section:
This article was submitted to Microbe and Virus Interactions with Plants, a section of the journal Frontiers in Microbiology

Received: *04 March 2020*
Accepted: *13 July 2020*
Published: *04 August 2020*

Citation:
Wang D, Sun S, Ren Y, Li S, Yang X and Zhou X (2020) RepA Promotes the Nucleolar Exclusion of the V2 Protein of Mulberry Mosaic Dwarf-Associated Virus. Front. Microbiol. 11:1828. doi: 10.3389/fmicb.2020.01828

INTRODUCTION

Plant viruses are obligate intracellular parasites that have long caused significant yield losses to crops and are continuously threatening crop cultivation worldwide. With limited coding capacities, plant viruses usually encode multifunctional viral proteins that play important roles in several steps of a virus life cycle. The functional specification of these multifunctional viral proteins is often

related to their differential interaction with host plant and viral components and somewhat depends on their dynamic localization to various subcellular compartments (Medina-Puche and Lozano-Duran, 2019). Understanding how viral proteins manipulate plant subcellular organelles would provide cues to depict protein function *in vivo*.

The plant nucleolus is the prominent subnuclear structure of cells that comprises several functional subcompartments such as fibrillar centers, a dense fibrillary component, a granular component, nucleolar vacuoles, nucleonema, and nucleolar chromatin (Stepinski, 2014). Besides its well-known role in ribosome RNA synthesis, the nucleolus plays critical roles in cell cycle regulation and responses to biotic and abiotic stresses (Kalinina et al., 2018). Although many plant RNA viruses replicate in the cytoplasm of host cells, an increasing number of viral proteins have been shown to localize, at least at some stage during infection, in the nucleolus (Hiscox, 2007). Examples include the umbravirus groundnut rosette virus (GRV) ORF3 protein (Kim et al., 2007), barley stripe mosaic virus (BSMV, hordeivirus) Triple Gene Block1 (TGB1) (Li et al., 2018), potyvirus VPg (Rajamäki and Valkonen, 2009), rice stripe virus (tenuivirus) P2 (Zheng et al., 2015), and the P20 protein encoded by bamboo mosaic virus (BaMV, potexvirus) satellite RNA (satRNA) (Chang et al., 2016). Viral proteins may subsequently utilize nucleolar functions for assembly of viral ribonucleoprotein (RNP) particles, virus replication, and movement, and to counteract plant antiviral defense (Kalinina et al., 2018).

Unlike RNA viruses, geminiviruses are a group of circular single-stranded DNA (ssDNA) viruses that replicate in the nucleus. Based on their genome organization, host range, and insect vector, geminiviruses have been classified into nine genera, namely, *Becurtovirus*, *Begomovirus*, *Capulavirus*, *Curtovirus*, *Eragrovirus*, *Grablovirus*, *Mastrevirus*, *Topocuvirus*, and *Turncurtovirus* (Zerbini et al., 2017). The genome of geminiviruses contains either one or two DNA molecules (2.7–3.0 kb) that is (are) encapsidated in twinned icosahedral particles. After uncoating, viral ssDNA is released into host cells and subsequently converted into double-stranded DNA (dsDNA) in the nuclei of differentiated plant cells (Gutierrez, 1999; Jeske, 2009). These dsDNAs can be packaged into viral minichromosomes that serve as templates for transcription, further replication, and the synthesis of progeny ssDNA that is encapsidated by the capsid protein to form virions (Gutierrez, 1999; Jeske, 2009; Hanley-Bowdoin et al., 2013). Assembly of geminivirus particles also occurs in the nucleus, and large aggregates consisting of geminivirus particles have been observed in the nuclei of infected plant cells (Rushing et al., 1987). Due to the extensive reliance of geminivirus life cycle on nuclear activities, many geminivirus proteins, such as Replication initiator protein (Rep) and transcription activator protein, target to the plant nucleus (Maio et al., 2019). As the nucleolus is the critical sub-domain of a plant nucleus, it is reasonable that the nucleus-replicating geminiviruses could interact with the immediately accessible nucleolus. For example, coat protein (CP), the unique protein required for geminivirus capsids formation, insect vector transmission, and nuclear shuttling of viral DNA of monopartite geminiviruses, is accumulated mainly in the nucleolus of both insect and tobacco cells (Kunik et al., 1998; Fondong, 2013). Reminiscent of the differential localization of CPs associated to the infection of animal DNA viruses, such as ssDNA Adeno-associated virus type 2 (Wistuba et al., 1997) and dsDNA human polyomavirus JC (Shishido-Hara et al., 2000), CP of a begomovirus tomato yellow leaf curl virus (TYLCV) is temporally excluded outside of the nucleolus in the progression of virus infection (Wang et al., 2017). This dynamic virus-dependent subnuclear localization of CP might underpin its different functions, highlighting the importance of observing the subcellular localization of viral proteins in the context of virus infection.

The V2/AV2 open reading frame, located upstream of the *CP* gene, is present in the virion-sense strand of different geminiviruses but not in members of the New World bipartite begomoviruses. The V2/AV2 protein of several geminiviruses has been identified as a suppressor of posttranscriptional gene silencing (PTGS) and transcriptional gene silencing (TGS) (Glick et al., 2008; Wang et al., 2014, 2018, 2019; Luna and Lozano-Durán, 2020). V2/AV2 is also involved in viral systemic infection, possibly by interacting with CP and facilitating nuclear export of CP to shuttle CP-mediated DNA export between the nucleus and cytoplasm (Poornima et al., 2011; Zhao et al., 2020). Although some functions of V2/AV2, such as the role in suppression of PTGS, are conserved across tested geminivirus species and genera (Luna and Lozano-Durán, 2020), the subcellular localization of V2/AV2 seems to vary in different species. The GFP-tagged V2 protein of monopartite begomoviruses, TYLCV, tomato leaf curl virus, tomato leaf curl Java virus, and a curtovirus beet curly top virus, is reported to localize to the perinuclear, cytoplasm, and endoplasmic reticulum of plant cells (Rojas et al., 2001; Sharma et al., 2011; Luna et al., 2017). TYLCV V2 is also demonstrated to form cytoskeleton-dependent aggregates that play an important role in TYLCV infection (Moshe et al., 2015), and to interact with AGO4 in the cajal body to suppress TGS (Ding and Lozano-Duran, 2020; Wang et al., 2020). The AV2 protein of a bipartite begomovirus, Indian cassava mosaic virus (ICMV), targets to cell periphery and to punctate spots that indicate plasmodesmal localization. ICMV AV2 also accumulates in nuclei in pairs of globular inclusions before it reaches the cells' periphery and the adjacent cells (Rothenstein et al., 2007). Grapevine red blotch-associated virus (GRBaV) V2 localizes to the nucleoplasm, Cajal bodies, and cytoplasm, and is redirected to the nucleolus upon coexpression with the nucleus and Cajal body-associated protein fibrillarin 2 (Fib2) (Guo et al., 2015). The V2 protein of a distinct monopartite geminivirus, Mulberry mosaic dwarf-associated virus (MMDaV), was shown to localize to both subnuclear foci and cytoplasm of the epidermal cells of *Nicotiana benthamiana* plants (Yang et al., 2018). Most of these experiments, however, have studied the subcellular localization of V2 in the absence of virus infection. Whether the localization of V2 is different in the context of virus infection remains to be evaluated. Since MMDaV V2 shows low sequence homology with the V2 proteins encoded by other geminiviruses (Ma et al., 2015), it is particularly interesting to investigate its subcellular localization in detail.

In this study, we analyzed the dynamic subcellular localization of MMDaV V2 in *N. benthamiana* in the absence or presence of MMDaV infection. We show that the MMDaV V2 protein colocalizes with the nucleolar protein fibrillarin in the nucleolus upon transient expression of V2 in the epidermal cells of *N. benthamiana*. Strikingly, we find that the V2 protein is excluded from the nucleolus to nucleoplasm in the context of MMDaV infection. We also demonstrate that the RepA interacts with V2 and mediates the change of V2 subcellular localization.

MATERIALS AND METHODS

Plant Growth

Wild-type *N. benthamiana* and transgenic *N. benthamiana* plants expressing a red fluorescent protein (RFP)-tagged histone 2B nuclear marker protein (RFP-H2B plants) (Martin et al., 2009) were grown in an insect-free growth room at 25°C under a 16 h light/8 h dark cycle.

Plasmid Construction

The *RepA*, *V2*, and *V3* genes from MMDaV (GenBank accession number KP303687) (Ma et al., 2015), the $V2^{dm61-77aa}$ from pGEM-T-$V2^{dm61-77aa}$ (Yang et al., 2018) and the coding sequences of the *fibrillarin 2* gene of *N. benthamiana* cDNA (GenBank accession number AM269909, NbFib2) were cloned into pENTR-D/TOPO entry vector without stop codon by standard protocols (Invitrogen, Beijing, China) to yield pENTR-RepA, pENTR-V2, pENTR-V3, pENTR-$V2^{dm61-77aa}$, and pENTR-NbFib2, respectively. For subcellular localization analysis, NbFib2 and RepA was gateway-cloned into plant binary vectors pEarleyGate102 [N-terminal cyan fluorescent protein (CFP) fusion] and pGWB454 (N-terminal RFP fusion) to yield Fib2-RFP and RepA-CFP, respectively (Earley et al., 2006; Nakagawa et al., 2007). The expression vectors, GFP-V2 and GFP-$V2^{dm61-77aa}$, containing fusions to an enhanced green fluorescent protein (eGFP) were constructed previously (Yang et al., 2018). To produce bimolecular fluorescence complementation (BiFC) vectors, the entry clones were transferred to gateway compatible 201-YN vector to yield a fusion with the N-terminal fragment of yellow fluorescent protein (nYFP) or the 201-YC vector as a fusion with the C-terminal fragment of YFP (cYFP) as described (Lu et al., 2010). To generate the bait and prey plasmids for yeast two-hybrid assays, the full-length fragment of RepA, V2, and NbFib2 was amplified using TransStart FastPfu high-fidelity DNA polymerase following the manufacturer's instructions (Transgene, Beijing, China) and then cloned into the *Eco*RI-*Bam*HI site of the yeast GAL4 DNA-binding domain vector pGBKT7 and the yeast GAL4 activation domain vector pGADT7 (Clontech, China), respectively. The oligonucleotide primers used to generate the plasmids are listed in **Supplementary Table S1**. All inserts were confirmed by DNA sequencing.

A two-tandem repeat of MMDaV was cloned into the pBinPLUS vector to generate the infectious clone of MMDaV (Yang et al., unpublished). The recombinant plant binary pCHF3 vectors expressing the individual ORFs of MMDaV (*V1, V3, V4, V5, RepA,* and *Rep*) were constructed in a previous study (Yang et al., 2018).

Transient Expression by Agro-Infiltration

The resulting plant expression constructs were individually transformed into the *Agrobacterium tumefaciens* strain C58C1. The infectious clone of MMDaV was electroporated into *A. tumefaciens* strain EHA105. Agrobacteria cells carrying these constructs were individually cultured, resuspended with the infiltration buffer containing 10 mM $MgCl_2$, 10 mM MES (pH5.8), and 100 μM acetosyringone, and infiltrated into 4-week-old wild-type *N. benthamiana* or RFP-H2B transgenic *N. benthamiana* leaves as described (Yang et al., 2018). For co-infiltration experiments, *A. tumefaciens* cultures harboring different constructs were adjusted to an optical density OD_{600} = 1.0 and mixed in equal proportion before infiltration.

Confocal Microscopy

Imaging of fluorescent proteins in the epidermal cells of agroinfiltrated *N. benthamiana* or RFP-H2B plants was performed on a laser-scanning confocal microscope (LSM880; Carl Zeiss, Jena, Germany) at 36–48 hours post-infiltration (hpi). Leaf tissues were examined using a Zeiss c-Apochromat 40 × 1.2 water immersion Korr objective. The GFP fluorophore was excited with 488-nm laser lines and emission was detected at 500–550 nm. To avoid chlorophyll auto-fluorescence, the RFP fluorophore was excited with 561-nm laser lines and emission was detected at 600–630 nm. The YFP fluorophore was excited with 514-nm laser lines and emission was detected at 519–587 nm. The CFP fluorophore was excited with 458-nm laser lines and emission was detected at 470–500 nm. For every experimental sample, at least three independent biological replicates were examined. Images were processed with Zeiss ZEN software.

Plant RNA Extraction and Analysis

Total RNA was extracted from infiltrated leaf regions of RFP-H2B plants using TRIzol reagent (Invitrogen, Carlsbad, CA, United States) following the manufacturer's instructions. Complementary DNA (cDNA) was synthesized from 1 μg of total RNA using PrimeScript RT reagent Kit with genomic DNA Eraser (Takara, Dalian, China). Expression of the individual ORF of MMDaV was detected by reverse transcription PCR (RT-PCR) from the synthesized cDNA as previously described (Yang et al., 2018).

Analysis of Protein Expression

Total plant proteins were extracted from infiltrated leave patches as described (Yang et al., 2011). Supernatant of extracted proteins was resolved by 12.5% SDS-PAGE, and transferred to nitrocellulose membranes which were then blocked and probed with primary antibodies raised against GFP (Roche Applied Science, Basel, Switzerland), HA (Santa Cruz, California, CA, United States), or FLAG (Sigma-Aldrich, St Louis, MO, United States). After washing, the membranes were incubated with a secondary peroxidase-conjugated goat antimouse antibody (Cell Signaling Technology, Boston, MA, United States).

The results were visualized using a chemiluminescence detection system (Tianneng, Shanghai, China).

Yeast Two-Hybrid Assays

GAL4-based yeast two-hybrid (Y2H) assays were carried out following the Clontech yeast protocol handbook. In brief, both plasmids containing fusion proteins with the GAL4 activation domain and DNA-binding domain were cotransformed into the yeast strain Y2H Gold and plated onto a selective medium lacking tryptophan and leucine (SD/-Trp/-Leu) at 30°C for 3–5 days to select for doubly transformed yeast cells. Transformants were then transferred to the selective medium lacking leucine, histidine, and tryptophan (SD/-Leu/-His/-Trp) containing 5 mM 3-amino-1,2,4-triazole (3-AT) or the selective medium lacking adenine, histidine, leucine and tryptophan (SD/-Ade/-His/-Leu/-Trp) and cultured at 30°C for 3–5 days to identify possible interaction by activation of reporter genes His3 and/or Trp.

RESULTS

V2 Colocalizes With Fibrillarin in the Nucleolus

To better understand the subcellular localization of MMDaV V2, we took advantage of the transgenic *N. benthamiana* plants expressing RFP-H2B (hereafter designated as RFP-H2B plants). These plants contain a 2 × 35 Spro:RFP-H2B expression cassette which allow us to monitor the nucleoplasm but not the nucleolus of plant cells (Martin et al., 2009). We set out to transiently infiltrate the agrobacteria cultures harboring the GFP-V2 fusion construct (GFP was fused to the N-terminal of V2) into the leaves of RFP-H2B plants and visualized the fluorescence by confocal laser-scanning microscopy (CLSM) at 36 hpi. As a control, agrobacteria cultures containing construct solely expressing GFP was infiltrated into the leaves of RFP-H2B plants. Consistent with the previous study (Yang et al., 2018), V2 accumulates in the cytoplasm and nucleus (**Supplementary Figure S1A**). A close-up view of the nucleus showed that V2 accumulated to the subnuclear bodies of varying numbers (from approximately three to 12, with a mean number of about six), and these subnuclear bodies formed aggregates in about 25% of the observed cells (n = 60) (**Supplementary Figure S1B**). Despite of the varied number of subnuclear bodies in different cells, V2 was observed to target to a subnuclear dot resembling a localization within the nucleolus in all the detected cells (**Figure 1A**). This was in contrast to the GFP alone infiltrated RFP-H2B plant leaves, where GFP was excluded from the nucleolar regions (**Figure 1A**).

To further establish the ability of MMDaV V2 to localize in the nucleolus, we began to determine if the V2 protein colocalizes with fibrillarin, one of the major nucleoprotein that is considered as a typical marker for the subnuclear compartment (Zheng et al., 2016). As described previously (Zheng et al., 2016), confocal imaging of *N. benthamiana* plant leaves expressing NbFib2-RFP with GFP showed that NbFib2 localized to the nucleolus and Cajal body of the epidermal cells of *N. benthamiana* plant leaves (**Figure 1B**). Besides, GFP was excluded from the nucleolar regions in *N. benthamiana* leaves co-infiltrated with GFP and NbFib2-RFP (**Figure 1B**). However, *N. benthamiana* plant leaves expressing GFP-V2 and NbFib2-RFP and imaged by CLSM showed clear colocalization of V2 with NbFib2 mainly in the nucleolus (**Figure 1B**), indicating that V2 is present in the nucleolus of plant cells.

V2 Interacts With NbFib2

As confocal microscopy suggests a colocalization of V2 and NbFib2 in the nucleolus of plant cells, a Y2H assay was performed to determine whether V2 directly interacts with NbFib2. V2 and NbFib2 was cloned into both of the yeast two-hybrid "prey" (Y2H) pGADT7 and "bait" pGBKT7 vectors to produce AD and BD fusions, and the bait and prey plasmids were then cotransformed to yeast strain Y2H Gold. Cotransformation of murine tumor suppressor p53 and simian virus 40 large T antigen (T) was used as a positive control and that of human lamin (Lam) and T as a negative control. Similar to the positive control, robust growth of yeast transformants containing BD-NbFib2 and AD-V2 was observed on the selective medium lacking histidine, leucine, and tryptophan supplementing with 5 mM 3-AT, whereas yeast transformants harboring AD-V2 with the empty BD vector or BD-NbFib2 with the empty AD vector failed to grow on the selective triple dropout medium, suggesting the specific interaction between NbFib2 and V2 in yeast cells (**Figure 2A**). NbFib2-V2 interaction was then confirmed in plant cells using BiFC. While no signal was detected for the negative control combination of V2–V3, YFP signal was evident in the cells co-infiltrated with the BiFC combinations of V2-NbFib2 (**Figure 2B**). As shown in **Figure 2B**, coexpression of V2 fused to the N-terminal of YFP (V2-nYFP) and NbFib2 fused to the C-terminal of YFP (NbFib2-cYFP) or NbFib2-nYFP and V2-cYFP reconstituted YFP fluorescence primarily in the nucleolus and weakly in the nucleoplasm in about 67% of the YFP-detectable cells (n = 60), and occasionally in some structures around/outside the nucleus in about 33% of the cells (**Figure 2B**), indicating that V2 interacts with NbFib2.

Since mutation of the predicted nuclear localization signal (NLS, from amino acids 61–77) of MMDaV V2 abolished its subnuclear foci localization and PTGS suppression activity (Yang et al., 2018), we performed a BiFC assay to evaluate whether this MMDaV V2 mutant interacts with NbFib2. As shown in **Figure 2B**, the NLS mutant of V2 did not interact with NbFib2 (**Figure 2B**). We then detected whether the NLS mutant is able to colocalize with NbFib2. In contrast to the wild-type V2 protein, the NLS mutant of V2 localized to the nucleoplasm and cytoplasm, while NbFib2 localized to the nucleolus (**Figure 2C**). Immunoblot analysis of total protein from infiltrated leave samples showed that the NLS mutant does not affect the stability of the V2 protein (**Figure 2D** and **Supplementary Figure S2**). These results suggest that V2, but not the V2 NLS mutant, colocalizes and interacts with NbFib2.

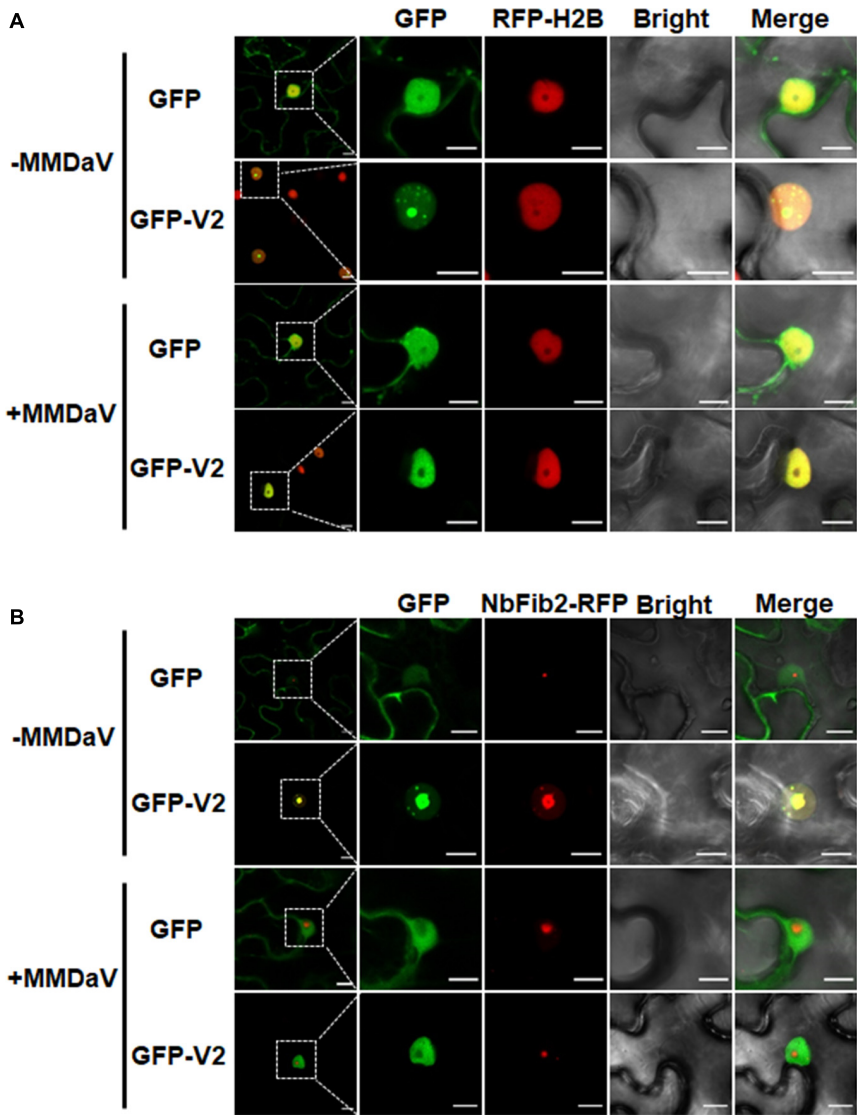

FIGURE 1 | V2 localization within the nucleolus is modulated in the presence of mulberry mosaic dwarf-associated geminivirus (MMDaV). **(A)** Subcellular localization of green fluorescent protein (GFP) or GFP-V2 fusion in the absence or presence of MMDaV infection in transgenic *Nicotiana benthamiana* plants expressing red fluorescent protein (RFP)-tagged histone 2B (RFP-H2B). RFP-H2B was used as a nuclear marker. **(B)** Colocalization analysis of V2 and fibrillarin 2 (NbFib2) in the absence or presence of MMDaV in *N. benthamiana* plants. To create an environment mimicking MMDaV infection, the infectious clone of MMDaV was infiltrated into RFP-H2B or *N. benthamiana* leaves 12 h prior to the infiltration of GFP or GFP-V2. Images were taken using Zeiss LSM 880 confocal laser scanning microscope at 36 hours post infiltration (hpi) of GFP or GFP-V2. This experiment was done three times and more than 20 cells were observed per sample and replicate. A representative image is shown for each set. The corresponding region in the white box in column 1 is magnified and shown from Column 2 to Column 5. Scale bars correspond to 10 μm.

V2 Nucleolar Accumulation Is Modulated in the Context of Virus Infection

To assess whether the subcellular localization of V2 varies during virus infection, the infectious clone of MMDaV was infiltrated into RFP-H2B plant leaves 12 h prior to the infiltration of agrobacteria cultures of GFP or GFP-V2 to create a cellular environment mimicking a natural viral infection. As shown in **Figure 1A**, MMDaV infection modulated the accumulation of V2 in the nucleus. In particular, the distribution of GFP-V2 displayed relocalization throughout the nucleoplasm but not to the nucleolus in all detected cells ($n = 60$). However, coexpression of GFP with MMDaV did not cause any profound shift in the localization of GFP (**Figure 1A**). Western blot analysis of total protein from infiltrated leave patches with the antibody against GFP showed that both GFP and GFP-V2 were expressed in the absence or presence of MMDaV (**Supplementary Figure S3**). Since V2 colocalizes with NbFib2 in the nucleolus in the absence of MMDaV infection, we next investigated whether V2 and NbFib2 could still colocalize in the nucleolus in the presence of virus infection. To this end, infectious clone of

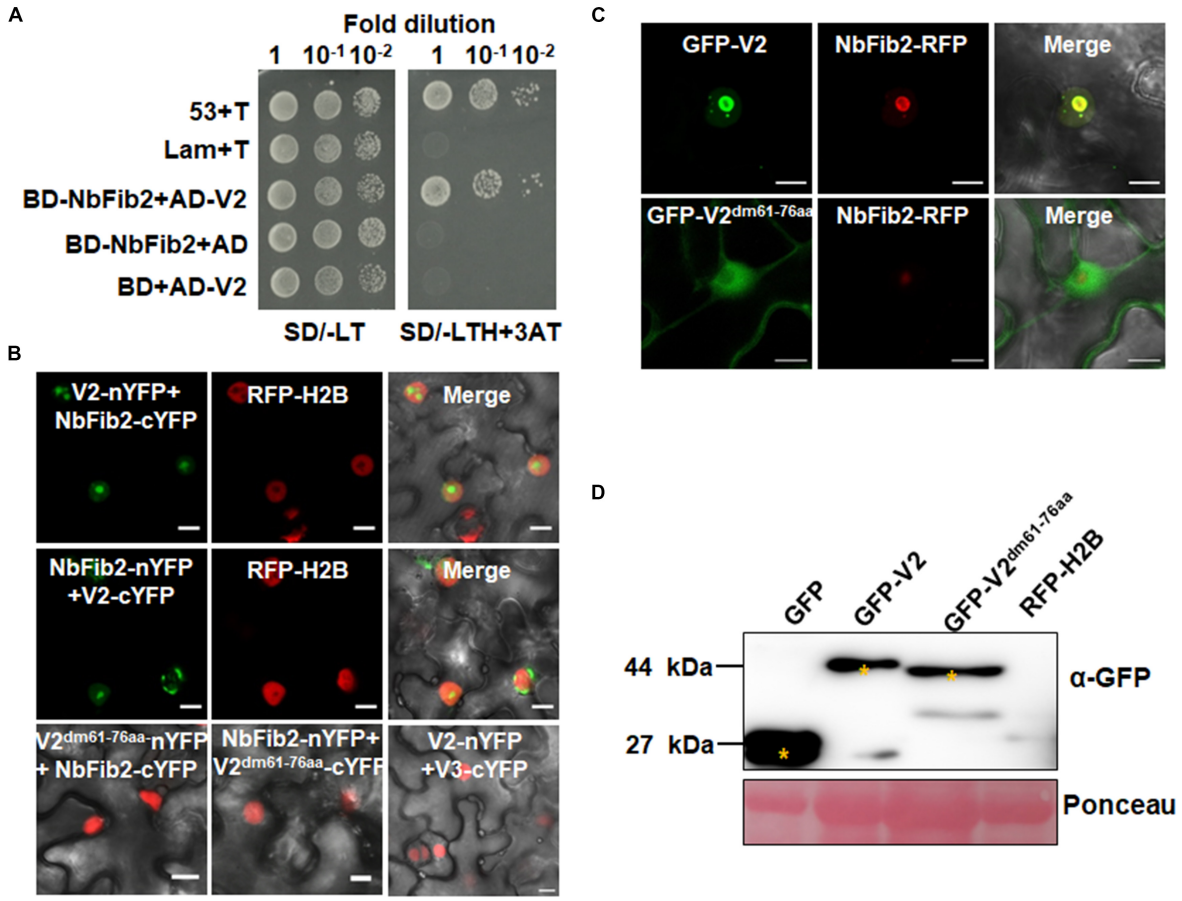

FIGURE 2 | V2 interacts with NbFib2. **(A)** Yeast two-hybrid assay showing the interaction between V2 and NbFib2 in yeast cells. Full-length NbFib2 was expressed as GAL4 DNA-binding domain fusion (BD, bait) and V2 was expressed as GAL4 activation domain fusion (AD, prey) in yeast cells of the strain Y2H Gold. The interaction of p53 and T was used as a positive control, and cotransformation of Lam and T was used as a negative control. Growth on the plates lacking leucine and tryptophan (SD/-LT) indicates successful transformation of both prey and bait vectors, respectively. Interaction between NbFib2 and V2 is indicated by growth of yeast cells on media also lacking histidine supplementing with 5 mM 3-amino-1,2,4-triazole (SD/-LTH + 3-AT). **(B)** Bimolecular fluorescence complementation assay (BiFC) assay showing the interaction between NbFib2 and V2 in plant cells. Constructs containing N-terminal YFP fusion (nYFP) and C-terminal YFP fusion (cYFP) fusions were infiltrated into RFP-H2B plant leaves. Combinations of BiFC constructs are shown at the top of each panel. Images were taken using a Zeiss LSM 880 confocal laser scanning microscope at 48 hpi. Reconstituted YFP signals resulting from V2-NbFib2 interaction are displayed as a false-green color. RFP-H2B served as a nuclear marker. Note that deletion of the predicted nuclear localization signal (from amino acid 61–76) of V2 abolishes its interaction with NbFib2. **(C)** Colocalization analysis of NbFib2 with V2 and V2 mutant in the epidermal cells of *N. benthamiana* by Zeiss LSM 880 confocal laser scanning microscope at 36 hpi. At least 60 cells from three repeats were examined. Scale bars correspond to 10 μm. **(D)** Immunoblot of proteins from RFP-H2B plant leaves infiltrated with construct as indicated using anti-GFP antibody. Ponceau staining of the large subunit of Rubisco serves as a loading control.

MMDaV was infiltrated into *N. benthamiana* leaves 12 h before the coinfiltration of GFP-V2 with NbFib2-RFP. Using confocal microscopy, we observed that V2 could not colocalize with NbFib2 in the nucleolus in the context of MMDaV infection, i.e., NbFib2 accumulated mainly in the nucleolus, whereas V2 was found in the nucleoplasm (**Figure 1B**), suggesting that the capability of V2 localizing to the nucleolus changes in the context of MMDaV infection.

RepA Interacts With V2 and Excludes V2 From the Nucleolus

In animal viruses and TYLCV, virus-regulated dynamic localization of CPs is contributed to another viral protein(s) (Wistuba et al., 1997; Shishido-Hara et al., 2000). For example, the Rep protein of TYLCV can mediate the nucleolar exclusion of CP (Wang et al., 2017). Unlike all the identified monopartite geminiviruses, the distinct monopartite geminivirus MMDaV encodes five ORFs (V1, V2, V3, V4, and V5) and two ORFs (C1 or RepA, and C2 or Rep) on the virion-sense and the complementary-sense strands, respectively (Ma et al., 2015). To test whether any of another viral protein(s) of MMDaV is responsible for the differential localization of V2 associated with MMDaV infection, agrobacteria cultures harboring the construct of GFP-V2 was transiently infiltrated into RFP-H2B plant leaves together with bacterium cultures containing pCHF3 plasmids expressing each of the viral proteins including V1, V3, V4, V5, RepA, and Rep independently. Similar to what was

seen in GFP-V2 alone infiltrated RFP-H2B plants, co-infiltration of GFP-V2 with any of the five proteins (V1, V3, V4, V5, and Rep) was not able to recapitulate the MMDaV-induced nucleolar exclusion of V2. Strikingly, when GFP-V2 was coinfiltrated with RepA, it no longer showed a nucleolar accumulation and instead was more evenly distributed throughout the nucleoplasm in all detected 60 cells (**Figure 3**). RT-PCR amplification of the individual MMDaV ORFs from the leaf disks used for confocal

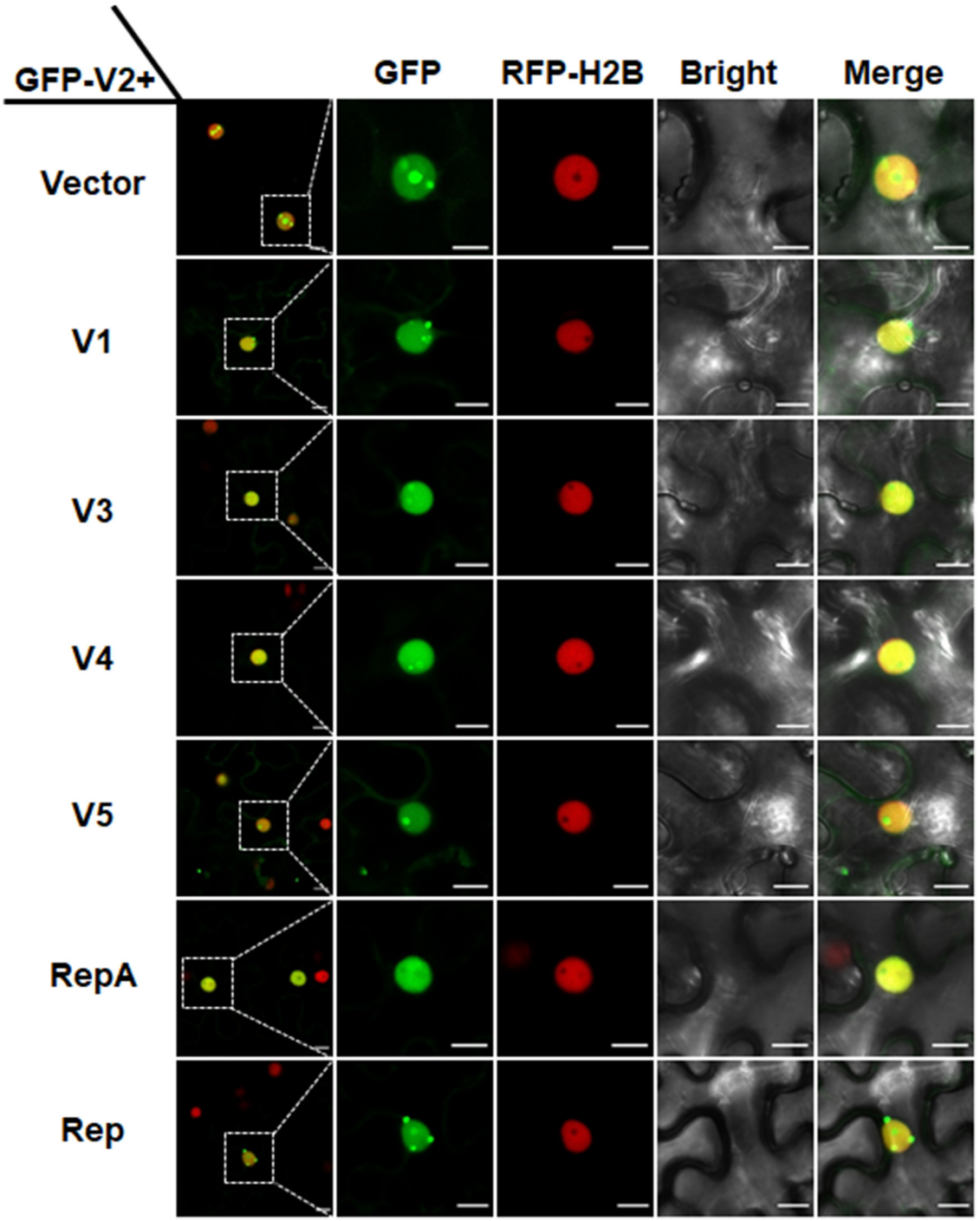

FIGURE 3 | RepA-dependent nucleolar exclusion of V2. RFP-H2B plant leaves were infiltrated with *Agrobacterium tumefaciens* cultures carrying constructs to express GFP-V2 and the other six individual ORFs (V1, V3, V4, V5, RepA, and Rep) of MMDaV. Fluorescence was visualized under a Zeiss LSM 880 confocal laser scanning microscope at 36 hpi. The corresponding region in the white box in column 1 is magnified and shown from Column 2 to Column 5. RFP-H2B was used as a nuclear marker. This experiment was done three times and more than 20 cells were observed per sample and replicate. Scale bars correspond to 10 μm.

microscopy confirmed the expression of viral genes from the binary vectors (**Supplementary Figure S4**), indicating that RepA is sufficient to exclude V2 from the nucleolus.

As RepA is sufficient to exclude V2 from the nucleolus, it raised the possibility that there might be a direct interaction between RepA and V2. To test the hypothesis, we explored both the Y2H and BiFC assay to examine the interaction of V2 and RepA. While the fusion protein BD-RepA interacted with the AD-V2 fusion, no activation of the reporter gene was observed when BD-RepA with AD or BD and AD-V2 was expressed in the yeast cells (**Figure 4A**). Further examination of the potential RepA-V2 interaction by the BiFC assay showed that the fluorescence due to the reconstitution of YFP *in planta* was only observed in the nucleoplasm by the BiFC combination of RepA and V2 (**Figure 4B**). However, no YFP signal was visible in any combination of the negative controls V2-nYFP + V3-cYFP, V3-nYFP + V2-cYFP, RepA-nYFP + V3-cYFP, and V3-nYFP + RepA-cYFP (**Figure 4B**), suggesting that V2 physically interacts with RepA. Collectively, our results reveal that RepA interacts with V2 and redistributes V2 from the nucleolus to nucleoplasm.

RepA Excludes the Site of V2–V2 Interactions From the Nucleolus

Self-interaction of viral proteins play critical roles in many steps of the virus infection cycle. To determine whether V2 interacts with itself and whether RepA has any impact on V2 self-interaction, we first tested the self-interaction of V2 in yeast cells. Growth of yeast transformants harboring AD-V2 and BD-V2 in selective yeast medium plates lacking adenine, histidine, leucine, and tryptophan indicated the self-interaction of V2 in yeast cells (**Figure 5A**). The capacity for self-interaction of V2 was further determined by the BiFC assay. Coexpression of V2 fused to the N-terminal of YFP (V2-nYFP) and V2 fused to the C-terminal of YFP (V2-cYFP) reconstituted

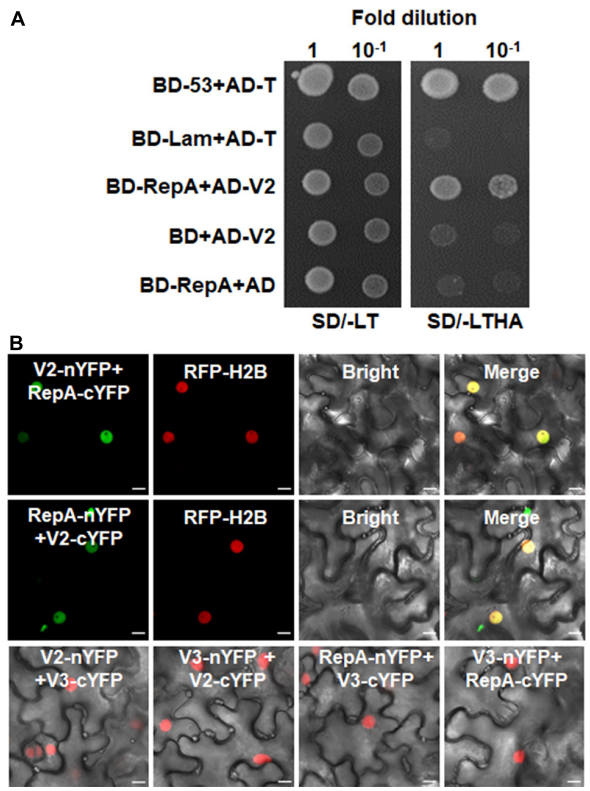

FIGURE 4 | RepA interacts with V2 in yeast and plant cells. **(A)** Yeast two-hybrid assay showing the interaction between RepA and V2 in yeast cells. Growth of yeast cotransformants containing the BD-RepA and AD-V2 fusions on the plates lacking leucine, tryptophan, histidine, and adenine (SD/-LTHA) indicates specific interaction between RepA and V2. **(B)** BiFC assay showing the interaction between RepA and V2 in plant cells. Combinations of BiFC constructs are shown at the top of each panel. Images were taken using a Zeiss LSM 880 confocal laser scanning microscope at 48 hpi. Reconstituted YFP signals as a consequence of V2-RepA interaction are depicted as a false-green color. RFP-H2B served as a nuclear marker.

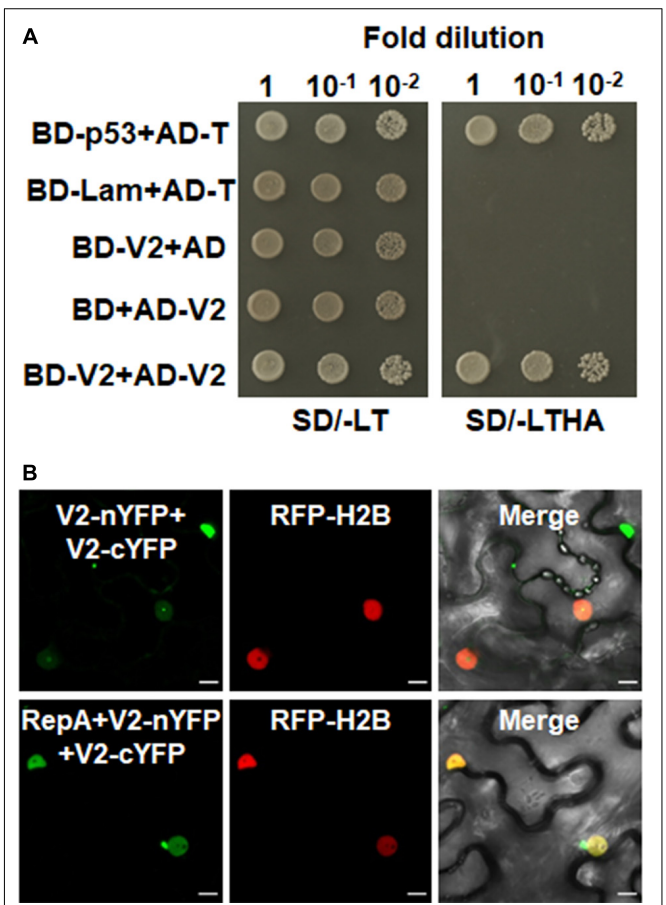

FIGURE 5 | RepA changes the site of V2–V2 self-interaction. **(A)** Self-interaction of V2 determined by yeast two-hybrid assay. **(B)** BiFC assays in leave cells of RFP-H2B plants. Self-interaction of V2 in the absence or presence of RepA was examined at 48 hpi using a confocal microscope. YFP signal resulting from interacting protein combinations are indicated as green. RFP-H2B was a marker for the nucleus. Note that the sites of V2–V2 self-interaction was excluded from the nucleolus by RepA. Images are representative of three independent experiments, in each of which at least 20 cells were examined. Scale bars correspond to 10 μm.

YFP fluorescence mainly in the nucleolus and weakly in the nucleoplasm (**Figure 5B**). However, when V2-nYFP and V2-cYFP was coexpressed with RepA, the reconstituted YFP fluorescence was reduced in the nucleolus and redistributed to the nucleoplasm in all the YFP-detectable cells (n = 60) (**Figure 5B**), suggesting that RepA also has a profound influence on the sites of V2–V2 interaction.

RepA Changes the Interaction Site of V2 and NbFib2

As V2 colocalized and interacted with NbFib2 in the nucleolus, we tried to determine whether RepA mediates nucleolar exclusion of V2 by impacting the V2-NbFib2 interaction. For this purpose, a CFP-tagged RepA (RepA-CFP) construct was generated and coexpressed with the BiFC combination of V2 and NbFib2. Interestingly, when RepA-CFP was coexpressed with NbFib2-nYFP and V2-cYFP in RFP-H2B plant leaves, an altered pattern of BiFC signal distribution was detected in infiltrated cells. Coexpression of the RepA-CFP protein with NbFib2-nYFP and V2-cYFP consequently redistributed the V2-NbFib2 complex out of the nucleolus to the nucleoplasm (**Figure 6**). Exclusion of the V2-NbFib2 complex from the nucleolus was also detected upon the infiltration of *N. benthamiana* plant leaves with MMDaV, NbFib2-nYFP, and V2-cYFP (**Figure 6**). These data shows that RepA is able to redirect the V2-NbFib2 complexes to the nucleoplasm during MMDaV infection.

DISCUSSION

Geminiviruses are known to have a limited coding capacity and have compensated for this restriction by encoding multifunctional viral proteins to make use of host biosynthetic machinery and to suppress multiple layers of plant immune responses to achieve a successful infection (Shunmugiah et al., 2017; Yang et al., 2019). Perhaps as a consequence, geminivirus multifunctional proteins could be distributed in various compartments of a plant cell to establish contacts with different host and viral components to fulfill their multiple tasks. In this study, we compared the subcellular localization of MMDaV V2 in non-infected and infected plant cells. We observed the modulated subcellular distribution of V2 in response to MMDaV infection. While the V2 protein accumulates in the nucleolus upon transient expression in the epidermal cells of *N. benthamiana* plants, V2 is excluded from the nucleolus in cells infected with MMDaV. This localization difference of V2 is associated to the presence of the RepA protein of MMDaV.

Viral proteins targeting the nucleus generally rely on a nuclear localization signal consisting of a short stretch of basic residues that allows interaction with the nuclear import proteins, importins, mediating entry into the nucleus via the nuclear pore complex (Lange et al., 2007). In contrast, despite many different sequences that are able to direct plant or viral proteins to the nucleolus have been identified, there is no consensus signal for nucleolar localization. The localization of a viral protein to the nucleolus largely attributes to direct or indirect interaction with other nucleolar proteins (Kalinina et al., 2018). We have shown here that the MMDaV V2 protein colocalizes with NbFib2 in the nucleolus of plant cells. The specific interaction between V2 and NbFib2 was confirmed by both the yeast two-hybrid and BiFC assays. Fib2 is a key component of several ribonucleoproteins that has been implicated to interact with an increasing number of viral proteins. The outcomes of viral protein and Fib interactions vary depending on different viruses. On the one hand, viral proteins,

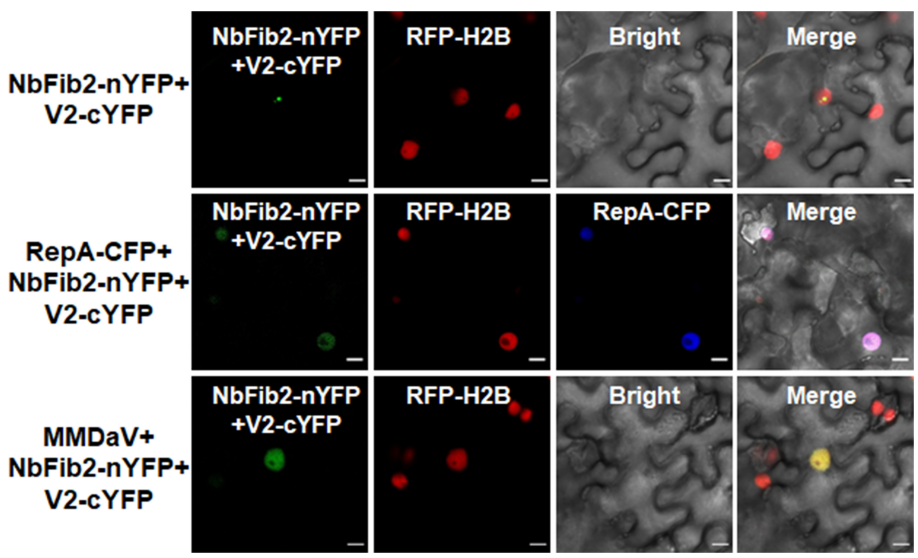

FIGURE 6 | Representative images showing the impact of RepA and MMDaV on the localization of V2-NbFib2 complex. Agrobacteria cultures harboring a cyan fluorescent protein-tagged RepA (RepA-CFP) or infectious clone of MMDaV was coexpressed with the BiFC combination constructs of NbFib2-V2. Images were captured at 48 hpi. Scale bars correspond to 10 μm.

such as BSMV TGB1, GRV ORF3, and the P20 protein of BaMV satRNA, hijack Fib2 for virus cell-to-cell or systemic movement (Kim et al., 2007; Chang et al., 2016; Li et al., 2018). One the other hand, viral proteins may associate with Fib to counter RNA silencing-based host defense (Rajamäki and Valkonen, 2009). Previously, it was shown that deletion of the basic motif encompassing amino acids 61 to 76 abolished the subnuclear localization and PTGS suppression activity of MMDaV V2 (Yang et al., 2018). In the present study, we showed that this MMDaV V2 mutant could neither interact nor colocalize with NbFib2. It would be interesting to determine whether V2-NbFib2 interaction is required for V2 to suppress RNA silencing.

Besides its accumulation in the nucleolus, MMDaV V2 also targets to other subnuclear foci outside of the context of virus infection. Note that the numbers of the subnuclear foci are approximations as it is difficult to assess due to their unclear boundaries and aggregation in the nucleus in some cases (**Supplementary Figure S1B**). Interestingly, targeting to subnuclear bodies have also been observed for GRBaV V3, though what the GRBaV-containing subnuclear bodies correspond to needs further study (Guo et al., 2015). It is also interesting to note that TYLCV CP can be detected in numerous nuclear foci in the context of virus infection. This virus-induced CP-targeting nuclear speckles can partially colocalize with markers of sites of RNA processing, raising the possibility of CP in interference with RNA metabolism (Wang et al., 2017). Further identification of the subnuclear bodies at which MMDaV V2 localizes would give a better understanding of the subcellular localization and potential biological role of MMDaV V2.

Strikingly, V2 is excluded from the nucleolus to the nucleoplasm in plant cells infected with MMDaV. Although this virus-dependent exclusion of V2 from the nucleolus might reflect more the natural situation in the viral infection process, we cannot rule out the possibility of temporal and spatial distribution of V2 to the nucleolus. Transporting of viral protein to different subcellular compartments has also been implicated to play critical roles in functional specification of plant viruses. For example, the nuclear-cytoplasmic compartmentalization of cucumber mosaic virus (CMV) 2b presumably maximizes the benefit for CMV by regulating the balance between virus accumulation and damage to the host (Du et al., 2014). Nucleocytoplasmic shuttling of tomato leaf curl Yunnan Virus (TLCYnV) C4 is critical for its function as a pathogenicity factor (Mei et al., 2018). Localization of the TYLCV V2 protein to the cajal body is required for V2 to interact with AGO4 and to suppress DNA methylation-mediated TGS against TYLCV (Ding and Lozano-Duran, 2020; Wang et al., 2020). Although very little is understood about the biological significance of MMDaV V2 translocation in virus infection, it raises a new perspective that the exclusion of V2 to the nucleoplasm might represent a new role for V2.

We also presented evidence that the dynamic localization of V2 and V2–V2 self-interaction site is RepA-dependent. We found that RepA redirects the V2-NbFib2 complex from the nucleolus to the nucleoplasmic sites. As RepA is involved in geminivirus replication, RepA-V2 interaction-mediated nucleolar exclusion of V2 might imply a link between virus replication and silencing suppression. Recruitment of the BSMV γb protein by the αa viral replication protein to the chloroplast membrane site of BSMV replication enhances the helicase activities of αa in unwinding of dsRNA duplexes and promotes BSMV replication (Zhang et al., 2017). It needs to be determined whether the nuclear export of V2 has any effect on RepA function or virus replication.

CONCLUSION

We have shown that MMDaV V2 displays a differential subcellular localization pattern in response to MMDaV infection. We also show that RepA interacts with V2 and mediates the nucleolar exclusion of V2. As many different viruses target the nucleolus to aid virus infection, the study of the interaction of viral proteins with the nucleolus will provide insight into the mechanisms of viral manipulating host cell functions which could lead to the design of novel antiviral strategies.

DATA AVAILABILITY STATEMENT

All datasets generated for this study are included in the article/**Supplementary Material**.

AUTHOR CONTRIBUTIONS

DW, SS, YR, and XY performed the experiments. All the authors contributed to the experimental design and interpretation. XY, DW, and XZ wrote the manuscript with contributions from all authors.

FUNDING

This work was financially supported by the National Natural Science Foundation of China (31672004 and 31972245) and National Key Research and Development Program of China (2016YFD0300701).

ACKNOWLEDGMENTS

The authors thank Michael Goodin (University of Kentucky) for providing RFP-H2B transgenic *N. benthamiana* seeds.

SUPPLEMENTARY MATERIAL

The Supplementary Material for this article can be found online at: https://www.frontiersin.org/articles/10.3389/fmicb.2020.01828/full#supplementary-material

REFERENCES

Chang, C.-H., Hsu, F.-C., Lee, S.-C., Lo, Y.-S., Wang, J.-D., Shaw, J., et al. (2016). The nucleolar fibrillarin protein is required for helper virus-independent long-distance trafficking of a subviral satellite RNA in plants. *Plant Cell* 28, 2586–2602. doi: 10.1105/tpc.16.00071

Ding, Y., and Lozano-Duran, R. (2020). The cajal body in plant-virus interactions. *Viruses* 12:250. doi: 10.3390/v12020250

Du, Z., Chen, A., Chen, W., Liao, Q., Zhang, H., Bao, Y., et al. (2014). Nuclear-cytoplasmic partitioning of cucumber mosaic virus protein 2b determines the balance between its roles as a virulence determinant and an RNA-silencing suppressor. *J. Virol.* 88, 5228–5241. doi: 10.1128/JVI.00284-14

Earley, K. W., Haag, J. R., Pontes, O., Opper, K., Juehne, T., Song, K., et al. (2006). Gateway-compatible vectors for plant functional genomics and proteomics. *Plant J.* 45, 616–629. doi: 10.1111/j.1365-313X.2005.02617.x

Fondong, V. N. (2013). Geminivirus protein structure and function. *Mol. Plant Pathol.* 14, 635–649. doi: 10.1111/mpp.12032

Glick, E., Zrachya, A., Levy, Y., Mett, A., Gidoni, D., Belausov, E., et al. (2008). Interaction with host SGS3 is required for suppression of RNA silencing by tomato yellow leaf curl virus V2 protein. *Proc. Natl. Acad. Sci. U.S.A.* 105, 157–161. doi: 10.1073/pnas.0709036105

Guo, T. W., Vimalesvaran, D., Thompson, J. R., Perry, K. L., and Krenz, B. (2015). Subcellular localization of grapevine red blotch-associated virus ORFs V2 and V3. *Virus Genes* 51, 156–158. doi: 10.1007/s11262-015-1205-x

Gutierrez, C. (1999). Geminivirus DNA replication. *Cell Mol. Life Sci.* 56, 313–329. doi: 10.1007/s000180050433

Hanley-Bowdoin, L., Bejarano, E. R., Robertson, D., and Mansoor, S. (2013). Geminiviruses: masters at redirecting and reprogramming plant processes. *Nat. Rev. Microbiol.* 11, 777–788. doi: 10.1038/nrmicro3117

Hiscox, J. A. (2007). RNA viruses: hijacking the dynamic nucleolus. *Nat. Rev. Microbiol.* 5, 119–127. doi: 10.1038/nrmicro1597

Jeske, H. (2009). Geminiviruses. *Curr. Top. Microbiol. Immunol.* 331, 185–226. doi: 10.1007/978-3-540-70972-5_11

Kalinina, N. O., Makarova, S., Makhotenko, A., Love, A. J., and Taliansky, M. (2018). The multiple functions of the nucleolus in plant development, disease and stress responses. *Front. Plant Sci.* 9:132. doi: 10.3389/fpls.2018.00132

Kim, S. H., MacFarlane, S., Kalinina, N. O., Rakitina, D. V., Ryabov, E. V., Gillespie, T., et al. (2007). Interaction of a plant virus-encoded protein with the major nucleolar protein fibrillarin is required for systemic virus infection. *Proc. Natl. Acad. Sci. U.S.A.* 104, 11115–11120. doi: 10.1073/pnas.0704632104

Kunik, T., Palanichelvam, K., Czosnek, H., Citovsky, V., and Gafni, Y. (1998). Nuclear import of the capsid protein of tomato yellow leaf curl virus (TYLCV) in plant and insect cells. *Plant J.* 13, 393–399. doi: 10.1046/j.1365-313x.1998.00037.x

Lange, A., Mills, R. E., Lange, C. J., Stewart, M., Devine, S. E., and Corbett, A. H. (2007). Classical nuclear localization signals: definition, function, and interaction with importin alpha. *J. Biol. Chem.* 282, 5101–5105. doi: 10.1074/jbc.R600026200

Li, Z., Zhang, Y., Jiang, Z., Jin, X., Zhang, K., Wang, X., et al. (2018). Hijacking of the nucleolar protein fibrillarin by TGB1 is required for cell-to-cell movement of Barley stripe mosaic virus. *Mol. Plant Pathol.* 19, 1222–1237. doi: 10.1111/mpp.12612

Lu, Q., Tang, X., Tian, G., Wang, F., Liu, K., Nguyen, V., et al. (2010). Arabidopsis homolog of the yeast TREX-2 mRNA export complex: components and anchoring nucleoporin. *Plant J.* 61, 259–270. doi: 10.1111/j.1365-313X.2009.04048.x

Luna, A. P., and Lozano-Durán, R. (2020). Geminivirus-encoded proteins: not all positional homologs are made equal. *Front. Microbiol.* 11:878. doi: 10.3389/fmicb.2020.00878

Luna, A. P., Rodriguez-Negrete, E. A., Morilla, G., Wang, L., Lozano-Duran, R., Castillo, A. G., et al. (2017). V2 from a curtovirus is a suppressor of post-transcriptional gene silencing. *J. Gen. Virol.* 98, 2607–2614. doi: 10.1099/jgv.0.000933

Ma, Y., Navarro, B., Zhang, Z., Lu, M., Zhou, X., Chi, S., et al. (2015). Identification and molecular characterization of a novel monopartite geminivirus associated with mulberry mosaic dwarf disease. *J. Gen. Virol.* 96, 2421–2434. doi: 10.1099/vir.0.000175

Maio, F., Arroyo-Mateos, M., Bobay, B. G., Bejarano, E. R., Prins, M., and van den Burg, H. A. (2019). A lysine residue essential for geminivirus replication also controls nuclear localization of the tomato yellow leaf curl virus Rep protein. *J. Virol.* 93:e01910-18. doi: 10.1128/jvi.01910-18

Martin, K., Kopperud, K., Chakrabarty, R., Banerjee, R., Brooks, R., and Goodin, M. M. (2009). Transient expression in *Nicotiana benthamiana* fluorescent marker lines provides enhanced definition of protein localization, movement and interactions in planta. *Plant J.* 59, 150–162. doi: 10.1111/j.1365-313X.2009.03850.x

Medina-Puche, L., and Lozano-Duran, R. (2019). Tailoring the cell: a glimpse of how plant viruses manipulate their hosts. *Curr. Opin. Plant Biol.* 52, 164–173. doi: 10.1016/j.pbi.2019.09.007

Mei, Y., Wang, Y., Hu, T., Yang, X., Lozano-Duran, R., Sunter, G., et al. (2018). Nucleocytoplasmic shuttling of geminivirus C4 protein mediated by phosphorylation and myristoylation is critical for viral pathogenicity. *Mol. Plant* 11, 1466–1481. doi: 10.1016/j.molp.2018.10.004

Moshe, A., Belausov, E., Niehl, A., Heinlein, M., Czosnek, H., and Gorovits, R. (2015). The Tomato yellow leaf curl virus V2 protein forms aggregates depending on the cytoskeleton integrity and binds viral genomic DNA. *Sci. Rep.* 5:9967. doi: 10.1038/srep09967

Nakagawa, T., Kurose, T., Hino, T., Tanaka, K., Kawamukai, M., Niwa, Y., et al. (2007). Development of series of gateway binary vectors, pGWBs, for realizing efficient construction of fusion genes for plant transformation. *J. Biosci. Bioeng.* 104, 34–41. doi: 10.1263/jbb.104.34

Poornima, P. C. G., Ambika, M. V., Tippeswamy, R., and Savithri, H. S. (2011). Functional characterization of coat protein and V2 involved in cell to cell movement of Cotton leaf curl Kokhran virus-Dabawali. *PLoS One* 6:e26929. doi: 10.1371/journal.pone.0026929

Rajamäki, M.-L., and Valkonen, J. P. T. (2009). Control of nuclear and nucleolar localization of nuclear inclusion protein a of Picorna-Like Potato virus A in Nicotiana apecies. *Plant Cell* 21, 2485–2502. doi: 10.1105/tpc.108.064147

Rojas, M. R., Jiang, H., Salati, R., Xoconostle-Cazares, B., Sudarshana, M. R., Lucas, W. J., et al. (2001). Functional analysis of proteins involved in movement of the monopartite begomovirus. Tomato yellow leaf curl virus. *Virology* 291, 110–125. doi: 10.1006/viro.2001.1194

Rothenstein, D., Krenz, B., Selchow, O., and Jeske, H. (2007). Tissue and cell tropism of Indian cassava mosaic virus (ICMV) and its AV2 (precoat) gene product. *Virology* 359, 137–145. doi: 10.1016/j.virol.2006.09.014

Rushing, A. E., Sunter, G., Gardiner, W. E., Dute, R. R., and Bisaro, D. M. (1987). Ultrastructural aspects of tomato golden mosaic virus infection in tobacco. *Phytopathology* 77, 1231–1236.

Sharma, P., Gaur, R. K., and Ikegami, M. (2011). Subcellular localization of V2 protein of Tomato leaf curl Java virus by using green fluorescent protein and yeast hybrid system. *Protoplasma* 248, 281–288. doi: 10.1007/s00709-010-0166-0

Shishido-Hara, Y., Hara, Y., Larson, T., Yasui, K., Nagashima, K., and Stoner, G. L. (2000). Analysis of capsid formation of human polyomavirus JC (Tokyo-1 Strain) by a eukaryotic expression system: splicing of late RNAs, translation and nuclear transport of major capsid protein VP1, and capsid assembly. *J. Virol.* 74, 1840–1853. doi: 10.1128/jvi.74.4.1840-1853.2000

Shunmugiah, V., Ramesh, P. P. S., Prasad, M., Praveen, S., and Pappu, H. R. (2017). Geminiviruses and plant hosts: a closer examination of the molecular arms race. *Viruses* 9:256. doi: 10.3390/v9090256

Stepinski, D. (2014). Functional ultrastructure of the plant nucleolus. *Protoplasma* 251, 1285–1306. doi: 10.1007/s00709-014-0648-6

Wang, B., Li, F., Huang, C., Yang, X., Qian, Y., Xie, Y., et al. (2014). V2 of tomato yellow leaf curl virus can suppress methylation-mediated transcriptional gene silencing in plants. *J. Gen. Virol.* 95, 225–230. doi: 10.1099/vir.0.055798-0

Wang, B., Yang, X., Wang, Y., Xie, Y., and Zhou, X. (2018). Tomato yellow leaf curl virus V2 interacts with host histone deacetylase 6 to suppress methylation-mediated transcriptional gene silencing in plants. *J. Virol.* 92:e00036-18. doi: 10.1128/JVI.00036-18

Wang, L., Tan, H., Wu, M., Jimenez-Gongora, T., Tan, L., and Lozano-Duran, R. (2017). Dynamic virus-dependent subnuclear localization of the capsid protein from a geminivirus. *Front. Plant Sci.* 8:2165. doi: 10.3389/fpls.2017.02165

Wang, L. P., Ding, Y., He, L., Zhang, G. P., Zhu, J. K., and Lozano-Duran, R. (2020). A virus-encoded protein suppresses methylation of the viral genome in the Cajal body through its interaction with AGO4. *bioRxiv*. doi: 10.1101/811091

Wang, Y., Wu, Y., Gong, Q., Ismayil, A., Yuan, Y., Lian, B., et al. (2019). Geminiviral V2 protein suppresses transcriptional gene silencing through interaction with AGO4. *J. Virol.* 93:e01675-18. doi: 10.1128/JVI.01675-18

Wistuba, A., Kern, A., Weger, S., Grimm, D., and Kleinschmidt, J. A. (1997). Subcellular compartmentalization of adeno-associated virus type 2 assembly. *J. Virol.* 71, 1341–1352. doi: 10.1128/jvi.71.2.1341-1352.1997

Yang, X., Guo, W., Li, F., Sunter, G., and Zhou, X. (2019). Geminivirus-associated betasatellites: exploiting chinks in the antiviral arsenal of plants. *Trends Plant Sci.* 24, 519–529. doi: 10.1016/j.tplants.2019.03.010

Yang, X., Guo, W., Ma, X., An, Q., and Zhou, X. (2011). Molecular characterization of tomato leaf curl China virus, infecting tomato plants in China, and functional analyses of its associated betasatellite. *Appl. Environ. Microbiol.* 77, 3092–3101. doi: 10.1128/AEM.00017-11

Yang, X., Ren, Y., Sun, S., Wang, D., Zhang, F., Li, D., et al. (2018). Identification of the potential virulence factors and RNA silencing suppressors of Mulberry mosaic dwarf-associated geminivirus. *Viruses* 10:472. doi: 10.3390/v10090472

Zerbini, F. M., Briddon, R. W., Idris, A., Martin, D. P., Moriones, E., Navas-Castillo, J., et al. (2017). ICTV virus taxonomy profile: *Geminiviridae*. *J. Gen. Virol.* 98, 131–133. doi: 10.1099/jgv.0.000738

Zhang, K., Zhang, Y., Yang, M., Liu, S., Li, Z., Wang, X., et al. (2017). The Barley stripe mosaic virus γb protein promotes chloroplast-targeted replication by enhancing unwinding of RNA duplexes. *PLoS Pathog.* 13:e1006319. doi: 10.1371/journal.ppat.1006319

Zhao, W., Wu, S., Barton, E., Fan, Y., Ji, Y., Wang, X., et al. (2020). Tomato yellow leaf curl virus V2 protein plays a critical role in the nuclear export of V1 protein and viral systemic infection. *Front. Microbiol.* 11:1243. doi: 10.3389/fmicb.2020.01243

Zheng, L., Du, Z., Lin, C., Mao, Q., Wu, K., Wu, J., et al. (2015). Rice stripe tenuivirus p2 may recruit or manipulate nucleolar functions through an interaction with fibrillarin to promote virus systemic movement. *Mol. Plant Pathol.* 16, 921–930. doi: 10.1111/mpp.12220

Zheng, L., Yao, J., Gao, F., Chen, L., Zhang, C., Lian, L., et al. (2016). The subcellular localization and functional analysis of fibrillarin2, a nucleolar protein in *Nicotiana benthamiana*. *Biomed. Res. Int.* 2016:2831287. doi: 10.1155/2016/2831287

Conflict of Interest: The authors declare that the research was conducted in the absence of any commercial or financial relationships that could be construed as a potential conflict of interest.

frontiers in Plant Science

ORIGINAL RESEARCH
published: 06 August 2020
doi: 10.3389/fpls.2020.01201

A Temporal Diversity Analysis of Brazilian Begomoviruses in Tomato Reveals a Decrease in Species Richness between 2003 and 2016

Tadeu Araujo Souza[1,2], *João Marcos Fagundes Silva*[3], *Tatsuya Nagata*[3], *Thaís Pereira Martins*[2,3], *Erich Yukio Tempel Nakasu*[2] and *Alice Kazuko Inoue-Nagata*[1,2]*

[1] Department of Plant Pathology, University of Brasilia, Brasilia, Brazil, [2] Laboratory of Virology, Embrapa Vegetables, Brasilia, Brazil, [3] Department of Cell Biology, University of Brasilia, Brasilia, Brazil

Understanding the molecular evolution and diversity changes of begomoviruses is crucial for predicting future outbreaks of the begomovirus disease in tomato crops. Thus, a molecular diversity study using high-throughput sequencing (HTS) was carried out on samples of infected tomato leaves collected between 2003 and 2016 from Central Brazil. DNA samples were subjected to rolling circle amplification and pooled in three batches, G1 (2003–2005, N = 107), G2 (2009–2011, N = 118), and G3 (2014–2016, N = 129) prior to HTS. Nineteen genome-sized geminivirus sequences were assembled, but only 17 were confirmed by PCR. In the G1 library, five begomoviruses and one capula-like virus were detected, but the number of identified viruses decreased to three begomoviruses in the G2 and G3 libraries. The bipartite begomovirus tomato severe rugose virus (ToSRV) and the monopartite tomato mottle leaf curl virus (ToMoLCV) were found to be the most prevalent begomoviruses in this survey. Our analyses revealed a significant increase in both relative abundance and genetic diversity of ToMoLCV from G1 to G3, and ToSRV from G1 to G2; however, both abundance and diversity decreased from G2 to G3. This suggests that ToMoLCV and ToSRV outcompeted other begomoviruses from G1 to G2 and that ToSRV was being outcompeted by ToMoLCV from G2 to G3. The possible evolutionary history of begomoviruses that were likely transferred from wild native plants and weeds to tomato crops after the introduction of the polyphagous vector *Bemisia tabaci* MEAM1 and the wide use of cultivars carrying the *Ty-1* resistance gene are discussed, as well as the strengths and limitations of the use of HTS in identification and diversity analysis of begomoviruses.

Keywords: begomovirus, capulavirus, diversity, population, geminivirus, resistance gene, metagenomics

OPEN ACCESS

Edited by:
Ralf Georg Dietzgen, The University of Queensland, Australia

Reviewed by:
Enrique Moriones, University of Málaga, Spain
Lawrence Kenyon, World Vegetable Center, Taiwan

***Correspondence:**
Alice Kazuko Inoue-Nagata
alice.nagata@embrapa.br

Specialty section:
This article was submitted to Virology, a section of the journal Frontiers in Plant Science

Received: *29 February 2020*
Accepted: *23 July 2020*
Published: *06 August 2020*

Citation:
Souza TA, Silva JMF, Nagata T, Martins TP, Nakasu EYT and Inoue-Nagata AK (2020) A Temporal Diversity Analysis of Brazilian Begomoviruses in Tomato Reveals a Decrease in Species Richness between 2003 and 2016. Front. Plant Sci. 11:1201. doi: 10.3389/fpls.2020.01201

INTRODUCTION

The cultivation of tomato (*Solanum lycopersicum*) is challenging due to its susceptibility to several pathogens, including begomoviruses (family *Geminiviridae*; genus *Begomovirus*), a major group of plant pathogens found in tropical and subtropical regions (Rojas et al., 2018). Begomoviruses present small, circular, single-stranded (ss) DNA genomes and are transmitted by whiteflies of the

Bemisia tabaci cryptic species complex. The genome is composed of either two components (bipartite)—DNA-A and DNA-B—each comprising ~2.6 kb or a single component (monopartite, corresponding to the DNA-A component of bipartite begomoviruses) of ~2.8 kb (Fauquet et al., 2003; Brown et al., 2012). The rate of 91% genome-wide nucleotide identity of the complete genome (or DNA-A for bipartite begomoviruses) is used as threshold for species demarcation in the genus *Begomovirus* (Brown et al., 2015).

Begomoviruses exhibit high mutation and recombination rates, both within and among species, resulting in the rapid adaptive evolution and emergence of new variants and species (Duffy et al., 2008; Rocha et al., 2013; Silva et al., 2014; Lima et al., 2017). Historically, the first reported begomoviral disease in tomatoes in Brazil was caused by the tomato golden mosaic virus (TGMV), a New World (NW) bipartite begomovirus, in the 1960s (Costa, 1976). The disease is characterized by distorted growth and yellow to light green mosaic in leaves and is transmitted by whiteflies (Matyis et al., 1975). Thereafter, the disease was either not reported or was at an undetectable level in the country. It is speculated that this low occurrence of begomoviruses in tomato plants was due to the host preference of the *B. tabaci* populations present in Brazil at that time, presumably of the cryptic species *B. tabaci* New World (NW), previously known as biotype A. However, after the introduction of the species *B. tabaci* Middle East Asia Minor 1 (MEAM1) in the early 1990s the situation changed, as MEAM1 is more polyphagous and readily attracted to tomatoes; this resulted in a fast and widespread occurrence of begomoviral diseases in Brazil (Faria et al., 1997; Ribeiro et al., 2003; Fernandes et al., 2006; Castillo-Urquiza et al., 2008). Unlike whiteflies of the NW, MEAM1 has a broad range of hosts and is believed to have transferred native viruses from weeds and wild plants to cultivated tomato plants (Castillo-Urquiza et al., 2008; Barreto et al., 2013). Currently, 25 species of tomato-infecting begomoviruses have been described in Brazil (e.g., Flores et al., 1960; Matyis et al., 1975; Ribeiro et al., 2003; Fernandes et al., 2006; Castillo-Urquiza et al., 2008; Fernandes et al., 2008; Albuquerque et al., 2012; Rocha et al., 2013). Bipartite begomoviruses, especially tomato severe rugose virus (ToSRV; Inoue-Nagata et al., 2016; Rojas et al., 2018; Mituti et al., 2019), are the most predominant in tomato plants. The monopartite tomato mottle leaf curl virus (ToMoLCV) (Vu et al., 2015) has also been largely reported in tomato plants and causes severe symptoms such as chlorotic spots, interveinal chlorosis, mottling, mosaic, leaf distortion, and stunting (Inoue-Nagata et al., 2016).

Traditionally, the most common preventive measures for begomoviral disease control are the application of insecticides against the vector and the use of resistant cultivars (Lapidot and Friedmann, 2002; Hurtado et al., 2012). To date, genes of the series *Ty-1* to *Ty-6* (and a few others such as *tcm-1* and *ty-5*) were reported to provide resistance/tolerance to tomato yellow leaf curl virus (TYLCV), the most widespread begomovirus in the world (e.g., Zamir et al., 1994; Giordano et al., 2005; Anbinder et al., 2009; Ji et al., 2009; Hutton et al., 2012; Bai et al., 2018; Gill et al., 2019); some of these genes can provide a moderate level of control against NW begomoviruses (Giordano et al., 2005; Boiteux et al., 2007; Aguilera et al., 2011). For example, an experimental heterozygous hybrid carrying *Ty-1* was less infected and displayed milder or no symptom under infection of the Brazilian begomoviruses tomato rugose mosaic virus (ToRMV) and tomato yellow vein streak virus (ToYVSV), and thus classified as tolerant to these viruses (Boiteux et al., 2007). These resistance genes have been successfully introgressed into tomato lines in breeding programs. Of those, many commercial tomato hybrids carrying the *Ty-1*/*Ty-3* (allelic) genes (Verlaan et al., 2013) are largely in use in Brazil (Pereira-Carvalho et al., 2015). *Ty-1*/*Ty-3* encode a plant RNA-dependent RNA polymerase, which activates transcriptional gene silencing with an increase in viral genome methylation (Verlaan et al., 2013; Butterbach et al., 2014). In plants that carry resistance alleles, viral accumulation continues, although at lower levels than in susceptible plants (Zamir et al., 1994; Belabess et al., 2016).

Based on the overwhelming diversity of begomoviruses in tomato plants in Brazil and the prevalence of only two begomovirus species (Inoue-Nagata et al., 2016; Rojas et al., 2018; Mituti et al., 2019), we hypothesize that several native begomoviruses were introduced from wild and weed plants to tomato and that their diversity decreased over time after intensive interactions between viruses, vectors, hosts, and environmental factors. Furthermore, the broad use of resistant tomato cultivars carrying *Ty*-like may also have influenced the begomovirus population dynamics in the field, as reported earlier for tomato yellow leaf curl disease (García-Andrés et al., 2009). This hypothesis assumes that selective pressure is posed by resistance genes, limiting species diversity over the years in a local environment. In this study, we estimated genetic diversity changes in begomoviruses that infect tomato plants in an important tomato-growing region in Central Brazil through ~14 years. For temporal analysis, begomovirus-infected plant samples were divided into three groups, and all begomovirus sequences were identified using high-throughput sequencing (HTS) data. Subsequently, species-specific PCR and Sanger sequencing were done to confirm the sequences.

MATERIALS AND METHODS

Collection of Tomato Samples and Detection of Begomovirus

Symptomatic tomato leaves (with chlorotic spots, interveinal chlorosis, and leaf curling; **Supplementary Figure 1**) were collected from 2003 to 2016 in a ~400 km^2 area comprising Taquara and Pipiripau, located at the Federal District, at altitudes varying from 905 to 1225 m above sea level (**Supplementary Table 1**)—two of the major tomato production areas in Central Brazil. In this region, tomatoes are grown for the fresh market. Begomovirus infections were previously confirmed by total DNA extraction using the CTAB method (Doyle and Doyle, 1990) and PCR amplification using universal primers (PAR1c496 and PAL1v1978; Rojas et al., 1993). To analyze temporal population change in the genetic variants of begomovirus, we divided the

samples into three groups according to the collection year: G1 (2003, 2004, 2005; N = 107), G2 (2009, 2010, 2011; N = 118), and G3 (2014, 2015, 2016; N = 129). Fields visited in G1 to G3 (**Supplementary Table 1**) equally represented the surveyed area.

Diversity Analysis of Begomoviruses by Rolling Circle Amplification and RFLP

Circular viral DNA was amplified in individual samples by rolling circle amplification (RCA) using the illustra TempliPhi DNA amplification kit (GE Healthcare, Milwaukee, USA), following the manufacturer's instructions and random hexamer primers, which efficiently amplifies circular DNA molecules at random. Each RCA product was digested with MspI and the digestion profile was analyzed by 1% agarose gel electrophoresis.

HTS of RCA Products From Each Group and Identification of Begomoviruses

Three independent libraries were prepared, each containing a different pool of RCA products, namely G1, G2, and G3 (as above). The libraries were prepared using the TruSeq DNA sample preparation v.2 kit and sequenced using 100 bp paired-end reads on the Illumina Hiseq 2000 platform (Macrogen Inc., Seoul, South Korea). The HTS reads were trimmed using Trimmomatic (Bolger et al., 2014), and the contigs were *de novo* assembled using Velvet and MEGAHIT v1.1.3 (Phred = 34, 71 k-mer) (Zerbino and Birney, 2008; Li et al., 2015). The sequences assembled by these two assemblers were transferred to Geneious 8.1.9 (Biomatters, Auckland, New Zealand) and subjected to a BLAST search against the geminivirus reference database (downloaded from NCBI on 28/01/2019). The short contigs (<100 nucleotides) or those containing repeated sequences were re-blasted for confirmation. For every detected virus from contigs of both assemblers, the reference sequence was used to map the reads in Geneious (using the map to reference tool), and thus consensus sequences were assembled. After manual verification of the genome coverage, only a fully covered genome was considered for further analyses. Pairwise comparisons of the full genome were performed using Sequence Demarcation Tool program (SDT, Muhire et al., 2014). To confirm the presence of various begomoviruses detected in the pooled samples by HTS analyses, PCR with specific primers for complete/partial genomic regions (**Supplementary Table 2**) was performed using the three pooled samples. Then primers were designed to amplify the complete DNA-A and DNA-B segments (**Supplementary Table 2**) of the confirmed viruses in the pooled samples, and the amplicons were directly sequenced by the Sanger method at Macrogen, both by using PCR primers and primer walking. More than one primer pair were used for some viruses (**Supplementary Table 2**).

Estimation of Intraspecies Diversity of ToMoLCV and ToSRV Sequences

Genetic diversity and population dynamics of begomoviruses through time were estimated using the HTS data. In this analysis, the reads were mapped to three reference databases comprising all ToMoLCV, ToSRV, and begomovirus sequences available in GenBank using BWA MEM v.0.7.17 (Li, 2013) with a seed length (-k) of 55 nucleotides. We opted for using the number and frequency of unique k-mers extracted from the aligned reads to estimate the diversity in order to mitigate cross alignments between different species, which should be common considering the 91% nucleotide identity thresholds for species demarcation (Brown et al., 2015). Twenty-seven mers were extracted and counted from the reads that aligned to each database using SAMtools v1.9 (Li et al., 2009) and Jellyfish v.2.2.3 (Marçais and Kingsford, 2011). Shannon entropy (Shannon, 1948) was calculated for each data set based on the frequency of each unique 27-mer. The number of reads aligned to each database was used to calculate the relative abundance of ToSRV and ToMoLCV for each sample group. To investigate whether the diversity of ToSRV and ToMoLCV significantly changed over time, we aligned previously extracted reads mapped to the genomes of these viruses in order to annotate single nucleotide polymorphisms (SNP) with LoFreq (Wilm et al., 2012). Thereafter, the entropy of each SNP was calculated and the cumulative sum of the entropy was used to perform the Wilcoxon signed-rank tests between two time points.

Ty-1 Detection in Individual Total DNA Samples

Considering that *Ty*-1 is the most common resistance gene introgressed in commercial cultivars in Brazil, PCR was performed to confirm its the presence in individual samples, as described by Prasanna et al. (2015). The amplicons were digested with HinfI and polymorphism was evaluated. The DNA profile from cultivars carrying *Ty-1* yields a single ~1 kb DNA fragment, in contrast to the ~0.6 kb fragment in those not carrying the gene.

Detection of the Major Begomoviruses in Individual Samples

The four most frequent begomoviruses in the data sets were selected: ToSRV, ToMoLCV, tomato golden vein virus (TGVV), and Sida micrantha mosaic virus (SiMMV). Thereafter, PCR was performed to evaluate their presence in individual total DNA samples within groups G1, G2, and G3 (primers listed in **Supplementary Table 2**).

Phylogenetic Analysis

Phylogenetic analyses were performed with the complete set of DNA-A and DNA-B sequences of all viruses identified in this study. All sequences related to these viruses were retrieved from GenBank and aligned using MUSCLE. The phylogenetic tree was constructed using the Tamura-Nei model (Tamura and Nei, 1993) and the maximum likelihood statistical method with 3000 repetitions included in the MEGAX program (Kumar et al., 2018). The reference sequence of the most closely related virus detected by BLAST search was used as outgroup.

RESULTS

Diversity Analysis by RCA-RFLP

A collection of begomoviruses sampled in the Taquara and Pipiripau regions was used for begomovirus diversity analysis

(**Supplementary Table 1**). A subset of these samples was divided into three groups according to the collection year: G1 (2003–2005), G2 (2009–2011), and G3 (2014–2016). The circular DNAs of individual samples from each group were amplified by RCA and digested with MspI for a preliminary evaluation of the diversity of begomoviruses in the samples, as viruses of the same species share a similar digestion profile. Summing the length of each fragment showed the genome size of the begomovirus to be ~2.7 kb for monopartite viruses and ~5.2 kb for bipartite viruses. The digestion profiles were analyzed individually and grouped into 17 distinct pattern profiles (representative profiles shown in **Figure 1**). The size of potential begomovirus genomes was estimated to range from 2.7–9.6 kb (numbers below the electrophoresis image, **Figure 1**), suggesting the presence of a monopartite begomovirus in some samples and mixed infections in others. In the G1 group, most of the profiles were mixed infection types, as the sum exceeded 6.7 kb (**Figure 1A**). In contrast, samples of the G2 and G3 groups likely contained either a monopartite or bipartite begomovirus (**Figures 1B, C**). Nine digestion profiles were observed in G1, seven were observed in G2 and only three in G3 (**Figure 1**). This suggested a local decrease in begomovirus diversity over time. Two identical profiles were observed in G2 and G3 (profiles 10 and 12, **Figures 1B, C**), indicating that the same viruses were potentially present in these groups, whereas those patterns observed in G1 were not found in the other groups. From these results, we concluded that a substantial change in the diversity of begomovirus species occurred in the evaluated time.

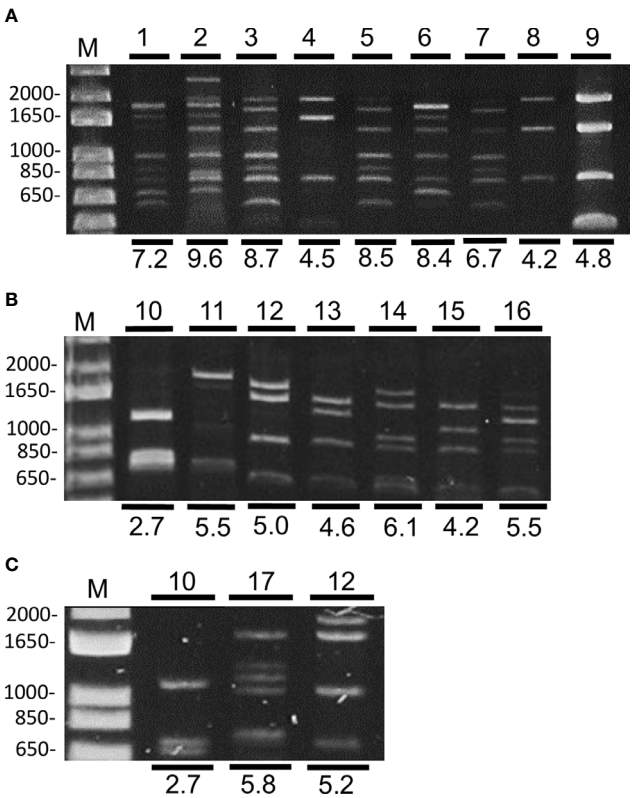

FIGURE 1 | Restriction enzyme digestion profiles of begomoviruses amplified by RCA and digested with MspI on 1% agarose gel, observed in representative samples of G1 **(A)**, G2 **(B)**, and G3 **(C)**. The estimated sum of each genome fragment (in kbp) is indicated below the restriction profile. M = 1 kb plus DNA ladder (Thermo Fisher Scientific).

A Gradual Decrease in Begomovirus Diversity From 2003 to 2016 Is Confirmed by Metagenomic Studies

Illumina sequencing generated a total of 25,522,962 reads from G1 (2003–2005), 21,442,638 reads from G2 (2009–2011), and 19,960,206 reads from G3 (2014–2016) (**Supplementary Table 3**). Removal of adapter residues and low-quality sequences yielded > 18,000,000 final reads each (**Supplementary Table 3**). Two assembling programs, Velvet and MEGAHIT, were evaluated for the number and size of the contigs. The number of contigs was higher for Velvet (**Supplementary Table 4**); however, they were in average shorter (141 to 1,089 bp) than those from the MEGAHIT assembler (406 to 2,631) (**Supplementary Table 5**). The BLAST results of contigs by both assemblers were highly similar, with contigs sharing high identities with seven viruses in G1, three in G2, and three in G3 (**Supplementary Tables 4** and **5**). Only one complete genome sequence containing 2,631 bases and sharing 98.29% identity with an isolate of ToMoLCV (**Supplementary Table 5**) was assembled. The remaining contigs were partial sequences of either DNA-A or DNA-B components.

After all reads were fine mapped using the reference sequence of the viruses corresponding to each contig, 19 genome-sized (~2.6 kb) sequences were assembled with full coverage (**Table 1**). In one case, when the reads were mapped to the ToMoLCV reference sequence (KX896398), the consensus sequence shared 89.47% identity with ToMoLCV accession KC706615, and 87.87% with the reference sequence, being distinct from the sequence assembled by MEGAHIT. This sequence was identified as Bego1:BR:G1, a potentially new begomovirus. In contrast, the consensus ToMoLCV sequence assembled by MEGAHIT (**Supplementary Table 5**) shared 91.97% with the ToMoLCV reference sequence. Hence, these two ToMoLCV-like sequences were included in **Table 1**.

In the G1 group, seven begomoviruses were identified from 10 segments: (1) SiMMV (DNA-A), (2, 3) tomato chlorotic mottle virus (ToCMoV; DNA-A and DNA-B), (4, 5) TGVV (DNA-A and DNA-B), (6) ToMoLCV (monopartite), (7) ToRMV (DNA-A), (8, 9) ToSRV; (DNA-A and DNA-B), and (10) Bego1:BR:G1 (DNA-A) (**Table 1**). In addition, the genome of another geminivirus, the capula-like virus (11) tomato apical leaf curl virus [ToALCV, monopartite; Vaghi Medina et al., 2018)] was identified. Although SiMMV is a bipartite begomovirus, its DNA-B sequence could not be detected. The DNA-B of ToRMV was not found, but it is known to share a high nucleotide identity to ToSRV (Silva et al., 2014). Several reads were mapped to ToYVSV sequences (data not shown), which is highly related to TGVV. In fact, all ToYVSV-like reads were clearly mapped to TGVV sequences, and the ToYVSV genome could not be assembled using our data.

TABLE 1 | Consensus viral sequences identified by high-throughput sequencing in individual libraries G1, G2, and G3 and nucleotide comparison with reference sequence of the closest begomovirus.

Group		Identification/Genomic component	Consensus length[1]	Coverage	Reads	Closest begomovirus	Percentage identity (%)[2]	Reference accession[3]
1	1	SiMMV : BR:G1 DNA-A	2691	100	2 610 718	SiMMV DNA-A	89.12 [94.09]	AJ557451
	2	ToCMoV : BR:G1 DNA-A	2622	100	4 503 800	ToCMoV DNA-A	92.12	AF490004
	3	ToCMoV : BR:G1 DNA-B	2577	100	1 566 484	ToCMoV DNA-B	85.78 [92.65]	AF491306
	4	TGVV : BR:G1 DNA-A	2563	100	2 628 102	TGVV DNA-A	98.01	JF803254
	5	TGVV : BR:G1 DNA-B	2530	100	736 932	TGVV DNA-B	99.37	JF803265
	6	ToMoLCV : BR:G1	2631	100	2 137 458	ToMoLCV	91.97	KX896398
	7	ToRMV : BR:G1 DNA-A	2620	100	6 629 911	ToRMV DNA-A	96.07	AF291705
	8	ToSRV : BR:G1 DNA-A	2592	100	8 275 251	ToSRV DNA-A	99.38	DQ207749
	9	ToSRV : BR:G1 DNA-B	2572	100	4 349 407	ToSRV DNA-B	99.53	EF534708
	10	Bego1:BR:G1	2632	100	2 507 736	ToMoLCV	87.87 [89.47]	KX896398
	11	ToALCV : BR:G1	2875	100	32 211	ToALCV	95.23	MG491196
2	1	SiMMV : BR:G2 DNA-A	2693	100	2 507 684	SiMMV DNA-A	89.23 [92.75]	AJ557451
	2	ToMoLCV : BR:G2	2631	100	3 485 577	ToMoLCV	91.52	KX896398
	3	ToSRV : BR:G2 DNA-A	2593	100	7 891 080	ToSRV DNA-A	99.50	DQ207749
	4	ToSRV : BR:G2 DNA-B	2572	100	4 838 835	ToSRV DNA-B	99.38	EF534708
3	1	ToMoLCV : BR:G3	2633	100	6 739 860	ToMoLCV	92.12	KX896398
	2	ToSRV : BR:G3 DNA-A	2593	100	3 498 480	ToSRV DNA-A	98.92	DQ207749
	3	ToSRV : BR:G3 DNA-B	2570	100	4 739 156	ToSRV DNA-B	98.25	EF534708
	4	Bego2:BR:G3	2617	100	2 067 809	BGMV DNA-A	89.30 [90.44]	M88686

[1]*Sequences are in* ***Supplementary Table 6***.

[2]*Nucleoitide identity of the genome-wide consensus sequence with the reference genome, calculated by SDT (Muhire et al., 2014). In square brackets, comparison with the closest begomovirus sequence for those with identity <91%, SiMMV G1 DNA-A compared to JX415187, ToCMoV G1 DNA-B to KC706562, ToMoLCV G1 to KC706615, SiMMV G2 DNA-A to JX415194, BGMV G3 to KJ939806.*

[3]*Accession number of the reference sequences.*

From the G2 group, three viral genomes were assembled (**Table 1**): (1) SiMMV (DNA-A), (2) ToMoLCV, and (3, 4) ToSRV (DNA-A and DNA-B). These three viruses were also detected in G1, suggesting that they are well-adapted to the tomato crop and remained in the evaluated region. The SiMMV sequences from G1 and G2 shared 95.13% nucleotide identity, indicating that they belonged to the same strain (i.e., > 94% nucleotide identity). They shared <90% genome-wide nucleotide identity with the reference sequence of SiMMV (AJ557451, **Table 1**). However, the closest match of SiMMV DNA-A of G1 was SiMMV accession JX415187 (from *Sida* sp.) sharing 94.09% identity, and of G2 was SiMMV accession JX415194 (from *Sida santaremnensis*) with 92.75% identity; thus, they were identified as SiMMV isolates: SiMMV : BR:G1 and SiMMV : BR:G2, respectively. Similar to the results for G1, the DNA-B of SiMMV was undetected. This suggests that SiMMV DNA-A might use the ToSRV DNA-B if SiMMV needs DNA-B for infection, as the three viruses—SiMMV, ToSRV, and the monopartite ToMoLCV—were detected in G2 samples. Another possibility is that the DNA B from this particular virus was under a detectable level or was outcompeted by other small circular DNA templates.

In G3, three viruses were identified: (1) ToMoLCV, (2, 3) ToSRV (DNA-A and DNA-B), and Bego2:BR:G3 (DNA-A) (**Table 1**). The genome of Bego2:BR:G3 shares 89.30% nucleotide identity with bean golden mosaic virus (BGMV) accession M88686 (reference sequence), and 90.44% with the closest begomovirus, the BGMV accession KJ939806; and it was provisionally named as Bego2. A BGMV DNA-B-like sequence was not found in the HTS reads. This result implies that ToMoLCV and ToSRV persisted in the area for over 14 years, whereas the other six viruses detected in G1 were not detected in the last samplings (G2 and G3). By comparing the sequences of ToSRV, ToMoLCV, and SiMMV from the three groups, nucleotide identities ranging from 95.13% to 99.80% were obtained, indicating their genomes accumulated non-lethal mutations. Furthermore, a thorough search for begomovirus-related satellites yielded no results for the three HTS data sets.

Intraspecies Diversity Analysis

Two parameters, unique k-mer count and Shannon entropy of unique k-mers, were used to estimate intraspecies diversity of ToMoLCV and ToSRV, the viruses found in all three groups, and of all begomoviruses for the G1, G2, and G3 data sets (**Table 2**). Additionally, total Shannon entropy, based on the frequency of each SNP of ToMoLCV and ToSRV, was calculated and the cumulative sum was used to test for a significant increase or decrease in diversity based on the Wilcoxon signed-rank test (**Figure 2**). The number of unique 27-mers of ToSRV and ToMoLCV compared to that of all begomoviruses suggests that these two species share several 27-mers. The overall diversity of begomoviruses decreased from 2003 to 2016 (G1–G3); conversely, the diversity of ToMoLCV increased from G1 to G3 and that of ToSRV increased from G1 to G2 but decreased from G2 to G3 (**Table 2**). Overall, the genetic diversity of ToSRV and ToMoLCV varied according to their relative abundance, however, the diversity of ToSRV DNA-B alone decreased from G2 to G3 while its relative abundance increased (**Table 2**). Based on total Shannon entropy, the diversity of SNPs followed a similar trend (**Table 2**), although in this case the diversity of DNA-B of ToSRV at G3 was smaller than that at G1. Importantly, in the latter diversity analysis, indels and epistasis are not accounted for.

TABLE 2 | Genetic diversity and relative abundance of ToSRV, ToMoLCV and all begomoviruses detected from 2003 to 2016.

Group		Virus	Unique 27-mers	27-mer Shannon entropy	Total SNP Shannon entropy	Total number of reads	Relative abundance
1	1	ToMoLCV	248 458	11.24	13.39	428 057	0.02
	2	ToSRV	3 493 062	14.07	72.31	11 606 934	0.67
	3	ToSRV DNA-A	2 099 063	13.12	29.77	7 718 716	0.45
	4	ToSRV DNA-B	1 448 480	13.24	42.53	3 888 218	0.22
	5	Begomovirus	6 555 088	15.20	NA	17 136 500	1
2	1	ToMoLCV	1 240 059	13.13	38.77	2 584 634	0.18
	2	ToSRV	4 369 323	14.59	112.57	11 714 792	0.81
	3	ToSRV DNA-A	2 446 504	13.58	51.52	7 531 010	0.52
	4	ToSRV DNA-B	2 002 928	13.91	61.04	4 183 782	0.29
	5	Begomovirus	5 611 647	15.02	NA	14 349 739	1
3	1	ToMoLCV	1 762 003	13.38	42.84	5 833 049	0.45
	2	ToSRV	2 340 172	14.25	73.73	6 867 494	0.53
	3	ToSRV DNA-A	1 159 760	13.37	39.67	2 943 937	0.23
	4	ToSRV DNA-B	1 222 633	13.29	34.05	3 923 557	0.30
	5	Begomovirus	4 079 349	14.84	NA	12 771 519	1

All Wilcoxon signed-rank tests of the cumulative SNP entropy between two time points were significant ($P < 1e\text{-}16$). Although SNPs appear to be concentrated in two regions of the ToMoLCV genome at G1, this result should be looked at with caution. These polymorphisms are located at the beginning or at the end of coding regions and likely represent cross alignment of reads from closely related species.

Validation of Begomovirus Sequences Identified by HTS Using PCR and Sequencing

To demonstrate that the geminivirus sequences were not artifacts of the assembly programs, we performed PCR using species-specific primers (**Supplementary Table 2**). Based on the assembled, complete sequences, primers were designed to amplify the entire or partial DNA-A of TGVV, SiMMV, ToMoLCV, ToSRV, ToCMoV, Bego1, Bego2, ToRMV, and ToALCV, producing amplicons of ~0.5 to ~2.9 kbp (**Supplementary Table 2**). SiMMV detection was confirmed in G1 and G2, TGVV, ToCMoV, ToALCV, ToRMV, and Bego1 in G1, Bego2 in G3, and ToMoLCV and ToSRV in pooled samples of G1, G2, and G3 (**Figure 3**). Furthermore, PCR-specific to the DNA-B sequences (**Supplementary Table 2**) confirmed the presence of DNA-B of ToSRV, ToCMoV, and TGVV in the corresponding group, but not of SiMMV DNA-B in the three groups (data not shown). These results confirmed the begomovirus identification by analyzing the HTS data sets of G1, G2, and G3.

Next, PCR was performed to amplify the complete genome (DNA-A and DNA-B, **Supplementary Table 2**) of each virus in the pools and hence to compare with the HTS-assembled sequences. The amplicons were directly sequenced and used to assemble the final consensus sequence (**Table 3**). The amplicon of ToRMV resulted in a ToSRV sequence, and the one of Bego1 in a ToMoLCV sequence. Alignments of the HTS-assembled ToRMV and Bego1 sequence with other begomovirus sequences showed that the ToRMV sequence was in fact a chimera between ToSRV and ToCMoV sequences, and Bego1 a chimera between ToMoLCV and ToSRV sequence, i.e., artifact sequences. Therefore, these two viruses, ToRMV and Bego1, were eliminated from the analysis. The Bego2 amplicon resulted in a sequence sharing >91% nucleotide identity with the DNA-A reference sequence of BGMV, and thus it was renamed BGMV : BR:G3 (**Table 3**).

The PCR-derived sequences shared >97% nucleotide identities with the corresponding HTS-derived sequences, except for SiMMV : BR:G1 DNA-A, SiMMV : BR:G2 DNA-A, and BGMV : BR:G3 (**Table 3**). The PCR amplicon sequence of SiMMV from G1 diverged almost 10% from the HTS consensus, while from G2 about 5%. The PCR amplicon sequence of BGMV shared 89.56% with the HTS-derived sequence, but 96.48% with the BGMV reference sequence (**Table 3**). The sequences of ToALCV from PCR and from HTS were completely identical, suggesting a highly homogenous population with genomes with minor point mutations. From 19 genomes, two (ToRMV and Bego1) were not confirmed, and two (SiMMV G1 and BGMV G3) were >9% divergent from the HTS-assembled sequence.

The number of reads used to assemble the begomovirus genomes out of the total reads in G2 and G3 was 93.12% and 90.33%, respectively. This indicates that <10% of reads were not mapped to begomovirus sequences. However, in G1 the reads exceed in 12.33% (26,840,363 out of 23,894,300; **Table 1**, **Supplementary Table 3**) from the total obtained reads. It clearly shows that some reads were used to assemble more than one genome, i.e., the genomes share short regions of high identity among the viruses. It makes the assembling process complex in the case of mixed population of highly related viruses. We hypothesized that this has caused incongruent assembly of SiMMV in G1 and BGMV in G3, and also of ToRMV and Bego1 in G1.

In a phylogenetic analysis of the complete genomes, the HTS-assembled sequences and the PCR-assembled sequences tightly clustered for most genomes (**Supplementary Figure 2**). The two exceptions were the DNA-A of SiMMV and BGMV. The HTS-assembled SiMMV G1 and G2 sequences were grouped, but were more distantly separated to the majority of SiMMV sequences. In contrast, the PCR-based sequences were closer to the other SiMMV sequences. In the BGMV tree, the PCR-derived sequence tightly clustered with other BGMV sequences, while the Bego2 sequence was distant from all of them, suggesting that these particular sequences generated by HTS assembly were not reliable.

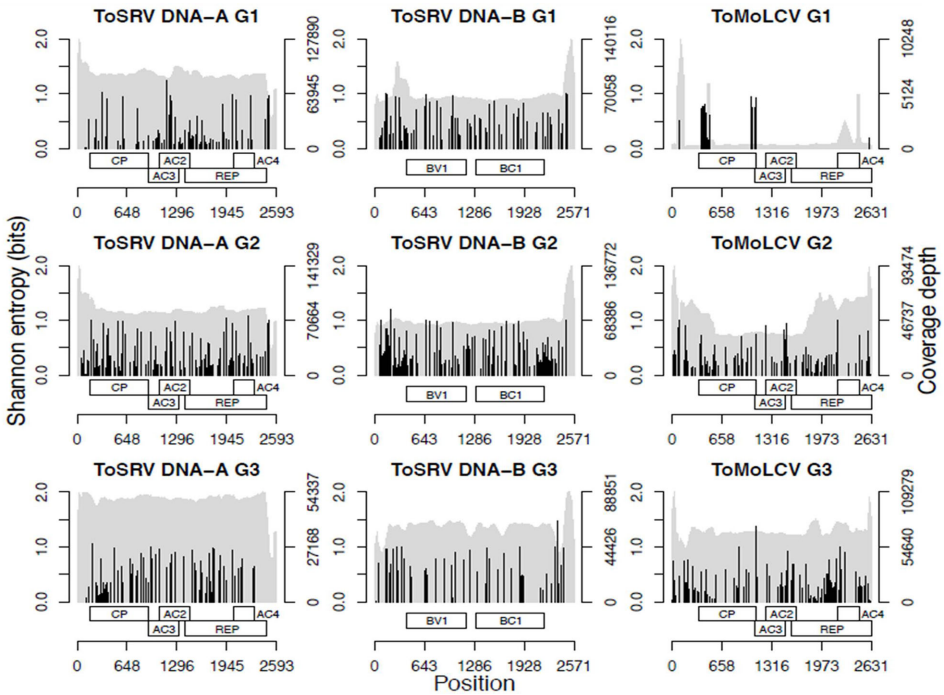

FIGURE 2 | Nucleotide diversity analysis of ToSRV and ToMoLCV showing coverage depth (gray) and Shannon entropy for the SNPs (black) and a representation of genome organization.

Detection of Selected Begomoviruses in Individual Total DNA Samples

It became clear that begomovirus diversity varied through time as did the prevalence of the viruses in each group. The four most frequent begomoviruses were: (1) SiMMV, (2) TGVV, (3) ToMoLCV, and (4) ToSRV. Consequently, to understand the frequency of each virus over time in the groups, we performed species-specific PCR to detect each of the four viruses in individual samples (**Figure 4**). In the G1 samples, a high detection rate of TGVV (100%) and ToSRV (99%) was observed, clearly indicating mixed infections. Approximately 21% of the plants were infected with ToMoLCV and 17% with SiMMV. In plants from G2 and G3, TGVV was not detected in any sample. SiMMV was detected in 4% of the samples in G2 and absent in G3. The rate of plants infected with ToSRV decreased from 99% in 2003–2005 to 83% in 2009–2011, and to 45% in 2014–2016. In contrast, ToMoLCV detection rate increased over time, from 21% in 2003–2005 to 47% in 2009–2011, and to 74% in 2014–2016, indicating that ToSRV and ToMoLCV were the most predominant viruses in this region.

Detection of the Resistance Gene *Ty-1* in the Samples

The variation in begomovirus species composition and the shift in the predominant virus from samples collected between 2003 and 2016 were striking. Several factors may have contributed to this variation, but an increase in the use of resistant cultivars may have been one of the most important factors. Assuming *Ty-1* to be the major resistance gene in Brazilian commercial hybrids, PCR was performed to detect this gene in individual samples of the three groups (**Figure 5**). *Ty-1* was detected in 14% of G1 samples, suggesting that 86% plants were susceptible to begomovirus infection. In G2 and G3, the rate of *Ty-1* positive samples increased dramatically to 71% and 55%, respectively, indicating that it is an important trait for the growers.

DISCUSSION

HTS provides an easy and fast means for sequencing of viral genomes present in infected plant samples at a large scale (e.g., Idris et al., 2014; Rodríguez-Negrete et al., 2019). Although viral DNA could be directly sequenced, we enriched the circular DNA using RCA prior to library preparation for specifically targeting begomoviruses (Idris et al., 2014). Two *de novo* assembling programs, Velvet (Zerbino and Birney, 2008) and MEGAHIT (Li et al., 2015) were used. Although Velvet produced a high number of contigs, they were shorter than those from MEGAHIT, as reported by Blawid et al. (2017) and Jo et al. (2017) (**Supplementary Tables 4 and 5**). Velvet reduces the chances of missing low frequent reads, which may not assemble to a detectable contig by other assemblers that generate longer contigs, being this an advantage of this method (Blawid et al., 2017). MEGAHIT, on the other hand, produces longer contigs,

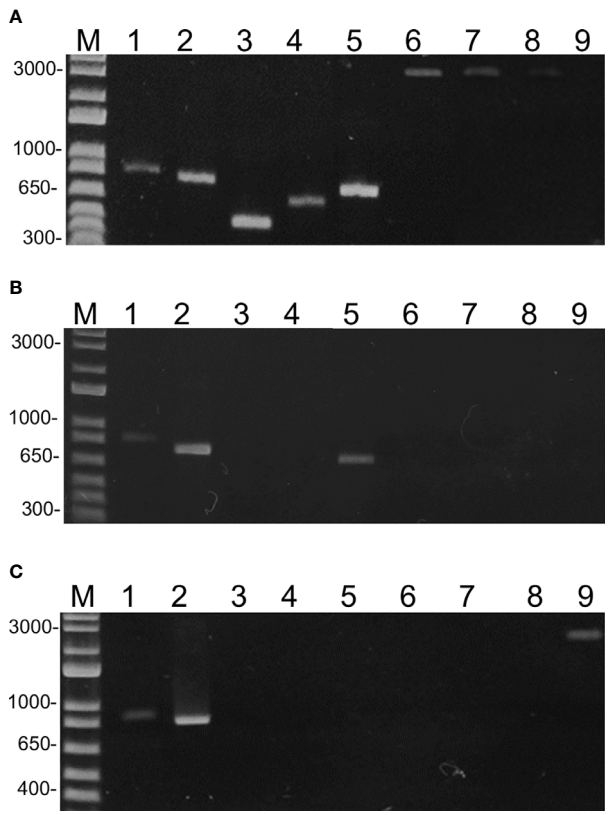

FIGURE 3 | Electrophoretic analysis of PCR amplicons on 1% agarose gel from pooled RCA samples of the G1 **(A)**, G2 **(B)**, and G3 **(C)** groups. PCR was performed using specific primers (**Supplementary Table 1**) for ToSRV (1), ToMoLCV (2), TGVV (3), ToCMoV (4), SiMMV (5), ToALCV (6), ToRMV (7), Bego1 (8), and Bego2 (9). M = 1 kb plus DNA ladder (Thermo Fisher Scientific).

which facilitates the assembling step and has a high sensitivity (Blawid et al., 2017). The final list of viruses was the same for both assemblers (**Table 1**, **Supplementary Tables 4** and **5**), indicating that the results were robust. However, the strategy of using 100 bp paired-end reads generated on the Illumina Hiseq 2000 platform for pooled highly related begomovirus samples proved to be challenging and could not be used as a stand-alone technique, as the final consensus sequence was significantly divergent in five (ToRMV, Bego1, Bego2, SiMMV G1 and SiMMV G2) out of 19 genomes. In the case of begomoviruses, it is therefore sensible that users avoid pooling samples, instead making use of barcoding to individualize samples, or by taking advantage of systems that generate longer sequences. Nevertheless, the analyses provided important information, such as the detection and identification of several begomoviruses and of one capula-like virus in the samples, which would be unlikely detected using traditional techniques as PCR/sequencing. Also important, it enabled the analysis of their diversity within the sampling pool, and through the three time points along the selected tomato cultivation area.

Analysis of ToSRV and ToMoLCV reads in the three libraries (**Figure 2**) showed that the coverage depth along the genome was reasonably uniform. A higher number of reads was concentrated at intergenic region of ToSRV, which may be related to overlapping reads in the common region shared by DNA-A and DNA-B. Exceptions were observed for ToMoLCV reads in G1 and G2, possibly correlating with highly conserved genomic regions among begomoviral species, and thus sharing many identical or near identical reads.

The uniform coverage of reads in the genome of ToSRV and ToMoLCV (**Figure 2**) also suggests that the amplification steps introduced by RCA and HTS were not biased and the entire genome was evenly covered. We do not discard, though, the possibility that an amplification bias was produced during the RCA step that could have introduced some artifacts.

We observed a remarkable population change in begomoviruses that infect tomatoes in the Federal District, Brazil, from 2003 to 2016. This study focused on samplings carried out within ~14 years, collected in an area of approximately 400 km^2. This region is an important tomato-growing area of the Brasilia greenbelt, where tomato is intensively planted throughout the year. In the G1 sample set (2003–2005), containing isolates collected approximately ten years after the introduction of *B. tabaci* MEAM1 and after the first report of begomovirus in tomatoes in this region (Ribeiro et al., 1994), we detected six geminivirus species (including one capula-like virus). A decrease in species richness was observed between 2007–2016, with only three species detected in each group (**Table 3**). The high rate of mixed infection in G1 suggests that the prevalence of begomovirus was high in the area and the plants were susceptible to begomovirus infection. Thereafter, a decrease in the number of begomovirus species and intraspecies diversity was observed (**Table 3**). Although it confirmed our initial hypothesis of continuous reduction of viral diversity following their transfer from wild and weed plants to a new cultivated plant, this phenomenon was not observed for tomato yellow leaf curl virus (TYLCV) in China (5-year survey; Yang et al., 2014) or tomato yellow leaf curl Sardinia virus (TYLCSV) in Spain (8-year survey; Sánchez-Campos et al., 2002). However, Font et al. (2007) reported that the number of haplotypes of TYLCV and TYLCSV was reduced and resulted in the prevalence of one haplotype with low genetic diversity in a time span of four years. Furthermore, in a study on begomovirus diversity, focused on pepper golden mosaic virus (PepGMV) and pepper huasteco yellow vein virus (PHYVV), on chiltepin in Mexico, Rodelo-Urrego et al. (2013) reported a reduction in coat protein sequence diversity within a 4-year sampling period (2007–2010) and attributed it to the level of landscape heterogeneity and not the effect of virus-host co-evolution. We speculate that after the invasion of MEAM1, which colonized myriad plants (crops and wild and weed hosts) in the early 1990s, the vectors transferred indigenous begomovirus populations from these plants to tomatoes (Castillo-Urquiza et al., 2008; García-Arenal and Zerbini, 2019), thereby resulting in an explosion of begomoviruses in the highly permissive tomato plants. Later, intense anthropic actions, such as cultivation on a commercial-scale, host uniformity, and lower crop diversity, contributed to a high degree of viral competition, and thus the selection of the

TABLE 3 | Consensus viral sequences identified by sequencing PCR amplicons in libraries G1, G2, and G3 and comparison with HTS and reference sequences.

Group		Identification/Genomic component	Genome length (Accession)[1]	Comparison with HTS[2]	Comparison with reference[3]
1	1	SiMMV : BR:G1 DNA-A	2676 (MT733803)	90.84*	94.39
	2	ToCMoV : BR:G1 DNA-A	2622 (MT733804)	98.09	92.75*
	3	ToCMoV : BR:G1 DNA-B	2536 (MT733805)	97.50	85.03*
	4	TGVV : BR:G1 DNA-A	2561 (MT733806)	98.71	98.20
	5	TGVV : BR:G1 DNA-B	2534 (MT733807)	99.37	98.93
	6	ToMoLCV : BR:G1	2631 (MT733810)	99.89	91.98*
	7	ToSRV : BR:G1 DNA-A	2592 (MT733808)	99.77	99.15
	8	ToSRV : BR:G1 DNA-B	2570 (MT733809)	99.73	99.26
	9	ToALCV : BR:G1	2875 (MT135209)	100.00	95.23
2	1	SiMMV : BR:G2 DNA-A	2691 (MT733814)	95.10	92.00*
	2	ToMoLCV : BR:G2	2631 (MT733813)	98.59	92.36*
	3	ToSRV : BR:G2 DNA-A	2592 (MT733811)	99.88	99.50
	4	ToSRV : BR:G2 DNA-B	2570 (MT733812)	99.88	99.34
3	1	ToMoLCV : BR:G3	2631 (MT733817)	99.92	92.12*
	2	ToSRV : BR:G3 DNA-A	2592 (MT733815)	99.31	99.27
	3	ToSRV : BR:G3 DNA-B	2570 (MT733816)	97.82	97.04
	4	BGMV : BR:G3 DNA-A	2619 (MT733818)	89.56*	96.48

[1]*Accession number at GenBank.*
[2]*Nucleotide identity of the genome-wide PCR amplicon sequence with the corresponding genome assembled by HTS, calculated by SDT (Muhire et al., 2014).*
[3]*Nucleotide identity of the genome-wide sPCR amplicon sequence with the corresponding reference genome (see Table 1), calculated by SDT (Muhire et al., 2014).*
**Percent identity below 94%.*

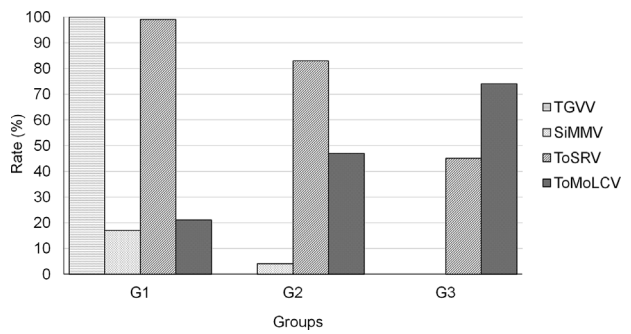

FIGURE 4 | Detection rate of TGVV, SiMMV, ToSRV, and ToMoLCV by PCR in individual total DNA from the G1 (2003–2005), G2 (2009–2011), and G3 (2014–2016) groups.

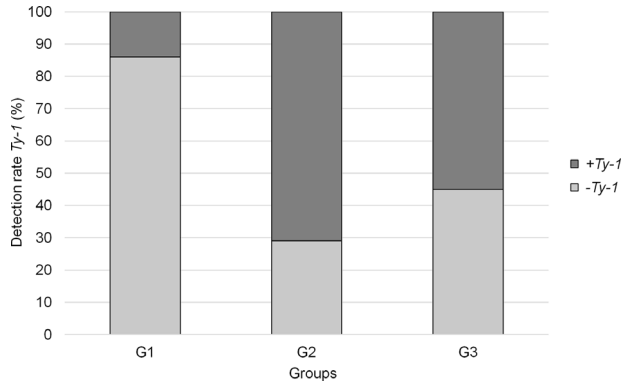

FIGURE 5 | Detection rate of *Ty-1* in individual total DNA from the G1 (2003–2005), G2 (2009–2011), and G3 (2014–2016) sample groups.

most fit, and on the decrease in the diversity of these begomoviruses, as also proposed by Pagán et al. (2012) and Rodelo-Urrego et al. (2013).

In this survey, six viruses, including the newly reported capula-like virus ToALCV with ~32,000 reads, were identified by HTS. ToALCV is a monopartite virus, and was recently described in Argentina (Vaghi Medina et al., 2018) and in the Federal District of Brazil (Batista et al., 2019). Thus, despite being recently described, the virus had been present in samples collected between 2003 and 2005. The vector of this virus is still unknown. DNA satellites associated to begomoviruses were not detected in our libraries, although alphasatellites have been previously reported in Brazil (Paprotka et al., 2010; Mar et al., 2017).

In this study, the use of >100 samples in at least eight farms for each grouping is believed to be sufficient to represent the begomovirus diversity in the region. One of the drawbacks of the sampling strategy was the selection of symptomatic plants. Although detecting begomoviral disease symptoms in resistant cultivars is simple, we may have generated a bias in searching for plants with stronger symptoms. However, in each field survey, an effort was made to cover all types of symptoms present in the area.

Notably, the DNA-A sequence of SiMMV was detected only in the G1 and G2 libraries, although at a low rate (**Figure 4**). SiMMV is usually associated with *Sida* spp., a widespread group of malvaceous weeds frequently found in association with tomato fields, and is an example of a virus that might be transferred from weeds to cultivated plants (Barreto et al., 2013). However, SiMMV DNA-B could not be detected by either HTS or PCR. As SiMMV DNA-A was found in G2 with ToSRV (always in mixed infection), it is possible that they share the DNA-B. This is because these two viruses are closely related and their DNA-A sequences share ~87% nucleotide identity. The analysis of the common region of all ToSRV and SiMMV

sequences assembled by HTS and PCR revealed an identical core-iterated sequence (GGTAG-GGTAG), except for the genome of SiMMV G1 assembled by PCR (GGGGT-GGGGA). Thus, it is possible that SiMMV DNA-A uses the ToSRV DNA-B for infection. Infectious clones prepared from a bipartite isolate of SiMMV, ToSRV, and G1 and G2 SiMMV DNA-A, tested in all possible combinations by inoculation in plants would clarify this relationship, and this study is underway. Furthermore, a BGMV isolate is expected to be a bipartite virus, but attempts to detect the DNA-B of a BGMV-like virus failed (data not shown). It means that it may also share the DNA-B of ToSRV or it behaves as a monopartite virus. The core-iterated sequence was (GGTGT-GGTGC) which is different from those of ToSRV. Another hypothesis is that when SiMMV or BGMV DNA-A coinfect a plant with a monopartite begomovirus, the viral derived proteins of the monopartite virus complement the DNA-A of SiMMV or BGMV. However, these hypotheses, and also the possibility that the DNA-B was under a detectable level, need to be further tested.

Due to the epidemic of begomovirus disease in the major tomato-growing regions in Brazil soon after the outbreak of MEAM1, (moderately) resistant cultivars became available and were largely used in the G2 group (**Figure 5**). Other resistance genes may be present in Brazilian cultivars but only the most prevalent gene, *Ty-1* (Pereira-Carvalho et al., 2015), was tested. We demonstrated that *Ty-1* was present in 55%–71% plants collected at later time points (**Figure 5**). We speculate that this might have produced a bottleneck effect during 2006–2008 and resulted in SiMMV, ToMoLCV and ToSRV to be filtered and survive the selection pressure. Even though the use of resistant cultivars is an effective strategy for disease control, it depends on the preference of growers. In many cases, susceptible cultivars have desired traits such as higher yield, resistance to other pathogens, and bigger fruit size and fruit quality (Boiteux et al., 2007; Rubio et al., 2010).

We estimated the rate of plants infected with the four prevalent viruses—ToSRV, ToMoLCV, TGVV, and SiMMV—by DNA-A-specific PCR. Only ToSRV and ToMoLCV were detected in all three groups (G1, G2, and G3). Although the number of plants infected with ToSRV decreased over time, the rate of ToMoLCV infection increased, outcompeting ToSRV (**Figure 4**). Whether ToMoLCV performs better during infection than ToSRV in resistant cultivars or if it is transmitted more efficiently by the MEAM1 population present in the area remains to be elucidated. The rate of mixed infection decreased over time, from 100% to almost 0%, after 13 years. The rate of mixed infection of two begomoviruses, PepGMV and PHYVV, also decreased from one year to another in cultivated chiltepin fields, which can be attributed to a decrease in host heterogeneity and an increase in host density (Pagán et al., 2012; Rodelo-Urrego et al., 2013), similar to what happened in the sampled area. It suggests that after their establishment in a specific crop, under a certain vector population in an intensively cultivated area, the co-existence of two begomoviruses in the same plant is not a common phenomenon. In fact, some regions may have reached this stage with the predominance of ToSRV in the major tomato-growing areas of the country (States of Goiás, São Paulo, and Minas Gerais, Mituti et al., 2019), ToMoLCV in the North-East region (Fernandes et al., 2008; Inoue-Nagata et al., 2016; Rojas et al., 2018), and tomato common mosaic virus (ToCmMV) in the states of Espírito Santo and Rio de Janeiro (Barbosa et al., 2016).

Interestingly, in the G1 library, ToSRV reads corresponded to a relative abundance of 0.67, implying that this virus was more prevalent than the others (**Table 2**). The increase in relative abundance to 0.81 in the G2 library confirms that it is most fit in this agricultural environment, such as continuous tomato cultivation, mild tropical climate, standard cultivation system, and the presence of *B. tabaci* MEAM1. However, this rate decreased in the G3 library, whereas that for ToMoLCV showed a substantial increase, similar to the tendency seen in G1–G2 (**Table 2**). Taken together, this result and the detection of these viruses in most individual samples (**Figure 4**) demonstrate that ToSRV and ToMoLCV were the most successful tomato plant viruses in the area. This result must be carefully analyzed since an amplification step by RCA was added prior to HTS, which may influence population profiles in the samples. Notably, the number of tomato samples was similar in all three groups in an attempt to reduce the bias introduced by the amplification step. In the field of virus genome analysis, Shannon entropy (**Table 2**) measures diversity, based on haplotype frequencies (Gregori et al., 2016), and demonstrates the abundance of unique sequences. In our case, we used 27-mers frequencies to circumvent the difficulties in assembling haplotypes from 100 bp reads. An increase in Shannon entropy index was observed in ToMoLCV (G1 to G3), but the decrease in ToSRV (G2 to G3) confirmed that ToMoLCV became more diverse (and more frequent) than ToSRV isolates. As expected under neutral selection, the diversity and population size of ToMoLCV and ToSRV varied accordingly overall (Kimura, 1983). Exceptionally, genetic diversity of ToSRV DNA-B decreased from G2 to G3 although its relative abundance increased, suggesting purifying selection.

ToSRV and ToMoLCV are considered successful begomoviruses in this production system. Future studies may reveal that only one—ToMoLCV—predominates, based on the tendency. This scenario may change dramatically as new resistance genes are being used for introgression into commercial tomato hybrids. During the surveyed period, only *B. tabaci* MEAM1 was detected in the area (data not shown). The first report of the invasive species *B. tabaci* Mediterranean (Med) in Brazil occurred in 2015 (Barbosa et al., 2015). To date, it has not been reported in the central region, although it is rapidly spreading in the country (Moraes et al., 2018). We speculate that the introduction of Med whiteflies can change the incidence, prevalence, and diversity of begomoviruses in our crops in the coming years.

DATA AVAILABILITY STATEMENT

The datasets generated for this study can be found in the GenBank. MT135209, MT733803, MT733804, MT733805, MT733806, MT733807, MT733808, MT733809, MT733810,

MT733811, MT733812, MT733813, MT733814, MT733815, MT733816, MT733817, MT733818.

AUTHOR CONTRIBUTIONS

TS and AI-N designed the experiments, and collected the samples. TS prepared the samples, analyzed the genetic polymorphism, performed the sequencing and validated the sequences. TS and TM amplified and sequenced the complete virus genomes. TS, JS, EN, TN and AI-N performed the bioinformatics analyses. TS, JS, TN, TM, EN and AI-N read, revised, and approved the manuscript.

FUNDING

The research leading to these results has received funding from the Fundação de Apoio à Pesquisa do Distrito Federal (Project 0193.001460/2016) and from the Fundação de Amparo à Pesquisa de São Paulo (Project 2018/18274-3).

ACKNOWLEDGMENTS

The authors thank Lucio Flavio Barbosa and Hamilton José Lourenço for technical assistance, and José Luiz Pereira for assistance in sample collection. The authors also thank Santiago Elena (CSIC, Spain) for relevant advices on intraspecific diversity analyses. TS is a recipient of CNPq scholarship. TN and AI-N are CNPq fellows.

SUPPLEMENTARY MATERIAL

The Supplementary Material for this article can be found online at: https://www.frontiersin.org/articles/10.3389/fpls.2020.01201/full#supplementary-material

REFERENCES

Aguilera, J. G., Hurtado, F. D., Xavier, C. A. D., Laurindo, B. S., Nick, C., Gil, M.Á., et al. (2011). Identificação dos genes *Ty*-2 e *Ty*-3 de resistência a begomovírus em genótipos de tomateiro. *Pesquisa Agropecuária Bras.* 46, 772–775. doi: 10.1590/s0100-204x2011000700014

Albuquerque, L. C., Varsani, A., Fernandes, F. R., Pinheiro, B., Martin, D. P., Ferreira, P. D. T. O., et al. (2012). Further characterization of tomato-infecting begomoviruses in Brazil. *Arch. Virol.* 157, 747–752. doi: 10.1007/s00705-011-1213-7

Anbinder, I., Reuveni, M., Azari, R., Paran, I., Nahon, S., Shlomo, H., et al. (2009). Molecular dissection of Tomato leaf curl virus resistance in tomato line TY172 derived from Solanum peruvianum. *Theor. Appl. Genet.* 119, 519–530. doi: 10.1007/s00122-009-1060-z

Bai, Y., Yan, Z., Pérez-de-Castro, A., Díez, M. J., Hutton, S. F., Visser, R. G. F., et al. (2018). Resistance to tomato yellow leaf curl virus in tomato germplasm. *Front. Plant Sci.* 9:1198:1198. doi: 10.3389/fpls.2018.01198

Barbosa, L. D. F., Yuki, V. A., Marubayashi, J. M., De Marchi, B. R., Perini, F. L., Pavan, M. A., et al. (2015). First report of Bemisia tabaci Mediterranean (Q biotype) species in Brazil. *Pest Manage. Sci.* 71, 501–504. doi: 10.1002/ps.3909

Barbosa, J. C., Albuquerque, L. C., Rezende, J. A., Inoue-Nagata, A. K., Bergamin Filho, A., and Costa, H. (2016). Occurrence and molecular characterization of Tomato common mosaic virus (ToCmMV) in tomato fields in Espírito Santo state, Brazil. *Trop. Plant Pathol.* 41, 62–66. doi: 10.1007/s40858-015-0064-2

Barreto, S. S., Hallwass, M., Aquino, O. M., and Inoue-Nagata, A. K. (2013). A study of weeds as potential inoculum sources for a tomato-infecting begomovirus in central Brazil. *Phytopathology* 103, 436–444. doi: 10.1094/phyto-07-12-0174-r

Batista, J. G., Melo, F. L., Pereira-Carvalho, R. C., Alves-Freitas, D. M. T., and Ribeiro, S. G. (2019). First report of tomato apical leaf curl virus infecting tomato in Brazil. *Plant Dis.* 103, 1443. doi: 10.1094/PDIS-09-18-1636-PDN

Belabess, Z., Peterschmitt, M., Granier, M., Tahiri, A., Blenzar, A., and Urbino, C. (2016). The non-canonical tomato yellow leaf curl virus recombinant that displaced its parental viruses in southern Morocco exhibits a high selective advantage in experimental conditions. *J. Gen. Virol.* 97, 3433–3445. doi: 10.1099/jgv.0.000633

Blawid, R., Silva, J. M. F., and Nagata, T. (2017). Discovering and sequencing new plant viral genomes by next-generation sequencing: description of a practical pipeline. *Ann. Appl. Biol.* 17, 301–314. doi: 10.1111/aab.12345

Boiteux, L. S., Oliveira, V. R., Silva, C. H., Makishima, N., Inoue-Nagata, A. K., Fonseca, M. E. D. N., et al. (2007). Reaction of tomato hybrids carrying the *Ty*-1 locus to Brazilian bipartite Begomovirus species. *Horticult. Bras.* 25, 20–23. doi: 10.1590/s0102-05362007000100005

Bolger, A. M., Lohse, M., and Usadel, B. (2014). Trimmomatic: a flexible trimmer for Illumina sequence data. *Bioinformatics* 30, 2114–2120. doi: 10.1093/bioinformatics/btu170

Brown, J. K., Fauquet, C. M., Briddon, R. W., Zerbini, M., Moriones, E., and Navas- Castillo, J. (2012). "Geminiviridae," in *Virus Taxonomy-Ninth Report of the International Committee on Taxonomy of Viruses*. Eds. A. M. Q. King, M. J. Adams, E. B. Carstens and E. J. Lefkowitz (San Diego, CA: Elsevier Academic Press), 351–373.

Brown, J., Zerbini, F. M., Navas-Castillo, J., Moriones, E., Ramos-Sobrinho, R., Silva, J., et al. (2015). Revision of Begomovirus taxonomy based on pairwise sequence comparisons. *Arch. Virol.* 160, 1593–1619. doi: 10.1007/s00705-015-2398-y

Butterbach, P., Verlaan, M. G., Dullemans, A., Lohuis, D., Visser, R. G., Bai, Y., et al. (2014). Tomato yellow leaf curl virus resistance by *Ty*-1 involves increased cytosine methylation of viral genomes and is compromised by cucumber mosaic virus infection. *Proc. Natl. Acad. Sci.* 111, 12942–12947. doi: 10.1073/pnas.1400894111

Castillo-Urquiza, G. P., Beserra, J. E. A., Bruckner, F. P., Lima, A. T., Varsani, A., Alfenas-Zerbini, P., et al. (2008). Six novel begomoviruses infecting tomato and associated weeds in Southeastern Brazil. *Arch. Virol.* 153, 1985–1989. doi: 10.1007/s00705-008-0172-0

Costa, A. S. (1976). Whitefly-transmitted plant diseases. *Annu. Rev. Phytopathol.* 14, 429–449. doi: 10.1146/annurev.py.14.090176.002241

Doyle, J. J., and Doyle, J. L. (1990). Isolation of plant DNA from fresh tissue. *Focus* 12, 39–40.

Duffy, S., Shackelton, L. A., and Holmes, E. C. (2008). Rates of evolutionary change in viruses: patterns and determinants. *Nat. Rev. Genet.* 9, 267–276. doi: 10.1038/nrg2323

Faria, J. C., Souza-Dias, J. A. C., Slack, S. A., and Maxwell, D. P. (1997). A new geminivirus associated with tomato in the State of São Paulo, Brazil. *Plant Dis.* 81:423. doi: 10.1094/pdis.1997.81.4.423b

Fauquet, C. M., Bisaro, D. M., Briddon, R. W., Brown, J. K., Harrison, B. D., Rybicki, E. P., et al. (2003). Revision of taxonomic criteria for species demarcation in the family Geminiviridae, and an updated list of begomovirus species. *Arch. Virol.* 148, 405–421. doi: 10.1007/s00705-002-0957-5

Fernandes, J. J., Carvalho, M. G., Andrade, E. C., Brommonschenkel, S. H., Fontes, E. P. B., and Zerbini, F. M. (2006). Biological and molecular properties of Tomato rugose mosaic virus (ToRMV), a new tomato-infecting begomovirus from Brazil. *Plant Pathol.* 55, 513–522. doi: 10.1111/j.1365-3059.2006.01395.x

Fernandes, F. R., de Albuquerque, L. C., de Britto Giordano, L., Boiteux, L. S., de Avila, A. C., and Inoue-Nagata, A. K. (2008). Diversity and prevalence of Brazilian bipartite begomovirus species associated to tomatoes. *Virus Genes* 36, 251–258. doi: 10.1007/s11262-007-0184-y

Flores, E., Silberschmidt, K., and Kramer, M. (1960). Observações de "clorose infecciosa" das malváceas em tomateiros do campo. *O Biológico* 26, 65–69.

Font, M. I., Rubio, L., Martinez-Culebras, P. V., and Jorda, C. (2007). Genetic structure and evolution of natural populations of viruses causing the tomato yellow leaf curl disease in Spain. *Virus Res.* 128, 43–51. doi: 10.1016/j.virusres.2007.04.003

García-Andrés, S., Tomás, D. M., Navas-Castillo, J., and Moriones, E. (2009). Resistance-driven selection of begomoviruses associated with the tomato yellow leaf curl disease. *Virus Res.* 146, 66–72. doi: 10.1016/j.virusres.2009.08.012

García-Arenal, F., and Zerbini, F. M. (2019). Life on the edge: geminiviruses at the interface between crops and wild plant hosts. *Annu. Rev. Virol.* 6, 411–433. doi: 10.1146/annurev-virology-092818-015536

Gill, U., Scott, J. W., Shekasteband, R., Ogundiwin, E., Schuit, C., Francis, D. M., et al. (2019). *Ty*-6, a major begomovirus resistance gene on chromosome 10, is effective against Tomato yellow leaf curl virus and Tomato mottle virus. *Theor. Appl. Genet.* 132, 1543–1554. doi: 10.1007/s00122-019-03298-0

Giordano, L. B., Silva-Lobo, V. L., Santana, F. M., Fonseca, M. E. N., and Boiteux, L. S. (2005). Inheritance of resistance to the bipartite Tomato chlorotic mottle begomovirus derived from Lycopersicon esculentum cv. *Tyking Euphytica* 143, 27–33. doi: 10.1007/s10681-005-1685-1

Gregori, J., Perales, C., Rodrigues-Frias, F., Esteban, J. I., Quer, J., and Domingo, E. (2016). Viral quasispecies complexity measures. *Virology* 493, 227–237. doi: 10.1016/j.virol.2016.03.017

Hurtado, F. D., Gil, M. A., Zubiaur, Y. M., Aguilera, J. G., Xavier, C. A. D., Zerbini Junior, F. M., et al. (2012). Sources of resistance in tomato to bipartite begomoviruses Tomato yellow spot virus and Tomato severe rugose virus. *Horticult. Bras.* 30, 639–644. doi: 10.1590/S0102-05362012000400013

Hutton, S. F., Scott, J. W., and Schuster, D. J. (2012). Recessive resistance to Tomato yellow leaf curl virus from the tomato cultivar Tyking is located in the same region as *Ty*-5 on chromosome 4. *HortScience* 47, 324–327. doi: 10.21273/HORTSCI.47.3.324

Idris, A., Al-Saleh, M., Piatek, M. J., Al-Shahwan, I., Ali, S., and Brown, J. K. (2014). Viral metagenomics: Analysis of begomoviruses by illumina high-throughput sequencing. *Viruses* 6, 1219–1236. doi: 10.3390/v6031219

Inoue-Nagata, A. K., Lima, M. F., and Gilbertson, R. L. (2016). A review of geminivirus diseases in vegetables and other crops in Brazil: current status and approaches for management. *Horticult. Bras.* 34, 8–18. doi: 10.1590/S0102-053620160000100002

Ji, Y., Scott, J. W., Schuster, D. J., and Maxwell, D. P. (2009). Molecular mapping of *Ty*-4, a new Tomato yellow leaf curl virus resistance locus on chromosome 3 of tomato. *J. Am. Soc. Hortic. Sci.* 134, 281–288. doi: 10.21273/jashs.134.2.281

Jo, Y., Choi, H., Kim, S. M., Kim, S. L., Lee, B. C., and Cho, W. K. (2017). The pepper virome: natural co-infection of diverse viruses and their quasispecies. *BMC Genomics* 18, 453. doi: 10.1186/s12864-017-3838-8

Kimura, M. (1983). *The neutral theory of molecular evolution* (Cambridge UP: Cambridge University Press). doi: 10.1017/CBO9780511623486

Kumar, S., Stecher, G., Li, M., Knyaz, C., and Tamura, K. (2018). MEGA X: molecular evolutionary genetics analysis across computing platforms. *Mol. Biol. Evol.* 35, 1547–1549. doi: 10.1093/molbev/msy096

Lapidot, M., and Friedmann, M. (2002). Breeding for resistance to whitefly transmitted geminiviruses. *Ann. Appl. Biol.* 140, 109–127. doi: 10.1111/j.1744-7348.2002.tb00163.x

Li, H., Handsaker, B., Wysoker, A., Fennell, T., Ruan, J., Homer, N., et al. (2009). The sequence alignment/map format and SAMtools. *Bioinformatics* 25, 2078–2079. doi: 10.1093/bioinformatics/btp352

Li, D., Liu, C. M., Luo, R., Sadakane, K., and Lam, T. W. (2015). MEGAHIT: an ultra-fast single-node solution for large and complex metagenomics assembly via succinct de Bruijn graph. *Bioinformatics* 31, 1674–1676. doi: 10.1093/bioinformatics/btv033

Li, H. (2013). Aligning sequence reads, clone sequences and assembly contigs with BWA-MEM. arXiv.org [Preprint]. Available at: https://arxiv.org/abs/1303.3997 (Accessed April 23, 2020).

Lima, A., Silva, J. C., Silva, F. N., Castillo-Urquiza, G. P., Silva, F. F., Seah, Y. M., et al. (2017). The diversification of begomovirus populations is predominantly driven by mutational dynamics. *Virus Evol.* 3, 1–14. doi: 10.1093/ve/vex005

Mar, T. B., Mendes, I. R., Lau, D., Fiallo-Olivé, E., Navas-Castillo, J., Alves, M. S., et al. (2017). Interaction between the New World begomovirus Euphorbia yellow mosaic virus and its associated alphasatellite: effects on infection and transmission by the whitefly Bemisia tabaci. *J. Gen. Virol.* 98, 1552–1562. doi: 10.1099/jgv.0.000814

Marçais, G., and Kingsford, C. (2011). A fast, lock-free approach for efficient parallel counting of occurrences of k-mers. *Bioinformatics* 27, 764–770. doi: 10.1093/bioinformatics/btr011

Matyis, J. C., Silva, D. M., Oliveira, A. R., and Costa, A. S. (1975). Purificação e morfologia do vírus do mosaico dourado do tomateiro. *Summa Phytopathol.* 1, 267–275.

Mituti, T., Moura, M. F., Macedo, M. A., Silva, T. N., Pinto, L. R., Costa, H., et al. (2019). Survey of begomoviruses and the crinivirus, tomato chlorosis virus, in solanaceous in Southeast/Midwest of Brazil. *Trop. Plant Pathol.* 44, 468–472. doi: 10.1007/s40858-019-00294

Moraes, L. A., Muller, C., Bueno, R. C. O. F., Santos, A., Bello, V. H., de Marchi, B. R., et al. (2018). Distribution and phylogenetics of whiteflies and their endosymbiont relationships after the Mediterranean species invasion in Brazil. *Sci. Rep.* 8 (1), 14589. doi: 10.1038/s41598-018-32913-1

Muhire, B. M., Varsani, A., and Martin, D. P. (2014). SDT: a virus classification tool based on pairwise sequence alignment and identity calculation. *PloS One* 9, 1–8. doi: 10.1371/journal.pone.0108277

Pagán, I., Gonzalez-Jara, P., Moreno-Letelier, A., Rodelo-Urrego, M., Fraile, A., Piñero, D., et al. (2012). Effect of biodiversity changes in disease risk: exploring disease emergence in a plant-virus system. *PloS Pathog.* 8, e1002796. doi: 10.1371/journal.ppat.1002796

Paprotka, T., Metzler, V., and Jeske, H. (2010). The first DNA 1-like alpha satellites in association with New World begomoviruses in natural infections. *Virology* 404, 148–157. doi: 10.1016/j.virol.2010.05.003

Pereira-Carvalho, R. C., Díaz-Pendón, J., Fonseca, M. E., Boiteux, L. S., Fernández-Muñoz, R., Moriones, E., et al. (2015). Recessive resistance derived from tomato cv. Tyking limits drastically the spread of tomato yellow leaf curl virus. *Viruses* 7, 2518–2533. doi: 10.3390/v7052518

Prasanna, H. C., Sinha, D. P., Rai, G. K., Krishna, R., Kashyap, S. P., Singh, N. K., et al. (2015). Pyramiding *Ty*2 and *Ty*3 genes for resistance to monopartite and bipartite tomato leaf curl viruses of India. *Plant Pathol.* 64, 256–264. doi: 10.1111/ppa.12267

Ribeiro, S. G., Melo, L. V., Boiteux, L. S., Kitajima, E. W., and Faria, J. C. (1994). Tomato infection by a geminivirus in the Federal District, Brazil. *Fitopatol. Bras.* 19, 330.

Ribeiro, S. G., Ambrozevicius, L. P., Avila, A. C., Bezerra, I. C., Calegario, R. F., Fernandes, J. J., et al. (2003). Distribution and genetic diversity of tomato-infecting begomoviruses in Brazil. *Arch. Virol.* 148, 281–295. doi: 10.1007/s00705-002-0917-0

Rocha, C. S., Castillo-Urquiza, G. P., Lima, A. T., Silva, F. N., Xavier, C. A., Hora-Júnior, B. T., et al. (2013). Brazilian begomovirus populations are highly recombinant, rapidly evolving, and segregated based on geographical location. *J. Virol.* 87, 5784–5799. doi: 10.1128/JVI.00155-13

Rodelo-Urrego, M., Pagán, I., González-Jara, P., Betancourt, M., Moreno-Letelier, A., Ayllón, M. A., et al. (2013). Landscape heterogeneity shapes host-parasite interactions and results in apparent plant–virus codivergence. *Mol. Ecol.* 22 (8), 2325–2340. doi: 10.1111/mec.12232

Rodríguez-Negrete, E. A., Morales-Aguilar, J. J., Domínguez-Duran, G., Torres-Devora, G., Camacho-Beltrán, E., Leyva-López, N. E., et al. (2019). High-Throughput Sequencing reveals differential begomovirus species diversity in non-cultivated plants in northern-pacific Mexico. *Viruses* 11:594. doi: 10.3390/v11070594

Rojas, M. R., Gilbertson, R. L., Russel, D. R., and Maxwell, D. P. (1993). Use of degenerate primers in the polymerase chain reaction to detect whitefly-transmitted geminiviruses. *Plant Dis.* 77, 340–347. doi: 10.1094/PD-77-0340

Rojas, M. R., Macedo, M. A., Maliano, M. R., Soto-Aguilar, M., Souza, J. O., Briddon, R. W., et al. (2018). World Management of Geminiviruses. *Annu. Rev. Phytopathol.* 56, 637–677. doi: 10.1146/annurev-phyto-080615-100327

Rubio, F., García-Martínez, S., Alonso, A., Grau, A., Valero, M., and Ruiz, J. J. (2010). Introgressing resistance genes into traditional tomato cultivars: effects on yield and quality. *Acta Hortic.* 935, 29–33. doi: 10.17660/ActaHortic.2012.935.3 Abstract retrieved from Abstracts in XXVIII International Horticultural Congress on Science and Horticulture for People (IHC2010).

Sánchez-Campos, S., Díaz, J. A., Monci, F., Bejarano, E. R., Reina, J., Navas-Castillo, J., et al. (2002). High genetic stability of the begomovirus Tomato yellow leaf curl Sardinia virus in southern Spain over an 8-year period. *Phytopathology* 92 (8), 842–849. doi: 10.1094/PHYTO.2002.92.8.842

Shannon, C. E. (1948). A mathematical theory of communication. *Bell System Tech. J.* 27, 379–423. doi: 10.1002/j.1538-7305.1948.tb01338.x

Silva, F. N., Lima, A. T., Rocha, C. S., Castillo-Urquiza, G. P., Alves-Júnior, M., and Zerbini, F. M. (2014). Recombination and pseudorecombination driving the evolution of the begomoviruses Tomato severe rugose virus (ToSRV) and Tomato rugose mosaic virus (ToRMV): two recombinant DNA-A components sharing the same DNA-B. *Virol. J.* 11:66. doi: 10.1186/1743-422x-11-66

Tamura, K., and Nei, M. (1993). Estimation of the number of nucleotide substitutions in the control region of mitochondrial DNA in humans and chimpanzees. *Mol. Biol. Evol.* 10, 512–526. doi: 10.1093/oxfordjournals.molbev.a040023

Vaghi Medina, C. G., Teppa, E., Bornancini, V. A., Flores, C. R., Marino-Buslje, C., and López Lambertini, P. M. (2018). Tomato apical leaf curl virus: a novel, monopartite geminivirus detected in tomatoes in Argentina. *Front. Microbiol.* 8:2665:2665. doi: 10.3389/fmicb.2017.02665

Verlaan, M. G., Hutton, S. F., Ibrahem, R. M., Kormelink, R., Visser, R. G., Scott, J. W., et al. (2013). The tomato yellow leaf curl virus resistance genes *Ty*-1 and *Ty*-3 are allelic and code for DFDGD-class RNA–dependent RNA polymerases. *PloS Genet.* 9, 1–11. doi: 10.1371/journal.pgen.1003399

Vu, S., Melgarejo, T. A., Chen, L., Souza, J. O., Macedo, M. A., Inoue-Nagata, A. K., et al. (2015). Evidence that tomato mottle leaf curl virus from Northeastern Brazil is an indigenous New World monopartite begomovirus. *Phytopathology* 105, 143. doi: PHYTO-105-11-S4.1

Wilm, A., Aw, P. P. K., Bertrand, D., Yeo, G. H. T., Ong, S. H., Wong, C. H., et al. (2012). LoFreq: a sequence-quality aware, ultra-sensitive variant caller for uncovering cell-population heterogeneity from high-throughput sequencing datasets. *Nucleic Acids Res.* 40, 11189–11201. doi: 10.1093/nar/gks918

Yang, X. L., Zhou, M. N., Qian, Y. J., Xie, Y., and Zhou, X. P. (2014). Molecular variability and evolution of a natural population of tomato yellow leaf curl virus in Shanghai, China. *J. Zhejiang Univ. Sci. B.* 15 (2), 133–142. doi: 10.1631/jzus.B1300110

Zamir, D., Ekstein-Michelson, I., Zakay, Y., Navot, N., Zeidan, M., Sarfatti,, et al. (1994). Mapping and introgression of a tomato yellow leaf curl virus tolerance gene, *Ty*-1. *Theor. Appl. Genet.* 88, 141–146. doi: 10.1007/bf00225889

Zerbino, D. R., and Birney, E. (2008). Velvet: algorithms for de novo short read assembly using de Bruijn graphs. *Genome Res.* 18, 821–829. doi: 10.1101/gr.074492.107

Conflict of Interest: The authors declare that the research was conducted in the absence of any commercial or financial relationships that could be construed as a potential conflict of interest.

Advantages of publishing in Frontiers

OPEN ACCESS
Articles are free to read for greatest visibility and readership

FAST PUBLICATION
Around 90 days from submission to decision

HIGH QUALITY PEER-REVIEW
Rigorous, collaborative, and constructive peer-review

TRANSPARENT PEER-REVIEW
Editors and reviewers acknowledged by name on published articles

Frontiers
Avenue du Tribunal-Fédéral 34
1005 Lausanne | Switzerland

Visit us: www.frontiersin.org
Contact us: frontiersin.org/about/contact

REPRODUCIBILITY OF RESEARCH
Support open data and methods to enhance research reproducibility

DIGITAL PUBLISHING
Articles designed for optimal readership across devices

FOLLOW US
@frontiersin

IMPACT METRICS
Advanced article metrics track visibility across digital media

EXTENSIVE PROMOTION
Marketing and promotion of impactful research

LOOP RESEARCH NETWORK
Our network increases your article's readership